

Modelling land-use futures in the context of climate change mitigation

The role of land use in global climate change mitigation and its connection to the water-land-energy-food-climate nexus

Jonathan Doelman

Modelling land-use futures in the context of climate change mitigation

The role of land use in global climate change mitigation and its connection to the water-land-energy-food-climate nexus.

J.C. Doelman

Modelling land-use futures in the context of climate change mitigation

The role of land use in global climate change mitigation and its connection to the water-land-energy-food-climate nexus.

J.C. Doelman, 2023

Provided by thesis specialist Ridderprint, ridderprint.nl

Printing Ridderprint

Layout and design Indah Hijmans, persoonlijkproefschrift.nl

Cover design Indah Hijmans

ISBN 978-94-6483-094-1

Modelling land-use futures in the context of climate change mitigation

The role of land use in global climate change mitigation and its connection to the water-land-energy-food-climate nexus

Het modelleren van toekomstig landgebruik in de context van klimaatmitigatie

De rol van landgebruik in mondiale klimaatmitigatie in relatie tot de water-land-energie-voedsel-klimaat nexus
(met een samenvatting in het Nederlands)

Proefschrift

ter verkrijging van de graad van doctor aan de
Universiteit Utrecht
op gezag van de
rector magnificus, prof.dr. H.R.B.M. Kummeling,
ingevolge het besluit van het college voor promoties
in het openbaar te verdedigen op

vrijdag 16 juni 2023 des middags te 2.15 uur

door

Jonathan Cornelis Doelman

geboren op 22 maart 1989
te Amsterdam

Promotor:

Prof. dr. D.P. van Vuuren

Copromotor:

Dr. E. Stehfest

Beoordelingscommissie:

Prof. dr. M. Banse

Prof. dr. J. Pongratz

Dr. A. Popp

Prof. dr. ir. M.G. Rietkerk

Prof. dr. B. Wicke

The research reported in this thesis was carried out at the 'Climate, Air and Energy' department of the 'PBL Netherlands Environmental Assessment Agency' in The Hague, and the 'Copernicus Institute for Sustainable Development, Faculty of Geosciences, Utrecht University' in Utrecht. The research was funded by European Union's Seventh Framework Programme FP7/2007-2013 under grant agreement n° 603542 LUC4C and grant agreement n°290693 FOODSECURE, and European Union's Horizon 2020 research and innovation programme, under grant agreement n°689150 SIM4NEXUS.

Table of Contents

Abbreviations and Units	10
1 Introduction	15
1.1. Land and climate change	16
1.2. Land use and climate change mitigation	18
1.3. Land use, sustainable development, and the water-land-energy-food-climate nexus	21
1.4. Modelling land-use futures in the context of global environmental change	22
1.5. The IMAGE integrated assessment model framework	24
1.6. Aim of the thesis	27
1.7. Outline	27
2 Exploring SSP land-use dynamics using the IMAGE model: Regional and gridded scenarios of land-use change and land-based climate change mitigation	31
Abstract	32
2.1. Introduction	33
2.2. Methods	35
2.2.1. The IMAGE 3.0 model framework	35
2.2.2. The SSP storylines and climate mitigation targets	38
2.2.3. Scenario implementation	40
2.3. Results	45
2.3.1. Global land-use dynamics in SSP baseline scenarios	45
2.3.2. Regional land-use dynamics in SSP reference scenarios	50
2.3.3. Impacts of land-based climate change mitigation on land dynamics	53
2.3.4. Greenhouse gas consequences of baseline and mitigation scenarios	55
2.4. Discussion and Conclusions	57
Acknowledgements	60
3 The role of peatland degradation, protection and restoration for climate change mitigation in the SSP scenarios	63
Abstract	64
3.1. Introduction	65
3.2. Methods	66
3.2.1. The IMAGE 3.2 model framework	66
3.2.2. Peatland implementation	67
3.2.3. Scenario description	67
3.2.4. Sensitivity analysis	69

3.3. Results	69
3.3.1. Land-use dynamics	69
3.3.2. GHG emissions dynamics	72
3.3.3. Sensitivity to varying peatland estimates	75
3.4. Discussion	77
3.5. Conclusions	80
Data availability statement	80
4 Afforestation for climate change mitigation: potentials, risks and trade-offs	83
Abstract	84
4.1. Introduction	85
4.2. Materials and Methods	87
4.2.1. The IMAGE model framework	87
4.2.2. Overview of afforestation method	88
4.2.3. Biophysical potential of afforestation	90
4.2.4. Costs of afforestation	91
4.2.5. Scenario definitions	93
4.3. Results	94
4.3.1. MAC curves	94
4.3.2. Mitigation scenarios	96
4.4. Discussion	101
Acknowledgements	105
5 Making the Paris Agreement climate targets consistent with food security objectives	107
Abstract	108
5.1. Introduction	109
5.2. Methods	110
5.2.1. Models	110
5.2.2. Scenario implementation	112
5.3. Results	119
5.3.1. Food security effects of land-based mitigation	119
5.3.2. Preventing negative effects of land-based mitigation on food security	122
5.4. Discussion	124
5.5. Conclusions	126
Acknowledgements	126

6	Quantifying synergies and trade-offs in the global water-land-food-climate nexus using a multi-model scenario approach	129
	Abstract	130
	6.1. Introduction	131
	6.2. Methods	133
	6.2.1. Model descriptions	133
	6.2.2. Scenario description	134
	6.2.3. Indicator description	139
	6.3. Results	140
	6.3.1. Irrigation water withdrawal	140
	6.3.2. Natural land share	142
	6.3.3. Food price index	143
	6.3.4. AFOLU GHG emissions	144
	6.3.5. Nitrogen surplus in agriculture	145
	6.3.6. Trade-offs and synergies	146
	6.4. Discussion	150
	6.5. Conclusions	152
7	Summary and conclusions	155
	7.1. Introduction and research questions	156
	7.2. Main findings	157
	7.2.1. How will land use develop in the long term under various scenarios at the global and regional scale?	157
	7.2.2. What can be the role of land use in achieving stringent climate targets?	160
	7.2.3. How important are trade-offs and synergies between land-based climate mitigation and other societal goals in the water-land-energy-food-climate nexus?	165
	7.2.4. How can these trade-offs be minimized and synergies be maximized?	168
	7.3. Suggestions for future research	171
	7.4. Policy recommendations	174
8	Samenvatting en conclusies	177
	8.1. Inleiding en onderzoeksvragen	178
	8.2. Voornaamste bevindingen	180
	8.2.1. Hoe zal landgebruik zich op lange termijn ontwikkelen in uiteenlopende scenario's op wereldwijde en op regionale schaal?	180
	8.2.2. Welke rol kan landgebruik vervullen in het realiseren van strikte klimaatdoelstellingen?	182

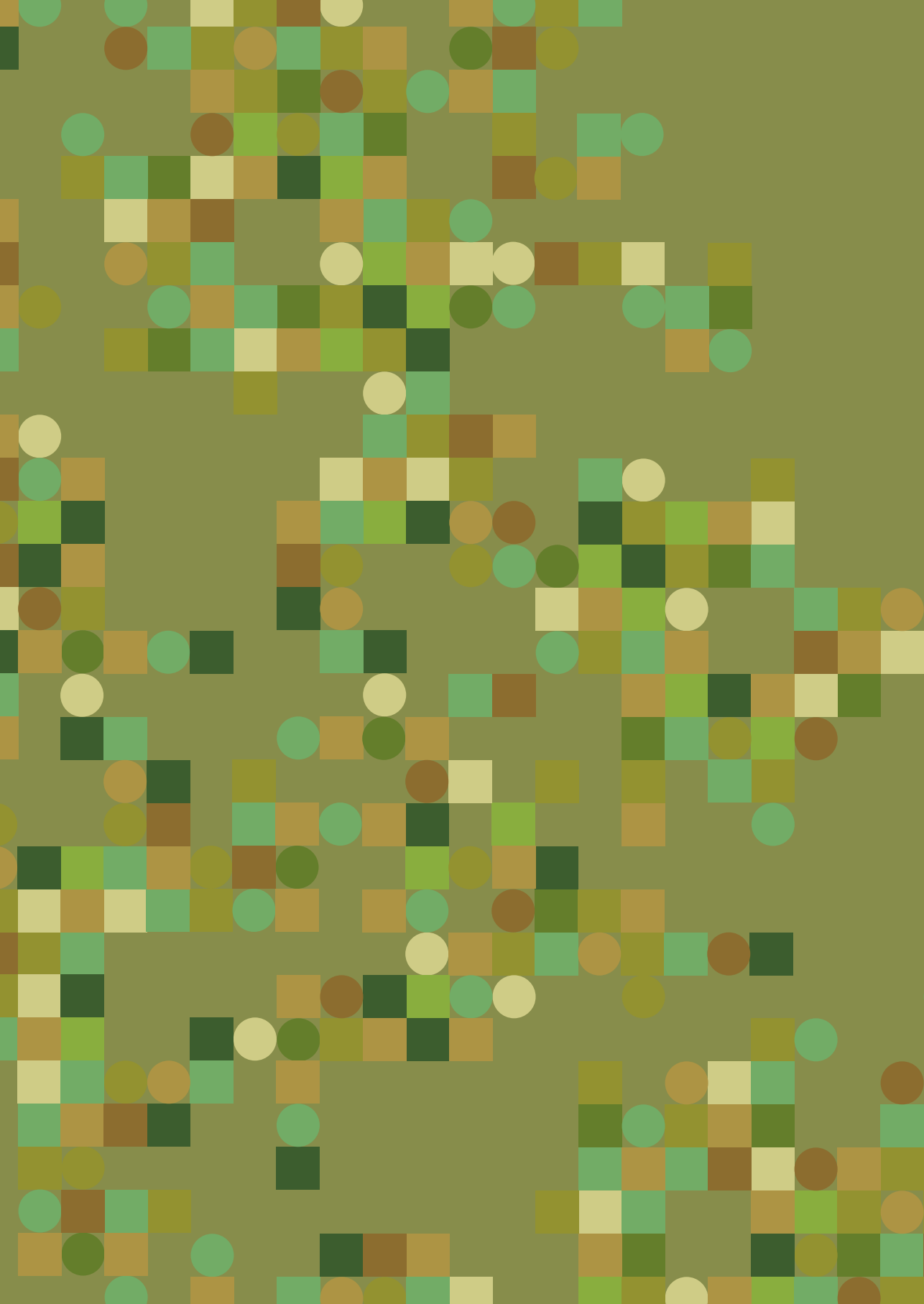
8.2.3. Hoe belangrijk zijn uitruilen en synergieën tussen land-gebaseerde klimaatmitigatie en andere maatschappelijke doelen in de water-land-energie-voedsel-klimaat nexus?	189
8.2.4. Hoe kunnen uitruilen worden geminimaliseerd en synergieën gemaximaliseerd?	192
8.3. Suggesties voor toekomstig onderzoek	195
8.4. Beleidsaanbevelingen	198
Supplementary Information	201
S2. Exploring SSP land-use dynamics using the IMAGE model: Regional and gridded scenarios of land-use change and land-based climate change mitigation	202
S3. The role of peatland degradation, protection and restoration for climate change mitigation in the SSP scenarios	222
S4. Afforestation for climate change mitigation: potentials, risks and trade-offs	238
S4.1 Estimating risk-adjusted discount rates	238
S4.2 Estimating maximum afforestation rate	238
S4.3 Construction of MAC curves and implementation in FAIR-SimCAP	238
S4.4 Food security indicators	238
S5. Making the Paris Agreement climate targets consistent with food security objectives	254
S6. Quantifying synergies and trade-offs in the global water-land-food-climate nexus using a multi-model scenario approach	258
S6.1 Supplementary material figures	258
S6.2 Extended model description MAgPIE	264
S6.3 Extended model description IMAGE	266
S6.4 Extended description of modelling procedures and key model differences	269
S6.5 Extended information scenario assumptions	272
References	278
Acknowledgements	302
Curriculum Vitae	306
List of publications	308
This thesis	308
Other publications	308

Abbreviations and Units

%	percentage
°C	degree Celsius
AFOLU	Agriculture, Forestry and Other Land Use
BC	Black Carbon
BECCS	Bioenergy with Carbon Capture and Storage
C	Carbon
cap	capita
CCS	Carbon Capture and Storage
CDR	Carbon Dioxide Removal
CGE	Computable General Equilibrium
CH₄	Methane
CHN	China region
CMIP	Coupled Model Intercomparison Project
CO	Carbon Oxide
CO₂	Carbon Dioxide
CO₂-eq	Carbon Dioxide Equivalent
COP	Conference of the Parties
CSA	Central and South America
DGVM	Dynamic Global Vegetation Model
DOC	Dissolved Organic Carbon
EFR	Environmental Flow Requirements
ESA-CCI	European Space Agency Climate Change Initiative
EUR	Western and Central Europe
FAIR	Framework to Assess International Regimes for the differentiation of commitments model
FAO	Food and Agriculture Organization
FRA	Forest Resource Assessment
GCM	Global Circulation Model
GDP	Gross Domestic Product
GHG	Greenhouse gas
GLOBIO	Global Biodiversity model
GLOBIOM	Global Biosphere Management Model
GNM	Global Nutrient Model
Gt	gigatonne
GTAP	Global Trade Analysis Project

GWP	Global Warming Potential
H₂O	Water
ha	hectare
HWSD	Harmonized World Soil Database
HYDE	History database of the Global Environment
IAM	Integrated Assessment Model
IMAGE	Integrated Model to Assess the Global Environment
IMPACT	International Model for Policy Analysis of Agricultural Commodities and Trade
IPCC	Intergovernmental Panel on Climate Change
ISIMIP	Inter-Sectoral Impact Model Intercomparison Project
JKO	Japan, Korea and Oceania
kcal	kilocalorie
km³	cubic kilometres
LPJmL	Lund-Potsdam-Jena managed Land
LUC	Land-Use Change
LUH	Land-Use Harmonization
LULUCF	Land Use, Land-Use Change and Forestry
MAC	Marginal Abatement Cost
MAGICC	Model for the Assessment of Greenhouse Gas Induced Climate Change
MAGNET	Modular Applied GeNeral Equilibrium Tool
MAgPIE	Model of Agricultural Production and its Impact on the Environment
MEN	Middle East, and Northern Africa
Mha	megahectare
Mt	megatonne
N	Nitrogen
N₂O	Nitrous Oxide
NAM	North America
NH₃	Ammonia
NMVOG	Non-Methane Volatile Organic Compound
Non-CO₂	All other GHGs than CO ₂
Nox	Nitrogen Oxides
O₃	Ozone
OC	Organic Carbon
OECD	Organisation for Economic Co-operation and Development
P	Phosphorus

PBs	Planetary Boundaries
PFT	Plant Functional Type
RCA	Russia and Central Asia
RCP	Representative Concentration Pathways
REDD	Reducing Emissions from Deforestation and forest Degradation
RQ	Research Question
SAS	South Asia
SDGs	Sustainable Development Goals
SEA	Southeast Asia
SI	Supplementary Information
SimCAP	Simple Model for Climate Policy assessment
SO_x	Sulfur Oxides
SSA	Sub-Saharan Africa
SSP	Shared Socio-economic Pathway
tCO₂	tonne CO ₂
TIMER	The IMAGE Energy Regional Model
UN	United Nations
UNCCD	United Nations Convention to Combat Desertification
UNFCCC	United Nations Framework Convention on Climate Change
US\$	United States Dollar
USA	United States of America
VOC	Volatile Organic Compound
W/m²	watts per square meter
WDPA	World Database on Protected Areas
WLEFC	Water-Land-Energy-Food-Climate
yr	year



CHAPTER 1

Introduction



1.1. Land and climate change

Land, i.e. the Earth's terrestrial surface, plays a central role in the climate system. Two types of processes determine the interactions between land and climate: biogeophysical and biogeochemical processes (Bonan, 2016; Jia et al., 2019) (Figure 1-1). The first set, i.e. biogeophysical processes, concerns the exchanges of energy and water between land and the atmosphere. The amount of incoming solar radiation that is absorbed and warms the Earth's surface depends on the reflectivity of the land (i.e. the albedo). This varies from the very high reflectivity of snow to the low reflectivity of darker surfaces such as forests. Long-wave radiation also warms the Earth's surface, where the amount of incoming long-wave radiation depends on the well-known greenhouse effect, which is driven by gases in the atmosphere such as water vapour (H₂O), carbon dioxide (CO₂), methane (CH₄), nitrous oxide (N₂O) and ozone (O₃). What happens with the absorbed radiation depends on 1) the emissivity of the surface, which determines long-wave radiation heat loss, and 2) surface roughness and the availability of water that determine sensible heat loss (conduction and convection) and energy loss through evapotranspiration. The latter process, in turn, is key for cloud formation. The second set of processes, i.e. biogeochemical processes, relate to the exchange of elements between land and the atmosphere, such as CO₂ and other greenhouse gases and aerosols. The balance between photosynthesis and respiration of vegetation, as well as the decomposition of dead organic matter, determines whether land acts as a sink or a source of CO₂, in turn greatly influencing atmospheric CO₂ concentrations. Other natural processes also cause greenhouse gas (GHG) emissions; for example, wetlands can act as major sources of CH₄ (Lunt et al., 2019). Additionally, aerosols originating on land play a role, with mineral and carbonaceous aerosols interacting with cloud formation and volatile organic compounds (VOCs) influencing O₃ concentrations (Szogs et al., 2017). Palaeoclimatology has shown that land, through biogeophysical and biogeochemical processes, tipped the balance in prehistoric climate change events. For example, the formation of great ice caps on land in the northern hemisphere has forced the Earth into an ice age for ten thousands of years (Zalasiewicz and Williams, 2012). In more recent times, humans have drastically changed the Earth's terrestrial surface, thereby greatly impacting interactions between land and climate.

Over the last ten years (2011-2020), global temperatures were, on average, 1.09°C (0.95°C-1.2°C) warmer than during pre-industrial times (1850-1900), with a higher temperature increase over land of 1.59°C (1.34°C-1.83°C) (IPCC, 2021). These observed changes result from increasing GHG concentrations in the atmosphere, which is predominantly caused by the large-scale use of fossil fuels by human society (Shukla et al., 2022). However, human activities directly linked to land, i.e. land use, also play a significant role. Large-scale deforestation and clearing of other natural lands for agriculture or forestry have been major sources of CO₂ emissions for centuries. In fact, an estimated 34% of cumulative CO₂ emissions since 1750 has resulted from land-use change (Friedlingstein et al., 2022). And although the share of land use, land-use change and forestry (LULUCF) emissions in total CO₂ emissions decreased substantially as a result of rapidly increasing fossil fuel emissions, today, they

are still responsible for about 10% of annual anthropogenic GHG emissions (Jia et al., 2019). Agriculture is also a major source of other GHGs, most notably CH_4 and N_2O , responsible for 13% of total annual GHG emissions (Jia et al., 2019). CH_4 emissions mainly result from large-scale cattle rearing, most importantly from ruminants such as cows and sheep that digest food with the help of microorganisms (enteric fermentation), but also from rice production, which takes place in flooded fields leading to anoxic decomposition of organic material. N_2O emissions are predominantly caused by the application of synthetic fertilizer used to grow crops, but emissions also result from the manure that is excreted by animals. While these biogeochemical processes predominantly drive anthropogenic climate change at the global scale, biogeophysical processes play a critical role in local scale dynamics. This effect can be observed with satellite data in regions with ongoing deforestation, such as the Amazon in Brazil, where temperatures increase on average by about 1°C locally due to deforestation (Alkama and Cescatti, 2016). Conversely, deforestation in the boreal zones locally leads to cooling as the bare soil is often covered by snow, leading to much higher reflectivity. The expansion of built-up areas also has strong local effects. Buildings and paved surfaces absorb solar radiation, limit evapotranspiration, and change air circulation patterns causing warming, the so-called urban heat island effect (Oke, 1982; Ward et al., 2016).

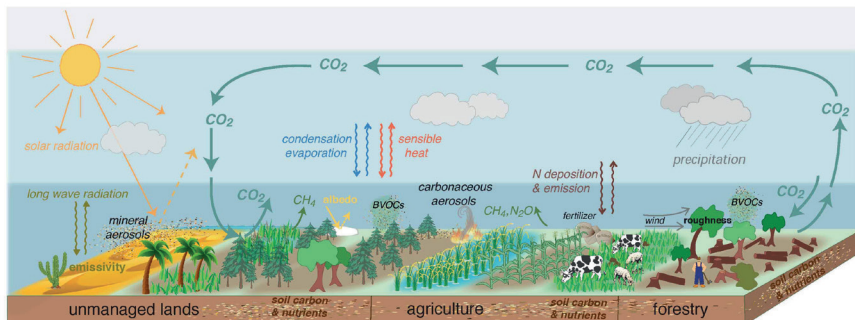


Figure 1-1: Illustration of the processes and interactions between land and the atmosphere that affect the climate system (adopted from IPCC special report on Climate Change and Land (IPCC, 2019a).

In short, it is clear that the role of land and land use is critical to take into account in climate change research. This is reflected by the fact that already in the first report of the United Nations' (UN) Intergovernmental Panel on Climate Change (IPCC) in 1990, emissions from agriculture, forestry and deforestation are explicitly accounted for (Berntal et al., 1990). Moreover, two special reports on land and land use in the context of climate change have been published by the IPCC: the special report on Land Use, Land-Use Change and Forestry in 2000 and, more recently, the Special Report on Climate Change and Land in 2019 (IPCC, 2019a; Watson et al., 2000).

1.2. Land use and climate change mitigation

In 2015, the Conference of the Parties (COP) of the United Nations Framework Convention on Climate Change (UNFCCC) agreed in Paris to limit global warming to well below 2 degrees and to pursue efforts to limit warming to 1.5 degrees (UNFCCC, 2015). As discussed previously, land plays a crucial role in the climate system and land use and land-use change are drivers of climate change. Consequently, reducing emissions from the so-called agriculture, forestry and other land use (AFOLU) sector is essential to achieve the goals of the Paris Agreement. Additionally, land plays a crucial role in technologies to sequester carbon, thereby taking CO₂ out of the atmosphere (also called negative emissions or carbon dioxide removal (CDR)) (Smith et al., 2016). The options to reduce AFOLU emissions or to sequester carbon using land are called land-based climate change mitigation measures. They are a central topic in this thesis that is introduced in more detail in this section. A distinction is made between the protection of natural ecosystems, the restoration and expansion of forests and wetlands, the reductions of emissions in agriculture through technical measures, increased sequestration of carbon in agricultural lands, demand-side measures such as dietary change, and the production and use of bioenergy. The relative potential of these various mitigation options, as estimated with a sectoral approach (Roe et al., 2019), is shown in Figure 1-2. In this thesis, the role of many of these mitigation options is investigated in a dynamic way using scenario analysis (the dashed options shown in Figure 1-2 are not included in the thesis).

Over the last decade, emissions from land-use change and forest degradation have been estimated at 4.0 GtCO₂/yr (Friedlingstein et al., 2022), albeit with a large uncertainty range of 1.5-6.6 GtCO₂/yr due to different estimation methods and data uncertainties. This is predominantly because of deforestation and forest degradation of tropical forests, but also the conversion of other natural lands, e.g. wetlands and savannahs, add to this number. Additionally, drainage of peatlands that are rich in organic matter causes decomposition causing GHG emissions estimated at 1.3-1.9 GtCO₂-eq/yr (Joosten, 2010; Leifeld and Menichetti, 2018). Consequently, preventing the continuation of natural ecosystem clearing is widely recognized as a high potential and relatively cost-effective measure to mitigate GHG emissions (Humpenöder et al., 2020; Kindermann et al., 2008; Overmars et al., 2014; Popp et al., 2014), with also important co-benefits for biodiversity conservation (Leclère et al., 2020)(see section 1.3). The recognition of the importance of these measures is illustrated by the Reducing Emissions from Deforestation and forest Degradation (REDD+) agreement at the UNFCCC CoP19 in Warsaw, where countries agreed on rules to regulate and promote measures limiting deforestation and forest degradation (la Viña et al., 2016).

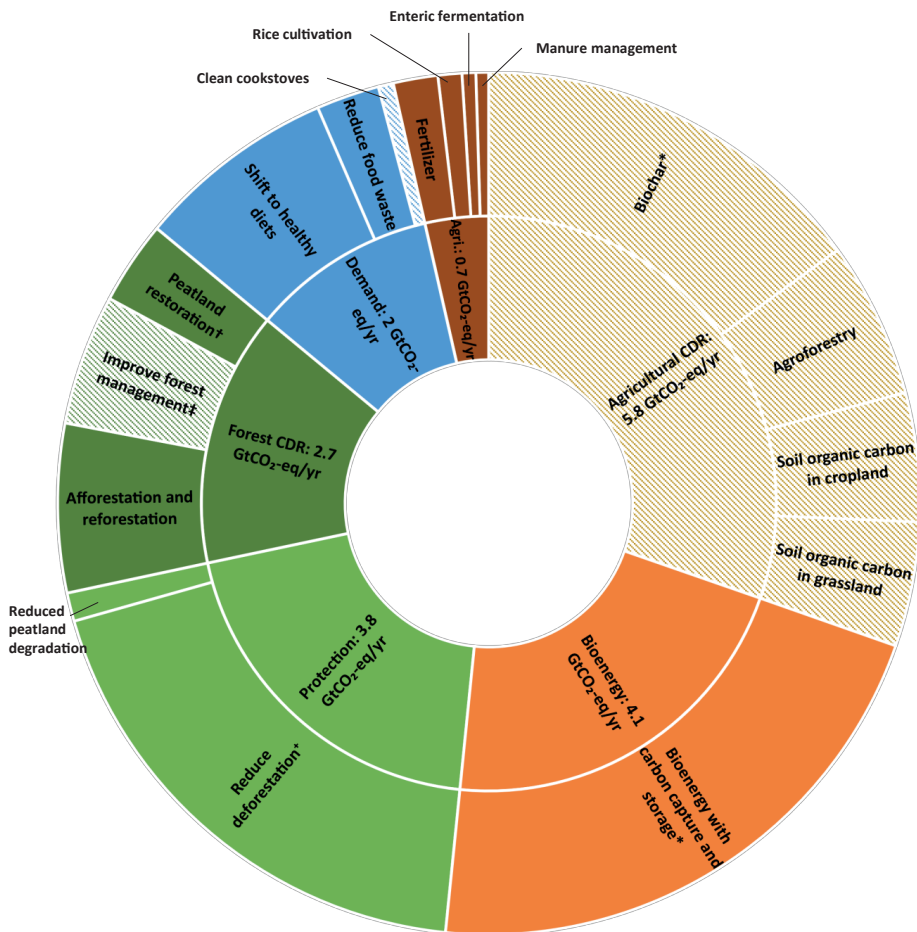


Figure 1-2: Estimated shares of cost-effective (less than \$100/tCO₂-eq/yr) land-based mitigation potentials for a range of categories based on a sectoral literature review, averaged in terms of GtCO₂-eq/yr over the 2020-2050 period, as compiled by Roe et al. (2021). The solid categories are addressed in this thesis whereas the dashed categories are not. Note that these estimates are not by definition additive as they are based on sectoral estimates that do not account for competing effects between measures, i.e. the maximum total potential land-based mitigation potential in 2020-2050 would be lower than the sum of the different categories displayed in this figure (*includes 90% fossil fuel substitution effect, †includes reduced mangrove loss, ‡includes grassland and savanna fire management, †includes mangrove restoration).

Forest or natural ecosystem-based CDR measures include expanding forest area through afforestation or reforestation, restoration of peatlands and wetlands, and improved forest management. The key similarity between these measures is that they increase carbon stocks on the land, thereby taking carbon out of the atmosphere. This may prove essential to achieving ambitious climate goals (van Vuuren et al., 2013). For afforestation and reforestation, a wide range of estimates is reported in the literature, from 0.5 GtCO₂/yr using 84 Mha from 2020 to 2050 (Busch et al., 2019) up to 10.3 GtCO₂/yr using 678 Mha by

2030 (Griscom et al., 2017). There are concerns, however, such as the competition with food production that might lead to food security issues, but also with permanency as climate change might increase the risk of forest fire reducing the capacity of forests to keep carbon out of the atmosphere (Keenan, 2015). Changes in forest management to increase carbon storage in forests while maintaining timber production also has substantial potential, for example by reduced impact logging and longer rotation cycles (Lauri et al., 2014; Sasaki et al., 2016).

Technical mitigation measures in agriculture provide a range of opportunities to reduce emissions from food production. For example, CH₄ emissions can be reduced by providing feed additives to ruminants to reduce enteric fermentation, by alternate flooding and drainage of paddy fields used for rice production, or by decreased exposure of manure (Harmsen et al., 2019; Lucas et al., 2007). For N₂O, more efficient fertilizer use or application of nitrification inhibitors could reduce emissions. It is, however, impossible to reduce emissions from agriculture to zero (Gernaat et al., 2015), highlighting the importance of CDR options to compensate for these emissions (van Vuuren et al., 2018). Another challenge is the potential for technical mitigation measures to be adopted at scale in the agricultural sector, as many smallholder farmers who produce one-third of the world's food face financial barriers and require knowledge and training (Edelenbosch et al., 2022).

There are various techniques to increase carbon stocks in agricultural lands without abandoning the agricultural use of the land. This can be achieved by increasing the number of trees in agricultural lands, also known as agroforestry (Chapman et al., 2020), by increasing soil carbon stocks through leaving additional residues on the field or reducing tillage (Lutz et al., 2019; Scharlemann et al., 2014), or by applying biochar which could also have substantial yield benefits (Lehmann et al., 2021; Schmidt et al., 2021). These techniques have received quite some attention in the context of the United Nations Convention to Combat Desertification (UNCCD), specifically in studies for the Global Land Outlook (van der Esch et al., 2022), where also the co-benefits between climate, biodiversity, water availability and food security are highlighted. Substantial estimates are reported in the literature, but concerns have been raised about the feasibility of these estimates, for example, regarding the availability of organic material needed to increase soil organic carbon levels or produce biochar (Janzen et al., 2022). In this thesis, CDR in agricultural land is not addressed, but it is a key topic for further research.

Demand-side changes have relatively recently been recognized as a part of the land-based mitigation option portfolio. Stehfest et al. (2009) were one of the first to clearly show the strong link between diets and climate change, highlighting that reducing meat consumption has strong benefits for climate. Since then, a large array of studies has been published on this topic, stressing the potential of reduced meat consumption as well as reductions in food waste for climate change mitigation (Bajželj et al., 2014; Poore and Nemecek, 2018; Springmann et al., 2018). In addition, the link between reduced meat consumption and health

has been identified as an important co-benefit (Willett et al., 2019). Even more recently, the potential of artificial meat as an option to reduce GHG emissions started to receive attention in the literature (Humpenöder et al., 2022; van Vuuren et al., 2018).

Bioenergy can mitigate climate change by replacing fossil fuels, thereby reducing the carbon footprint of the energy system (Daioglou, 2016). If energy generation based on biomass is combined with carbon capture and storage (CCS), this can create negative emissions, making it an interesting climate change mitigation technology (Smith et al., 2016; van Vuuren et al., 2013). This mitigation option combines the land and energy system and, therefore, can only partially be considered a land-based mitigation measure. It is, however, directly dependent on the production of biomass on land and for that reason included in this thesis. The use of bioenergy for climate mitigation has seen fierce debate in politics and society as well as in the scientific community. Key scientific concerns are the uncertainty around (indirect) land-use change effects of increased bioenergy demand potentially leading to higher GHG emissions than conventional fossil fuels (Daioglou et al., 2017; Hanssen et al., 2020; Searchinger et al., 2008), as well as negative effects on biodiversity (Immerzeel et al., 2014) and food security (Hasegawa et al., 2020).

1.3. Land use, sustainable development, and the water-land-energy-food-climate nexus

Land not only plays a key role in the climate system but also in many other socio-economic and environmental processes: for example, the provision of food, energy and water depend (at least partly) on land and are essential resources to sustain people's lives. Land also forms the substrate for natural ecosystems sustaining biodiversity. The importance of land to sustainably provide resources for people's livelihoods and to protect the environment has been recognized in the Sustainable Development Goals (SDGs) (UN, 2015) and the planetary boundaries (PBs) (Rockström et al., 2009; Steffen et al., 2015). The SDGs and PBs include many targets representing an array of sustainable development and global environmental change dimensions. The scientific community investigating climate scenarios and climate change policy has, in recent years, expanded into sustainable development, aiming to design future pathways that limit climate change to well below 2°C as well as achieve SDG and PB targets (Frank et al., 2021; Humpenöder et al., 2018; van Vuuren et al., 2015). This thesis aims to contribute to that ambition.

To study multiple interconnected sectors representing different dimensions of sustainable development and global environmental change, a nexus approach is useful. This approach recognizes that components of a system are inherently interconnected and must be investigated and managed in an integrated, holistic manner (Hoff, 2011). In this thesis the water-land-energy-food-climate (WLEFC) nexus is assessed, which broadens the scope from reaching climate change mitigation targets to also achieve targets related to water, land,

energy, and food. For water, this concerns the availability of sufficient and clean water for human use (SDG6), preserving freshwater ecosystems (SDG14) and the PB on excessive water use. Examples of key interactions are the effects of increased crop production on irrigation water use and limited availability for human consumption (Bonsch et al., 2016; de Vos et al., 2021), the expansion of hydropower on river flow affecting aquatic biodiversity (Gernaat et al., 2017; Vörösmarty et al., 2010), increased fertilizer use and animal manure in agriculture negatively affecting water quality which in turn impacts aquatic biodiversity (Beusen et al., 2022; Janse et al., 2019), and changes in water availability caused by climate change (Konapala et al., 2020). For land, the focus is on terrestrial biodiversity (SDG15) and the PB on land-use change. Key interactions are the expansion of agricultural land for food or energy use resulting in deforestation and loss of natural ecosystems (Popp et al., 2014; Schipper et al., 2020), as well as increased nitrogen deposition from agriculture and energy generation negatively affecting biodiversity (Bobbink et al., 2010). For energy, energy availability is highly interconnected with other components of the WLEFC nexus (SDG7), with changes in availability of traditional and modern bioenergy due to land protection or climate change impacts on yields (Dagnachew et al., 2020; Gernaat et al., 2021), or forest degradation due to excessive use of traditional biofuels. For the food component of the nexus, food security is a high priority for sustainable development (SDG2) and plays a key role in the nexus: Increased food production can improve food security but might lead to further land-use expansion and GHG emissions (van Meijl et al., 2020). Conversely, climate change impacts on yields and reduced water availability for irrigation might negatively affect food security (Hasegawa et al., 2015a). Finally, climate as a specific component of the nexus is important as highlighted by SDG13, the PB on climate change and the Paris Agreement, and it is directly affected by land-use change, energy generation and agriculture through GHG emissions (IPCC, 2019a).

1.4. Modelling land-use futures in the context of global environmental change

The previous sections have shown that land use is highly relevant in the context of climate change, global environmental change and sustainable development. Therefore, it is important to understand how land use may develop in the future. The scenario-based approach applied in this thesis is suitable for this purpose. Scenarios can be defined as plausible descriptions of how the future might develop, as based on a coherent and internally consistent set of assumptions about the key relationships and driving forces (IPCC, 2000a; van Vuuren, 2007). This approach is specifically useful as the dynamics of land use are highly uncertain with complex underlying driving forces such as demography and economics, technological change, human decision-making, and environmental policies that all interact (Stehfest et al., 2019). As climate change and climate policy are a key topic of interest, the scenarios assessed in this thesis are mostly long-term – i.e. up to the end of the 21st century – because climate change is a slow process where current emissions and land-use change have impacts over many decades to come, and also because climate policy aiming to stabilize

climate change is a long-term endeavour. Two types of scenarios are assessed: explorative scenarios and normative scenarios. Explorative scenarios describe the future under a pre-defined set of assumptions to see how the future could develop. A typical example is the Shared Socio-economic Pathway (SSP) baseline scenarios (Chapter 2) (Riahi et al., 2017). Normative scenarios assess futures that achieve a certain predefined goal – for example a 2°C target (Chapter 2, 3 and 4) or nexus goals on nature protection or water extraction (Chapter 6) – thereby showing how certain targets could be achieved. A key purpose of scenarios is to describe plausible futures (either with or without targets) to facilitate debate between scientists, policy makers and stakeholders. Additionally, scenarios are useful to quantify to what extent different climate change mitigation or sustainable development measures might compete for the same resources – e.g. land – under future circumstances or whether measures are, in fact, synergistic or have trade-offs with non-related targets.

To gain insight in the role of land use in global environmental change and climate change mitigation policy, understanding of the global food and agricultural system is essential. An estimated 80% of deforestation worldwide is driven by agriculture (Kissinger et al., 2012) and agriculture is the main driver of terrestrial biodiversity loss (Tilman et al., 2017). Moreover, agriculture is responsible for 70% of freshwater use mainly for irrigation (FAOSTAT, 2020) and the main cause of a doubling of nitrogen (N) and phosphorus (P) input in the environment during the 20th century (Beusen et al., 2016). Over the last decades, the increase of agricultural production has worsened these impacts: from 1961 to 2020, global crop production increased by 270% and livestock production by 210% (FAOSTAT, 2022). Interestingly, on average during this period only 10% of the global crop production increase was achieved through expansion of agricultural land, while 90% was the result of intensification related to increased inputs such as fertilizer and pesticides (39%) or irrigation expansion (9%), but also due to increases in total factor productivity which relates to for example improved agronomic practices and better crop varieties (43%)(USDA-ERS, 2022a). While land-use expansion is clearly linked to land-use change (LUC) emissions and natural ecosystem loss, agricultural intensification is also a major driver of global environmental change through for example increases in water and nutrient use. On the other hand, the increases in production have enabled improved food security. The share of underweight population reduced from 15% to 10% from 1965 to 2015, although the absolute number did increase due to population growth (Bodirsky et al., 2020). At the same time however, overconsumption increased causing the obese share of the world population to grow from 2% to 10% indicating a major health crisis that also severely affects the environment and highlights the stark inequality of the global food system. On top of these developments, also demand for bioenergy increased adding more pressure to the food and agricultural system. In the USA currently about 40% of all maize production is used to generate biofuels (USDA-ERS, 2022b). To project these dynamics into the future, agro-economic models are used. These models represent costs of agricultural production, food, land, and inputs such as fertilizer, as well as changes in demand for food and bioenergy. Changes in key drivers such as population, income, land availability and technological change together determine how the food and agricultural system develops

in the future. Examples of agro-economic models that develop land-use scenarios in the context of global environmental change are GLOBIOM (Havlík et al., 2011), MAGPIE (Dietrich et al., 2019), IMPACT (Robinson et al., 2015) and MAGNET (Woltjer et al., 2014). In this thesis, MAGNET is applied as part of the IMAGE framework (see Section 1.5).

The actual processes, impacts and feedbacks of land-use change and the interaction with the environmental system play out on the local scale, although influenced by global and regional dynamics. Exactly where land-use change takes place, even within a country, can make a significant difference: for example, the location of agricultural expansion is key for the GHG emissions that occur due to conversion (e.g. was the original land cover forest or savannah) (Daioglou et al., 2017), but also the crop yield that can be achieved in a certain location due to biophysical as well as socio-economic factors differs substantially (van der Hilst, 2018). In addition, biodiversity impacts are highly local and depend critically on the spatial distribution and heterogeneity of land cover types (Hoskins et al., 2016). Therefore, assessments at high spatial resolution are an important topic in land-use studies. Observations of land cover change based on remote sensing data are available at very high resolution, for example the ESA-CCI data with 300-meter grid cell resolution time series data from 1992 up to 2020 (Hollmann et al., 2013). Observations of deforestation are available at an even higher resolution of 30 meters (Hansen et al., 2013). Land-use modelling typically takes place at slightly coarser resolution for computational reasons, but also due to data limitations as not all relevant information (e.g. population density, yield estimates or climate variables) is available at the same very high resolution as the land cover observations. Most models represent the agro-economy on the level of world regions and then downscale to a spatial resolution of 0.5 arc-degree (± 50 km at the equator) (Dietrich et al., 2014; Hasegawa et al., 2017) or 5 arc-minute (± 9 km at the equator) (Stehfest et al., 2014; van Asselen and Verburg, 2013), subsequently linking back relevant feedbacks to the regional agro-economic models. For biodiversity assessments higher resolution allocation models exist at 30 or 10 arc-second resolution (± 1 km and ± 300 m, respectively) (Hoskins et al., 2016; Schipper et al., 2020), but in these approaches the number of land-use types represented is much more limited. Next to the spatial resolution, considerable variation is present in the allocation procedures with different models projecting very different spatial explicit land-use futures indicating a key topic of uncertainty (Prestele et al., 2016).

1.5. The IMAGE integrated assessment model framework

As discussed in the previous sections, land use plays a key role in climate change, global environmental change and sustainable development. Vice versa, land-use dynamics are also influenced by these developments. Consequently, land-use futures can only be understood by using an integrated approach that takes these different dimensions into account. In this thesis, the IMAGE integrated assessment model framework is applied. IMAGE was developed

to investigate interactions between human activities and the environment to explore long-term global environmental change and policy options in the areas of climate, land, and sustainable development (Stehfest et al., 2014). Therefore, the IMAGE integrated assessment model framework is well suited to study land-use futures. For some of the analyses in this thesis, also the land system model MAgPIE is used (Dietrich et al., 2019)(Chapter 6). MAgPIE covers similar sectors and dynamics as IMAGE and is therefore interesting for model comparison exercises (SI Section S6.2)

The IMAGE model framework comprises several interlinked models that focus on different components of the human or the earth system (Figure 1-3) (for extended model descriptions, see SI Section S6.3). The IMAGE-LandManagement model represents agricultural land use, natural land cover, forestry and livestock systems at the grid level with 5 arc-minute spatial resolution. The model describes 16 crop types, 5 livestock types and 5 bioenergy types (van Vuuren et al., 2021). The land-use allocation algorithm applies empirically-based statistical suitability layers derived from ESA-CCI land-use change data (Cengic et al., 2023). IMAGE-LandManagement is dynamically coupled to the dynamical global vegetation model (DGVM) LPJmL, which represents the carbon and hydrological cycles as well as crop growth for rainfed and irrigated agriculture at half-degree spatial resolution (Müller et al., 2016; Schaphoff et al., 2018b, 2018a). It is a process-based model that applies the concept of multiple plant functional types (PFTs) categorized according to biophysical characteristics. The agricultural economy is represented by the multi-regional, static, applied computable general equilibrium (CGE) model MAGNET, which is based on neoclassical economic theory and builds on the standard GTAP model (Hertel, 1997; Woltjer et al., 2014). It covers all sectors of the economy but represents land use in relatively high detail by modelling land as an explicit production factor described by a land-supply curve. The process-based simulation model TIMER models the energy system in high technological detail and represents key processes such as supply, conversion and demand of energy (van Vuuren et al., 2021). The simple climate model MAGICC is used to calculate climate change effects based on emissions from the land-use and energy systems (Meinshausen et al., 2011), emulating results from large-scale global circulation models (GCMs). Changes in temperature and precipitation are downscaled to the grid level with a pattern-scaling approach based on bias-corrected ISIMIP data (Frieler et al., 2017). The climate policy model FAIR-SimCAP uses marginal abatement cost (MAC) curves to determine cost-optimal emission pathways to achieve specific climate targets (den Elzen et al., 2008). Finally, the GNM model uses land use and agricultural production data to model the nutrient and phosphorus cycles, calculating nutrient balances and concentrations in the environment (Beusen et al., 2015).

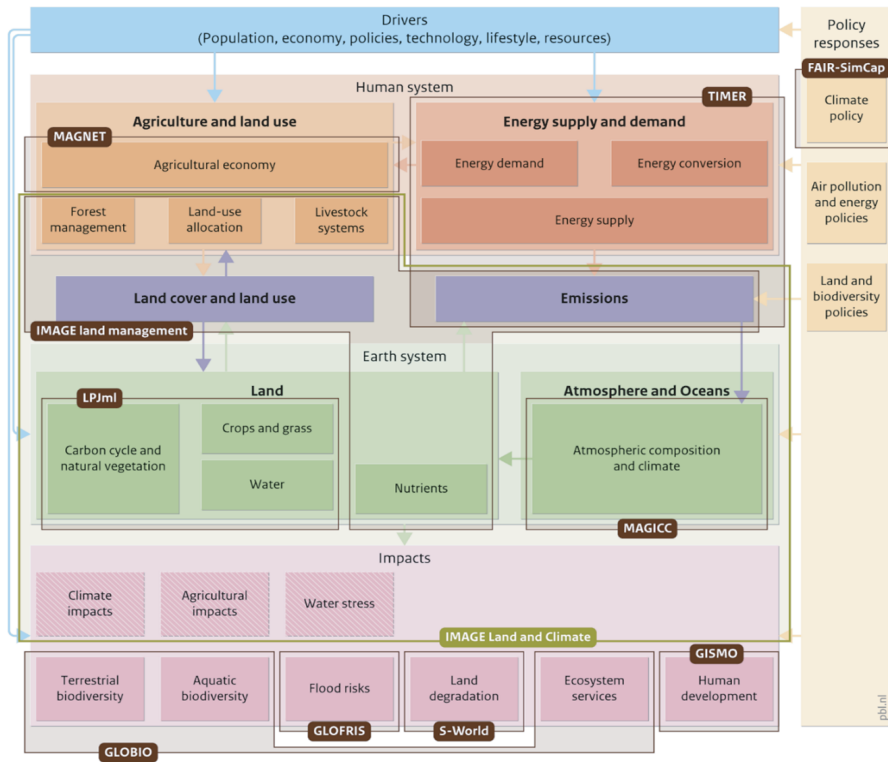


Figure 1-3: Schematic representation of the IMAGE model framework showing different model components and their interactions, as well as the specific models that represent them (Stehfest et al., 2014).

1.6. Aim of the thesis

Land use is one of the drivers of climate change and has an important role to play in climate change mitigation to achieve the Paris Agreement goals. Land use is also a critical factor in many other global environmental change and sustainable development issues. Therefore, understanding and quantifying how land use may develop in the future is essential to prepare for the challenges ahead and to be able to assess the role of potential response strategies. Scenario analyses using integrated assessment models are a suitable tool for this task. This thesis aims to contribute to our understanding of land use futures in the context of climate change mitigation by seeking answers to the following research questions (RQs):

1. How will land use develop in the long term under various scenarios at the global and regional scale?
2. What can be the role of land use in achieving stringent climate targets?
3. How important are trade-offs and synergies between land-based climate mitigation and other societal goals in the water-land-energy-food-climate nexus?
4. How can these trade-offs be minimized and synergies be maximized?

1.7. Outline

This thesis is structured along the research questions introduced in Section 1.6. First, an explorative scenario analysis is presented using the SSPs to investigate long-term land-use futures at the global and regional scale (**Chapter 2**). Second, the potential role of various land-based mitigation options in different scenarios aiming for stringent mitigation targets is quantified, with detailed analyses of peatland protection and restoration, and afforestation (**Chapters 2, 3 and 4**). Third, the trade-offs and synergies of land-based climate change mitigation measures with developments in the WLEFC nexus are quantified (**Chapters 3, 4, 5 and 6**). Fourth, various options are investigated that may prevent the negative effects of land-based mitigation or other WLEFC nexus measures and make optimal use of co-benefits (**Chapter 5 and 6**). Finally, a summary of the thesis and the answers to the research questions are provided in English and Dutch (**Chapter 7 and 8**). A detailed description of the different chapters and their relation to the research questions is provided here and in Table 1-1:

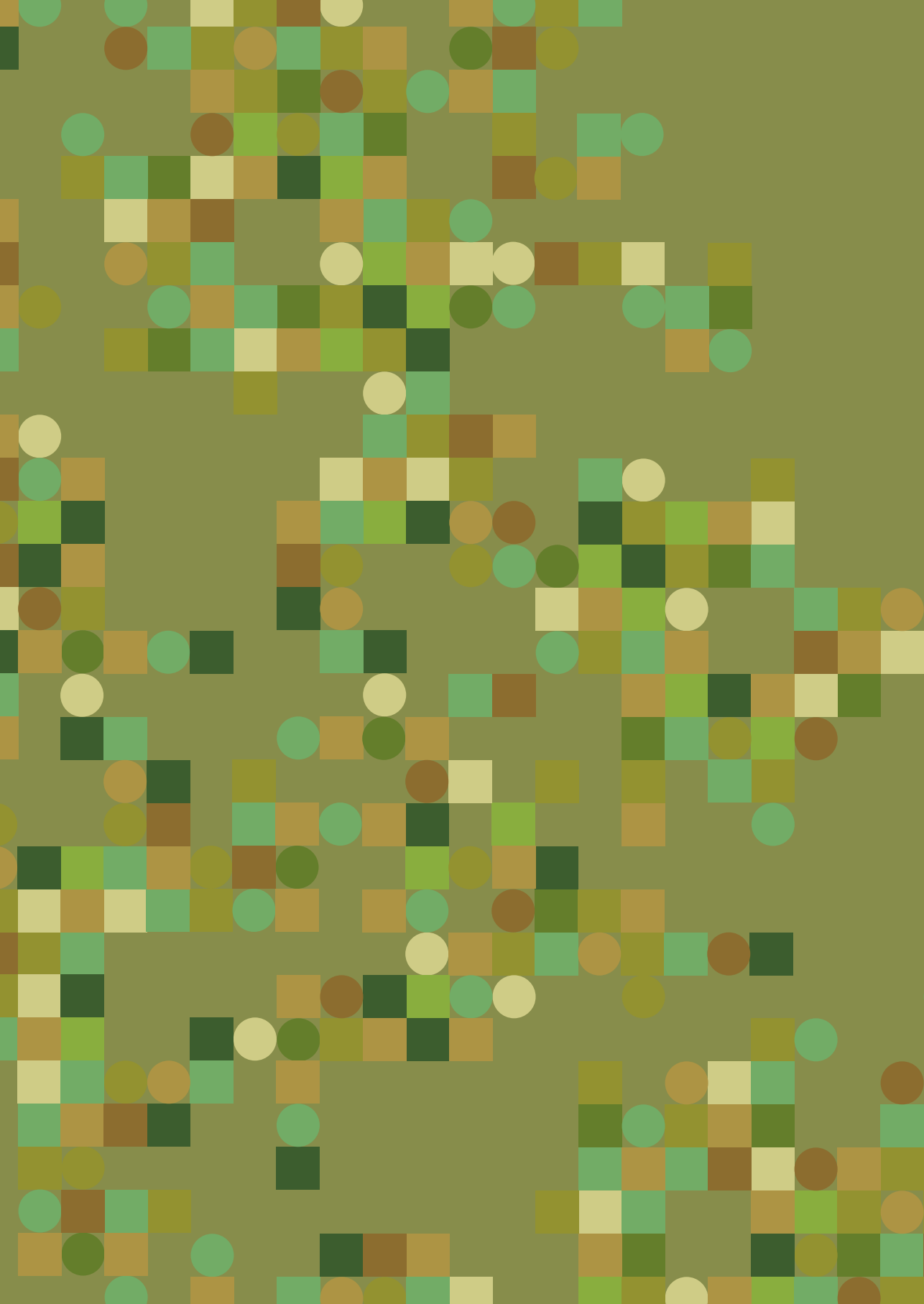
- **Chapter 2:** *Exploring SSP land-use dynamics using the IMAGE model: Regional and gridded scenarios of land-use change and land-based climate change mitigation.* This chapter introduces the SSP scenarios as developed with the IMAGE 3.0 model with a focus on land use at the global, regional, and gridded scale. Baseline scenarios for the five different SSPs are assessed representing a range of land-use futures (**RQ1**). In addition, mitigation scenarios are presented based on SSP1 and SSP2 aiming for increasingly ambitious climate goals down to the 1.5°C target using a variety of land-based mitigation options (**RQ2**). Finally, also the impacts of the scenarios on climate and food security are discussed

as well as the role of bioenergy, covering the land, energy, food and climate components of the nexus (**RQ3**).

- **Chapter 3:** *The role of peatland degradation, protection and restoration for climate change mitigation in the SSP scenarios.* A deep-dive is made into the effects of peatland degradation on climate change as well as the potential role of peatland protection and restoration in climate change mitigation pathways (**RQ2**).
- **Chapter 4:** *Afforestation for climate change mitigation: potentials, risks and trade-offs.* Another deep-dive is made into afforestation as a land-based mitigation strategy, investigating potentials and costs and how large the role of afforestation could be in stringent climate change mitigation scenarios (**RQ2**). In addition, the impacts of afforestation on land-use dynamics and food security are studied (**RQ3**).
- **Chapter 5:** *Making the Paris Agreement climate targets consistent with food security objectives.* This chapter provides a detailed assessment of food security impacts of large-scale land-based mitigation measures such as bioenergy or afforestation (**RQ3**). Subsequently, additional agricultural intensification and dietary change are introduced as measures to prevent negative effects on food security (**RQ4**).
- **Chapter 6:** *Quantifying synergies and trade-offs in the global water-land-food-climate nexus using a multi-model scenario approach.* The water-land-food-climate nexus is investigated using a scenario approach with two integrated assessment models (IMAGE and MAgPIE) (**RQ3**). Various measures are introduced that aim to improve different components of the nexus to analyse how to maximize synergies and minimize trade-offs (**RQ4**).

Table 1-1: Relation between research questions and thesis chapters.

Chapter	RQ1	RQ2	RQ3	RQ4
2: SSP land use				
3: Peatland				
4: Afforestation				
5: Food security				
6: WLFC nexus				

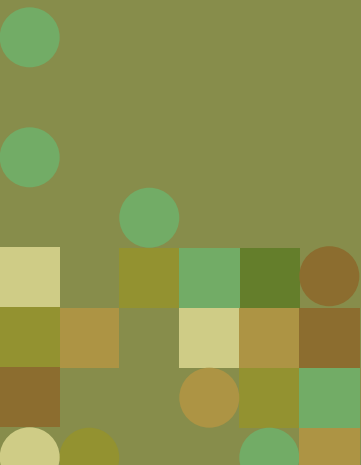


CHAPTER 2

Exploring SSP land-use dynamics using the IMAGE model: Regional and gridded scenarios of land-use change and land-based climate change mitigation

Jonathan C. Doelman, Elke Stehfest, Andrzej Tabeau, Hans van Meijl, Luis Lassaletta, David E.H.J. Gernaat, Kathleen Hermans, Mathijs Harmsen, Vassilis Daioglou, Hester Biemans, Sietske van der Sluis, Detlef P. van Vuuren

“Exploring SSP land-use dynamics using the IMAGE model: Regional and gridded scenarios of land-use change and land-based climate change mitigation” Global Environmental Change 48 (2018): 119-135



Abstract

Projected increases in population, income and consumption rates are expected to lead to rising pressure on the land system. Ambitions to limit global warming to 2°C or even 1.5°C could also lead to additional pressures from land-based mitigation measures such as bioenergy production and afforestation. To investigate these dynamics, this paper describes five elaborations of the Shared Socio-economic Pathways (SSP) using the IMAGE 3.0 integrated assessment model framework to produce regional and gridded scenarios up to the year 2100. Additionally, land-based climate change mitigation is modelled aiming for long-term mitigation targets including 1.5°C. Results show diverging global trends in agricultural land in the baseline scenarios ranging from an expansion of nearly 826 Mha in SSP3 to a decrease of more than 305 Mha in SSP1 for the period 2010-2050. Key drivers are population growth, changes in food consumption, and agricultural efficiency. The largest changes take place in Sub-Saharan Africa in SSP3 and SSP4, predominantly due to high population growth. With low increases in agricultural efficiency this leads to expansion of agricultural land and reduced food security. Land use also plays a crucial role in ambitious mitigation scenarios. First, agricultural emissions could form a substantial component of emissions that cannot be fully mitigated. Second, bioenergy and reforestation are crucial to create net negative emissions reducing emissions in SSP2 in 2050 by 8.7 Gt CO₂/yr and 1.9 Gt CO₂/yr, respectively (1.5°C scenario compared to baseline). This is achieved by expansion of bioenergy area (516 Mha in 2050) and reforestation. Expansion of agriculture for food production is reduced due to REDD policy (290 Mha in 2050) affecting food security especially in Sub-Saharan Africa indicating an important trade-off of land-based mitigation. This set of SSP land-use scenarios provides a comprehensive quantification of interacting trends in the land system, both socio-economic and biophysical. By providing high resolution data, the scenario output can improve interactions between climate research and impact studies.

2.1. Introduction

The land system plays a crucial role in human development, providing key products and ecosystem services such as food, fibre, shelter and freshwater (Foley et al., 2005). The demands that humanity places on the land system have increased substantially over the last century. As the global population increased to over 7 billion people, total land use increased from 13% of global land area in 1900 to 35% in 2000 (Klein Goldewijk et al., 2011). Moreover, less than 25% of the world's ice-free area is still free from human influences (Ellis and Ramankutty, 2008). As the global population (KC and Lutz, 2017), income (Dellink et al., 2017) and food consumption (Alexandratos and Bruinsma, 2012; Popp et al., 2017) are expected to continue to increase, it is likely that human demands placed on the land system will continue to increase as well. A key question is what the increase in demand for products and ecosystem services implies for the sustainability of the land system (Erb et al., 2016; Foley et al., 2011; Lambin and Meyfroidt, 2011; Smith et al., 2010).

Global land use plays an important role in climate change. Emissions from agriculture, forestry and other land use (AFOLU) are estimated to be responsible for around 24% of anthropogenic greenhouse gas (GHG) emissions in 2010 (Smith, 2013). CO₂ emissions from land-use change and forestry have been more-or-less stable from 1970-2010 at approximately 5 Gt CO₂/yr, showing a tentative decrease from 2000-2010 while increasing again in the last five years (Quéré et al., 2016). CH₄ and N₂O emissions from land use have shown a continuous increase with growing crop and animal production: from around 3.7 Gt CO₂eq and 1.3 Gt CO₂eq in 1970 respectively, to 4.3 Gt CO₂eq and 2.1 Gt CO₂eq in 2010 (JRC/PBL, 2012). These emissions are especially relevant for policies aiming to limit global mean temperature change to 2°C or even 1.5°C, as technical potential to reduce CH₄ and N₂O emissions is limited (Gernaat et al., 2015). The land system is also important in climate change mitigation policies as it provides the possibility to generate negative emissions through afforestation and bioenergy with carbon capture and storage (BECCS) that are crucial in ambitious mitigation scenarios (van Vuuren et al., 2013).

Many key driving forces of the future land system are inherently uncertain, ranging from socio-economic variables such as population, wealth, human and livestock diets, waste and urbanization to biophysical parameters such as climate, yields, the carbon cycle and hydrological cycle. Their interactions determine what land-use futures might look like. In several earlier scenario studies, different land-use scenarios have been developed to quantify the possible consequences of different socio-economic development patterns (Popp et al., 2013; Schmitz et al., 2014; Smith et al., 2010; Strengers et al., 2004). The Shared Socio-economic Pathway (SSP) scenario framework builds on this work by defining five scenarios that together describe a wide set of different socio-economic futures (O'Neill et al., 2017; Riahi et al., 2017). The SSPs can be combined with different long-term mitigation targets based on the Representative Concentration Pathways (RCP) (van Vuuren et al., 2011) to produce

a scenario matrix that allows assessment of different climate policy strategies (van Vuuren et al., 2012).

Land-use scenarios are used for many applications, both in traditional climate research (Ciais et al., 2014; Jones et al., 2016) and beyond in studies on e.g. biodiversity (Alkemade et al., 2009), nutrient cycles (Beusen et al., 2015) and flood risks (Winsemius et al., 2013). Here, we present a consistent set of scenarios as developed with the IMAGE model (Stehfest et al., 2014). The IMAGE 3.0 model is a comprehensive integrated assessment model (IAM) that combines regional agro-economic, energy and climate policy modelling (26 regions) with land-use, dynamic vegetation and hydrological modelling on a geographic grid (5 and 30 arc-minute grid cells). This set-up allows the development of high resolution data, available online at regional¹ and gridded² levels meeting the demand of different scientific communities.

In van Vuuren et al. (2017b), the overall elaboration of the SSP scenarios in IMAGE 3.0 was described. Here, we specifically focus on the land-use components of these scenarios. In doing so, the article adds to the existing literature on possible land-use trends for the SSPs. First, the article gives a detailed presentation of a set of scenarios developed with one IAM, thus providing a consistent set across SSPs and mitigation targets and providing the detail required to understand model-specific land-use dynamics as presented before in multi-model analyses (Hurtt et al., 2011; Popp et al., 2017). Second, the article for the first time discusses high resolution land-use results of the SSPs. Third, the article presents spatially-explicit results of land-use dynamics of the IMAGE 1.5°C scenarios. We use the set of scenarios to answer the following questions: 1) What are potential land-use futures? 2) What are geographic hotspots of change where large changes in the land system can occur? 3) What is the role of land use in climate change mitigation?

The paper start with a description of the IMAGE 3.0 framework with a focus on the land-use components of the model (Section 2.2.1), followed by a description of the SSP storylines and climate change mitigation targets (Section 2.2.2) and the implementation of the scenarios in IMAGE (Section 2.2.3). Subsequently, results of land-use dynamics in the baselines are presented on the global (Section 2.3.1) and (sub-)regional scale (Section 2.3.2), followed by results of the mitigation scenarios (Section 2.3.3) and the implications for greenhouse gas emissions (Section 2.3.4). Finally, conclusions, model uncertainties and effects on the results are discussed (Section 2.4).

1 Regional data available for download: <http://themasites.pbl.nl/models/image/index.php/Download>.

2 Gridded data available for download: <https://data.knmi.nl/datasets?q=PBL>.

2.2. Methods

2.2.1. The IMAGE 3.0 model framework

IMAGE 3.0³ is an integrated assessment modelling framework that simulates the interactions between human activities and the environment (Stehfest et al., 2014), to explore long-term global environmental change and policy options in the areas of climate, land and sustainable development. The framework comprises a number of sub-models describing land use, agricultural economy, the energy system, natural vegetation, hydrology, and the climate system (Figure 1-3). In the description, we focus on the land-related components of IMAGE and their interactions (Figure 2-1). The sub-models operate at different spatial resolutions. The socio-economic components work at the level of 26 regions while the environmental components work at the grid level to take into account heterogeneities in environmental circumstances. Interaction between the models takes place through upscaling and downscaling algorithms. For example, crop productivity is modelled at the grid level and subsequently aggregated to the regional level for the exchange with the agricultural economy (MAGNET) and energy system (TIMER). Similarly, land use in IMAGE-LandManagement is represented at 5 arc-minute resolution, and aggregated to 30 arc-minute resolution for the data exchange with LPJmL. Next to differences in spatial resolution, sub-models are either hard- or soft-coupled. For example, IMAGE-LandManagement is hard-coupled to LPJmL which means that data is exchanged on an annual basis (see also Müller et al. (2016)). In contrast, IMAGE-LandManagement is soft-coupled to TIMER through an iterative process of scenario data exchange. A sequence of data-exchange procedures ensures that relevant feedbacks represented in different sub-models are taken into account. A detailed description of all parameters exchanged between the various IMAGE sub-models is available³.

IMAGE-LandManagement determines the area and location of cropland on a 5 arc-minute geographical grid required to fulfil the demand for production of 7 crop classes (temperate cereals, rice, maize, tropical cereals, pulses, roots and tubers, oil crops) calculated by MAGNET. The historical locations and areas of cropland and grazing land are based on the HYDE database (Klein Goldewijk et al., 2011) which is consistent with FAO statistics (FAOSTAT, 2013). For each region in each time step crop production is calculated using gridded potential yields from LPJmL, locations of cropland in the previous time step and a regional management factor (calibrated to historical yields from FAO and future yield trends according to MAGNET). If production is higher than demand, cropland is abandoned on the least productive locations. If production is lower than demand, cropland is expanded following an empirical allocation algorithm with four drivers: potential crop yield as modelled by LPJmL, accessibility from Nelson (2008), population density from the HYDE database (Klein Goldewijk et al., 2010), and terrain slope index from the Harmonized World Soil Database (Fischer et al., 2008). The algorithm is based on regional multi-linear regression models fitted to explain current

3 For more background info visit the online IMAGE documentation: http://themasites.pbl.nl/models/image/index.php/Welcome_to_IMAGE_3.0_Documentation.

cropland and grazing land distribution. Next to land-use allocation, IMAGE-LandManagement includes a model for livestock production in five classes (beef, dairy, pigs, poultry, sheep and goats) for 26 regions in intensive and extensive systems taking into account large variations between regions in feed composition, feed efficiency, genetic animal productivity and age at slaughter (Bouwman et al., 2005). The livestock production module determines the amount of feed crops and grass required to fulfil demand for animal production as calculated by MAGNET. Expansion or abandonment of grazing land depends on demand for grass and follows the same allocation procedure as cropland. IMAGE-LandManagement also computes timber production in four forest management systems: clear cut, selective cut (conventional or reduced impact logging) and wood plantations.

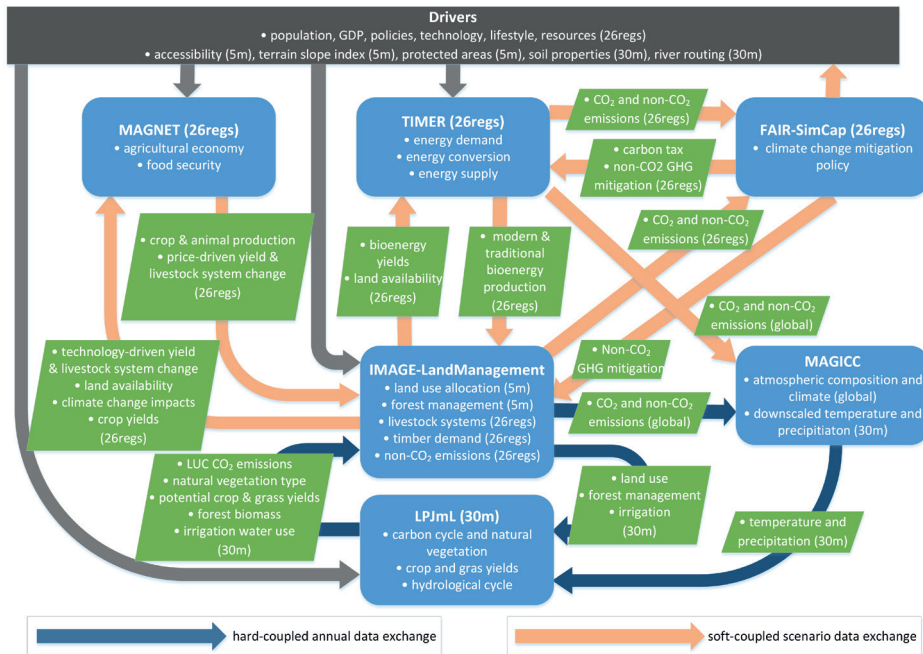


Figure 2-1: Schematic overview of the IMAGE framework focusing on the land-use components and interactions. Dark-blue arrows indicate hard-coupled interactions between sub-models (annual data exchange). Orange arrows indicate soft-coupled interaction using an iterative exchange of scenario data (scenario data exchange). 'Global', '26regs', '30m' and '5m' indicates data exchange or model operation at a global level, 26 regions levels, 30 arc-minute grid or 5 arc-minute grid, respectively.

MAGNET is a multi-regional, multi-sectoral, applied general equilibrium model (Woltjer et al., 2014) based on neo-classical microeconomic theory and it is an extension of the standard GTAP model (Hertel, 1997). The core of MAGNET is an input-output model, which links industries in value added chains from primary goods to final goods and services for consumption. Input and output prices are endogenously determined by the markets to

achieve supply and demand equilibrium. The agricultural sector is represented in high detail compared to standard CGE models. Developments in productivity are driven by a combination of assumptions on autonomous technological change provided by IMAGE-LandManagement and by economic processes as modelled by MAGNET (i.e. substitution between production factors). Land is modelled as an explicit production factor described by a land supply curve, constructed with land availability data provided by IMAGE-LandManagement (van Meijl et al., 2006). MAGNET provides information on agricultural demand, production, trade, and intensification or extensification of crop yields and livestock systems to IMAGE-LandManagement.

The dynamic vegetation model LPJmL (Müller et al., 2016) is an integral part of IMAGE (hard-coupled to IMAGE-LandManagement and MAGICC, annual data exchange) and simulates crop yields, grassland productivity, vegetation dynamics, and carbon and water cycles on a half degree geographic grid (Bondeau et al., 2007; Sitch et al., 2003). LPJmL is based on the concept of multiple plant functional types (PFTs) that are categorized according to biophysical characteristics. Both natural and crop PFTs are represented. Data on potential yields of the various crops and grasslands are provided to IMAGE-LandManagement. In return, IMAGE-LandManagement provides data on agricultural land use, irrigation and forest management, and MAGICC provides data on climate to LPJmL. Carbon and water cycle variables such as land-use change (LUC) CO₂ emissions, carbon uptake and irrigation water use are returned to IMAGE-LandManagement.

The energy system is modelled for 12 primary energy carriers and 26 regions by the energy model TIMER (van Vuuren, 2007). This is a simulation model that quantifies long-term trends in energy use using algorithms based on previous system states. Demand for bioenergy forms an important connection with IMAGE-LandManagement. Depending on bioenergy prices (determined by land supply, productivity of biomass for bioenergy, labour and capital costs, and learning dynamics) and other trends in the energy system (e.g. prices of competing energy sources) a certain demand for bioenergy is calculated by TIMER. The potential supply for bioenergy is calculated in IMAGE-LandManagement according to a set of sustainability rules: only abandoned agricultural lands and natural grass lands can be used, and bioenergy cannot directly compete with food (Hoogwijk et al., 2003). The potential yield of bioenergy biomass is calculated by LPJmL, and bioenergy land use is implemented in IMAGE-LandManagement. Preferably it is allocated on abandoned agricultural land. If no abandoned land is available, bioenergy is allocated on natural grasslands

Land-use CO₂ emissions are calculated by grid-level process modelling of LUC and forestry in IMAGE-LandManagement and LPJmL. Non-CO₂ emissions (CH₄, N₂O, CO, NH₃, NO_x, SO_x, NMVOC, BC, OC) from land and agriculture are calculated from various activity data combined with emission factors that are calibrated to the historical period (SI Table 2-4). Together with emissions from energy and industry this determines total projected emissions. An implementation of the simple climate model MAGICC 6.0, is used to determine atmospheric

concentrations, radiative forcing and global mean temperature change (Meinshausen et al., 2011). MAGICC emulates the behaviour of more complex climate models. Based on patterns of precipitation and temperature change in complex climate models, global mean temperature change and changes in precipitation are downscaled to a geographical grid at half degree resolution. Non-CO₂ emissions are converted to CO₂-eq for comparability using 100-year lifetime global warming potentials according to the IPCC (Solomon, 2007).

The climate policy model FAIR-SimCAP is used to determine global emission pathways with a long term climate target (den Elzen et al., 2008). FAIR-SimCAP uses carbon prices and marginal abatement cost curves (MACs) representing costs of mitigation actions to determine a cost optimal emission pathway. MACs on CO₂ mitigation in the energy sector are calculated by the TIMER model, including the use of BECCS. Mitigation potentials of non-CO₂ GHGs are based on Lucas et al. (2007). The ambition level of REDD and reforestation of degraded forest areas is roughly calibrated to the carbon price using Kindermann et al. (2008).

2.2.2. The SSP storylines and climate mitigation targets

The SSP storylines describe the key developments in the SSPs for the baseline and the mitigation scenarios (O'Neill et al., 2017). The storylines were used to derive demographic (KC and Lutz, 2017) and economic scenarios (Dellink et al., 2017)(Table 2-1, Figure 2-1). We earlier provided a description of the overall implementation of the SSP storylines in IMAGE (van Vuuren et al., 2017b). Here, we focus on the land-use components. Relevant storyline elements are supply, demand and trade of agricultural commodities, dietary preferences, agricultural efficiencies, policy on LUC, and climate change mitigation (Table 2-1 for SSP storyline elements and SI Table 2-1 for IMAGE SSP assumptions).

The SSP storylines are combined with climate-change mitigation targets to assess the role of land use and LUC in climate change and to investigate the effect of climate change mitigation policy on land-use dynamics. Five long term targets are used to define the mitigation scenarios: 6.0 W/m², 4.5 W/m², 3.4 W/m², 2.6 W/m² and 1.9 W/m². The first four scenarios correspond to the forcing targets of the initial set of RCP scenarios where 2.6 W/m² has a 66% likelihood to limit global warming to 2°C (van Vuuren et al., 2011). The 1.9 W/m² target has a 66% likelihood to limit global warming to 1.5°C and has been added in response to the adoption of the Paris Agreement which aims “to limit the temperature increase to 1.5°C above pre-industrial levels” (UNFCCC, 2015).

Table 2-1: Scenario-specific characteristics of important drivers of land-use dynamics

	SSP1	SSP2	SSP3	SSP4		SSP5
	Sustainability	Middle of the Road	Fragmentation	High income regions	Medium income regions	Fossil-Fueled development
Population (billion) (2050/2100)	8.5 / 7.0	9.2 / 9.1	10.0 / 12.8	9.2 / 9.5	9.2 / 9.5	8.6 / 7.4
GDP(thousand 2005 US\$ per capita) (2050/2100)	34 / 81	25 / 59	18 / 22	25 / 38	25 / 38	44 / 139
Globalization of trade	Highly globalized	Moderately globalized	Less globalized	Highly globalized	Highly globalized	Highly globalized
Animal product consumption	Reduced preference for animal products	Current preference for animal products	High preference for animal products	Current preference for animal products	High preference for animal products	High preference for animal products
Land-use change regulation	Strict regulation	Moderate regulation	Little regulation	Strict regulation	Moderate regulation	Moderate regulation
Crop yield improvement	High yield improvement	Moderate yield improvement	Low yield improvement	High yield improvement	Medium yield improvement	High yield improvement
Livestock system efficiency	High efficiency improvement	Moderate efficiency improvement	Low efficiency improvements	High efficiency improvement	Moderate efficiency improve-ment	High efficiency improvement
Effectiveness land-based mitigation	Very effective	Moderately effective	Not effective	Moderately effective	Moderately effective	Very effective

First, five baseline scenarios are developed to calculate how land use and climate change evolve in a world without mitigation policy. Subsequently, mitigation policies are introduced in each baseline scenario to achieve the defined targets. This leads to a set of 25 scenarios (SI Table 2-3). Some combinations are missing, for example in SSP1 the baseline radiative forcing is lower than the 6.0 W/m^2 target. In other scenarios the lower targets cannot be reached: 1.9 W/m^2 is infeasible for SSP3, SSP4 and SSP5, and 2.6 W/m^2 is infeasible for SSP3. Finally, a set of eight counterfactual scenarios are performed in which deployment of bioenergy is prevented in the energy and the land system in order to quantify the role of bioenergy in climate change mitigation.

2.2.3. Scenario implementation

In this section, the methodology through which the scenario-specific characteristics have been implemented in IMAGE are described (see also SI Table 2-1). In all scenarios climate feedbacks are taken into account in the natural system, e.g. through climate change effects on the carbon cycle. The climate impacts are calculated on the basis of greenhouse gas emissions of each scenario driven by both land-use and energy system trends. Effects of climate change on the socio-economic system are excluded, i.e. the effects of climate change on crop and grass yields and subsequently on agricultural economy are not taken into account. The standard approach in IMAGE does take climate change effects on the socio-economic system into account, however in the SSP design it was decided not to include these feedbacks. This design is implemented in the RCP (van Vuuren et al., 2011) as well as the SSP process (Riahi et al., 2017) to facilitate consistent estimates of impacts, adaptation and vulnerability in follow-up research.

2.2.3.1. Agricultural demand and trade

Food consumption patterns form important drivers of land use (Stehfest et al., 2009). In our analysis food consumption is assumed to be a function of population and income as well as the SSP storyline. Based on the storyline, animal product consumption in SSP1 is assumed to be 30% lower than the consumption level projected by the MAGNET model without this preference shift. Conversely, in SSP3 and SSP5 animal product consumption is assumed to be 30% higher than projected without the preference shift. It is also assumed that losses in the food supply chain differ between the scenarios. Currently, food losses and waste throughout the chain range from e.g. 19% for cereals in Sub-Saharan Africa to 60% for roots and tubers in Northern America (Gustavsson et al., 2011). Reflecting this wide variation and consistent with the storylines, in SSP1 a 33% reduction in losses in the food supply chain and at the household level is assumed related to increased environmental awareness. In SSP3 a 33% increase in losses is assumed related to the growing share of inefficient supply chains in developing countries. In SSP5 also 33% increase in food losses is assumed reflecting a consumption oriented society.

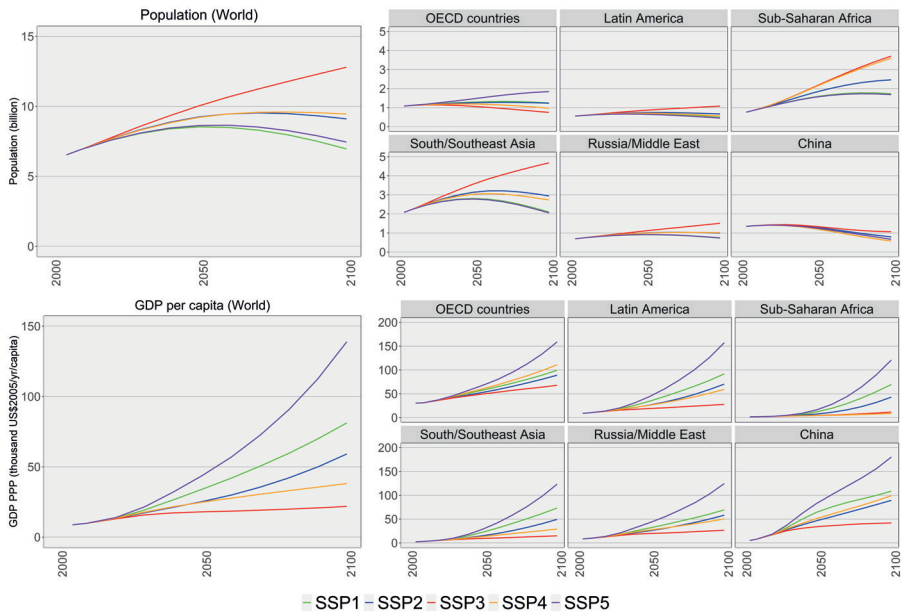


Figure 2-2: Scenario-specific trajectories of population (KC and Lutz, 2017) and GDP per capita (Dellink et al., 2017) for the world and six aggregated regions (see also SI Table 2-2)

International trade is encouraged or discouraged by a wide variety of legislation and trade tariffs (Tokarick, 2006). To reflect these effects in the various scenarios, assumptions on import taxes are made based on the storylines: in SSP3 import taxes are assumed to increase by 10% due to regional rivalry. In contrast, all trade tariffs are assumed to be removed in SSP1 and SSP5 reflecting increased globalization. In SSP4, it is assumed that trade tariffs are removed in the high/middle-income regions, while import taxes are increased by 10% in low-income regions to represent inequality between world regions. In SSP2 trade tariffs and subsidies are assumed to stay at current levels.

2.2.3.2. Land availability

In IMAGE, some land is considered unavailable for agricultural production due to biophysical reasons such as low productivity (<10% of maximum potential yield of the three most productive crop types from LPJmL), steep slopes (>45°), permafrost, ice cover (Fischer et al., 2008), or wetlands (Lehner and Döll, 2004). Land is also excluded for other reasons such as nature conservation in protected areas (based on WDPA (IUCN, 2015)) and urban areas (Klein Goldewijk et al., 2010). In addition, 10% of available land is excluded based on the assumption that subpixel heterogeneity and infrastructure makes part of the land unavailable for agricultural use (Fritz et al., 2013; Verburg et al., 2009). Lastly, also areas that have low probability to be converted to agriculture according to the IMAGE-LandManagement land-use allocation algorithm are excluded (Mandryk et al., 2015). This results in a global land availability for cropland and grazing land of 6717 Mha. This includes 4899 Mha that is already

in use as cropland or grazing land, implying that 1819 Mha is available for possible land-use expansion (Figure 2-2). Compared to the literature this is a medium to high estimate (Eitelberg et al., 2015).

Further scenario-specific restrictions on land availability are assumed in order to reflect storyline-driven efforts towards environmental conservation. In SSP1, SSP2 and SSP5, and in SSP4 medium/high-income regions, protected areas are expanded to achieve the Aichi biodiversity target in which 17% of terrestrial environments are protected (CBD, 2010). Protected areas are expanded in natural areas as computed by IMAGE-LandManagement in the year 2010, with a preference close to current protected areas according to the WDPA (IUCN, 2015). In addition, in each country 17% of each biome present is protected if possible. In SSP1 and in the high-income regions of SSP4 it is assumed that areas excluded from agricultural expansion are increased to cover 30% of the land. This is in line with the storyline on substantial land regulation, e.g. to ensure sustainable ecosystem services. In SSP3 and the low-income regions of SSP4, all available land can be converted to agriculture.

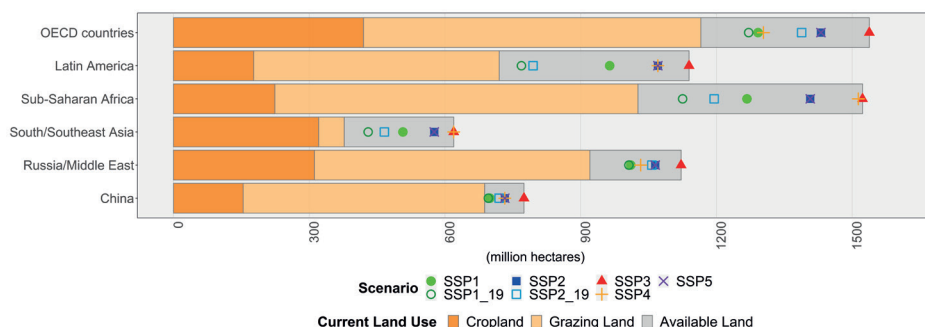


Figure 2-3: Regional land use in 2010, assumed maximum amount of available land, and scenario-specific assumptions on available land for the baseline and two 1.5°C mitigation scenarios (1.9 W/m²)

2.2.3.3. Agricultural efficiencies

Agricultural efficiencies are calculated on the basis of a projected base-level improvement in technology and management, in combination with price-driven yield increases leading to substitution between production factors as calculated endogenously in MAGNET. For SSP2, the overall regional crop yield changes are calibrated to the FAO Agricultural Outlook (Alexandratos and Bruinsma, 2012). It is assumed that 50% of the improvement is autonomous while the other 50% is price driven. For the other SSPs, the autonomous improvement has been derived from SSP2 using a correlation with GDP. As a result, advances in crop yields are high in SSP5 and SSP1, low in SSP3 and distributed across regions in SSP4.

Fertilizer application rates in SSP2 are based on the FAO Agricultural Outlook (Alexandratos and Bruinsma, 2012). It is assumed that in SSP1, SSP5 and high-income regions of SSP4,

fertilizer efficiency improvement is 20% higher than SSP2 based on environmental concerns or technological improvements. Only in Sub-Saharan Africa where nutrient mining currently occurs (Lassaletta et al., 2014) does the application rate go up. In SSP3 and low-income regions of SSP4, 20% lower fertilizer efficiency improvements are assumed due to limited agricultural improvements.

Developments in the efficiency of livestock systems in SSP2 are also derived from the FAO Agricultural Outlook (Alexandratos and Bruinsma, 2012). Important characteristics are production performance and feed rations. In IMAGE-LandManagement a distinction is made between intensive (mixed and industrial) and extensive (pastoral) systems for ruminants. It is assumed that production in existing extensive systems remains stable. Additional demands for animal products are supplied by intensive systems (Bouwman et al., 2005). In SSP1 and SSP5, livestock system efficiencies are assumed to increase faster related to continued economic growth: less efficient regions experience 50% convergence with the most efficient regions. In contrast, in SSP3 the efficiency improvements are assumed to stagnate. In SSP4, high/middle-income regions show continued efficiency improvements whereas low-income regions experience stagnation. The density of animals on grazing land is determined by MAGNET accounting for competing demands for land between grazing land and cropland.

2.2.3.4. Irrigation

Irrigated area projections in SSP2 are based on the FAO Agricultural Outlook (Alexandratos and Bruinsma, 2012): region specific growth rates of irrigated harvested area from 2005 to 2050 are applied to the 2005 areas equipped for irrigation. For 2050-2100 the 2030-2050 growth rate is assumed to continue. Irrigated area growth rates in SSP1 are assumed to be 50% lower than SSP2 because of low population growth and concerns about unsustainable water use. In contrast, in SSP3 growth rates are assumed to be 50% higher than SSP2 related to high population growth. SSP5 is assumed to follow the same trend as SSP2, while in SSP4 high/medium/low income regions are assumed to follow the projections of SSP1/SSP2/SSP3, respectively.

Improvement of irrigation efficiency is implemented as a gradual closure of the gap between withdrawal and consumption. In SSP2, irrigation is assumed to depend on the relative increase in irrigated area as an indicator of regional investment in improved irrigation technology (0.2%/yr on new areas). In SSP1, the efficiency gap is assumed to decrease by 0.1%/yr on all irrigated areas which is in line with the sustainability storyline and recommendations by the FAO to improve irrigation systems in order to reduce water footprints (Molden, 2007). The same efficiency change is assumed in SSP5 related to high economic growth and investments. In SSP3 on the other hand, efficiency is assumed to remain at 2005 levels. In SSP4 high/medium/low income regions are assumed to follow the projections of SSP1/SSP2/SSP3, respectively.

2.2.3.5. Urban areas

Urban area development directly follows the approach of Klein Goldewijk et al. (2010). Urban population and population density are used to calculate urban area per country using a bell-shaped curve based on historical urban densities, which is subsequently downscaled on a 5 arc-minute grid.

2.2.3.6. Forestry

Global demand for timber is determined by the demand for fuelwood and industrial roundwood. Demand for fuelwood is modelled by the energy model TIMER, and is a function of access policies, poverty and the size of the rural population (Daioglou et al., 2012). Demand for industrial roundwood is determined by multiplying population with scenario-specific per capita demand. In SSP2 per capita demand increases by 5% up to 2100. In SSP1 global average per capita demand is reduced by 10% due to environmental awareness, while in SSP5 per capita demand increases by 40% due to high economic growth and consumption. In SSP3 and SSP4 per capita demands decrease by 10% and 5% respectively as the share of population living in poverty increases substantially. Production of timber and fuelwood can be done through clear cut, selective cut (reduced or high impacts) or wood plantations dependent on the storyline. In SSP3, we assume that the current systems persist, resulting in high impact selective logging in developing regions, while in SSP1 wood plantations and reduced impact logging are prevalent for biodiversity concerns.

The FAO's Forest Resource Assessment (FRA) provides detailed information on historical deforestation rates (FAO, 2015). Using historical data on expansion of agriculture from FAO, however, leads to considerably lower deforestation rates than reported by the FRA. In IMAGE it is therefore assumed that the differences are caused by additional reasons, e.g. unsustainable forestry preventing regrowth of natural forests, mining or illegal logging. To account for this, a historically calibrated rate of additional forest degradation is implemented. The trend is assumed to continue in the near future. In the environmentally aware world of SSP1 additional forest degradation is assumed to go to zero in 2040, while in the fragmented and underdeveloped world of SSP3 it continues until 2060.

2.2.3.7. Land-based climate change mitigation

In scenarios that aim to meet a specific climate target, three types of land-based climate change mitigation are implemented: bioenergy, REDD (avoided deforestation) and reforestation of degraded forest areas. Bioenergy demand is determined by the energy model TIMER based on bioenergy yield, the carbon price, dynamics in the energy system, and land availability following a food-first principle. REDD is implemented by protecting areas with high carbon stocks according to Ruesch and Gibbs (2008), i.e. by further limiting the land supply (Figure 2-3). Three increasingly strict protection levels are defined at 200, 150 and 100 ton C/ha. Reforestation on degraded forest areas restores areas that have been degraded for reasons other than agriculture. Two levels of reforestation are defined: either half or all of the degraded forest areas are reforested.

The demand for bioenergy in climate change mitigation scenarios is linked to the carbon price required to reach the mitigation target in the IMAGE framework in competition with other mitigation options (discussed in more detail in van Vuuren et al. (2017b)). The levels of REDD and reforestation are not linked to this price but roughly calibrated to abatement curves on avoided deforestation (Kindermann et al., 2008)(Table 2-2). Next to that, as land-based mitigation is assumed to be moderately successful in SSP2 and SSP4 and unsuccessful in SSP3, the levels of REDD and deforestation are relatively lower in those scenarios than would be expected if solely the carbon price is considered.

Table 2-2: levels of REDD and reforestation implemented in the mitigation scenarios. REDD is defined through a carbon density threshold: high REDD 100 t C/ha, medium REDD 150 t C/ha, low REDD 200 t C/ha. Full reforestation assumes that all degraded forests are restored, half reforestation assumes that half of degraded forests are restored. Missing scenarios are infeasible.

Climate target (W/m ²)	SSP1	SSP2	SSP3	SSP4	SSP5
1.9	High REDD, full reforestation	High REDD, full reforestation	-	-	-
2.6	High REDD, full reforestation	Medium REDD, full reforestation	-	Medium REDD, full reforestation	High REDD, full reforestation
3.4	Medium REDD, full reforestation	Low REDD, half reforestation	No REDD, no reforestation	Low REDD, half reforestation	Medium REDD, full reforestation
4.5	Low REDD, half reforestation	No REDD, no reforestation	No REDD, no reforestation	No REDD, no reforestation	Low REDD, half reforestation
6.0		No REDD, no reforestation	No REDD, no reforestation	No REDD, no reforestation	No REDD, no reforestation

2.3. Results

2.3.1. Global land-use dynamics in SSP baseline scenarios

2.3.1.1. Demand for agricultural products, bioenergy and wood

Agricultural production (Figure 2-4) is a dominant factor in observed LUC patterns. In all scenarios crop production for food and feed increases, ranging from 46% in SSP1 to 73% in SSP5 in 2010-2050. For 2010-2100, the increase ranges from 48% in SSP1 to 91% in SSP3. The production growth in all scenarios is predominantly driven by continued population and per capita income (GDP) growth up to 2050 (Figure 2-2). In addition, high production in SSP3 and SSP5 is caused by dietary preference for animal products and high food losses and waste. The opposite characteristics are present in SSP1 leading to relatively low production growth. Production in 2050 in SSP5 is higher than in SSP3, even though population is substantially

lower (8.6 and 10 billion resp.). The difference is caused by high levels of consumption driven by high per capita income increase in SSP5, as opposed to a large share of the population living in poverty in SSP3 with limited increases in per-capita consumption. Change in grass production ranges from -13% in SSP1 to 50% in SSP3 in 2010-2050, and from -35% in SSP1 to 89% in SSP3 in 2010-2100. The large variation results from differences in dietary preference for animal products and from increased efficiency in livestock production systems. The latter involves substitution in the feed composition of livestock with larger shares of feed crops relative to grass resulting in lower grass production and higher crop production in SSP1 and SSP5. As a consequence of this, land abandonment in SSP1 mostly occurs on grazing land areas (Figure 2-6 and SI Figure 2-7). This is less so the case in SSP5 due to higher animal product consumption and less incentive to abandon agricultural land for ecosystem restoration.

Production of biomass for bioenergy increases in all scenarios as it becomes a standard component of the energy mix, up to 4.0 Gt/yr in SSP1 in 2100. Demand for wood production decreases by 23% in SSP1 in 2010-2100, mostly due to specific policies focused on access to modern energy and reduced poverty leading to lower shares of traditional fuel such as fuel wood and charcoal. In contrast, wood production increases by 46% in SSP3 in 2010-2100 due to population growth leading to high timber demand and a large poor population creating high demand for traditional fuels.

2.3.1.2. Agricultural efficiency

Next to production, agricultural efficiency is an important factor determining the amount of land required to meet demand for agricultural products. Trends in globally averaged cereal yields show an overall increase in the productivity of cropping systems (Figure 2-5). In SSP1 and SSP2 yields increase 50% from 3.2 t/ha today to 4.8 t/ha in 2100. In SSP5, yields increase up to 5.2 t/ha. In SSP3 and SSP4, increases are slightly lower with yields going up 41% to 4.5 t/ha in 2100.

Livestock system efficiencies determine the amount of feed and grass required to produce animal products. Efficiencies (expressed as dry matter animal product output as a percentage of total dry matter feed and grass input) differ greatly between types of animal products with 10.3% for pigs and poultry, 7.9% for dairy cattle and 1.1% for beef cattle in 2010 (Figure 2-5). From 2010-2100, especially SSP1 and SSP5 show large improvements, up to 12% for dairy cattle. In SSP3 and SSP4 however a reduction in efficiency down to 6.2% and 6.7%, respectively, takes place. This results from low technological improvements and large production increases in areas with low efficiency, most notably Sub-Saharan Africa.

2.3.1.3. Land-use change

LUC varies substantially between the SSP scenarios (Figure 2-6, Figure 2-10). SSP3 shows the largest global increase in total cropland and grazing land amounting to 826 Mha for the period 2010-2050, after which it continues at a slower pace to a total increase of 1011 Mha

for 2010-2100. In contrast, SSP1 shows a decrease of 305 Mha in 2010-2050 and 682 Mha in 2010-2100. For SSP2, SSP4 and SSP5, cropland and grazing land increases by 424 Mha, 459 Mha and 655 Mha respectively in 2010-2050. After 2050, cropland and grazing land levels out resulting in a total increase of 412 Mha in SSP2, 423 Mha in SSP4 and 510 Mha in SSP5 for the period 2010-2100.

Changes in forest area are mostly driven by changes in agricultural land. In addition, forestry and additional forest degradation have a substantial impact when forest is assumed not to regenerate after timber harvesting. This results in a large decrease of 529 Mha in forest area compared to today in SSP3 in 2010-2100. In SSP1 a large increase of 296 Mha takes place in 2010-2100 as natural forest regrowth occurs on abandoned agricultural land, most notably in northern and eastern Europe, the eastern USA and eastern China (SI Figure 2-9).

The increase in irrigated cropland in SSP2 is 59 Mha in 2010-2100 representing 27% of total cropland increase, indicating investment in existing cropland to achieve higher yields. This is also evident in SSP1 where irrigated cropland increases by 24 Mha even though total cropland decreases. In SSP3 on the other hand, irrigated cropland represents only 16% of total cropland increase in 2010-2100 as cropland expansion mostly takes place in poor regions. Biomass plantation area for bioenergy is high in SSP1 after 2050 reaching 162 Mha in 2100 due to efforts to move away from a fossil-fuel based energy system. In SSP4, bioenergy area increases quickly due to self-sufficiency concerns up to 172 Mha in 2050.

Increases in built-up area range from 49 Mha in SSP3 to 74 Mha in SSP5 in 2010-2100. These estimates depend on population growth and rates of urbanization (Jiang and O'Neill, 2017). This explains low increases in SSP3, because even though this scenario shows high population growth, levels of urbanization are low. On the other extreme, while global population in SSP5 is going down by the end of the century, built-up areas grow fast as almost the entire population urbanizes.

2.3.1.4. Food security

Globally averaged per capita food available for consumption increases in all scenarios (Figure 2-7). SSP3 shows an increase of 3% going from 2891 kcal/cap/day today to 2966 kcal/cap/day in 2100 indicating limited improvements in food security (van Meijl et al., 2020). In contrast, SSP5 shows an increase of 20% going to 3466 kcal/cap/day in 2100. Food available for consumption is substantially lower in SSP1 compared to SSP5, even though per capita GDP (an important determinant of food availability) is high in both SSP1 and SSP5 (Figure 2-2). This is due to lower levels of food losses and lower income elasticity representing a less consumption oriented society (SI Table 2-1).

Variations in globally averaged food prices are large. In SSP1 a 58% decrease in prices occurs, while in SSP3 prices increase by 251% (Figure 2-7). These differences are in part determined by developments in agricultural efficiency and overall demand. For example, in SSP1

agricultural and supply chain efficiency increases substantially, while the increase in demand for agricultural commodities is relatively low. This results in a reduction of food prices. This is the opposite of SSP3, where low increases in agricultural efficiency, an inefficient food supply chain and large increases in demand generate high food prices.



Figure 2-4: Global production of food/feed crops, grass for livestock, biomass for bioenergy and wood for timber and fuel in 2010, 2050 and 2100 in five baseline scenarios.

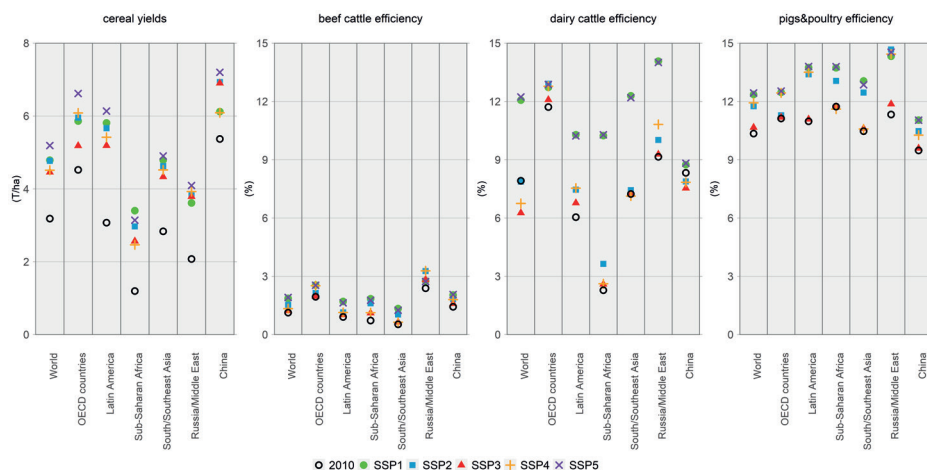


Figure 2-5: Cereal yields (incl. temperate cereals, rice, maize, tropical cereals) and livestock efficiencies (dry matter animal product output as a percentage of total dry matter feed and grass input for beef, dairy, and pigs and poultry respectively) in 2010 and 2100 for five baseline scenarios

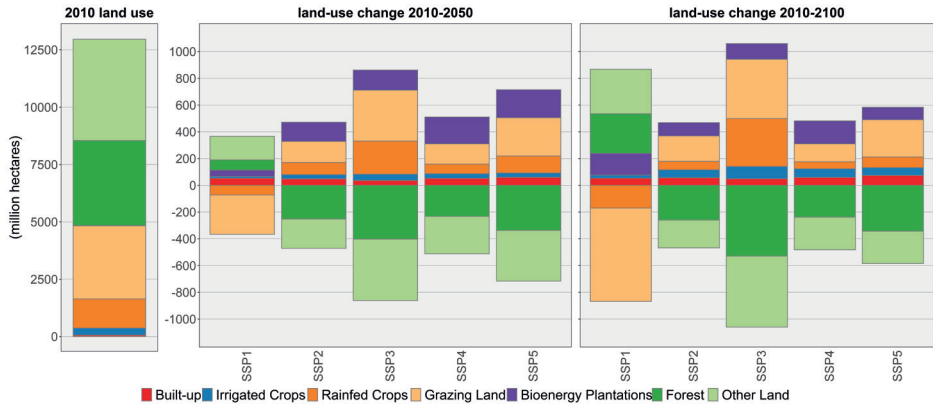


Figure 2-6: Global land use in 2010, and global LUC for 2010-2050 and 2010-2100 for seven land-use classes in five baseline scenarios. Degraded forests are classified as other land.

2

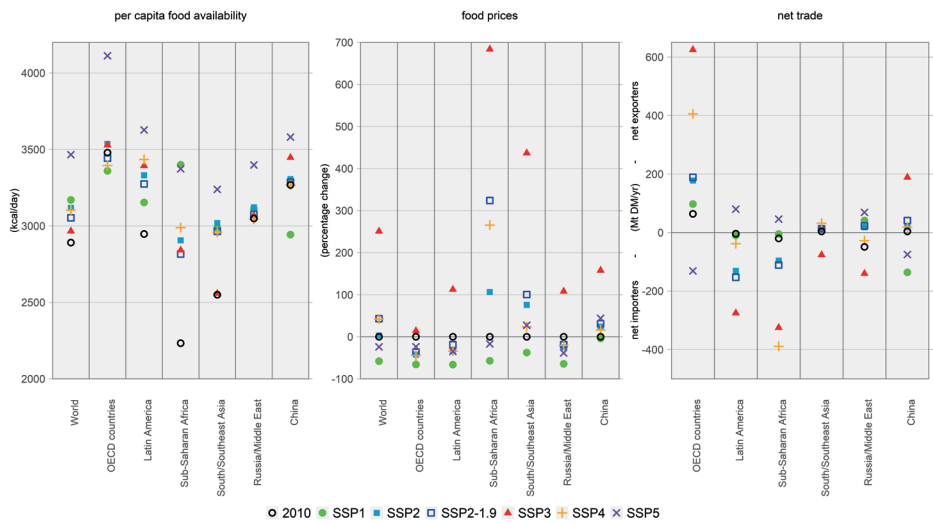


Figure 2-7: Agro-economic indicators for 2010 and 2100 for five baseline scenarios and the SSP2 1.5°C mitigation scenario (1.9 W/m²) scenario: per capita food availability of food crops and animal products in kcal/cap/day, changes in average food prices, and net trade between the regions.

2.3.2. Regional land-use dynamics in SSP reference scenarios

The *OECD countries* (excl. Turkey, Mexico, Chile) show a decrease in agricultural land in SSP1, SSP2 and SSP4 in 2010-2100, up to 236 Mha in SSP1 (Figure 2-8). The reduction mostly happens on grazing land, predominantly due to intensification in the livestock sector (e.g. in the eastern USA, SI Figure 2-7). In SSP3 a substantial increase of 163 Mha takes place, partly in response to high land pressure in other regions. In addition, although agricultural efficiency is already relatively high in the OECD countries, a continued increase is projected with cereal yields rising from 4.5 t/ha to 6.0 t/ha in SSP2 creating higher crop production on similar land areas. As per capita food availability increases only slightly in most scenarios (Figure 2-7) and population mostly decreases (Figure 2-2) this results in a production surplus that is traded with other regions to make up for production shortages elsewhere: in SSP2 net export increases from 64 Mt in 2010 to 178 Mt in 2100.

Projected change in agricultural area in *Latin America* ranges from a reduction of 73 Mha in SSP1 to an increase of 207 Mha in SSP3 in 2010-2100. Per capita food availability increases in all scenarios resulting in increased production (Figure 2-9). In SSP1, the livestock sector intensifies substantially, and food losses and dietary preferences for animal products are reduced, leading to abandonment of grazing land. Abandonment takes place in relatively productive areas (predominantly north-western Brazil, SI Figure 2-7) leading to high potential for bioenergy production. In the other SSPs higher demand is mostly met by increases in agricultural land along the arc of deforestation in Brazil and the Gran Chaco region in Bolivia, Argentina and Paraguay (Figure 2-10). In contrast, in Central America possibilities for agricultural expansion are limited leading to import dependency.

Sub-Saharan Africa experiences the most extreme LUC of all regions in the various scenarios. SSP3 and SSP4 show an increase in agricultural area from 1015 Mha in 2010 to 1439 Mha and 1406 Mha respectively in 2100. Most expansion occurs on the rims of the Congo basin which is severely encroached, and smaller natural areas still left in Western Africa are all converted (Figure 2-10). Only SSP1 shows a decrease of grazing land, though cropland is still expanding. A key driver is the growth of population. Despite the large expansion of cropland and grazing land, agricultural demand cannot be fulfilled within the region requiring high levels of net import from other regions. In SSP4, 389 Mt in food commodities are imported compared to a regional crop production of 930 Mt. This implies an increasing dependency of Sub-Saharan Africa on food imports which might reduce food security. This is also illustrated by food prices which increase by 266% in SSP4 and 684% in SSP3.

Agricultural land in *South/Southeast Asia* changes relatively little in 2010-2100 ranging from a reduction of 29 Mha in SSP1 to an increase of 125 Mha in SSP3, even though population increases substantially by 2100. This is partially due to low animal product consumption and especially low beef consumption for cultural reasons resulting in low demand for grass which is a major cause for LUC in other regions. On the other hand, crop production doubles to 2033 Mt in SSP2. The limited effect on cropland is due to India which is a dominant country in

South/Southeast Asia that has little potential for agricultural expansion. As a consequence, intensification is high in all scenarios leading to 53-73% higher yields. On the other hand, the effects on food security in SSP3 are large as food prices increase by 437% and food availability does not improve in the aggregated region. Food availability even deteriorates in India from 2493 kcal/cap/day in 2010 to 2357 kcal/cap/day in 2100.

The *Russia/Middle East* region (also including Northern Africa, Central Asia, Turkey, Ukraine and Belarus) show varying developments. In Russia and Central Asia grazing land is abandoned due to intensification in the livestock system. In addition, Ukraine and Russia increase their net export as yields increase on the large cropland areas that are currently not intensively used. On the other hand, in Northern Africa and the Middle East agricultural production on relatively unproductive land continues, even though these areas cannot fulfil demand of an increasing population. Consequently, these regions remain net importers of food crops.

Contrary to most other regions, *China* shows reductions in agricultural land in all scenarios. This is a consequence of the downward trends in the population projections in combination with substantial intensification in both crop yields and the livestock sector. Furthermore, even though meat consumption in China increases substantially this predominantly consists of pork as opposed to large shares of beef in OECD and Latin America. As pork is mostly fed with crops and residues this requires substantially less land thus reducing land demand in China. Therefore, afforestation trends that have been observed in recent years are projected to continue up to 152 Mha in SSP1 as a consequence of abandoning agricultural land.

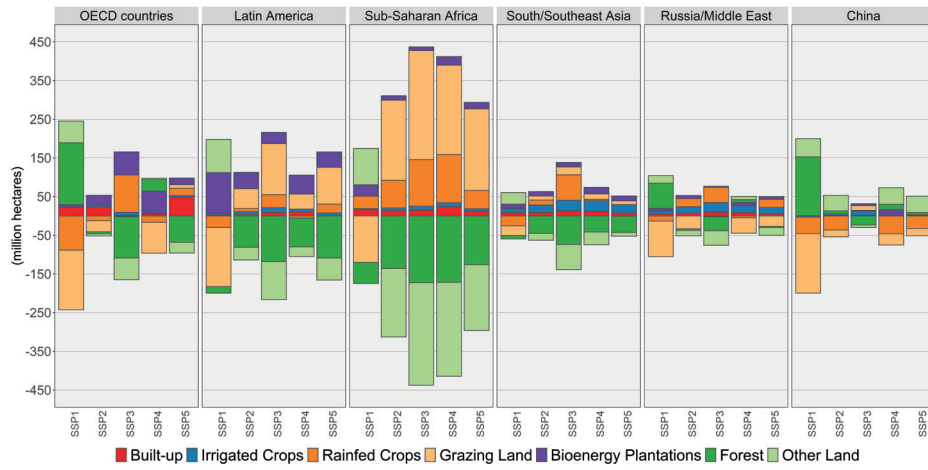


Figure 2-8: Regional LUC for 2010-2100 for seven land-use classes in five baseline scenarios. Degraded forests are classified as other land.

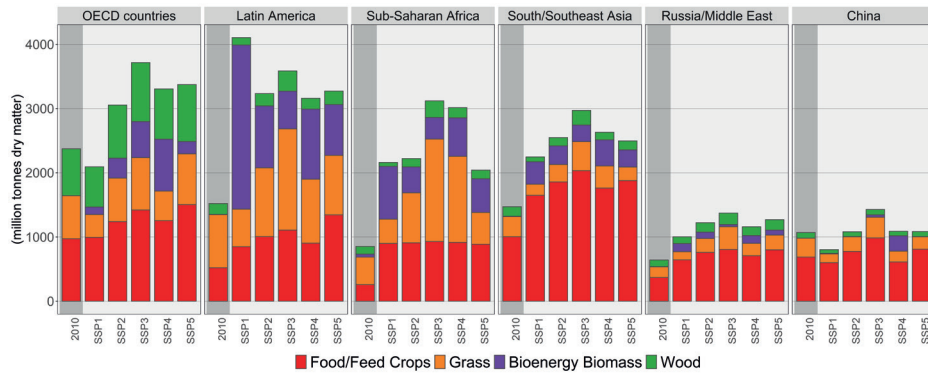


Figure 2-9: Regional agricultural production in 2010 and 2100 for five baseline scenarios.

Land-use change: 2010 – 2100

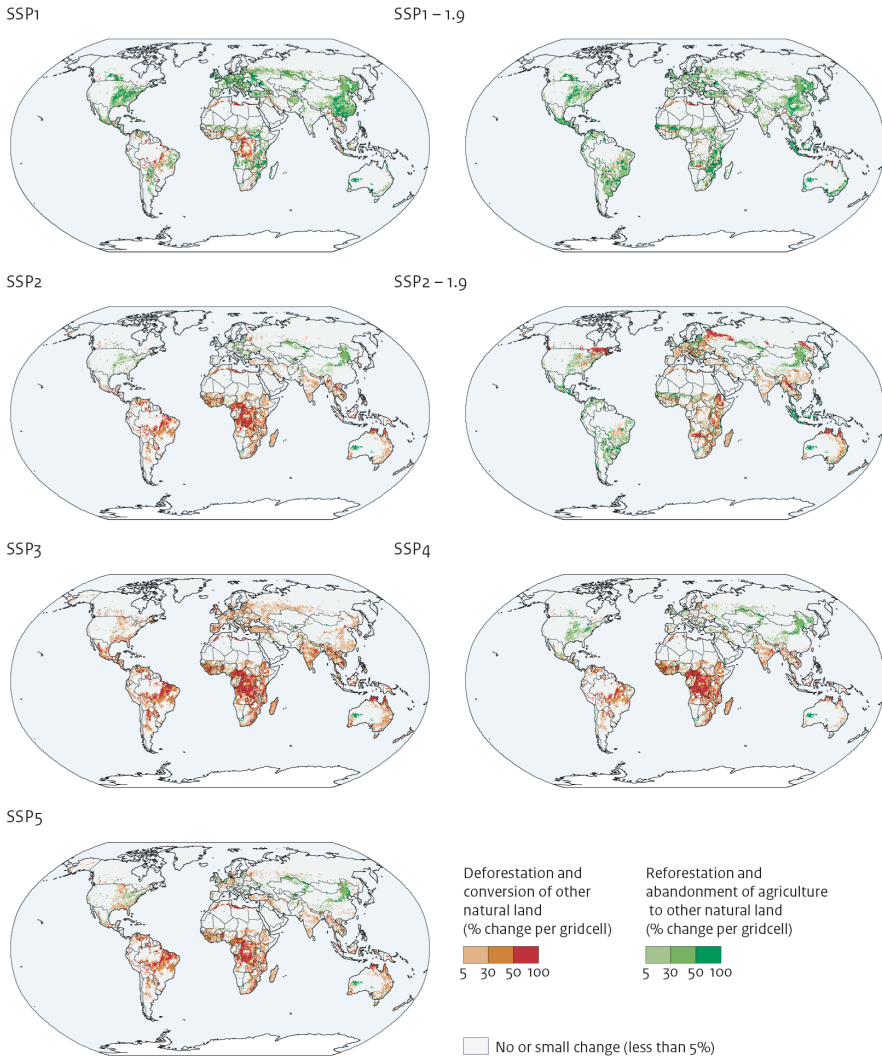


Figure 2-10: Change in land use (percentages of grid cells) between 2010 and 2100; deforestation and conversion of other natural land to agriculture (red) and reforestation and abandonment of agriculture to other natural land (green) for five baseline scenarios and two 1.5°C mitigation scenarios (1.9 W/m²).

2.3.3. Impacts of land-based climate change mitigation on land dynamics

Three types of land-based climate change mitigation are implemented: bioenergy, REDD (avoided deforestation) and reforestation of degraded forest areas. Implementation of large-scale bioenergy production (partly in combination with carbon capture and storage)

is an essential mitigation strategy to reach ambitious climate targets (Daioglou, 2016). In mitigation scenarios with a 2.6 W/m² (2°C) or a 1.9 W/m² (1.5°C) target this results in large increases in area used for bioenergy production in 2010-2100, ranging from 363 Mha in SSP1-2.6 and 225 Mha in SSP2-2.6, to 391 Mha in SSP1-1.9 and 414 Mha in SSP2-1.9 (Figure 2-11). Almost all biomass for bioenergy is produced on plantations with fast-growing grass species or short-rotation coppice woody species that are suitable for second generation bioenergy. Allocation preferably takes place on abandoned agricultural land, most notably in central Europe, southern China and eastern USA, and on natural grasslands in central Brazil, eastern and southern Africa, and Northern Australia (SI Figure 2-8). The 1.9 W/m² target is very ambitious in an SSP2 world, requiring large-scale bioenergy deployment early in the century (516 Mha in 2010-2050) as well as using forest areas in temperate and boreal regions (notably Canada and Russia) with the assumption that replaced wood biomass is used for timber or bioenergy. Following the sustainability criteria applied in IMAGE, bioenergy production takes place on areas that are not required for food production, consequently not affecting any of the agro-economic indicators.

Areas that are addressed by REDD policy are located in regions with high density carbon stocks, predominantly the tropical areas. Therefore, land availability is reduced most in Latin America, Sub-Saharan Africa and South/Southeast Asia (Figure 2-3). In SSP2-1.9 all forest with a carbon density higher than 100 t C/ha is protected leading to 311 Mha less cropland and grazing land compared to the baseline (2010-2100)(Figure 2-11). REDD has the largest effect on agricultural land use in Sub-Saharan Africa as this region is projected to have the highest agricultural land expansion in the baseline scenario (Figure 2-8). In addition, the policy negatively affects food security shown by a reduction in food availability (from 2905 in SSP2 to 2816 kcal/cap/day in SSP2-1.9) and a sharp increase in food prices (306% in SSP2-1.9 compared to 106% in SSP2)(Figure 2-7). Also globally the effects of REDD are substantial: total agricultural production is reduced by 220 Mt and food prices rise by 40% in SSP2-1.9 compared to SSP2 in 2100.

REDD together with reforestation of degraded forest areas leads to substantial increases in forest area in the mitigation scenarios compared to the baseline scenarios: in 2100 forest area is respectively 220 Mha and 404 Mha higher than the baseline in SSP1-2.6 and in SSP2-2.6. In SSP2-1.9, the stringency of the mitigation target leads to more bioenergy production to achieve more negative emissions thus limiting the difference to 254 Mha compared to SSP2 in 2100.

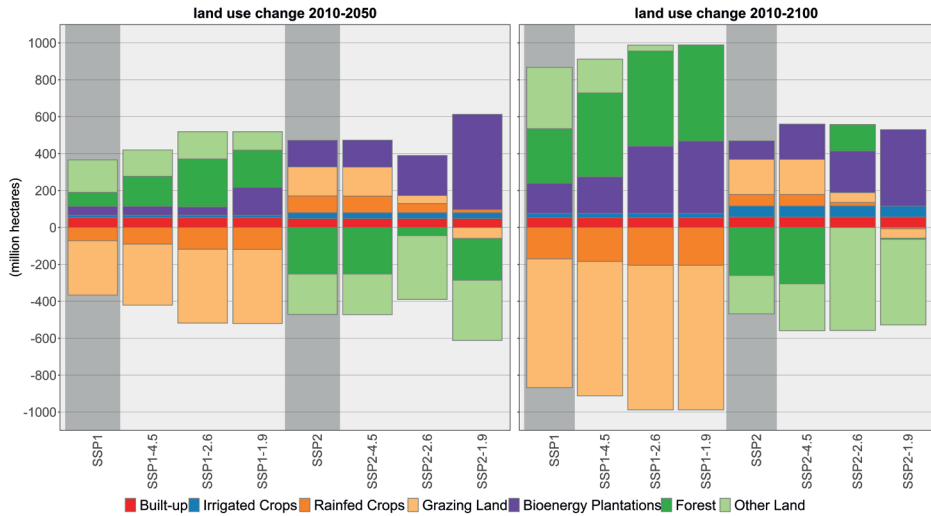


Figure 2-11: Global LUC in 2010-2050 and 2010-2100 for the SSP1 and SSP2 baseline and three increasingly ambitious mitigation targets: 4.5, 2.6 and 1.9. Degraded forests are classified as other land.

2.3.4. Greenhouse gas consequences of baseline and mitigation scenarios

Emissions from agriculture and LUC are estimated to make up 20.6% of total emissions in 2010 (Figure 2-12). With large increases in total emissions in the baselines (e.g. in SSP2 up to 74.8 Gt CO₂eq/yr in 2050 and 94.2 Gt CO₂eq/yr in 2100) the share of agriculture and LUC emission reduces to 18.0% in 2050 and 8.1% in 2100. This is even more extreme in SSP5 where total emissions in 2100 increase to 136.3 Gt CO₂eq/yr reducing the share of agriculture and LUC to only 4.1% (SI Figure 2-3). In contrast, in mitigation scenarios the relative share of agricultural emissions increases as emissions of energy, industry and LUC decrease dramatically. In 2100 agricultural emissions of CH₄ and N₂O are the largest source of net emissions in many ambitious mitigation scenarios (SSP1-2.6, SSP1-1.9, SSP2-2.6, SSP2-1.9) because of the limited reduction potential (Gernaat et al., 2015).

LUC CO₂ emissions result from deforestation and reforestation. In 2050 all baseline scenarios except SSP1 are still a net source of LUC CO₂ emissions ranging from 5.0 Gt CO₂/yr to 7.1 Gt CO₂/yr in SSP5 and SSP3 respectively (SI Figure 2-3). In 2100, only SSP3 continues to be a net source with 1.4 Gt CO₂/yr whereas the other scenarios have near zero emissions (SSP2 and SSP4) or negative emissions up to -2.4 Gt CO₂/yr in SSP1 due to reductions in agricultural land. REDD and reforestation create more negative emissions due to faster reductions in LUC and due to reforestation of degraded forests. In SSP1-2.6 in 2050 emissions are -1.6 Gt CO₂/yr compared to -0.2 Gt CO₂/yr in the SSP1 baseline, while in SSP2-2.6 emissions are 2.6 Gt CO₂/yr compared to 5.0 Gt CO₂/yr in the SSP2 baseline. From the 2.6 W/m² target to the 1.9 W/m² target LUC emissions are slightly higher again: -0.6 Gt CO₂/yr in SSP1-1.9 and 3.1 Gt CO₂/yr in SSP2-1.9 in 2050. This is caused by increased land use for bioenergy production,

resulting in reduced reforestation area and conversion of areas with relatively low carbon density to bioenergy production.

Approximately half of present-day CH₄ land-use emissions are caused by the livestock sector. Other land-use CH₄ sources are rice production, burning of biomass and agricultural waste. Projected emissions of the livestock sector depend on the total demand for animal products (particularly ruminants) and production efficiency. Projected emissions from biomass burning depend on LUC trends, and emissions from rice production and agricultural waste burning depend on crop production. Total projected emissions range from SSP3 with 6.1 Gt CO₂eq/yr in 2050 and 6.9 Gt CO₂eq/yr in 2100, to SSP1 with 3.7 Gt CO₂eq/yr in 2050 and 3.2 Gt CO₂eq/yr in 2100 respectively. In the mitigation scenarios emissions are reduced dependent on the carbon price as there is substantial abatement potential: in SSP2-1.9 CH₄ emissions are reduced by 40% in 2050 and 48% in 2100 compared to the SSP2 baseline. CH₄ mitigation is already relatively high in 2050 because it is estimated to be a cheap measure compared to other mitigation options (Lucas et al., 2007) and because mitigation needs to be implemented very fast in case of a 1.9 W/m² target.

Land-use emissions of N₂O are predominantly determined by synthetic fertilizer application and livestock excretion. Emissions turn out highest in SSP3 with 4.4 Gt CO₂eq/yr in 2100 as synthetic fertilizer use is high due to inefficient fertilizer application in combination with high demand. Manure production is also high due to high demand and inefficient livestock systems requiring large numbers of animals. SSP1 has the lowest N₂O emissions with 2.5 Gt CO₂eq/yr in 2100 due to lower demand and higher efficiencies in livestock systems and fertilizer application. The identified mitigation potentials are moderate with reductions of 9% in 2050 and 7% in 2100 in SSP2-1.9 compared to the SSP2 baseline. Mitigation of N₂O emissions is partially counteracted by higher levels of fertilizer use due to large-scale bioenergy production.

Mitigation through bioenergy by replacement of fossil fuels and BECCS are crucial components of ambitious mitigation scenarios. Preventing bioenergy use in the energy system causes increased emissions from fossil fuels. In addition, climate change mitigation is hampered as negative emissions from BECCS are made impossible. On the other hand, LUC emissions from the expansion of bioenergy plantations are reduced (SI Figure 2-8). A set of counterfactual scenarios in which deployment of bioenergy is prevented in the energy and the land system is used to quantify this effect. In the moderately ambitious mitigation scenarios SSP1-4.5 and SSP2-4.5 (4.5 W/m² ≈ 3°C) bioenergy plays a moderate role with a difference of 5.9 Gt CO₂/yr and 3.8 Gt CO₂/yr respectively in 2100 (Figure 2-12). However, in ambitious mitigation scenarios bioenergy is crucial to achieve negative emissions: in SSP1-2.6 and SSP2-2.6 bioenergy is responsible for an annual reduction of 13.8 Gt CO₂/yr and 9.6 Gt CO₂/yr respectively in 2100. Reductions in 2100 in SSP1-1.9 and SSP2-1.9 are even larger with 17.3 Gt CO₂/yr and 13.4 Gt CO₂/yr respectively. An important characteristic of the 1.9 W/m² mitigation scenarios is that mitigation measures are implemented faster to be able

to stay within the carbon budget: in 2050 reductions through bioenergy are 7.5 Gt CO₂/yr in SSP1-1.9 compared to 1.4 Gt CO₂/yr in SSP1-2.6, and 8.7 Gt CO₂/yr in SSP2-1.9 compared to 7.6 Gt CO₂/yr in SSP2-2.6. Generally, the role of bioenergy is larger in SSP1 than in SSP2 because of abandonment of grazing land which lowers biomass prices.

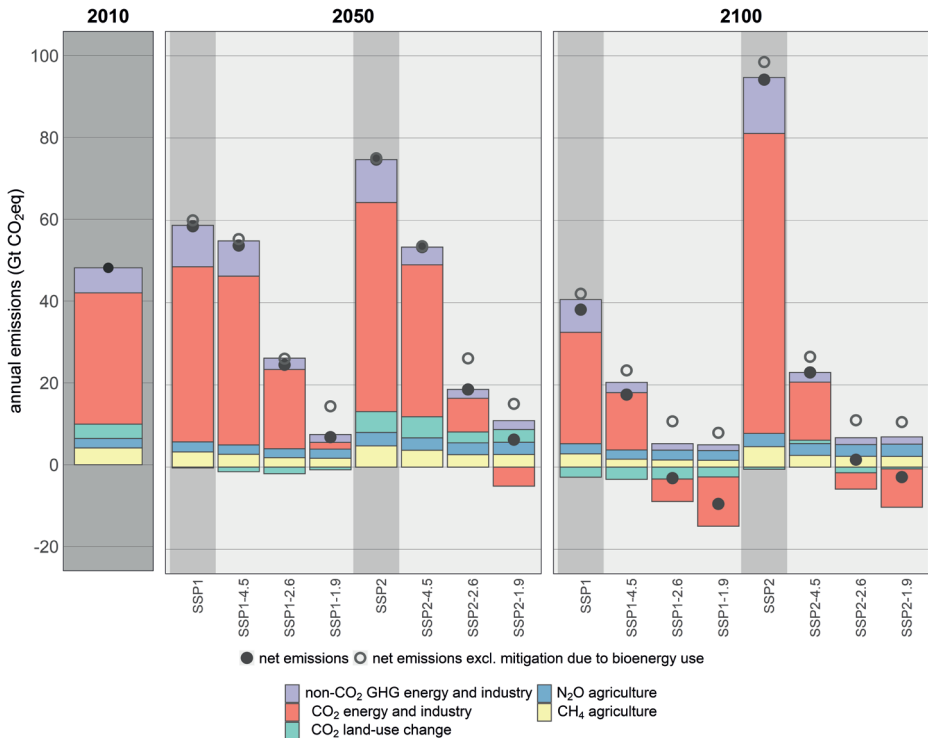


Figure 2-12: GHG emissions in 2010, 2050 and 2100 from energy and industry, LUC including reforestation, and agriculture, net emissions and net emissions without mitigation due to bioenergy for two baseline scenarios and six mitigation scenarios.

2.4. Discussion and Conclusions

The results from the IMAGE SSP baseline scenarios show large variations in potential land-use futures. The most prominent LUC trends are in agricultural land use, ranging from large decreases in SSP1 to large increases in SSP3. The most striking hotspot of change is Sub-Saharan Africa, which shows the largest increases in agricultural land use of all regions in almost all scenarios causing large-scale deforestation. Key drivers are population growth, changes in food consumption depending on per capita GDP, and agricultural efficiency. In Sub-Saharan Africa these drivers lead to agricultural expansion and increasing import dependency in SSP3 and SSP4, while in SSP1 land use stabilizes and net trade is near zero. The

difference in SSP3 and SSP4 compared to SSP1 indicates that major benefits can be gained in Sub-Saharan Africa from improved agricultural efficiency and reduced population growth, as also suggested by Billen et al. (2015). Large yield gaps exist in Sub-Saharan Africa with potential for increased production (Mueller et al., 2012; Neumann et al., 2010; van Ittersum et al., 2013). Utilization of this potential could improve food security and at the same time reduce deforestation, although it is very uncertain if these intensification processes are feasible (van Ittersum et al., 2016).

In contrast to Sub-Saharan Africa, China and the OECD countries show decreases in agricultural land use and increases in net export in nearly all scenarios. This is partly due to continued improvements in agricultural efficiencies, which is in line with historically observed trends. However, it is questioned if crop improvements can continue in the future because biological limits may have been reached (Grassini et al., 2013). If increases in agricultural efficiency stagnate in developing regions, reforestation on former agricultural land and net export of food could be negatively affected. A more detailed representation of the different components responsible for yield increases (Fischer et al., 2014) is required to improve long-term projections.

Indicators of food security discussed in this paper are food availability and food prices (indicative of food accessibility). Although this is a limited set that does not take into account differences between population groups within regions (FAO, 1996; Hasegawa et al., 2015b) it allows to identify hotspots of change in the land-system in a different way from LUC. South/Southeast Asia is the most extreme in SSP3 as food availability remains at the same level (India even experiences a deterioration) whereas it increases in all other regions. Moreover, food prices increase sharply. This implies that SSP3 assumptions such as limited international trade, slow yield improvements, and high population growth result in major threats to food security. Specifically in India, food security is also affected by low land availability which limits the possibility to expand agricultural land. This highlights the necessity for India to invest in yield improvement and to limit population growth. It also indicates the importance of land availability as a model parameter. Estimates of land availability are uncertain and vary substantially (Eitelberg et al., 2015): possible improvements could come from empirical data on soil quality to exclude areas unsuitable for cropland, or spatially explicit costs of conversion related to original land-use and accessibility. Next to that, the effects of land scarcity on agriculture and land-use change is uncertain (Lambin, 2012), and the way in which models handle these effects differs.

The set of scenarios presented in this paper provides high resolution gridded land-use data (Figure 2-10, SI Figure 2-4 to 2-11). In IMAGE, the land-use allocation algorithm for cropland and pasture is based on a regional empirical multiple linear regression model fitting a selection of potential drivers of land-use change to current land use (Section 2.2.1), which is an improvement over the rule-based approach of previous IMAGE versions (Alcamo et al., 1998). This is similar to the CLUMondo model which uses a regional logistic regression

model that combines a large selection of potential drivers with the current distribution of land systems (van Asselen and Verburg, 2013). The disadvantage of this approach is that it is unknown whether future land-use expansion will follow the current land-use distribution patterns, due to changing drivers of LUC. A solution to this issue is fitting the model to historical data of land-use **change**, preferably based on satellite observations. The recently published land cover time series of the ESA climate change initiative provides data from 1992-2015 that might prove suitable for this purpose (Hollmann et al., 2013). Next to land-use expansion, abandonment of agricultural land is an important process in some scenarios (e.g. SSP1). In IMAGE-LandManagement abandonment takes place on locations with the lowest productivity which is consistent with historical land abandonment in Europe, for example in the Mediterranean regions of France. Specific biodiversity policies could however alter this process as productive agricultural land is converted for nature restoration, therefore necessitating a more advanced approach to land abandonment. Lastly, allocation in larger regions comprising countries with very different political and economic characteristics is important. For example, Western Africa covers both Nigeria and the Democratic Republic of the Congo where the former experiences high economic growth rates and the latter continuous to be affected by conflict. Multilevel modelling including national and gridded level variables could improve this (Neumann et al., 2011).

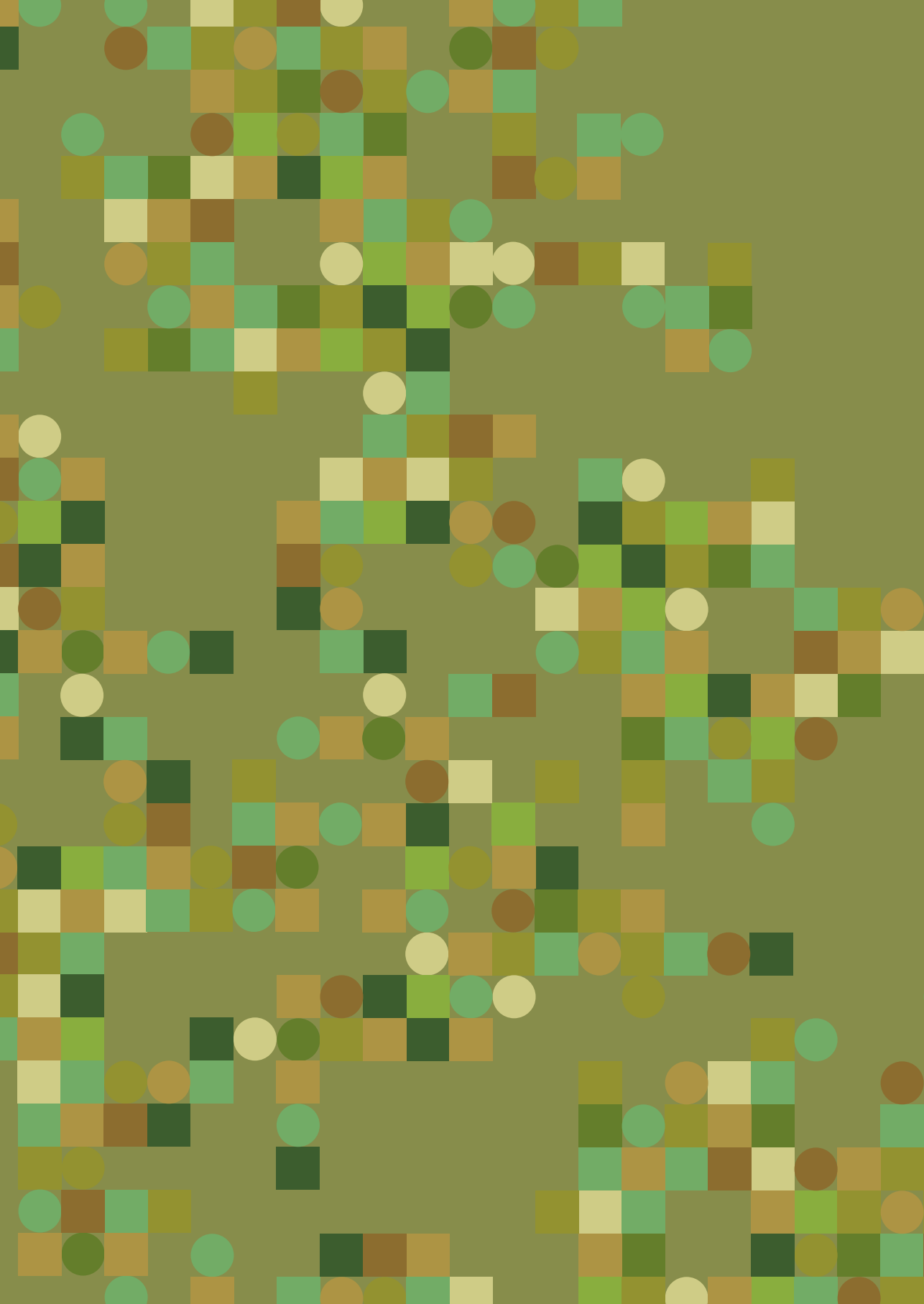
The results of the mitigation scenarios show that land use plays an important role in climate change mitigation. As GHG emissions were not reduced sufficiently in the recent past and are most likely not sufficiently reduced in the near future, and as not all emissions from the energy and the land system can be reduced to zero (e.g. CH₄ and N₂O emissions from agriculture) negative emissions through BECCS and afforestation are needed to achieve ambitious climate targets (van Vuuren et al., 2013). Especially in 1.5°C scenarios very large increases in production of bioenergy are required already by 2050. A trade-off of land-based mitigation might be negative effects on food security: in Sub-Saharan Africa, the implementation of REDD causes a reduction in food availability and a sharp increase in food prices. Another trade-off is caused by large-scale expansion of bioenergy plantations in non-forest ecosystems which probably negatively affects biodiversity (ten Brink et al., 2010). These effects indicate that land-based climate mitigation in developing regions might have severe consequences that are in conflict with the achievement of sustainable development goals (SDG) such as no poverty, zero hunger and life on land (UN, 2015). Therefore, large-scale land-based mitigation will have to be accompanied by additional policies to reduce or avoid trade-offs, especially in the food system. In IMAGE, the effects of land-based mitigation on the land system could be underestimated as bioenergy and afforestation do not compete with agriculture. Other IAM models that participated in the development of the SSP scenarios show a stronger effect of climate policy on land use, which is most noticeable comparing SSP2 and SSP2-2.6 (SI Figure 2-2) in MESSAGE-GLOBIOM (Havlik et al., 2012), REMIND-MagPIE (Popp et al., 2011) and GCAM4 (Wise et al., 2014). It is likely that large-scale land-based mitigation will have consequences for various SDGs. Modelling these interactions and trade-offs is an important field of research for the IAM community.

By design, the SSP scenarios do not include impacts of climate change on the land system. Analyses show that climate change may have a substantial and predominantly negative effect on crop yields on a global scale, especially if CO₂ fertilization is excluded (Asseng et al., 2013; Müller et al., 2015; Rosenzweig et al., 2014). The impact of CO₂ fertilization is uncertain. On a regional scale however, climate change can have a beneficial effect on crop yields, typically on high latitudes. Climate impacts (negative and positive) will have a substantial impact on the agro-economic system (Nelson et al., 2014). The IMAGE 3.0 model framework couples the dynamic vegetation model LPJmL to the simple climate model MAGICC and the agro-economic model MAGNET making it very suitable to assess climate change impacts throughout the land system. For example, if the severe climate change impacts in the case of SSP3 are accounted for (about 4°C warming in 2100), this would lead to reduced yields in South Asia and Sub-Saharan Africa and increasing yields in USA, Europe and Russia. As a consequence, the southern regions will be more dependent on food imports and food security will be worse. In other studies, we have estimated the impacts of climate change on the IMAGE SSP scenarios (van Meijl et al., 2018).

An important purpose of the RCP-SSP scenario framework is “to strengthen cooperation between integrated-assessment modellers, climate modellers, and vulnerability, impact and adaptation researchers” (van Vuuren et al., 2012). Land use is a crucial interface between many of these research fields. The publication of this set of land-use scenarios aims to facilitate this cooperation. Various studies implementing the IMAGE SSP scenario are currently in progress. Biogeochemical and biogeophysical climate change effects in ambitious mitigation scenarios are disentangled using the Community Earth System Model (Hurrell et al., 2013). The scenarios are used to assess impacts on biodiversity with the GLOBIO model (Alkemade et al., 2009), and nitrogen and phosphorus cycles are investigated by implementing the scenarios in the Global Nutrient Model (GNM)(Beusen et al., 2015). Finally, the scenarios will be part of the Land-Use Harmonization (LUH2) project (Hurtt et al., 2011) which will provide input to the Coupled Model Intercomparison Project Phase 6 (CMIP6).

Acknowledgements

The authors would like to thank the researchers of other research groups involved in the SSPs as the development of the IMAGE scenarios greatly benefited from the constructive comments received throughout the process. Liesbeth de Waal and Rineke Oostenrijk are gratefully acknowledged for their technical support. The development of the IMAGE SSPs also benefited from the funding of the European Union’s Seventh Framework Programme FP7/2007-2013 under grant agreement n° 603542 (LUC4C).

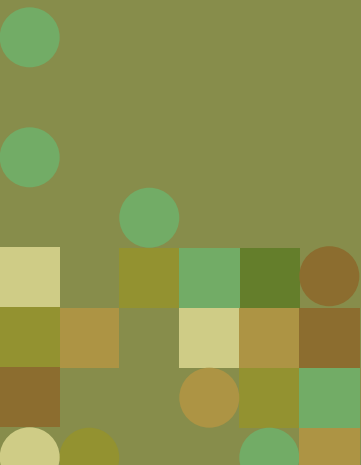


CHAPTER 3

The role of peatland degradation, protection and restoration for climate change mitigation in the SSP scenarios

J.C. Doelman, W. Verhagen, E. Stehfest, D.P. van Vuuren

Provisionally accepted in Environmental Research: Climate



Abstract

Peatlands only cover a small fraction of the global land surface (~3%) but store large amounts of carbon (~600 GtC). Drainage of peatlands for agriculture results in the decomposition of organic matter, leading to greenhouse gas (GHG) emissions. As a result, degraded peatlands are currently responsible for 2-3% of global anthropogenic emissions. Preventing further degradation of peatlands and restoration (i.e. rewetting) are therefore important for climate change mitigation. In this study, we show that land-use change in three SSP scenarios with optimistic, recent trends, and pessimistic assumptions leads to peatland degradation between 2020 and 2100 ranging from -7 to +10 Mha (-23% to +32%), and a continuation or even an increase in annual GHG emissions (-0.1 to +0.4 GtCO₂-eq/year). In default mitigation scenarios without a specific focus on peatlands, peatland degradation is reduced due to synergies with forest protection and afforestation policies. However, this still leaves large amounts of GHG emissions from degraded peatlands unabated, causing a cumulative CO₂ emission from 2020 to 2100 in an SSP2-1.5°C scenario of 73 GtCO₂. In a mitigation scenario with dedicated peatland restoration policy, GHG emissions from degraded peatlands can be reduced to nearly zero without major effects on projected land-use dynamics. This underlines the opportunity of peatland protection and restoration for climate change mitigation and the need to synergistically combine different land-based mitigation measures. Peatland location and extent estimates vary widely in the literature; a sensitivity analysis implementing various spatial estimates shows that especially in tropical regions degraded peatland area and peatland emissions are highly uncertain. The required protection and mitigation efforts are geographically unequally distributed, with large concentrations of peatlands in Russia, Europe, North America and Indonesia (33% of emission reductions are located in Indonesia). This indicates an important role for only a few countries that have the opportunity to protect and restore peatlands coupled with global benefits from climate change mitigation.

3.1. Introduction

Peatlands only cover a small fraction of the global land surface (~3%) but have a disproportionately large contribution to several of the current global sustainability issues (Dargie et al., 2017; Loisel et al., 2014; Page et al., 2011; Scharlemann et al., 2014). They are important for the global climate (Leifeld and Menichetti, 2018), provide unique habitat to species of conservation concern (Posa et al., 2011; Saarimaa et al., 2019) and are important for water and nutrient regulation (Grand-Clement et al., 2013; Loisel et al., 2014; Ritson et al., 2016). Total carbon stocks in peatland soils are estimated at around 600 GtC (2200 GtCO₂) (Yu et al., 2010), which is four to five times the remaining carbon budget to limit global warming to 1.5 degrees (IPCC, 2021). This underscores the importance of keeping carbon stored in peatlands to achieve the goals of the Paris Agreement (UNFCCC, 2015). Recent studies in the Congo basin found peatland areas with formerly unknown large carbon stocks that are at risk of degradation, highlighting that peatlands could play an even larger role in climate change than previously thought (Crezee et al., 2022; Dargie et al., 2017).

Drainage of peatlands for agriculture, forestry or peat extraction results in large emissions of carbon dioxide (CO₂) as well as smaller amounts of other greenhouse gasses (GHGs) such as nitrous oxide (N₂O) and methane (CH₄). Several studies have estimated the contribution of degraded peatlands to GHG emissions. Global estimates currently range between 1.3 Gt CO₂-eq/yr to 1.9 Gt CO₂-eq/yr (Joosten, 2010; Leifeld and Menichetti, 2018), which is 2.3%-3.4% of annual global anthropogenic GHG emissions (56 GtCO₂-eq/year in 2010-2019)(IPCC, 2022). Halting the expansion of peatland drainage would stop the increase of contemporary peatland emissions but would not reduce them because the complete decomposition of peat soils may take centuries. Restoration of high water levels in degraded peatlands could reverse this process, halting the decomposition of organic matter and keeping carbon stored in the soil (Jaenicke et al., 2010; Wilson et al., 2016). This so-called rewetting of peatland even results in sequestration of CO₂ but at the same time leads to higher methane emissions (Abdalla et al., 2016). Compared to peatland degradation, however, rewetting of peatlands has major net climate benefits.

Peatland degradation is tightly linked to agricultural activity, for example, with expansion of palm oil plantations on peatlands in Indonesia (Miettinen et al., 2012) and intensively managed pasture lands on peat soils in the Netherlands (van den Born et al., 2016). Assessing how future changes in agricultural land use may affect peatlands is key to understand how the status of peatlands and their role in climate change may develop in the future. Reducing peatland emissions can also contribute significantly to climate change mitigation (Humpenöder et al., 2020; Leifeld et al., 2019). In this study, we investigate how different land-use scenarios affect peatlands, what the impacts are on GHG emissions, what the role of peatland restoration is in achieving climate change mitigation targets, and how large uncertainties are. To this purpose, we use the IMAGE 3.2 integrated assessment model framework (Stehfest et al., 2014; van Vuuren et al., 2021). Specifically, we assess three different

Shared Socioeconomic Pathway scenarios (SSPs): the optimistic SSP1, the middle-of-the-road SSP2, and the pessimistic SSP3. In addition, we assess how much protection of non-degraded peatlands and restoration of degraded peatlands can contribute to mitigating climate change in deep mitigation pathways under these three different socio-economic futures. Finally, we look into a key uncertainty of peatland emission projections regarding estimates of the location and extent of peatland area that vary considerably in the literature. Compared to existing literature, this study provides a more detailed analysis of peatland degradation under multiple socio-economic futures using baseline as well as mitigation assumptions. Assessments are presented both at the global and the regional scale. In addition, we address model uncertainty by operationalizing these scenarios in a different integrated assessment model and for the first time we quantify the uncertainty arising from varying estimates of peatland extent.

3.2. Methods

3.2.1. The IMAGE 3.2 model framework

The IMAGE 3.2 integrated assessment model framework⁴ is designed to explore future global environmental change due to socio-economic developments and to assess potential response strategies (Stehfest et al., 2014; van Vuuren et al., 2021). It includes the human system with detailed descriptions of the energy and land-use systems, and the natural system with representations of natural vegetation dynamics, the hydrological cycle and the climate system. This study focuses on an application in the land system models of the framework. Land is represented in the IMAGE-LandManagement model at 5 arc-minutes resolution with crop production, livestock systems, bioenergy production, forestry and natural land. Agro-economic trends are determined through coupling to the computable general equilibrium model MAGNET (Woltjer et al., 2014) that uses information on land availability, changes in crop and livestock efficiency and impacts on crop yields of climate change and water shortages from IMAGE to calculate developments in the food system. Projections are made at the level of 26 world regions (SI Figure 3-1). IMAGE uses food system data from MAGNET such as demand for crop and livestock production and trends in intensification or extensification to project gridded land use in the future. Expansion of agricultural land is allocated at the grid-level using empirically based statistical suitability layers derived from ESA-CCI land-use change data (Cengic et al., 2023). Gridded land use and climate change are implemented in the dynamic global vegetation model LPJmL which represents the carbon and hydrological cycles as well as crop growth for rainfed and irrigated agriculture (Müller et al., 2016; Schaphoff et al., 2018b).

4 For more information on the IMAGE model visit the online documentation: <http://models.pbl.nl/image>.

3.2.2. Peatland implementation

A gridded map with fractional coverage of peatland at 5 arc-minutes resolution has been created to include peatland dynamics in the IMAGE model. The map is based on the S-world global soil map (Stoorvogel, 2014), which is a high-resolution soil map (30 arc-seconds) combining data from the Harmonized World Soil Database (Nachtergaele et al., 2012) with multiple other auxiliary data sources. Specifically, all histosols (Folic, Terric, Fibric, Thionic and Gelic Histosols) were classified as peatland, whereas all other soils were assumed not to contain peatlands. This binary classification at 30 arc-seconds is then aggregated to fractions at 5 arc-minutes.

The peatland map is combined with gridded agricultural land use in the IMAGE-LandManagement model. It is assumed that at the 5 arc-minutes level each share of agricultural land use (including 16 food crop types, 5 bioenergy crop types and grazing land) is proportionally located on peatland and non-peatland area present in each grid cell, implying that each agricultural land-use fraction is multiplied by the peatland fraction. The resulting peatland fractions with agricultural land use are assumed to be degraded. All other peatland fractions are assumed to be non-degraded. This is a simplification that may lead to over or underestimation of the degraded peatland fractions. If agriculture on peatland is abandoned during the scenario period (i.e. after the year 2015) it is assumed to be restored (i.e. rewetted). This is an optimistic assumption as restoration can be costly, but in the context of this study we consider it appropriate as the goal is to assess the maximum potential role of peatland restoration for climate change mitigation. We define restoration as halting the decomposition process typically by raising the water table, i.e. this does not imply full hydro-ecological restoration which is more difficult and costly to achieve. Aboveground carbon dynamics for deforestation due to land-use change or forest regrowth after abandonment are calculated using default vegetation dynamics of the LPJmL model. Due to data limitations historical peatland restoration is not included.

The degraded and rewetted peatland fractions are multiplied by land area and annual peatland emissions factors based on the IPCC guidelines (IPCC, 2014a; Wilson et al., 2016). Emission factors for CO₂, CH₄, N₂O, and dissolved organic carbon (DOC, eventually also emitted as CO₂), are specified per biome (boreal, temperate and tropical) based on the IMAGE biome classification and per degraded land-use type (SI Table 3-2 to SI Table 3-5) differentiating between croplands, grasslands and plantations. This results in total anthropogenic emissions from peatland degradation and restoration. Natural peatlands are also sources of GHG emissions, but these are non-anthropogenic and, therefore, not addressed in this study.

3.2.3. Scenario description

Three SSP scenarios are implemented in this study covering a substantial range of possible land-use futures (Doelman et al., 2018; van Vuuren et al., 2021). The core of these scenarios is formed by GDP and population projections (Dellink et al., 2017; KC and Lutz, 2017), which,

together with narrative-based assumptions, shape the scenarios (SI Table 3-1). SSP2 is characterized as a world where historical developments continue, with population growth levelling off slowly, continued economic growth, no major changes to current levels of globalized trade, continued technological development, increases in meat consumption in line with growth in welfare and no major improvements in environmental regulation such as nature protection (O'Neill et al., 2017). SSP1 has a more optimistic outlook where the population starts to decrease by 2050, and people continue to become wealthier but are also more environmentally aware with relatively lower meat consumption and better protection of ecosystems. SSP3 has the most pessimistic outlook. Here, the global population grows strongly to more than 12 billion by the end of the century. Moreover, due to a lack of cooperation, international trade and technology development stagnate, leading to less economic growth and slow improvement of food security. In the scenario, nature protection is unsuccessful, and strong resource demand increases pose major environmental risks.

Table 3-1: Overview of scenarios and their key differences implemented in this study

Scenario name	Radiative forcing in 2100 (W/m ²)	Climate change mitigation policy (energy, industry and land use)	Peatland protection and restoration
SSP1	5.0		
SSP2	6.2		
SSP3	6.7		
SSP1-1.9-D	1.9	X	
SSP2-1.9-D	1.9	X	
SSP3-2.6-D	2.6	X	
SSP1-1.9-P	1.9	X	X
SSP2-1.9-P	1.9	X	X
SSP3-2.6-P	2.6	X	X

The three SSP baseline scenarios (i.e. without climate policy) are combined with ambitious climate mitigation targets to investigate the potential and impacts of climate policies required to achieve stringent targets (Table 3-1). For SSP1 and SSP2, the 1.9 W/m² target is implemented which is in line with the 1.5°C temperature goal. In SSP3, the 2.6 W/m² target is used (in line with 2°C) because the 1.9 W/m² goal is infeasible due to the high challenges to mitigation. In the default setting (denoted by the suffix D) all standard, cost-optimal climate policies are included, such as upscaling of renewables, higher energy efficiencies in the energy use in end-use sectors and production, as well as forest protection, afforestation and non-CO₂ mitigation in the land-use sectors (Doelman et al., 2020, 2018; van Vuuren et al., 2021, 2017b). Peatland protection and restoration are not included in the default scenarios but are added in the peatland scenarios (denoted by the suffix P) to assess the effects of peatland policy on climate change mitigation and land-use dynamics. Peatland protection is implemented as strict protection after 2020 of all grid cells with more than 10% peatland area share. Peatland restoration is implemented as forced abandonment of all agricultural

lands between 2020 and 2030 (linearly) in grid cells with more than 10% peatland area share. These protection and restoration measures are highly ambitious and optimistic. This is in line with the stringent goals of 1.5°C and 2°C, but it is important to note that these are maximal potential estimates of peatland mitigation that do not take feasibility concerns into account.

3.2.4. Sensitivity analysis

Mapping peatlands at the global scale is a difficult task, given differences in how peatlands are defined, and inconsistencies in data availability and quality, resulting in a wide range of estimates for peatland area and carbon stocks (Minasny et al., 2019). In this study, we choose to use the S-world global soil map, which is a reclassification of the HWSO soil map (Stoorvogel et al., 2017), as our default peatland extent estimate. This map has relatively conservative estimates in the tropical regions which are shown to be highly uncertain (Section 3.3). Therefore it is used as default out of a precautionary principle. There are various other approaches available in the literature, including 1) soil map reclassification methods similar to the default approach used in this study (Hiederer and Köchy, 2011), 2) assessments based on inventories (Humpeöder et al., 2020; Tanneberger et al., 2017), 3) expert-based modelling (Gumbricht et al., 2017) and 4) machine-learning algorithms (Melton et al., 2022). In addition to our default map, we select five global spatial-explicit estimates of peatland area that are integrated in the IMAGE model to analyze the related uncertainty and its effect on GHG emissions estimates. These are the meta-studies by 1) Leifeld and Manichetti (2018) and 2) Xu et al. (Xu et al., 2018) that both combine multiple data sources to compile peatland maps; the inventory-based approach by 3) Humpeöder et al. (2020) who downscale inventory data from Joosten (2010) to the grid level; the machine-learning based approach from 4) Melton et al. (2022); and the expert-based model approach by 5) Gumbricht et al. (2017), which is complemented by the default S-world data for the temperate and boreal zones because the data is only available for the tropical zones.

3.3. Results

3.3.1. Land-use dynamics

The SSP scenarios show very different land-use futures under baseline assumptions (Figure 3-1). SSP2 and SSP3 show strong increases in agricultural land of 680 Mha and 1090 Mha (2020-2100 period) due to population growth and increased welfare resulting in growing food demand. SSP1 shows a strong reduction in grazing land (-850 Mha) due to increased welfare coupled with lower demand for meat as well as increased efficiency. Cropland does still increase slightly on the global level (+110 Mha), mainly due to expansion in Sub-Saharan Africa while in other regions such as the USA and China cropland decreases (SI Figure 3-2). Agricultural expansion typically comes at the cost of natural land which decreases strongly in SSP2 and SSP3 (-730 and -1130 Mha, respectively) while it increases in SSP1 (+700 Mha). Built-up area also plays a role with relatively modest increases in all SSPs (+39 to +45 Mha). Land-use change in the baseline scenarios leads to additional peatland degradation in SSP2 and

SSP3 of 7 and 10 Mha, respectively, in the 2020-2100 period (Figure 3-2b). This corresponds to a 21% and 32% increase in degraded peatlands, respectively, compared to 31 Mha degraded peatlands in 2020. The increases are very geographically focused, with 67% of the expansion in SSP2 taking place in only two regions: Indonesia and Rest of South America (Figure 3-2c and SI Figure 3-3). This specifically implies continued conversion and drainage of the tropical peatland forests of Indonesia (Sumatra, Borneo and New Guinea) as well as losses in the Peruvian Amazon and the coastal areas of British Guyana and Surinam (SI Figure 3-4). In SSP1 the global reduction in agricultural land leads to a reduction in degraded peatland of 7 Mha. Especially in the first half of the century in some regions still some non-degraded peatland (i.e. natural) is lost because reductions in agricultural land mainly take place later in the century, resulting in about 9 Mha of restored peatland (rewetted) by 2100.

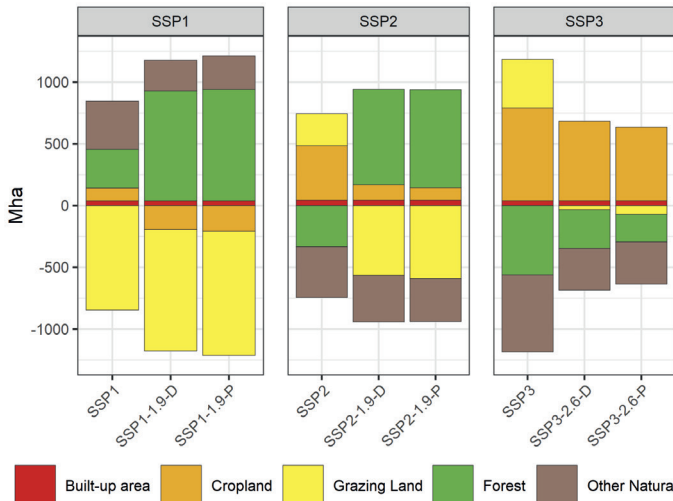


Figure 3-1: Global land-use change for five main land-use categories in the 2020-2100 period.

In the default mitigation scenarios aiming for a maximum warming of 1.5°C or 2°C, land-based mitigation policies are implemented leading to major changes in land-use dynamics. In all scenarios forest protection is implemented to reduce deforestation emissions. These measures limit increases in agricultural land as expansion into forested areas is prohibited. Additionally, cropland area is dedicated to the production of crops or biomass for bioenergy in order to replace fossil fuels as well as to capture and store carbon (BECCS). In SSP1 and SSP2, also large-scale reforestation is implemented resulting in reductions of agricultural land use. In SSP3 no afforestation takes place as land-based mitigation is assumed to be less successful. These policies result in strong increases in forest area in SSP1 and SSP2 (+890 and +770 Mha, respectively, in 2020-2100), and reduced deforestation in SSP3 (-250 Mha) mostly from reductions in grazing land (Figure 3-1). Although not specifically targeted in the default mitigation scenarios, forest protection and afforestation partly overlap with peatland

resulting in restoration of peatlands. Especially in SSP1-1.9-D and SSP2-1.9-D, this results in substantial restoration of 16 and 14 Mha of peatland, respectively (Figure 3-2b). Again, the dynamics are very unevenly spread between world regions, with most of the restoration taking place in regions with historically large degraded peatland areas, notably Russia+ (25%), Indonesia+ (15%), USA (12%) and Western Europe (12%) (Figure 3-2c). Canada on the other hand observes a small increase in degraded peatland due to expansion of bioenergy. In SSP3-2.6-D a modest decrease in degraded peatland is found (1 Mha). In some regions in SSP2-1.9-D still a reduction in non-degraded peatland area occurs (Figure 3-2c), even though there also is a substantial increase in peatland restoration. This notably occurs in Western Europe and USA due to changes in agricultural land distribution (e.g. due to productivity changes from climate change) and highlights the importance of peatland protection which is not included in SSP2-1.9-D. Despite the co-benefits between some mitigation policies and peatland restoration, still a large area of degraded peatland remains in the default mitigation scenarios by the end of the century, ranging from 18 Mha in SSP1-1.9-D to 40 Mha in SSP3-2.6-D.

To fully make use of the mitigation potential of peatland, we assume additional policy in the mitigation scenarios to protect and restore peatlands. Consequently, nearly all degraded peatlands are restored in the 2020-2030 period (30-31 Mha) requiring small additional reductions in cropland and grazing land in the peatland mitigation scenarios compared to the default mitigation scenarios. Logically, most of the changes take place in the regions with historically large degraded peatland areas (Indonesia, Russia, Ukraine, Europe and North America). Additionally, also regions where expansion of agriculture on peatland occurred see changes in land-use distribution to non-peatland locations. Most notably in the Rest South America region, agricultural expansion is located to non-peatland areas and also slightly more agricultural expansion takes place in this region because of trade effects from peatland protection and restoration in other world regions. The changes to global land-use dynamics due to peatland policy are modest, which is also reflected by small effects on global food security indicators: Food prices in 2100 increase by 0.3%-5.1% and food demand decreases by 0.8%-1.3% in the peatland mitigation scenarios compared to the default mitigation scenarios (SI Figure 3-10 and SI Figure 3-11). However, regional differences are stark, with most notably much stronger increases in Indonesia where prices increase by 44%-48% and food demand decreases by 4.6%-5.2% (SI Figure 3-12 and SI Figure 3-13).

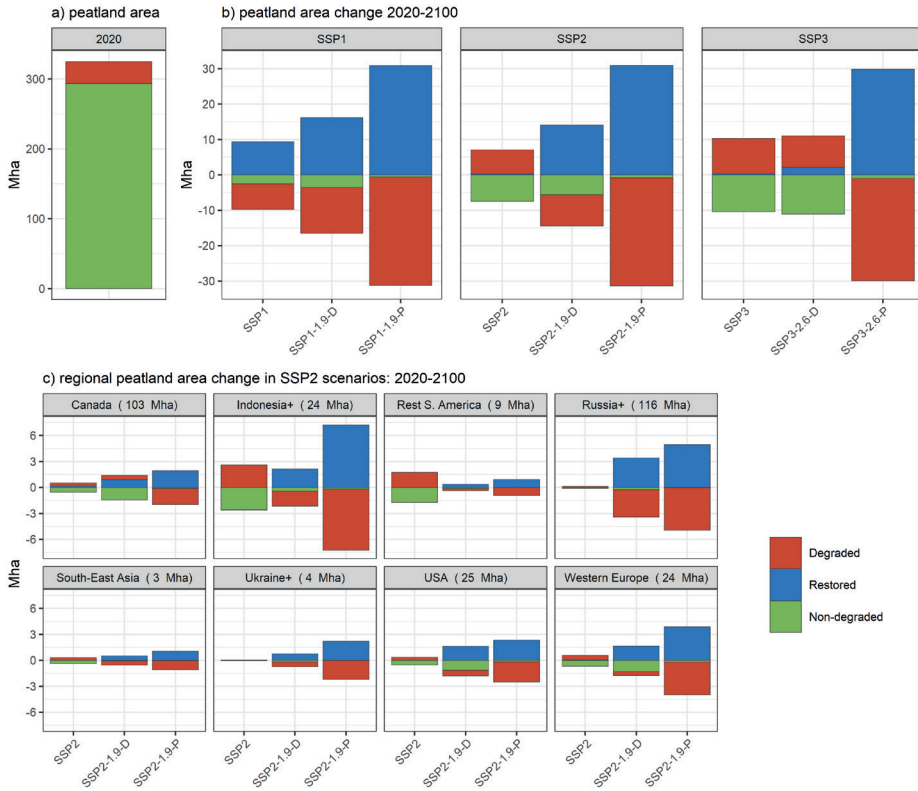


Figure 3-2: a) Peatland area in 2020, b) changes in global peatland area in all scenarios in the 2020-2100 period, c) changes in peatland area in the SSP2 scenarios in 8 selected regions representing 80% of historical degraded peatland area and 88% of peatland conversion in the SSP2 baseline scenario. Between brackets the total peatland area in each region is shown.

3.3.2. GHG emissions dynamics

The SSP scenarios show a substantial range in GHG emissions from the agriculture, forestry and other land use (AFOLU) sector by the end of the century. With strong increases in SSP3 from 10.8 GtCO₂-eq/yr in 2020 up to 16.9 GtCO₂-eq/yr in 2100 (Figure 3-3a)(CO₂-equivalents of CH₄ and N₂O are calculated using 100-year time horizon global warming potentials (GWP100)). In SSP1 on the other hand, emissions are reduced to 6.0 GtCO₂-eq/yr by 2100. Deforestation continues in the baseline SSP2 and SSP3 scenarios throughout the century resulting in substantial AFOLU CO₂ emissions, while in SSP1 a small negative net CO₂ flux occurs due to abandonment of agricultural land. Non-CO₂ emissions in SSP2 and SSP3 show substantial increases due to growth of the agricultural sector, while in SSP1 a modest decrease takes place. Emissions from peatland form 10% of annual AFOLU emissions in 2020 (1.1 GtCO₂-eq/yr), which in turn is comprised of 90% CO₂ emissions as almost all emissions result from degrading peatlands. The remaining share is predominantly N₂O (Figure 3-3b). By the end of the century emissions from peatlands have increased substantially in SSP2 (1.4 GtCO₂-eq/

yr) and SSP3 (1.6 GtCO₂-eq/yr) while a modest decrease occurs in SSP1 (1.0 GtCO₂-eq/yr). The relative importance has changed however, with peatlands representing 15% of total remaining positive AFOLU emissions in SSP1 compared to 9% of total AFOLU emissions in SSP3. The emissions are very unevenly distributed, with 30% of 2020 emissions originating from Indonesia which increases further to 33% in SSP2 by 2100 (Figure 3-3c). The boreal and temperate regions also have substantial emission shares, with 12% and 10% from Russia and Western Europe, respectively, but these are not projected to increase much when recent trends are assumed to continue (SSP2). The strongest relative increase takes place in the Rest South America region, with 185% increase in emissions.

The default mitigation scenarios show strong decreases in AFOLU emissions: In all scenarios non-CO₂ emissions are reduced by 39% to 50% compared to baseline levels, due to technical mitigation measures as well as reductions in food consumption. CO₂ emissions go strongly negative in SSP1-1.9-D and SSP2-1.9-D as afforestation is applied at scale. In SSP3-2.6-D CO₂ emissions are reduced by 47%, but remain positive as afforestation is assumed to be infeasible in line with the scenario narrative. Peatland emissions decrease slightly in SSP3-2.6-D (-6% compared to baseline in 2100) as not all peatland degradation is prevented by forest protection measures. In fact in Russia an increase in peatland degradation occurs as cropland expansion is prevented in the tropics due to forest protection measures leading to displacement of crop production to Russia, among others (SI Figure 3-2). On the other hand, in SSP2-1.9-D a strong reduction in peatland emissions takes place (-39%) as agricultural land diminishes compared to the baseline due to forest protection and afforestation resulting in restoration of peatlands. The emission reduction in SSP1-1.9-D is relatively smaller (-24%) than in SSP2-1.9-D because already in the SSP1 baseline a substantial reduction in agricultural land occurs resulting in less relative improvement in the mitigation scenario.

Dedicated peatland restoration policies result in major reductions in peatland emissions in all peatland scenarios (Figure 3-3b). CO₂ emissions and N₂O emissions go down quickly, and even modest CO₂ sequestration is assumed in boreal regions as reported by Wilson et al. (2016) (SI Table 3-2 to SI Table 3-5). Methane emissions increase from the large area of restored peatlands, up to 78-81 MtCO₂-eq/yr by 2100. However, these emissions are negligible compared to CO₂ and N₂O emissions from degrading peatlands. Mirroring the fact that the bulk of peatlands emissions comes from certain regions, also the emissions reductions are focused in a few geographic locations, most notably again Indonesia, but also Russia and Western Europe. Even though Indonesia only has slightly more restored peatland area than Russia and Western Europe, it does have a much larger share of emissions reduction because peatland emissions per area in the tropics are much higher than in the temperate and boreal zones.

Comparing cumulative CO₂ emissions from peatland in the 2020-2100 period to cumulative emissions in the energy and industry sector and the AFOLU sector emphasizes the importance of including peatland protection and restoration in climate change mitigation policy (Table

3-2). In the default mitigation scenarios, peatland CO₂ emissions make up large shares of the CO₂ budgets as projected in the scenarios: 21% in the SSP3-2.6-D scenario, 25% in the SSP1-1.9-D scenario and 49% of the SSP2-1.9-D scenario. Including peatland policies greatly reduces these shares to 2%-3%. As the effect of these policies on land-use dynamics and, therefore, on the food and agricultural system are fairly limited at the global scale, including peatland protection and restoration is a critical component of a policy package making stringent mitigation targets feasible without major negative impacts on food security. However, the possibility, or responsibility, to implement these policies is very unequally divided between world regions, highlighting a key challenge.

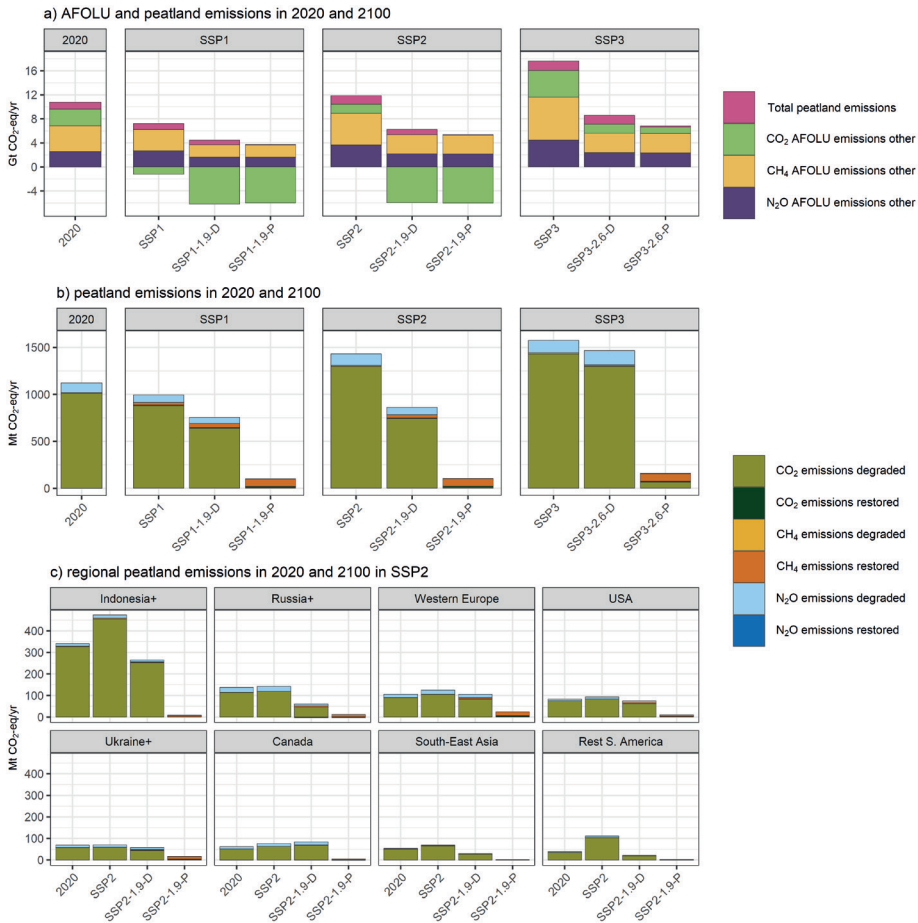


Figure 3-3: a) Global GHG emissions from the AFOLU sector (excluding peatland) for CO₂, N₂O and CH₄ and total GHG emissions from peatlands, b) global peatland GHG emissions distinguished by source from degraded or rewetted peatlands and by GHG and c) selected regional GHG emissions distinguished by source from degraded or rewetted peatlands and by GHG. Emissions are defined in terms of CO₂-equivalents calculated using 100-year time horizon global warming potentials (GWP100).

Table 3-2: Cumulative CO₂ emissions from energy and industry, AFOLU, peat degradation and total in the 2020-2100 period.

Cumulative CO ₂ emissions (GtCO ₂) in the 2020-2100 period	Energy and industry emissions	AFOLU emissions (excl. peatlands)	Peatland emissions	Total
SSP1	2767	50	78	2895
SSP1-1.9-D	486	-285	65	266
SSP1-1.9-P	486	-291	6	201
SSP2	3904	308	96	4309
SSP2-1.9-D	259	-183	73	149
SSP2-1.9-P	259	-193	6	73
SSP3	4323	452	103	4879
SSP3-2.6-D	114	257	96	467
SSP3-2.6-P	114	212	10	336

3.3.3. Sensitivity to varying peatland estimates

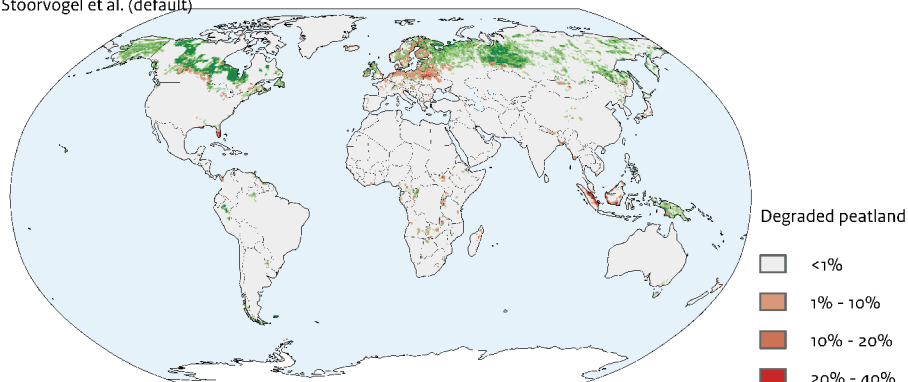
Spatial-explicit estimates of peatland area extent vary greatly in the literature. The integration of five additional estimates of peatland area in IMAGE provides the opportunity to assess the sensitivity of our degraded peatland area and emissions projections to these estimates. Table 3-3 shows the total peatland area, degraded peatland area in 2020 and 2100, and cumulative peatland CO₂ emissions from this sensitivity at the global scale and disaggregated to tropical and temperate & boreal regions. Degraded peatland areas vary widely, from 31 to 96 Mha in 2020 and from 38 to 123 Mha in 2100. This is also reflected in the cumulative CO₂ emissions that range from 87 GtCO₂ to 344 GtCO₂. The approach based on Stoorvogel et al. (2017), which is the default method in this study, yields results that are in line with other studies. However, the sensitivity analysis shows various higher estimates of degraded peatlands and GHG emissions indicating that we may underestimate peatland degradation in some locations. The highest estimate is found using the map from Leifeld and Manichetti (2018). As this map is considered an 'upper estimate of the possible global peatland area extent', it is to be expected that this is the highest estimate both in degraded peatland area and GHG emissions. The largest variation in the projections is found in the tropical regions, most notably in South America and Sub-Saharan Africa: emissions in the Rest South America region range from 34 MtCO₂-eq/yr to 1.5 GtCO₂-eq/yr in 2100, and emissions in Western Africa range from 25 to 800 MtCO₂-eq/yr. This is mainly due to the higher estimates of current peatland extent in the tropics in Gumbricht et al (2017) and Leifeld and Manichetti (2018) highlighting the uncertainty of peatland extent in the tropical regions of the world (Table 3-3). The importance of tropical peatlands in South America and Sub-Saharan Africa is in line with Gumbricht et al. (2017) that highlighted the underestimation of peatland in the Amazon basin, as well as with recent publications on the extent of peatland stocks in the Congo basin (Crezee et al., 2022; Dargie et al., 2017)(Figure 3-4).

Table 3-3: Peatland area estimates in 2020 and cumulative CO₂ emission estimates for the 2020-2100 period in the SSP2 baseline scenario using different peatland area maps. Results are shown at the global level and disaggregated in predominantly tropical regions and temperate and boreal regions.

Global	Total peatland area in 2020 (Mha)	Degraded peatland area in 2020 (Mha)	Degraded peatland area in 2100 (Mha)	Cumulative CO2 emissions in the 2020-2100 period (GtCO2)
Default (Stoorvogel et al.)	325	31	38	96
Gumbricht et al.	440	66	86	241
Humpenöder et al.	407	35	43	116
Leifeld and Manichetti	920	96	123	344
Melton et al.	386	54	69	193
Xu et al.	440	32	39	87
Tropical regions				
Default (Stoorvogel et al.)	46	13	18	57
Gumbricht et al.	150	41	59	188
Humpenöder et al.	54	17	23	75
Leifeld and Manichetti	197	66	91	279
Melton et al.	105	31	46	146
Xu et al.	42	5	11	33
Temperate&boreal regions				
Default (Stoorvogel et al.)	279	18	20	39
Gumbricht et al.	289	25	27	53
Humpenöder et al.	354	18	20	41
Leifeld and Manichetti	724	30	32	65
Melton et al.	281	22	23	47
Xu et al.	398	27	28	53

Peatland extent in SSP2 in 2100 - natural and degraded

Stoorvogel et al. (default)



Gumbrecht et al.

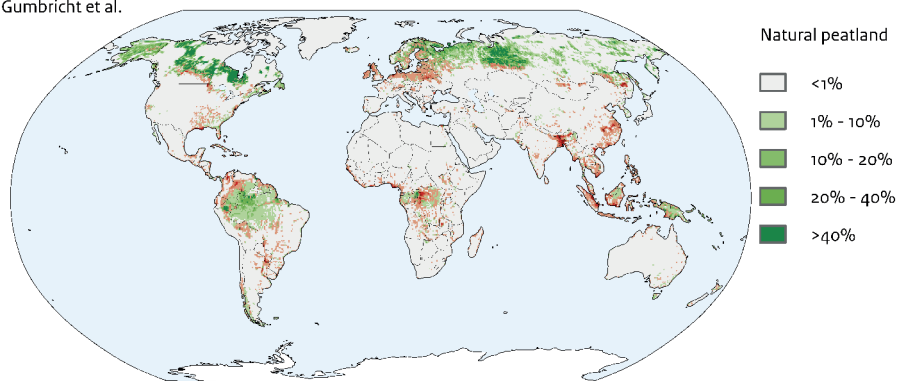


Figure 3-4: Spatial-explicit degraded and non-degraded peatland areas in 2100 in SSP2 for the default peatland map used in this study (Stoorvogel et al., 2017) and one sensitivity peatland map based on Gumbrecht et al. (2017) (for other sensitivity maps see SI Figure 3-8 and SI Figure 3-9). Data is aggregated to the percentage peatland area of total land area per half degree grid cell. When grid cells have both degraded and natural peatlands only the degraded percentage is shown.

3.4. Discussion

Here we show the important role that peatland protection and restoration plays in global climate mitigation. Various other studies have investigated the role of peatland degradation in climate change. A comparison with these other studies shows that our estimates are on the lower end of the range in terms of degraded peatland area and GHG emissions in the historical period. For total degraded peatland area on the global scale we estimate 31 Mha in 2020, where other studies report 43 Mha in 2008 (Joosten, 2010), and 51 Mha (Leifeld and Menichetti, 2018) and 46 Mha in 2015 (Humpenöder et al., 2020). For GHG emissions

we report 1.1 GtCO₂-eq/yr, where Leifeld and Menichetti (2018) report 1.9 GtCO₂-eq/yr and Humpenöder et al. (2020) 1.5 GtCO₂-eq/yr. Joosten (2010) only reports CO₂ emissions of 1.3 GtCO₂/yr, which is slightly higher than the 1.0 GtCO₂/yr found here. A key difference is the fact that in our study only degradation due to agriculture is taken into account while peatland degradation is also caused by forestry or peat extraction, although agriculture is estimated to be responsible for 87% of degrading peatland emissions and therefore the largest source (Joosten, 2010). Also, a relatively conservative peatland extent map has been implemented, as shown in the sensitivity analysis, where degraded peatland areas are shown to range between 31 and 96 Mha in 2020 depending on the map used. Nonetheless, it is found that peatland degradation plays a key role in climate change and climate change mitigation which confirms the findings from other studies.

The projections of peatland degradation presented in this study range between -7 to +10 Mha from 2020 to 2100 under baseline conditions on the global scale. The default mitigation scenarios show decreases between -1 to -16 Mha, while in the peatland mitigation scenarios by assumption nearly all peatland is restored (30-31 Mha). Leifeld et al. (2019) made a projection of future peatland degradation based on recent historical conversion rates resulting in the loss of 11 Mha between 2015 and 2100. Humpenöder et al (2020) report peatland degradation of 10 Mha between 2015 and 2100 assessed with the MAgPIE model in an SSP2 mitigation scenario aiming for 2°C (RCP 2.6). Both studies find conversion rates up to the end of the century similar to the pessimistic baseline estimate reported here (SSP3). A notable difference with Humpenöder et al (2020) is that their SSP2 mitigation scenario shows strong conversion of peatlands mainly due to large-scale expansion of agriculture for bioenergy production, while in this study land-based mitigation in fact results in lower peatland degradation due to reduced forest conversion and afforestation. This illustrates how different implementations or assumptions on land-based mitigation will result in very different estimates of peatland conversion without dedicated peatland policies. All studies concur however that full restoration and rewetting of peatlands is essential to optimally use the climate change mitigation potential of peatlands.

We show that on the global scale, peatland policies cause modest changes in land-use change dynamics and on food security. However, locally, impacts can be much larger. This is reflected by food security effects in Indonesia that are much stronger compared to other regions in our scenario results. The assumption that all agricultural land on peatlands is fully abandoned would have major impacts on the livelihoods of farmers in those locations. To address these impacts, follow-up research should include management options to limit decomposition of peat soils but also continue agricultural production. One option is paludiculture which is proposed as a farming practice where water levels are kept at near-surface to preserve peat while still using the land for agriculture using adapted management techniques (UNEP, 2022).

A key uncertainty in the methodology concerns the implementation of constant emission factors as adopted from the IPCC (2014) and Wilson et al. (2016). Emission factors may

vary markedly depending on water table depths that can be different due to management regimes. Shallow peat deposits may be fully oxidized even after a few years resulting in much lower emissions factors than during the initial degradation phase (Hooijer et al., 2012). As the analysis presented in this study is not constrained by the depth of peat deposits this implies we might overestimate emissions. Cross-checking showed that cumulative gridded emissions exceed gridded soil carbon stocks of S-world (Stoorvogel et al., 2017) by 15%. However this stock estimate excludes carbon stocks in peatland soils deeper than 1 meter, which are common but not reliably mapped at the global scale. This indicates that full oxidization of peatland soils most likely will not constrain peatland emissions substantially before the end of the century. Next to uncertainty of degraded peatland emission factors, also the factors for peatland restoration are highly uncertain. This is most notably in the tropics where 'rewetting as a management practice is still in its infancy' and emission factors are based on surrogate data (Wilson et al., 2016). Climate change impacts on peatlands emissions are excluded even though higher temperatures and reduced rainfall could amplify the decomposition process (Leng et al., 2019), and also emissions of peat fires are not considered. Although peat fires can cause large emissions peaks they are typically temporary whereas constant emissions from drainage are, over a longer time horizon, the larger source of GHG emissions (Page and Hooijer, 2016). Despite the fact that constant emission factors are a simplification, including emissions from peatland degradation is key to include in scenarios assessing the effects of land use on climate change. More dynamics related to the depth of peatland soils, peat fires and climate change impacts are beyond the scope of this study but are important directions of future research.

Another source of uncertainty regards spatial-explicit land-use allocation: As peatlands are typically concentrated in certain geographic locations, allocation of agricultural expansion in one location or another within a region can greatly affect GHG emissions. In this study only the IMAGE model is applied, but differences in land-use allocation between land-use models have been shown to be substantial (Prestele et al., 2016). Overlaying peatland maps with land-use projections from different land-use models could provide a quantification of this uncertainty, but is beyond the scope of this study.

As highlighted here, the mitigation challenge of restoring peatlands is unequally distributed between world regions, with one third of projected GHG emission reductions located in Indonesia. Moreover, the sensitivity analysis showed that tropical peatland conversion may be underestimated in our study indicating risks of peatland degradation in the Amazon and Congo basins. For peatland degradation and restoration, similar to preventing deforestation and the potential of afforestation, the largest risk of impacts on climate change as well as the largest potential for climate change mitigation is located in the tropical regions of the world (Doelman et al., 2020). At the same time these are also among the poorer regions of the world that from an equity perspective should not have to carry most of the burden of preventing dangerous climate change (Höhne et al., 2014; van den Berg et al., 2020) underlining a key challenge of preventing peatland degradation and peatland restoration. On the other

hand, large areas of potential peatland restoration are also located in rich countries, most notably Western Europe and the USA, that have lower GHG emissions per hectare but still considerable potential to prevent continued climate change impacts of peatland degradation.

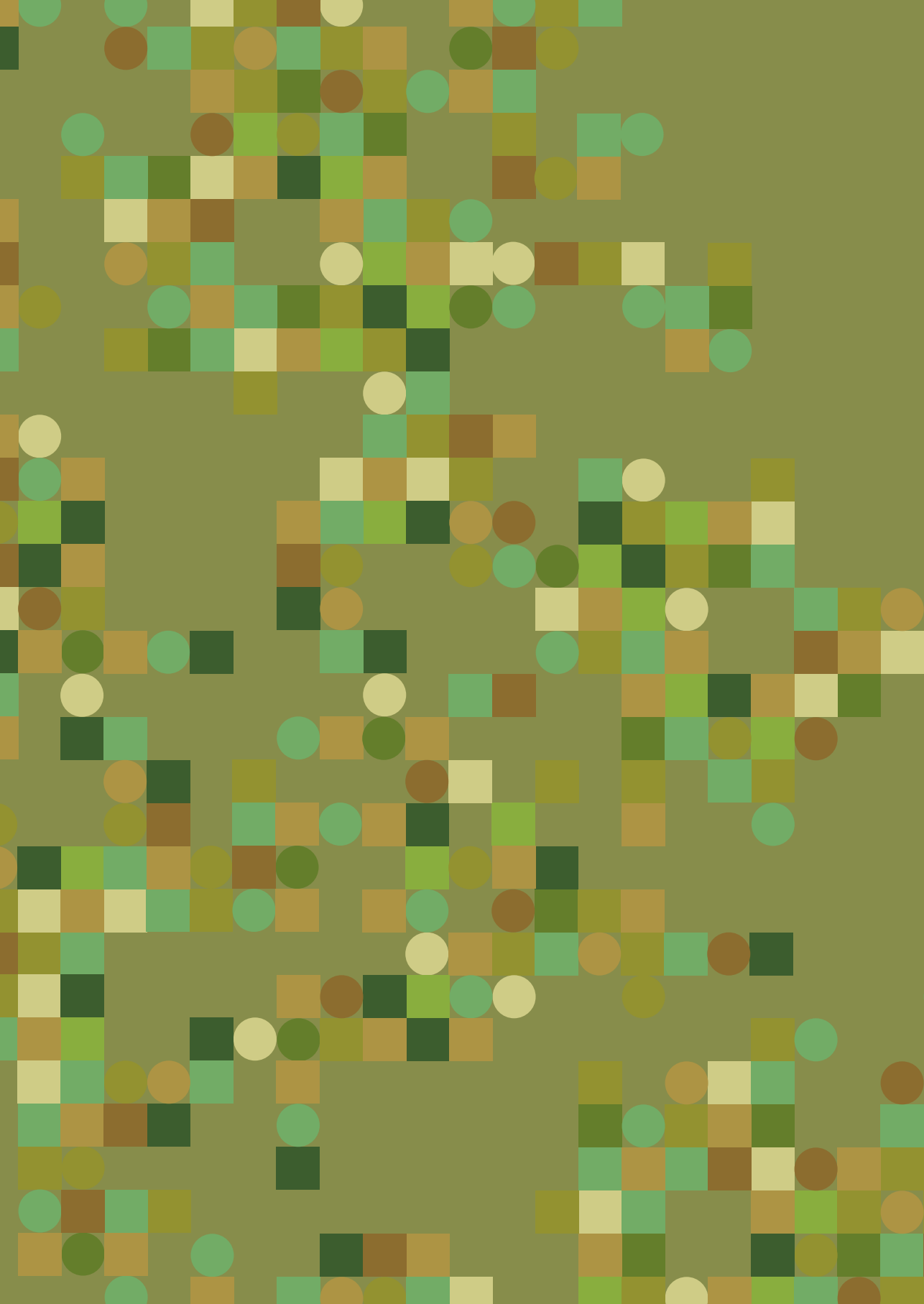
3.5. Conclusions

In this article, we presented an analysis of peatland degradation and restoration in three SSP scenarios under baseline assumptions and with climate change mitigation targets both excluding and including specific peatland protection and restoration measures. It is shown that future peatland degradation may vary substantially depending on socio-economic assumptions, with a moderate reduction in degraded peatlands in SSP1 (-7 Mha) and substantial expansion of peatland degradation in SSP3 (+10 Mha). Default mitigation scenarios (without specific peatland policies) substantially reduce peatland emissions due to synergies with forest protection and afforestation policies, but still leave substantial amounts of GHG emissions from degraded peatlands unabated, that amount to 65 to 96 GtCO₂ cumulatively. If dedicated peatland protection and restoration policies are implemented to prevent further peatland degradation and to restore currently degraded peatlands, these emissions are reduced to less than 10 GtCO₂ cumulatively making ambitious mitigation targets better feasible without major changes required to land-use dynamics. This emphasizes the need to synergistically combine land-based mitigation measures such as forest and peatland protection and peatland restoration and afforestation.

The responsibility to protect and restore peatlands is unequally distributed between regions, with one-third of required GHG emissions reductions located in one country (Indonesia) where prevention of additional peatland degradation is essential as well as restoration of already degraded peatlands. A large potential for peatland restoration is found in temperate and boreal regions such as Europe, North America and Russia, while these regions do not show high risk for additional peatland degradation. In contrast, in South America peatland degradation is projected to expand substantially while its current extent of degraded peatlands is fairly limited. A sensitivity analysis shows that our study may underestimate future peatland degradation in tropical regions, notably the Amazon and Congo basin

Data availability statement

The data presented in this study are deposited in the following Zenodo database: <https://doi.org/10.5281/zenodo.7681342>.

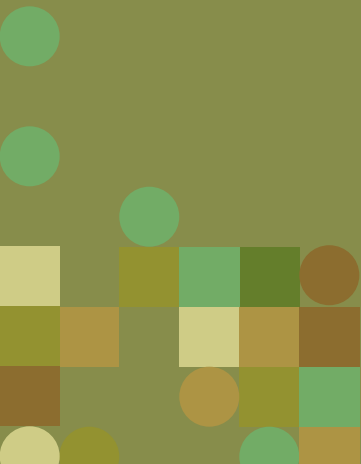


CHAPTER 4

Afforestation for climate change mitigation: potentials, risks and trade-offs

Jonathan C. Doelman, Elke Stehfest, Detlef P. van Vuuren, Andrzej Tabeau, Andries F. Hof, Maarten C. Braakhekke, David E.H.J. Gernaat, Maarten van den Berg, Willem-Jan van Zeist, Vassilis Daoglou, Hans van Meijl, Paul Lucas

"Afforestation for climate change mitigation: potentials, risks and trade-offs"
Global Change Biology 26 (2020): 1576-1591



Abstract

Afforestation is considered a cost-effective and readily available climate change mitigation option. In recent studies afforestation is presented as a major solution to limit climate change. However, estimates of afforestation potential vary widely. Moreover, the risks in global mitigation policy and the negative trade-offs with food security are often not considered. Here, we present a new approach to assess the economic potential of afforestation with the IMAGE 3.0 integrated assessment model framework. In addition, we discuss the role of afforestation in mitigation pathways and the effects of afforestation on the food system under increasingly ambitious climate targets. We show that afforestation has a mitigation potential of 4.9 GtCO₂/yr at 200 US\$/tCO₂ in 2050 leading to large-scale application in an SSP2 scenario aiming for 2°C (410 GtCO₂ cumulative up to 2100). Afforestation reduces the overall costs of mitigation policy. However, it may lead to lower mitigation ambition and lock-in situations in other sectors. Moreover, it bears risks to implementation and permanence as the negative emissions are increasingly located in regions with high investment risks and weak governance, for example in Sub-Saharan Africa. Afforestation also requires large amounts of land (up to 1100 Mha) leading to large reductions in agricultural land. The increased competition for land could lead to higher food prices and an increased population at risk of hunger. Our results confirm that afforestation has substantial potential for mitigation. At the same time, we highlight that major risks and trade-offs are involved. Pathways aiming to limit climate change to 2°C or even 1.5°C need to minimize these risks and trade-offs in order to achieve mitigation sustainably.

4.1. Introduction

Ambitious climate change mitigation scenarios aiming to limit global warming to 2°C or less require very rapid reductions in greenhouse gas (GHG) emissions (Clarke et al., 2014; van Vuuren et al., 2013). Even if stringent policies are adopted, it is likely that negative CO₂ emissions will become indispensable to achieve the Paris Agreement climate goal as shown in many mitigation scenario studies (Rogelj et al., 2018; van Vuuren et al., 2018, 2017a). The need for such negative emissions highlights the role of land use in the context of mitigation. While emissions from agriculture, forestry and other land use (AFOLU) are responsible for around 24% of anthropogenic GHG emissions in 2010 (Smith, 2013), land use also plays a critical role in two key negative emission options. First, through the production of bioenergy in combination with carbon capture and storage (BECCS) (Azar et al., 2010). Second, through the expansion of forest area (afforestation) increasing the storage of CO₂ in terrestrial vegetation (Canadell and Raupach, 2008). This study focuses on the role of afforestation in climate change mitigation, where we define afforestation to include reforestation as well as afforestation both of which are defined by the IPCC as the establishment of trees on non-treed land (IPCC, 2000b).

The economic potential of afforestation for climate change mitigation has been assessed before using dedicated forestry models and integrated assessment models (IAMs) (Benítez et al., 2007; Calvin et al., 2014; Humpenöder et al., 2014; Kindermann et al., 2008; Sathaye et al., 2006; Sohngen and Sedjo, 2006; Strengers et al., 2007). Estimates vary widely depending on model characteristics and scenario assumptions, with cumulative sequestration until the year 2100 ranging from 176 GtCO₂ using 231 Mha of land at \$220/tCO₂ (Sathaye et al., 2006) to 700 GtCO₂ using 2800 Mha of land at \$1165/tCO₂ (Humpenöder et al., 2014). Other studies use more data-driven approaches, for example Busch et al. (2019) who use data on agricultural prices and data on forest conversion from satellites to estimate a potential of 15.1 GtCO₂ in 2050 at \$50/tCO₂. Most studies find that already at low CO₂ prices (<\$50/tCO₂) afforestation is economically feasible. However, the wide range in results indicates it is very uncertain at what scale and at what costs afforestation is feasible.

Recent studies by Griscom et al. (2017), Lewis et al. (2019) and Bastin et al. (2019) that looked into the biophysical potential of afforestation using data-driven approaches received a lot of attention. They find high potentials: Griscom et al. (2017) present a sequestration rate of 10.3 GtCO₂/yr using 678 Mha by 2030, Lewis et al. (2019) find 154 GtCO₂ on 350 Mha over a time period of 70 years, and Bastin et al. (2019) show a potential of 752 GtCO₂ using 900 Mha without specifying a time period. These studies state that afforestation is a major solution to climate change, however they do not assess costs of afforestation or how it compares to other mitigation options. Moreover, they assume that afforestation – despite its large extent – does not occur on agricultural areas and thus does not affect food security. This highlights a fundamental divide in afforestation studies concerning the areas assumed to be available for afforestation.

Estimates in the literature show that the largest share of afforestation potential lies in tropical regions (Benítez et al., 2007; Griscom et al., 2017; Kreidenweis et al., 2016). The tropical regions are dominated by developing countries with high investment risks and weak governance implying substantial risk to the success of mitigation policies (Iyer et al., 2015). Despite these risks, afforestation is a negative-emission technology that plays a crucial role in many existing scenarios aiming for 2°C or 1.5°C (Riahi et al., 2017; Rogelj et al., 2018). Calvin et al. (2014) show for one stylized scenario that large-scale afforestation reduces cumulative mitigation policy costs but also diminishes mitigation efforts in energy and industry. Otherwise, the policy implications and risks of afforestation in mitigation pathways received little attention.

Large-scale afforestation requires land that is most likely also needed to provide other land-based services such as food production. As a consequence, food security may be affected. Food security is defined by the FAO by four dimensions: availability (i.e. sufficient quantities of food), access (i.e. adequate resources to obtain food), utilization (i.e. nutritious and safe diets) and stability (i.e. the temporal dimension of the other three dimensions)(FAO, 2008). When considering a role for afforestation in climate change mitigation, it is crucial to take the trade-off with food security into account. A number of studies have assessed the food security effects of land-based mitigation including bioenergy production, taxing of agricultural emissions and in some cases afforestation (Frank et al., 2017; Hasegawa et al., 2018, 2015a; van Meijl et al., 2018). These studies indicate that land-based mitigation can put severe pressure on food security, however the extent to which this can be ascribed to afforestation remains unclear. Kreidenweis et al. (2016) do show that large-scale afforestation can lead to a fourfold increase in global food prices, an indicator of access to food. However, the effect on other dimensions of food security is not discussed. Explicitly addressing food security risks is key if afforestation is considered in mitigation strategies.

Here we assess the global economic potential of afforestation for climate change mitigation in increasingly ambitious mitigation scenarios following the SSP-RCP scenario framework (van Vuuren et al., 2012) using the IMAGE 3.0 model framework (Stehfest et al., 2014). We present regional marginal abatement cost (MAC) curves that are based on grid-level forest growth potentials from the LPJmL model, region-specific estimates of afforestation costs, cost effects of land scarcity and risk-adjusted investment decisions. Our approach provides a new estimate of afforestation potential to the literature with high geographic detail. The presented approach is coupled with the climate policy model FAIR-SimCAP (den Elzen et al., 2008) and the energy simulation model TIMER (van Vuuren, 2007). This integration makes it possible to compare afforestation to a large number of other climate change mitigation options in the energy, industry and agricultural sectors, and is used to analyze how and to what extent afforestation changes mitigation pathways. Next to that, the approach is coupled to the agro-economic model MAGNET (Woltjer et al., 2014) and the health model GISMO (Lucas et al., 2019). This is used to provide a detailed analysis of the potential effects of afforestation on food security, which is assessed along two dimensions of the FAO definition

of food security (FAO, 2008): For access to food we present the indicator food price, and for availability of food we assess food availability per capita and the number of people at risk of hunger. Compared to the existing literature our study focuses on the isolated effects of afforestation on mitigation pathways and food security. In this way we provide a detailed assessment of the risks and trade-offs of this mitigation strategy, which is an important component in many scenarios aiming to prevent dangerous climate change.

In Section 4.2 a detailed description of the methodology to model afforestation and how the approach is integrated in the IMAGE framework is provided, followed by an overview of the implemented scenarios. Section 4.3 4.2 presents the mitigation potential of afforestation, analyses the emission trajectories in the mitigation scenarios, and shows resulting land-use dynamics and food security effects. Where possible, results are presented for 10 aggregated regions (see SI Table 4-1: IMAGE regions, aggregated regions used in the paper and income levels used in color labelling and description of results.). Furthermore, a sensitivity analysis is presented investigating a number of crucial variables as well as uncertainty related to climate change and CO₂ fertilization. Finally, Section 4.4 reflects on the methodology and results, compares results to existing literature and summarizes conclusions.

4.2. Materials and Methods

4.2.1. The IMAGE model framework

Our analysis is performed with the IMAGE 3.0⁵ integrated assessment modelling framework. The IMAGE framework is used to simulate interactions between human activities and the environment to explore long-term global environmental change and policy options in the areas of climate, land use and sustainable development (Stehfest et al., 2014). It comprises a number of sub-models describing land use, the agricultural economy, the energy system, natural vegetation, hydrology, and the climate system (Figure 1-3 and Figure 2-1). Agriculture, forestry and land-use dynamics are modelled on the grid-level in the IMAGE-Land Management land-use model (Doelman et al., 2018). Demand for crop and livestock products, trends in agricultural intensification and trade dynamics are provided by the computable general equilibrium model (CGE) MAGNET (Woltjer et al., 2014). Gridded land-use dynamics are implemented in the dynamic global vegetation model LPJmL to model effects on the carbon and hydrological cycle (Bondeau et al., 2007; Sitch et al., 2003). LPJmL provides data on potential crop and grass yields, land-use change emissions and irrigation water use. The simulation model TIMER represents the energy system with high technological detail for 12 primary energy carriers including bioenergy (van Vuuren, 2007). The demand for bioenergy is determined by TIMER based on grid-level land availability in IMAGE-LandManagement. Greenhouse-gas (GHG) emissions from energy, industry and land use are input to the simple

5 For more background info, see the detailed, online IMAGE documentation: http://themasites.pbl.nl/models/image/index.php/Welcome_to_IMAGE_3.0_Documentation.

climate model MAGICC, which emulates complex climate models to calculate global mean temperature change (Meinshausen et al., 2011). The climate policy model FAIR-SimCAP uses marginal abatement cost curves to determine cost-optimal emission pathways to achieve specific climate targets (den Elzen et al., 2008). Finally, data on food availability, energy use and climate change are input to the GISMO model, which calculates changes in human development in relation to the global environment (Lucas et al., 2019).

4.2.2. Overview of afforestation method

To investigate afforestation as a climate change mitigation option data from different sub-models of the IMAGE framework is used (Figure 4-1). The biophysical potential of forest growth is provided by LPJmL (Section 4.2.3). Current and projected land use in a baseline scenario is provided on a grid-basis by IMAGE-LandManagement (Section 4.2.5). The value of agricultural land use is taken from the agro-economic model MAGNET (Woltjer et al., 2014)(Section 4.2.4.1), and other cost components are taken from sources in the literature (Section 4.2.4.2).

To calculate if and how much afforestation takes place in a scenario, these data are combined as follows: It is assumed that cropland, pasture and degraded forest land as projected in a baseline scenario are available for afforestation. For each grid cell (5x5 arc-minutes) in each time step (5 years) during the scenario period (2010-2100), a comparison is made whether it is more profitable to use the land for agriculture or to afforest for climate change mitigation. Climate change mitigation policy is driven by a global CO₂ price. To determine the profitability of an investment, it is common to calculate the net present value (NPV). This is the present value of all future cash flows subtracted by the present investment costs, opportunity costs and other costs (Clarke et al., 2008; Shabman et al., 2002). The NPV is calculated using equation 3.1:

$$NPV_i = \sum_{t=1}^T \frac{(Cseqrev_{i,t} - landrent_{i,t} - monitorcost_{i,t})}{(1+r)^t} - conversioncost_i \quad (3.1)$$

where NPV is the net present value at location i at time step t ; $Cseqrev$ is the annual revenue of carbon sequestration, which is the product of the CO₂ price and the carbon stored annually in the vegetation and soil; $landrent$ is the annual economic return to land for agricultural land use (crop or livestock production), which is assumed as the opportunity cost and depends on the amount of afforestation in previous time steps (Section 4.2.4.1); $monitorcost$ is the annually returning cost to monitor carbon stocks; $conversioncost$ is the initial investment cost of afforestation that is required at the start of afforestation (conversion/preparation of the land and planting of trees)(Section 4.2.4.2); T is the time horizon, which is the period of time that is considered to determine the profitability of an investment. It is assumed to be 30 years, which is a common period for a carbon sequestration project to decide whether or not to invest (Humpenöder et al., 2014; Winsten et al., 2011); r is the discount rate. Instead

of a uniform discount rate we use region-specific risk-adjusted discount rates to account for differences in investment risks between regions. These can be notably higher in developing regions that also have high afforestation potential (Benítez et al., 2007; Iyer et al., 2015). World bank data on national lending rates is used as this represents the annual rate of return that is required for a landowner to make an investment profitable. A simple exponential relation between lending rates and GDP per capita for the period 1996-2015 is fitted to derive regional discount rates, resulting in a range of 6.3% in the USA to 20.7% in Eastern Africa in 2010 (SI Section S4.1 and SI Table 4-2). This relation is assumed to also hold in future periods.

Afforestation is assumed to take place if the investment is profitable, i.e. if the NPV is positive. All grid cells that can potentially be afforested are sorted according to their NPV, and afforestation is allocated to the most profitable locations. Grid cells with average carbon sequestration of less than 0.5 ton C/ha/yr during the first 30 years after planting are excluded to ensure forest growth can be sustained. Once forest is established it is not converted back to agriculture at a later point in time, thus excluding the risk of non-permanence (Dutschke, 2001). To prevent unrealistically fast conversion of agricultural land to forest in case of very high CO₂ prices, a maximum afforestation rate is assumed of 0.4%/yr relative to total agricultural land, on a regional scale. This assumption represents a limit to the speed at which climate policy is adopted by (i.e. by landowners, policy makers, forestry experts). Limits to the rate of change in response to climate policies are observed, for example in bioenergy policies in the UK (Alexander et al., 2013) and are also an important assumption in the modelling of different climate change mitigation policies (den Elzen et al., 2008). However, historically afforestation has not occurred at the scale investigated in this study. Therefore, the maximum afforestation rate is based on examples of expansion of palm oil in Indonesia and soy bean in Brazil that have shown rates of change in the order of magnitude as assumed here (SI Section S4.2 and SI Figure 4-1). We test the impact of this critical assumption in a sensitivity analysis (Section 4.3.2.4).

We use a stand-alone tool (afforestation-tool) to calculate afforestation dependent on a prescribed CO₂ price trajectory (Figure 4-1). First, stylized CO₂ price trajectories are implemented to create MAC curves for afforestation that show regional mitigation achieved at increasing CO₂ prices (SI Section S4.3). These MAC curves are then implemented in the FAIR-SimCAP model (den Elzen et al., 2008), which determines the cost-optimal CO₂ price trajectory by comparing afforestation to other mitigation options (in the energy system and in agriculture) to achieve a pre-defined climate target (Section 4.2.5). The afforestation-tool is then used again to calculate the afforestation area of the cost-optimal CO₂ price trajectory. This area is subsequently implemented in MAGNET, IMAGE-LandManagement and LPJmL to calculate effects on the food system, land use, carbon and hydrological cycles. Food availability from MAGNET is input to GISMO to determine the population at risk of hunger (SI Section S4.4). The CO₂ price trajectory from FAIR-SimCAP is implemented in TIMER to determine energy system dynamics. Bioenergy use is also determined by TIMER based on land availability from IMAGE-LandManagement assuming only other land that is not available

for food production or afforestation is available for bioenergy production (Daioglou et al., 2019; Hoogwijk et al., 2009). While this assumption implies we do not capture interactions between food and bioenergy production, it does allow to compare afforestation to the energy system and emission dynamics of bioenergy use and to assess the direct effect of afforestation on food security.

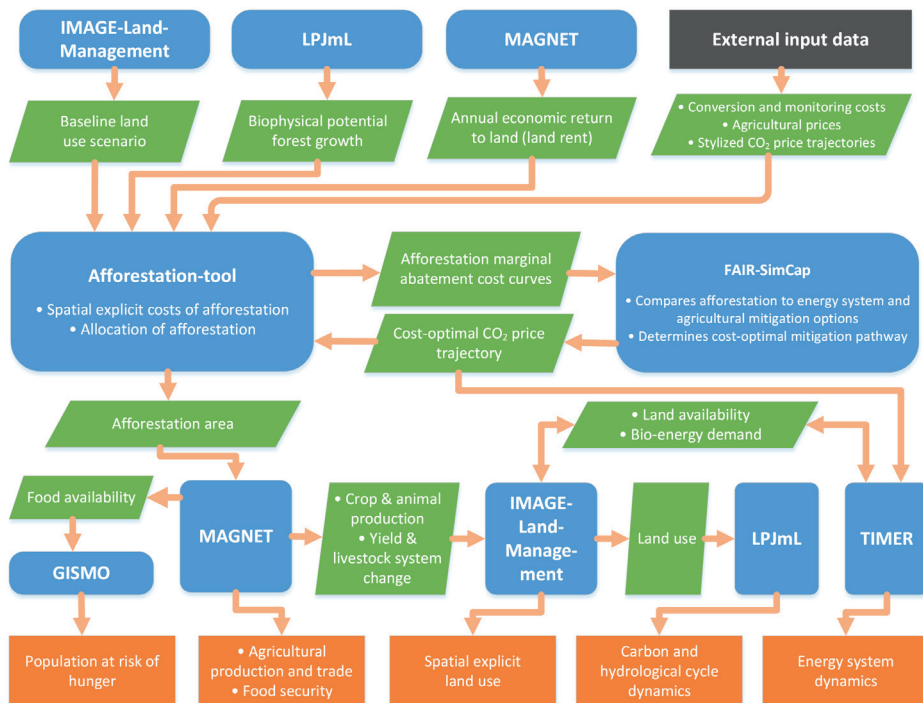


Figure 4-1: Schematic overview of afforestation modelling procedure.

4.2.3. Biophysical potential of afforestation

Biophysical potential of forest growth on a grid-basis is modelled using LPJmL (Bondeau et al., 2007; Sitch et al., 2003)(Figure 4-2). In this study we use the new forest plantation functional types (FPFT) that have been developed to represent planted forests (Braakhekke et al., 2019). Tree growth is simulated for three FPFTs (temperate, tropical, and boreal). These are based on the natural plant functional types (PFTs) “temperate broadleaved summergreen tree”, “tropical broadleaved evergreen tree”, and “boreal needle-leaved evergreen tree”. Compared to natural PFTs, a newly established FPFT stand has a high initial planting density representing the planting of forest saplings and prevention of competition with other plant species as opposed to the gradual establishment and natural succession assumed in natural PFTs. The growth rates of the FPFTs are calibrated to forest plantation data from the literature. In addition, constraints on carbon use efficiency and maximum biomass are used to ensure

that carbon fluxes and storage are realistic compared to their natural counterparts. No forest management after establishment such as irrigation, fertilization or thinning is assumed. The resulting growth rates are substantially higher than natural forest growth rates, but lower than intensively managed forest plantations (see for more info Braakhekke et al. (2019)). Therefore, this representation of forest plantations can be described as a planted forest in line with the FAO definition (FAO, 2018a) with minimal management after establishment.

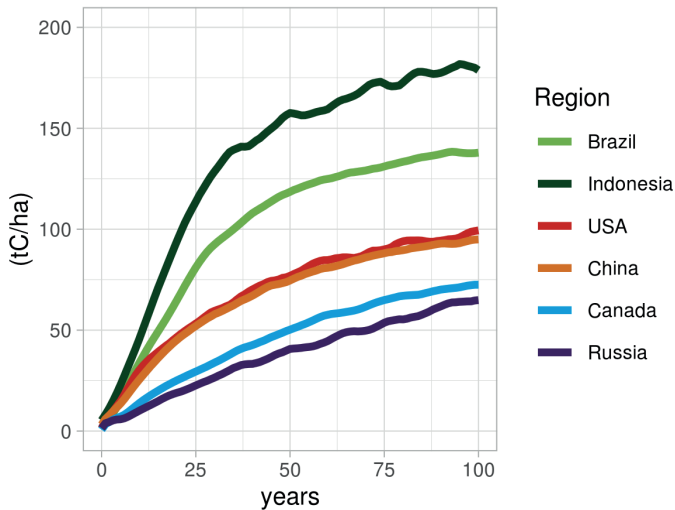


Figure 4-2: Potential average cumulative carbon sequestration of forest plantations on current agricultural land that can sustain forest growth (>0.5 tC/ha/yr growth in first 30 years after planting) in six selected regions: two predominantly tropical regions (Brazil and Indonesia), two predominantly temperate regions (USA and China) and two predominantly boreal regions (Canada and Russia).

4.2.4. Costs of afforestation

4.2.4.1. Opportunity costs

An important component of the investment decision for afforestation (Equation 3.1) is the opportunity cost of land. In this study afforestation competes with agriculture. Therefore, the opportunity cost is the annual economic return to land of agriculture. We use here the opportunity costs as calculated by the computable general equilibrium model MAGNET. MAGNET is an extension of the GTAP model and database (Hertel, 1997). GTAP has detailed information on the value added of the agricultural sector, which is distributed over the production factors land, labour and capital. The share of the value added related to land is the economic return to land from agriculture, also known as the land rent. Land rent from MAGNET is available at a resolution of 26 regions (SI Table 4-4) while afforestation is implemented at the grid-level. Therefore a downscaling of land rent is applied using grid-

based yields from LPJmL calibrated to FAOSTAT (2017), and prices of IMAGE crop types and grass derived from World Bank, FAO and FAPRI data SI Table 4-3.

MAGNET includes agricultural land as an explicit production factor described by a land-supply curve (Woltjer et al., 2014). The value of land rent changes in scenario projections due to various factors, e.g. due to economic development and population growth leading to higher demand for agricultural products, due to substitution between land, labour and capital, or due to increasing scarcity of land as the additional land available for agriculture is depleted. These changes are included in the investment decision (Equation 3.1) and depend on location and time. MAGNET does not explicitly include afforestation. For the purpose of this study a model setup is developed in which agricultural land use in MAGNET can exogenously be reduced by a prescribed land area requirement, in this case for afforestation (Figure 4-3): The land supply curve is shifted to the left resulting in a new equilibrium leading to adjusted food prices, food consumption, trade and agricultural efficiency. To take the effect of increasing land rent into account in the afforestation decision, a set of stylized scenarios is created where agricultural land is linearly reduced. The land rent values from these scenarios are interpolated to create a detailed look-up table of land rents dependent on the reduction in agricultural land SI Table 4-5. These are subsequently applied in the NPV calculation to include the effect of higher afforestation area on land rent.

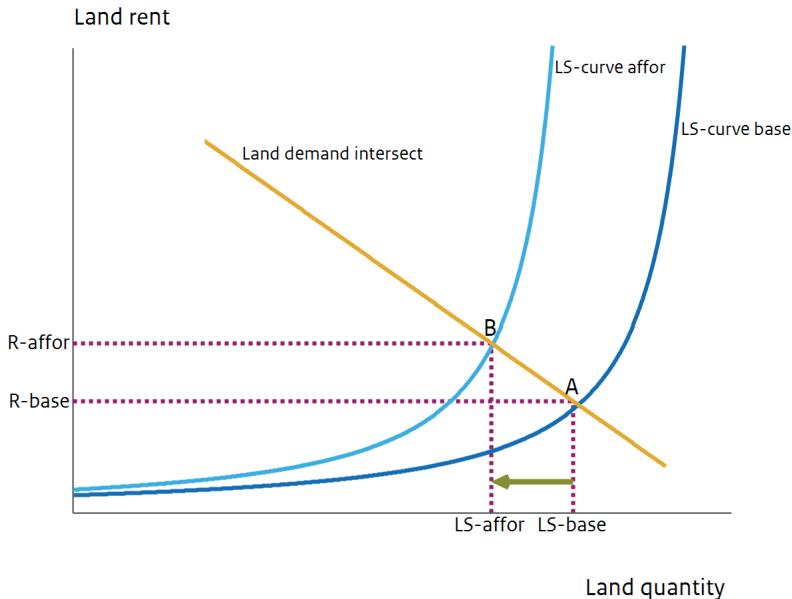


Figure 4-3: Graphic representation of agricultural land supply curves for a baseline and an afforestation scenario (LS-curve base in dark blue and LS-curve affor in light blue, respectively). The green arrow indicates a prescribed reduction in agriculture. The baseline scenario equilibrium land supply (LS-base) and land rent (R-base) in point **A** shift following the land demand intersect (yellow) to a new afforestation scenario equilibrium land supply (LS-affor) and land rent (R-affor) in point **B**.

4.2.4.2. Conversion and monitoring costs

A study by Winsten et al. (2011), focusing on afforestation specifically for carbon sequestration in the north-eastern USA, is used to estimate conversion and monitoring costs. Winsten et al. (2011) sent questionnaires to foresters to investigate the costs of conversion. The conversion costs specifically comprise site preparation, planting, maintenance (e.g. mowing, weeding, herbicides, tilling, herbivore control), and replanting costs. In this study, we take the average value of these costs across all states considered in the Winsten study. Conversion costs are assumed to be an initial cost, i.e. no additional future costs are taken into account. This is in line with the minimal forest management assumed in LPJmL (Section 4.2.3). Monitoring of carbon stocks to check if a land owner is eligible for carbon sequestration payments is estimated at \$71.70 per hectare for a 20-year project (Winsten et al., 2011). For this estimate, a discount rate of 4% was used, implying an annual cost of \$5.25 per hectare for the USA.

In order to use the data in other world regions we assume that 50% are capital costs from e.g. machine use or fence building that are considered to be equal globally. The other 50% are assumed to be labour costs depending on regional differences in wages for low-skilled labour. As a proxy for this, regional GDP/capita relative to the USA is used. This results in total costs for conversion ranging from \$862 per hectare in Eastern Africa to \$1633 per hectare in the USA (SI Table 4-4). While this is a simplistic procedure, the resulting cost range is similar to other studies (Humpenöder et al., 2014; Sathaye et al., 2006). The same method is applied to scale monitoring costs between regions resulting in a range of \$2.66/ha/yr in Eastern Africa to \$5.25/ha/yr in the USA. For the projection period, the costs of conversion and of monitoring for the USA are assumed to increase at the same rate as GDP/capita. In other regions, the development of GDP/capita relative to the USA is used to scale costs (SI Table 4-6).

4.2.5. Scenario definitions

A set of 11 scenarios is defined to investigate the role of afforestation in increasingly stringent mitigation scenarios (Table 4-1). The baseline scenario is the IMAGE 'middle of the road' SSP2 scenario (van Vuuren et al., 2017b). Crucial drivers of SSP2 are population, which continues to grow until 2050 and shows a slight decrease from 2050 to 2100, and GDP, which continues to grow in all regions until the end of the century (SI Figure 4-4). The developments in agricultural land are based on the interactions between projections of food demand, agricultural efficiency and the economy. Degraded forest estimates are derived from the historical difference in deforestation due to agricultural expansion and deforestation according to FAO's Forest Resource Assessment (for more detail see Doelman et al. (2018)). The SSP2 baseline scenario results in a change in radiative forcing of around 6.5 W/m². To assess the effect of increasingly ambitious mitigation targets the baseline is combined with a number of climate mitigation targets: 6.0 W/m², 4.5 W/m², 3.4 W/m², 2.6 W/m² and 1.9 W/m² (Table 4-1). The first four scenarios correspond to the forcing targets of the RCP scenarios (van Vuuren et al., 2011), where 2.6 W/m² has a 66% likelihood to limit global warming to 2 °C (Rogelj et al., 2011). The 1.9 W/m² target has a 66% likelihood to limit global

warming to 1.5 °C and reflects the ambitions expressed in the 2016 Paris Agreement (Rogelj et al., 2018). Next to the scenarios with afforestation, an additional set of scenarios with the same climate targets are defined as reference cases where afforestation as mitigation policy is excluded. In all scenarios except the baseline, avoided deforestation policy is implemented under the assumption that this is cheaper than afforestation (based on Kindermann et al. (2008)); all forests with carbon stocks of 10 tC/ha or higher are protected (Doelman et al., 2018; Overmars et al., 2014). We exclude climate impacts in this set of scenarios to improve interpretability of the results, but include it in the sensitivity analysis.

Table 4-1: Description of implemented scenarios.

climate target (radiative forcing (W/m ²))	afforestation	no afforestation (reference)
no target	-	SSP2-baseline
6.0	SSP2-6.0-A	SSP2-6.0-R
4.5	SSP2-4.5-A	SSP2-4.5-R
3.4	SSP2-3.4-A	SSP2-3.4-R
2.6	SSP2-2.6-A	SSP2-2.6-R
1.9	SSP2-1.9-A	SSP2-1.9-R

In addition, we define a number of sensitivity tests to investigate the importance of various parameter settings that are central to the afforestation methodology: the discount rates, the time horizon, the conversion and monitoring costs, and the maximum afforestation rate. In addition, climate change effects with and without CO₂ fertilization are tested (for details see SI Table 4-7). The sensitivity tests are implemented by rerunning a scenario with a pre-determined CO₂ price with one of the selected parameters changed in a positive or negative direction. We perform the sensitivity for three scenarios with different climate mitigation targets with increasing ambition: SSP2-4.5-A, SSP2-3.4-A and SSP2-2.6-A. The sensitivity is assessed by investigating the effect on cumulative carbon sequestration (2010-2100).

4.3. Results

4.3.1. MAC curves

Our results show there is moderate potential for climate change mitigation through afforestation at low prices: globally at US\$50/tCO₂ we find 0.75 GtCO₂/yr in 2030, 1.5 GtCO₂/yr in 2050 and 1.1 GtCO₂/yr in 2100 (Figure 4-4). More than half of the potential at low cost is located in Latin America, which is related to low land prices, high forest growth rates and relatively lower discount rates than other tropical regions with similarly high growth rates. In 2100, the potential is lower than in 2050 due to higher costs related to continued economic

growth and higher land prices because of increased land scarcity. The potential is lower in 2030 compared to 2050 due to limits on how fast afforestation area can expand.

The potential from afforestation increases substantially with higher CO₂ prices: globally at US\$200/tCO₂ there is a potential of 2.7 GtCO₂/yr in 2030, 4.9 GtCO₂/yr in 2050 and 5.8 GtCO₂/yr in 2100. At these prices there is increased potential in temperate regions, notably North America and China with 0.6 and 0.5 GtCO₂/yr respectively in 2050. Afforestation is relatively more expensive in these regions due to high land prices and lower forest growth rates. The potential in Russia and Central Asia remains limited with 0.12 GtCO₂/yr in 2050, which is caused by relatively low growth rates in boreal forests. At very high CO₂ prices of over US\$500/tCO₂ the potential increases slightly to 0.18 GtCO₂/yr (see SI Figure 4-3).

At all CO₂ price levels Latin America and Sub-Saharan Africa are responsible for at least 50% of the climate change mitigation potential from afforestation. This is mostly related to large land areas that can potentially be afforested, high forest growth rates and higher absolute carbon stocks that can be reached per land area compared to temperate or boreal forests (see Figure 4-2). While we do take into account higher risks of investment in these regions through risk-adjusted discount rates, this only affects the price at which afforestation becomes economically feasible but does not change the maximum potential .

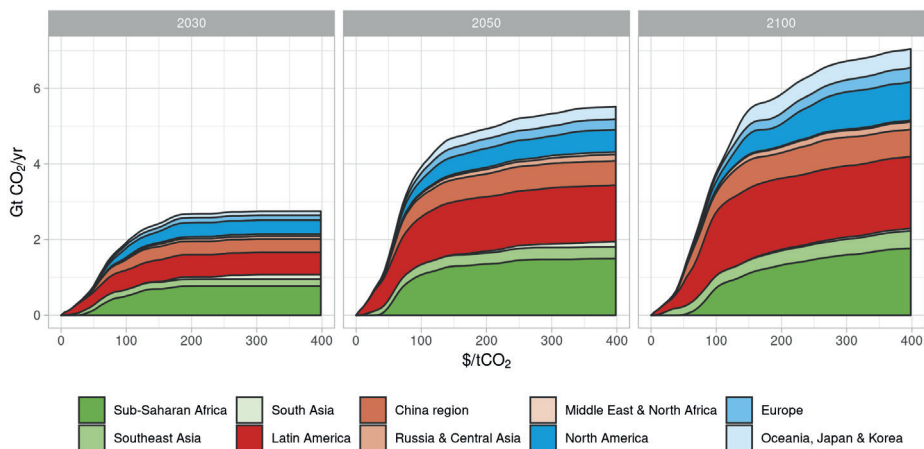


Figure 4-4: Marginal abatement cost (MAC) curves of carbon sequestration through afforestation in 10 aggregated regions (SI Table 4-1) in years 2030, 2050 and 2100. Based on stylized linear CO₂ price trajectories that increase from \$0/tCO₂ in 2020 to CO₂ price as shown on the Y-axis in 2030, 2050 and 2100. For clarity, the graphs are limited to 400 US\$/tCO₂. MAC curves up to \$1000 US\$/tCO₂ are presented in SI Figure 4-3.

4.3.2. Mitigation scenarios

4.3.2.1. CO₂ emissions

To achieve an ambitious mitigation target of 2.6 W/m² substantial reductions of emissions from the energy, industry and land sectors are implemented (Figure 4-5a). In addition, negative emissions from afforestation and BECCS are used to achieve the mitigation target. In the SSP2-2.6-A scenario afforestation is implemented as soon as mitigation policy starts (from 2020 onwards) as it is available at relatively low costs compared to other mitigation options. BECCS is implemented from 2030 onwards when CO₂ prices have risen up to a level where the technology has become profitable. By the end of the century, negative emissions of 5.0 GtCO₂/yr and 3.1 GtCO₂/yr result from afforestation and BECCS, respectively. Cumulatively, negative emissions from afforestation are similar until 2100 in the stringent mitigation scenarios SSP2-2.6-A and SSP2-1.9-A with 430 and 450 GtCO₂ respectively, as nearly the maximum afforestation potential is utilized in these scenarios (Figure 4-5b). Emissions from land-use change and forestry in these scenarios persist as avoided deforestation policy is not immediately effective and because of bioenergy expansion on other natural land. In SSP2-3.4-A and SSP2-4.5-A, less stringent climate targets result in comparatively lower levels of carbon sequestration from afforestation of 250 and 64 GtCO₂, respectively. The SSP2-6.0-A scenario does not include any afforestation as the amount of climate policy required to achieve this low ambition target is very limited: only 270 GtCO₂ reduction is required, which is achieved through other cheaper options.

Including afforestation as a mitigation option has a major impact on mitigation policy in other sectors. Afforestation is a relatively cheap option that reduces overall mitigation costs as indicated by lower average CO₂ prices in all scenarios (Figure 4-5c): for example, the 2020-2100 average is 240 US\$/tCO₂ in SSP2-2.6-A compared to 430 US\$/tCO₂ in SSP2-2.6-R. While this means that climate policy is cheaper, it also means that less investments are made in mitigation options in the energy sector such as electrification of industry, decarbonization of transport and large-scale deployment of renewable energy sources. This implies lower ambitions in the decarbonization of sectors in energy and industry leading to 27% higher emissions in these sectors in the 2.6 W/m² afforestation scenario compared to the reference scenario.

Lower reductions in energy and industry are mirrored by increased reliance on negative emissions. In SSP2-3.4-A, SSP2-2.6-A and SSP2-1.9-A cumulative negative emissions increase by 92%, 95% and 57% respectively compared to their respective reference scenarios (Figure 4-5b). This indicates an important risk as mitigation pathways including large-scale negative emissions could lead to lock-in situations in sectors that are more expensive to decarbonize (Anderson and Peters, 2016). Moreover, afforestation causes a larger share of total negative emissions to be located in low income regions: 31% in SSP2-2.6-A compared to 17% in SSP2-2.6-R (Figure 4-5d). This indicates a higher risk for implementation and permanence when mitigation occurs in regions with high investment risks and weak governance. In contrast,

afforestation does reduce negative emissions from BECCS, which has also been criticized as a high-risk mitigation strategy (Searchinger et al., 2017): for example, compared to their respective reference scenarios the 2.6 and 3.4 W/m² afforestation scenarios involve 13% and 26% less negative emissions from BECCS, respectively.

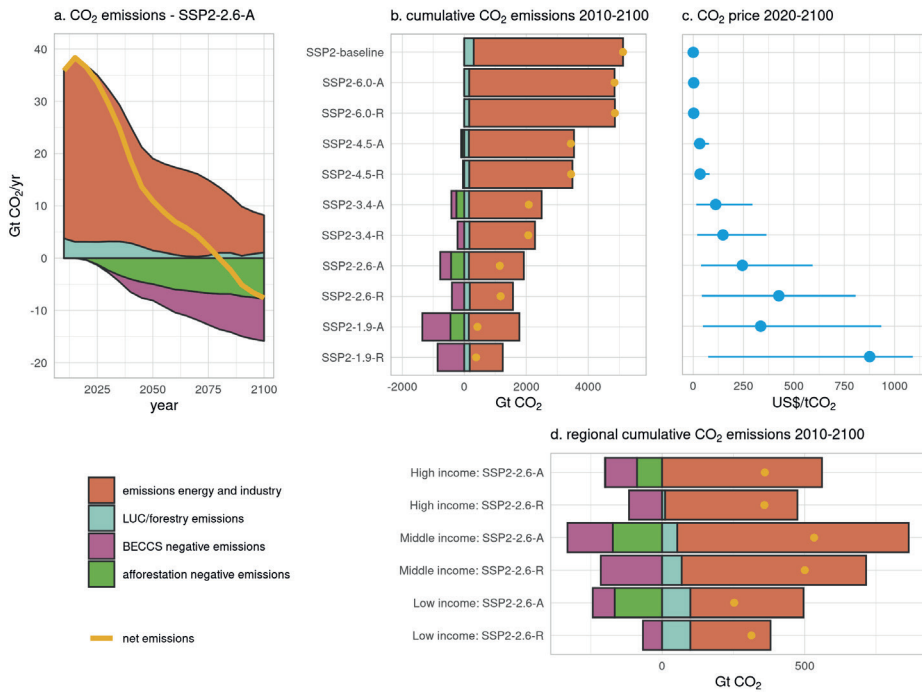


Figure 4-5: CO₂ emissions in baseline and mitigation pathways: a) Annual CO₂ emissions from SSP2-2.6-A, b) cumulative CO₂ emissions from 2010-2100 for all scenarios, c) average and range of CO₂ prices from 2020-2100 for all scenarios, and d) cumulative CO₂ emissions from SSP2-2.6-A and SSP2-2.6-R for high, middle and low income regions.

4.3.2.2. Land use

At moderate and high levels of CO₂ prices, afforestation is an economic alternative to agriculture, and therefore agricultural area is converted to forests. The largest reductions are in pasture land because this is the largest share of land in the baseline, because it is cheaper than cropland, and because there is substantial potential for intensification in the livestock sector for example substituting feed from grass with feed from crops (Figure 4-6). In the more stringent scenarios also cropland for food and feed production is reduced as high food prices lead to additional intensification as well as reduced food demand. In all mitigation scenarios the land use for bioenergy increases to allow for additional climate policy, mostly at the cost of other natural lands with low carbon stocks such as savannahs.

SSP2-3.4-A, SSP2-2.6-A and SSP2-1.9-A already have substantial afforestation by 2050 (120, 440 and 470 Mha, respectively), and forests continue to expand towards 2100 (up to 740, 1090 and 1150 Mha, respectively). SSP2-4.5-A only shows forest expansion after 2050 as climate policy is postponed due to the low ambition target (230 Mha in 2100), while SSP2-6.0-A does not show any afforestation because CO₂ prices are too low to make it profitable. SSP2-1.9-A also shows a reduction in other forests as bioenergy plantations replace managed forests in temperate and boreal regions in order to supply sufficient bioenergy to achieve the 1.9 W/m² target. Degraded forest lands are afforested in nearly all scenarios as these are relatively cheap lands.

Notable hotspots of land-use change for afforestation are South America, China, USA, and Sub-Saharan Africa (Figure 4-4; SI Figure 4-5), because these are regions that currently have large agricultural areas as well as high potential forest growth rates. Arid regions such as Northern Africa and the Middle East show limited afforestation as forest growth rates are very low. On the other hand, for example India also shows limited afforestation because land rents are high due to high population pressure leading to high demand for agricultural products. This limiting effect is further enhanced during the scenario period as the population of India is projected to continue to increase.

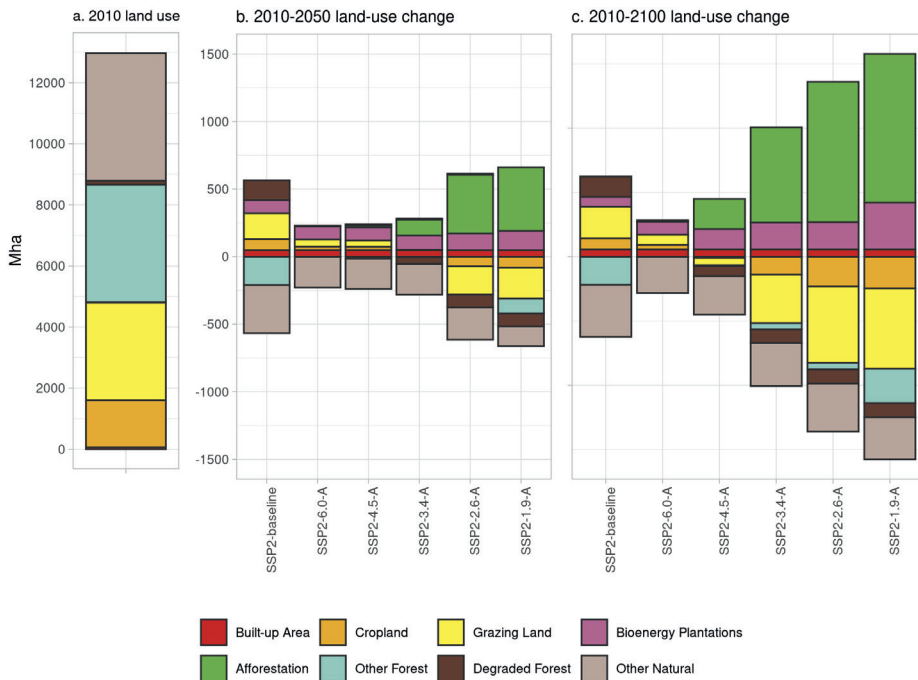


Figure 4-6: a) Land use in 2010. Land-use change in b) 2010-2050 and c) 2010-2100 for the scenarios with afforestation.

4.3.2.3. Food security

If afforestation is implemented in cost-optimal mitigation policy across all sectors it is likely to affect food security (Hasegawa et al., 2018, 2015a), though additional measure can counteract these consequences (Doelman et al., 2019; Fujimori et al., 2018). Here we calculate how afforestation and reductions in agricultural land could negatively affect prices and food security. Our results show increasing food prices, reduced food availability (SI Figure 4-6 and SI Figure 4-7) and, as a consequence, negative impacts on the population at risk of hunger (Figure 4-7). In the baseline scenario, the population at risk of hunger is projected to decrease from 795 million in 2010 to 415 million in 2050, and to 209 million in 2100. In the reference scenarios (SSP2-6.0/1.9-R in Figure 4-7) avoided deforestation policy limits this decrease to 504 million in 2050 and 275 million in 2100. Bioenergy is assumed only to occur on other lands not required for agriculture or afforestation and therefore does not affect food security (see Section 4.2.2). In SSP2-2.6-A, improvements in food security do not continue resulting in 716 million people at risk of hunger in 2100. This implies an additional 441 million people at risk of hunger due to afforestation for climate change mitigation. In 2100 in the SSP2-4.5-A, SSP2-3.4-A, SSP2-1.9-A scenarios an additional 29 million, 176 million and 517 million people are at risk of hunger, respectively.

Regionally, the effects differ greatly with the majority of the population at risk of hunger living in Sub-Saharan Africa and South Asia (Figure 4-7). In 2010, there is still a substantial risk of hunger in China, however this decreases to near zero in 2100 in the SSP2-baseline. In stringent mitigation scenarios, the risk of hunger in China is not much affected, which is partly due to a declining population by the end of the century limiting the pressure on the food system (SI Figure 4-4). In Sub-Saharan Africa in contrast, the population at risk of hunger decreases by 56% in the baseline from 2010 to 2100, while in SSP2-2.6-A it increases by 86%. In part this is due to continued population growth in Sub-Saharan Africa as the share of the population at risk of hunger still decreases. However, also the increase in food prices, which causes a decline in food availability, has a strong effect (SI Figure 4-6 and SI Figure 4-7).

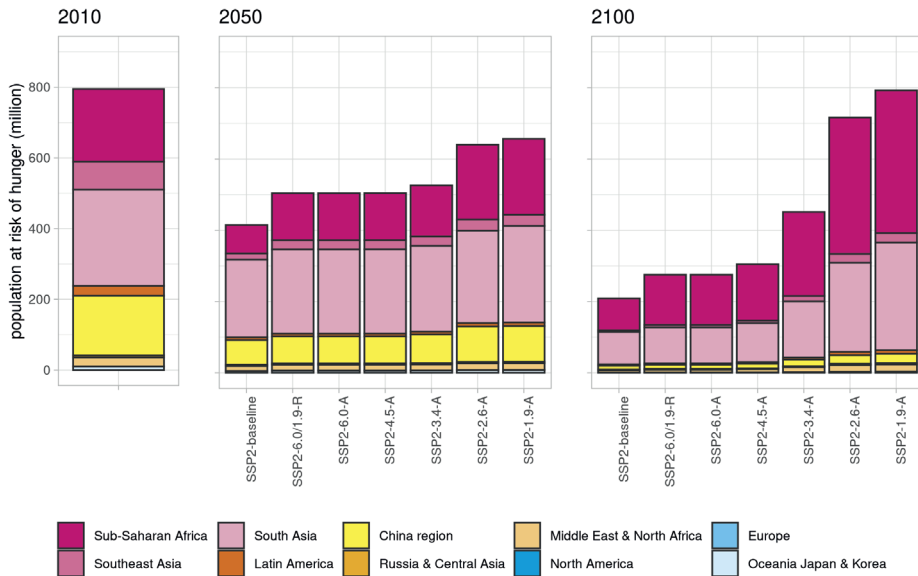


Figure 4-7: Population at risk of hunger in 10 aggregated regions in 2010, 2050 and 2100 for the baseline scenario, the reference scenarios (combined in one bar as food security effects are equal), and the afforestation scenarios.

4.3.2.4. Sensitivity analysis

To test the importance of different parameter settings we performed a sensitivity analysis (Figure 4-8) (for details see Section 4.2.5 and SI Table 4-7). It is shown that the importance of the various parameters differs substantially depending on the stringency of the climate target, i.e. at the level of the CO₂ price. At relatively low or moderate CO₂ prices (SSP2-4.5-A and SSP2-3.4-A: \$32/tCO₂ and \$112/tCO₂ on average in 2020-2100, respectively) most parameters have a substantial impact: for example, a shorter time horizon leads to a strong reduction in cumulative carbon sequestration in SSP2-4.5A and SSP2-3.4-A (-54% and -31%, respectively) due to less carbon uptake over a shorter time period implying lower expected profit. Lower afforestation costs or reduced discount rates lead to a strong increase in cumulative carbon sequestration (ranging from 13% to 29%) as investments are profitable at lower CO₂ prices. The 4.5 W/m² and 3.4 W/m² scenarios result in substantial climate change. Therefore, including the effect of changes in temperature and precipitation in combination with CO₂ fertilization leads to increases in cumulative carbon sequestration (+30% and +18%, respectively) as the fertilization effect has a dominant positive impact on tree growth. Climate change without CO₂ fertilization has a moderate negative impact on cumulative carbon sequestration (-5% and -2%, respectively).

In a scenario with high CO₂ prices (SSP2-2.6-A: \$244/tCO₂ on average in 2020-2100) the maximum afforestation rate is a crucial parameter that strongly affects cumulative carbon sequestration (-44% and +30% for the negative and positive case, respectively). In contrast,

afforestation costs and discount rates have a small effect in this scenario (ranging from -11% to +3%) because the value of CO₂ sequestration is so high that nearly all investments are profitable. This highlights the importance of estimating how fast carbon policy can be adopted, which is an important uncertainty in mitigation scenarios, most notably at high CO₂ prices. Climate change and CO₂ fertilization have a limited effect in SSP2-2.6-A (-2% and +9% for the negative and positive case, respectively) as the global increase in temperature is kept below 2°C thus preventing large effects on tree growth.

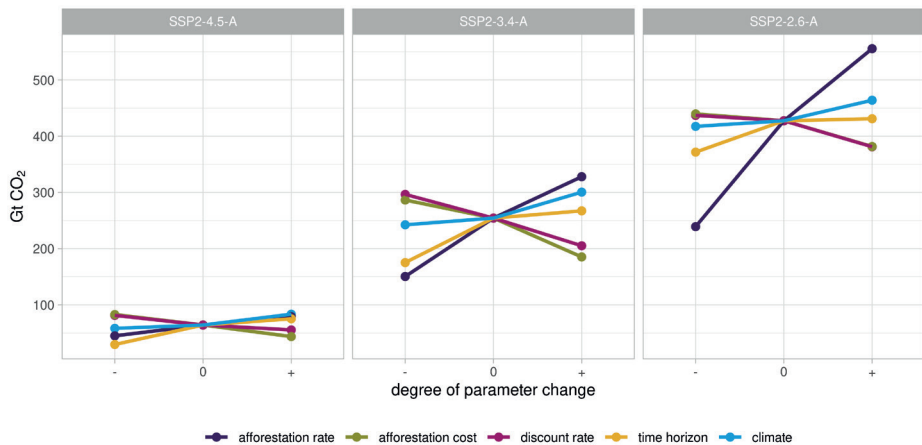


Figure 4-8: Sensitivity of cumulative carbon sequestration (2010-2100) from afforestation to selected parameter settings for three mitigation scenarios with relatively low, moderate and high CO₂ prices. Settings varied for afforestation rate (0.2% (-), 0.4% (0), 0.6% (+)), afforestation costs (global low costs (Eastern Africa)(-), region-specific costs (0), global high costs (USA)(+)), discount rate (global low discount rate (USA)(-), region-specific discount rates (0), global high discount rate (USA)(+)), time horizon (10 (-), 30 (0), 50 (+) years), and climate change effects (climate change without CO₂ fertilization (-), no climate change (0), climate change with CO₂ fertilization(+))(for details see SI Table 4-7).

4.4. Discussion

In this study we show that afforestation has moderate potential for negative emissions at low CO₂ prices (1.5 Gt CO₂/yr in 2050 at US\$50/tCO₂) and high potential at higher CO₂ prices (4.9 Gt CO₂/yr in 2050 at US\$200/tCO₂). When applying afforestation in scenarios aiming for 2.6 W/m², cumulative carbon sequestration in 2100 amounts to 410 GtCO₂ leading to forest expansion of 1110 Mha. This order of magnitude is similar to previous studies. Calvin et al. (2014) investigate a scenario including afforestation with the GCAM model aiming for an end-of-the-century radiative forcing of 3.7 W/m² and find an area use of approximately 1000 Mha resulting in cumulative carbon sequestration of about 590 GtCO₂. Humpenöder et al. (2014) test linear carbon tax scenarios up to \$194, \$1165 and \$1942 per tCO₂ with the MAgPIE model, yielding cumulative carbon sequestration from afforestation of respectively 400 GtCO₂, 700 GtCO₂ and 800 GtCO₂, with area requirements of respectively 2000 Mha, 2800 Mha and 3000

Mha. The SSP2 scenario aiming for 2.6 W/m² developed with the GLOBIOM model (Fricko et al., 2017) shows cumulative carbon sequestration by the year 2100 of 215 GtCO₂ with an afforestation area of 830 Mha. Sathaye et al. (2006) find 176 GtCO₂ using 230 Mha of land with an exponential carbon tax up to \$175/tCO₂ in 2100 using the GCOMAP forestry model. In comparison to these studies our results are in the middle of the range both for cumulative carbon sequestration and average carbon sequestration per hectare of land afforested.

Global estimates of forest growth rates vary widely (van Minnen et al., 2008). Previous studies use either a stylized growth curve (Humpenöder et al., 2014; Kyle et al., 2011) or natural forest growth from vegetation models (Krause et al., 2017). Natural forest growth in vegetation models underestimates potential growth rates of trees as no seeding, planting or management is taken into account (Braakhekke et al., 2019). This study uses forest plantations because if afforestation is actively implemented for the purpose of climate change mitigation it is likely that some form of management is implemented to enhance tree growth. To achieve high growth rates, intensive management such as planting of specialized tree species, fertilization, thinning or irrigation may be required (Laclau et al., 2005; Stape et al., 2010). However, such intensive management may impact the nutrient and hydrological cycles. Moreover, forest plantations in non-forest biomes or plantations consisting of exotic species may negatively affect biodiversity (Bremer and Farley, 2010; Hall et al., 2012). For this reason, in this study we implement afforestation as planted forest without active management after establishment. Taking into account different management intensities is an important research priority as it affects the potential of forest-based mitigation options as well as its trade-offs with nutrient and water cycles and biodiversity.

Including afforestation as a climate change mitigation policy in stringent mitigation scenarios has important trade-offs with other policy domains. Because afforestation is relatively cheap, it is preferred in our scenarios over other more expensive policies such as electrification of industry, decarbonization of transport and large-scale deployment of renewable energy sources. As a result, the average 2020-2100 CO₂ price required to achieve, for example, the 2.6 W/m² target is reduced by 50% in a scenario with afforestation compared to a reference scenario indicating that afforestation could reduce the overall costs of climate change mitigation. At the same time, in SSP2-2.6-A emissions from energy and industry remain substantially higher and the reliance on negative emissions to achieve the mitigation target is nearly doubled. The latter issue is a crucial risk as it is argued that dependency on future negative emissions reduces the incentive to invest in decarbonization of the energy and industry sectors today leading to lock-in situations in carbon-intensive sectors (Anderson and Peters, 2016). Also, it is argued that negative emissions could at a later stage prove infeasible or less effective, leaving society without technologies to undo the damage (Kantha and Dooley, 2016). This risk is reinforced by our finding that a large share of the afforestation takes place in middle and low income regions (notably Latin America and Sub-Saharan Africa) that are currently characterized by weak governance and continued deforestation trends (Harris et al., 2012; Rochedo et al., 2018). Whether large-scale afforestation is feasible in

these regions is very uncertain. An additional risk in regions with weak governance is non-permanence, i.e. that forests can be cleared again at a later stage reversing previous benefits to climate mitigation. Moreover, it is uncertain how forests will respond to climate change where a loss of carbon stocks due to increasing droughts, fire or diseases could also limit the effectiveness of afforestation (Keenan, 2015). Many of the IAM scenarios that feed into the IPCC assessments include large-scale afforestation to achieve the 2°C or 1.5°C targets. An important direction of research is the development of scenarios achieving stringent mitigation targets without high-risk strategies such as negative emissions or afforestation in middle and low income regions.

Our results indicate that afforestation policy could pose a risk to food security due to the reductions in agricultural land. The stringent scenarios aiming for 2.6 W/m² or 1.9 W/m² show that the population at risk of hunger remains at similar levels as in 2010 as opposed to a strong decrease in the baseline scenario. The number of people at risk of hunger in Sub-Saharan Africa and South Asia increases substantially due to afforestation. These regions are most sensitive to hunger as average food availability is relatively low causing a decrease in food availability to directly lead to an increase in number of people at risk of hunger. These findings are consistent with other studies investigating the effect of land competition from land-based mitigation such as avoided deforestation, afforestation and bioenergy, and the effects of carbon pricing on agricultural emissions (Frank et al., 2017; Hasegawa et al., 2018, 2015a; Kreidenweis et al., 2016; Tabeau et al., 2017; van Meijl et al., 2018), showing strong increases in food prices, reduced food consumption and increased populations at risk of hunger. These results however are very uncertain, especially in long-term scenarios. For one, the sensitivity of consumers to food price changes (i.e. food demand elasticity) is highly debated, with empirical evidence showing very low elasticities in high-income regions (Muhammad et al., 2011) and some IAMs assuming zero elasticity of food demand (Kreidenweis et al., 2016). On the other hand, empirical evidence does show higher elasticities in low-income regions (Muhammad et al., 2011) and most models do include food demand elasticities (Nelson et al., 2014). Next to this, it is argued that economic models are not suitable to assess long-term projections of food demand as they are calibrated to trends in the recent past and do not take into account physical constraints (Bijl et al., 2017). Especially when assessing major shocks to the system such as those from large-scale afforestation, economic models are argued not to be suited for the major transitions that could be required. Therefore, the food security results that are presented in this paper need to be considered in light of substantial uncertainties.

Nonetheless, a recurring notion in the literature is that achieving a stable climate should not be achieved at the cost of reduced food security. This is in line with the ambitions of the Sustainable Development Goals that promote zero hunger (SDG2) as well as climate action (SDG13)(UN, 2015). Therefore, when considering afforestation for climate change mitigation, it is crucial to take food security trade-offs into account, even though the quantification of the effects is associated with high uncertainty. There are many possibilities to prevent negative

impacts of land-based mitigation on food security: 1) enhanced agricultural productivity e.g. through closure of yield gaps (Doelman et al., 2019; Neumann et al., 2010; van Ittersum et al., 2013), 2) dietary change leading to reduced consumption of animal products (Bajželj et al., 2014; Stehfest et al., 2009), 3) inclusive climate policies that compensate affected people (Fujimori et al., 2018), 4) or prohibiting land-based mitigation policy in regions that are sensitive to negative food security impacts (Frank et al., 2017). Furthermore, due to its relative competitiveness and the large trade-offs, it can be questioned whether afforestation and the agricultural sector should be confronted with the same CO₂ price as the energy and industry sector. More likely, land-based climate policy should be stimulated through support and incentives for climate change mitigation, or managed by regulation. Still, as land use is responsible for a large share of GHG emissions and as it plays a key role in negative emission technologies, it is inevitable that land-based mitigation will have to play a role in a solution to climate change. Hence, when developing mitigation strategies involving afforestation or any other type of land-based mitigation, the trade-offs with food security as well as possible solutions need to be explicitly taken into account.

The results in this study project afforestation under ambitious mitigation policy to be economic in almost all world regions that are reasonably suitable for forest growth. The largest potential is realized in tropical regions, however also boreal regions such as Russia and Canada show a substantial increase in forest area. The effectiveness of afforestation for climate change mitigation in boreal regions, which have substantial snow cover during part of the year, might be counteracted by biophysical climate feedbacks due to decreasing albedo. Changes in albedo can cause local warming limiting the net effect of reduced CO₂ concentrations (Alkama and Cescatti, 2016; Schaeffer et al., 2006). Conversely, expansion of forests in tropical regions can enhance evapotranspiration leading to local cooling effects thus increasing its effectiveness (Jackson et al., 2008). Including these effects in the analysis might substantially change the mitigation potential as well as land-use dynamics (Jones et al., 2015; Kreidenweis et al., 2016).

A crucial parameter is the maximum afforestation rate, especially in scenarios with high CO₂ prices as shown by the sensitivity analysis (see Section 4.3.2.4). The maximum afforestation rate is a simple assumption representing how easy agricultural land can be converted into forest. However, especially at high CO₂ prices it can be argued that other mechanisms such as implementation mechanisms, local governance and adoption rates are more important determinants of the rate of afforestation (Alexander et al., 2013). Independent of the methodological approach, land conversion elasticities derived from historical data, or other mechanisms reflecting assumed rates of change or adoption of technology play a crucial role in land-use modelling.

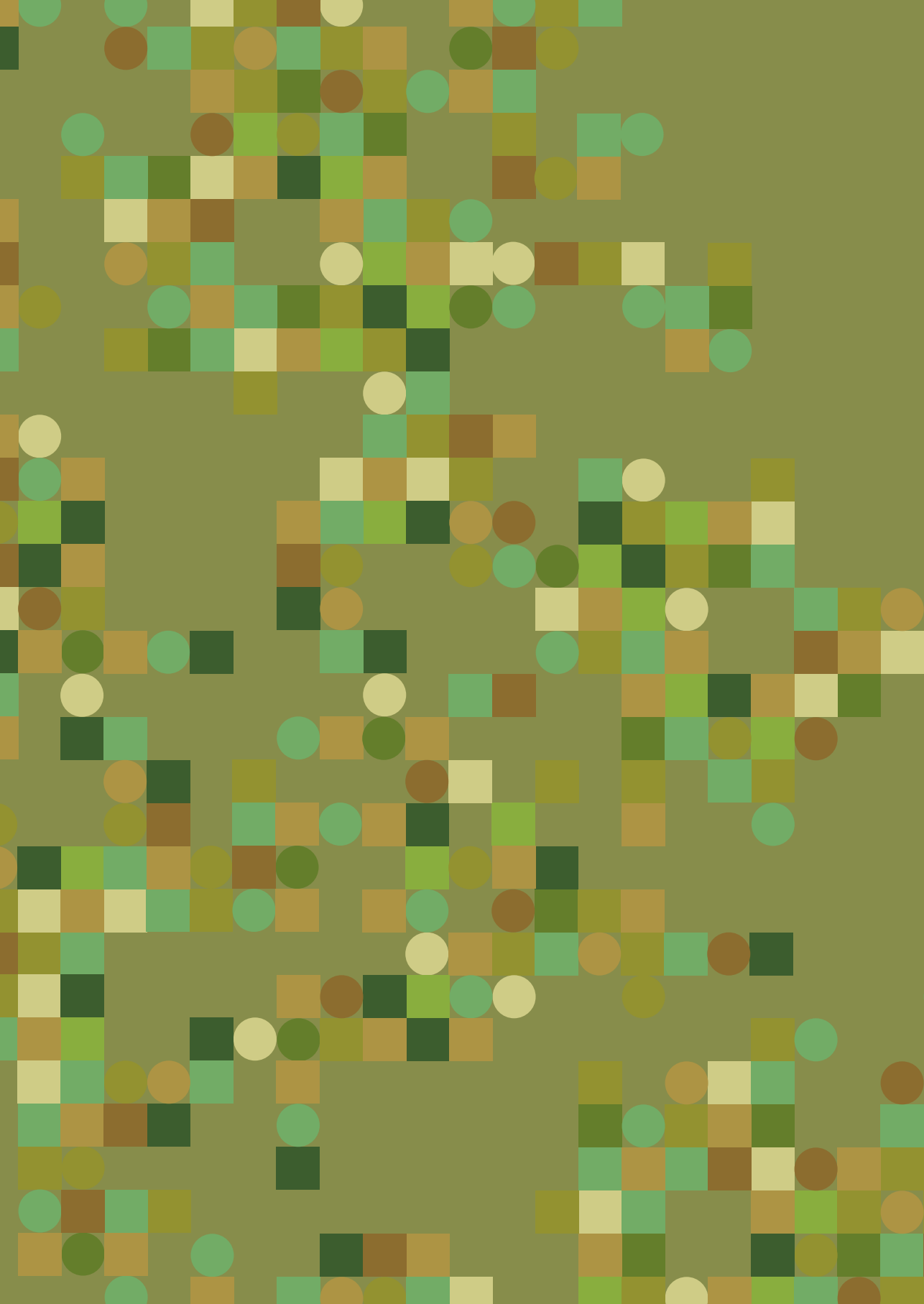
An important assumption in this study is that agricultural land is reduced for afforestation only. This approach clearly shows the pros, cons and dynamics of afforestation and makes it possible to assess the food security and mitigation policy effects of afforestation only.

However, in reality there will be competition between land use for afforestation and other land-based activities such as bioenergy production or biodiversity protection. It might be more efficient from a mitigation perspective to use forest areas for production of biomass for bioenergy while also maintaining carbon stocks (Lauri et al., 2014), or to use biomass to substitute emission-intensive materials such as concrete or steel (Leskinen et al., 2018). A comprehensive, grid-based comparison combining afforestation potentials as presented in this study and emission-factors of biomass supply chains as presented in Daiglou et al. (2017) might be able to answer this question.

In this study we have shown that moderate potential for afforestation for climate change mitigation exists at low costs (1.5 GtCO₂/yr at \$50/tCO₂ in 2050) and high potential at moderate costs (4.9 GtCO₂/yr at \$200/tCO₂ in 2050). Including afforestation cost-optimally as a mitigation option in scenarios for stringent climate targets results in a strong decrease in CO₂ prices indicating that afforestation can substantially reduce overall mitigation costs. At the same time, afforestation may lead to lower mitigation ambition and lock-in situations in sectors in energy and industry. Moreover, major risks exist regarding implementation and permanence as the negative emissions are increasingly located in regions with high investment risks and weak governance. Next to this, afforestation in our 2°C scenario causes reductions in agricultural land leading to competition with food production. Consequently, food security could be at risk as shown by an increased population at risk of hunger, most notably in Sub-Saharan Africa and South Asia. These food security effects are a crucial trade-off of large-scale afforestation. Recent publications have presented afforestation as one of the main solutions to prevent dangerous climate change (Bastin et al., 2019; Griscom et al., 2017; Lewis et al., 2019). While afforestation indeed has substantial potential for mitigation, we show that there are also major risks and trade-offs involved. Pathways aiming to limit climate change to 2°C or even 1.5°C need to minimize these risks and trade-offs in order to achieve mitigation sustainably.

Acknowledgements

Liesbeth de Waal and Alja Vrieling are gratefully acknowledged for their technical support. This study benefited from the funding of the European Union's Seventh Framework Programme FP7/2007-2013 under grant agreement n° 603542 (LUC4C).

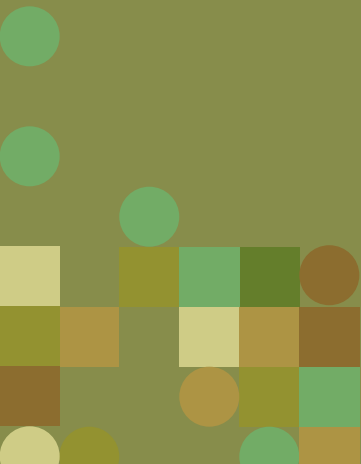


CHAPTER 5

Making the Paris Agreement climate targets consistent with food security objectives

Jonathan Doelman, Elke Stehfest, Andrzej Tabeau, Hans van Meijl

"Making the Paris Agreement climate targets consistent with food security objectives." Global food security 12 (2019): 93-103.



Abstract

Climate change mitigation is crucial to limit detrimental impacts of climate change on food production. However, cost-optimal mitigation pathways consistent with the Paris Agreement project large-scale land-based mitigation for bioenergy and afforestation to achieve stringent climate targets. Land demand from land-based mitigation leads to competition with food production, raising concerns that climate policy (SDG13 – climate action) conflicts with food security objectives (SDG2 – zero hunger). In this study we use the computable general equilibrium model MAGNET and the IMAGE integrated assessment model to quantify the food security effects of large-scale land-based mitigation. Subsequently, we implement two measures to prevent reduced food security: increased agricultural intensification and reduced meat consumption. We show that large-scale land-based mitigation (~600 Mha in 2050) leads to increased food prices (11%), reduced food availability (230 kcal/cap/day) and substantially more people at risk of hunger (230 million) compared to the baseline scenario in 2050, most notably in developing regions. Land-based mitigation also leads to yield increases (9%) and intensified ruminant production (11%). Additional crop yield improvement (9%) and intensification in ruminant production (3%) could prevent the negative effect of mitigation on food security. Introducing a reduction in meat consumption in high- and middle-income regions reduces required crop yield improvement (7%) and ruminant intensification (2%). Our study highlights the importance of transparency about food security effects in climate change mitigation scenarios. In addition, it provides an example of explicitly including measures to limit negative trade-offs in mitigation scenarios. In this way, we show how the Paris Agreement can be made consistent with food security objectives and how multiple Sustainable Development Goals can be achieved.

5.1. Introduction

The Paris Agreement aims to limit global warming to well below 2 degrees above pre-industrial levels and to pursue 1.5 degrees (UNFCCC, 2015). One important reason to limit global warming is the threat it poses to food production, as explicitly stated in the Paris Agreement as well as the original United Nations Framework Convention on Climate Change (UN, 1994). Indeed, many studies show that climate change is projected to have severe negative impacts on crop yields which leads to reduced food security and highlights the importance of climate change mitigation (Nelson et al., 2014; Rosenzweig et al., 2014; von Lampe et al., 2014; Zhao et al., 2017). The importance of food security and climate change mitigation is also emphasized by the United Nations Sustainable Development Goals (SDGs) that have specific goals for both: zero hunger (SDG2) and climate action (SDG13). This underlines the importance of achieving the Paris Agreement climate target to ensure food security.

The recently published IPCC special report on 1.5 degree as well as many scenario studies conclude that to limit climate change in line with the Paris Agreement requires substantial negative emissions (IPCC, 2018; Riahi et al., 2017; Rogelj et al., 2018). These negative emissions are needed to compensate for excessive emissions in the early stages of a decarbonization pathway and for emissions that are difficult to mitigate fully such as in agriculture. In most mitigation scenarios this is realized via large-scale afforestation (Calvin et al., 2014; Humpenöder et al., 2014) and bioenergy with carbon capture and storage (BECCS) (Azar et al., 2010; van Vuuren et al., 2013). These land-based mitigation technologies require large areas of land which can lead to competition for land between food production and climate change mitigation. As a consequence, food prices might rise causing negative effects on food security (Frank et al., 2017; Hasegawa et al., 2015a; Kreidenweis et al., 2016). Recent studies have shown that by the year 2050 the impact of land-based mitigation on food security could even be larger than the negative impact of climate change (Hasegawa et al., 2018; van Meijl et al., 2018). This raises the concern that the Paris Agreement climate target and food security objectives are conflicting and cannot be achieved simultaneously.

However, there are opportunities on the supply and demand side of the food system to limit the negative effects of afforestation and BECCS on food security. The productivity of crop and livestock production systems varies widely between regions, with efficient production in developed regions such as USA and Western Europe as opposed to inefficient production in developing regions such as Sub-Saharan Africa and Southern Asia. Closing yield gaps through improved fertilization, increased irrigation and better management could lead to major increases in productivity (Mueller et al., 2012; Neumann et al., 2010; van Ittersum et al., 2013). Similarly, livestock systems have substantial opportunity for intensification transitioning from grassland-based systems to mixed systems and through improved animal management (Havlík et al., 2014; Herrero et al., 2016). In this way, increased efficiency on the supply side of the food system would reduce land requirements and thus limit the effect of

competition between food production and land-based mitigation on food security. On the demand side of the system, dietary change reducing consumption of livestock products and substituting them by crops has large potential to reduce land requirements because crop production requires less resources (including land) than livestock production (Bajželj et al., 2014; Poore and Nemecek, 2018; Stehfest et al., 2009). A transition to diets with less livestock products would therefore limit the negative effect of land competition on food security.

Solutions to the conflicting nature of climate mitigation and food security have not been formally included in scenario analyses. In this study, we explore how negative effects of land-based mitigation on food security can be prevented by implementing measures on the supply and demand side of the food system – specifically through enhanced agricultural intensification and through dietary change. In this way, we investigate how the climate targets from the Paris Agreement can be made consistent with food security objectives. To quantify this, we perform a model-based analysis using the agro-economic model MAGNET (Woltjer et al., 2014) in combination with the IMAGE integrated assessment model (Stehfest et al., 2014). First, we perform a detailed analysis of the effect of ambitious land-based mitigation on various dimensions of food security. Secondly, we investigate how much agricultural intensification is required to prevent negative effects of land-based mitigation from a food security perspective. Thirdly, we explore how dietary change, through reduced consumption of livestock products, could lower the required level of intensification to maintain food security. For expositional convenience, we make the assessment explicit at the level of six world regions (SI Table 5-1) in order to highlight regional differences in food security effects and food system changes.

5.2. Methods:

5.2.1. Models

5.2.1.1. MAGNET

The Modular Applied GeNeral Equilibrium Tool (MAGNET)(Woltjer et al., 2014) is based on the standard GTAP model (Hertel, 1997), which is a multi-regional, static, applied computable general equilibrium (CGE) model based on neoclassical microeconomic theory. It covers all sectors of the economy (agriculture, manufacturing and services) and all regions and major countries in the world. The core of MAGNET is an input-output model, which links industries in value added chains from primary goods to final goods and services for consumption. Input and output prices are endogenously determined by the markets to achieve supply and demand equilibrium. The agricultural sector is represented in high detail compared to standard CGE models. In MAGNET, factor markets are divided (segmented) into agricultural and non-agricultural labour and capital. This reflects empirical evidence on imperfect mobility of labour (de Janvry et al., 1991), and is thus an improvement above other CGEs which assume perfect mobility. Land is modelled as an explicit production factor described

by a land-supply curve, which specifies the relation between total agricultural land supply and the real land price given constraints related to biophysical availability (potential area of suitable land) and institutional factors (agricultural and urban policy, conservation of nature). The land supply curve is constructed with land availability data provided by IMAGE (Dixon et al., 2016; van Meijl et al., 2006).

Households are assumed to distribute income across savings and (government and private) consumption expenditures according to fixed budget shares following a Cobb-Douglas (CD) expenditure function. Private consumption expenditures are allocated across commodities by introducing a richer representation of income effects in the demand system. In particular, marginal budget shares vary with the expenditure level using a non-homothetic constant differences of elasticity (CDE) expenditure function. Government consumption is allocated across commodities according to fixed budget shares using a CD expenditure function. Labour, capital and natural resources are fully employed in each region and the aggregated supply of each factor equals its demand (equilibrium). Thus, factor markets are competitive between sectors but not between regions. MAGNET assumes that that products traded internationally are differentiated by country of origin following the Armington assumption. This assumption generates smaller and more realistic responses of trade to price changes than implied by models of homogeneous products (Armington, 1969).

5.2.1.2. IMAGE 3.0

IMAGE 3.0⁶ is an integrated assessment modelling framework that simulates the interactions between human activities and the environment (Stehfest et al., 2014), to explore long-term global environmental change and policy options in the areas of climate, land and sustainable development. IMAGE consists of various sub-models describing land use, agricultural economy, the energy system, natural vegetation, hydrology, and the climate system. Most socio-economic processes are modelled at the level of 26 regions. Most environmental processes are modelled on the grid-level at 30 or 5 arc-minutes resolution. Data exchange takes place either through hard-coupling with annual exchange of data, or soft-coupling using an iterative approach of scenario data exchange.

Agriculture, forestry and land-use dynamics are modelled on the grid-level in the IMAGE-Land Management model (Doelman et al., 2018). Demand for crop and livestock products, trends in agricultural intensification and trade dynamics are provided by MAGNET (Section 5.2.1.1). Gridded land-use dynamics are implemented in the dynamic global vegetation model LPJmL to model effects on the carbon and hydrological cycle (Bondeau et al., 2007; Sitch et al., 2003). LPJmL provides data on potential crop and grass yields, land-use change emissions and irrigation water use. The simulation model TIMER represents the energy system with high technological detail for 12 primary energy carrier including bioenergy (van Vuuren, 2007). Land use for the production of bioenergy as determined by TIMER is implemented on

6 For more background info visit the online IMAGE documentation: www.pbl.nl/image.

the grid-level in IMAGE-LandManagement. Greenhouse-gas (GHG) emissions from energy, industry and land use are input to the simple climate model MAGICC which emulates complex climate models to calculate global mean temperature change (Meinshausen et al., 2011). Finally, data on food availability, energy use and climate change are input to the GISMO model which calculates changes in human development in relation to the global environment (Hilderink et al., 2008).

5.2.1.3. Food security indicators

The Food and Agricultural Organization (FAO) distinguishes four dimensions of food security: availability, access, utilization, and stability (FAO, 1996). In this study we present indicators covering the first two of these dimensions as these are well-represented in the implemented models. The availability dimension is represented by two indicators. First, food availability which is defined as ‘kilocalories per capita per day available for consumption’ as calculated by the MAGNET model. Second, ‘the number of people at risk of hunger’ which is a fraction of the population below a minimum level of dietary energy requirements following a method proposed by the FAO (FAO, 2008). It is calculated using the GISMO model (Hilderink et al., 2008) and is based on food availability data from MAGNET, a coefficient of variation dependent on GDP per capita as proposed by Hasegawa et al. (2015b) and region, sex and age specific dietary energy requirements. The food access dimension relates to people’s food purchasing power and therefore to food prices, dietary patterns, and income developments (Lele et al., 2016). This dimension is represented by two indicators calculated by MAGNET. First, the average price development of food including primary agricultural products and processed foods, which neglects the income dimension. Second, as a proxy for the food purchasing power we use the price development of a food consumption basket in relation to income developments of a particular income group. Specifically, we calculate the change in food purchasing power for a cereal diet of unskilled workers working in agriculture (cereal sector) and other sectors by subtracting the change in wages from the change in the price level of the cereal diet.

5.2.2. Scenario implementation

5.2.2.1. Baseline

As a baseline scenario we use the ‘1% World’ scenario (ONEPW) from the FOODSECURE project (van Dijk et al., 2020). The four stakeholder-based FOODSECURE scenarios are designed along two dimensions of equality and sustainability. The ‘1% World’ scenario describes a world where wealth is very unequally distributed. However, people do care about sustainability and protection of biodiversity and the environment. There is substantial investment in technology leading to high technological development in the agricultural sector ensuring that everyone is fed and to ensure protection of biodiversity and the environment. We choose this scenario as it describes an unequal world open to sustainability issues such as mitigating climate change. Moreover, in the 1% World scenario food security increases throughout the scenario period highlighting the difference between improving food security in a baseline scenario

and negative impacts on food security in a mitigation scenario. In addition, the scenario does not include dietary change which is important to analyse the potential of reduced livestock product consumption.

Globally, wealth increases with average GDP rising from 9,500 US\$/capita to 21,300 US\$/capita (Table 5-1; Figure 5-1). However, regional differences remain very large with GDP in the OECD countries increasing up to 77,400 US\$/capita whereas Sub-Saharan Africa achieves 2,900 US\$/capita. Similarly, global population continues to rise up to 9.6 billion people, with the largest increases in developing regions. The global share of people living in Sub-Saharan Africa and South/South-East Asia increases from 12% to 19% and from 32% to 34%, respectively. Exogenous land productivity improvements are high, especially in developing regions (Sub-Saharan Africa and South/Southeast Asia) as agricultural productivity catches up with global standards related to high technological development. Agricultural land availability is low in developed regions (<20% of current agricultural land) as large areas are excluded from agricultural expansion due to high environmental protection standards.

Table 5-1: Macro-economic and land supply assumptions in the baseline scenario, and land-based mitigation assumption in LBM mitigation scenario.

Regions	GDP	Population	GDP per capita	Exogenous land productivity improvement	Share of current agricultural land in total available land (%) in 2010	Average land supply elasticity	Land-based mitigation in 2050 (% agricultural land reduction relative to baseline)
	Average annual growth (%) (2010-2050)						
World	2.9	0.8	2.0	1.0	74	0.08	15
OECD countries	2.2	0.5	1.7	0.7	83	0.02	13
Latin America	3.1	0.8	2.3	0.8	63	0.23	28
Russia/Middle East	3.5	0.9	2.6	1.1	83	0.03	11
Sub-Saharan Africa	3.9	1.9	2.1	1.6	67	0.09	15
South/Southeast Asia	4.6	1.0	3.6	1.4	63	0.18	12
China+	4.4	-0.1	4.5	0.4	89	0.02	12

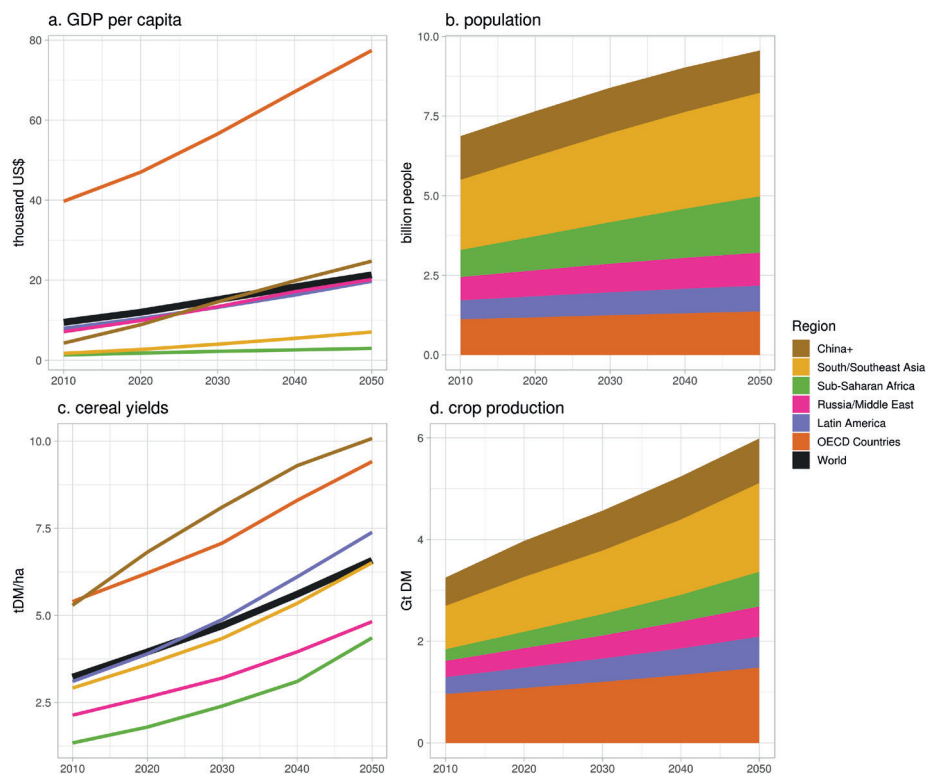


Figure 5-1: GDP, population, yield and crop production in the '1% World' (ONEPW) scenario.

5.2.2.2. Land-based mitigation

MAGNET does not model land-based mitigation directly. Therefore, the land area required for land-based mitigation is implemented exogenously and forces a certain reduction in actual agricultural land use over the scenario period (Figure 5-3). As a consequence, also the land-supply curve of MAGNET is shifted in line with the implemented land area requirement. Figure 5-2 shows a graphic representation of the approach. In the baseline scenario, no distinction is made between total land supply and agricultural land supply. Land demand is shown by the yellow line which intersects in point A providing total land supply (LS) and land price in the baseline scenario (P-base). In a mitigation scenario, total land supply (LS-tot) is distinguished from agricultural land supply (LS-agr) where the difference is accounted for by the land-based mitigation area. The agricultural land supply curve is shifted to the left (less supply) to accommodate the area required (green arrow) leading to a new equilibrium in point B at a higher land price (P-LBM). The restricted land use results in adjusted food prices, food consumption, trade and agricultural efficiency which consequently affect food security (Tabeau et al., 2017).

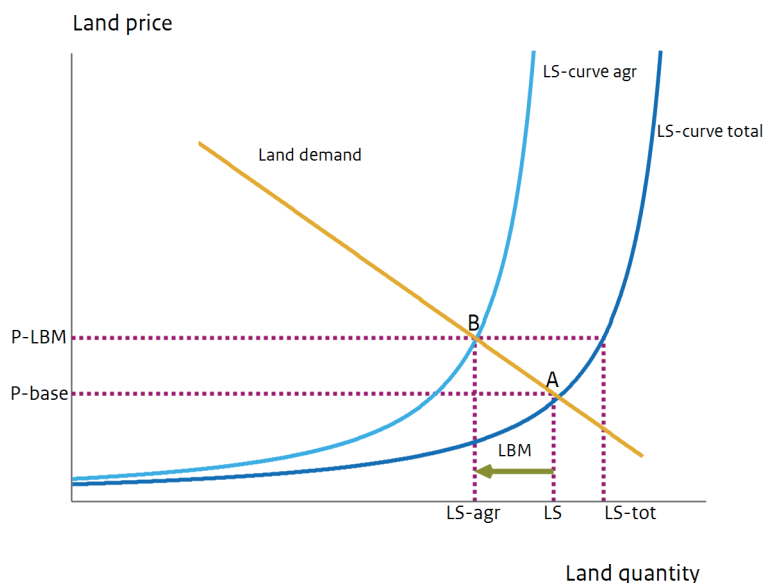


Figure 5-2: Graphic representation of total land supply curve (LS-curve total) and agricultural land supply curve (LS-curve agr). In a baseline scenario land demand (yellow line) is in equilibrium in point A with land supply LS and land price P-base. In a mitigation scenario total land supply (LS-tot) is distinguished from agricultural land supply (LS-agr) where the difference is land-based mitigation (LBM, green arrow). The agricultural land supply curve is shifted to accommodate this area leading to a new equilibrium in point B at a higher land price (P-LBM).

Areas required for land-based mitigation to achieve the Paris Agreement climate target are derived from literature on the SSP scenarios as implemented by several integrated assessment models (IAMs) in a coordinated effort (Popp et al., 2017). Across-model average areas of land-based mitigation (i.e. afforestation and bioenergy with and without CCS) are calculated for the SSP2 scenario combined with an RCP 1.9 climate change target for five world regions as presented in Rogelj et al. (2018). We decided to use this scenario as it is the most ambitious climate-change mitigation target in recent literature which is highly relevant in the current discussions on achieving the 1.5-degree target. We take the average land-based mitigation area from four models: AIM/CGE (Fujimori et al., 2014), GCAM4 (Wise et al., 2014), GLOBIOM (Havlík et al., 2014) and REMIND-MAGPIE (Popp et al., 2014). The land-based mitigation area varies substantially between the models ranging from 410 Mha (AIM/CGE) to 950 Mha (GCAM4) in 2050. These results represent the state-of-the-art of land-based mitigation estimates to achieve stringent climate targets, illustrating the large uncertainty that is present in the literature. We use the average reduction in cropland for food and feed and the reduction in grazing land per world region of the four aforementioned models. Globally, this implies a reduction in agricultural land use of ~600 Mha compared to baseline. In absolute terms, the largest change takes place in Latin America with a 28% reduction in agricultural land use compared to baseline levels (160 Mha)(Table 5-1). The changes in other regions range from 11% to 15%.

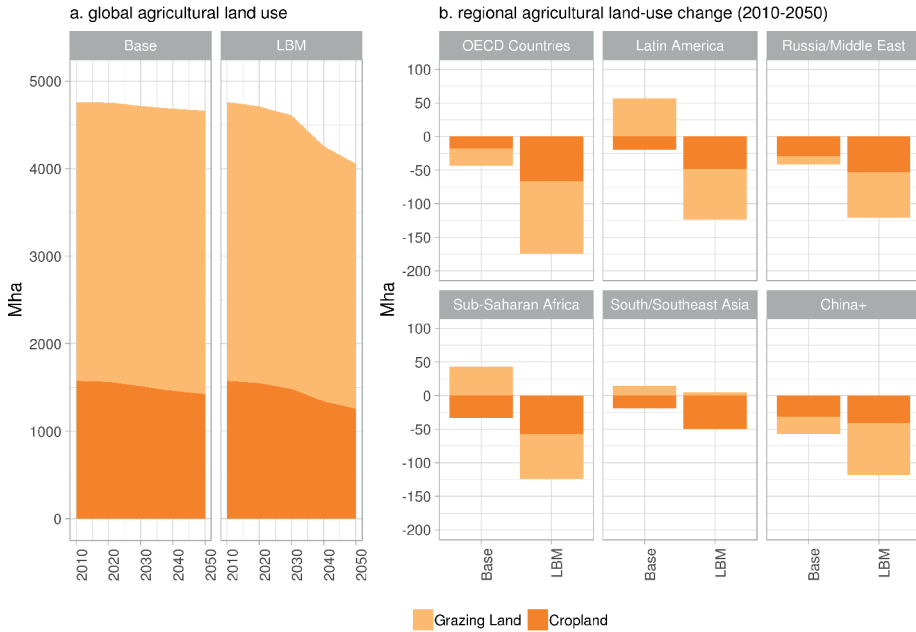


Figure 5-3: a) Global cropland for food/feed and grazing land in baseline and LBM mitigation scenario and b) regional land-use change in baseline and LBM mitigation scenario

5.2.2.3. Agricultural intensification

Additional agricultural intensification, e.g. through closure of the yield gap or increased efficiency in the livestock sector, can prevent negative effects of land-based mitigation on food security. To investigate the level of required intensification, a scenario is designed to keep average agricultural price in a mitigation scenario at the same level as in the baseline scenario in each region. To achieve this, the average agricultural price is exogenously fixed at the baseline level. The level of land productivity in the agricultural sector is endogenously determined (increasing uniformly across all agricultural commodities) within the model run for each region. In this way, we assume that the average agricultural price change caused by mitigation is compensated by additional intensification in the agricultural sectors. The model endogenously determines the level of agricultural intensification required in each region to absorb the effect of land-based mitigation on average agricultural price. By fixing average agricultural prices on baseline levels, also total food availability is similar to the baseline because prices levels are the same as in the baseline and income levels are close to the baseline.

5.2.2.4. Diet change

Next to agricultural intensification, changes in diet towards less meat consumption reduces demand for agricultural land, and thus can help to prevent negative effects of land-based mitigation on food security. To test how diet change can help to reduce concerns for food security a low meat diet pattern is introduced. A reduction in the consumption of ruminant and non-ruminant meat is implemented by exogenously prescribing meat consumption. In contrast to the standard settings, consumer preferences concerning meat are endogenously determined. Total food consumption volume is kept constant to assure that the reduction in meat is replaced by consumption of crops and dairy products. To achieve this, consumer preferences concerning overall food consumption are also endogenously determined. The low meat diet changes include strong reductions in China and Latin America (from 640 to 370 kcal/cap/day and from 420 to 270 kcal/cap/day, respectively, from baseline to diet scenario) and moderate reductions in Russia/Middle East and the OECD countries (from 240 to 130 kcal/cap/day and from 560 to 470 kcal/cap/day, respectively, from baseline to diet scenario resp.). No reductions are assumed in Sub-Saharan Africa and South/Southeast Asia as meat consumption in these regions is already comparatively low. The implemented changes are modest compared to the recommended meat consumption of 92 kcal/cap/day in the recently proposed healthy diet from sustainable food systems by Willett et al. (2019).

5.2.2.5. Scenario definitions

Four scenarios are implemented in this study (Table 5-2). As described in Section 5.2.2.1, the ONEPW scenario is used as a baseline (Base). To investigate the effect of land-based mitigation on food security, the baseline is combined with a prescribed land area for land-based mitigation derived from IAMs (Section 5.2.2.2) in the Land-Based Mitigation (LBM) scenario. In the LBM-Yield scenario yields are endogenously increased to achieve food prices as in the baseline scenario (Section 5.2.2.3). Additional diet change is implemented in the LBM-Diet-Yield scenario and yields remain endogenously determined to achieve baseline food prices (Section 5.2.2.4). Land-based mitigation, agricultural intensification and dietary change are implemented in the MAGNET model; subsequently, trends in agricultural demand, production, intensification and trade are implemented in IMAGE to determine spatial explicit land-use dynamics and number of people at risk of hunger (Section 5.2.1). As the focus of this paper is the impact of land-based mitigation on food security we do not consider negative effects of climate change on food security.

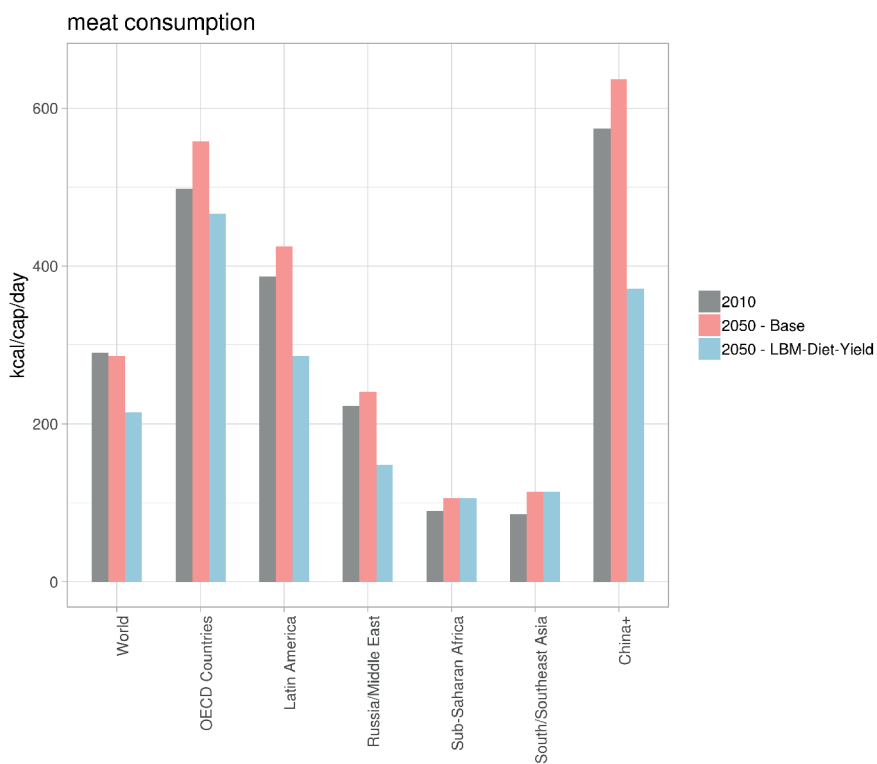


Figure 5-4: Meat consumption changes as implemented in the LBM-Diet-Yield scenario.

Table 5-2: Table with definitions of implemented scenarios, land-based mitigation is based on several IAM 1.5 degree scenarios (see Section 5.2.2.2).

Scenario name	Start settings	Land-based mitigation	Yield increase to achieve baseline food prices	Preference change for low-meat diet
Base	ONEPW	-	-	-
LBM	ONEPW	~600 Mha	-	-
LBM-Yield	ONEPW	~600 Mha	Yes	-
LBM-Diet-Yield	ONEPW	~600 Mha	Yes	Yes

5.3. Results

5.3.1. Food security effects of land-based mitigation

In the baseline scenario major improvements in food security are achieved. The availability dimension of food security shows an increase of global average food availability by 230 kcal/cap/day (Figure 5-5a) and a decrease in the number of people at risk of hunger of 402 million (Figure 5-6), from 2010 to 2050. Regionally, the largest changes take place in the developing regions with strong increases in food availability in Sub-Saharan Africa and South/Southeast Asia (500 and 560 kcal/cap/day resp. from 2010 to 2050) driven by high increases in per capita income (Figure 5-1a) and by strong technological growth in crop productivity, especially in developing regions that are catching up with developed regions. This trend is also reflected in the number of people at risk of hunger which decreases by 254 million people in South/Southeast Asia from 2010 to 2050. In Sub-Saharan Africa, characterised by low GDP per capita growth, the reduction is only 35 million people from 2010 to 2050 as the average food availability is still lower than in other regions, and because the fraction of people at risk of hunger is reduced but the absolute number of people is strongly increasing. China, with a much higher GDP per capita growth, shows a reduction in number of people at risk of hunger, even though food availability is going down slightly. This is possible as the coefficient of variation decreases with the high increase in GDP resulting in improved distribution of food across the population.

The access dimension of food security also improves in the baseline scenario. Aggregated food prices show a moderate decrease of 4% by 2050 on the global level. Regionally, stronger decreases take place most notably in Latin America and Russia/Middle East (14% and 19% resp. by 2050). Increases in food prices occur in South/Southeast Asia and China, among others related to continued population growth in combination with limited possibilities to expand agricultural land (Table 5-1: Macro-economic and land supply assumptions in the baseline scenario, and land-based mitigation assumption in LBM mitigation scenario. Table 5-1). At the same time, purchasing power more than doubles for unskilled workers in other sectors than agriculture as a result of increasing wages in combination with reducing food prices in most regions (Figure 5-5d). Unskilled workers in the cereal sector experience less improvement in food purchasing power than their equivalent in other sectors due to lower increase in wages that are partly induced by the lower agricultural prices and the segmentation of the labour market (Figure 5-5c).

Land-based mitigation in the LBM scenario leads to increased land scarcity, from a food production perspective, which negatively affects food prices and food security. As a consequence, the improvements in food availability are reduced with global average food availability 100 kcal/cap/day lower in LBM in 2050 compared to the baseline. The same effect takes place in the number of people at risk of hunger, with 232 million more people at risk of hunger in LBM in 2050 compared to the baseline. Regionally, reductions in food availability are fairly similar between regions (3%-5% in LBM in 2050 compared to Base). However, the

number of people at risk of hunger is unevenly distributed with 181 million people extra in Sub-Saharan Africa and South/Southeast Asia compared to 51 million people in other regions (LBM compared to Base in 2050). This is due to the relatively low food availability compared to other regions which increases the number of people below the threshold indicating risk of hunger. Globally averaged food prices go up by 11% in LBM compared to the baseline in 2050, with a very strong increase in South/Southeast Asia (32%) due to the tight land market. Purchasing power goes down for all unskilled labour mainly driven by the higher food prices.

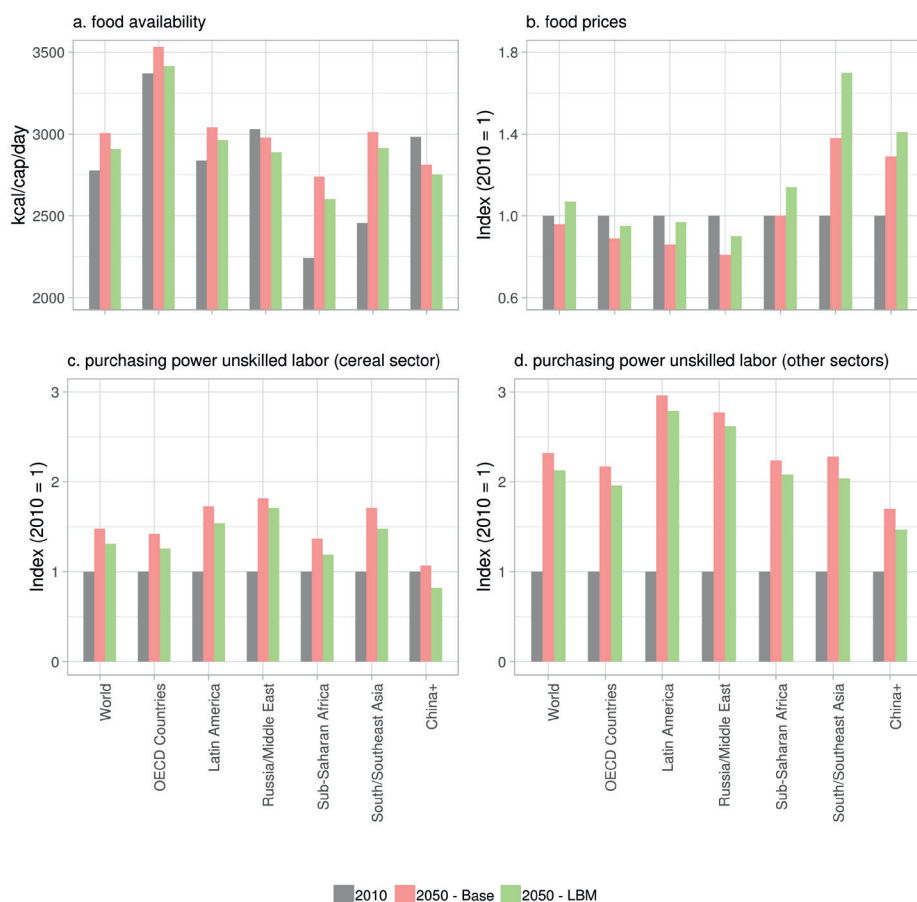


Figure 5-5: Global and regional a) food availability, b) food prices, purchasing power of unskilled labour in c) the cereal sector and in d) other sectors in the baseline and LBM scenarios for 2010 and 2050.

Land-based mitigation also affects crop and livestock intensification through price-induced substitution effects. As land prices increase relatively to wages and capital rents, land will be substituted by capital and labour in agriculture and consequently leads to a higher land productivity. This partially counterbalances the negative effect of land-based mitigation on

food security. Globally averaged crop yields in 2050 increase due to intensification by an additional 8% in the LBM scenario compared to the baseline (Figure 5-7). This is caused by the increased land competition and induced higher land prices due to land-based mitigation which causes a 13% reduction in agricultural land in LBM compared to Base. Crop yields increase more due to intensification with further reduction in agricultural land. For example, in 2050 in Latin America agricultural land is reduced by 22% and yields increase by 21% in LBM compared to the baseline, while in South/Southeast Asia agricultural land is reduced by 11% and yields increase by 5%.

Production of ruminant products such as meat and dairy is predominantly grass-based and responsible for two thirds of agricultural land use. Total ruminant production (in ton dry matter) relative to grassland area provides an indication of ruminant production system efficiency. In 2050 in the LBM scenario, ruminant efficiency increases by 11% compared to baseline due to reduced land availability. Between regions, efficiency increases vary from 6% in South/Southeast Asia to 18% in Latin America in 2050 in LBM compared to the baseline, roughly at similar levels as crop yield increases. In Sub-Saharan Africa however, the ruminant efficiency increase is substantially higher with 12% compared to a crop yield increase of 6% in 2050 in LBM compared to the baseline. This is related to low initial ruminant efficiency.

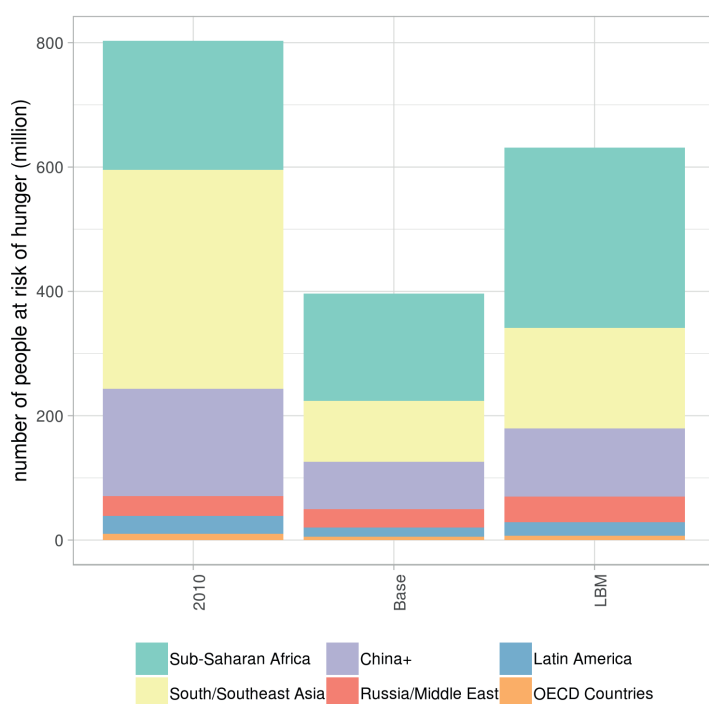


Figure 5-6: Number of people at risk of hunger in 2010, in 2050 in the baseline scenario and in 2050 in the LBM scenario.

5.3.2. Preventing negative effects of land-based mitigation on food security

To prevent negative effects of land-based mitigation on food security, we increase agricultural intensification until food prices and food availability are at the same level as the baseline scenario. It is shown that, in 2050 on the global level, an additional 9% increase in crop yields and an additional 3% increase in ruminant efficiency is sufficient to prevent negative food security impacts of land-based mitigation, as is shown by comparing the LBM-Yield scenario to the LBM scenario in (Figure 5-7). The larger increase in crop yields compared to ruminant efficiency is due to the relatively higher cost share of cropland compared to grassland in agricultural prices. As our exercise returns food prices to baseline level through increases in capital and labour to boost land productivity, more production factors are needed in the crop sector than the livestock sector leading to higher increases in crop yield than in ruminant efficiencies. Regionally, additional crop yield increases range from 5% in China to 12% in the OECD countries (LBM-Yield compared to LBM in 2050). Changes in ruminant efficiency range from a 9% increase in Latin America to a 0.5% decrease in efficiency in OECD countries (LBM-Yield compared to LBM in 2050). The decrease in OECD countries is also due to the abovementioned effect that the majority of production factors is needed to stimulate crop productivity.

To investigate how diet change helps to limit negative effects on food security we reduce meat consumption and subsequently analyse how much agricultural intensification is still required to achieve food prices and food availability as in the baseline scenario. On the global level, the required crop yield increase is 2% lower and the required ruminant efficiency increase is 1% lower in the LBM-Diet-Yield scenario compared to the LBM-Yield scenario in 2050. The beneficial effects are more substantial on the regional level, most notably in Latin America and China as in these regions we implement the largest reductions in meat consumption (Figure 5-4). In Latin America, little additional improvement in crop yield or ruminant efficiency is required to achieve baseline food security (<2% when comparing LBM and LBM-Diet-Yield in 2050). In China, crop yield improvements required to achieve baseline food prices and food availability in LBM-Diet-Yield in 2050 are even below those in the LBM scenario, however improvements in ruminant efficiency are not substantial. In Sub-Saharan Africa and South/Southeast Asia, crop yields and ruminant efficiencies slightly increase as they do not experience reduced demand internally, but do slightly increase their export of crops due to increased demand from other regions. Counterintuitively, Russia/Middle East also shows an increase in both crop yields and ruminant efficiency. This is due to increased crop exports and a substantial shift from meat to dairy products, respectively. The shift to dairy products results in increased ruminant efficiency as dairy is substantially more productive than meat per unit of grassland.

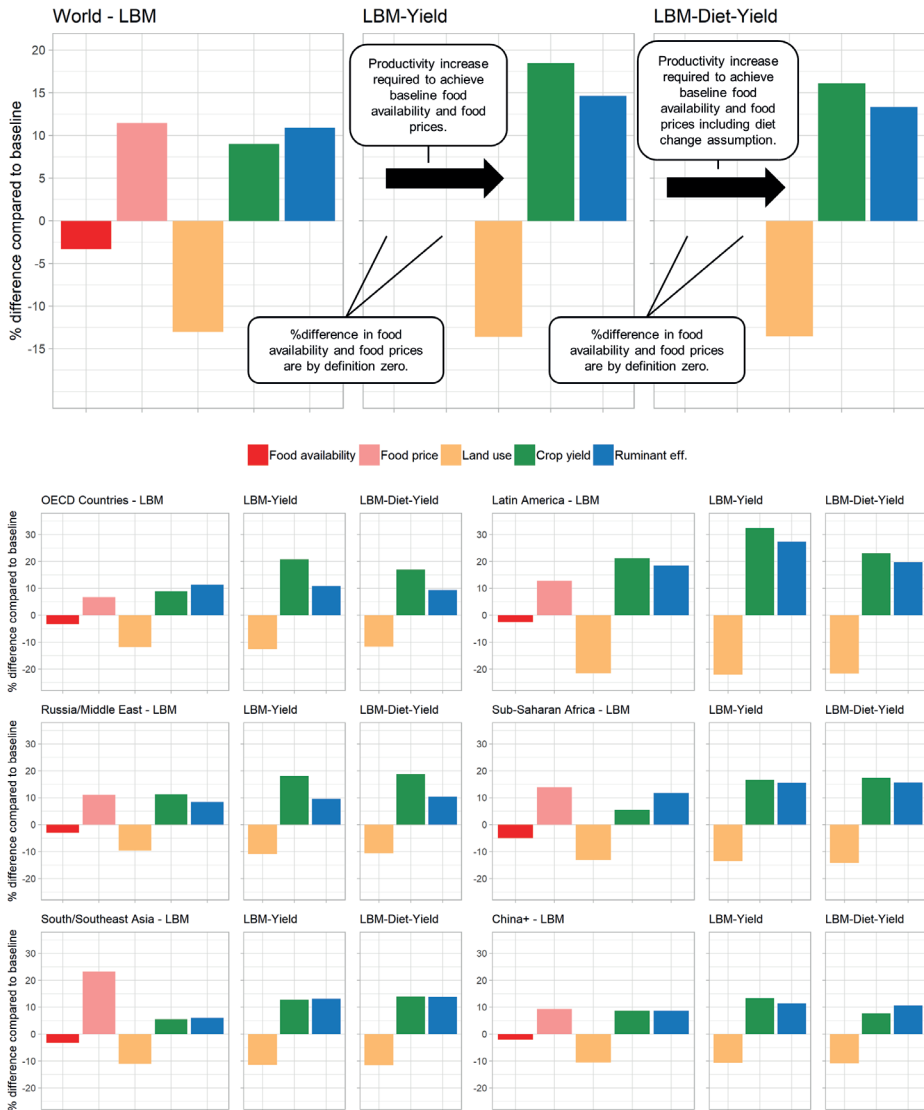


Figure 5-7: Percentage difference in food availability, food prices, land use, crop yields and ruminant efficiency (ruminant meat and dairy production divided by grassland area) for the LBM, LBM-Yield and LBM-Diet-Yield scenarios compared to the baseline scenario on the global and the regional level. Comparing LBM to LBM-Yield shows the increases in yield and ruminant efficiency required to achieve zero change in food availability and food prices compared to the baseline scenario. Comparing LBM to LBM-Diet-Yield shows the increases in yield and ruminant efficiency required to achieve zero change in food availability and food prices compared to the baseline scenario when additional diet change is assumed.

5.4. Discussion

Land-based mitigation as implemented in this study is based on four IAMs that assume uniformly implemented carbon price globally, i.e. in the energy, agriculture and forestry sectors. These results generally represent the most cost-optimal solution to climate change mitigation, however whether the scale at which BECCS and afforestation are applied in response to this uniform carbon price will in reality be feasible from a governance and a social-acceptance perspective is an open question (Nemet et al., 2018). Assuming that large-scale land-based mitigation is realistic, the results of this paper show that a cost-optimal approach across all sectors has significant trade-offs with food security. This is confirmed by other studies with IAMs that have assessed the effect of land-based climate change mitigation reporting significant rises in food prices (Calvin et al., 2014; Kreidenweis et al., 2016), decreased food availability and increasing numbers of people at risk of hunger (Frank et al., 2017; Hasegawa et al., 2018, 2015a; van Meijl et al., 2018). The sensitivity of food consumption to changes in food prices, i.e. the food demand elasticity, is highly debated. Empirical analyses show that food demand elasticities are low, most notably in high-income countries (Muhammad et al., 2011). Elasticities vary substantially between agro-economic models, with some models assuming zero elasticity (MAGPIE (Lotze-Campen et al., 2008)) or zero elasticity of all staple crops (GCAM (Calvin et al., 2014)). A model intercomparison of 9 agro-economic models showed that the elasticity of food demand to food price change in MAGNET is in the middle range compared to other models (Nelson et al., 2014), however especially under large shocks such as the land-based mitigation areas implemented in this study it is uncertain how food demand will exactly be affected. This implies that uncertainties in food demand elasticities play a fundamental role in food security assessments and therefore require continued research as well as transparent communication of assumptions.

Our results show that additional agricultural intensification can prevent negative effects of land-based mitigation on food security. Historically, cereal yields have shown a continuous linear increase since 1961 (SI Figure 5-1)(FAOSTAT, 2020), with a doubling over the 1970-2010 period. An additional increase of 9% in crop yields (LBM compared to LBM-Yield in 2050) is required on the global level to maintain food security at baseline levels, which is equal to 4 years of historical cereal yield increases. Regionally, historical cereal yield increases in 1970-2010 ranged from 53% in Russia/Middle East to 154% in China+. The regional additional crop yield increases required to maintain food security ranges from 5% to 12% which is well within this range. These yield increases do need to take place in addition to baseline yield increases. The ONEPW scenario used in this scenario shows an increase in yields from 2010 to 2050 of slightly over 100%. This implies a continuation of historical trends which is in line with the scenario assumption on high investment in technological developments leading to strong increases in agricultural productivity. Compared to other scenarios in the literature these yield projections are on the high end (Alexandratos and Bruinsma, 2012; FAO, 2018b; Popp et al., 2017), but baseline projections of yields are very uncertain and the high yields are consistent with the technology-oriented world view in this ONEPW scenario. It is widely acknowledged that there is major potential for increased production in developing regions

with large yield gaps (Mueller et al., 2012; Neumann et al., 2010; van Ittersum et al., 2013); for developed countries, however, studies argue that yield levels will not continue to increase at historical rates, but rather level off due to biological limits of crop productivity (Grassini et al., 2013). Negative impacts of climate change, which are very uncertain and not included in this study, might further reduce the possible future increase in crop yields (Rosenzweig et al., 2014; Zhao et al., 2017). In conclusion, although baseline projections of yields are uncertain, the additional yield requirements to ensure food security are modest compared to historical yield trends.

Ruminant efficiencies have historically shown a linear increase with a total increase of 70%⁷ over the period 1970-2010 (SI Figure 5-2 and SI Figure 5-3). In the scenario period, improvements continue linearly with a 50% improvement from 2010 to 2050. The required intensification to maintain food security is modest in our results (3% in LBM-Yield compared to LBM). Livestock system efficiencies vary widely, most notably between developed and developing regions (Bouwman et al., 2005; Herrero et al., 2013), indicating high potential for efficiency improvements. This is confirmed by studies focusing on climate mitigation benefits of increased livestock efficiencies (Havlík et al., 2014; Herrero et al., 2016). On the other hand, a substantial share of ruminant production takes place on marginal lands through traditional, smallholder production systems (McDermott et al., 2010) where intensification might be infeasible. Still, as our results only show a modest acceleration in ruminant efficiency improvements our estimates seem to be relatively conservative compared to the potential of livestock intensification discussed in the literature. Our results show more intensification in the crop sector than in the livestock sector even though the latter also has large intensification potential. Part of the reason for this is that we considered intensification in both sectors simultaneously through changing land productivity. Follow-up research might consider both options separately to identify differences between these approaches.

Multiple studies have shown the benefits of reduced livestock product consumption as it has large potential to reduce land requirements because crop production requires less resources (including land) than livestock production (Bajželj et al., 2014; Frank et al., 2019; Stehfest et al., 2009). This study confirms that reduced meat consumption also helps to reduce impacts on food security through reduced land demand. On the global scale, the effects in our results are limited as we only reduce meat consumption in high- and middle-income countries, while meat consumption still increases moderately in low-income countries. In regions with large changes however (Latin America, China+), the effects are also large leading to lower agricultural intensification requirements. As our assumptions are above recommended intake levels in all high- and middle-income regions (Willett et al., 2019) (Section 5.2.2.4), the role of diet change could in fact be larger than presented in this study. On the other hand, a major uncertainty is how a lifestyle change such as reduced meat consumption can in practice be achieved.

7 This value is a correction compared to the original publication which erroneously stated 60%. The corrected value does not affect the conclusions of the article.

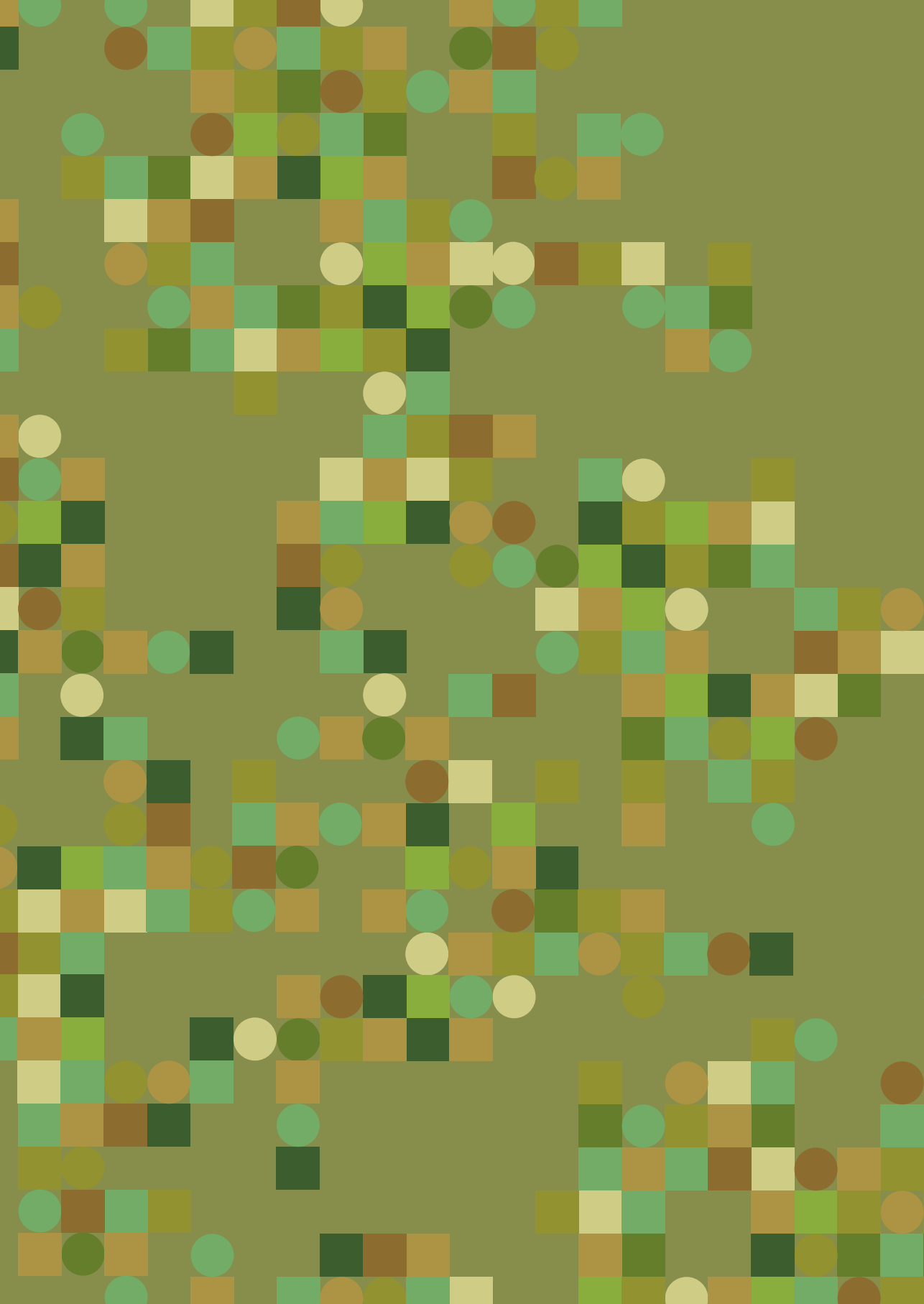
5.5. Conclusions

Climate change mitigation is important to prevent negative impacts of climate change on food production. However, in this study we show that large-scale land-based mitigation in cost-optimal pathways consistent with the Paris Agreement also leads to negative impacts on food security due to competition for land. On the global level, we show that both the availability and the access to food, two important dimensions of food security, are significantly reduced compared to baseline levels due to large-scale land-based mitigation. On the regional level, especially developing regions are affected as the number of people at risk of hunger increases most notably in Sub-Saharan Africa and South/Southeast Asia. Possible solutions to limit the negative effects of land-based mitigation on food security are additional agricultural intensification and dietary change. We explicitly include these options in our scenarios, showing that a modest increase in crop yields and livestock efficiency can prevent negative effects on food security, although the feasibility of future yield increases remains an important uncertainty. Reduced meat consumption lowers the required improvements, most notably in regions where meat consumption is currently relatively high.

Achieving food security for all (SDG2) as well as preventing climate change (SDG13) are important aspects of a sustainable future as defined by the Sustainable Development Goals. Both our study and various other studies have identified the negative effects on food security that arises in cost-optimal pathways that mitigate climate change. Scenario studies need to be transparent about this trade-off and where possible include explicit policy to prevent negative effects. Our study provides an example of explicitly including measures to prevent negative trade-offs in scenarios. In this way, we show how pathways in line with the Paris Agreement can be made consistent with food security objectives and how multiple Sustainable Development Goals can be achieved.

Acknowledgements

The authors gratefully acknowledge the support of the European Union's Seventh Framework programme FP7/2007-2011 under Grant Agreement n°290693 FOODSECURE. The views expressed are the sole responsibility of the author(s) and do not necessarily reflect the views of the European Commission.



CHAPTER 6

Quantifying synergies and trade-offs in the global water-land-food-climate nexus using a multi-model scenario approach

Jonathan C. Doelman, Felicitas D. Beier, Elke Stehfest, Benjamin L. Bodirsky, Arthur H.W. Beusen, Florian Humpenöder, Abhijeet Mishra, Alexander Popp, Detlef P. van Vuuren, Lotte de Vos, Isabelle Weindl, Willem-Jan van Zeist, Tom Kram

"Quantifying synergies and trade-offs in the global water-land-food-climate nexus using a multi-model scenario approach" Environmental Research Letters 17 (2022): 045004



Abstract

The human-earth system is confronted with the challenge of providing a range of resources for a growing and more prosperous world population while simultaneously reducing environmental degradation. The Sustainable Development Goals and the Planetary Boundaries define targets to manage this challenge. Many of these are linked to the land system, such as biodiversity, water, food, nutrients and climate, and are strongly interconnected. A key question is how measures can be designed in the context of multi-dimensional sustainability targets to exploit synergies. To address this, a nexus approach is adopted that acknowledges the interconnectedness between the important sub-systems water, land, food, and climate. This study quantifies synergies and trade-offs from ambitious interventions in different components of this Water-Land-Food-Climate nexus at the global scale. For this purpose, a set of six harmonized scenarios is simulated with the MAGPIE and IMAGE models. The multi-model approach improves robustness of the results while shedding light on variations coming from different modelling approaches. Our results show that measures in the food component towards healthy diets with low meat consumption have synergies with all other nexus dimensions: Increased natural land improving terrestrial biodiversity (+4% to +8%), lower greenhouse gas emissions from land (-45% to -58%), reduced irrigation water withdrawals to protect or restore hydrological environmental flows (-3% to -24%), and reductions in nitrogen surpluses (-23% to -35%). Climate mitigation measures in line with the Paris Agreement have trade-offs with the water and food components of the nexus, as they adversely affect irrigation water withdrawals (+5% to +30% in 2050 compared to reference scenario) and food prices (+1% to +20%). The analysis of a scenario combining all measures reveals how certain measures are in conflict while others reinforce each other. This study provides an example of a nexus approach to scenario analysis providing input to the next generation of pathways aiming to achieve multiple dimensions of sustainable development.

6.1. Introduction

The human population is expected to grow to around 9.4-10.1 billion people in 2050 and to become wealthier (Dellink et al., 2017; UN, 2019). These developments lead to continued increases in the use of key natural resources such as land, water, and energy, thereby further aggravating environmental degradation throughout the world (FAO, 2018b; UNCCD, 2017). A crucial question is how the provision of natural resources to sustain societies can be reconciled with maintaining a sustainable state of the environment and how this can be achieved. Climate change impacts further exacerbate these challenges (IPCC, 2019b).

The ambition to achieve sustainable resource use and protect the environment along multiple dimensions is manifested in the Sustainable Development Goals (SDGs) (UN, 2015) and the Planetary Boundaries (PBs) (Rockström et al., 2009; Steffen et al., 2015). The SDGs and PBs cover a wide range of topics including socio-economic targets on energy and food security as well as environmental ambitions on excessive nutrient use and climate change. Implementing policies to achieve certain goals without considering interactions might negatively impact other goals. For example, climate change mitigation could involve large-scale bioenergy deployment which might negatively affect food security and terrestrial biodiversity (Hasegawa et al., 2015a; Smith et al., 2016). On the other hand, policies might also synergistically benefit other targets, for example achieving universal electricity access in Sub-Saharan Africa could greatly reduce respiratory diseases as well as deforestation (Dagnachew et al., 2018). Understanding these interlinkages and accounting for potential synergies and trade-offs is crucial to design effective policies and to achieve policy coherence (Nilsson et al., 2016; UNEP, 2019).

To take many relevant relationships into account, a nexus approach is useful. It recognizes that components of a system are inherently interconnected and must be investigated and managed in an integrated, holistic manner (Hoff, 2011). A meta-study investigating the literature on the water-energy-food nexus found that only 30% of nexus studies applied quantitative methods (Albrecht et al., 2018). The majority of these studies focus on the local or regional scale (Karlberg et al., 2015; Yang et al., 2016). Nexus studies with a global perspective have been relatively few, although the number is increasing (Humpenöder et al., 2018; Obersteiner et al., 2016; OECD, 2017; van Vuuren et al., 2019). To our knowledge this is the first multi-model study on the global nexus. While modelling at the global scale inherently involves simplifications and high uncertainty, the global scale of the challenges concerned makes it important to also assess them on the global level in addition to local and regional studies. Global-level modelling studies make it possible to define overall targets, to guide policy ambitions and to pinpoint risks for policy coherence. Integrated assessment models, originally designed to study the interactions between the energy, land, and climate systems, are developing their representation of multiple sustainable development dimensions and the nexus (van Soest et al., 2019). As they already represent numerous human-environment

interactions and possible policy interventions, they are well-suited for global quantitative nexus assessments (Johnson et al., 2019).

The goal of this study is to quantify synergies and trade-offs in the Water-Land-Food-Climate (WLFC) nexus based on a multi-model scenario analysis at the global scale while also accounting for local relationships. The analysis uses a set of scenarios with harmonized assumptions and input that focus on aspects broadly related to the land system such as biodiversity, water, food, nutrients and climate. The four components of the WLFC nexus are selected as developments in each of these components affects and is affected by the other components. Furthermore, they are at the core of the PB concept (Rockström et al., 2009; Steffen et al., 2015) and central to the SDGs (UN, 2015). Six scenarios are simulated: one business-as-usual scenario, four scenarios focusing on measures in individual nexus components, and one scenario combining measures in all nexus components. The scenario focusing on water addresses excessive water use and negative implications for aquatic biodiversity (Vörösmarty et al., 2010), which corresponds to the PBs on freshwater use and the nitrogen cycle as well as to SDG6 on Clean Water. The scenario focusing on land represents an ambitious conservation scheme that protects half of the Earth to support terrestrial biodiversity (Wilson, 2016), which responds to the PBs on biodiversity loss, the nitrogen cycle and land-use change and to SDG15 on Life on Land. The scenario focusing on food addresses the importance of healthy diets and their impact on the environment (Springmann et al., 2018; Stehfest et al., 2009), in line with the EAT-Lancet report proposing healthy diets from sustainable food systems (Willett et al., 2019) and SDG2 on Zero Hunger. The scenario focusing on climate aims to limit climate change to reduce its risks and impacts in line with the Paris Agreement (UNFCCC, 2015) as well as the PB on climate change and SDG13 on Climate Action. In all the scenarios, climate change impacts and adaptation are taken into account. The scenarios are analysed using the following set of indicators: Irrigation water withdrawal, natural land, food prices, land-based GHG emissions and nitrogen surpluses in agriculture.

The scenarios are implemented in two models: The land-systems modelling framework MAgPIE 4.3 (Dietrich et al., 2019) and the integrated assessment model IMAGE 3.2 (Stehfest et al., 2014; van Vuuren et al., 2021). Both models cover the WLFC nexus in high detail and are extensively applied to study these topics (Humpenöder et al., 2018; Van Vuuren et al., 2019). While the representation of biophysical components (crop yields, water and carbon) is similar in both models, the solution concepts and methods differ. MAgPIE is a partial equilibrium model of the agricultural sector, which is solved recursive dynamically with the objective function of cost minimization (optimization model). IMAGE combines a global general equilibrium approach with a grid-based analysis and high biophysical detail. By implementing these scenarios in two models the variation in results dependent on modelling approaches is highlighted: this provides additional insights and improves the robustness of the results.

6.2. Methods

In this study, we implement a set of six scenarios with harmonized assumptions covering different components of the nexus in the MAgPIE and IMAGE models. The models are described in Section 6.2.1 and in further detail in SI Sections S6.2 and S6.3. Detailed descriptions of the scenarios, assumptions and input data are provided in Section 6.2.2 and SI Section S6.5. The results are analysed and compared across models, scenarios and at the global and regional level using a set of five indicators as described in Section 6.2.3. Additional detail on the modelling procedures and key differences and similarities in IMAGE and MAgPIE is provided in SI Section S6.4.

6.2.1. Model descriptions

6.2.1.1. Model of Agricultural Production and Its Impact on the Environment (MAgPIE)

The MAgPIE 4.3 modular open-source land-systems modelling framework⁸ (Dietrich et al., 2019) simulates possible future land-use patterns and crop production using a recursive dynamic partial equilibrium approach (Lotze-Campen et al., 2008) (for detailed model description see SI Section S6.2). Based on biogeophysical inputs at 30 arc-minute spatial resolution from the global dynamic vegetation, crop and hydrology model LPJmL (Bondeau et al., 2007; Müller and Robertson, 2014), country-level socio-economic data and policy scenarios, it derives optimal land-use patterns and future land-use changes. The objective is to meet global food (Bodirsky et al., 2020), feed (Weindl et al., 2017b, 2017a), material and bioenergy demand (Popp et al., 2011) while taking international trade (Schmitz et al., 2012), resource constraints (land, water, and nutrient availability), biophysical conditions (spatially explicit crop and pasture yields, carbon densities) and possible future socio-economic scenarios into account.

To determine the optimal amount, type, and location of agricultural production, MAgPIE's constrained optimization follows a global production cost minimization approach (Popp et al., 2011). Future food demand is estimated based on food intake, dietary composition, and food waste. Food intake is projected based on population size, per capita income, sex and age structure, and the population's physical activity level, while dietary composition and food waste ratio depend in the model solely on per-capita income (Bodirsky et al., 2020). Feed demand depends on regional livestock production and regionally-dynamic feed efficiencies and dynamic feed basket composition feed (Weindl et al., 2017b, 2017a). Bioenergy demand is set exogenously (Klein et al., 2014; Kriegler et al., 2017; Popp et al., 2011), but MAgPIE endogenously determines the optimal location of the three biomass types (bioenergy grasses, bioenergy trees, and residues). Climate change affects production via

⁸ The MAgPIE modular framework code is open-source and can be found on GitHub: <https://github.com/magpiemodel/magpie>. The code is comprehensively documented under <https://rse.pik-potsdam.de/doc/magpie/4.3/> and a model description is available in the model description article published in Geosci. Model Dev. (<https://gmd.copernicus.org/articles/12/1299/2019/>).

its impacts on available water and attainable yields that are provided by LPJmL leading to adaptation in the food system such as changes in crop type, spatial relocation within a region, international trade, irrigation, or management intensification. GHG emissions arise from the transformation of natural land into cropland or pastureland as well as from livestock and cropland production. N₂O emissions are accounted for in the Nitrogen (N) flow module (Bodirsky et al., 2014, 2012) that transforms all biomass flows into N flows.

6.2.1.2. Integrated Model to Assess the Global Environment (IMAGE)

IMAGE 3.2 is an integrated assessment modelling framework⁹ that simulates the interactions between human activities and the environment (Stehfest et al., 2014) to explore long-term global environmental change and policy options in the areas of climate, land, and sustainable development (for detailed model description see SI Section S6.S6.3). IMAGE consists of various sub-models describing land use, agricultural economy, the energy system, natural vegetation, hydrology, and the climate system. Socioeconomic processes are modelled at the level of 26 regions. Most environmental processes are modelled on the grid-level at 30 or 5 arc-minutes resolution.

Agriculture, forestry, and land-use dynamics are modelled on the IMAGE-LandManagement model's grid-level (Doelman et al., 2018). Demand for crop and livestock products, trends in agricultural intensification, and trade dynamics are provided by the economic general equilibrium model MAGNET (Woltjer et al., 2014). Gridded land-use dynamics are implemented in the dynamic global vegetation model LPJmL to model effects on the carbon and hydrological cycle (Müller et al., 2016; Schaphoff et al., 2018b) and to the global nutrient model (GNM) to model the nitrogen and phosphorus cycles (Beusen et al., 2015). LPJmL provides data on potential crop and grass yields, land-use change emissions, and irrigation water use while considering the impact of climate change. Adaptation to climate change in the food system is included by informing MAGNET about the regional impact of climate change leading to changes in agricultural production and trade flows. The simulation model TIMER represents the energy system with high technological detail for 12 primary energy carriers, including bioenergy. Land use for the production of bioenergy as determined by TIMER is implemented on the grid-level in IMAGE-LandManagement. GHG emissions from energy, industry, and land use are inputs to the simple climate model MAGICC, which emulates complex climate models to calculate global mean temperature change (Meinshausen et al., 2011). The climate policy model FAIR-SimCAP uses MAC curves to determine cost-optimal emission pathways to achieve specific climate targets (den Elzen et al., 2008).

6.2.2. Scenario description

In this study, six scenarios are analysed over the period from 2015 to 2050 to shed light on nexus synergies and trade-offs. The reference (REF) scenario is the baseline for all scenarios. The WATER, LAND, FOOD and CLIMATE scenarios focus on improvements in one component

⁹ For more information on the IMAGE model visit the online documentation: <http://models.pbl.nl/image>.

of the WLFC nexus each. The TOTAL scenario aims for improvements in all nexus components. Climate impacts and adaptation effects are considered an integral aspect of each nexus component and are accounted for in all scenarios. Specifically, impacts on crop yields, water use and availability, and natural vegetation growth are included, which are key impacts in the WLFC nexus (for more detail see Section 6.2.1 and SI Section S6.2 and S6.3). In the REF, WATER, LAND and FOOD scenarios the RCP 6.0 is used representing impacts under a likely climate change pathway without widespread implementation of climate change mitigation measures (Hausfather and Peters, 2020). In the CLIMATE and TOTAL scenarios RCP 2.6 is used representing impacts with climate change mitigation measures in line with a 2°C target (van Vuuren et al., 2011). Climate data in line with these RCPs are adopted from the Inter-Sectoral Impact Model Intercomparison Project (ISMIP), specifically using results from the IPSL-CM5a-LR model (Frieler et al., 2017). The scenarios are described in more detail in the following sections and Table 6-1.

6.2.2.1. Reference scenario

The REF scenario represents a *business-as-usual* future where trends do not shift markedly from historical patterns. The main drivers follow updated SSP2 scenario trends (O'Neill et al., 2017; Popp et al., 2017): This includes continued uneven economic growth with some countries experiencing substantial growth while in other countries growth remains below global average. Population growth levels off slowly as no additional efforts are implemented to speed up the demographic transition. Pressure on the natural system increases from growing demand for food and other biomass uses and climate change.

6.2.2.2. Water scenario

In the WATER scenario, the focus is on preventing excessive water use and adverse impacts on aquatic ecosystems, in line with the PBs on freshwater use and the nitrogen cycle and SDG6. To achieve this, the quantity of water withdrawals is limited to ensure sufficient water flows in the hydrological system and fertilizer use efficiency is increased to improve water quality. In IMAGE, environmental flow requirements are implemented following the variable monthly flow (VMF) method developed by Pastor et al. (2014) where 60%, 45% and 30% of the mean monthly natural flow is reserved for ecosystems in low, intermediate and high flow periods, respectively. MAgPIE follows the method outlined in Smakthin et al. (2004) that derives the baseflow (low flow requirements) based on the 90th percentile of monthly discharge and high flow requirements based on mean annual runoff depending on the variability of the river flows (Bonsch et al., 2015). In both models, environmental flow protection measures imply that water withdrawals for irrigation and other uses cannot exceed a prescribed quantity as this would reduce water levels below the respectively prescribed minimum flow requirement. To reduce the impact of excessive nitrogen runoff in the environment on aquatic biodiversity (Howarth et al., 2011), fertilizer use efficiency is assumed to improve to 70% in MAgPIE. In IMAGE, 70% convergence to a maximum achievable NUE based on (Zhang et al., 2015) is assumed (SI Section S6.5.4).

6.2.2.3. Land scenario

In the LAND scenario, the aim is to stop the conversion of natural ecosystems and terrestrial biodiversity loss by an ambitious area-based conservation effort preserving half of the Earth's land to protect nature as proposed in the literature (Pimm et al., 2018; Wilson, 2016). For this purpose, a map of protected areas developed by Kok et al. (2020) is implemented. This map protects - where possible - 50% of the terrestrial area in each ecoregion (Dinerstein et al., 2017) (SI Figure 6-8; SI Section S6.5.3). Expansion of agriculture in these locations is not allowed. To reduce the impact of nitrogen deposition on terrestrial biodiversity (Bobbink et al., 2010), fertilizer use efficiency is assumed to improve to 70% in MAGPIE. In IMAGE 70% convergence to a maximum NUE is assumed (SI Section S6.5.4).

6.2.2.4. Food scenario

Dietary change towards healthy daily caloric intake, lower meat consumption and increased vegetable and pulses consumption can have considerable health benefits (Willett et al., 2019) and environmental co-benefits reducing GHG emissions and limiting pressure on the land system (Springmann et al., 2018; Stehfest et al., 2009). Also, there is very large potential to reduce waste in the food system, which could further lower agricultural production required to feed the global population (Gustavsson et al., 2011). In the FOOD scenario, ambitious changes in the food system are assumed towards the year 2050 by implementing a transition towards healthy diets proposed by Willett et al. (2019), which includes a strong reduction in meat consumption in regions that currently have intake above healthy levels (SI Section S6.5.2). Additionally, a reduction in food waste is assumed in line with SDG target 12.3 which aims to halve per capita global food waste and losses at consumer level and along the production and supply chains (UN, 2015). In IMAGE this is implemented as a 50% reduction in food waste in all regions. In MAGPIE food waste is reduced to a maximum of 20% of food intake, which is in line with the IMAGE assumption as this amounts to 50% reduction of current food waste ratios in high-income countries.

6.2.2.5. Climate scenario

In the CLIMATE scenario, global warming is limited to 2°C above preindustrial temperatures by 2100 to reduce the risks and impacts of climate change (IPCC, 2014b). Climate mitigation measures are implemented in both models based on a GHG price as calculated by FAIR-SimCAP (climate policy module of IMAGE) in line with a 2.6 W/m² radiative forcing target (SI Table 6-1): The global GHG price increases up to 55 US\$/tCO₂ in 2030 and 87 US\$/tCO₂ in 2050, which is substantially higher than the average European emission trading scheme price in 2010-2020 of about 12 US\$/tCO₂ (Sandbag, 2021) and in line with 2°C scenarios in the literature (Rogelj et al., 2018). The GHG price steers technical mitigation in non-CO₂ GHG emissions based on marginal abatement cost curves (MACC) (Harmsen et al., 2019) and protection of all forests and other carbon-rich land cover types (Overmars et al., 2014; Popp et al., 2014). The same bioenergy demand from mitigation measures in the energy system is implemented in both IMAGE and MAGPIE, as derived from the energy module of IMAGE (SI Table 6-1) (Daioglou et al., 2019). This increases up to 96 EJ/yr in 2050, a strong increase

compared to the 4.65 EJ/yr used in 2015 (IEA, 2017), which is required to achieve the ambitious 2°C mitigation goal. In line with reduced N₂O emissions from fertilizer based on the MACC information fertilizer efficiency is assumed to increase moderately, with 65% in MAgPIE and by 50% in IMAGE relative to the maximum NUE (Section S6.5.4). For IMAGE, climate mitigation measures are implemented in MAGNET through reductions in land supply due to forest protection, which affects the food system and therefore also food prices. Bioenergy expansion is assumed not to affect food prices based on a food-first approach (Daioglou et al., 2019). In MAgPIE, mitigation measures affect the food system because of land demand for forest protection, bioenergy use and afforestation (for more detail see Section S6.5.1).

6.2.2.6. Total scenario

In the TOTAL scenario, all measures are combined to investigate how they might reinforce or counteract one another (Table 6-1). This includes among others protection of forests and carbon-rich natural land for climate mitigation as well as protection for terrestrial biodiversity purposes, the introduction of healthy diets and reduced food waste, and limitations on water extraction. As improvements in fertilizer use efficiency are implemented in the CLIMATE, LAND, and WATER scenarios, we assume that the measures partially add up implying a very large improvement in fertilizer efficiency in the TOTAL scenario: We assume a 75% increase in MAgPIE and an 80% increase in IMAGE relative to the maximum NUE (SI Section S6.5.4).

Table 6-1: Overview of scenario-specific assumptions and settings.

Measures	SCENARIO					TOTAL
	REF	WATER	LAND	FOOD	CLIMATE	
Environmental flow requirements		Limit water extraction, ensuring sufficient water to ensure a fair condition of aquatic ecosystems				Limit water extraction, ensuring sufficient water to ensure a fair condition of aquatic ecosystems
Biodiversity protection			Biodiversity protection extended to 50% of all terrestrial ecoregions by 2050			Biodiversity protection extended to 50% of all terrestrial ecoregions by 2050
Fertilizer efficiency		Large improvement in fertilizer efficiency	Large improvement in fertilizer efficiency		Moderate improvement in fertilizer efficiency	Very large improvement in fertilizer efficiency
Diet change				Diet change towards healthy diets by 2050 as proposed by Willet et al., 2019		Diet change towards healthy diets by 2050 as proposed by Willet et al., 2019
Food waste				50% reduction in food waste		50% reduction in food waste
GHG price					GHG price for 2°C climate mitigation 2030: 55 US\$/tCO ₂ 2050: 87 US\$/tCO ₂	GHG price for 2°C climate mitigation 2030: 55 US\$/tCO ₂ 2050: 87 US\$/tCO ₂
Bioenergy production					Bioenergy for 2°C climate mitigation 2030: 61 EJ/yr 2050: 96 EJ/yr	Bioenergy for 2°C climate mitigation 2030: 61 EJ/yr 2050: 96 EJ/yr
Climate impacts	RCP 6.0	RCP 6.0	RCP 6.0	RCP 6.0	RCP 2.6	RCP 2.6

6.2.3. Indicator description

A set of indicators as described in the following sections is used to analyse and compare outcomes under different scenarios. All indicators are endogenous results from the models and underlying model dynamics are described in detail in Section 6.2.1 and SI Sections S6.S6.2 and S6.S6.3. All indicators are presented and described at the global and the regional level. The regional results are presented at the level of 10 world regions (SI Figure 6-1): North America (NAM), Central and South America (CSA), Middle East, and Northern Africa (MEN), Sub-Saharan Africa (SSA), Western and Central Europe (EUR), Russia and Central Asia (RCA), South Asia (SAS), China region (CHN), Southeast Asia (SEA), and Japan, Korea and Oceania (JKO). Additionally, these regions are categorized into different income classes, i.e., high (NAM, EUR, JKO), middle (CSA, MEN, RCA, CHN), and low (SSA, SAS, SEA). Finally, in Section 3.6 we analyse synergies and trade-offs by comparing the percentage change in each indicator in each scenario compared to the REF scenario in 2050.

6.2.3.1. Irrigation water withdrawal

Excessive freshwater use has major impacts on aquatic biodiversity as well as on the availability of water for human use (Vörösmarty et al., 2010). Water use for irrigation in agriculture is responsible for about 70% of freshwater use globally and therefore of crucial importance. Here we present irrigation water withdrawal, which is an endogenous output of both IMAGE and MAgPIE, defined as the total amount of water in km³ per year extracted for irrigation of crops.

6.2.3.2. Natural land share

The loss of natural ecosystems due to the expansion of human land use has been the dominant reason for terrestrial biodiversity loss historically (IPBES, 2019). Projected development in the share of natural land is therefore a relevant indicator for the impact of human land use on terrestrial biodiversity. To understand the underlying dynamics of these changes, in the results section we present the developments in seven major land-use classes in terms of land-use change from 2015 to 2050 in million hectares (Mha): rainfed and irrigated cropland, grazing land, bioenergy, built-up area, forest and other natural land. The simplified indicator share of natural land as presented in the synergies and trade-off analysis includes the two land-use classes forest and other natural land and is calculated as the sum of these two classes divided by total terrestrial land area. We do not account for changes in managed forest.

6.2.3.3. Food price index

Changes in the price of primary agricultural products are presented as a simple indicator of food security (van Meijl et al., 2020). Both IMAGE and MAgPIE include food prices for a large range of commodities: In the result section we discuss aggregated prices for crop, livestock and total agricultural products to provide additional insight in underlying dynamics. The indicator shows the impact of different nexus measures on the affordability of food and pressure in the food system. It should however be cautioned that final food prices are

considerably higher than agricultural commodity prices due to processing and marketing, and that any price variation also gets diluted by the value-added in up-stream supply chains that we do not simulate here. For IMAGE and MAgPIE, the development of average primary agricultural products prices is represented by the Laspeyres index based on a constant food basket in the year 2015. For MAgPIE, the food price index is corrected for the GHG emissions tax revenue to exclude the effect that GHG taxes are passed through to consumers (Section S6.5.1). The indicator is an index of aggregated changes in food prices from 2015 to 2050.

6.2.3.4. AFOLU GHG emissions

Total changes in GHG emissions from the agriculture, forestry, and other land use (AFOLU) sectors are assessed as these are indicative of the role of the WLFC nexus on climate change (IPCC, 2019). GHG emissions from the AFOLU sector result from numerous activities: Carbon dioxide (CO₂) emissions are predominantly caused by land-use change like the conversion of natural land to agricultural land. Methane (CH₄) and nitrous oxide (N₂O) emissions are mainly caused by agricultural activities such as organic and inorganic fertilizer application, manure management, enteric fermentation from ruminants, and rice production. The indicator used in this study comprises total AFOLU GHG emissions from all aforementioned sectors in terms of CO₂-equivalents.

6.2.3.5. Nitrogen surplus in agriculture

Excessive nitrogen input into the environment has detrimental effects on terrestrial and aquatic biodiversity (Bobbink et al., 2010; Howarth et al., 2011), human health, and the suitability of surface water for human use (van Vliet et al., 2021). As human impacts on the nitrogen cycle are dominated by agriculture (Liu et al., 2010), the surplus of nitrogen in the agricultural system (including crop and livestock production) is a good indicator of improving or worsening developments. It describes the difference between the total inputs (sum of nitrogen in manure, fertilizer, deposition and fixation) and output (nitrogen removed by crop and grass harvest and grazing), which can enter the environment in different forms of nitrogen. The indicator represents total surplus of nitrogen in agriculture in million tons of nitrogen per year (Mt N/yr).

6.3. Results

6.3.1. Irrigation water withdrawal

Total global irrigation water withdrawals in the historical period (2015) differ slightly between MAgPIE and IMAGE with 1850 and 2020 km³/yr, respectively (Figure 6-1). Regional discrepancies are larger, with relatively more withdrawals in MAgPIE in low-income regions and more withdrawals in IMAGE in middle-income regions, which is a consequence of differences in irrigation efficiency assumptions, spatial distribution of crop types and cropping intensity of irrigated areas between the models. As estimates for contemporary irrigation water withdrawal show variations up to 30% (Wisser et al., 2008) the estimates

in IMAGE and MAgPIE are fairly well aligned. For the future, MAgPIE shows a substantial increase in water withdrawals in the REF scenario (+240 km³/yr in 2015-2050) resulting from the expansion irrigated areas (Figure 6-2), while withdrawals in IMAGE are nearly constant due to small irrigated area increases and higher water use efficiency.

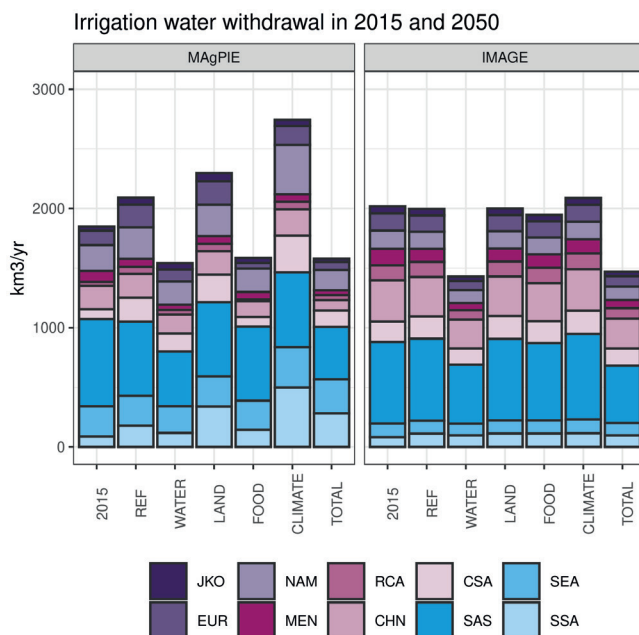


Figure 6-1: Irrigation water withdrawal in IMAGE and MAgPIE for all regions in 2015 and for all scenarios in 2050 for different regions (high-income: Japan, Korea and Oceania (JKO), North America (NAM), Western and Central Europe (EUR); middle-income: Middle East, and Northern Africa (MEN), Russia and Central Asia (RCA), China region (CHN) Central and South America (CSA); low-income: Sub-Saharan Africa (SSA), South Asia (SAS), Southeast Asia (SEA)).

The measures in the different scenarios mainly affect irrigation water withdrawals in MAgPIE that includes endogenous investments into irrigation infrastructure and therefore is flexible to expand irrigated areas, while irrigated area development in IMAGE is set exogenously and does not change between the scenarios (Section 6.3.2). MAgPIE projects increases in water withdrawals in the LAND and CLIMATE scenarios (+450 and +780 km³/yr in 2050, resp.), mainly in low-income regions and in the case of the CLIMATE scenario for North America. These additional irrigated agricultural areas are due to the pressure on the agricultural system resulting from land protection in both scenarios and additional demand for crop production for bioenergy in the CLIMATE scenario. This leads to higher food prices, making it more worthwhile to invest in irrigation to increase crop production (Section 3.3 for further details). In IMAGE, where irrigated areas are set exogenously, only the CLIMATE scenario shows slightly higher withdrawals (+70 km³/yr compared to REF in 2050) as lower levels of CO₂ fertilization reduce irrigation efficiency due to higher transpiration levels. The restriction of

irrigation water availability that allows fulfilling environmental flow requirements has a large impact on irrigation water withdrawals in both MAgPIE and IMAGE, resulting in a reduction of -550 and -570 km³/yr respectively in WATER compared to REF in 2050. In the FOOD scenario lower meat consumption and food waste reduce irrigation water withdrawals with a similar order of magnitude in MAgPIE (-510 km³/yr compared to REF in 2050) and even lead to lower water withdrawals than in 2015 (-260 km³/yr compared to 2015).

6.3.2. Natural land share

Changes in natural land (forest and other natural land) (Figure 6-6) are a result of developments in land use by humans, predominantly for agriculture. Both MAgPIE and IMAGE show a substantial increase in agricultural land in the REF scenario in the 2015-2050 period (Figure 6-2). In MAgPIE, this results from expansion in cropland (+440 Mha) while grazing land is slightly reduced (-30 Mha). In IMAGE, both cropland and grazing land expand (+340 and +140 Mha, resp.). A substantial share of IMAGE cropland expansion results from increased demand for bioenergy (100 Mha), projected also under business-as-usual conditions while it remains very low up to 2050 in MAgPIE. IMAGE also includes the expansion of built-up area (40 Mha), although this is assumed not to change between the scenarios. Because of these land-use dynamics, natural land decreases substantially in REF in MAgPIE (-400 Mha) as well as IMAGE (-520 Mha), with the largest losses occurring in Sub-Saharan Africa in both models (SI Figure 6-4).

Natural land is reduced slightly more in WATER than in REF in both MAgPIE and IMAGE, as yield reductions on irrigated cropland due to irrigation restrictions lead to higher agricultural land requirements to fulfil crop demand. In the LAND scenario, a substantial expansion of protected areas leads to a significant reduction in agricultural land expansion, resulting in lower natural land losses than REF and WATER. In the FOOD scenario, dietary change with lower demand for livestock products drives reductions in grazing land and cropland. IMAGE shows a stronger reduction than MAgPIE as in MAgPIE extensification of grazing land (i.e., reducing animals per hectare) is allowed, while in IMAGE this is assumed not to take place. Consequently, MAgPIE still shows a slight reduction in natural land while IMAGE shows a small increase. The abandonment of grazing land in IMAGE typically occurs on lands with relatively low productivity that often coincide with other natural lands, leading to a small increase in this land-use category in the FOOD scenario. The strongest abandonment takes place in IMAGE in Central and South America where livestock production systems typically use a lot of land per animal, resulting in a strong increase in natural land share SI Figure 6-4. In the CLIMATE scenario, protection of forests and other carbon-rich natural lands leads to reduced deforestation, preventing forest loss in both models. In MAgPIE a small increase in forest area is observed as afforestation in line with current national climate policies is included. Simultaneously, a substantial increase in bioenergy production occurs. In the TOTAL scenario the combination of dietary change with pressure on land from protection for biodiversity and forest for climate mitigation leads to substantial reductions in grazing land in both models and reductions in cropland in MAgPIE. Bioenergy increases

and counteracts the positive impact on natural land in both models, resulting in eventually only slight increases in natural land.

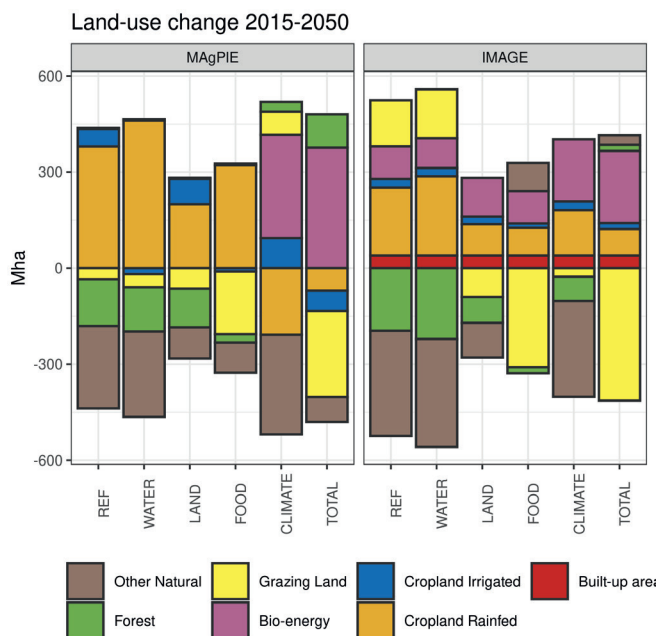


Figure 6-2: Global land-use change in IMAGE and MAgPIE in the 2015-2050 period for all scenarios for 7 land-use categories. Negative values indicate area reduction in a land-use category, positive values indicate expansion of a land-use category.

6.3.3. Food price index

In the business-as-usual REF scenario, livestock prices increase both in MAgPIE and IMAGE (+15% and +6%, resp.) (Figure 6-3). This is due to strong increases in demand for ruminant meat and dairy products in developing regions such as Sub-Saharan Africa and South Asia (SI Figure 6-5), which causes a relative scarcity of grazing land in these regions leading to higher prices. Crop prices are almost stable in MAgPIE (-2%) while they show a moderate decrease in IMAGE (-14%). In IMAGE, the WATER scenario shows less of a decrease in crop prices compared to the REF scenario due to reduced crop productivity from the reduced application of irrigation in line with environmental flow restrictions (-2% compared to -14%). The same process occurs in MAgPIE, but the assumption on improved fertilizer efficiency outbalances its effects, resulting in negligible change compared to REF. The LAND and CLIMATE scenarios result in increases in food prices due to land protection and increased demand for bioenergy increasing the pressure on the agro-economic system. In FOOD, the opposite effect occurs as diet change leads to reduced demand which lowers the pressure on the agro-economic system leading to strong decreases in both models, most notably in IMAGE. In TOTAL, the latter effect dominates, leading to the second-lowest prices of all scenarios, although the

opposite effects of natural land protection, lower irrigated yields and demand for bioenergy somewhat reduce the price decreases. Climate change also impacts agricultural prices with increases in tropical regions due to negative climate change impacts on crop yields. In boreal regions, prices decrease due to positive climate change impacts on crop yields. However, the effect is still quite moderate by the year 2050 and on the global level these counteracting effects level out. Therefore, in our results the impacts of the nexus measures on agriculture prices dominate.

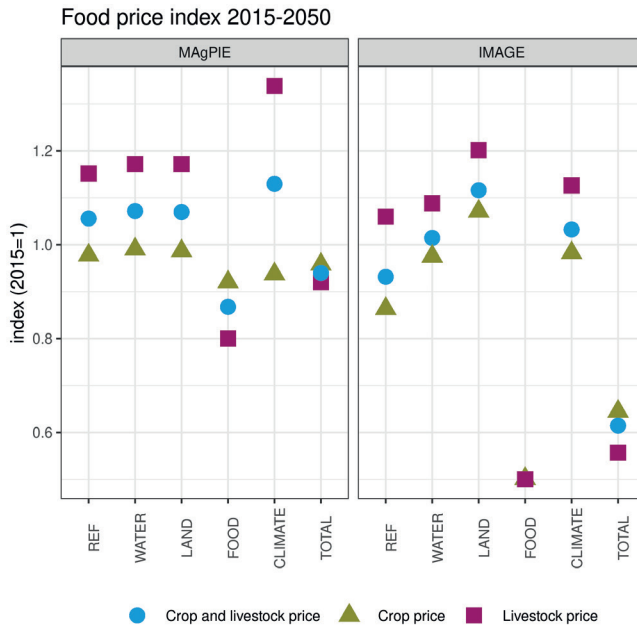


Figure 6-3: The globally averaged food price index in IMAGE and MAgPIE for crops, livestock, and crops and livestock combined for the 2015-2050 period.

6.3.4. AFOLU GHG emissions

Both MAgPIE and IMAGE project an increase of GHG emissions from 2015 to 2050 in the REF scenario due to continued expansion of agricultural land and higher agricultural production (Figure 6-4) (5.6 and 4.3 GtCO₂-eq., resp.). The LAND scenario, on the other hand, shows substantial reductions in CO₂ emissions as agricultural land expansion is restricted, leading to less conversion of natural land. The same is the case for the FOOD scenario, where also non-CO₂ GHG emissions from agriculture are much lower due to reduced food and feed production. In the CLIMATE scenario, emissions are also substantially reduced due to protection of forests and other carbon-rich natural lands and mitigation measures in agriculture leading to lower emissions from land-use change and reduced non-CO₂ GHG emissions. Emission reductions vary widely between regions, with the largest reductions

in land-use change CO₂ emissions in SSA and CSA and major reductions in agricultural non-CO₂ emissions in SAS and CHN (SI Figure 6-6). In the TOTAL scenario, the strongest emission reduction of all scenarios is achieved due to the combination of all measures: In 2050, emissions are reduced by 12.5 and 7.9 GtCO₂-eq compared to REF in MAgPIE and IMAGE, respectively.

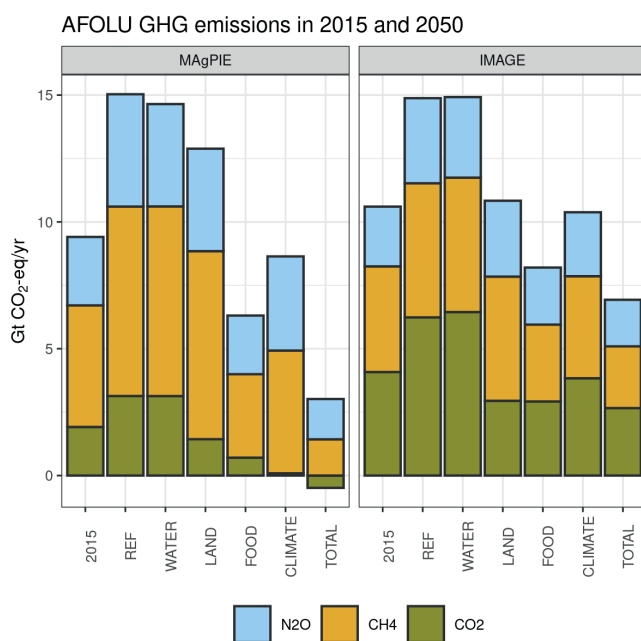


Figure 6-4: Global CO₂, CH₄, and N₂O emissions in IMAGE and MAgPIE in 2015 and in 2050 for all scenarios for the AFOLU sector.

6.3.5. Nitrogen surplus in agriculture

For the historical period (i.e., 2015), MAgPIE and IMAGE find surpluses of 146 and 132 Mt N/yr, respectively (Figure 6-5). Both models show a strong increase of this surplus in REF up to 2050 (+79 and +47 Mt N/yr compared to 2015, resp.). In MAgPIE the increases predominantly take place in high and low income regions while in IMAGE almost all increases take place in the low income regions.

The implemented measures lead to substantial decreases in nitrogen surpluses in nearly all scenarios. The only exception is the CLIMATE scenario in MAgPIE that only shows a relatively small reduction as the surplus reduction gained from higher fertilizer use efficiency is cancelled out by higher total fertilizer input for large-scale bioenergy production. The FOOD scenario also leads to lower nitrogen surpluses even though fertilizer use efficiency rates are assumed to be the same as in the REF scenario. This is because of lower total

crop production due to less food waste and reduced feed production, and lower losses in animal waste management due to the reduction in livestock product consumption. The TOTAL scenario shows very strong reductions in nitrogen surplus in both models, even below historical levels (-58 and -43 Mt N/yr compared to 2015 in MAGPIE and IMAGE, resp.), due to the combination of dietary change and strong increases in fertilizer use efficiency.

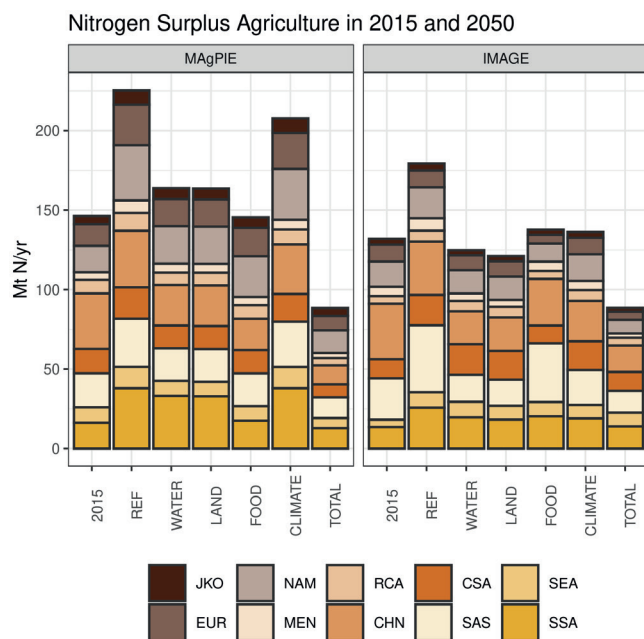


Figure 6-5: Regional nitrogen surplus in IMAGE and MAGPIE in 2015 and for all scenarios in 2050 for different regions (high-income: Japan, Korea and Oceania (JKO), North America (NAM), Western and Central Europe (EUR); middle-income: Middle East, and Northern Africa (MEN), Russia and Central Asia (RCA), China region (CHN) Central and South America (CSA); low-income: Sub-Saharan Africa (SSA), South Asia (SAS), Southeast Asia (SEA)).

6.3.6. Trade-offs and synergies

Here we compare the relative change of all indicators across scenarios, models, and regions by calculating the percentage difference in 2050 between the REF scenario and all other scenarios. These results are used to identify synergies and trade-offs, differences between regions, and robustness of these findings across models (Table 6-2 and Figure 6-6). Synergies and trade-offs are defined as, respectively, positive or negative effects on certain processes, as a consequence of measures that are not specifically targeted at these processes. In the scenarios considered in this study, this is represented by the indicators in each nexus scenario that represent a nexus component that is not the main focus of this particular scenario: For example, AFOLU emissions in the WATER scenario, or irrigation water withdrawal in the CLIMATE scenario.

In the WATER scenario, irrigation water withdrawal and nitrogen surplus in agriculture are specifically targeted by measures and therefore show substantial reductions both in MAGPIE and IMAGE. Food prices show a trade-off compared to REF (+9%) in IMAGE due to lower yields in irrigated agriculture as a result of environmental flow requirements, with a large regional variation as food prices increase much more in the Middle East (+68%) and Russia and Central Asia (+38%) because irrigation plays such an important role in food production in these regions. In MAGPIE the trade-off with food prices due to environmental flow requirements is much lower (+1%) because of the compensating effect of improved nitrogen use efficiencies reducing the costs of agricultural production.

In the LAND scenario, natural land area increases and the nitrogen surplus decreases as intended by the measures. In addition, both IMAGE and MAGPIE show synergies with AFOLU emissions (-14% to -27%) due to reduced deforestation and conversion of other agricultural lands. A trade-off is found in MAGPIE with irrigation water withdrawal (+10%) due to intensification of agriculture involving expansion of irrigation due to increased pressure in the food system. IMAGE shows a trade-off in food prices (+9%), also due to pressure in the food system.

The FOOD scenario shows substantial reductions in food prices (-18% to -46%) indicating positive trends in food security. In addition, synergies are found in both models with all other indicators: Irrigation water withdrawal (-3% to -24%), natural land area (+4% to +8%), nitrogen surplus in agriculture (-23% to -35%) and AFOLU emissions (-45% to -58%). Especially the reduction in meat consumption and reduced food waste results in less animal waste leading to nitrogen surpluses and GHG emissions, lower requirements for intensive irrigation and reduced agricultural area requirements increasing natural land area and strongly reducing CO₂ emissions from land-use change.

Table 6-2: Global percentage difference of scenario indicators in IMAGE and MAgPIE between the REF scenario and the nexus scenarios in 2050. Colour indication shows where strong synergies occur in green, weak synergies in light green, strong trade-offs in red, weak trade-offs in light red, indicators specifically targeted by measures in a particular scenario in blue, and no substantial change in grey.

Model	MAgPIE					IMAGE				
	Scenario	WATER	LAND	FOOD	CLIMATE	TOTAL	WATER	LAND	FOOD	CLIMATE
Water Withdrawal Irrigation	-26%	+10%	-24%	+31%	-25%	-28%	0%	-3%	+5%	-26%
Natural Land Area	0%	+2%	+4%	+2%	+6%	-1%	+4%	+8%	+2%	+8%
Nitrogen Surplus Agriculture	-27%	-27%	-35%	-8%	-61%	-30%	-32%	-23%	-24%	-51%
Food Price	+1%	+1%	-18%	+7%	-11%	+9%	+20%	-46%	+11%	-34%
AFOLU Emissions	-3%	-14%	-58%	-43%	-83%	0%	-27%	-45%	-30%	-53%

In the CLIMATE scenario, AFOLU emissions show strong decreases (-30% to -43%), although the FOOD scenario actually has larger decreases highlighting the potential for climate change mitigation from dietary change. The CLIMATE scenario involves a synergy with natural land share (+2%) in both models as a result of forest protection limiting land-use change. There is, however, a substantial regional variation with some regions showing a reduction in natural land due to expansion of bioenergy and reallocation of global agricultural production: E.g. in Sub-Saharan Africa in MAgPIE (-2.4%) or in IMAGE in Japan, Korea and Oceania (-3.0%) and Middle East and Northern Africa (-2.9%). Trade-offs are found with food prices (+7% to +11%) and irrigation water withdrawal (+5% to +31%) due to increased pressure on the land system from forest protection and increased demand for bioenergy production.

The TOTAL scenario combines all measures from the different nexus scenarios. This implies that all indicators are targeted and therefore no synergies or trade-offs can be analysed. It is interesting however to observe how some measures reinforce each other while others counteract one another. For example, the combined effect of improved nitrogen use efficiency and lower levels of livestock production results in a major decrease in the nitrogen surplus in agriculture (-51% to -61%). Similarly, the combined effects of lower livestock numbers with technical mitigation measures in agriculture results in large reductions in AFOLU emissions (-53% to -83%). On the other hand, the reduction in food prices due to dietary change is counteracted by higher pressure in the land system from land protection measures and increased bioenergy demand: Consequently, food prices still go down in the TOTAL scenario (-11% to -34%), but not as much as in the FOOD scenario (-18% to -46%).

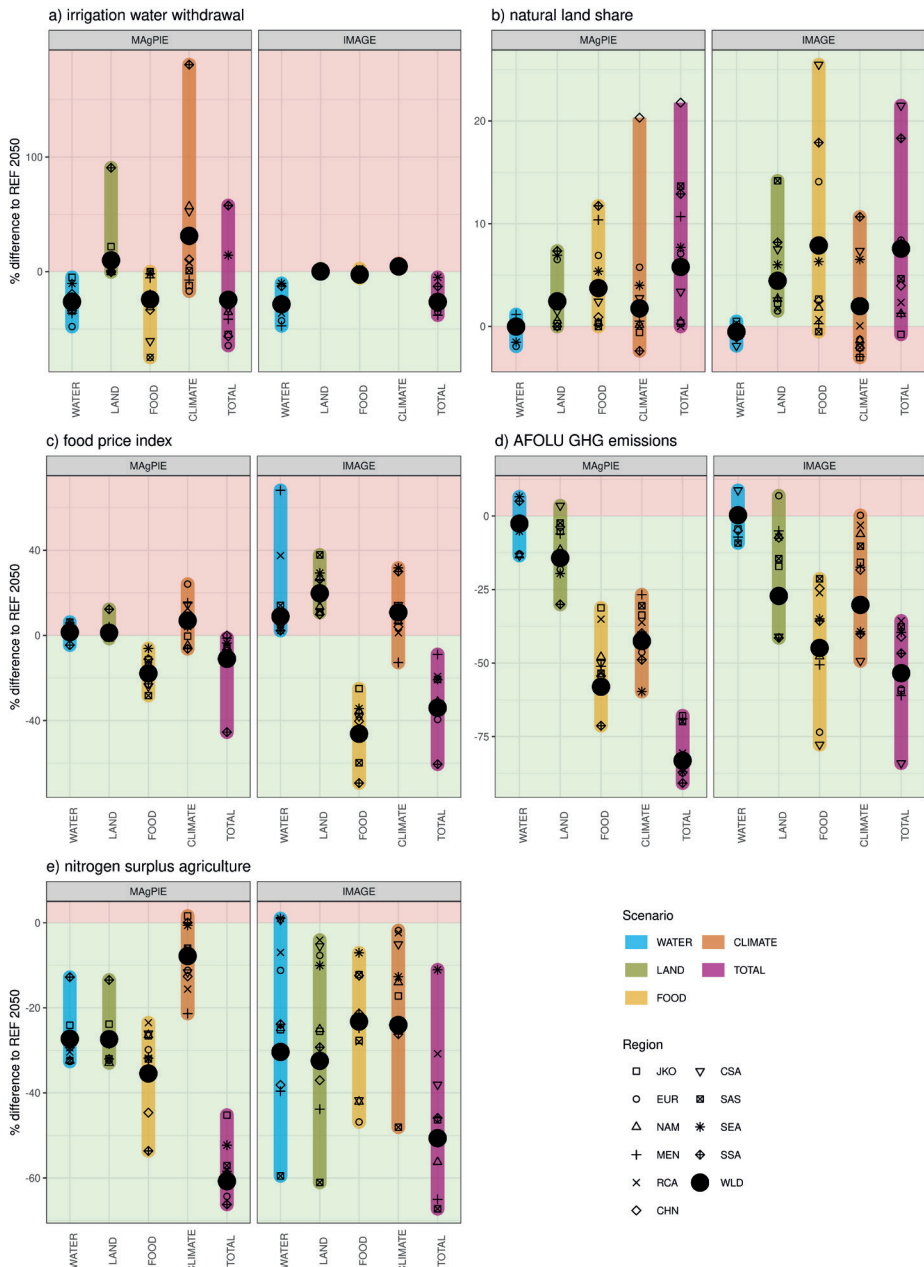


Figure 6-6: Percentage difference of scenario indicators in IMAGE and MagPIE between the REF scenario and the nexus scenarios in 2050 for the global total/average and regional variation: a) irrigation water withdrawal, b) natural land share, c) food price index, d) AFOLU GHG emissions, e) nitrogen surplus agriculture. The red shaded areas show in which cases the scenario projects a worsening performance compared to REF, the green shaded areas show in which cases the scenario projects an improved performance compared to REF. The graph also shows the regional results and their divergence, in case regional trends differ the bars in the graph become extended.

6.4. Discussion

The synergies and trade-offs analysis presented in this study generally finds similar results in both models providing more confidence in the results than in the case of a single model study. The trade-offs found between climate mitigation measures, increased pressure in the land-use system from land protection and higher food prices are found in both models and are confirmed by the literature (Fujimori et al., 2019; Hasegawa et al., 2018). The trade-off of climate mitigation measures (most notably bioenergy production) with water use is most clear in MAGPIE and less commonly considered in scenario studies on climate mitigation but also a known issue that warrants attention (Hayman et al., 2020; Stenzel et al., 2021). The strong synergy between diet change, climate change mitigation, excessive water use and nitrogen input into the environment is also a clear result from both models and confirmed in the literature (Obersteiner et al., 2016; Soergel et al., 2021; Springmann et al., 2018). The notion that a combined portfolio of measures in multiple dimensions of the nexus as shown in both models in the TOTAL scenario could lead to the best results for biodiversity (as implied by improvements in natural land share, water withdrawals and nitrogen surplus) is also shown by Leclère et al. (2020).

Given our goal to assess different dimensions of the WLFC nexus in two models at the same time, we choose to focus on the nexus components that are well represented in both models. Both models have a good representation of the nexus, but the focus on nexus dimensions related to the land system limits the study's scope somewhat. The nexus' energy component is taken into account by considering the impact of bioenergy use for climate mitigation. However, impacts of water availability on the energy system, such as for thermoelectric power generation or hydropower, or the effects of climate change on renewable energy supply (Gernaat et al., 2021; van Vliet et al., 2016), are not considered. Also, the water dimension of the nexus is considered only from the volumetric water quantity perspective as the metric of environmental flow requirements implies restrictions on human use volume to protect aquatic ecosystems by providing sufficient high and low flow quantities (Gerten et al., 2013), while both water quantity and water quality are also of crucial importance for human wellbeing (Bijl et al., 2018; van Vliet et al., 2021; Vörösmarty et al., 2010). Water quality is indirectly covered by the nitrogen surplus indicator.

For this study, five indicators were selected to simplify the comparison between models and scenarios. More indicators could have been added: For example, food price is a fairly simple indicator that does not reflect consumers' eventual purchasing power, which changes with increasing income. Other dimensions of food security, such as nutritional value or undernourishment, can provide additional interesting insights (van Meijl et al., 2020). Similarly, the natural land share and nitrogen budget only provide indirect indications of biodiversity impacts, while specialized biodiversity models have more direct indicators (Leclère et al., 2020). While irrigation water withdrawals represent about 70% of anthropogenic water use, it does not represent dynamics in the water use for energy, industry and households – which

is substantial – that might have more direct impact on communities (de Vos et al., 2021). In IMAGE these other uses are taken into account based on population, GDP and energy and industry system dynamics (Bijl et al., 2016). In MAgPIE an exogenously assumed fraction of water use is reserved for other uses.

Some key differences in individual scenario results between the two models result from differences in model setup. In IMAGE, irrigated cropland area is set exogenously (Doelman et al., 2018). It does not vary between the scenarios producing different irrigation water withdrawal dynamics compared to MAgPIE, where irrigated area is responsive to the agricultural intensification trends (Bonsch et al., 2015). Also, the nitrogen use efficiency assumptions play out differently in the models: In MAgPIE, the efficiency assumption makes it cheaper to intensify agriculture resulting in reduced food prices, while in IMAGE, nitrogen use efficiency is assumed not to affect food prices. In the integrated assessment modelling community several multi-model studies exist on GHG emissions, land-use change dynamics, and food security indicators (Frank et al., 2019; Hasegawa et al., 2018; Popp et al., 2017). For the water and nitrogen dimensions, such comparison studies have not been conducted yet, indicating an important direction of future research and model development.

Other indicators do show similar dynamics in both models across the scenarios, but still show interesting differences: AFOLU CO₂ emissions are lower in MAgPIE than in IMAGE (1.9 GtCO₂ and 4.1 GtCO₂ in 2015, respectively). The majority of these emissions result from land-use change which is notoriously uncertain as illustrated by the 2.9-8.1 GtCO₂ range reported by Friedlingstein et al. (2019). Part of the difference can be explained as IMAGE takes emissions from forestry and degraded peatlands into account whereas MAgPIE does not. Total irrigation water withdrawal is similar in MAgPIE and IMAGE (1850 km³ and 2010 km³, respectively). However, compared to the literature these estimates are on the low end of the range (Wada et al., 2013; Wisser et al., 2008). IMAGE and MAgPIE use the LPJmL model for irrigation estimates that (in this version) does not take into account unsustainable groundwater use from deep aquifers and multiple cropping cycles explaining part of this low estimate (Biemans et al., 2016; Wada et al., 2010).

Both models take climate impacts into account following either the RCP 6.0 or RCP 2.6 climate change trajectories. It should be noted though that the two trajectories start only to diverge strongly after the year 2050 (which is the focus of this assessment). Climate change impacts predominantly influence the results through changes in the biophysical system as modelled by LPJmL. Key processes that are affected are crop productivity, water availability and growth rates of natural vegetation. Various other climate impacts that might affect the Water-Land-Food-Climate nexus are excluded due to model or data limitations, e.g. the effect of heat stress on labour productivity (Orlov et al., 2021) or the effect of increasing water temperatures on aquatic biodiversity (Barbarossa et al., 2021). The effects on crops are central to the food system modelling in this study and involve substantial uncertainty. Generally, global gridded crop models simulate crop yield improvements in temperate and boreal regions and for C3

crops such as wheat, while reductions in crop yields are predominantly found in more tropical regions and in C4 crops such as maize (Jägermeyr et al., 2021; Rosenzweig et al., 2014). The LPJmL model used in this study also shows these patterns but is on the optimistic side of the model range. More empirically based studies typically find larger climate change impacts on crop yields indicating that our study might underestimate the effects of climate change on the food system (IPCC, 2019a). Moreover, the MAgPIE and IMAGE models do not consider climate-change induced extreme events such as storm or droughts. Due to the additional use of land for mitigation (e.g. reforestation and bioenergy) our study finds higher food prices in the CLIMATE scenario (RCP2.6) than in the REF scenario (RCP6.0), implying that mitigation measures (without looking at other objectives) lead to stronger impacts on food security than climate change in the baseline. Some earlier studies have also reached this conclusion (Hasegawa et al., 2018; van Meijl et al., 2018). These impacts can be prevented by smarter design of mitigation scenarios or using a part of GHG tax revenues to compensate food insecure households (Fujimori et al., 2019; Soergel et al., 2021).

In this study we explicitly choose to implement measures instead of policies. Especially at the global scale, designing and implementing policies capable of achieving the measures assumed here is a major challenge. For example, in our FOOD and TOTAL scenarios very ambitious changes in diets and food waste are assumed. Previous studies with similar dietary scenarios (Bodirsky et al., 2014; Springmann et al., 2018; Stehfest et al., 2009; Stevanović et al., 2017) also showed the high impacts of such changes. Given that diets high in livestock protein and high food waste only appeared within the last decades (Bodirsky et al., 2020), a transformation to healthy diets and low food waste seems technically possible. It is however an open research question how such a large-scale behavioural change can be achieved. If diet change shall be incentivized via the price, extremely high prices would be required to achieve this transformation within current elasticities (Latka et al., 2021). It seems therefore evident, that price-based measures cannot achieve this transformation alone, but also food environments and food preferences need to be addressed, e.g. through healthy food options in canteens and awareness raising campaigns. The step from measures to policies is beyond the scope of this study but should be a key direction of follow-up research.

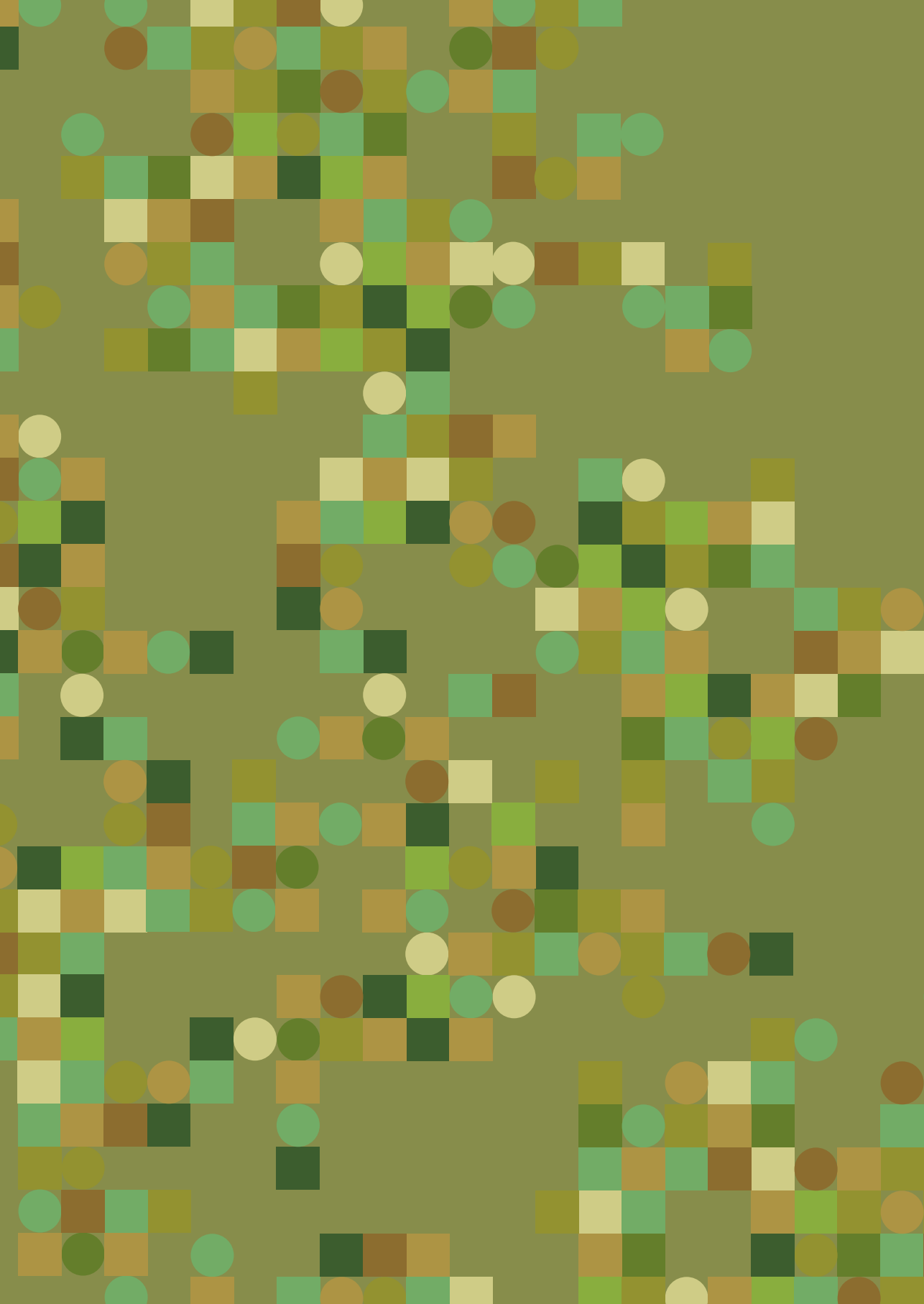
6.5. Conclusions

This article presents a model comparison study with harmonized scenarios quantifying dynamics in all components of the Water-Land-Food-Climate nexus. Broadly, the models find similar results for the synergies and trade-offs that are quantified. Trade-offs are identified resulting from climate mitigation measures and land protection for biodiversity purposes, affecting irrigation water withdrawals (+5% to +30%) and food prices (+1% to +20%) indicating excessive freshwater use and food security risks. A clear synergy is found between food measures and all other nexus dimensions: Dietary change including reduced meat consumption and less food waste results in lower irrigation water withdrawal (-3%

to -24%), higher natural land areas (+4% to +8%), reduced AFOLU GHG emissions (-45% to -58%), and lower nitrogen surpluses (-23% to -35%). This reaffirms the potential of changes in the food system, although it is recognized that the feasibility of measures at the scale implemented in this study is difficult to assess and crucial questions remain how to design and implement policies that can achieve the implementation of these ambitious measures. While the models agree in broad terms, some substantial variations are present: The most considerable differences are found in the water and nitrogen indicators, signifying that model development and future research should focus on these components. In conclusion, this study provides an example of a nexus approach to scenario development where all dimensions are considered providing input to the next generation of pathways aiming to achieve multiple dimensions of sustainable development in line with the Planetary Boundaries and the Sustainable Development Goals.

Acknowledgements

The research benefited from funding under the European Union's Horizon 2020 research and innovation programme, under grant agreement no 689150 SIM4NEXUS. In addition, it received funding from the SHAPE project which is part of AXIS, an ERA-NET initiated by JPI Climate, and funded by FORMAS (SE), FFG/BMWFW (AT), DLR/BMBF (DE, Grant No. 01LS1907A-B-C), NWO (NL) and RCN (NO) with co-funding by the European Union (Grant No. 776608). It also received funding from the European Union's Horizon 2020 research and innovation programme under grant agreement No 776479 (COACCH), and 031B0787B (FOCUS). We acknowledge the support by the German Federal Environmental Foundation (DBU) through a scholarship for FB.



CHAPTER 7

Summary and conclusions



7.1. Introduction and research questions

The land area of the Earth greatly influences climate dynamics through biogeophysical and biogeochemical processes. These processes concern, respectively, the exchange of energy and water, and the exchange of greenhouse gasses (GHGs) such as CO₂, CH₄ and N₂O, between land systems and the atmosphere. By using the Earth's land surface, humans have greatly altered it – leading to significant environmental impacts. Historically, climate change has mostly been caused by fossil fuel combustion. Still, land use, land-use change and forestry (LULUCF) have caused an estimated 34% of cumulative anthropogenic CO₂ emissions since 1750. Over time, the contribution of CO₂ from LULUCF declined to around 10% of annual global anthropogenic GHG emissions. At the same time, agriculture is responsible for about 13% of global GHG emissions in the form of non-CO₂ GHG emissions.

The importance of land and land use in climate dynamics means that land has a role in preventing dangerous climate change. First, it is essential to significantly reduce the 23% of annual GHG emissions from the agriculture, forestry and other land use (AFOLU) sector to make ambitious climate targets feasible. Second, land is key to various techniques to remove carbon from the atmosphere (so-called negative emissions or carbon dioxide removal (CDR)). Any measures to limit climate change directly linked to land use are termed land-based mitigation measures. Six categories of measures can be distinguished: 1) the protection of natural ecosystems to reduce emissions, for example, by preventing deforestation, 2) the restoration and expansion of forests and wetlands resulting in carbon sequestration in vegetation and soils, 3) the reductions of emissions in agriculture through technical measures such as improved manure management or precision farming, 4) increased sequestration of carbon in agricultural lands through for example application of biochar or increased tree cover in agricultural lands (agroforestry), 5) demand-side measures such as dietary change, 6) the production of bioenergy to replace fossil fuels and to sequester CO₂ using carbon capture and storage (CCS).

In addition to climate, land is central to many other sustainable development issues and environmental challenges. For example, it is essential for the provision of resources such as food, energy and water, as well as to sustain terrestrial biodiversity. The importance to sustainably provide resources for people's livelihoods and to protect the environment has been recognized in the Sustainable Development Goals (SDGs) (UN, 2015) and the planetary boundaries (PBs) (Rockström et al., 2009). These include targets on an array of sustainable development and global environmental change dimensions. A useful approach to study different dimensions of sustainable development and environmental change is the nexus concept which recognizes that components of a system are inherently interconnected and must be investigated and managed in an integrated, holistic manner. In this thesis, the water-land-energy-food-climate (WLEFC) nexus is addressed, taking into account trade-offs and synergies between these different systems in achieving multiple goals.

Scenario analysis can be used to explore the role of land use in climate change and climate change mitigation, and for other societal goals related to the WLEFC nexus. Scenarios can be defined as plausible descriptions of how the future might develop based on a coherent and internally consistent set of assumptions about the key relationships and driving forces (IPCC, 2000a). An important ambition of the scientific community is to develop scenarios that achieve both climate and other environmental and sustainability goals such as the PBs and the SDGs. In this thesis, we use exploratory scenarios that investigate how the future might develop under pre-defined assumptions, as well as normative scenarios that aim for pre-defined targets and describe pathways that could achieve these goals. Examples of targets are stabilizing global warming, nature protection or limits to water extraction. These scenarios are developed using the IMAGE integrated assessment model framework (Stehfest et al., 2014): It describes the human and natural system, their interactions and how these may develop into the future and is therefore well-suited to study land use, climate change and the WLEFC nexus. For some of the analyses and for model comparison purposes, also the land system model MAgPIE is used (Dietrich et al., 2019).

Specifically, the following research questions are addressed in this thesis:

1. How will land use develop in the long term under various scenarios at the global and regional scale?
2. What can be the role of land use in achieving stringent climate targets?
3. How important are trade-offs and synergies between land-based climate mitigation and other societal goals in the water-land-energy-food-climate nexus?
4. How can these trade-offs be minimized and synergies be maximized?

7.2. Main findings

7.2.1. How will land use develop in the long term under various scenarios at the global and regional scale?

The IMAGE elaboration of the SSP scenarios presented in Chapter 2 explores a wide range of land-use futures driven by assumptions on, among others, population and economic growth, lifestyle change, environmental awareness, (de)globalization and technological progress. The IMAGE 3.0 SSP scenarios were developed as part of a large multi-model effort (O'Neill et al., 2013; Riahi et al., 2017). The population assumptions in the scenario range from +36 million people (SSP1) to +5.9 billion people (SSP3) and per capita income (i.e. GDP) ranging from a factor 2 increase (SSP3) to a factor 16 increase (SSP5), for the 2010-2100 period (O'Neill et al., 2017). A key goal of the SSP scenarios is to cover the uncertainty range of land-use futures.

The SSP scenarios project changes in agricultural land ranging from -680 Mha (SSP1) to +1010 Mha (SSP3) and changes in natural land from -1060 Mha (SSP3) to +630 Mha (SSP1) depending on varying socio-economic futures and scenario assumptions (Figure 7-1).

These developments are a combination of different trends. In the Middle-of-the-Road scenario SSP2, continued income growth (+550% in 2010-2100) drives an increase in food consumption (+280 kcal/cap/day i.e. 8% in 2010-2100). In combination with population growth, this leads to strong increases in agricultural production of an additional 2700 Mt/yr crops and 160 Mt/yr livestock by the year 2100 (70% and 60%, respectively). This drives the expansion of cropland (+120 Mha, both rainfed and irrigated) and grazing land (+190 Mha). The built-up area expands (+60 Mha) due to population growth and urbanization, and bioenergy plantations also expand (+100 Mha) due to developments in the energy system that, also in a baseline scenario (i.e. without climate change mitigation policy), moves to relatively more renewables. All these expansions come at the cost of natural land (-470 Mha). In the Sustainability scenario SSP1, agricultural land decreases substantially (-680 Mha) due to lower population growth, improved agricultural efficiency due to technological development, stricter nature protection and a relative reduction in meat consumption due to more environmental awareness. On the other hand, the Regional Rivalry scenario SSP3 shows a strong increase in agricultural land (+1010 Mha) due to high population growth, stagnating technological developments and limited nature protection, resulting in large losses of natural land. The Fossil-fuelled Development scenario SSP5 also as a substantial expansion of agricultural land (+510 Mha), even though population changes are similar to SSP1, due to major increases in per capita food demand as the world population grows increasingly richer and consumption continues to grow strongly. The Inequality scenario SSP4 on the global level shows similar levels of expansion (+420 Mha) as SSP2, but with strong regional differences due to major inequalities between world regions.



Figure 7-1: Global land use in 2010 and global land-use change in the 2010–2050 and 2010–2100 period for seven land-use classes in the five SSP scenarios, based on IMAGE 3.0 as presented in Chapter 2.

Land-use trends differ strongly on the regional and local level: agricultural land increases in Sub-Saharan Africa and Latin America in almost all SSPs, while in the OECD countries and China agricultural land decreases in most SSPs. Although global developments are major drivers of land-use change, regional characteristics result in strong variation at the regional and local scale. The SSPs can provide insights into the differences. In Sub-Saharan Africa and Latin America, nearly all scenarios (except SSP1) show increases in agricultural land leading to deforestation and conversion of other natural land (Figure 2-8): Continued ecosystem loss is projected in the arc of deforestation in Brazil, the Gran Chaco in Bolivia, Paraguay and Argentina, the Congo Basin and the tropical rainforests of Western Africa (Figure 7-2). In Sub-Saharan Africa, the expansion is mainly driven by population growth which drives higher demand for agricultural production. In Latin America, on the other hand, populations stabilize in most scenarios: Land-use change is mostly a result of higher per capita consumption and expansion of extensively used grazing lands. A key similarity between Sub-Saharan Africa and Latin America is the high availability of land suitable for agricultural expansion: As a result, a substantial share of demand is fulfilled by land expansion as opposed to intensification. This is different from South and Southeast Asia, most notably India, where little additional land is available. As a result, additional demand has to be fulfilled mostly by agricultural intensification or more food imports. If this is not possible negative effects on food security follow. In most scenarios, the OECD regions and China see a moderate decrease in agricultural land use due to stable or decreasing populations and relatively small changes in per capita consumption levels. As a result of further intensification, OECD regions frequently still see an increase in agricultural production enabling higher exports.

Land-use change: 2010 – 2050

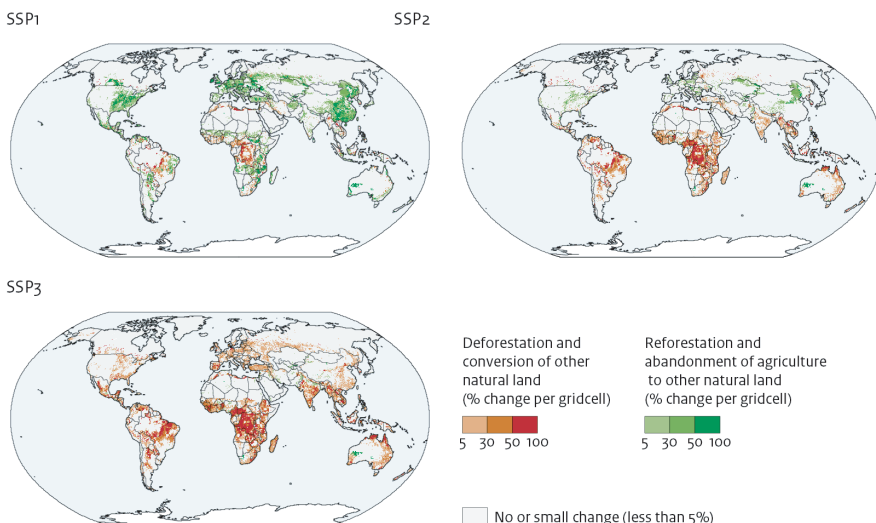


Figure 7-2: Change in land use (percentages of grid cells) between 2010 and 2050; deforestation and conversion of other natural land (red) and reforestation and abandonment of agriculture to other natural land (green) for SSP1, SSP2 and SSP3 based on IMAGE 3.0 as presented in Chapter 2.

7.2.2. What can be the role of land use in achieving stringent climate targets?

In baseline scenarios without climate policy, the share of AFOLU emissions in total emissions becomes smaller over the century (Table 7-1). The SSP baseline scenarios (i.e. without any climate policy) mostly show strong increases in GHG emissions up to the end of the century. The most extreme SSP5 scenario goes up to 130 GtCO₂-eq/yr in 2100, which means a tripling of current emissions, leading to about a 4-5°C temperature increase (IPCC, 2021). This is the result of much higher wealth and consumption levels and high dependency of the energy system on fossil fuels such as coal, which is fortunately considered an unlikely pathway (Hausfather and Peters, 2020). The share of AFOLU emissions in total emissions becomes smaller towards the end of the century in all scenarios: from 21% in 2010 to 13% in 2100 in SSP3 and SSP4, down to just 4% in SSP5. A key dynamic causing this effect is the slowing down of population growth in most scenarios, whereas wealth mostly does continue to grow. Income growth has the strongest impact on food demand when people move away from extreme poverty because the food demand elasticity (i.e. the percentage change in food demand with a percentage change in income) strongly decreases with higher income (Bijl et al., 2017; Muhammad et al., 2011). In the first half of the century, food demand growth continues at a similar pace as demand for energy and industrial goods. In the second half of the century, population growth slows down; moreover, food demand becomes less sensitive to income growth as people, on average, are richer. These trends result in a stabilization of food demand. As a consequence, non-CO₂ GHG emissions also stabilize as these are directly linked to total agricultural production. Land-use change (LUC) emissions go to zero as no additional agricultural land is needed or, in some cases, even go negative as agricultural efficiency continues to improve, resulting in a reduction of total agricultural land (SI Figure 2-3). Meanwhile, emissions from energy and industry do continue to increase, resulting in smaller shares of AFOLU emissions in total emissions.

Table 7-1: Emissions for the energy, industry and AFOLU sectors, and the share of AFOLU emissions of total emissions in the five baseline SSP scenarios, in 2010, 2050 and 2100 based on IMAGE 3.0 as presented in Chapter 2 in terms of GtCO₂-eq/yr using 100-year time horizon global warming potentials (GWP100) (see also Figure 2-12).

2010	2010				
Energy and industry emissions (GtCO ₂ -eq/yr)	38.2				
AFOLU emissions (GtCO ₂ -eq/yr)	9.9				
AFOLU share of total (%)	21%				
2050	SSP1	SSP2	SSP3	SSP4	SSP5
Energy and industry emissions (GtCO ₂ -eq/yr)	52.6	61.3	64.2	54.0	93.4
AFOLU emissions (GtCO ₂ -eq/yr)	5.9	13.5	17.1	14.4	14.9
AFOLU share of total (%)	10%	18%	21%	21%	14%
2100	SSP1	SSP2	SSP3	SSP4	SSP5
Energy and industry emissions (GtCO ₂ -eq/yr)	35.0	86.6	87.4	53.3	130.7
AFOLU emissions (GtCO ₂ -eq/yr)	3.2	7.7	12.6	7.8	5.6
AFOLU share of total (%)	8%	8%	13%	13%	4%

Dedicated peatland protection and restoration measures have substantial mitigation potential (96 GtCO₂ in 2020-2100 in SSP2) without large impacts on global land-use change compared to default mitigation scenarios. Chapter 3 presents a new assessment of the role of peatland degradation, protection and restoration in SSP scenarios. Gridded estimates of peatland extent are integrated into IMAGE and combined with spatial explicit land use and IPCC-based emission factors to determine emissions of peatland degradation in baseline and mitigation scenarios. Baseline scenarios find substantial increases in degraded peatland area and GHG emissions in SSP2 and SSP3, compared to a moderate decrease in SSP1. In default mitigation scenarios (i.e. without dedicated peatland protection and restoration measures), peatland emissions decrease due to synergies with forest protection and afforestation policy. Still, the share of total emissions remains high, with 65 to 96 GtCO₂ cumulatively left unabated. Dedicated peatland policy fully restoring degraded peatlands can bring peatland emissions to nearly zero without major effects on projected land-use dynamics. This underlines the opportunity of peatland policy for climate change mitigation and the need to combine different land-based mitigation measures synergistically. The possibility to protect and restore peatlands is, however, unequally distributed between regions, with one-third of required GHG emissions reductions located in one country (Indonesia) where prevention of additional peatland degradation is essential as well as restoration of already degraded peatlands. A large potential for peatland restoration is found in temperate and boreal regions such as Europe, North America and Russia, while these regions do not show high risk for additional peatland degradation. In contrast, in South America peatland degradation is projected to expand substantially while its current extent of degraded peatlands is fairly limited.

In cost-optimal scenarios afforestation for climate mitigation plays a major role as a carbon dioxide removal option (430 GtCO₂ cumulatively in SSP2-2.6), allowing to achieve stringent climate targets at lower costs. A newly developed methodology to assess afforestation potential in competition with the agricultural sector is presented in Chapter 4: Grid-based estimates of tree growth as modelled with LPJmL (Braakhekke et al., 2019) are combined with region-specific estimates of afforestation costs, price effects of land scarcity and risk-adjusted investment decisions. This data is used to produce marginal abatement cost curves that are implemented in the climate policy model FAIR-SimCAP to compare afforestation to other climate change mitigation options in the energy, industry and agricultural sectors. It is shown that afforestation has large potential for mitigation at relatively low prices, where an SSP2 scenario with cost-optimal policy (i.e. policy that achieves targets at the lowest costs) aiming for 2°C maximum warming uses 430 GtCO₂ of negative emissions from afforestation. This also lowers the mitigation costs, as indicated by a lower CO₂ price (240 US\$/tCO₂ compared to 430 US\$/tCO₂ on average in 2020-2100)(Figure 7-3). The higher dependence on negative emissions is a risk as it could lead to lock-in situations in sectors that are more expensive to decarbonize (Anderson and Peters, 2016). A cost-optimal approach to afforestation also leads to a higher dependence of climate policy on action in low-income regions. In a scenario with afforestation 31% of CDR is implemented

in low-income regions compared to 17% in a scenario where afforestation is excluded as a mitigation option (mainly afforestation and bioenergy with CCS, comparison between SSP2-2.6-A and SSP2-2.6-R).

In cost-optimal scenarios land-based climate change mitigation can provide annual emission reductions of 28%-33% and 28%-44% in 2050 and 2100, respectively, depending on scenario characteristics. Figure 7-4 and Table 7-2 show the role of land-based mitigation measures in relation to total mitigation in other energy (i.e. not bio-energy) and industry (based on IMAGE 3.2 scenarios presented in Chapter 3). Land-based mitigation (incl. bioenergy and its fossil-fuel substitution effect, similar analysis as presented in Section 2.3.4) amounts to 16-21 GtCO₂-eq/yr in 2050 and 20-26 GtCO₂-eq/yr in 2100 (Figure 7-4). Especially in SSP1-1.9, the share of land-based mitigation is high, i.e. 44% in 2100 (Table 7-2). The reason for this is that land-based mitigation is often cheaper than mitigation in energy and industry (see also Chapter 4), which means that if the total mitigation requirement is relatively small land-based mitigation takes a relatively high share. This explains the high share of land-based mitigation in SSP1-1.9 compared to the relatively lower share in SSP3-2.6 (28% in 2100).

Non-CO₂ mitigation plays a larger role in scenarios with strong increases in agricultural production, up to 6.2 GtCO₂-eq/yr in SSP3-2.6 in 2100. Non-CO₂ mitigation in agriculture (e.g. improved manure management or feed additives to reduce enteric fermentation) leads to emission reductions of 1.4-4.5 GtCO₂-eq/yr in 2050 and 2.7-7.3 GtCO₂-eq/yr in 2100. It is a relatively cheap measure, so with high GHG prices typically present in deep mitigation scenarios, the maximum potential is used (Harmsen et al., 2019). The potential is highest in SSP3 because high population growth leads to strong increases in food demand and inefficient agriculture leads to relatively higher emission per ton food production. Logically, higher total emissions also increases the potential to mitigate emissions. Importantly, these emissions cannot be fully mitigated, and therefore remaining emissions need to be (partly) compensated by negative emissions (Gernaat et al., 2015).

The potential to reduce emissions by avoided deforestation directly depends on baseline deforestation trends. The contribution of avoided deforestation ranges between near zero in SSP1-1.9 to 6.8 GtCO₂-eq/yr in SSP3 in 2050. This is directly dependent on projected deforestation in the baseline scenario. Typically in SSP2 and SSP3 strong continuation of deforestation is projected, with forest losses of respectively 330 and 560 Mha between 2020 and 2100 leading to high emissions. In contrast, in SSP1 due to modest increases in food demand, high agricultural efficiency and an environmentally aware society deforestation is eliminated in the baseline and therefore avoided deforestation does not have a role as a mitigation option.

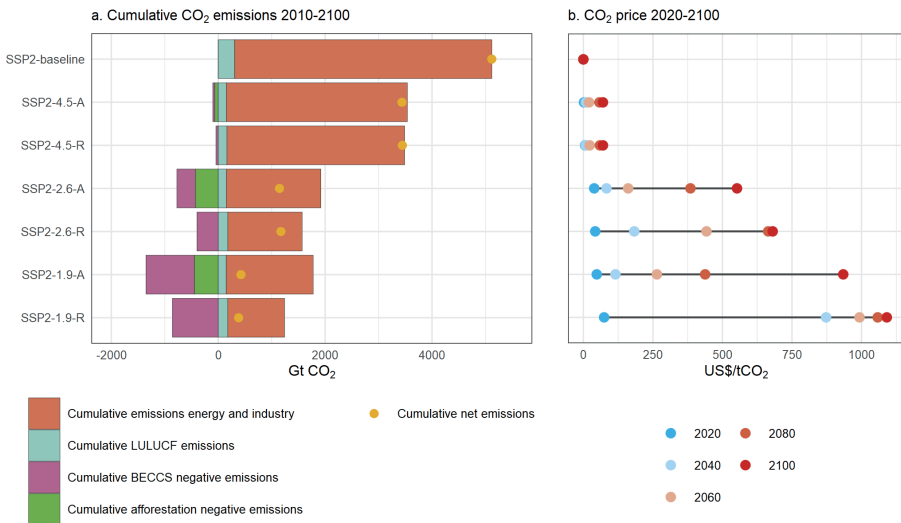


Figure 7-3: Selected scenarios assessed in Chapter 4 using IMAGE 3.0 aiming for maximum warming of 4.5, 2.6 or 1.9 W/m² either with afforestation as a mitigation option (indicated by suffix A (Afforestation)) or without afforestation as a mitigation option (indicated by suffix R (Reference)). The results show (a) cumulative CO₂ emissions in 2010-2100 and (b) CO₂ prices in selected years from 2020 to 2100.

Afforestation and peatland protection and restoration are important mitigation measures with 5.3 and 1.2 GtCO₂-eq/yr in 2050 in SSP2-1.9. Afforestation is responsible for 8%-13% of total mitigation in SSP1-1.9 and SSP2-1.9, indicating the critical role of afforestation in cost-optimal mitigation scenarios. In SSP3-2.6 afforestation has a relatively smaller role (~1%) as limits on afforestation as a mitigation measure are assumed in the SSP3 narrative. The potential of peatland protection and restoration is around 2% in all mitigation scenarios indicating that is a modest but non-negligible component of the climate change mitigation portfolio.

Bioenergy plays a critical role in cost-optimal scenarios with a share in total mitigation of 9%-23%. The production of bioenergy and its use in the energy system is an effective mitigation option as it can replace the use of fossil fuel with an option with much lower net CO₂ emissions. Additionally, it has the capacity to remove CO₂ from the atmosphere when applied in combination with carbon-capture and storage (CCS). In the cost-optimal mitigation scenarios presented in this thesis (Figure 7-4) the net mitigation effect can be as high as 13.5 GtCO₂-eq/yr (in SSP3-2.6 in 2100), higher than any other land-based mitigation category. Especially in SSP1 the share of bioenergy is high compared to other mitigation options (23% in 2100), because large-scale abandonment of agricultural land makes land cheaply available for biomass production. However, extensive use of bioenergy for climate mitigation has received criticism related to mitigation efficacy concerns and negative impacts on biodiversity and food security (Hasegawa et al., 2020; Searchinger et al., 2017). Scenarios aiming to achieve

stringent climate mitigation targets with limited bioenergy use have been an important topic of study in recent years (Edelenbosch et al., 2022; van Vuuren et al., 2018)

Dietary change and food waste reduction have major climate change mitigation potential of 6.7 GtCO₂eq/yr in 2050. Demand-side measures such as changes in diet and food waste reduction are not part of default cost-optimal mitigation scenarios as presented earlier. In Chapter 6 an SSP2 scenario is assessed (FOOD) where a transition towards healthy diets as proposed by the EAT-Lancet commission (Willett et al., 2019) is implemented. This includes reduced meat and dairy consumption and lower total calorie intake in middle- and high-income regions. In addition, food waste is reduced (Gustavsson et al., 2011). It is shown that by the year 2050, these changes reduce GHG emissions by 6.7 GtCO₂eq/yr, which is equal to 10% of the total required mitigation effort in SSP2-1.9. It is important to note that this mitigation potential cannot simply be added to the land-based mitigation potential as estimated based on the default mitigation scenarios. The GHG emission reductions attributed to diet change result from lower agricultural non-CO₂ emissions (mainly from livestock) and forest regrowth on abandoned agricultural land (mainly grazing land), therefore reducing the potential of non-CO₂ mitigation potential and afforestation as estimated in cost-optimal scenarios.

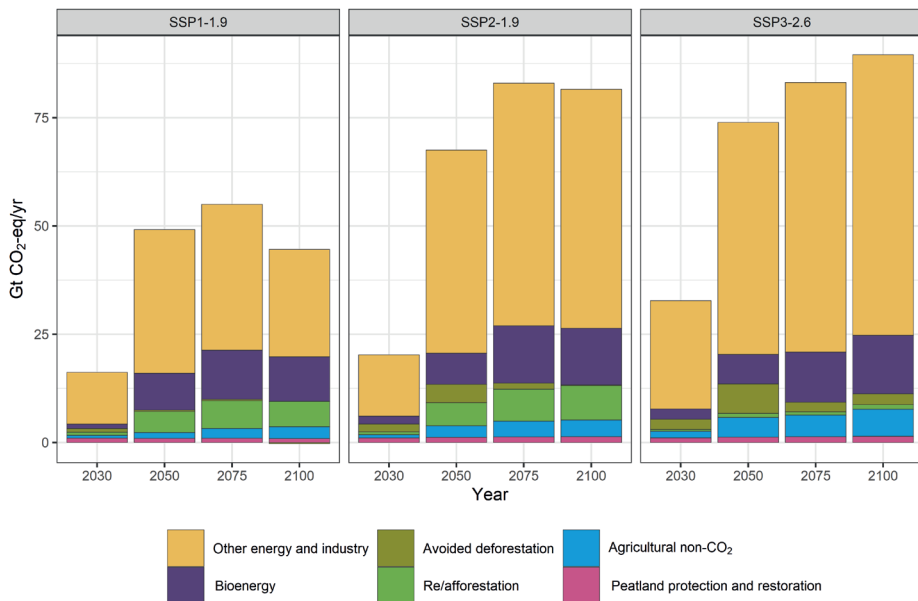


Figure 7-4: Annual global mitigation (i.e. difference in emissions between baseline and mitigation scenario) in SSP1-1.9, SSP2-1.9 and SSP3-2.6 in GtCO₂-eq/yr (GWP100) per land-based mitigation option and energy and industry in 2030, 2050, 2075 and 2100. Results are based on IMAGE 3.2 scenarios as presented in Chapter 3. Bioenergy mitigation includes carbon-capture and storage and fossil-fuel substitution effect, and is corrected for land-use change effects, based on the method presented in Section 2.3.4.

Table 7-2: Mitigation shares per land-based mitigation option and energy and industry in 2050 and 2100 derived from annual GHG emissions (see Figure 7-4). Results are based on IMAGE 3.2 scenarios as presented in Chapter 3. Bioenergy mitigation includes carbon-capture and storage and fossil-fuel substitution effect, and is corrected for land-use change effects, based on the method presented in Section 2.3.4.

2050	SSP1-1.9	SSP2-1.9	SSP3-2.6
Avoided deforestation	1%	6%	9%
Re/afforestation	10%	8%	1%
Agricultural non-CO2	3%	4%	6%
Peatland protection and restoration	2%	2%	2%
Bioenergy	17%	11%	9%
Other energy and industry	67%	69%	72%
2100	SSP1-1.9	SSP2-1.9	SSP3-2.6
Avoided deforestation	0%	0%	3%
Re/afforestation	13%	10%	1%
Agricultural non-CO2	6%	5%	7%
Peatland protection and restoration	2%	2%	2%
Bioenergy	23%	16%	15%
Other energy and industry	56%	68%	72%

7.2.3. How important are trade-offs and synergies between land-based climate mitigation and other societal goals in the water-land-energy-food-climate nexus?

Forest protection can lead to less expansion of agricultural land and thus prevent deforestation. However, it also leads to displacement of land use to other natural lands. Strict protection of forests to limit deforestation emissions leads to an increase in forest area compared to the baseline, e.g. by 120 Mha in 2050 in the CLIMATE scenario from IMAGE 3.2 (Chapter 6, similar to SSP2-2.6, see Figure 6-2). The reduced loss of natural forest is an important synergy with terrestrial biodiversity. However, by only protecting natural ecosystems with high aboveground carbon content, a displacement of agricultural expansion to other ecosystems takes place that have lower aboveground carbon content but also unique biodiversity value, e.g. natural grasslands such as savannahs and steppes. This can be seen in SSP2-2.6 (Chapter 2) where forest increases by 400 Mha compared to the baseline while other natural lands decrease by 250 Mha.

Bioenergy can play a role in climate change mitigation but has strong trade-offs with natural land and therefore terrestrial biodiversity. As discussed in the previous section, bioenergy could play a large role in achieving stringent climate targets. This does however

require large areas of land, e.g. 410 Mha by 2100 in IMAGE 3.0 in SSP2-1.9 (Chapter 2) and 320 Mha by 2050 in the CLIMATE scenario by MAgPIE (Chapter 6). The expansion of bioenergy lands partly uses agricultural land that was used for food production leading to food security effects (see next section), but also takes place on natural lands impacting terrestrial biodiversity. As expansion of agricultural land for bioenergy is typically implemented in mitigation scenarios that also include forest protection measures to limit LUC emissions, new bioenergy area usually leads to a reduction in non-forest ecosystems.

In ambitious mitigation pathways afforestation could lead up to 1090 Mha of additional forest area by 2100 in SSP2-2.6. Impacts on biodiversity could be positive or negative depending on tree species used and management intensity. At moderate and high CO₂ prices afforestation is an economically viable alternative to agriculture and therefore agricultural land is converted to forest when cost-optimal competition is allowed in deep mitigation scenarios (Chapter 4). In an SSP2-2.6 scenario where the value of CO₂ is on average 240 US\$/tCO₂ in the 2020-2100 period this leads to strong increases in forest area up to 1090 Mha by the end of the century. In this thesis we assume planted forest with minimum management afterwards. No specific assumptions are made on tree species due to model limitations. If exotic tree species are used in locations where naturally non-forest ecosystems occur, for example Eucalypt plantations in savannah ecosystems, afforestation has strong trade-offs with biodiversity (Bremer and Farley, 2010; Hall et al., 2012). In contrast, reforestation with native tree species could in fact be synergistic with terrestrial biodiversity goals.

The impact of climate policy on agriculture can severely affect food security with 110-135 million more people at risk of hunger in 2050 compared to baseline levels, with the bulk of the effect occurring in Sub-Saharan Africa and South/Southeast Asia. Competition for land between food production and land-based mitigation measures limits the capacity to produce food leading to higher food prices and consequently reduced food availability and security (Chapters 2, 4, 5, 6). These impacts can be evaluated along FAO's four food security dimensions: availability, access, utilization and stability (FAO, 1996; van Meijl et al., 2020). The number of people at risk of hunger is a key indicator of food availability which also takes inequality and healthy levels of food intake into account. Analyses with IMAGE 3.2 show that in baseline scenarios the number of people at risk of hunger decreases from 670 million in 2020 to 240-410 million in 2050, mainly due to income growth, with the lowest estimate in SSP1 and the highest in SSP3 (Figure 7-5). If large-scale land-based mitigation is implemented an extra 110-140 million people could be at risk of hunger in 2050, due to increased competition for land and resources in the food system. By the end of the century the effects could be even stronger (Chapter 4), however these long-term food security estimates are uncertain as food demand elasticities are based on recent time periods and might not be applicable for the long term (Bijl et al., 2017).

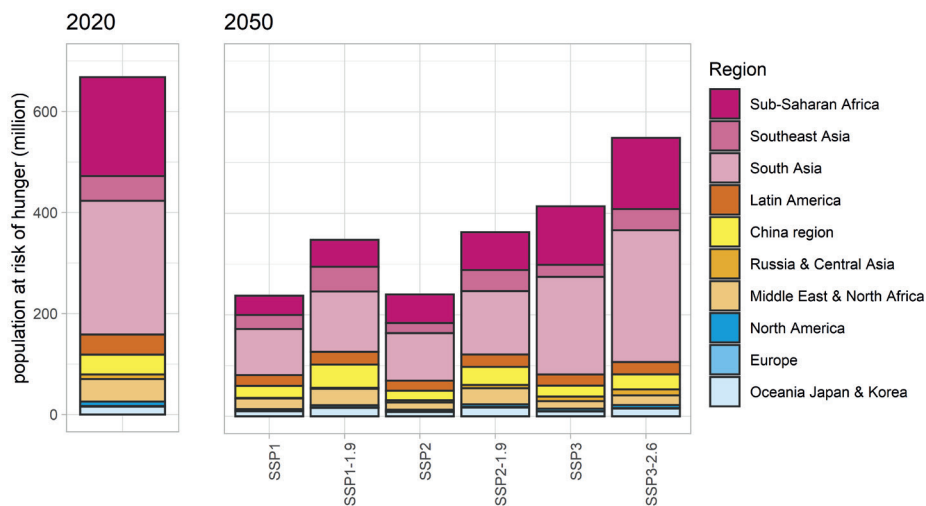


Figure 7-5: Number of people at risk of hunger in 2020, and in 2050 in baseline scenarios SSP1, SSP2 and SSP3 and in mitigation scenarios SSP1-1.9, SSP2-1.9 and SSP3-2.6. Results based on IMAGE 3.2 scenarios presented in Chapter 3.

Land-based mitigation could lead to a substantial increase in freshwater extraction for irrigation, up to 540 km³ extra (+31%) compared to the baseline in 2050, but this depends on model characteristics and assumptions. The analysis of irrigation water use in IMAGE 3.2 and MAGPIE in the CLIMATE scenario in Chapter 6 shows that water use could increase between +70 and +540 km³ in a mitigation scenario compared to a baseline scenario. MAGPIE shows substantially increased withdrawals due to expansion of irrigated area for bioenergy production and as part of enhanced agricultural intensification due to pressure on the food system from emission pricing and land protection. In IMAGE 3.2, bioenergy is assumed not to be irrigated as part of a set of sustainability assumptions and irrigation area is not affected by agricultural intensification. Lower CO₂ fertilization in a mitigation scenario does reduce irrigation efficiency leading to slightly higher levels of water withdrawal. This indicates that water use could be a strong trade-off of land-based mitigation, but the estimated effects depend on model characteristics and assumptions.

The increase in agricultural production in a baseline scenario could cause a strong rise in nitrogen surplus (+36% to +54%) indicating risks for water quality and biodiversity. In a climate mitigation scenario, this surplus is reduced (-8% to -24%) due to synergies with N₂O mitigation policies. Continued growth in agricultural production leads to strong growth in fertilizer use for crop production and manure resulting from livestock production. This leads to more N₂O emissions to the atmosphere exacerbating climate change and nitrogen emissions to the soil and surface water reducing water quality and damaging terrestrial and aquatic biodiversity. The nitrogen surplus, i.e. the amount of nitrogen that is not taken up by

agricultural crops, is a suitable indicator to assess the magnitude and risk of these processes. In a baseline scenario strong increases take place from 2015 to 2050 both in IMAGE 3.2 (+47 MtN/yr i.e. +36%) and MAgPIE (+79 MtN/yr, i.e. +54%)(REF scenario, Chapter 6, Figure 6-4). In a mitigation scenario, the nitrogen surplus is reduced (-17 MtN/yr to -43 MtN/yr, i.e. -8% to -24% in 2050 compared to baseline level), due to higher nitrogen use efficiencies in line with mitigation policies aiming to reduce N₂O emissions. Applied measures are for example more efficient fertilizer use, application of nitrification inhibitors, and improved manure management. This indicates an important synergy between climate policy and excessive nitrogen in the land and water components of the nexus.

7.2.4. How can these trade-offs be minimized and synergies be maximized?

Additional agricultural intensification of 17% in crop yields and 14% in ruminant efficiency compared to baseline intensification from 2010 to 2050 would be sufficient to prevent negative impacts of land-based mitigation on food security. In Chapter 5 an analysis is made of the effect of large-scale land-based mitigation on food security. Subsequently, it is calculated at what level of additional agricultural intensification food prices are the same as baseline levels. It is shown that 17% increase in crop yields and 14% increase in ruminant efficiency (tonnes of ruminant meat and dairy per hectare of grazing land) from 2010 to 2050 compared to the baseline levels would be sufficient to remedy negative food security impacts (Figure 7-6). Historically, cereal yields have seen a continuous linear increase since 1961 and a doubling of yields in the 1970-2010 period (global average). Ruminant efficiency increased by 70% over the same period. In that context, 18% for crops and 15% for ruminants seems realistic in the 2010-2050 time period. However, these increases do need to be achieved on top of baseline efficiency increases of 100% and 50%, respectively, resulting in trends that are on the high end of scenarios in the literature (van Zeist et al., 2020). Large potential for yield improvement exists in developing countries with large yield gaps (van Ittersum et al., 2013), but at the same time it is questioned whether yields can continue to increase at historical rates or whether biological limits to crop productivity are being reached (Grassini et al., 2013). Moreover, a key question is whether agricultural intensification can be achieved sustainably without trade-offs to other components of the nexus such as water use and biodiversity (Seppelt et al., 2020).

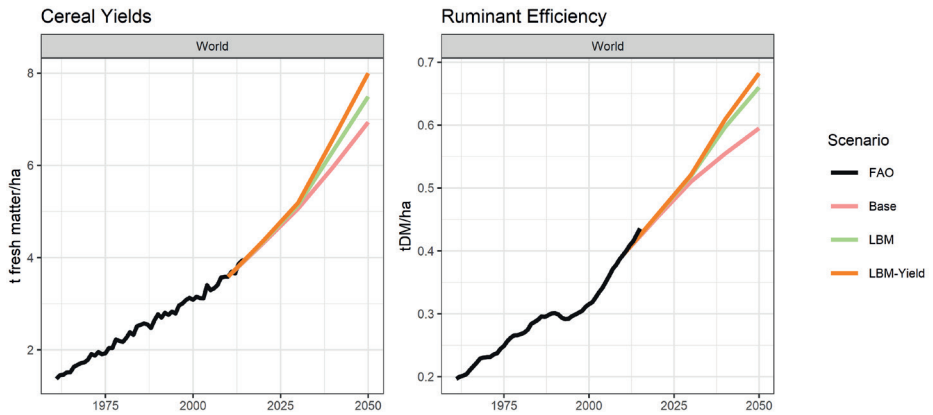


Figure 7-6: Cereal yields and ruminant efficiency (ruminant meat and dairy production divided by grassland area) for historical period based on FAO and scenario period for three scenarios: a business-as-usual scenario (Base), a scenario with large-scale land-based mitigation such as bioenergy and afforestation (LBM), and a scenario with large-scale land-based mitigation and additional agricultural intensification to prevent negative food security impacts (LBM-Yield) (see for more detail Chapter 5). Projected cereal yields and ruminant efficiencies are corrected to 2015 FAO values.

Lower demand in the food system from changes such as lower meat consumption, healthy diets and less food waste have co-benefits in all components of the WLEFC nexus. To investigate the role of demand-side changes in the food system and impacts in the WLEFC nexus, scenarios are implemented where diets are changed in line with healthy diets as proposed by the EAT-Lancet commission (FOOD scenario, Chapter 6) (Willett et al., 2019). This includes reduced meat and dairy consumption and lower total calorie intake in middle- and high-income regions, and increased calorie intake up to healthy levels in low-income regions. For example in Western Europe, this involves a reduction in daily meat consumption per person from on average 280 grams today to 50 grams in 2050. In addition, lower food waste is implemented as especially in high-income regions this is an extra cause of high food demand (Gustavsson et al., 2011). It is shown that demand-side changes have strong synergies with all components of the WLEFC nexus (Table 7-3). AFOLU GHG emissions are strongly reduced (-45% to -58% in 2050 relative to baseline in IMAGE and MAgPIE, resp.), most notably due to less livestock production reducing non-CO₂ emissions (meat production is reduced from 430 Mt per year today to 280 Mt/yr in 2050, compared to 590 Mt/yr in the reference scenario), but also due to strongly reduced deforestation as no more agricultural expansion is required and even restoration of natural land due to agricultural abandonment takes place. These dynamics also directly relate to an increase in natural land area (+4% to +8%) indicating the benefits for terrestrial biodiversity. Similarly, the nitrogen surplus is greatly reduced (-23% to -35%) mainly due to less manure from livestock production which is beneficial for both aquatic and terrestrial biodiversity. Also, the requirements for irrigation water withdrawal are substantially lower (-3% to -24%) as a consequence of reduced pressure in the food system. In Chapter 6, the effects on the energy system are not investigated, however in Chapter 2, it is shown that moderate reductions in meat consumption in SSP1,

in combination with other scenario assumptions, greatly increased the availability of land leading to high levels of bioenergy deployment indicating synergies between reduced food demand and energy availability. Finally, in Chapter 5, it is shown that a moderate reduction in meat consumption could limit the productivity increase needed to prevent negative food security effects.

Protection of natural ecosystems benefits biodiversity and reduces GHG emissions. However, additional measures such as yield increases or dietary change are needed to prevent negative impacts on food security and irrigation water use. An ambitious conservation effort is implemented in the LAND scenario in Chapter 6, aiming to preserve half of the Earth's terrestrial area for nature (Pimm et al., 2018; Wilson, 2016). The scenario analysis with IMAGE 3.2 and MAgPIE shows that this measure indeed leads to a substantial increase in the natural land area (+2% to +4%), indicating the benefits for biodiversity. In addition, it also substantially limits AFOLU GHG emissions (-14% to -27%) due to less conversion of natural lands. On the other hand, the limits on agricultural expansion increase the pressure on the agricultural system leading to higher food prices (+20% in IMAGE), highlighting a trade-off with food security. Moreover, increased water withdrawals for irrigation (+10% in MAgPIE) indicate a trade-off with water availability and aquatic biodiversity. To minimize these trade-offs, additional measures are required, for example, higher levels of agricultural intensification or dietary changes.

Restrictions on the extraction of freshwater for irrigation benefit aquatic biodiversity but have trade-offs with food security, most notably in arid regions. Improved irrigation efficiency could mitigate these impacts. Excessive water use might negatively affect aquatic biodiversity: A measure to prevent this is the restriction of water extraction in line with environmental flow requirements (EFR) (Smakhtin et al., 2004). If such a measure is implemented globally, as tested in the WATER scenario (Chapter 6), it reduces irrigation water withdrawal by 26% to 28%. The trade-offs of these restrictions are very unevenly distributed, as some regions rely much more on irrigated agriculture than others. Most notably, Northern Africa, the Middle East and Central Asia would be severely impacted by major increases in food prices, indicating risks to food security (+30% in Russia and Central Asia and +60% in Middle East and Northern Africa in 2050 in IMAGE 3.2). As the agricultural sector needs to compensate for the loss of production on irrigated lands, this could even lead to expansion of agriculture elsewhere, in turn affecting natural land, which is reduced by 1% in IMAGE 3.2 as a consequence of agricultural expansion. To prevent the trade-offs of EFR, additional measures are needed. Improved irrigation efficiency, which is not assessed in this thesis, could alleviate the aforementioned issues for example by switching from surface to sprinkler or drip irrigation thereby greatly increasing the amount of agricultural production that can be achieved per litre of water (Jägermeyr et al., 2015).

Increasing nitrogen use efficiency for the purpose of limiting negative biodiversity effects has synergies with climate policy and could reduce food prices. In the nexus scenario assessment of Chapter 6 improvements in nitrogen use efficiency are a specific measure to reduce the nitrogen surplus in agriculture and to limit the effects of excessive nitrogen on terrestrial and aquatic biodiversity (WATER and LAND scenarios). Due to lower application rates of synthetic fertilizer also the emissions of N₂O are reduced indicating an important synergy with climate policy. Additionally, in MAgPIE modest reductions in food prices are observed due to lower fertilizer costs indicating some improvement in food security.

Table 7-3: Global percentage difference of scenario indicators in IMAGE and MAgPIE between the REF scenario and the nexus scenarios in 2050 (Chapter 6). Colour indication shows where strong synergies occur in green, weak synergies in light green, strong trade-offs in red, weak trade-offs in light red, indicators specifically targeted by measures in a particular scenario in blue, and no substantial change in grey.

Model Scenario	MAgPIE					IMAGE				
	WATER	LAND	FOOD	CLIMATE	TOTAL	WATER	LAND	FOOD	CLIMATE	TOTAL
Water Withdrawal Irrigation	-26%	+10%	-24%	+31%	-25%	-28%	0%	-3%	+5%	-26%
Natural Land Area	0%	+2%	+4%	+2%	+6%	-1%	+4%	+8%	+2%	+8%
Nitrogen Surplus Agriculture	-27%	-27%	-35%	-8%	-61%	-30%	-32%	-23%	-24%	-51%
Food Price	+1%	+1%	-18%	+7%	-11%	+9%	+20%	-46%	+11%	-34%
AFOLU Emissions	-3%	-14%	-58%	-43%	-83%	0%	-27%	-45%	-30%	-53%

7.3. Suggestions for future research

The studies presented in this thesis highlight several topics where further research is warranted. These concern model developments and improved cooperation and integration between research fields.

Integrated modelling of all land-based mitigation options. As discussed in the introduction on land-based climate change mitigation measures (Section 1.2), not all mitigation options are addressed in this thesis nor are all possible mitigation options represented in the IMAGE model. It is a challenge for all integrated assessment modelling teams to keep up to date with ongoing research and integrate every new mitigation measure in their models. This is also evident in Roe et al (2021) where the scope of the sector-based assessment of mitigation potentials is larger than the assessment based on the IAMs. It is key that IAMs continue to

integrate new mitigation options, especially because these models are the best tools to assess whether different mitigation options compete with one another as this might limit the total potential of measures which is not taken into account in sectoral assessments. This is the case, for instance, for CDR measures in agriculture such as increased soil carbon storage or addition of biochar. These measures depend on the availability of crop residues or dedicated biomass crops that are currently assumed to be used for bioenergy (Daioglou et al., 2016). The same goes for agroforestry, that is projected on large areas of agricultural land that in mitigation scenarios may be converted to forest for climate mitigation purposes. Assessing the potential of agricultural CDR measures must be done in an integrated manner with transparent scenario assumptions. IAMs are well-suited for this task but continued research and model development is essential.

Location and process-specific modelling of agricultural intensification and its limits.

From 1961 to 2020 on average 90% of annual growth in global crop production was achieved through intensification of existing cropland as opposed to expansion of cropland (USDA-ERS, 2022a). This highlights the crucial role of agricultural intensification in fulfilling food demand. At the same time, intensification is the cause of environmental issues such as the loss of biodiversity in agricultural landscapes, excessive freshwater use, soil erosion, and eutrophication of rivers and lakes. Finding a balance between using the land for the provision of food and the role of land in ecosystem services is a key question. Grid-based modelling of agricultural intensification could help to answer this question, especially because many of these processes are highly location-specific. In addition, improved representation of the different drivers of intensification is required such as changes in fertilizer and pesticide use, increased mechanization, more productive crop varieties or better agronomic knowledge. In the approach used in this thesis, the ratio between agricultural expansion and intensification to fulfil agricultural demand is determined at the world-region level where aggregated yield and land supply shocks related to environmental issues are taken into account. If location and driver-specific limits to intensification can be set, for example related to biodiversity hotspots, sensitivity to soil erosion, water depletion, or riparian zones to limit nutrient and pesticide leaching, a more detailed assessment can be made of the processes and impacts of agricultural intensification. Such an approach can also show the consequences of limits to intensification within regions where the impacts occur, making the step from large-scale global challenges to local solutions more comprehensible and easier to communicate to policymakers.

Expanded modelling of climate impacts and more explicit modelling of climate adaptation. This thesis did not focus on climate impacts and adaptation, even though these are important topics in relation to climate policy and, therefore, important fields of further research. A key issue is the wide range in estimates of climate impact on crop yields (Jägermeyr et al., 2021), where a better understanding of the effects of CO₂ fertilization, drought, heat stress and extreme events is important to take the impacts of yield changes in land-use futures better into account. In addition, other impacts on the agricultural sector,

such as the effects of heat stress on labour, are usually excluded. These could have severe effects, though, and for that reason should be integrated (de Lima et al., 2021; Hertel and de Lima, 2020). Finally, adaptation to climate change is often implicitly included, for example, changes in trade between regions due to climate impacts on crop yields or changes in crop sowing seasons due to different precipitation regimes. Conversely, other adaptation options might not be included due to model limitations even though they could help to mitigate climate change impacts, for example the possibility to further expand irrigation. It could help to make the role of adaptation more explicit in order to understand the challenges society will face due to climate change and make the possibilities of adaptation clearer for policymakers to act on them.

Expanded modelling of nexus and sustainable development linkages to develop comprehensive sustainable development pathways. In this thesis, several nexus linkages and sustainable development topics were explicitly quantified and discussed in detail. At the same time, many linkages and dimensions of sustainable development are not represented. It is key to expand the number of modelled linkages between nexus components and dimensions of sustainable development. Eventually, scenarios should be developed that can outline comprehensive future pathways that achieve sustainability both from a social and environmental perspective while taking trade-offs and synergies into account. To achieve this, further integration between different modelling and research fields is needed. For example, the impacts of land-use change and intensification on biodiversity could be integrated in agro-economic modelling to dynamically consider the impacts on biodiversity and its benefits and explore economically optimal transition pathways. Also, the interactions between the energy system and the nexus can be further integrated: for example, the effects of water shortages on power generation; the effects of hydropower on water availability and biodiversity; and the effect of biodiversity protection measures on hydropower potential. Finally, the effects on human well-being need to become a standard component of assessments. Food security already receives quite some attention, whereas health and poverty could equally be part of the core set of indicators that are assessed.

Learning from social sciences to model land system transitions. The land-use projections presented in this thesis are based on neoclassical economic theory, which is the core of the agro-economic modelling. This type of modelling implicitly takes human behaviour into account based on relations built on historical data. However, major transitions to, for example, different diets can only be implemented in a stylized manner. Better understanding and representation of human behaviour and decision-making might improve the realism of the land system projections and also give more concrete options for policy-makers and society in general to achieve such transitions. To this end, the integrated assessment modelling community should improve the cooperation with social sciences. Interesting examples that are moving in this direction are agent-based modelling of European land-system change (Brown et al., 2019) and behavioural modelling of diet change (Eker et al., 2019).

7.4. Policy recommendations

The results of this thesis are ultimately intended to advise policy-makers on the role of the land sector in limiting global warming to well below two degrees while protecting the environment and achieving sustainable development. The key policy recommendations can be summarized as follows.

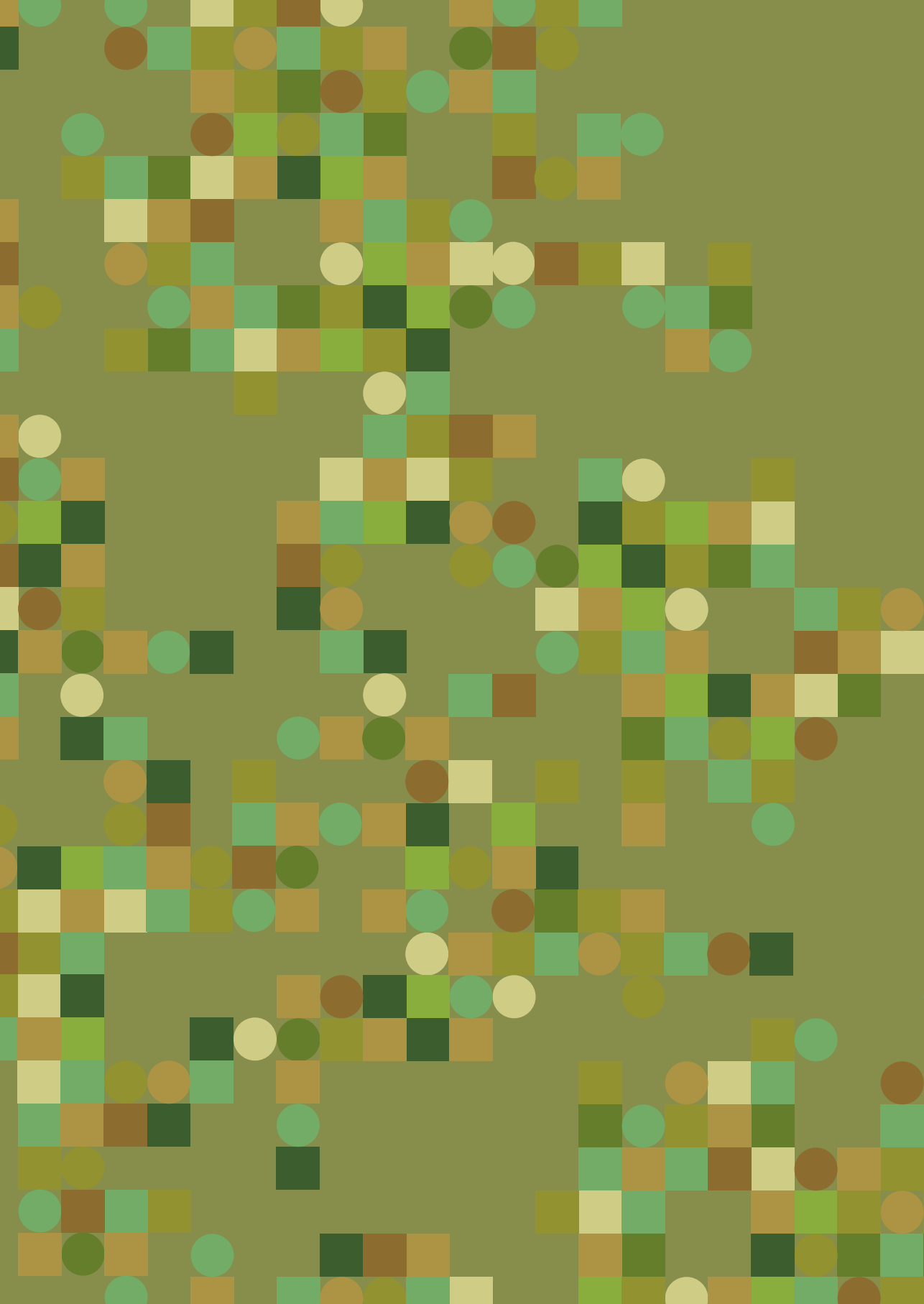
Land-based mitigation can provide a large contribution to limiting climate change, however policy should not be over-reliant on the land sector due to risks of trade-offs and feasibility concerns. Land-based mitigation can deliver a major share of climate change mitigation needed to achieve ambitious mitigation targets, with 28%-33% of total mitigation in 2050 related to land in cost-optimal mitigation pathways. However, these mitigation measures have risks for trade-offs, most notably with food security due to competition for land, with biodiversity due to large-scale use of bioenergy and afforestation, and excessive water and fertilizer use due to agricultural intensification. In addition, a large share of the potential is located in developing regions where continued economic development is required to improve living standards in line with the SDGs. Moreover, the implementation of measures depends on farmers and other land owners involving feasibility concerns. Therefore, the estimated potential of land-based mitigation needs to be treated with caution and net-zero strategies should not be over-reliant on the land sector. When land-based mitigation is included as an important contributor, it should be carefully planned using a nexus approach that accounts for environmental requirements as well as the needs of people dependent on the land.

Peatland protection and restoration are efficient climate mitigation measures that deserve attention of policy-makers. Protection of natural peatlands and restoration of degraded peatlands are very effective mitigation measures with large GHG benefits per hectare. They can contribute about 2% of total mitigation, with relatively small impacts on global land-use dynamics. Therefore they deserve the attention of policy-makers. A critical challenge however is the unequal geographic distribution of peatland mitigation potential where few countries have the opportunity to implement policy.

Demand-side measures such as diet change and food waste reductions are no-regret policy options as they greatly reduce GHG emissions and other environmental impacts and benefit health. Reduced meat and dairy consumption, lower food waste and healthy levels of food intake substantially reduce GHG emissions from the food system and also reduce other environmental challenges, e.g. biodiversity loss, eutrophication and excessive water extraction. Therefore, policies that discourage the consumption of animal products or stimulate plant-based alternatives are no-regret options. In addition, investments should be made to reduce food waste, for example by improved supply chain management or increased consumer awareness. In addition to the environmental benefits, dietary change has major health benefits (Willett et al., 2019) underscoring it as a no-regret option.

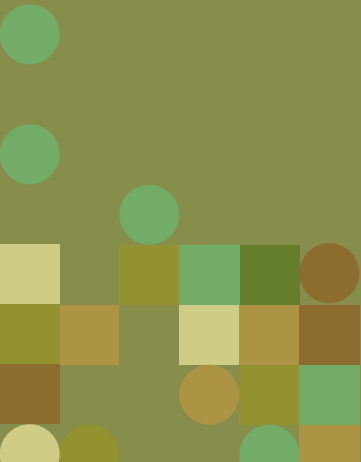
Protection of natural lands is key to reduce deforestation emissions and to protect biodiversity, but needs to be combined with investments in agricultural development to prevent negative food security effects. The protection of natural ecosystems is essential both to prevent GHG emissions and to stop biodiversity loss. However, especially in developing countries strict limits on the expansion of agriculture can have major negative effects on food security, especially in countries where growth of the population and the economy is expected to continue. Therefore, protection measures need to be combined with investments in agriculture to prevent negative trade-offs and to facilitate the economic development of poorer countries in line with the SDGs.

Improved nitrogen use efficiency is critical to reduce negative impacts on biodiversity and has co-benefits with climate change mitigation. More efficient use of fertilizers, both synthetic and organic (i.e. manure), reduces the impacts of excessive nitrogen concentrations on water quality and aquatic biodiversity, as well as on terrestrial biodiversity. Additionally, it also lowers the emissions of nitrous oxide which is a major GHG. Therefore policies to prevent the negative effects of nitrogen on biodiversity align well with climate mitigation efforts and should be a key policy ambition.



CHAPTER 8

Samenvatting en conclusies



8.1. Inleiding en onderzoeksvragen

Het landareaal van de Aarde heeft grote invloed op het klimaat door biogeofysische en biogeochemische processen. Deze processen betreffen de interactie tussen het landsysteem en de atmosfeer van, respectievelijk, energie en water, en van broeikasgassen (BKG) zoals CO₂, CH₄ en N₂O. De mens heeft het landoppervlak van de aarde ingrijpend veranderd door gebruik te maken van het land, met grote effecten op het milieu tot gevolg. Historisch gezien is klimaatverandering vooral veroorzaakt door verbranding van fossiele brandstoffen. Desalniettemin hebben landgebruik, landgebruiksverandering en bosbouw (*land use, land use change and forestry*, LULUCF) naar schatting 34% van de cumulatieve door mensen gegenereerde CO₂-emissies sinds 1750 veroorzaakt. In de loop van de tijd nam de bijdrage van CO₂ uit LULUCF af tot ongeveer 10% van de jaarlijkse wereldwijde door mensen gegenereerde uitstoot van BKG. Maar evenzeer geldt dat landbouw verantwoordelijk is voor ongeveer 13% van de mondiale uitstoot van BKG in de vorm van niet-CO₂ BKG-emissies.

Het belang van land en landgebruik voor het klimaat betekent dat land een rol moet spelen in het voorkomen van gevaarlijke klimaatverandering. Ten eerste is het voor de haalbaarheid van ambitieuze klimaatdoelstellingen essentieel om het huidige aandeel van 23% door de uitstoot van landbouw, bosbouw en ander landgebruik (*agriculture, forestry and other land use*, AFOLU) op het totaal aan BKG-emissies drastisch te verminderen. Ten tweede heeft land een sleutelrol in verschillende technieken waarmee koolstof uit de atmosfeer kan worden verwijderd (zogenaamde negatieve emissies of koolstofdioxide verwijdering (*carbon dioxide removal*, CDR)). Alle maatregelen ter beperking van klimaatverandering die direct verband houden met landgebruik worden hier benoemd als land-gebaseerde mitigatiemaatregelen. Er kunnen zes categorieën maatregelen worden onderscheiden: 1) bescherming van natuurlijke ecosystemen om uitstoot te verminderen, bijvoorbeeld door het voorkomen van ontbossing; 2) herstel en uitbreiding van bossen en draslanden waardoor koolstof in vegetatie en bodem wordt vastgelegd; 3) vermindering van uitstoot door landbouw met behulp van technische maatregelen zoals verbeterd mestmanagement en precisielandbouw; 4) vergroting van koolstofvastlegging in landbouwgrond bijvoorbeeld door toepassing van *biochar* of het aanplanten van bomen in landbouwgebied (*agroforestry*); 5) maatregelen aan de vraagzijde, bijvoorbeeld door veranderingen in het voedingspatroon; 6) productie van bio-energie ter vervanging van fossiele brandstoffen en ter vastlegging van CO₂ met behulp van het afvangen en opslaan van koolstof (*carbon-capture and storage*, CCS).

Naast klimaat heeft land een sleutelrol in vele andere kwesties betreffende duurzame ontwikkeling en milieuproblematiek. Zo is land essentieel voor de voorziening van hulpbronnen als voedsel, energie en water, en voor de instandhouding van biodiversiteit. De Duurzame Ontwikkelingsdoelen (*Sustainable Development Goals*, SDGs) (UN, 2015) en de planetaire grenzen (*planetary boundaries*, PBs) (Rockström et al., 2009) beschrijven het belang van duurzame hulpbronnenvoorziening op het levensonderhoud van mensen en de bescherming van het leefmilieu. De SDGs en PBs bevatten tevens doelstellingen voor de vele

dimensies van duurzame ontwikkeling en milieuproblematiek. Een nuttige benadering voor het bestuderen van de verschillende dimensies van duurzame ontwikkeling en mondiale milieuproblematiek is het nexus-concept dat ervan uitgaat dat componenten van een systeem inherent onderling verbonden zijn en daarom op integrale, holistische wijze moeten worden onderzocht en beheerd. In deze thesis wordt de water-land-energie-voedsel-klimaat (*water-land-energy-food-climate*, WLEFC) nexus op deze wijze benaderd, rekening houdend met mogelijke uitruilen en synergieën tussen de verschillende systemen bij het nastreven van verschillende doelstellingen.

Bij het onderzoeken van de rol van landgebruik in klimaatverandering, klimaatmitigatie en andere maatschappelijke doelstellingen die verband houden met de WLEFC-nexus kan gebruik worden gemaakt van scenario analyse. Scenario's worden gedefinieerd als aannemelijke beschrijvingen van toekomstige ontwikkelingen gebaseerd op een samenhangende en consistente set van aannames betreffende de essentiële relaties en drijvende krachten (IPCC, 2000a). Een belangrijke ambitie van de wetenschappelijke gemeenschap is de ontwikkeling van scenario's waarin zowel doelstellingen op het gebied van klimaat als andere milieu- en duurzaamheid-gerelateerde doelstellingen zoals PBs en SDGs worden gerealiseerd. In deze thesis gebruiken we zowel verkennende scenario's waarmee wordt onderzocht hoe de toekomst zich zou kunnen ontwikkelen op basis van vooraf gedefinieerde aannames, als normatieve scenario's gericht op vooraf gedefinieerde doelen en wegen waarlangs deze kunnen worden gerealiseerd. Voorbeelden van doelen zijn stabilisering van wereldwijde opwarming, bescherming van de natuur en begrenzing van wateronttrekking. Deze scenario's zijn ontwikkeld met behulp van het IMAGE *integrated assessment model* (IAM) (Stehfest et al., 2014). Hierin zijn het menselijk en het natuurlijk systeem beschreven, alsmede de interacties tussen beide en de mogelijke toekomstige ontwikkeling daarvan. IMAGE is daarom zeer geschikt om landgebruik, klimaatverandering en de WLEFC-nexus te bestuderen. Voor enkele analyses en ten behoeve van modelvergelijking wordt ook het *land system* model MAgPIE gebruikt (Dietrich et al., 2019).

Deze thesis behandelt de volgende specifieke onderzoeksvragen:

1. Hoe zal landgebruik zich op lange termijn ontwikkelen in uiteenlopende scenario's op wereldwijde en op regionale schaal?
2. Welke rol kan landgebruik vervullen in het realiseren van strikte klimaatdoelstellingen?
3. Hoe belangrijk zijn uitruilen en synergieën tussen land-gebaseerde klimaatmitigatie en andere doelen betreffende de water-land-energie-voedsel-klimaat nexus?
4. Hoe kunnen uitruilen worden geminimaliseerd en synergieën gemaximaliseerd?

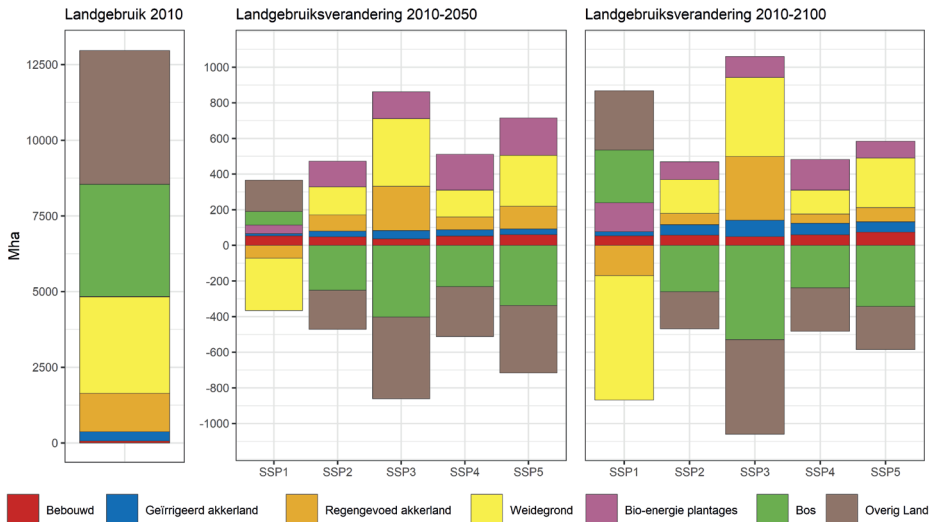
8.2. Voornaamste bevindingen

8.2.1. Hoe zal landgebruik zich op lange termijn ontwikkelen in uiteenlopende scenario's op wereldwijde en op regionale schaal?

In de IMAGE uitwerking van de SSP (*Shared Socioeconomic Pathway*) scenario's wordt een breed scala van toekomstige vormen van landgebruik, gebaseerd op aannames betreffende, onder meer, bevolking en economische groei, verandering van levensstijl, milieubewustzijn, (de)globalisering en technologische vooruitgang, onderzocht. De IMAGE 3.0 SSP scenario's zijn ontwikkeld als onderdeel van een groot multimodel project (O'Neill et al., 2013; Riahi et al., 2017). De aannames in de scenario's voor de periode 2010-2100 met betrekking tot bevolkingsprojectie variëren van +36 miljoen mensen (SSP1) tot +5.9 miljard mensen (SSP3). De aannames over inkomen per hoofd van de bevolking (*gross domestic product*, GDP) neemt toe met een factor 2 (SSP3) tot een factor 16 (SSP5) (O'Neill et al., 2017). Een belangrijk doel van de SSP scenario's is om meer inzicht te verkrijgen in de mate van onzekerheid van toekomstig landgebruik.

In de SSP scenario's worden veranderingen in landbouwareaal variërend van -680 Mha (SSP1) tot +1010 Mha (SSP3) en veranderingen in natuurlijk areaal variërend van -1060 Mha (SSP3) tot +630 Mha (SSP1) voorzien, afhankelijk van uiteenlopende sociaaleconomische ontwikkelingen en scenario aannames (Figuur 81). Deze ontwikkelingen zijn het resultaat van een combinatie van verschillende trends. In het *Middle-of-the-Road* scenario SSP2 heeft inkomensgroei (+ 550% in 2010-2100) een toename van de voedselconsumptie tot gevolg (+280 kcal per hoofd per dag, i.e. 8% in 2010-2100). Gecombineerd met bevolkingsgroei leidt dit tot een sterke toename van de agrarische productie, namelijk 2700 megaton gewasopbrengsten per jaar en 160 megaton dierlijke producten per jaar in 2100 (d.w.z. respectievelijk 70% en 60% toename). Dit leidt tot uitbreiding van akkerland (+120 Mha, zowel gevoed door neerslag als door irrigatie) en weidegrond (+190 Mha). Het bebouwde areaal groeit (+60 Mha) door bevolkingsgroei en verstedelijking en ook bio-energie plantages breiden uit (+100 Mha) door ontwikkelingen in de energievoorziening die ook in een referentiescenario (d.w.z. een scenario zonder klimaatmitigatiebeleid) leiden tot relatief meer gebruik van hernieuwbare bronnen. Al deze uitbreidingen gaan ten koste van natuurlijk land (-470 Mha). In het *Sustainability* scenario SSP1 slinkt het landbouwareaal aanzienlijk (-680 Mha) als gevolg van een geringere bevolkingstoename, verbeterde landbouwefficiëntie door technologische ontwikkeling, strengere natuurbescherming en een relatieve afname van de vleesconsumptie dankzij toegenomen milieubewustzijn. Het *Regional-Rivalry* scenario SSP3 daarentegen voorziet een sterke toename van landbouwareaal (+1010 Mha) door sterke bevolkingsgroei, stagnerende technologische ontwikkeling en beperkte natuurbescherming, met als gevolg grote verliezen van natuurlijk land. Ook het *Fossil-fueled development* scenario SSP5 leidt tot substantiële uitbreiding van het landbouwareaal (+510 Mha), al is de verandering in bevolking vergelijkbaar met SSP1, door de sterke groei van de voedselvraag per hoofd als gevolg van de steeds rijker wordende wereldbevolking en de navenante consumptiegroei.

Het *Inequality* scenario SSP4 voorziet op mondiaal niveau een vergelijkbare uitbreiding in landbouwareaal als SSP2 (+420 Mha), maar met grote regionale verschillen door ongelijkheid tussen werelddelen.

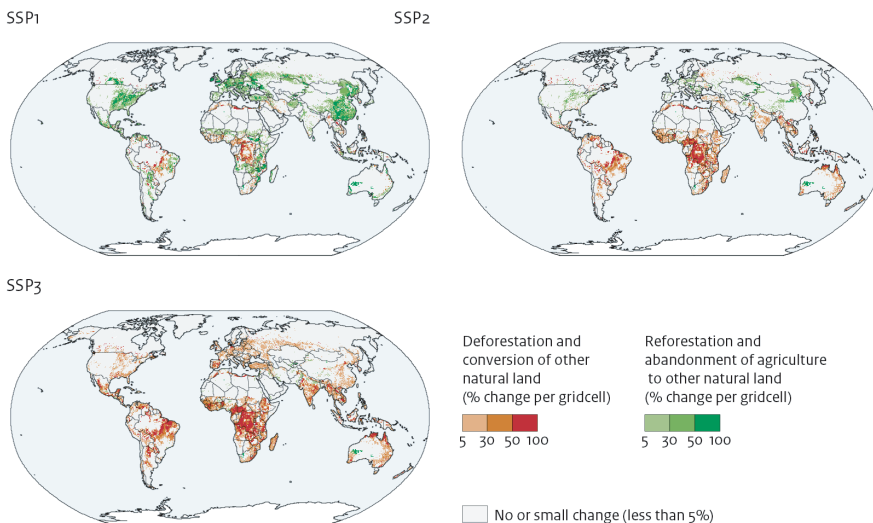


Figuur 8-1: Mondiaal landgebruik in 2010, verandering in landgebruik in de periodes 2010-2050 en 2010-2100 voor zeven landgebruiksklassen in de vijf SSP scenario's, gebaseerd op IMAGE 3.0 zoals besproken in hoofdstuk 2.

Trends in landgebruik verschillen sterk op regionaal en lokaal niveau: het landbouwareaal groeit in Sub-Sahara Afrika en in Latijns-Amerika in bijna alle SSPs, terwijl het landbouwareaal in de landen van de OESO en in China in de meeste SSPs afneemt. Al zijn mondiale ontwikkelingen in hoge mate bepalend voor veranderingen in landgebruik, toch kunnen regionale karakteristieken resulteren in grote variaties op regionale en lokale schaal. De SSPs bieden inzicht in die verschillen. In Sub-Sahara Afrika en Latijns-Amerika laten bijna alle scenario's (SSP1 uitgezonderd) groei van het landbouwareaal zien, leidend tot ontbossing en omzetting van ander natuurlijk land (Figuur 82): verder verlies van ecosystemen wordt voorzien in 'de boog van ontbossing' in Brazilië, de Gran Chaco in Bolivia, Paraguay en Argentinië, het Kongobekken en het tropisch regenwoud van West-Afrika. In Sub-Sahara Afrika wordt de uitbreiding vooral veroorzaakt door bevolkingsgroei die de vraag naar landbouwproductie opvoert. Daarentegen is de bevolking van Latijns-Amerika in de meeste scenario's stabiel: hier is verandering van landgebruik grotendeels het resultaat van hogere consumptie per hoofd en expansie van extensief begraaide weidegrond. Een belangrijke overeenkomst tussen Sub-Sahara Afrika en Latijns-Amerika is de ruime beschikbaarheid van land dat geschikt is voor agrarische expansie. Het gevolg hiervan is dat in een substantieel deel van de vraag wordt voorzien door uitbreiding van het landbouwareaal in plaats van door intensivering. Hierin verschillen deze regio's van Zuid-

en Zuidoost-Azië, en in het bijzonder van India, waar weinig extra landareaal beschikbaar is. Dit heeft tot gevolg dat in die regio's vooral aan de toenemende vraag moet worden voldaan door agrarische intensivering of door import van voedsel. Als dit niet mogelijk blijkt, resulteert dit in negatieve effecten op de voedselzekerheid. Voor de OESO-landen en China geldt dat als gevolg van de stabiele of afnemende bevolking de meeste scenario's een beperkte afname van agrarisch landgebruik laten zien en relatief kleine veranderingen in het niveau van consumptie per hoofd van de bevolking. Wel is in OESO-landen nog geregeld sprake van toename van agrarische productie door verdere intensivering, wat verruiming van het exportvolume mogelijk maakt.

Land-use change: 2010 – 2050



Figuur 8-2: Verandering in landgebruik (percentages per rastercel) tussen 2010 en 2050; ontbossing en conversie van ander natuurareaal (rood) en herbebossing en onttrekking aan landbouw van ander natuurareaal (groen) in SSP1, SSP2 en SSP3 op basis van IMAGE 3.0 zoals besproken in hoofdstuk 2.

8.2.2. Welke rol kan landgebruik vervullen in het realiseren van strikte klimaatdoelstellingen?

In referentiescenario's zonder klimaatmitigatiebeleid wordt het aandeel AFOLU-emissies in de totale uitstoot kleiner in de loop van de 21^e eeuw (Tabel 81). De SSP referentiescenario's (d.w.z. die zonder enig klimaatmitigatiebeleid) laten vooral sterke toename van BKG-emissies zien, oplopend naar het einde van de eeuw. In het meest extreme scenario SSP5 neemt dit toe tot 130 GtCO₂-eq/Jr in 2100, een verdrievoudiging van de huidige emissies die leidt tot een temperatuurstijging van 4-5°C (IPCC 2021). Dit komt door veel hogere welvaart- en consumptieniveaus en een grote afhankelijkheid van het energiesysteem gebaseerd op fossiele brandstoffen zoals steenkool. Gelukkig wordt deze

ontwikkeling onwaarschijnlijk geacht (Hausfather en Peters, 2020). Het aandeel AFOLU-emissies in de totale uitstoot wordt tegen het einde van de eeuw in alle scenario's kleiner: van 21% in 2010 tot 13% in 2100 in SSP3 en SSP4, tot slechts 4% in SSP5. Een belangrijke oorzaak voor deze ontwikkeling is de afvlakking van de bevolkingsgroei in de meeste scenario's, terwijl de welvaart in de meeste gevallen blijft groeien. Inkomensgroei heeft de meeste invloed op de voedselvraag daar waar mensen loskomen van extreme armoede, omdat de voedselvraagelasticiteit (d.w.z. de verhouding tussen het percentage verandering in vraag naar voedsel tot het percentage verandering in inkomen) sterk afneemt bij een hoger inkomen (Bijl et al., 2017; Muhammad et al., 2011). In de eerste helft van de eeuw groeit de vraag naar voedsel in hetzelfde tempo als de vraag naar energie en industriële goederen. In de tweede helft van de eeuw vlakt de bevolkingsgroei af en wordt de vraag naar voedsel bovendien minder beïnvloed door de inkomensgroei omdat mensen gemiddeld genomen rijker zijn. Deze trends resulteren in een stabilisering van de vraag naar voedsel, met als gevolg stabilisering van non-CO₂ BKG-emissies die immers direct verbonden zijn met de totale agrarische productie. De uitstoot door verandering van landgebruik gaat naar nul wanneer uitbreiding van landbouwareaal niet meer nodig is en wordt zelfs negatief waar agrarische efficiëntie verder toeneemt met verkleining van het totale landbouwareaal tot gevolg (SI Figuur 2-4). Intussen blijft de uitstoot van energie en industrie wel groeien, zodat het aandeel van de AFOLU-emissies in het totaal kleiner wordt.

Tabel 8-1: Emissies voor de sectoren energie, industrie en AFOLU en het aandeel AFOLU-emissies in de totale uitstoot volgens de vijf SSP referentiescenario's in 2010, 2050 en 2100, gebaseerd op IMAGE 3.0 zoals besproken in Hoofdstuk 2. In eenheden GtCO₂-eq/jr met gebruikmaking van een 100 jaar perspectief op potentiële mondiale opwarming (100-year time horizon global warming potentials, GWP100). (Zie ook Figuur 2-12)

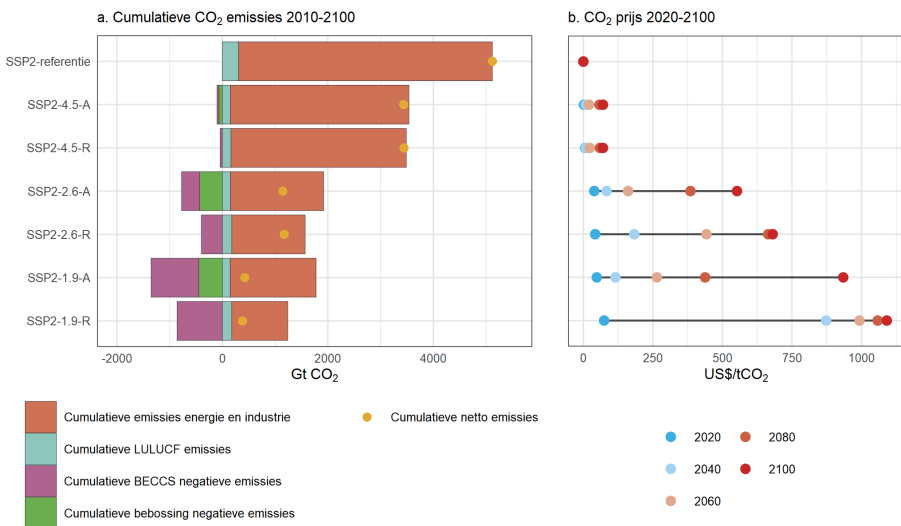
2010	2010				
Energie en industrie emissies (GtCO ₂ -eq/jr)	38.2				
AFOLU emissies (GtCO ₂ -eq/jr)	9.9				
Aandeel AFOLU van het total (%)	21%				
2050	SSP1	SSP2	SSP3	SSP4	SSP5
Energie en industrie emissies (GtCO ₂ -eq/jr)	52.6	61.3	64.2	54.0	93.4
AFOLU emissies (GtCO ₂ -eq/jr)	5.9	13.5	17.1	14.4	14.9
Aandeel AFOLU van het total (%)	10%	18%	21%	21%	14%
2100	SSP1	SSP2	SSP3	SSP4	SSP5
Energie en industrie emissies (GtCO ₂ -eq/jr)	35.0	86.6	87.4	53.3	130.7
AFOLU emissies (GtCO ₂ -eq/jr)	3.2	7.7	12.6	7.8	5.6
Aandeel AFOLU van het total (%)	8%	8%	13%	13%	4%

Gerichte maatregelen ter bescherming en herstel van veengebieden hebben, in tegenstelling tot maatregelen in standaard mitigatiescenario's, een hoge potentiële opbrengst aan klimaatmitigatie (96 GtCO₂ in 2020-2100 volgens SSP2) zonder grote

invloed op mondiale verandering in landgebruik. In Hoofdstuk 3 wordt een nieuwe analyse van de rol van degradatie, bescherming en herstel van veengebied in de SSP-scenario's gepresenteerd. Schattingen op basis van kaarten van de omvang van veengebieden worden toegepast in IMAGE en gecombineerd met ruimtelijk-expliciet landgebruik en op IPCC-bronnen gebaseerde uitstoot-data om de uitstoot door degradatie van veengebied in referentie- en mitigatiescenario's te bepalen. Referentiescenario's laten een sterke toename van gedegraderd veenareaal en BKG-emissies zien in SSP2 en SSP3 en in vergelijking hiermee een beperkte afname in SSP1. In standaard mitigatiescenario's (d.w.z. zonder gerichte maatregelen ter bescherming en herstel van veengebieden) neemt de uitstoot door veengebied af dankzij synergie met bosbescherming en bebossingsbeleid. Toch blijft, met een cumulatief onverminderde uitstoot van 96 GtCO₂, het aandeel in het totaal hoog. Beleid gericht op volledig herstel van gedegradeerde veengebieden kan de uitstoot van veengebied terugbrengen tot bijna nul zonder substantiële invloed op voorziene veranderingen in landgebruik. Deze bevinding onderstreept de meerwaarde van beleid gericht op veengebied voor klimaatmitigatie en de noodzaak om verschillende land-gebaseerde mitigatiemaatregelen in synergie in te zetten. Daarbij moet wel worden opgemerkt dat de mogelijkheden om veengebieden te beschermen en te herstellen ongelijk zijn verdeeld over de regio's. Een derde deel van de benodigde reductie van BKG-emissies uit veengebied moet komen uit Indonesië, waarbij preventie van verdere degradatie en herstel van reeds gedegradeerde veengebieden essentieel is. Veengebieden met groot potentieel voor herstel zijn te vinden in gematigde en boreale klimaatregio's zoals Europa, Noord-Amerika en Rusland. In deze regio's bestaat bovendien minder risico op een toename van gedegraderd veengebied. Daar tegenover staat Latijns-Amerika, waar een aanzienlijke uitbreiding van gedegraderd veengebied wordt voorzien terwijl het huidige areaal van gedegraderd veengebied juist tamelijk beperkt is.

In kostenefficiënte scenario's speelt bebossing met het oog op klimaatmitigatie een belangrijke rol als methode om koolstofdioxide te verwijderen uit de atmosfeer (cumulatief 430 GtCO₂ in SSP2-2.6), waardoor strikte klimaatdoelen tegen lagere kosten kunnen worden behaald. Een nieuwe methodiek om het potentieel van bebossing in concurrentie met de agrarische sector te analyseren wordt gepresenteerd in Hoofdstuk 4. Ruimtelijk-expliciete schattingen van boomgroei gemodelleerd in LPJmL (Braakhekke et al., 2019) worden gecombineerd met regio-specifieke schattingen van de kosten van bebossing, de prijseffecten van schaarste van land en risicogecorrigeerde investeringsbeslissingen. Deze data worden gebruikt om *marginal abatement cost curves* te maken die worden ingevoerd in het klimaatbeleid model FAIR-SimCAP om bebossing te vergelijken met andere mogelijkheden van klimaatmitigatie in de sectoren energie, industrie en landbouw. Hiermee wordt aangetoond dat bebossing grote potentie heeft voor klimaatmitigatie tegen relatief lage prijzen, waarmee in een SSP2 scenario met kostenefficiënt beleid (d.w.z. beleid dat doelen haalt tegen de laagste kosten) gericht op 2°C maximale opwarming 430 GtCO₂ aan negatieve emissies door bebossing wordt behaald. Hierdoor worden de kosten van klimaatmitigatie lager, gezien de lagere CO₂-prijs (240 US\$/t CO₂ vergeleken met het gemiddelde 430 US\$/t

CO₂ in de periode 2020-2100)(Figuur 83). Grotere afhankelijkheid van negatieve emissies vormt een risico omdat dit kan leiden tot *lock-in* situaties van mitigatiebeleid in sectoren waar decarbonisatie kostbaarder is (Anderson en Peters, 2016). Een kostenefficiënte benadering van bebossing leidt ook tot een grotere afhankelijkheid van klimaatbeleid van acties in lage-inkomens regio's. In een scenario met bebossing wordt 31% van CDR geïmplementeerd in lage-inkomens regio's in tegenstelling tot 17% in een scenario zonder bebossing (CDR betreft voornamelijk bebossing en bio-energie in combinatie met CCS, vergelijking tussen SSP2-2.6-A en SSP2-2.6-R).



Figuur 8-3: Scenario's, geanalyseerd in Hoofdstuk 4 met behulp van IMAGE 3.0, gericht op een maximale opwarming van 4.5, 2.6 of 1.9 W/m², hetzij mét inzet van bebossing als middel voor klimaatmitigatie (aangeduid met suffix A (Afforestation)), hetzij zonder inzet van bebossing als middel voor klimaatmitigatie (aangeduid met suffix R (Reference)). De uitkomsten tonen (a) de cumulatieve CO₂ emissies in de periode 2010-2100 en (b) de CO₂-prijzen in geselecteerde jaren in de periode 2010-2100.

In kostenefficiënte scenario's kan, afhankelijk van de karakteristieken van het betreffende scenario, land-gebaseerde klimaatmitigatie een jaarlijkse uitstootreductie van 28%-33% en 28%-44% in respectievelijk 2050 en 2100 opleveren. Figuur 84 en Tabel 82 tonen de rol van land-gebaseerde maatregelen gericht op mitigatie in verhouding tot de totale mitigatie in andere energiesectoren (d.w.z. niet-bio-energie) en de industrie. Land-gebaseerde mitigatie (incl. het vervangingseffect van bio-energie op fossiele brandstoffen, een analyse vergelijkbaar met die in Sectie 2.3.4) komt uit op 16-21 GtCO₂-eq/jr in 2050 en 20-26 GtCO₂-eq/jr in 2100 (Figuur 84). Vooral in SSP1-1.9 is het aandeel van land-gebaseerde mitigatie groot, nl. 44% in 2100 (Tabel 82). De reden hiervoor is dat land-gebaseerde klimaatmitigatie vaak goedkoper is dan mitigatie in energie en industrie, met als gevolg dat waar de totale mitigatiebehoefte relatief gering is, de land-gebaseerde mitigatie een relatief

groot aandeel levert. Dit verklaart het grote aandeel van land-gebaseerde klimaatmitigatie in SSP1-1.9 vergeleken met het relatief kleinere aandeel in SSP3-2.6 (28% in 2100).

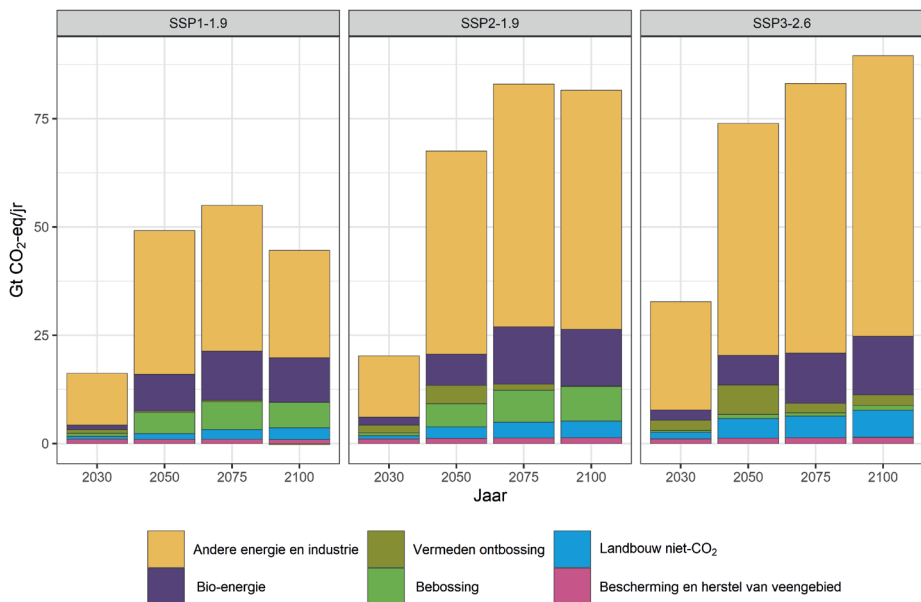
Mitigatie gericht op andere BKG dan CO₂ speelt een relatief grote rol in scenario's waarin sprake is van sterke groei van de agrarische productie, tot 6.2 GtCO₂-eq/jr in SSP3-2.6 in 2100. Niet-CO₂ mitigatiemaatregelen in de landbouw (bijvoorbeeld verbeterd mestmanagement of veevoeradditieven ter reductie van de uitstoot van methaan) leiden tot uitstootreducties van 1.4-4.5 GtCO₂-eq/jr in 2050 en 2.7-7.3 GtCO₂-eq/jr in 2100. Het gaat om relatief goedkope maatregelen die maximaal kunnen worden benut in scenario's met een grote mitigatiebehoefte en inherent hoge prijzen van BKG (Harmsen et al., 2019). Het benuttingspotentieel is het grootst in SSP3, waar sterke bevolkingsgroei leidt tot een grote toename van de vraag naar voedsel en inefficiënte landbouw een relatief hoge uitstoot per ton geproduceerd voedsel tot gevolg heeft. Uiteraard vergroot een hoge totale uitstoot het potentieel aan te mitigeren emissies. Van belang om op te merken is, dat deze emissies niet volledig gemitigeerd kunnen worden: de resterende uitstoot moet (ten dele) worden gecompenseerd door negatieve emissies (Gernaat et al., 2015).

Het potentieel aan te verminderen uitstoot door vermeden ontbossing is direct afhankelijk van de ontwikkelingen in ontbossing in referentiescenario's. De bijdrage van vermeden ontbossing varieert van bijna nul in SSP1-1.9 tot 6.8 GtCO₂-eq/jr in SSP3 in 2050. Dit is direct afhankelijk van voorziene ontbossing in het referentiescenario. In SSP2 en SSP3 wordt grote verdere ontbossing voorzien, met verlies aan bosareaal van respectievelijk 330 en 560 Mha in de periode 2020-2100 tot gevolg, leidend tot een hoge uitstoot. Daartegenover laat SSP1 de beëindiging van ontbossing zien door een bescheiden groei van de vraag naar voedsel, hoge agrarische efficiëntie en een sterk milieubewustzijn in de samenleving. Ontbossing heeft in dit scenario dus geen rol als mitigatiemaatregel.

Bebossing is samen met bescherming en herstel van veengebied een belangrijke mitigatiemaatregel met een opbrengst van respectievelijk 5.3 en 1.2 GtCO₂-eq/jr in 2050 volgens SSP2-1.9. Bebossing is verantwoordelijk voor 8%-13% van de totale mitigatie in SSP1-1.9 en SSP2-1.9. Bebossing is daarmee een bepalende factor in kostenefficiënte mitigatiescenario's. In SSP3-2.6 speelt bebossing een relatief kleinere rol (~1%) omdat in dit scenario beperktere mogelijkheden van bebossing als mitigatiemaatregel worden aangenomen. Het potentieel voor bescherming en herstel van veengebieden ligt rond de 2% in alle mitigatiescenario's. Deze maatregelen vormen dus een bescheiden, maar niet te verwaarlozen, component in het klimaatmitigatieportfolio.

Met een aandeel in de totale klimaatmitigatie van 9%-23% is bio-energie een bepalende factor in kostenefficiënte scenario's. De productie van bio-energie en het gebruik ervan in het energiesysteem zijn een effectieve mitigatiemaatregel omdat dit het gebruik van fossiele brandstoffen vervangt, met een veel lagere netto CO₂-uitstoot tot gevolg. Daar komt bij dat met deze maatregel CO₂ uit de atmosfeer kan worden verwijderd als hij wordt

gecombineerd met CCS. In de kostenefficiënte mitigatiescenario's die worden besproken in deze thesis (Figuur 84) kan de netto-opbrengst aan mitigatie oplopen tot 13.5 GtCO₂ eq/jr (in SSP3-2.6 in 2100). Dat is meer dan enige andere categorie van land-gebaseerde mitigatie. Vooral in SSP1 is het aandeel van bio-energie groot in vergelijking met andere mogelijkheden tot mitigatie, doordat verkleining van het landbouwareaal meer en (daardoor) goedkoper land oplevert voor de productie van biomassa. Daar staat tegenover dat vraagtekens zijn te plaatsen bij de grootschalige inzet van bio-energie voor klimaatmitigatie ten aanzien van de doeltreffendheid van deze maatregel en de negatieve invloed op biodiversiteit en voedselzekerheid (Hasegawa et al., 2017). De laatste jaren wordt meer onderzoek gedaan naar scenario's gericht op het realiseren van strikte klimaatmitigatiedoelstellingen waarbij slechts beperkt gebruik wordt gemaakt van bio-energie (Edelenbosch et al., 2022; van Vuuren et al., 2018).



Figuur 8-4: Jaarlijkse mondiale mitigatie (d.w.z. het verschil in uitstoot tussen een referentie- en een mitigatiescenario) in SSP1-1.9, SSP2-1.9 en SSP3-2.6 in GtCO₂-eq/jr (GWP100) per land-gebaseerde mogelijkheid voor klimaatmitigatie alsmede energie en industrie in 2030, 2050, 2075 en 2100. De opbrengsten zijn gebaseerd op IMAGE 3.2 scenario's besproken in Hoofdstuk 3. De opbrengst aan mitigatie middels bio-energie is inclusief die van het afvangen en opslaan van koolstof en de vervanging van fossiele brandstoffen en gecorrigeerd voor de effecten van verandering van landgebruik, conform de methode besproken in Sectie 2.3.4.

Tabel 8-2: Aandeel in het totaal van de verschillende mogelijkheden voor klimaatmitigatie alsmede energie en industrie in 2050 en 2100, afgeleid van de jaarlijkse uitstoot van BKG (Figuur 84). De opbrengsten zijn gebaseerd op IMAGE 3.2 scenario's besproken in Hoofdstuk 3. De opbrengst aan mitigatie door middel van bio-energie is inclusief die van het afvangen en opslaan van koolstof en de vervanging van fossiele brandstoffen en gecorrigeerd voor de effecten van verandering van landgebruik, conform de methode besproken in Sectie 2.3.4.

2050	SSP1-1.9	SSP2-1.9	SSP3-2.6
Vermeden ontbossing	1%	6%	9%
Bebossing	10%	8%	1%
Landbouw niet-CO2	3%	4%	6%
Bescherming en herstel van veengebied	2%	2%	2%
Bio-energie	17%	11%	9%
Andere energie en industrie	67%	69%	72%
2100	SSP1-1.9	SSP2-1.9	SSP3-2.6
Vermeden ontbossing	0%	0%	3%
Bebossing	13%	10%	1%
Landbouw niet-CO2	6%	5%	7%
Bescherming en herstel van veengebied	2%	2%	2%
Bio-energie	23%	16%	15%
Andere energie en industrie	56%	68%	72%

Verandering van het voedingspatroon en vermindering van voedselverspilling hebben een grote potentiële opbrengst aan klimaatmitigatie van 6.7GtCO₂-eq/jr in 2050.

Vraagrijde-gerichte maatregelen zoals verandering van het voedingspatroon en vermindering van voedselverspilling, zijn geen onderdeel van de standaard kostenefficiënte mitigatiescenario's die hiervoor zijn besproken. In Hoofdstuk 6 wordt een SSP2 scenario geanalyseerd (FOOD) waarin een transitie naar een gezond voedingspatroon zoals voorgesteld door de EAT-Lancet commissie (Willett et al., 2019) is geïmplementeerd. Hierin worden aannames gedaan over een lagere vlees- en zuivelconsumptie en een lagere totale calorie-inname in regio's met midden- en hoge inkomens. Ook wordt de voedselverspilling vermindert (Gustavsson et al., 2011). Aangetoond wordt dat deze veranderingen in 2050 leiden tot een vermindering van 6.7 GtCO₂-eq/jr uitstoot van BKG, gelijkstaand aan 10% van de totale vereiste klimaatmitigatie in SSP2-1.9. Een belangrijke kanttekening hierbij is dat deze potentiële opbrengst aan klimaatmitigatie niet zomaar kan worden opgeteld bij het potentieel aan land-gebaseerde klimaatmitigatie zoals die is ingeschat in de standaard mitigatiescenario's. De uitstoot van BKG vermindert door een verandering van het voedingspatroon wat resulteert in geringere agrarische uitstoot van niet-CO₂ BKG (voornamelijk door vee) en van bebossing op landbouwareaal dat niet meer nodig is voor de agrarische sector (voornamelijk weidegrond). Hierdoor neemt de potentiële opbrengst van niet-CO₂ klimaatmitigatie en van herbebossing, zoals ingeschat in kostenefficiënte scenario's, af.

8.2.3. Hoe belangrijk zijn uitruilen en synergieën tussen land-gebaseerde klimaatmitigatie en andere maatschappelijke doelen in de water-land-energie-voedsel-klimaat nexus?

Bosbescherming kan resulteren in een beperktere uitbreiding van agrarisch areaal en dus ontbossing voorkomen. Het kan echter ook leiden tot verplaatsing van landgebruik naar ander natuurlijk land. In vergelijking met het referentiescenario leidt strikte bosbescherming, gericht op het beperken van de uitstoot door ontbossing, tot een vergroting van het bosareaal, bijvoorbeeld met 120 Mha in het CLIMATE-scenario in IMAGE 3.2 (Hoofdstuk 6, vergelijkbaar met SSP2-2.6, zie Figuur 6-2). Het verminderde verlies van natuurlijk bos is een belangrijke synergie met biodiversiteit op land. Echter, wanneer alleen natuurlijke ecosystemen met hoog bovengronds koolstofvolume worden beschermd (zoals regenwouden), kan dit leiden tot verplaatsing van de expansie van agrarisch areaal naar ecosystemen met een lager bovengronds koolstofvolume die ook een unieke biodiversiteitswaarde vertegenwoordigen, bijvoorbeeld natuurlijke graslanden zoals savannes en steppes. Dit is te zien in SSP2-2.6 (Hoofdstuk 2) waar bosareaal toeneemt met 400 Mha in vergelijking met het referentiescenario, terwijl ander natuurlijk areaal afneemt met 250 Mha.

Bio-energie kan een rol spelen in klimaatmitigatie, maar gaat gepaard met substantiële uitruilen met natuurlijk areaal en dus met biodiversiteit op land. Zoals besproken in de vorige sectie kan bio-energie een belangrijk aandeel leveren in het behalen van strikte klimaatdoelen. Hiervoor zijn wel grote landarealen nodig, bijvoorbeeld 410 Mha in 2100 volgens SSP2-1.9 in IMAGE 3.0 (Hoofdstuk 2) en 320 Mha in 2050 in het CLIMATE scenario van MAgPIE (Hoofdstuk 6). Voor de expansie van bio-energie areaal wordt enerzijds landbouwareaal ingezet dat gebruikt werd voor voedselproductie, wat zijn weerslag heeft op de voedselzekerheid. Anderzijds wordt ook natuurlijk areaal gebruikt, met gevolgen voor de biodiversiteit op land. Omdat expansie van agrarisch areaal ten behoeve van bio-energie doorgaans onderdeel is van mitigatiescenario's die tevens maatregelen ter bescherming van bosareaal bevatten, gericht op uitstootbeperking door verandering van landgebruik, gaat een toename van bio-energie areaal meestal gepaard met een afname van niet-bos ecosystemen.

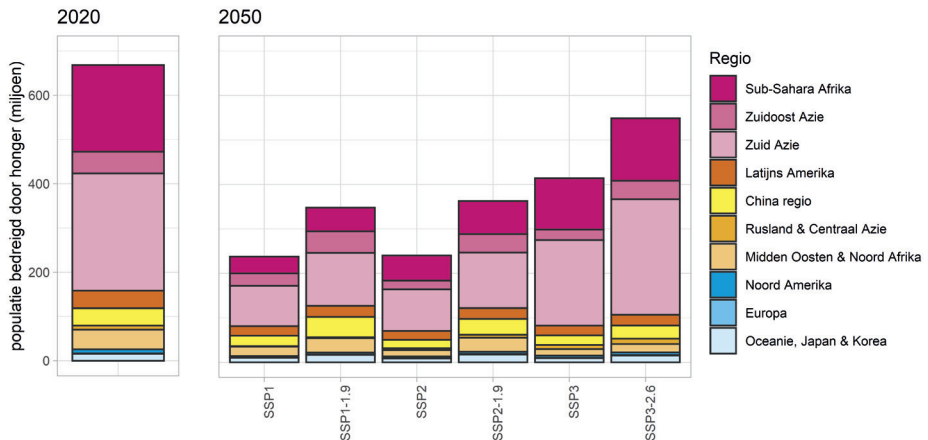
In een ambitieus mitigatiescenario als SSP2-2.6 kan bebossing uitkomen op 1090 Mha extra bosareaal in 2100. De invloed hiervan op biodiversiteit kan positief of negatief zijn, afhankelijk van de gebruikte boomsoorten en de intensiteit van het beheer. Als de prijs van CO₂ gemiddeld of hoog is, kan bebossing een economisch rendabel alternatief voor landbouw zijn. Het aanplanten van bos op voormalige landbouwgrond vindt plaats daar waar kostenefficiënte concurrentie mogelijk is in scenario's met een grote mitigatiebehoefte (Hoofdstuk 4). Zo zien we in een SSP2-2.6 scenario met een gemiddelde waarde van 240 US\$/t CO₂ in de periode 2020-2100 een grote uitbreiding van het bosareaal tot 1090 Mha tegen het einde van de eeuw. Deze thesis gaat uit van aangeplant bos met minimaal beheer.

Door beperkingen van het model zijn specifieke aannames met betrekking tot variaties in boomsoorten niet mogelijk. Waar exotische boomsoorten worden gebruikt in gebieden met natuurlijke niet-bos ecosystemen, bijvoorbeeld eucalyptusplantages in savanne-ecosystemen, leidt bebossing tot grote uitruileffecten met biodiversiteit (Bremer en Farley, 2010; Hall et al., 2012). Daar staat tegenover dat herbebossing met inheemse boomsoorten synergie kan opleveren met doelstellingen gericht op biodiversiteit op land.

Het effect van klimaatbeleid op landbouw heeft grote gevolgen voor de voedselzekerheid. In vergelijking met referentiescenario's dreigen 110-135 miljoen extra mensen honger te lijden in 2050. Deze gevolgen doen zich voornamelijk voor in Sub-Sahara Afrika en in Zuid-/Zuidoost-Azië. Concurrentie om land tussen voedselproductie enerzijds en land-gebaseerde mitigatiemaatregelen anderzijds, beperkt de capaciteit van voedselproductie wat leidt tot hogere voedselprijzen en een beperking van voedselbeschikbaarheid en voedselzekerheid (Hoofdstukken 2, 4, 5, 6). Deze gevolgen kunnen worden beoordeeld aan de hand van de vier dimensies van voedselzekerheid van de FAO: beschikbaarheid, toegang, benutting en stabiliteit (FAO, 1996; van Meijl et al., 2020). Het aantal mensen dat honger dreigt te lijden is een belangrijke indicator voor de dimensie voedselbeschikbaarheid, waarin ook ongelijkheid en niveaus van gezonde voedselinname zijn meegenomen. Analyses met behulp van IMAGE 3.2 tonen aan dat in referentiescenario's het aantal mensen dat honger dreigt te lijden afneemt van 670 miljoen in 2020 tot 240-410 miljoen in 2050. De belangrijkste oorzaak hiervan is inkomensgroei. De laagste inschatting van het aantal mensen bedreigd door honger is te vinden in SSP1, de hoogste in SSP3 (Figuur 85). Bij uitvoering van grootschalige land-gebaseerde klimaatmitigatie zouden in 2050 110-140 miljoen mensen extra honger kunnen lijden door de toegenomen concurrentie om land en om hulpbronnen in het voedselsysteem. Tegen het einde van de eeuw zouden deze effecten nog heviger kunnen zijn. Echter, schattingen rondom voedselzekerheid op de lange termijn zijn zeer onzeker, omdat aannames betreffende de voedselvraagelasticiteit zijn gebaseerd op recente tijdvakken en dus mogelijk niet toepasbaar op de langere termijn (Bijl et al., 2017).

Land-gebaseerde klimaatmitigatie kan leiden tot een substantiële toename van zoetwateronttrekking voor irrigatie, oplopend tot 540 km³ (+31%) in vergelijking met het referentiescenario in 2050. Deze uitkomst is wel afhankelijk van de karakteristieken en aannames in het model. Analyse van watergebruik voor irrigatie in het CLIMATE scenario van IMAGE 3.2 en MAgPIE (Hoofdstuk 6) toont aan dat zoetwateronttrekking in de vergelijking van een mitigatiescenario met een referentiescenario kan toenemen met +70 tot +540 km³. In MAgPIE is deze substantiële toename in onttrekking het gevolg van expansie van het geïrrigeerde areaal voor bio-energie productie en door toegenomen agrarische intensivering door BKG beprijzing en landbeschermingsmaatregelen. In IMAGE 3.2 voorkomen aannames met betrekking tot duurzaamheid dat het bio-energie areaal wordt geïrrigeerd en dat de oppervlakte aan geïrrigeerd areaal wordt beïnvloed door agrarische intensivering. Wel leidt, in een mitigatiescenario, geringere CO₂-bemesting tot afname van de irrigatie-efficiëntie, met

licht hogere volumes aan zoetwateronttrekking tot gevolg. Dit wijst erop dat watergebruik een belangrijke uitruil van land-gebaseerde mitigatie kan zijn. De geschatte opbrengsten zijn afhankelijk van de karakteristieken en aannames in het model.

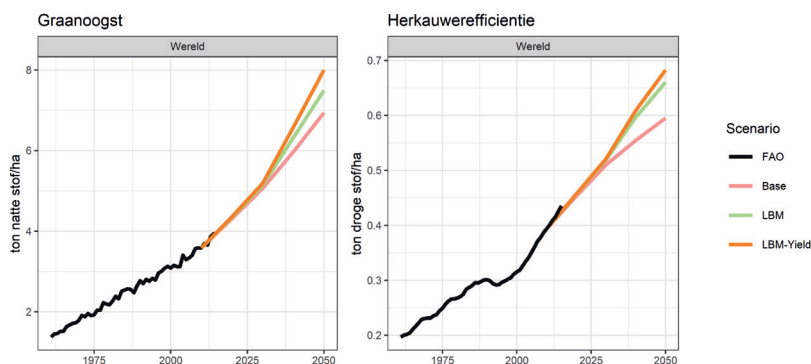


Figuur 8-5: Aantallen mensen bedreigd door honger in 2020 en 2050 volgens referentiescenario's SSP1, SSP2 en SSP3 en volgens mitigatiescenario's SSP1-1.9, SSP2-1.9 en SSP3-2.6. Opbrengsten gebaseerd op IMAGE 3.2 scenario's zoals besproken in Hoofdstuk 3.

In een referentiescenario kan toename van agrarische productie een sterke groei van het stikstofoverschot (+36% tot +54%) veroorzaken, met risico's voor de waterkwaliteit en biodiversiteit tot gevolg. In een klimaatmitigatiescenario wordt dit overschot kleiner (-8% tot -24%) dankzij N₂O mitigatiebeleid. Verdere groei van agrarische productie leidt tot een sterke toename van zowel het gebruik van kunstmest voor de productie van gewassen als een grotere mestopbrengst door veeteelt. Dit leidt tot meer uitstoot van N₂O in de atmosfeer die klimaatverandering verergert en neerslag van stikstof op land en oppervlaktewater veroorzaakt. Dit leidt vervolgens tot een afname van de waterkwaliteit en veroorzaakt schade aan de biodiversiteit op land en in water. Het stikstofoverschot, oftewel de hoeveelheid stikstof die niet wordt opgenomen door agrarisch gewas, is een goede indicator om de omvang en het risico van deze processen te beoordelen. Volgens een referentiescenario is sprake van sterke groei tussen 2015 en 2050, zowel in IMAGE 3.2 (+47 MtN/jr, i.e. +36%) als in MAgPIE (+79 MtN/jr, i.e. +54%)(REF scenario, Hoofdstuk 6, Figuur 6-4). In een mitigatiescenario neemt het stikstofoverschot af (-17 MtN/jr tot -43 MtN/jr, i.e. -8% tot -24% in 2050 in vergelijking met het referentieniveau). Dit is het gevolg van grotere efficiëntie in het gebruik van stikstof, conform mitigatiebeleid gericht op afname van de N₂O-uitstoot. Hiertoe ingezette maatregelen zijn onder meer efficiënter kunstmestgebruik, toepassing van nitrificatieremmers en verbeterd mestmanagement. Dit wijst op een belangrijke synergie tussen klimaatbeleid enerzijds en het voorkomen van overmatig stikstofgehalte in de componenten land en water van de nexus anderzijds.

8.2.4. Hoe kunnen uitruilen worden geminimaliseerd en synergieën gemaximaliseerd?

Aanvullende agrarische intensivering van 2010 tot 2050 ter grootte van 17% aan gewasopbrengsten en 14% aan herkauwerefficiëntie in vergelijking met intensivering in een referentiescenario zou voldoende zijn om te voorkomen dat land-gebaseerde klimaatmitigatie negatieve gevolgen heeft voor de voedselzekerheid. In Hoofdstuk 5 wordt het effect van grootschalige land-gebaseerde klimaatmitigatie op voedselzekerheid geanalyseerd. Vervolgens wordt berekend bij welk niveau van aanvullende agrarische intensivering de voedselprijzen gelijk zijn aan die op het referentieniveau. Deze berekening toont aan dat 17% toename van gewasopbrengsten en 14% toename aan herkauwerefficiëntie (aantal ton vlees en zuivel productie van herkauwers per hectare weidegrond) in vergelijking met het referentieniveau van 2010 tot 2050 voldoende is om negatieve gevolgen voor de voedselzekerheid te verhelpen (Figuur 86). De opbrengst van graanoogsten is lineair toegenomen sinds 1961 en verdubbeld in de periode 1970-2010 (mondiaal gemiddelde). Herkauwerefficiëntie is in dezelfde periode met 70% gegroeid. Zo bezien lijkt een toename van 18% graanoogst en 15% herkauwerefficiëntie in de periode 2010-2050 realistisch. Wel moet deze groei worden gerealiseerd in aanvulling op het referentieniveau van groei van respectievelijk 100% en 50%. Dit resulteert in relatief hoge trends ten opzichte van scenario's die in de literatuur beschreven zijn (van Zeist et al., 2020). In ontwikkelende landen met grote oogsttekorten is het potentieel voor oogstverbetering groot (van Ittersum et al., 2013). Maar het is de vraag of gewasopbrengsten in dit historische tempo kunnen blijven groeien of dat de biologische grenzen aan gewasproductie worden bereikt (Grassini et al., 2013). Bovendien is er de essentiële vraag of agrarische intensivering duurzaam kan worden gerealiseerd zonder uitruilen met andere componenten van de nexus zoals watergebruik en biodiversiteit (Seppelt et al., 2020).



Figuur 8-6: Graanoogsten en herkauwerefficiëntie (vlees- en zuivelproductie van herkauwers gedeeld door het areaal weidegrond) gebaseerd op FAO data in de historische periode en op drie scenario's in de toekomstige periode: een referentiescenario (Base), een scenario met grootschalige klimaatmitigatie zoals bio-energie en bebossing (LBM) en een scenario met grootschalige klimaatmitigatie aangevuld met agrarische intensivering ter voorkoming van negatieve gevolgen voor de voedselzekerheid (LBM-Yield) (voor meer detail zie Hoofdstuk 5). Voorziena graanopbrengsten en herkauwerefficiëntie gecorrigeerd naar FAO-waarden 2015.

Afnemende vraag in het voedselsysteem door veranderingen als minder vleesconsumptie, gezondere voedingspatronen en minder voedselverspilling heeft bijkomende voordelen in alle componenten van de WLEFC-nexus. Om de rol van vraagrijde-gerichte veranderingen in het voedselsysteem en de gevolgen daarvan op de WLEFC-nexus te kunnen onderzoeken worden scenario's ontwikkeld waarin voedingspatronen worden aangepast aan gezonde diëten zoals voorgesteld door de EAT-Lancet commissie (FOOD-scenario, Hoofdstuk 6)(Willett et al., 2019). Dit houdt onder andere een lagere vlees- en zuivelconsumptie in, een lagere totale calorie-inname in regio's met midden- en hoge inkomens, en een toegenomen calorie-inname tot gezonde niveaus in regio's met lage inkomens. Voor West-Europa komt dit uit op een afname van de gemiddelde dagelijkse vleesconsumptie van 280 gram nu naar 50 gram in 2050. Daarnaast wordt verminderde voedselverspilling aangenomen omdat die juist in regio's met hoge inkomens extra vraag naar voedsel met zich meebrengt (Gustavsson et al., 2011). Aangetoond wordt dat vraagrijde-gerichte veranderingen sterke synergie-effecten hebben met alle componenten van de WLEFC-nexus (Tabel 83). Bovendien wordt de AFOLU BKG uitstoot sterk gereduceerd (-45% tot -58% in 2050 in vergelijking met het referentiescenario in respectievelijk IMAGE en MAgPIE). Ten eerste door de verminderde veeteelt die leidt tot een afname van niet-CO₂ BKG uitstoot (productie van vlees neemt af van 430 Mt per jaar nu tot 280 Mt per jaar in 250, in vergelijking met 590 Mt per jaar in het referentiescenario). Maar ten tweede ook door de sterk afnemende ontbossing omdat agrarische expansie niet meer nodig is en er zelfs sprake is van herstel van natuurlijk land daar waar areaal aan de landbouw wordt onttrokken. Deze ontwikkelingen houden ook rechtstreeks verband met de groei van het natuurlijk landareaal (+4% tot +8%) wat wijst op voordelen voor biodiversiteit op land. Hetzelfde geldt voor de substantiële reductie van het stikstofoverschot (-23% tot -35%) - wat vooral het gevolg is van de lagere opbrengst aan mest uit de veeteelt - die voordelig is voor de biodiversiteit zowel in water als op het land. Door de verminderde druk in het voedselsysteem is ook de onttrekkingsbehoefte van water bestemd voor irrigatie substantieel kleiner (-3% tot -24%). In Hoofdstuk 6 worden de effecten op het energiesysteem niet onderzocht. Wel wordt in Hoofdstuk 2 aangetoond hoe in SSP1 gematigde reductie van de vleesconsumptie – in combinatie met andere aannames – de beschikbaarheid van landareaal sterk vergroot, leidend tot grotere inzet van bio-energie en wijzend op synergieën tussen afname van de vraag naar voedsel en energiebeschikbaarheid. Tenslotte wordt in Hoofdstuk 5 aangetoond dat een beperkte reductie van de vleesconsumptie kan leiden tot beperking van de benodigde groei van productiviteit die nodig is om de negatieve effecten op de voedselzekerheid te voorkomen.

Bescherming van natuurlijke ecosystemen bevoordeelt biodiversiteit en vermindert de uitstoot van BKG. Hierop zijn wel aanvullende maatregelen nodig met het oog op verhoging van oogstbrenngsten en verandering van voedingspatronen om negatieve gevolgen voor de voedselzekerheid en het gebruik van water voor irrigatie te voorkomen.

In het LAND-scenario (Hoofdstuk 6) is een ambitieuze conserveringsinspanning ontwikkeld, gericht op het behoud van de helft van het landareaal op aarde ten behoeve van natuur (Pimm et al., 2018; Wilson, 2016). Scenario-analyse met IMAGE 3.2 en MAgPIE toont aan dat

deze inspanning daadwerkelijk leidt tot een substantiële groei van het natuurlijk landareaal (+2% tot +4%), en wijst op de voordelen voor biodiversiteit. Bovendien heeft het, dankzij de verminderde conversie van natuurlijk landareaal, een sterke afname van AFOLU BKG uitstoot tot gevolg. Daartegenover staat dat begrenzing van de toename van landbouwareaal de druk op het agrarisch systeem opvoert, resulterend in hogere voedselprijzen (+20% in IMAGE). Dit wijst op een uitruileffect met voedselzekerheid. Bovendien wijst een toename van wateronttrekking ten behoeve van irrigatie (+10% in MAgPIE) op uitruileffecten met de beschikbaarheid van zoetwater en met biodiversiteit in water. Om deze effecten te minimaliseren zijn aanvullende maatregelen nodig, bijvoorbeeld agrarische intensivering en veranderingen in voedingspatronen.

Beperking van de zoetwateronttrekking ten behoeve van irrigatie komt ten goede van de biodiversiteit in water maar heeft uitruileffecten met voedselzekerheid, in het bijzonder in aride gebieden. Excessief watergebruik kan een negatieve invloed hebben op de biodiversiteit in water. Een manier om dit te voorkomen is beperking van de wateronttrekking conform minimale milieubeschermdende waterafvoereisen (*environmental flow requirements*, EFR) (Smakhtin et al., 2004). Wanneer zulk beleid mondiaal wordt ingevoerd, zoals onderzocht in het WATER-scenario (Hoofdstuk 6), wordt de wateronttrekking voor irrigatie met 26% tot 28% verminderd. De uitruileffecten van deze beperking zijn zeer ongelijk verdeeld vanwege de verschillen in afhankelijkheid van geïrrigeerde landbouw tussen de regio's. Vooral Noord-Afrika, het Midden-Oosten en Centraal-Azië zouden zwaar worden getroffen door deze maatregel, met een sterke stijging van de voedselprijzen en met risico's voor voedselzekerheid als gevolg (+30% in Rusland en Centraal Azië, en +60% in het Midden Oosten en Noord Afrika in 2050 in IMAGE 3.2). De noodzaak om het verlies van agrarische productie op geïrrigeerd land te compenseren kan zelfs leiden tot uitbreiding van landbouwareaal elders, met als gevolg een afname van natuurlijk landareaal met 1% in IMAGE 3.2. Om uitruileffecten van EFR te voorkomen zijn aanvullende maatregelen nodig. Verbeterde irrigatie-efficiëntie (die in deze thesis niet wordt geanalyseerd) kan de hierboven besproken effecten verminderen, bijvoorbeeld door over te gaan van oppervlakte-irrigatie naar sprinkler- of druppel-irrigatie. Deze efficiënte irrigatietechnieken maken een sterke groei van agrarische opbrengst per liter water mogelijk (Jägermeyer et al., 2015).

Verhoging van de efficiëntie in het gebruik van stikstof met het oog op beperking van de negatieve effecten op biodiversiteit levert synergieën op met klimaatbeleid en zou kunnen leiden tot verlaging van de voedselprijs. In de nexus-scenario-analyse van Hoofdstuk 6 vormen verbeteringen in de efficiëntie in stikstofgebruik een specifieke maatregel ter vermindering van het stikstofoverschot in de landbouw en ter beperking van de effecten van excessieve stikstofneerslag op de biodiversiteit op land en in water (de WATER en LAND-scenario's). N₂O-emissies worden ook gereduceerd door afnemend gebruik van synthetische kunstmest, wat wijst op een belangrijke synergie met klimaatbeleid. Bovendien wordt in MAgPIE een bescheiden verlaging van de voedselprijs voorzien, veroorzaakt door de lagere kosten van kunstmest. Dit duidt op een lichte verbetering van de voedselzekerheid.

Tabel 8-3: Mondiale procentuele verschillen in scenario-indicatoren in IMAGE en MagPIE tussen het REF scenario en de nexus scenario's in 2050 (Hoofdstuk 6). Kleuren geven aan waar sprake is van sterke synergieën (groen), zwakke synergieën (licht groen), sterke uitruilen (rood), zwakke uitruilen (licht rood), indicatoren waarop maatregelen in een bepaald scenario specifiek gericht zijn (blauw), geen noemenswaardige verandering (grijs).

Model Scenario	MAGPIE					IMAGE				
	WATER	LAND	FOOD	CLIMATE	TOTAL	WATER	LAND	FOOD	CLIMATE	TOTAL
Water onttrekking voor irrigatie	-26%	+10%	-24%	+31%	-25%	-28%	0%	-3%	+5%	-26%
Natuurlijk landareaal	0%	+2%	+4%	+2%	+6%	-1%	+4%	+8%	+2%	+8%
Stikstofoverschot in de landbouw	-27%	-27%	-35%	-8%	-61%	-30%	-32%	-23%	-24%	-51%
Voedselprijs	+1%	+1%	-18%	+7%	-11%	+9%	+20%	-46%	+11%	-34%
AFOLU BKG uitstoor	-3%	-14%	-58%	-43%	-83%	0%	-27%	-45%	-30%	-53%

8.3. Suggesties voor toekomstig onderzoek

Uit de studies besproken in deze thesis komen verschillende onderwerpen naar voren die nader onderzoek verdienen. Het betreft ontwikkeling van modellen en verbeterde samenwerking tussen, en integratie van, onderzoeksvelden.

Geïntegreerd modelleren van alle opties voor land-gebaseerde klimaatmitigatie. Zoals besproken in de introductie over land-gebaseerde maatregelen voor klimaatmitigatie (Sectie 1.2), behandelt deze thesis niet alle mogelijkheden voor mitigatie. Evenmin worden al deze mogelijkheden meegenomen in het IMAGE model. Het is een uitdaging voor alle teams die werken aan IAMs om *up to date* te blijven met voortgaand onderzoek en om elke nieuwe mitigatiemaatregel te integreren in de modellen. Dit blijkt ook uit Roe et al. (2021) waar de reikwijdte van de sector-gebaseerde beoordeling van mogelijkheden voor mitigatie, groter is dan de beoordeling op basis van de IAMs. Het is essentieel dat voortdurend wordt gewerkt aan de integratie van mitigatiemaatregelen in IAMs, in het bijzonder omdat deze modellen de beste instrumenten zijn om te beoordelen of verschillende mogelijkheden voor mitigatie met elkaar concurreren. Concurrentie zou immers het potentieel van alle maatregelen samen kunnen beperken, wat niet wordt meegenomen in sectorale analyses. Dit is bijvoorbeeld het geval bij maatregelen gericht op CDR in de landbouw, zoals verhoging van het volume grondgebonden koolstofopslag of toevoeging van *biochar*. Het slagen van deze maatregelen is afhankelijk van de beschikbaarheid van oogstresten of geormerkte biomassa oogsten, waarvan nu de aanname is dat ze worden gebruikt voor de productie van bio-energie (Daioglou et al., 2016). Hetzelfde geldt voor *agroforestry*, dat wordt voorzien voor grote landbouwvelden die volgens mitigatiescenario's in aanmerking komen voor bebossing met het oog op klimaatmitigatie. De beoordeling van de mogelijkheden van agrarische CDR-maatregelen moet geïntegreerd worden verricht, uitgaande van transparante

scenario-aannames. IAMs zijn hiervoor zeer geschikt, maar voortgaand onderzoek naar en ontwikkeling van de modellen is essentieel.

Mogelijkheden en beperkingen van plaats- en proces-specifiek modelleren van agrarische intensivering. In de periode 1961-2020 kwam gemiddeld 90% van de jaarlijkse groei van gewasopbrengsten voor rekening van intensivering van bestaand landbouwareaal, en dus niet van uitbreiding van dit areaal (USDA-ERS, 2022a). Dit betekent dat agrarische intensivering een cruciale rol speelt in de vervulling van de vraag naar voedsel. Tegelijkertijd veroorzaakt intensivering milieuproblemen zoals verlies van biodiversiteit in agrarische landschappen, excessief watergebruik, bodemerrosie en eutrofiëring van rivieren en meren. Daarom is het vinden van balans tussen landgebruik voor de voedselvoorziening en de rol van land in het bieden van ecosystemendiensten een belangrijke opdracht. Ruimtelijk expliciete modellering van agrarische intensivering kan helpen bij de uitvoering van deze opdracht, in het bijzonder omdat dergelijke processen sterk plaatsgebonden zijn. Bovendien is er behoefte aan een verbeterde weergave van de verschillende aanjagers van intensivering, zoals veranderingen in het gebruik van kunstmest en gewasbeschermers, toegenomen mechanisering, gewasvariëteiten met hogere opbrengst en grotere landbouwkundige kennis. In deze thesis wordt de verhouding tussen agrarische expansie en agrarische intensivering met het oog op vervulling van de agrarische vraag bepaald op het niveau van wereldregio's. Hierbij worden effecten op gewasopbrengst en landbeschikbaarheid die verband houden met milieuproblemen op geaggregeerde wijze in acht genomen. Wanneer het mogelijk wordt om plaats- en aanjager-specifieke beperkingen aan intensivering vast te stellen, bijvoorbeeld gerelateerd aan bijzondere plekken voor biodiversiteit, gevoeligheid voor bodemerrosie of verdroging, oeverzones ter beperking van het weglekken van voedings- en gewasbeschermingsstoffen, dan kan een meer gedetailleerde beoordeling worden uitgevoerd van processen en beïnvloedingen veroorzaakt door agrarische intensivering. Een dergelijke benadering maakt tevens zichtbaar wat de consequenties zijn van beperking van intensivering in regio's waar deze processen en beïnvloedingen zich voordoen. Hierdoor wordt de stap van grootschalige mondiale uitdagingen naar lokale oplossingen minder groot en ook makkelijker uit te leggen aan beleidsmakers.

Uitgebreidere modellering van de effecten van klimaatverandering en meer expliciete modellering van klimaatadaptatie. In deze thesis wordt de nadruk niet gelegd op de effecten van klimaatverandering en klimaatadaptatie, ook al zijn dit belangrijke onderwerpen voor klimaatbeleid en dus relevante onderzoeksvelden. Een cruciale kwestie is de grote onzekerheid in de schattingen van de effecten van klimaatverandering op gewasopbrengsten (Jägermeyer et al., 2021). Een beter begrip van de effecten van CO₂-bemesting, droogte, hittestress en extreme weersomstandigheden is van belang om de beïnvloeding van toekomstige vormen van landgebruik door schommelingen in gewasopbrengst in kaart te kunnen brengen. Daarnaast worden andere effecten op de agrarische sector, bijvoorbeeld de effecten van hittestress op arbeid, veelal uitgesloten. Deze effecten kunnen substantieel zijn en zouden daarom moeten worden geïntegreerd (de Lima et al., 2021;

Hertel en de Lima, 2020). Tenslotte wordt klimaatadaptatie vaak impliciet meegenomen, bijvoorbeeld als het gaat over veranderingen in de handel tussen regio's onder invloed van klimaatverandering op gewasopbrengsten, of over verandering van de zaaikalender door gewijzigde neerslagperiodes. Daar staat tegenover dat andere mogelijke vormen van klimaatadaptatie, bijvoorbeeld verdere uitbreiding van irrigatie, niet worden meegenomen door beperkingen van het model, ook als die klimaatmitigatie zouden kunnen ondersteunen. Explicitering van de rol van klimaatadaptatie kan leiden tot meer begrip van de uitdagingen waarvoor de samenleving door klimaatverandering wordt gesteld en tot verheldering van de mogelijkheden van klimaatadaptatie waarop beleidsmakers actie moeten ondernemen.

Vergroting van het aantal gemodelleerde verbindingen tussen de nexus en duurzame ontwikkeling, gericht op het ontwerpen van omvattende trajecten van duurzame ontwikkeling. In deze thesis zijn verschillende nexus-verbindingen en duurzame ontwikkelingsthema's expliciet gekwantificeerd en in detail besproken. Tegelijkertijd zijn vele verbindingen met en dimensies van duurzame ontwikkeling niet aan de orde gekomen. Het is belangrijk om het aantal gemodelleerde verbindingen tussen componenten van de nexus en dimensies van duurzame ontwikkeling te vergroten. Uiteindelijk moet dit leiden tot scenario's waarmee toekomstige integrale trajecten kunnen worden ontworpen die duurzaamheid vanuit sociaal én vanuit milieuperspectief bereikbaar maken en daarbij rekening houden met de effecten van uitruilen en synergieën. Om dit te realiseren is verdere integratie van verschillende modelleringsmethoden en onderzoeksvelden noodzakelijk. Zo zouden bijvoorbeeld de invloeden van intensivering van en veranderingen in landgebruik op biodiversiteit geïntegreerd kunnen worden in agro-economische modelleringen. Dit maakt het mogelijk om de dynamiek van beïnvloeding van biodiversiteit en de meerwaarde daarvan te overwegen en te zoeken naar economisch optimale transitietrajecten. Ook kunnen de interacties tussen het energiesysteem en de nexus verder worden geïntegreerd. Bijvoorbeeld de effecten van watertekorten op de opwekking van elektriciteit; de effecten van waterkrachtcentrales op de beschikbaarheid van water en de biodiversiteit; en de effecten van maatregelen ter bescherming van biodiversiteit op het vermogen aan waterkracht. Tenslotte behoort het menselijk welzijn een standaard component van deze beoordelingen te zijn. Er is al behoorlijk veel aandacht voor voedselzekerheid, maar bijvoorbeeld gezondheid en armoede zouden ook deel moeten uitmaken van de centrale set van indicatoren die worden beoordeeld.

Van sociale wetenschappen leren om transitie van landsystemen te modelleren. De trends in voorzien landgebruik die in deze thesis aan de orde worden gesteld zijn gebaseerd op de neoklassieke economische theorieën, de kern van de agro-economische modellering. Dit type modelleren houdt impliciet rekening met menselijk gedrag, op basis van relaties die voortbouwen op historische data. Belangrijke transities, bijvoorbeeld verandering van het voedingspatroon, kunnen echter alleen op gestileerde wijze worden geïmplementeerd. Beter begrip en betere weergave van menselijk gedrag en menselijke besluitvorming kunnen het realisme van de voorziene landsystemen verbeteren en tevens aan beleidsmakers en

de samenleving als geheel mogelijkheden bieden om zulke transitie te realiseren. Om dit te bereiken zou de IAM-gemeenschap de samenwerking met sociale wetenschappen moeten verbeteren. Interessante initiatieven in die richting zijn *agent-based* modelleren van verandering in Europese landsystemen (Brown et al., 2019) en gedragsmatig modelleren van verandering van voedingspatronen (Eker et al., 2019).

8.4. Beleidsaanbevelingen

De bevindingen van deze thesis zijn uiteindelijk bedoeld om beleidsmakers te adviseren aangaande de rol van de landsector in het beperken van mondiale opwarming tot ruim onder de twee graden met inachtneming van de bescherming van het milieu en het realiseren van duurzame ontwikkeling. De belangrijkste beleidsaanbevelingen kunnen als volgt worden samengevat.

Land-gebaseerde mitigatie kan een belangrijke bijdrage leveren aan de beperking van klimaatverandering. Vanwege de risico's van uitruilen en zorgen over haalbaarheid zou het beleid echter niet té afhankelijk van de sector land moeten zijn. Land-gebaseerde mitigatie kan een substantieel aandeel leveren in de klimaatmitigatie die nodig is om ambitieuze doelen te halen: tot 28%-33% van de totale mitigatie in 2050 in kostenefficiënte mitigatietrajecten. Deze mitigatiemaatregelen brengen echter de risico's van uitruileffecten met zich mee, met name ten aanzien van voedselzekerheid door concurrentie om land, ten aanzien van biodiversiteit door grootschalige toepassing van bio-energie en bebossing, en ten aanzien van excessief gebruik van water en kunstmest door intensivering van landbouw. Daar komt bij dat een groot deel van het betreffende landareaal gesitueerd is in ontwikkelende regio's waar voortgaande economische ontwikkeling is vereist om de levensstandaard conform de SDGs te verhogen. Bovendien is de implementatie van maatregelen afhankelijk van boeren en andere landeigenaren, een gegeven dat zorgen over de haalbaarheid met zich meebrengt. Daarom moeten schattingen van het mogelijke aandeel van de landsector met voorzichtigheid worden behandeld en mogen klimaatneutraliteit strategieën niet té afhankelijk zijn van land-gebaseerde mitigatie. Waar een grote bijdrage van land-gebaseerde mitigatie wordt aangenomen, moet dit volgens een zorgvuldige planning worden gedaan met een nexus-benadering die rekening houdt met zowel milieu-vereisten als de behoeften van mensen die afhankelijk zijn van het land.

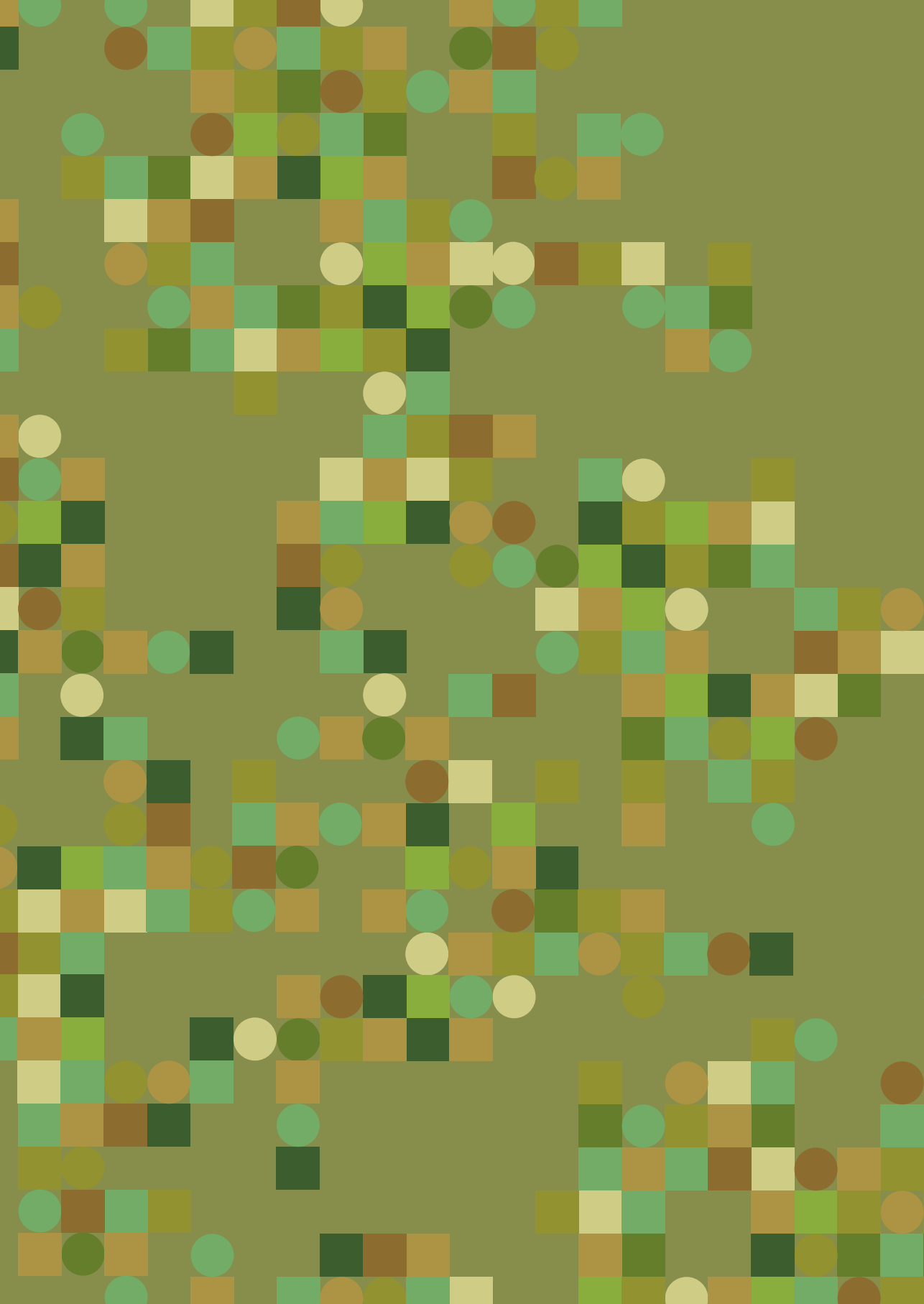
Bescherming en herstel van veengebied zijn belangrijke maatregelen voor klimaatmitigatie die aandacht van beleidsmakers verdienen. Bescherming van natuurlijk veenareaal en herstel van gedegradeerd veengebied zijn zeer effectieve mitigatiemaatregelen met hoge BKG-voordelen per hectare. Hiermee kan 2% van de totale vereiste mitigatie worden gerealiseerd met relatief weinig beïnvloeding op de mondiale ontwikkeling van landgebruik. Daarom verdienen deze maatregelen de aandacht van beleidsmakers. Wel

vormt de ongelijke geografische verdeling van veengebied dat kan bijdragen aan mitigatie een kritische uitdaging: er zijn maar weinig landen die hierop beleid kunnen maken.

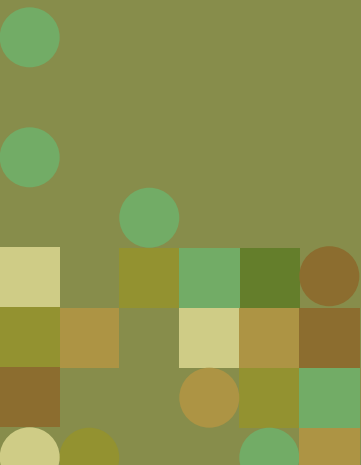
Vraagzijde-gerichte maatregelen zoals verandering van voedingspatroon en vermindering van voedselverspilling bieden win-win mogelijkheden, omdat ze enerzijds leiden tot sterke afname van uitstoot van BKG en van andere bedreigingen van het milieu, en anderzijds ten goede komen aan volksgezondheid. Lagere vlees- en zuivelconsumptie, minder voedselverspilling en gezonde niveaus van voedselinname reduceren de BKG-uitstoot van het voedselsysteem substantieel en verminderen tevens andere milieuproblemen, zoals biodiversiteitsverlies, eutrofiëring en overmatige wateronttrekking. Daarom is beleid dat de consumptie van dierlijke producten ontmoedigt en plantaardige alternatieven stimuleert een win-win mogelijkheid. Daarnaast zou moeten worden geïnvesteerd in vermindering van voedselverspilling, bijvoorbeeld door verbetering van het management van bevoorradingsketens en door versterking van consumentenbewustzijn. Verandering van voedingspatronen verbetert bovendien niet alleen het milieu, maar ook de volksgezondheid (Willett et al., 2019), wat het win-win karakter van deze maatregelen onderstreept.

Bescherming van natuurlijk landareaal is essentieel voor vermindering van emissies door ontbossing en voor bescherming van biodiversiteit, maar moet worden gecombineerd met investeringen in agrarische ontwikkeling om negatieve gevolgen voor de voedselzekerheid te voorkomen. Bescherming van natuurlijke ecosystemen is onmisbaar zowel ter voorkoming van uitstoot van BKG als ter beëindiging van het verlies van biodiversiteit. Echter, strikte grenzen aan de expansie van landbouw kunnen in het bijzonder in ontwikkelende landen de voedselzekerheid sterk negatief beïnvloeden. Dit geldt te meer voor landen met een verwachte verdere groei van de bevolking en economie. Daarom moeten beschermingsmaatregelen worden gecombineerd met landbouwinvesteringen om negatieve uitruileffecten te voorkomen en om economische ontwikkeling van armere landen conform de SDGs te faciliteren.

Verhoging van de efficiëntie in het stikstofgebruik is onmisbaar voor het verminderen van negatieve effecten op biodiversiteit en is tevens voordelig voor klimaatmitigatie. Grotere efficiëntie in het gebruik van meststoffen, zowel kunstmest als dierlijke mest, leidt tot verminderde effecten van excessieve stikstofconcentraties op de waterkwaliteit en de biodiversiteit in water en op land. Bovendien wordt hierdoor tevens de uitstoot van lachgas, een belangrijk BKG, verlaagd. Daarom complementeert beleid ter voorkoming van negatieve effecten van stikstof op biodiversiteit de inspanningen voor klimaatmitigatie. Het zou dus een ambitie met prioriteit moeten zijn.



SUPPLEMENTARY INFORMATION



S2. Exploring SSP land-use dynamics using the IMAGE model: Regional and gridded scenarios of land-use change and land-based climate change mitigation

SI Table 2-1: Scenario-specific characteristics used for the IMAGE SSP implementation

Scenario	SSP1	SSP2	SSP3	SSP4	SSP5
Trade in agricultural commodities	Abolishment of current import tariffs and introduction export subsidies by 2030	Current tariffs and subsidies.	Introduction of a 10% import tax for all agricultural products by 2050, for self-sufficiency concerns	Abolishment of import tariffs and introduction export subsidies in high/medium- income regions 10% import tax in low-income regions as they are excluded from the global market	Abolishment of current import tariffs and introduction export subsidies by 2030
Trade in energy carriers	No trade restrictions	No trade restrictions	Stronger reliance on domestic production.	Stronger reliance on domestic production in low-income regions, no trade restrictions in high/medium-income regions	No trade restrictions
Meat consumption	Low - Consumption of animal products 30% lower than endogenous outcome	Medium- endogenous model outcome	High - Consumption of animal products 30% higher than endogenous outcome,	Medium- endogenous model outcome	High - Consumption of animal products 30% higher than endogenous outcome,
Income elasticity	Slight decrease in income elasticity representing less consumption oriented society	Standard income elasticities	Slight increase in income elasticity representing more consumption oriented society	Standard income elasticities	Slight increase in income elasticity representing more consumption oriented society
Losses in food supply chain including waste at household level	Reduction of food losses by 33%.	Current levels of food losses	Increase of food losses by 33%.	Current levels of food losses	Increase of food losses by 33%

SI Table 2-1: Scenario-specific characteristics used for the IMAGE SSP implementation (continued)

Scenario	SSP1	SSP2	SSP3	SSP4	SSP5
Land-use change regulation	Strong – Protected areas are extended to achieve the Aichi target of 17%. Additionally, areas are protected to provide essential services in line with Aichi targets 14 and 15, adding up to a total 30% of terrestrial area unavailable for agricultural expansion.	Medium – Protected areas are extended to achieve the Aichi target of 17% of the terrestrial area, gradually implemented from 2010-2050.	Low – protected areas at current level.	Strong protection (as in SSP1) in high-income regions, medium production in middle-income regions (as in SSP2) and low protection (as in SSP3) in low-income regions	Medium – Protected areas are extended to achieve the Aichi target of 17% of the terrestrial area, gradually implemented from 2010-2050.
Agricultural productivity crops	High – crop yield increase as a function of GDP	Medium – following largely the projections by FAOs agricultural outlook	Low – crop yield increase as a function of GDP	Strong to low in high- to low-income regions respectively, as a function of GDP	Strong – crop yield increase as a function of GDP
Agricultural productivity livestock	High – Efficiency parameters achieve 50% convergence to the levels of the most efficient regions in SSP2	Medium - following largely the projections by FAOs agricultural outlook	Low - Efficiency stagnates at current regional levels	High to low in high- to low-income regions respectively	High- Efficiency parameters achieve 50% convergence to the levels of the most efficient regions in SSP2

SI Table 2-1: Scenario-specific characteristics used for the IMAGE SSP implementation (continued)

Scenario	SSP1	SSP2	SSP3	SSP4	SSP5
Irrigation area and efficiency	Irrigation area growth rate 50% lower than SSP2, irrigation efficiency increases by 0.1%/yr for all irrigated areas	Irrigation area increases following the FAO agricultural outlook of irrigated harvested area, irrigation efficiency increases by 0.2%/yr for newly irrigated areas	Irrigation area growth rate 50% higher than SSP2 Irrigation efficiency remains at current levels	Irrigation area and efficiency trends follow SSP1, SSP2 and SSP3 in high, middle and low-income regions respectively	Irrigation area increases following the FAO agricultural outlook of irrigated harvested area, irrigation efficiency increases by 0.1%/yr for all irrigated areas
Nutrient management	High efficiency - fertilizer use efficiency 20% higher than SSP2, fertilizer application rates increase in countries with nutrient mining	Medium efficiency - fertilizer use efficiency rates largely follow FAO agricultural outlook	Low efficiency - fertilizer use efficiency 20% lower than SSP2	Fertilizer use efficiencies follow SSP1, SSP2 and SSP3 in high/middle/low-income regions respectively	High efficiency - fertilizer use efficiencies 20% higher than SSP2, rates increase in countries with nutrient mining
Roundwood demand	Global average per capita demand decreases by 10%	Global average per capita demand increases by 5%	Global average per capita demand decreases by 10%	Global average per capita demand decreases by 5%	Global average per capita demand increases by 40%
Forest management	High increase in production from wood plantations and reduced impact logging	Moderate increase in production from wood plantations and clear cut systems	Current management systems are maintained	Management system changes follow SSP1, SSP2 and SSP3 in high/middle/low-income regions respectively	High increase in production from wood plantations and clear cut systems
Additional forest degradation	Additional forest degradation levels of by 2040	Additional forest degradation levels of by 2050	Additional forest degradation levels of by 2060	High-income regions level off by 2040, medium-income regions by 2050, low-income regions by 2060	Additional forest degradation levels of by 2050

SI Table 2-2: IMAGE regions, regional aggregation used in the paper and high/medium/low-income regions classification used in scenario development. The regional aggregation is added to prevent very large figures that hamper understanding. Regions that have reasonably similar economics and land dynamics are added together. The Russia/Middle East region is a bit mixed but characterized by relatively small land-use changes in all scenarios.

IMAGE region	Aggregated region	Income region (high/medium/low)
Canada	OECD countries	High
USA	OECD countries	High
Mexico	Latin America	Medium
Rest Central America	Latin America	Medium
Brazil	Latin America	Medium
Rest South America	Latin America	Medium
Northern Africa	Russia/Middle East	Low
Western Africa	Sub-Saharan Africa	Low
Eastern Africa	Sub-Saharan Africa	Low
South Africa	Sub-Saharan Africa	Medium
OECD Europe	OECD countries	High
Eastern Europe	OECD countries	Medium
Turkey	Russia/Middle East	Medium
Ukraine +	Russia/Middle East	Medium
Asia-Stan	Russia/Middle East	Medium
Russia +	Russia/Middle East	High
Middle East	Russia/Middle East	Medium
India	South/Southeast Asia	Low
Korea	OECD countries	High
China +	China	Medium
South-East Asia	South/Southeast Asia	Low
Indonesia +	South/Southeast Asia	Low
Japan	OECD countries	High
Oceania	OECD countries	High
Rest South Asia	South/Southeast Asia	Low
Rest Southern Africa	Sub-Saharan Africa	Low

SI Table 2-3: Description of scenario simulations performed

SSP	Baseline (endogenous radiative forcing result)	Mitigation to achieve 6.0 W/m ² (RCP6)	Mitigation to achieve 4.5 W/m ² (RCP4.5)	Mitigation to achieve 3.4 W/m ² (RCP3.4)	Mitigation to achieve 2.6 W/m ² (RCP2.6)	Mitigation to achieve 1.9 W/m ² (RCP1.9)	Counterfactual scenarios performed to quantify mitigation effect bioenergy
SSP1	SSP1 (5.0 W/m ²)	Baseline radiative forcing lower than mitigation target	SSP1-4.5	SSP1-3.4	SSP1-2.6	SSP1-1.9	SSP1-nobio, SSP1-4.5-nobio, SSP1-2.6-nobio, SSP1-1.9-nobio
SSP2	SSP2 (6.5 W/m ²)	SSP2-6.0	SSP2-4.5	SSP2-3.4	SSP2-2.6	SSP2-1.9	SSP2-nobio, SSP2-4.5-nobio, SSP2-2.6-nobio, SSP2-1.9-nobio
SSP3	SSP3 (6.8 W/m ²)	SSP3-6.0	SSP3-4.5	SSP3-3.4	Infeasible	Infeasible	
SSP4	SSP4 (6.1 W/m ²)	SSP4-6.0	SSP4-4.5	SSP4-3.4	SSP4-2.6	Infeasible	
SSP5	SSP5 (8.3 W/m ²)	SSP5-6.0	SSP5-4.5	SSP5-3.4	SSP5-2.6	Infeasible	

SI Table 2-4: Emission factors per activity level for all non-CO₂ emissions from agriculture and land use.

emission source	gas	sub-type	Activity	emission factor - median (min-max)	unit	comment	source
Enteric fermentation	CH ₄	dairy cattle	number of animals	70 (38 - 173)	kg CH ₄ / head	region specific emission factors for 2005 - time dependent	(IPCC, 2006)
		non-dairy cattle	number of animals	51 (25 - 66)	kg CH ₄ / head	region specific emission factors for 2005 - time dependent	(IPCC, 2006)
		pigs	number of animals	1.0 - 1.5	kg CH ₄ / head	region specific emission factors for 2005 - time dependent	(IPCC, 2006)
		sheep&goats	number of animals	5, 8	kg CH ₄ / head	region specific emission factors for 2005 - time dependent	(IPCC, 2006; JRC/PBL, 2012)
Animal waste	CH ₄	dairy cattle	number of animals	5.4 (1.0 - 63.3)	kg CH ₄ / 1000 head	region specific emission factors for 2005 - time dependent	(JRC/PBL, 2012)
		non-dairy cattle	number of animals	1.0 (0.95 - 6.93)	kg CH ₄ / 1000 head	region specific emission factors for 2005 - time dependent	(JRC/PBL, 2012)
		pigs	number of animals	2.6 (0.99 - 13.1)	kg CH ₄ / 1000 head	region specific emission factors for 2005 - time dependent	(JRC/PBL, 2012)
		poultry	number of animals	0.02 (0.01 - 0.36)	kg CH ₄ / 1000 head	region specific emission factors for 2005 - time dependent	(JRC/PBL, 2012)
	N ₂ O	sheep&goats	number of animals	0.19 (0.11 - 0.24)	kg CH ₄ / 1000 head	region specific emission factors for 2005 - time dependent	(JRC/PBL, 2012)
		stable	number of animals	0.004 (0.0003 - 0.01)	g N ₂ O-N/g N excretion	region specific emission factors for 2005 - time dependent	(JRC/PBL, 2012)
NH ₃	pasture	number of animals	0.02 (0.0005 - 0.04)	g N ₂ O-N/g N excretion	region specific emission factors for 2005 - time dependent	(JRC/PBL, 2012)	
	stable	number of animals	0.16 (0.024 - 0.44)	g NH ₃ -N/g N excretion	region specific emission factors for 2005 - time dependent	(JRC/PBL, 2012)	

SI Table 2-4: Emission factors per activity level for all non-CO₂ emissions from agriculture and land use. (continued)

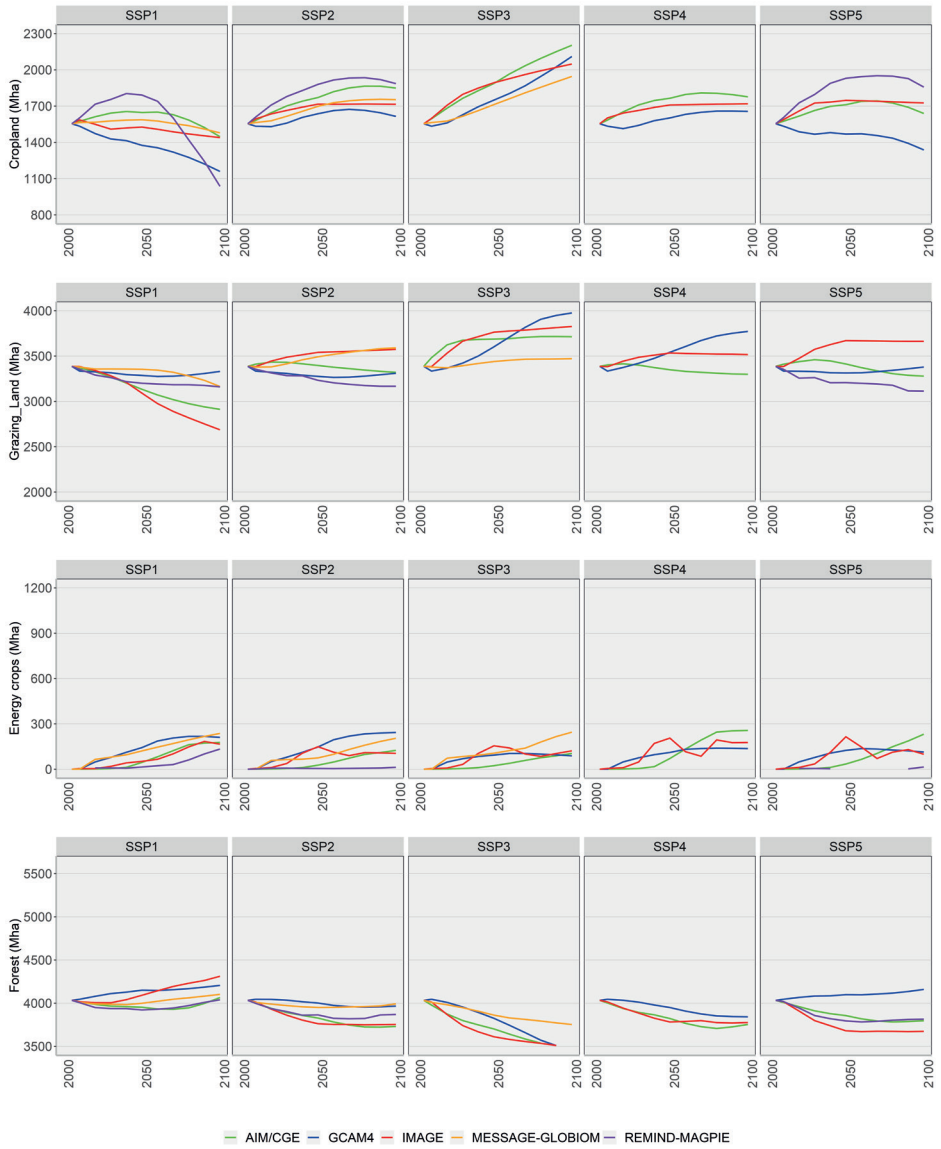
emission source	gas	sub-type	Activity	emission factor - median (min-max)	unit	comment	source
Animal waste (continued)		pasture	number of animals	0.08 (0.003 - 0.2)	g NH ₃ -N/g N excretion	region specific emission factors for 2005 - time dependent	(JRC/PBL, 2012)
	NOx	stable	number of animals	0.002 (0.0004 - 0.005)	g NOx-N/g N excretion	region specific emission factors for 2005 - time dependent	(JRC/PBL, 2012)
		pasture	number of animals	0.004 (0.0001 - 0.009)	g NOx-N/g N excretion	region specific emission factors for 2005 - time dependent	(JRC/PBL, 2012)
Wetland rice fields	CH ₄		area wetland rice	22.1 (8.4 - 44.3)	(Tg/km ²)	region specific emission factors for 2005 - time dependent	(JRC/PBL, 2012)
Synthetic fertilizer	N ₂ O		N fertilizer applied	0.01	g N ₂ O-N/g N applied		(IPCC, 2006)
	NH ₃		N fertilizer applied	0.16 (0.08 - 0.21)	g NH ₃ -N/g N applied	region specific emission factors for 2005 - time dependent	(JRC/PBL, 2012)
Manure fertilizer	NOx		N fertilizer applied	0.005	g NOx-N/g N applied		(Bouwman et al., 2002)
	N ₂ O		N fertilizer applied	0.01	g N ₂ O-N/g N applied		(IPCC, 2006)
	NH ₃		N fertilizer applied	0.26 (0.21 - 0.26)	g NH ₃ -N/g N applied	region specific emission factors for 2005 - time dependent	(JRC/PBL, 2012)
	NOx		N fertilizer applied	0.0055	g NOx-N/g N applied		(Bouwman et al., 2002)
Indirect emissions	N ₂ O	leaching and runoff	N fertilizer applied	0 - 0.0225	g N ₂ O-N/g N applied		(IPCC, 2006)
		deposition	NH ₃ and NOx emissions from agriculture	0.01	g N ₂ O-N/g N deposited		(IPCC, 2006)

SI Table 2-4: Emission factors per activity level for all non-CO₂ emissions from agriculture and land use. (continued)

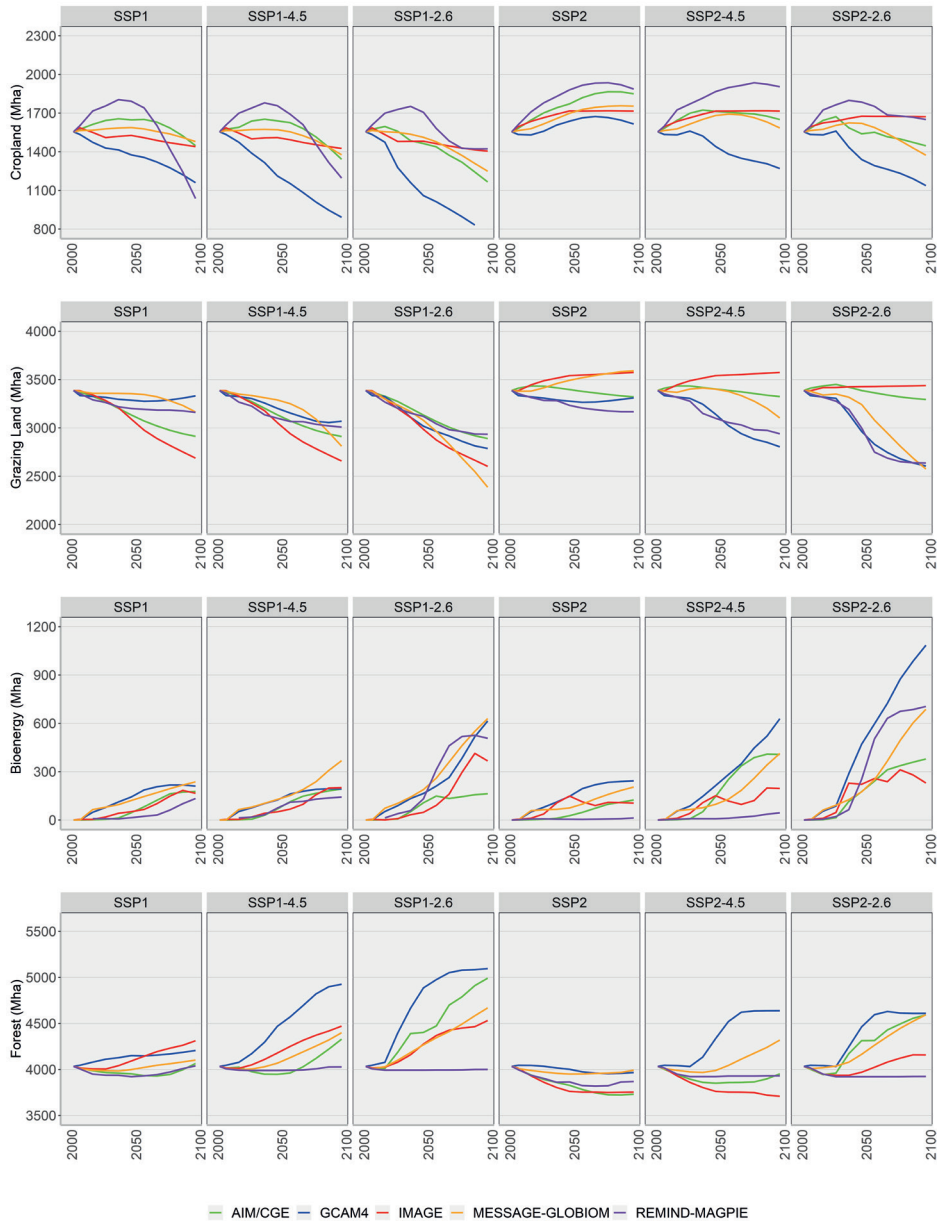
emission source	gas	sub-type	Activity	emission factor - median (min-max)	unit	comment	source
Savannah burning	CH ₄		carbon burnt	5	g CH ₄ /kg C		(JRC/PBL, 2012)
	N ₂ O		carbon burnt	0.265	g N/kg C		(JRC/PBL, 2012)
	CO		carbon burnt	57.143	g C/kg C		(JRC/PBL, 2012)
	NH ₃		carbon burnt	1.613	g N/kg C		(JRC/PBL, 2012)
	NOx		carbon burnt	1.585	g N/kg C		(JRC/PBL, 2012)
	SOx		carbon burnt	0.354	g S/kg C		(JRC/PBL, 2012)
	NMVOc		carbon burnt	7.708	g C /kg C		(JRC/PBL, 2012)
	BC		carbon burnt	0.48 (0.48 - 1)	g C/kg C		(Bond et al., 2004)
	OC		carbon burnt	3.4 (3 - 3.4)	g C/kg C		(Bond et al., 2004)
	Agricultural waste burning	CH ₄		carbon burnt	5.63	g C/kg C	
N ₂ O			carbon burnt	0.09	g N/kg C		(JRC/PBL, 2012)
CO			carbon burnt	103 (84 - 116)	g C/kg C	region specific emission factors for 2005 - time dependent	(JRC/PBL, 2012)
NH ₃			carbon burnt	2.23	g N/kg C		(JRC/PBL, 2012)
NOx			carbon burnt	2.41	g N/kg C		(JRC/PBL, 2012)
SOx			carbon burnt	0.6 (0.4 - 0.8)	g S / kg C	region specific emission factors for 2005 - time dependent	(JRC/PBL, 2012)
NMVOc			carbon burnt	14.58	g C/kg C		(JRC/PBL, 2012)

SI Table 2-4: Emission factors per activity level for all non-CO₂ emissions from agriculture and land use. (continued)

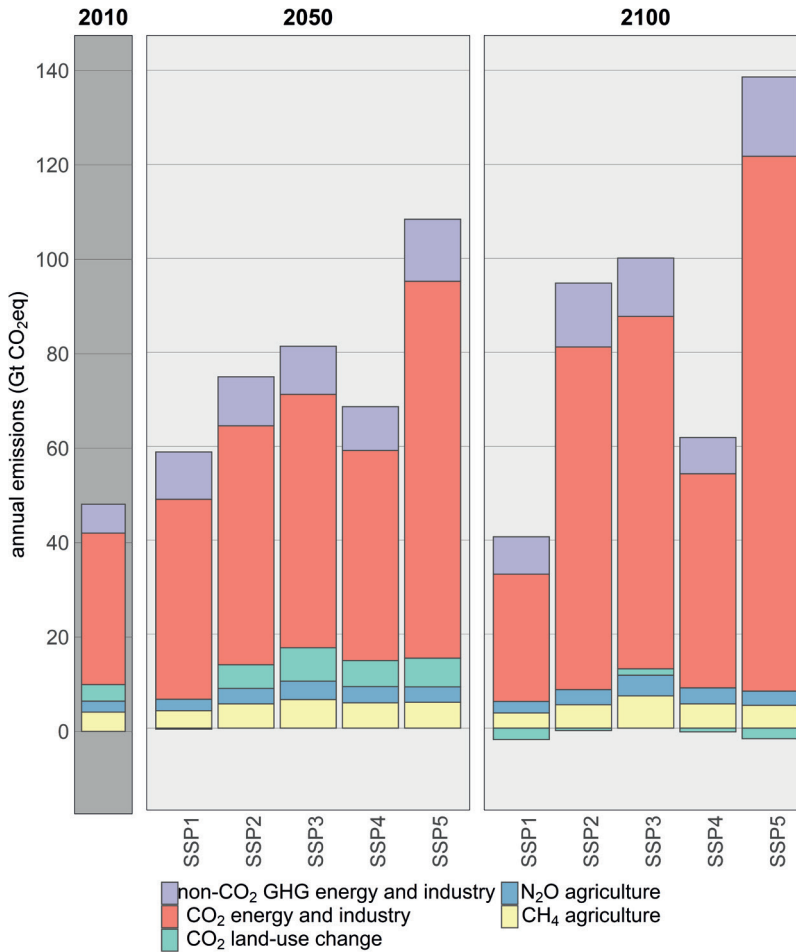
emission source	gas	sub-type	Activity	emission factor - median (min-max)	unit	comment	source
Agricultural waste burning (continued)	BC		carbon burnt	0.66 (0.56 - 0.66)	g C/kg C		(Bond et al., 2004)
	OC		carbon burnt	5.2 (5.2 - 8)	g C/kg C		(Bond et al., 2004)
Deforestation	CH ₄		carbon burnt	14.17	g C/kg C		(JRC/PBL, 2012)
	N ₂ O		carbon burnt	0.27	g N/kg C		(JRC/PBL, 2012)
	CO		carbon burnt	89.29	g C/kg C		(JRC/PBL, 2012)
	NH ₃		carbon burnt	2.57	g N/kg C		(JRC/PBL, 2012)
	NOx		carbon burnt	1.65	g N/kg C		(JRC/PBL, 2012)
	SOx		carbon burnt	0.78	g S/kg C		(JRC/PBL, 2012)
	NMVOC		carbon burnt	14.79	g C/kg C		(JRC/PBL, 2012)
	BC		carbon burnt	0.66 (0.56 - 0.66)	g C/kg C		(Bond et al., 2004)
	OC		carbon burnt	5.2 (5.2 - 8)	g C/kg C		(Bond et al., 2004)
Crops and decomposition of crops	NH ₃		crop area	250	kg N/km ²		(Bouwman et al., 2002)



SI Figure 2-1: land-use trends for cropland, grazing land, bioenergy plantations and forest in five IAMs for five baseline scenarios: AIM/CGE (Fujimori et al., 2014), GCAM (Wise et al., 2014), IMAGE (Stehfest et al., 2014), MESSAGE-GLOBIOM (Havlik et al., 2012) and REMIND-MAGPIE (Popp et al., 2011). The starting point is calibrated to 2005 FAO data.



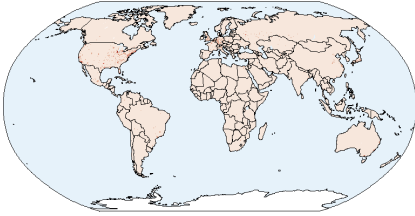
SI Figure 2-2: Land-use trends for cropland, grazing land, bioenergy plantations and forest in five IAMs for SSP1 and SSP2 baseline and two SSP1 and two SSP2 mitigation scenarios: AIM/CGE (Fujimori et al., 2014), GCAM (Wise et al., 2014), IMAGE (Stehfest et al., 2014), MESSAGE-GLOBIOM (Havlik et al., 2012) and REMIND-MAGPIE (Popp et al., 2011). The starting point is calibrated to 2005 FAO data.



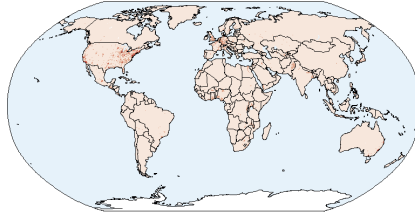
SI Figure 2-3: GHG emissions in 2010, 2050 and 2100 from energy and industry, LUC including reforestation, and agriculture, for five baseline scenarios

Built-up area

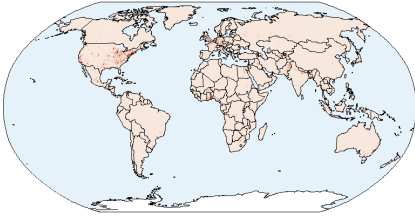
2010



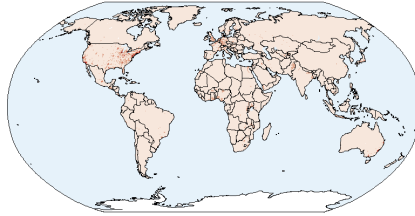
2100: SSP1



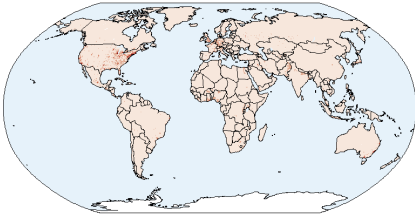
2100: SSP2



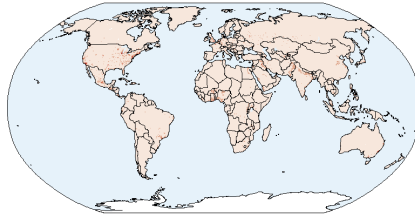
2100: SSP1-1.9



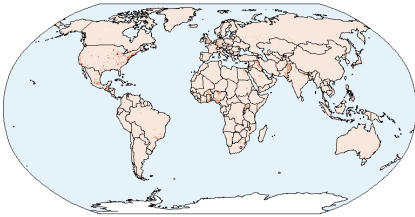
2100: SSP2-1.9



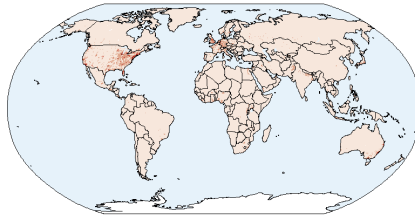
2100: SSP3



2100: SSP4



2100: SSP5



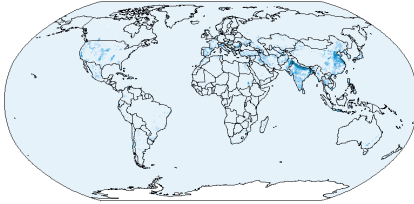
built-up area (% per gridcell)



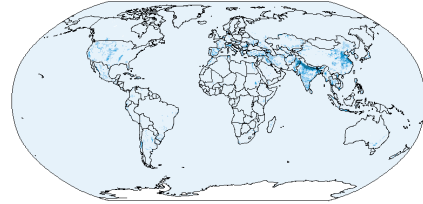
SI Figure 2-4: Built-up area in 2010 and in 2100 for five baseline scenarios and two 1.5°C mitigation scenarios (1.9 W/m²)

Irrigated food/feed cropland

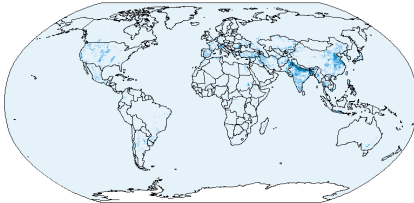
2010



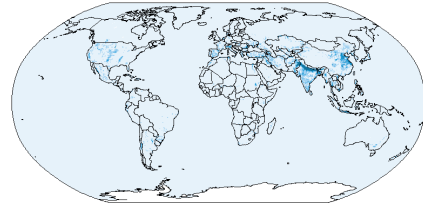
2100: SSP1



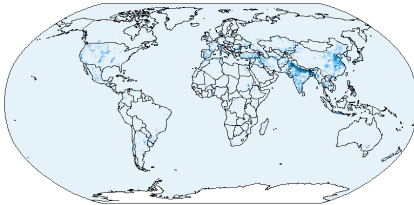
2100: SSP2



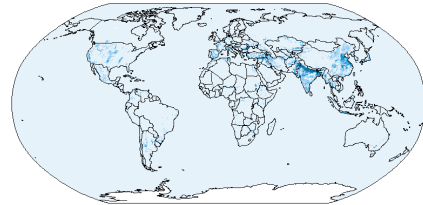
2100: SSP1-1.9



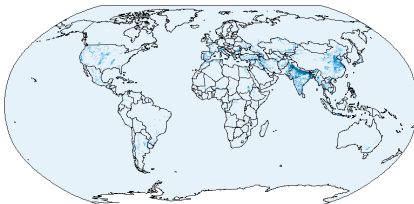
2100: SSP2-1.9



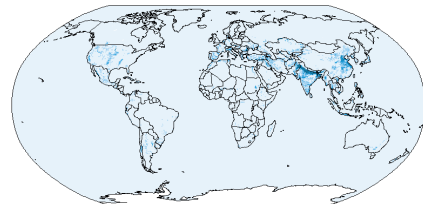
2100: SSP3



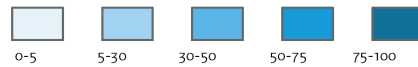
2100: SSP4



2100: SSP5



irrigated cropland for food/feed (% per gridcell)

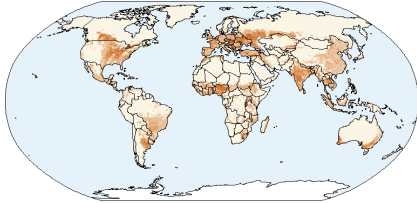


SI Figure 2-5: Irrigated cropland for food and feed production in 2010 and in 2100 for five baseline scenarios and two 1.5°C mitigation scenarios (1.9 W/m²)

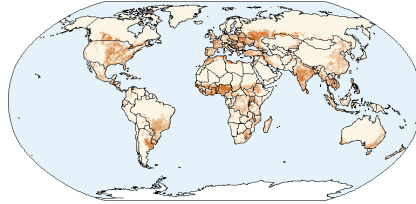
A

Rainfed food/feed cropland

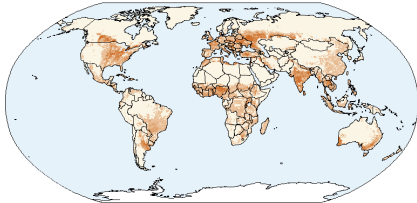
2010



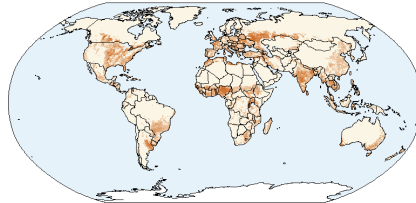
2100: SSP1



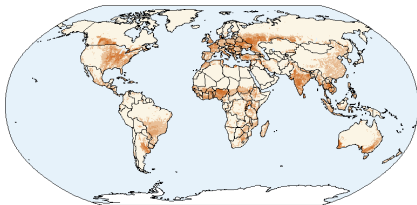
2100: SSP2



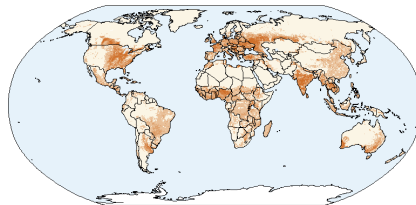
2100: SSP1-1.9



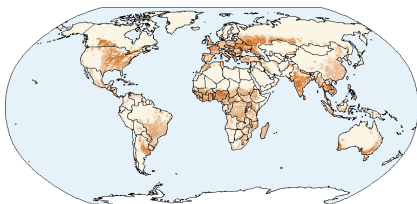
2100: SSP2-1.9



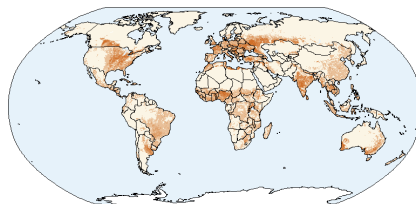
2100: SSP3



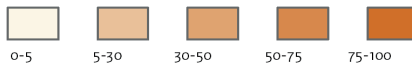
2100: SSP4



2100: SSP5



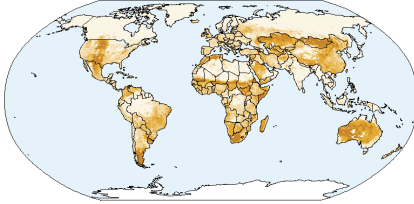
rainfed cropland for food/feed (% per gridcell)



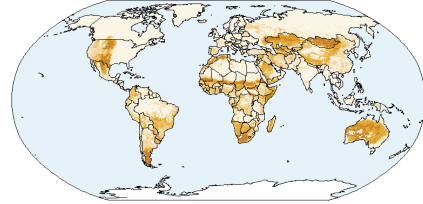
SI Figure 2-6: Rainfed cropland for food and feed production in 2010 and in 2100 for five baseline scenarios and two 1.5°C mitigation scenarios (1.9 W/m²)

Grazing land

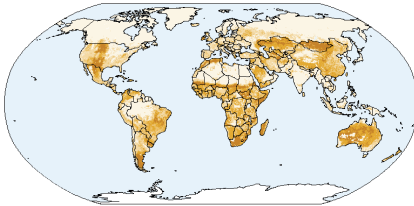
2010



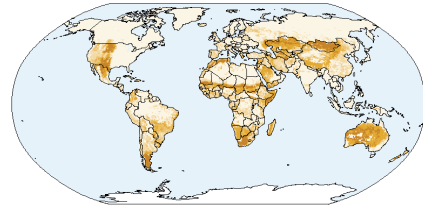
2100: SSP1



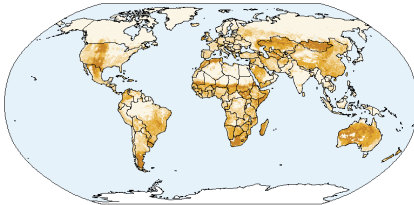
2100: SSP2



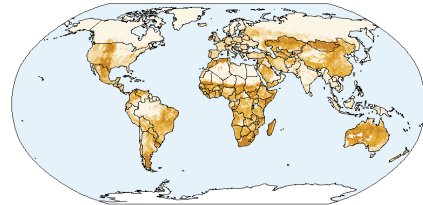
2100: SSP1-1.9



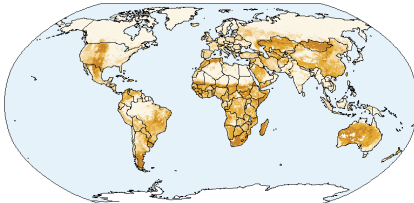
2100: SSP2-1.9



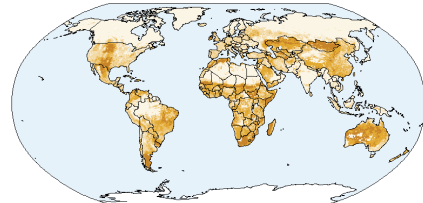
2100: SSP3



2100: SSP4



2100: SSP5



grazing land (% per gridcell)

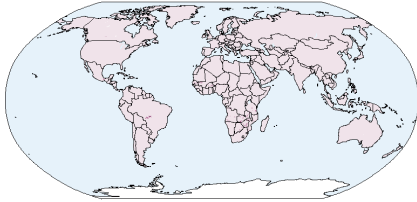


SI Figure 2-7: Grazing land in 2010 and in 2100 for five baseline scenarios and two 1.5°C mitigation scenarios (1.9 W/m²)

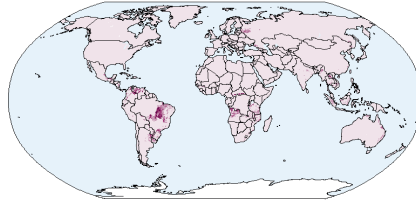
A

Bioenergy plantations

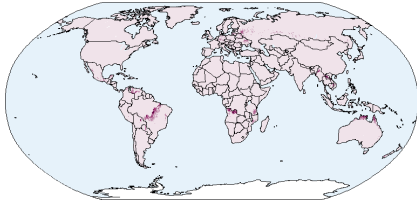
2010



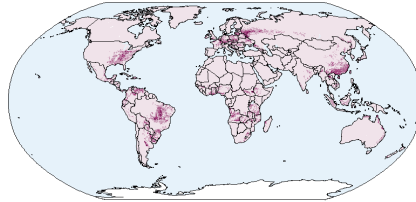
2100: SSP1



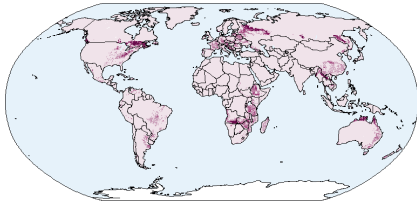
2100: SSP2



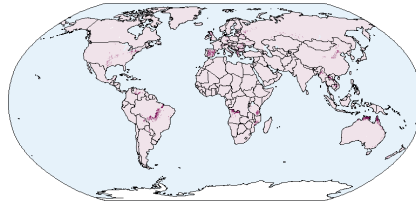
2100: SSP1-1.9



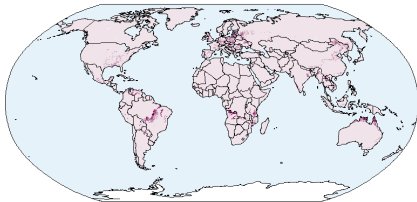
2100: SSP2-1.9



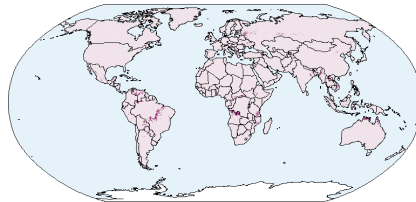
2100: SSP3



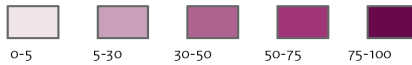
2100: SSP4



2100: SSP5



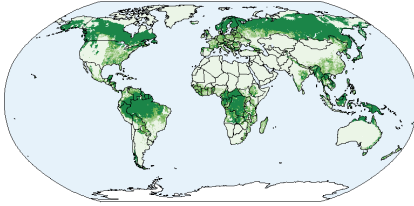
bioenergy plantations (% per gridcell)



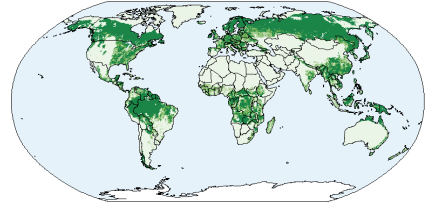
SI Figure 2-8: Bioenergy plantations in 2010 and in 2100 for five baseline scenarios and two 1.5°C mitigation scenarios (1.9 W/m²)

Forest

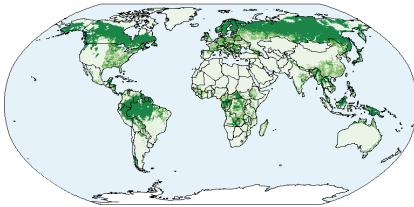
2010



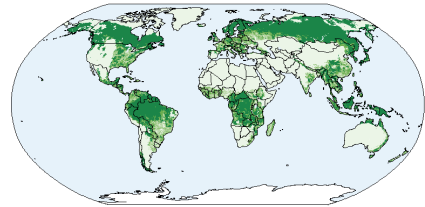
2100: SSP1



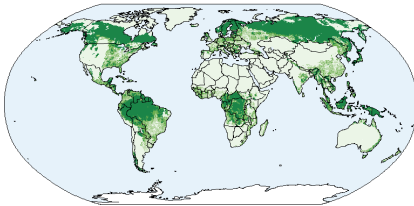
2100: SSP2



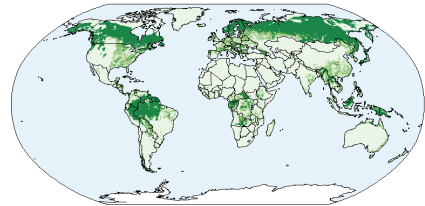
2100: SSP1-1.9



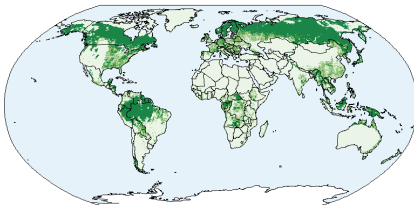
2100: SSP2-1.9



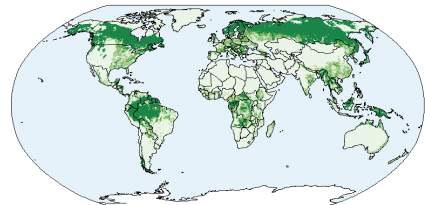
2100: SSP3



2100: SSP4



2100: SSP5



Forest (% per gridcell)

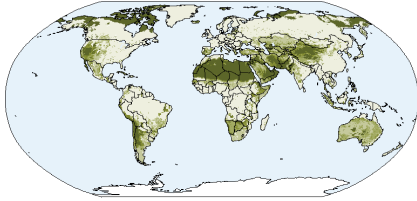


SI Figure 2-9: Forest cover in 2010 and in 2100 for five baseline scenarios and two 1.5°C mitigation scenarios (1.9 W/m²)

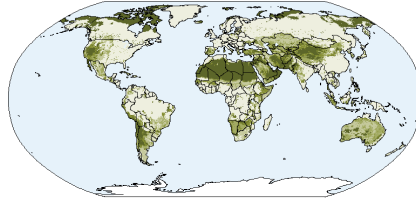
A

Other natural land

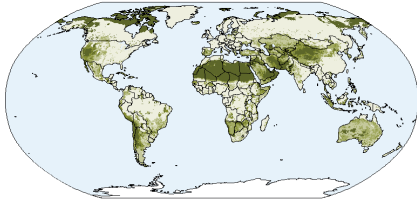
2010



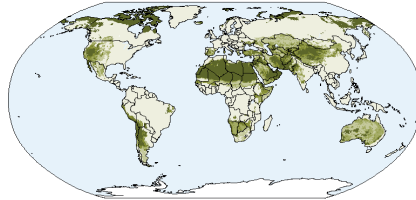
2100: SSP1



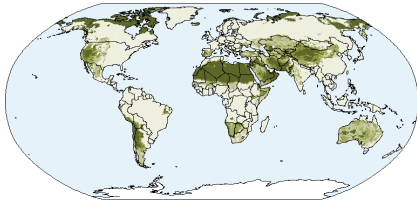
2100: SSP2



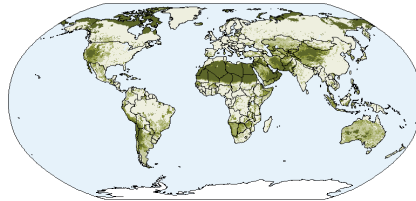
2100: SSP1-1.9



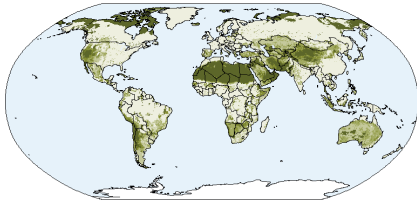
2100: SSP2-1.9



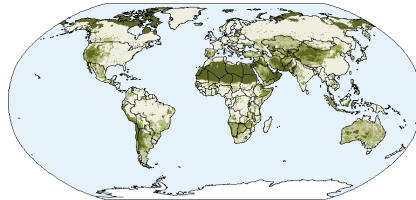
2100: SSP3



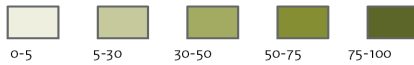
2100: SSP4



2100: SSP5



other natural land (% per gridcell)



SI Figure 2-10: Distribution of other natural land in 2010 and in 2100 for five baseline scenarios and two 1.5°C mitigation scenarios (1.9 W/m²)

S3. The role of peatland degradation, protection and restoration for climate change mitigation in the SSP scenarios

SI Table 3-1: Scenario-specific characteristics of key drivers of land-use dynamics

	SSP1 Sustainability (optimistic)	SSP2 Middle of the Road (business-as-usual)	SSP3 Fragmentation (pessimistic)
Population (billion) (2050/2100)	8.7 / 7.1	9.3 / 9.2	10.0 / 12.8
GDP (thousand 2010 US\$ per capita) (2050/2100)	22 / 61	18 / 50	12 / 13
Globalization of trade	Highly globalized	Moderately globalized	Less globalized
Animal product consumption	Reduced preference for animal products	Current preference for animal products	High preference for animal products
Land-use change regulation	Strict regulation	Moderate regulation	Little regulation
Crop yield improvement	High yield improvement	Moderate yield improvement	Low yield improvement
Livestock system efficiency	High efficiency improvement	Moderate efficiency improvement	Low efficiency improvements
Effectiveness land-based mitigation	Very effective	Moderately effective	Not effective

SI Table 3-2: Annual CO₂ emission factor for degraded and rewetted peatland (t C/ha/yr)

land cover type	degraded*			rewetted**		
	boreal	temperate	tropical	boreal	temperate	tropical
grass	5.7	5.0	9.6	-0.45	0.14	0.00
wheat	7.9	7.9	14.0	-0.45	0.14	0.00
rice	7.9	7.9	9.4	-0.45	0.14	0.00
maize	7.9	7.9	14.0	-0.45	0.14	0.00
tropical cereals	7.9	7.9	14.0	-0.45	0.14	0.00
other temperate cereals	7.9	7.9	14.0	-0.45	0.14	0.00
pulses	7.9	7.9	14.0	-0.45	0.14	0.00
soybeans	7.9	7.9	14.0	-0.45	0.14	0.00
temperate oil crops	7.9	7.9	14.0	-0.45	0.14	0.00
tropical oil crops	7.9	7.9	15.0	-0.45	0.14	0.00
temperate roots & tubers	7.9	7.9	14.0	-0.45	0.14	0.00

SI Table 3-2: Annual CO₂ emission factor for degraded and rewetted peatland (t C/ha/yr) (continued)

land cover type	degraded*			rewetted**		
	boreal	temperate	tropical	boreal	temperate	tropical
tropical roots & tubers	7.9	7.9	14.0	-0.45	0.14	0.00
sugar cane	7.9	7.9	14.0	-0.45	0.14	0.00
oil, palm fruit	7.9	7.9	11.0	-0.45	0.14	0.00
fruit and vegetables	7.9	7.9	14.0	-0.45	0.14	0.00
other non-food, luxury, spices	7.9	7.9	14.0	-0.45	0.14	0.00
plant based fibers	7.9	7.9	14.0	-0.45	0.14	0.00
grains (biofuel)	7.9	7.9	14.0	-0.45	0.14	0.00
oil crops (biofuel)	7.9	7.9	14.0	-0.45	0.14	0.00
sugarcrops (biofuel)	7.9	7.9	14.0	-0.45	0.14	0.00
woody biofuel	7.9	7.9	14.0	-0.45	0.14	0.00
non-woody biofuel	7.9	7.9	14.0	-0.45	0.14	0.00

*table 2.1 from IPCC 2013 wetland supplement; reclassified to IMAGE agricultural land-use categories

**table 2 from Wilson et al 2016, where applicable the average of nutrient poor and nutrient rich is used; reclassified to IMAGE agricultural land-use categories

SI Table 3-3: Annual CH₄ emission factor for degraded and rewetted peatland (kg CH₄/ha/yr)

land cover type	degraded*			rewetted**		
	boreal	temperate	tropical	boreal	temperate	tropical
grass	1.4	18.9	7.0	89.0	154.0	41.0
wheat	0.0	0.0	7.0	89.0	154.0	41.0
rice	0.0	0.0	143.5	89.0	154.0	41.0
maize	0.0	0.0	7.0	89.0	154.0	41.0
tropical cereals	0.0	0.0	7.0	89.0	154.0	41.0
other temperate cereals	0.0	0.0	7.0	89.0	154.0	41.0
pulses	0.0	0.0	7.0	89.0	154.0	41.0
soybeans	0.0	0.0	7.0	89.0	154.0	41.0
temperate oil crops	0.0	0.0	7.0	89.0	154.0	41.0
tropical oil crops	0.0	0.0	26.2	89.0	154.0	41.0
temperate roots & tubers	0.0	0.0	7.0	89.0	154.0	41.0
tropical roots & tubers	0.0	0.0	7.0	89.0	154.0	41.0
sugar cane	0.0	0.0	7.0	89.0	154.0	41.0
oil, palm fruit	0.0	0.0	0.0	89.0	154.0	41.0

A

SI Table 3-3: Annual CH₄ emission factor for degraded and rewetted peatland (kg CH₄/ha/yr) (continued)

land cover type	degraded*			rewetted**		
	boreal	temperate	tropical	boreal	temperate	tropical
fruit and vegetables	0.0	0.0	7.0	89.0	154.0	41.0
other non-food, luxury, spices	0.0	0.0	7.0	89.0	154.0	41.0
plant based fibers	0.0	0.0	7.0	89.0	154.0	41.0
grains (biofuel)	0.0	0.0	7.0	89.0	154.0	41.0
oil crops (biofuel)	0.0	0.0	7.0	89.0	154.0	41.0
sugarcrops (biofuel)	0.0	0.0	7.0	89.0	154.0	41.0
woody biofuel	0.0	0.0	7.0	89.0	154.0	41.0
non-woody biofuel	0.0	0.0	7.0	89.0	154.0	41.0

*table 2.3 from IPCC 2013 wetland supplement; reclassified to IMAGE agricultural land-use categories

**table 2 from Wilson et al 2016, where applicable the average of nutrient poor and nutrient rich is used; reclassified to IMAGE agricultural land-use categories

SI Table 3-4: Annual N₂O emission factor for degraded and rewetted peatland (kg N/ha/yr)

land cover type	degraded*			rewetted**		
	boreal	temperate	tropical	boreal	temperate	tropical
grass	9.50	4.70	5.00	0.06	0.07	0.94
wheat	13.00	13.00	5.00	0.06	0.07	0.94
rice	13.00	13.00	0.40	0.06	0.07	0.94
maize	13.00	13.00	5.00	0.06	0.07	0.94
tropical cereals	13.00	13.00	5.00	0.06	0.07	0.94
other temperate cereals	13.00	13.00	5.00	0.06	0.07	0.94
pulses	13.00	13.00	5.00	0.06	0.07	0.94
soybeans	13.00	13.00	5.00	0.06	0.07	0.94
temperate oil crops	13.00	13.00	5.00	0.06	0.07	0.94
tropical oil crops	13.00	13.00	3.30	0.06	0.07	0.94
temperate roots & tubers	13.00	13.00	5.00	0.06	0.07	0.94
tropical roots & tubers	13.00	13.00	5.00	0.06	0.07	0.94
sugar cane	13.00	13.00	5.00	0.06	0.07	0.94
oil, palm fruit	13.00	13.00	1.20	0.06	0.07	0.94
fruit and vegetables	13.00	13.00	5.00	0.06	0.07	0.94
other non-food, luxury, spices	13.00	13.00	5.00	0.06	0.07	0.94

SI Table 3-4: Annual N₂O emission factor for degraded and rewetted peatland (kg N/ha/yr) (continued)

land cover type	degraded*			rewetted**		
	boreal	temperate	tropical	boreal	temperate	tropical
plant based fibers	13.00	13.00	5.00	0.06	0.07	0.94
grains (biofuel)	13.00	13.00	5.00	0.06	0.07	0.94
oil crops (biofuel)	13.00	13.00	5.00	0.06	0.07	0.94
sugarcrops (biofuel)	13.00	13.00	5.00	0.06	0.07	0.94
woody biofuel	13.00	13.00	0.00	0.06	0.07	0.94
non-woody biofuel	13.00	13.00	5.00	0.06	0.07	0.94

*table 2.5 from IPCC 2013 wetland supplement; reclassified to IMAGE agricultural land-use categories

**table 4 from Wilson et al 2016, where applicable the average of nutrient poor and nutrient rich is used; reclassified to IMAGE agricultural land-use categories

SI Table 3-5: Annual DOC emission factor for degraded and rewetted peatland (t C/ha/yr)

land cover type	degraded*			rewetted**		
	boreal	temperate	tropical	boreal	temperate	tropical
grass	0.08	0.21	0.57	0.08	0.24	0.51
wheat	0.08	0.21	0.57	0.08	0.24	0.51
rice	0.08	0.21	0.57	0.08	0.24	0.51
maize	0.08	0.21	0.57	0.08	0.24	0.51
tropical cereals	0.08	0.21	0.57	0.08	0.24	0.51
other temperate cereals	0.08	0.21	0.57	0.08	0.24	0.51
pulses	0.08	0.21	0.57	0.08	0.24	0.51
soybeans	0.08	0.21	0.57	0.08	0.24	0.51
temperate oil crops	0.08	0.21	0.57	0.08	0.24	0.51
tropical oil crops	0.08	0.21	0.57	0.08	0.24	0.51
temperate roots & tubers	0.08	0.21	0.57	0.08	0.24	0.51
tropical roots & tubers	0.08	0.21	0.57	0.08	0.24	0.51
sugar cane	0.08	0.21	0.57	0.08	0.24	0.51
oil, palm fruit	0.08	0.21	0.57	0.08	0.24	0.51
fruit and vegetables	0.08	0.21	0.57	0.08	0.24	0.51
other non-food, luxury, spices	0.08	0.21	0.57	0.08	0.24	0.51
plant based fibers	0.08	0.21	0.57	0.08	0.24	0.51
grains (biofuel)	0.08	0.21	0.57	0.08	0.24	0.51
oil crops (biofuel)	0.08	0.21	0.57	0.08	0.24	0.51

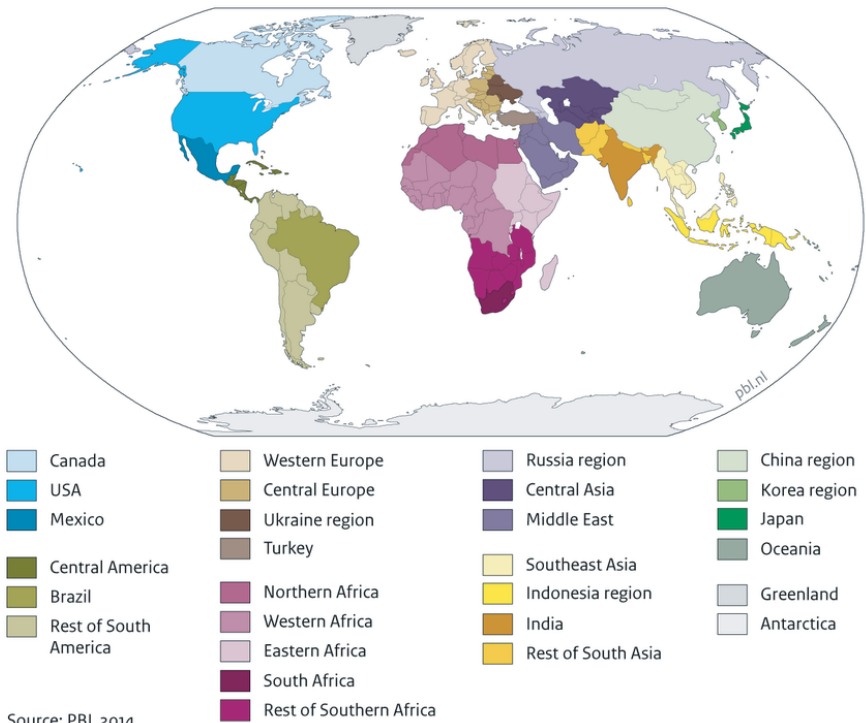
SI Table 3-5: Annual DOC emission factor for degraded and rewetted peatland (t C/ha/yr) (continued)

land cover type	degraded*			rewetted**		
	boreal	temperate	tropical	boreal	temperate	tropical
sugarcrops (biofuel)	0.08	0.21	0.57	0.08	0.24	0.51
woody biofuel	0.08	0.21	0.57	0.08	0.24	0.51
non-woody biofuel	0.08	0.21	0.57	0.08	0.24	0.51

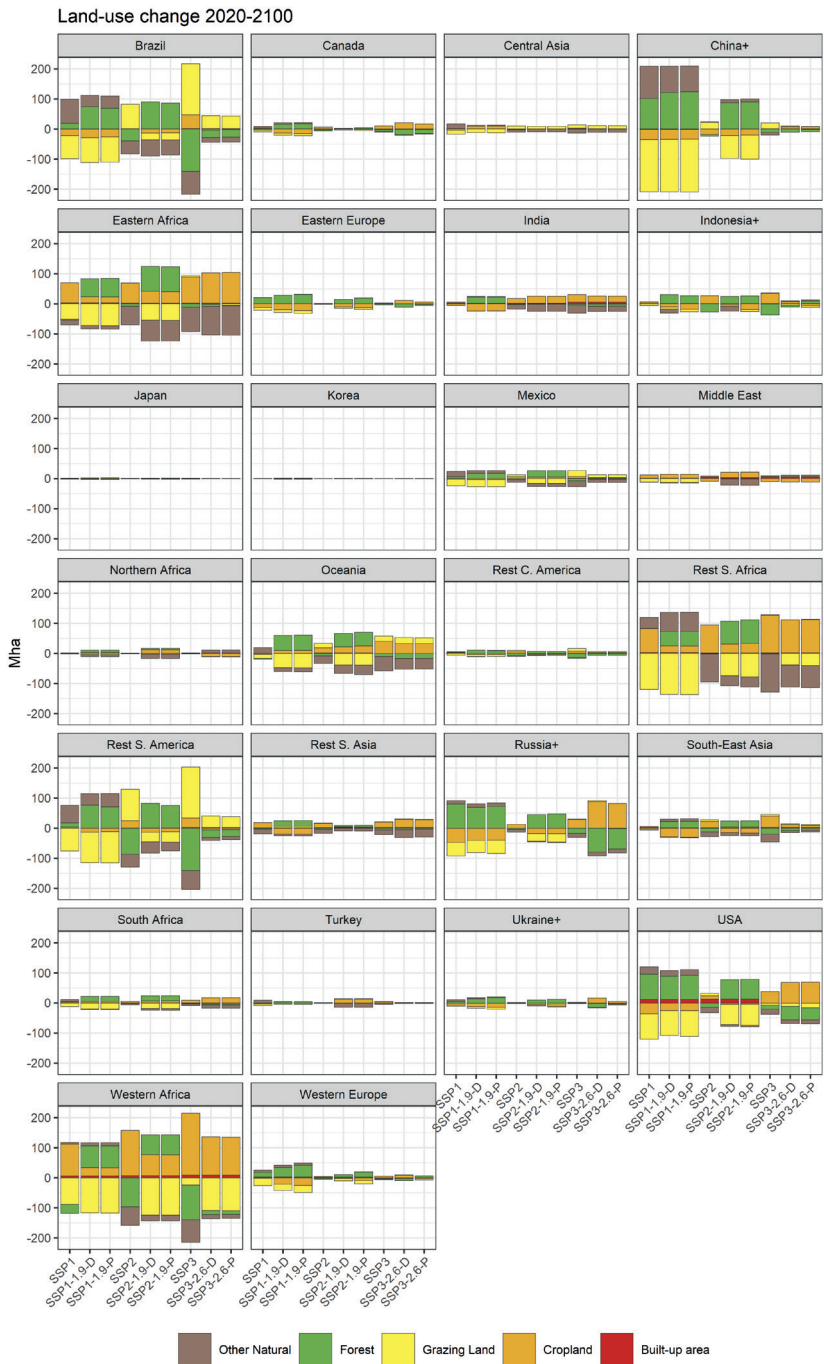
*table 2.2 from IPCC 2013 wetland supplement; reclassified to IMAGE agricultural land-use categories

**table 3 from Wilson et al 2016; reclassified to IMAGE agricultural land-use categories

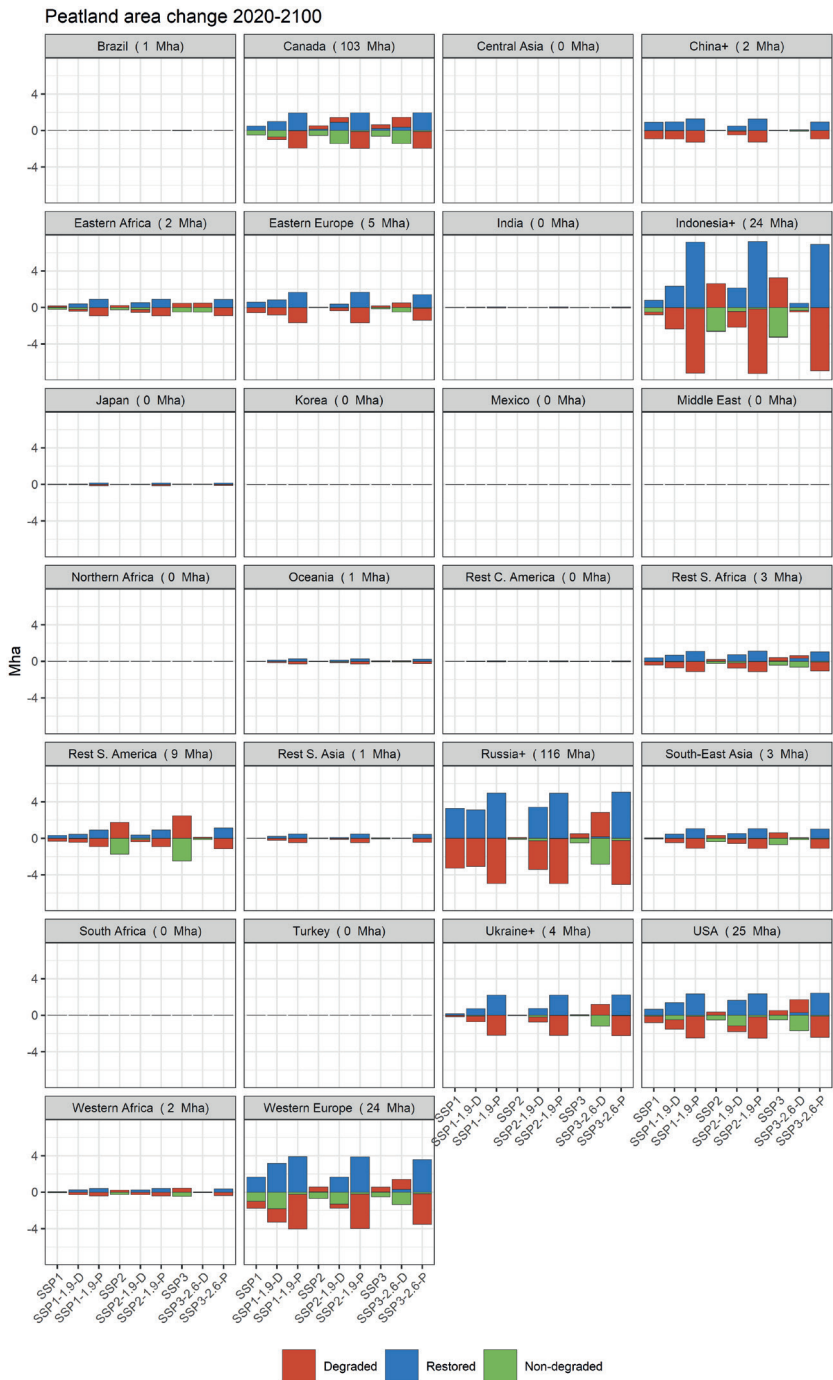
The 26 world regions in IMAGE 3.0



SI Figure 3-1: IMAGE 3.2 model world regions



SI Figure 3-2: Regional land-use change for five main land-use categories in the 2020-2100 period.



SI Figure 3-3: Changes in regional peatland area in all scenarios in the 2020-2100 period. Between brackets the total peatland area in each region is shown.

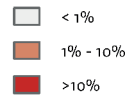
Peatland degradation and restoration - 2020-2100

SSP2

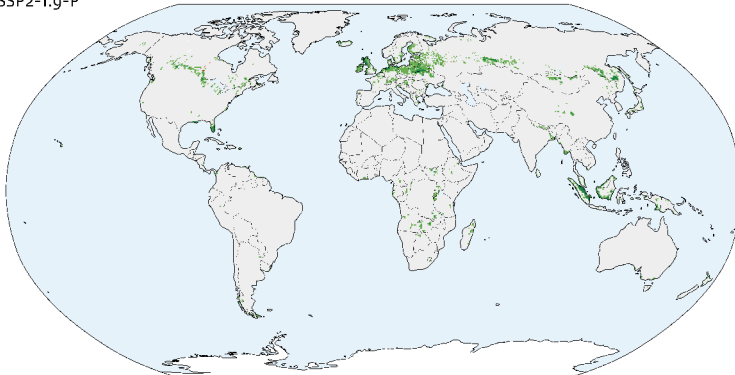


Peatland degradation

% change

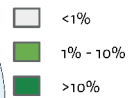


SSP2-1.9-P



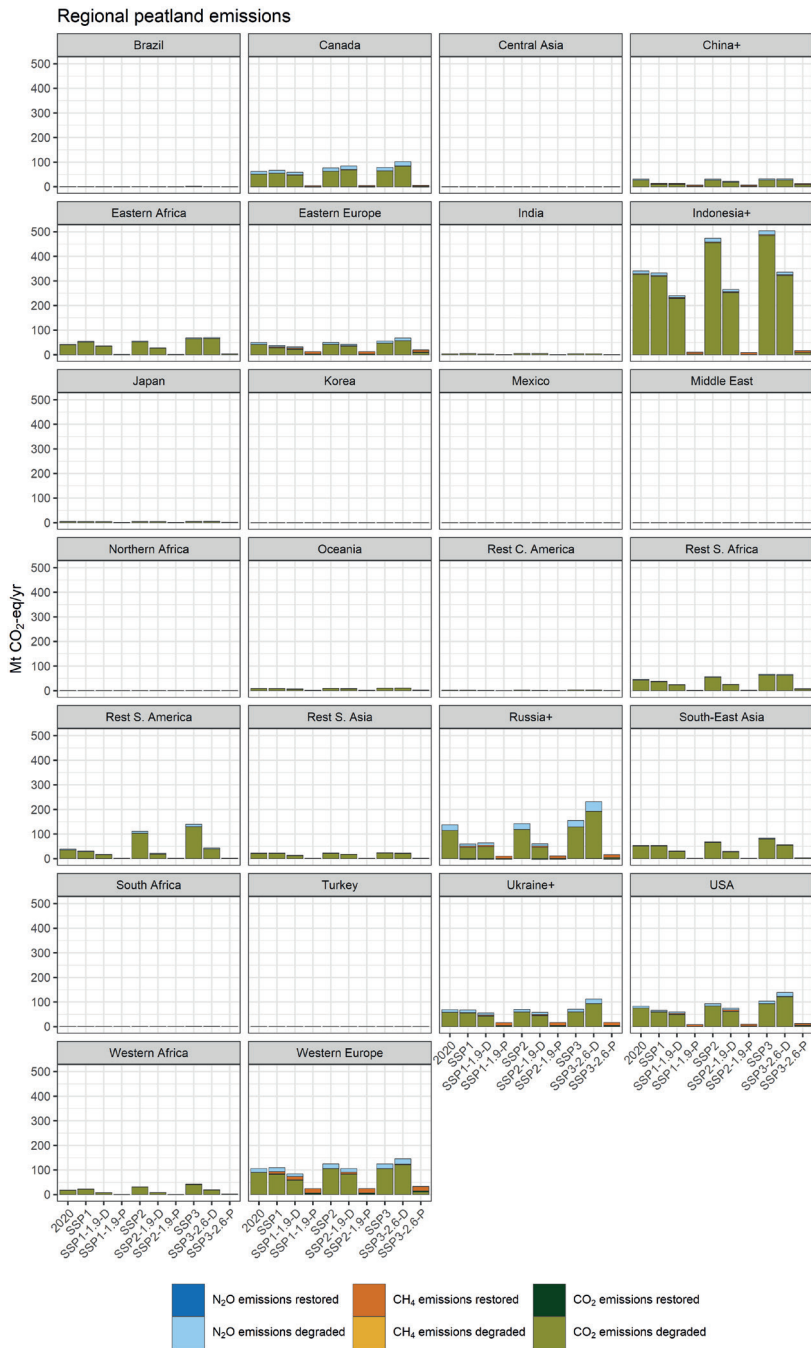
Peatland restoration

% change

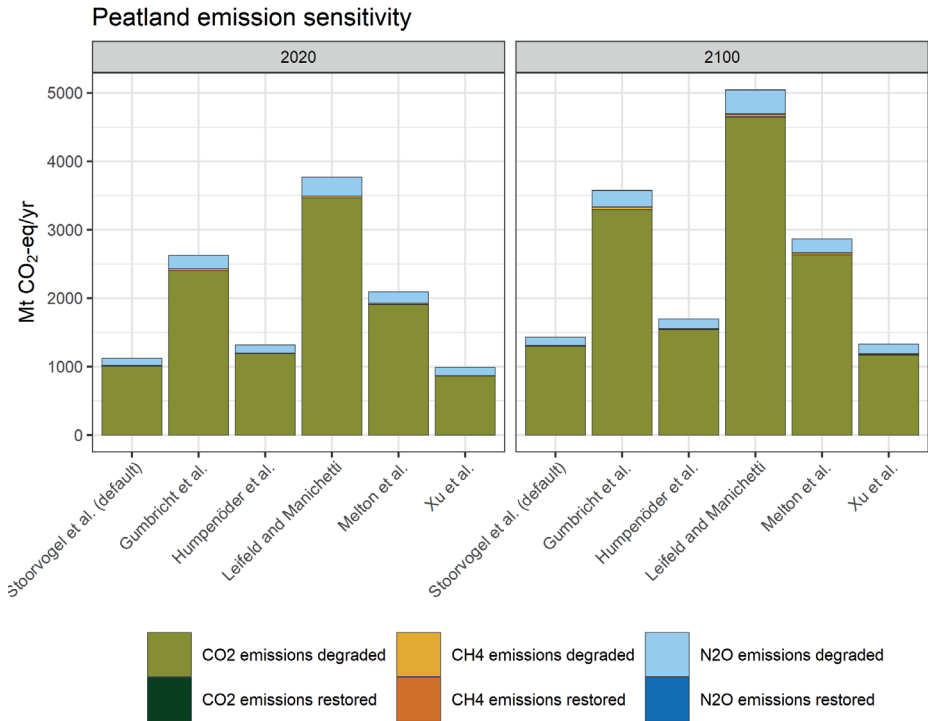


SI Figure 3-4: Maps of peatland degradation and restoration in SSP2 in SSP2-19-P in the 2020-2100 period with fractions change in degraded and restored peatlands at half degree resolution.

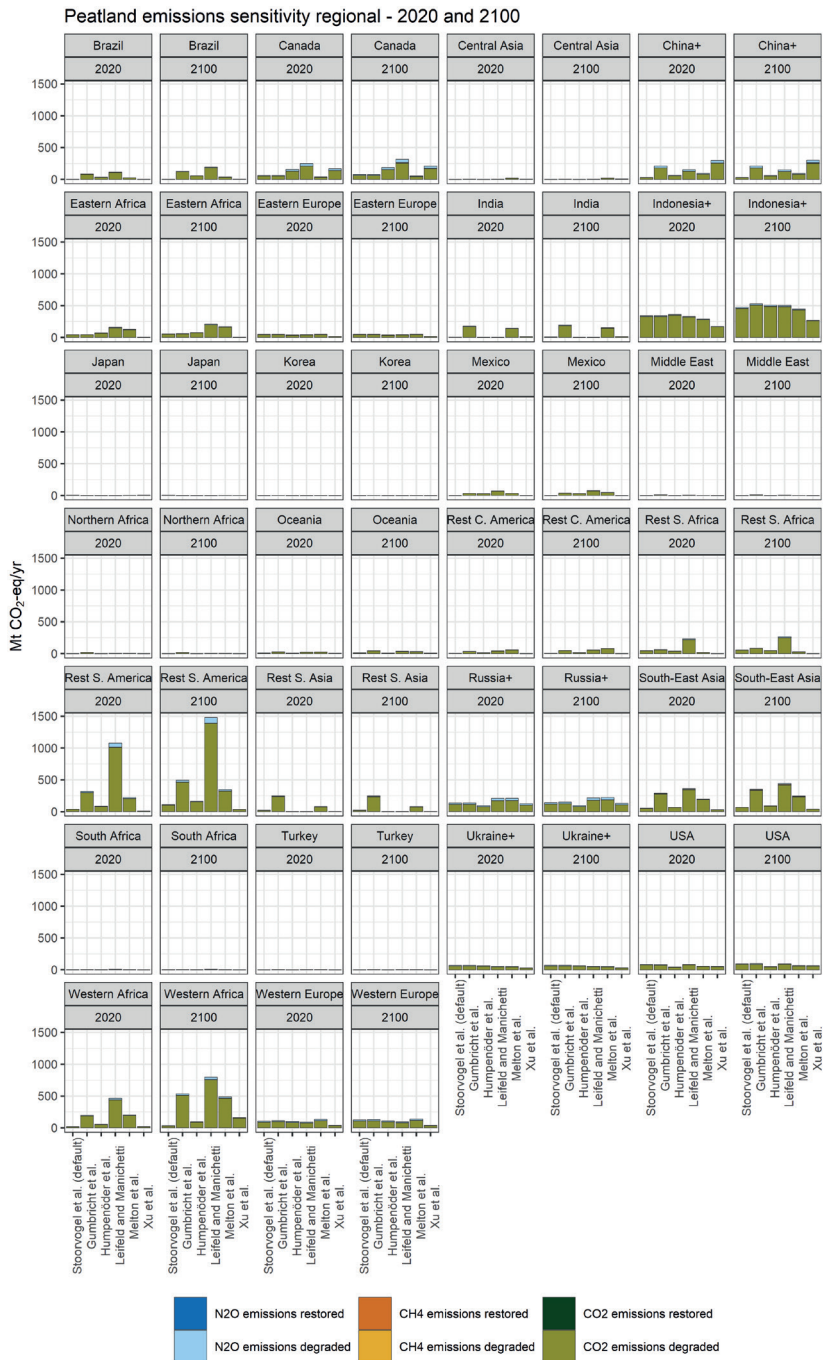
A



SI Figure 3-5: Regional peatland GHG emissions distinguished by source from degraded or rewetted peatlands and by GHG.



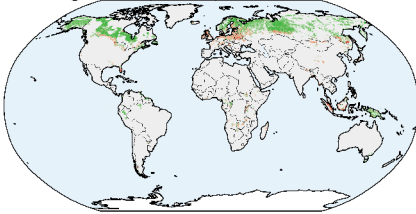
SI Figure 3-6: Global peatland emissions sensitivity in SSP2 scenario to varying peatland extent estimates.



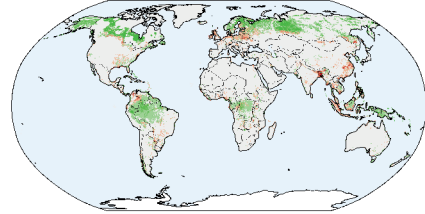
SI Figure 3-7: Regional peatland emissions sensitivity in SSP2 scenario to varying peatland extent estimates.

Peatland extent in 2020 (natural and degraded)

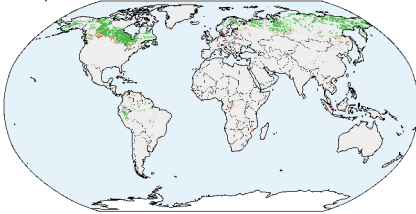
Stoorvogel et al. (default)



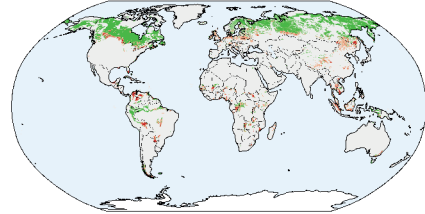
Gumbrecht et al.



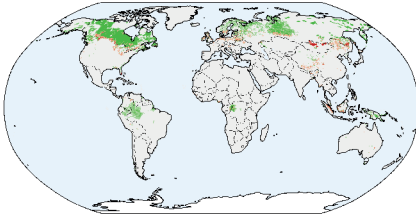
Humpenöder et al.



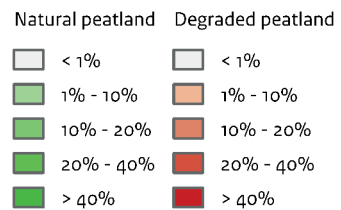
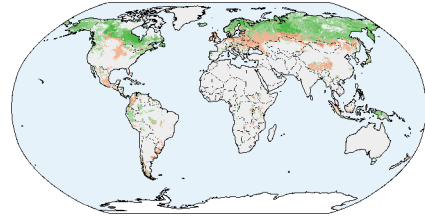
Leifeld and Manichetti



Melton et al.



Xu et al.

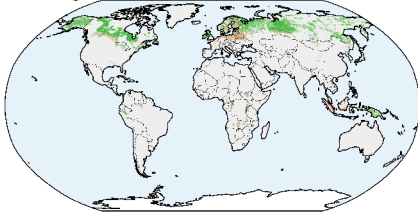


SI Figure 3-8: Spatial-explicit degraded and non-degraded peatland areas in 2020 for the default peatland map used in this study and five sensitivity peatland maps (see methods section for details). Data is aggregated to the percentage peatland area of total land area per half degree grid cell. When grid cells have both degraded and natural peatlands only the degraded percentage is shown.

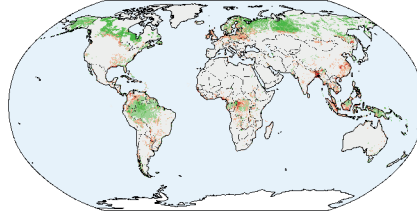
A

Peatland extent in 2100 (natural and degraded)

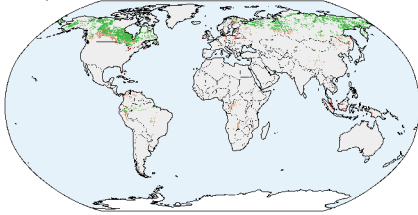
Stoorvogel et al. (default)



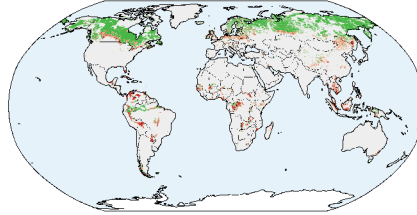
Gumbricht et al.



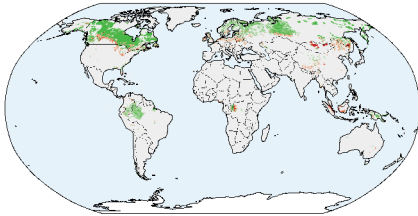
Humpenöder et al.



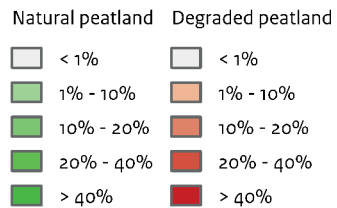
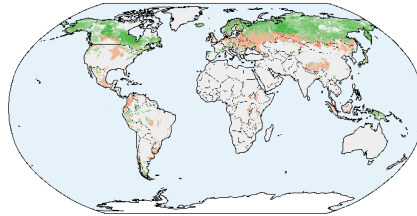
Leifeld and Manichetti



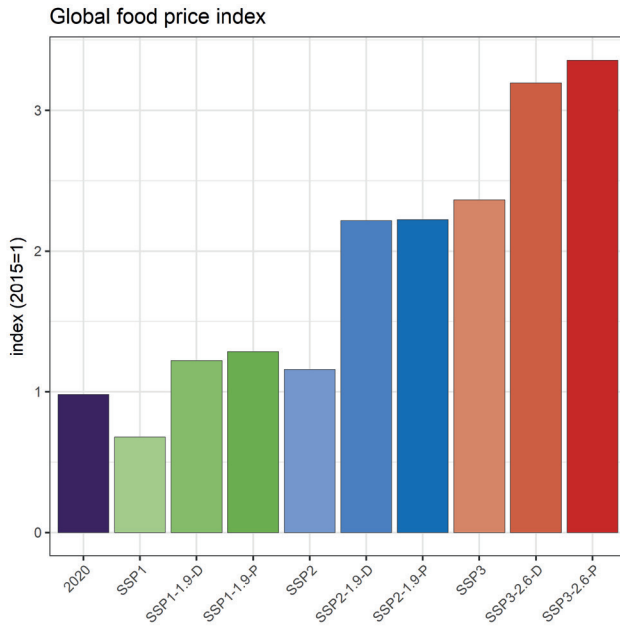
Melton et al.



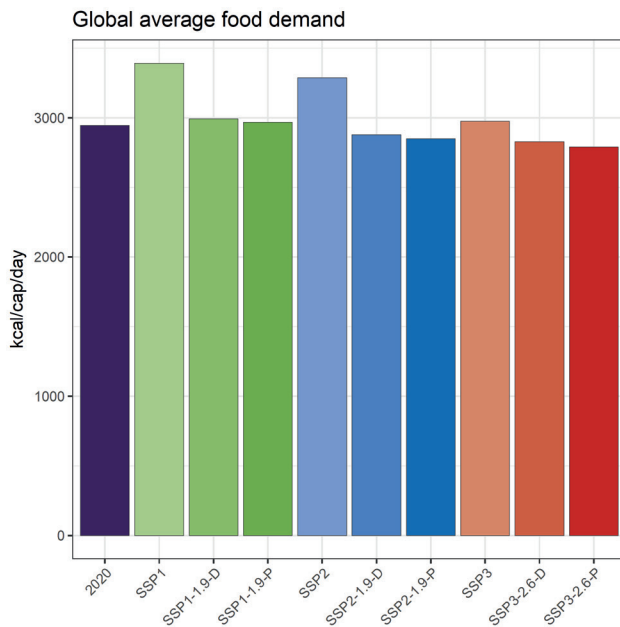
Xu et al.



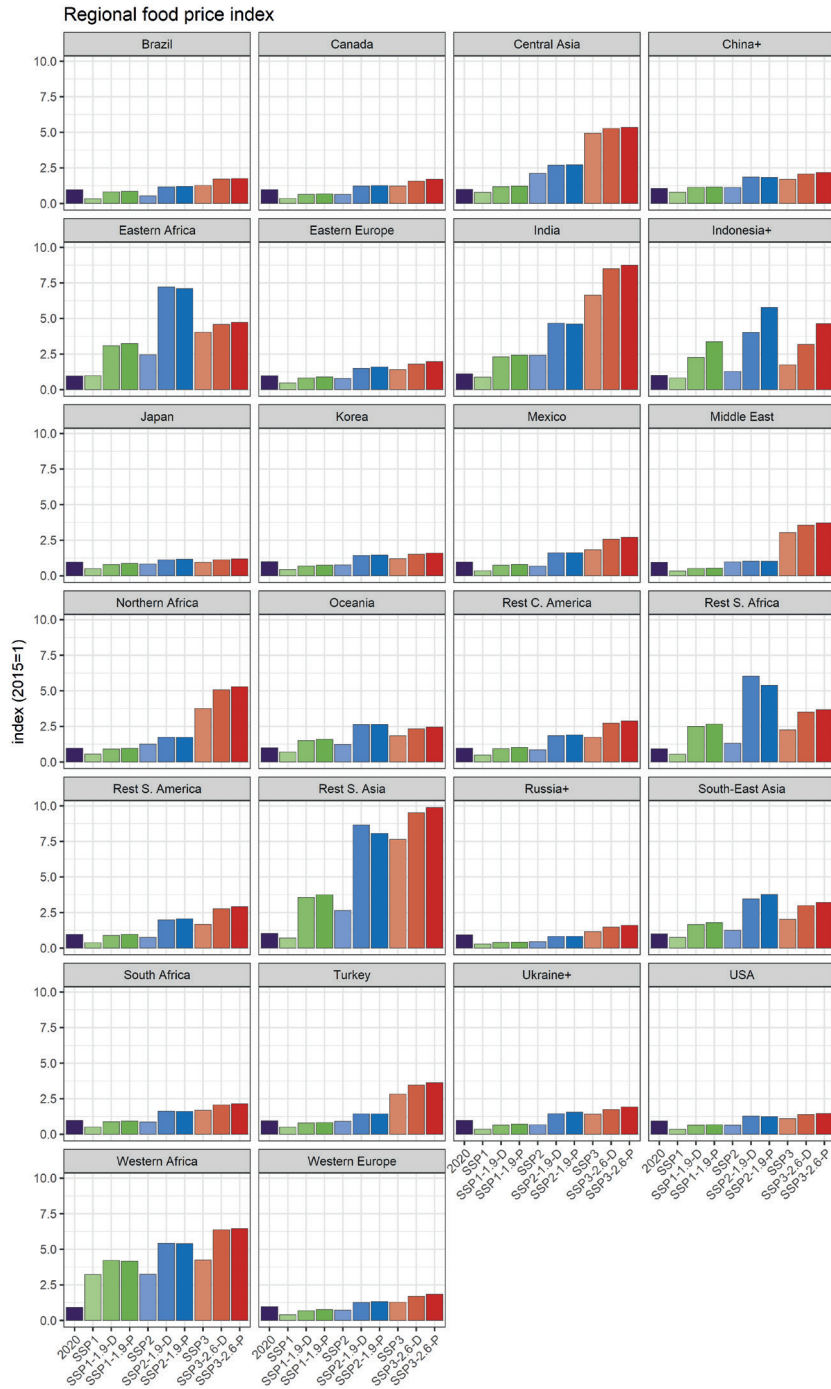
SI Figure 3-9: Spatial-explicit degraded and non-degraded peatland areas in 2100 in SSP2 for the default peatland map used in this study and five sensitivity peatland maps (see methods section for details). Data is aggregated to the percentage peatland area of total land area per half degree grid cell. When grid cells have both degraded and natural peatlands only the degraded percentage is shown.



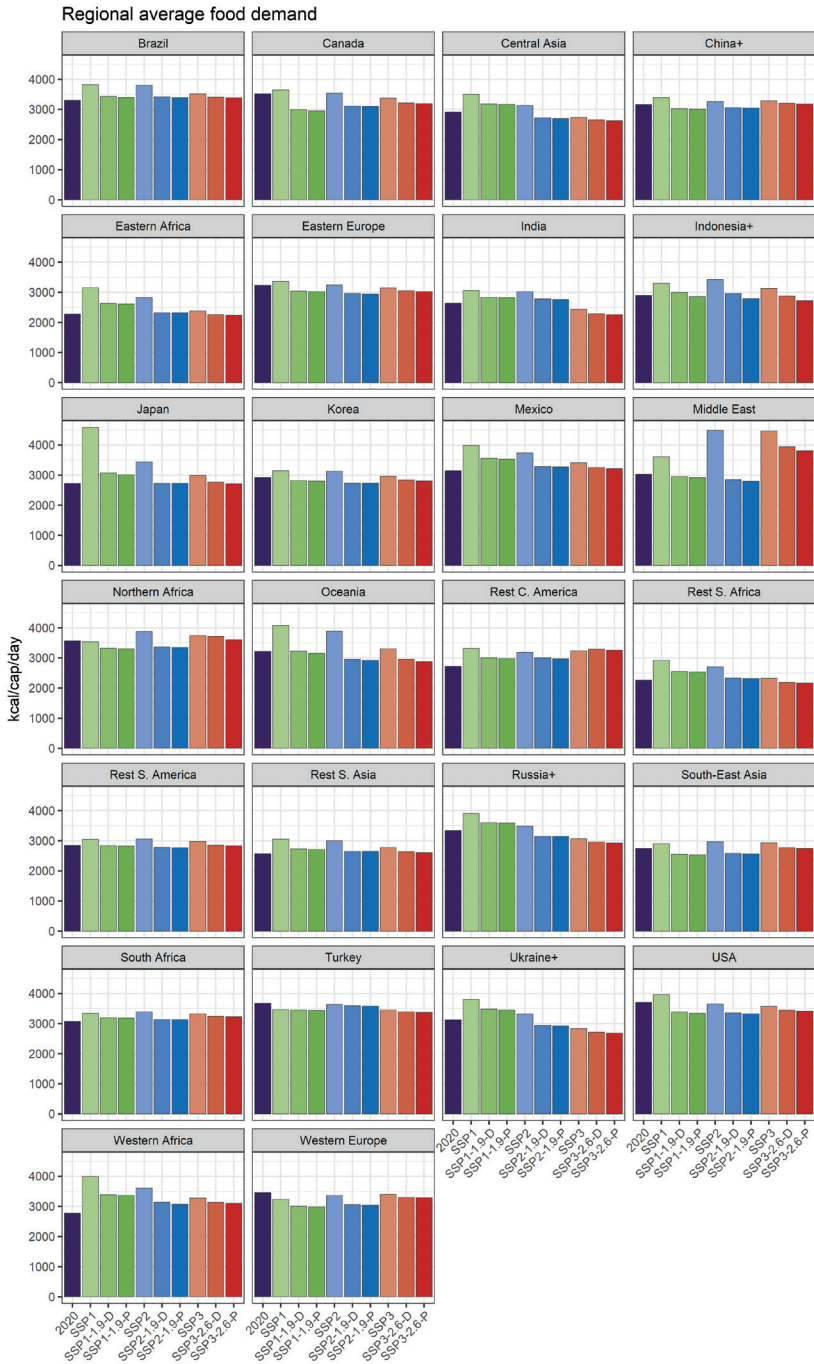
SI Figure 3-10: Global food price index (2015=1) in 2020 and 2100 for the 9 scenarios.



SI Figure 3-11: Global average food demand in kilocalories per capita per day in 2020 and 2100 for the 9 scenarios.



SI Figure 3-12: Regional food price index (2015=1) in 2020 and 2100 for the 9 scenarios.



SI Figure 3-13: Regional average food demand in kilocalories per capita per day in 2020 and 2100 for the 9 scenarios.

S4. Afforestation for climate change mitigation: potentials, risks and trade-offs

S4.1 Estimating risk-adjusted discount rates

Risk-adjusted discount rates reflect the region-specific risk of investment. Our region-specific discount rates are based on lending rates from the World Bank, as these represent the annual rate of return that is required for a land-owner to make an investment profitable. A simple exponential relation between lending rates and GDP per capita for the period 1996-2015 is fitted to derive regional discount rates. This relation is assumed to also hold in future periods. The resulting relation is $107.55 * GDP_{percapita}^{-0.268}$ with an R^2 of 0.38 (see SI Figure 4-2), which results in risk-adjusted discount rates ranging from 6.3% in the USA to 20.7% in Eastern Africa in 2010 (see SI Table 4-2).

S4.2 Estimating maximum afforestation rate

In order to define a maximum to the annual expansion of afforestation area in case of high CO_2 prices we analysed the rates of change of palm oil in Indonesia and of soy in Brazil. These examples are chosen as the countries overlap with regions in the IMAGE model, and as the expansion of these crops took place due to high demand for palm oil and soy on the world market resulting in fast expansion of crop area. While this is not the same as conversion of agricultural land to forest for climate policy, we do think it is a good example of a fast land-use transition related to market dynamics. SI Figure 4-1a and SI Figure 4-1c show areas of palm oil and soy compared to total agricultural land. SI Figure 4-1b and SI Figure 4-1d shows the shares of palm oil and soy respectively relative to total agricultural land. From 1980-2015, the period during which the area of palm oil in Indonesia increased substantially, on average the observed increase in the share of land compared to total agriculture was 0.42% per year. From 1970-2015, the period when soy area in Brazil increased substantially, on average the observed increase in the share of land compared to total agriculture was 0.37% per year.

S4.3 Construction of MAC curves and implementation in FAIR-SimCAP

The FAIR-SimCAP model uses MAC curves to determine CO_2 price pathways consistent with climate change mitigation targets. The afforestation-tool is run with 200 stylized CO_2 -price trajectories following a linear, cubic, or cubic-root shape, up to a specified CO_2 price (20-4000 US\$/tC with \$20 steps). The large number of runs with different trajectories makes sure that possible path-dependencies are taken into account. The output of these runs is used to construct region-specific MAC curves. This is then input to the FAIR-SimCAP model which determines a cost-optimal CO_2 price trajectory in line with a specific climate target by comparing MACs for afforestation, the energy system, and agriculture.

S4.4 Food security indicators

The MAGNET and GISMO models calculate the effect of the afforestation land-claims on the food system. Two important dimensions of food security are the availability and accessibility of food (FAO, 1996). In MAGNET these are represented by two indicators, respectively by *food*

availability which is defined as 'kilocalories per capita per day available for consumption', and by *food price* which is the value-weighted average price development of food including primary agricultural products and processed foods. In GISMO the availability dimension is represented by the more advanced indicator *prevalence of undernourishment* (population at risk of hunger), which is defined as the fraction of the population below the minimum level of dietary requirements. The calculation of prevalence of undernourishment is based on a method proposed by the FAO (FAO, 2008). It uses a lognormal distribution function of food availability over the population, determined by average food availability (kcal/cap/day) and a food distribution or inequality parameter (coefficient of variation). Food availability data from MAGNET is used, the coefficient of variation is a function of per capita GDP as used in Hasegawa et al. (2015b), and the minimum dietary energy requirement is derived by aggregating the region specific sex-age energy requirements weighted by the proportion of each sex and age group in the total population based on FAO data.

SI Table 4-1: IMAGE regions, aggregated regions used in the paper and income levels used in color labelling and description of results.

IMAGE region	Aggregated region	Income level
'Canada'	North America	High
'USA'	North America	High
'Mexico'	North America	High
'Central America'	Central and South America	Middle
'Brazil'	Central and South America	Middle
'Rest of South America'	Central and South America	Middle
'Northern Africa'	Middle East and Northern Africa	Middle
'Western Africa'	Sub-Saharan Africa	Low
'Eastern Africa'	Sub-Saharan Africa	Low
'South Africa'	Sub-Saharan Africa	Low
'Western Europe'	Western and Central Europe	High
'Central Europe'	Western and Central Europe	High
'Turkey'	Middle East and Northern Africa	Middle
'Ukraine region'	Russian region and Central Asia	Middle
'Kazakhstan region'	Russian region and Central Asia	Middle
'Russia'	Russian region and Central Asia	Middle
'Middle East'	Middle East and Northern Africa	Middle
'India'	South Asia	Low
'Korea region'	Japan, Korea and Oceania	High
'East Asia'	China region	Middle

SI Table 4-1: IMAGE regions, aggregated regions used in the paper and income levels used in color labelling and description of results. (continued)

IMAGE region	Aggregated region	Income level
'Southeast Asia'	Southeast Asia	Low
'Indonesia'	Southeast Asia	Low
'Japan'	Japan, Korea and Oceania	High
'Oceania'	Japan, Korea and Oceania	High
'Rest India'	South Asia	Low
'Rest Southern Africa'	Sub-Saharan Africa	Low

SI Table 4-2: region-specific discount rates for the scenario period for the years 2010, 2030, 2050 and 2100.

	2010	2030	2050	2100
Canada	6.5	6.1	5.7	4.9
USA	6.3	5.8	5.5	5.1
Mexico	9.6	8.5	7.4	5.4
Central America	11.3	9.6	8.0	5.3
Brazil	10.6	9.2	8.3	6.4
Rest of South America	11.1	9.3	8.1	6.0
Northern Africa	13.3	11.2	9.2	6.5
Western Africa	18.4	14.5	11.1	6.1
Eastern Africa	20.7	16.8	12.7	6.8
South Africa	10.6	8.9	7.7	5.9
Western Europe	6.5	6.2	5.8	4.7
Central Europe	9.5	8.1	7.2	5.7
Turkey	9.9	8.3	7.3	5.6
Ukraine region	13.5	10.9	9.1	6.7
Kazachstan region	14.2	10.3	8.7	6.9
Russia	10.4	8.6	7.6	6.3
Middle East	10.4	9.2	8.3	6.4
India	17.0	12.4	9.9	6.7
Korea region	8.3	6.9	6.2	5.1
East Asia	12.0	8.0	6.8	5.6
Southeast Asia	13.7	10.9	9.1	6.4
Indonesia	14.8	10.7	8.6	6.0

SI Table 4-2: region-specific discount rates for the scenario period for the years 2010, 2030, 2050 and 2100. (continued)

	2010	2030	2050	2100
Japan	6.5	6.1	5.7	4.7
Oceania	6.7	6.2	5.8	4.9
Rest India	19.0	15.1	12.0	7.2
Rest Southern Africa	17.4	14.3	11.6	6.3

SI Table 4-3: Average 2004-2014 commodity prices used to downscale land rent

IMAGE pasture/ crop class	Commodity price sources	Prices (2010 US\$)
Grass&Fodder	Hay farm price (2010US\$/mt) (FAPRI-MU 2017)	\$ 118.44
Temperate Cereals	Wheat, US SRW (2010US\$/mt) (World Bank)	\$ 224.31
Rice	Rice, Thai 5% (2010US\$/mt) (World Bank)	\$ 443.78
Maize	Maize (2010US\$/mt) (World Bank)	\$ 190.66
Tropical Cereals	Millet (2010US\$/mt) (World Bank)	\$ 150.88
Pulses	Dry beans Brazil (53%) & Chick peas India (25%) & Peas dry Canada (22%) (2010US\$/mt)(FAO)	\$ 625.82
Roots and Tubers	Potatoes China (57%) & Cassava Nigeria (43%) (2010US\$/mt)(FAO)	\$ 209.39
Oil crops	Oil palm fruits Indonesia (52%) & Soybeans USA (48%) (2010US\$/mt)(FAO)	\$ 229.68

SI Table 4-4: Area-weighted average land rent derived from MAGNET data, conversion costs and monitoring costs.

IMAGE region	2010 average land rent (2010 US\$/ha/yr)	Conversion costs (2010 US\$/ha)	Monitoring costs (2010 US\$/ha/yr)
Canada	\$ 48	\$ 1,531	\$ 4.92
USA	\$ 96	\$ 1,634	\$ 5.25
Mexico	\$ 81	\$ 983	\$ 3.16
Central America	\$ 197	\$ 908	\$ 2.92
Brazil	\$ 37	\$ 930	\$ 2.99
Rest of South America	\$ 58	\$ 915	\$ 2.94
Northern Africa	\$ 45	\$ 866	\$ 2.78
Western Africa	\$ 27	\$ 832	\$ 2.67
Eastern Africa	\$ 11	\$ 826	\$ 2.66

SI Table 4-4: Area-weighted average land rent derived from MAGNET data, conversion costs and monitoring costs. (continued)

IMAGE region	2010 average land rent (2010 US\$/ha/yr)	Conversion costs (2010 US\$/ha)	Monitoring costs (2010 US\$/ha/yr)
South Africa	\$ 7	\$ 931	\$ 2.99
Western Europe	\$ 380	\$ 1,513	\$ 4.86
Central Europe	\$ 247	\$ 991	\$ 3.18
Turkey	\$ 160	\$ 967	\$ 3.11
Ukraine region	\$ 71	\$ 864	\$ 2.78
Kazakhstan region	\$ 11	\$ 856	\$ 2.75
Russia	\$ 80	\$ 938	\$ 3.01
Middle East	\$ 16	\$ 939	\$ 3.02
India	\$ 526	\$ 837	\$ 2.69
Korea region	\$ 2,569	\$ 1,105	\$ 3.55
China	\$ 260	\$ 890	\$ 2.86
Southeast Asia	\$ 319	\$ 862	\$ 2.77
Indonesia	\$ 452	\$ 850	\$ 2.73
Japan	\$ 1670	\$ 1,547	\$ 4.97
Oceania	\$ 14	\$ 1,435	\$ 4.61
Rest India	\$ 526	\$ 830	\$ 2.67
Rest Southern Africa	\$ 7	\$ 835	\$ 2.68

SI Table 4-5: MAGNET land rent in look-up table derived from three selected stylized linear agricultural reduction scenarios.

year	2010				2050				2100				
	percentage agricultural reduction.	baseline	4%	8%	12%	baseline	4%	8%	12%	baseline	10%	20%	30%
Canada	\$ 48	\$ 209	\$ 269	\$ 348	\$ 454	\$ 238	\$ 238	\$ 348	\$ 454	\$ 238	\$ 424	\$ 810	\$ 1,708
USA	\$ 96	\$ 194	\$ 244	\$ 312	\$ 403	\$ 154	\$ 154	\$ 312	\$ 403	\$ 154	\$ 291	\$ 588	\$ 1,305
Mexico	\$ 81	\$ 176	\$ 220	\$ 281	\$ 363	\$ 176	\$ 176	\$ 281	\$ 363	\$ 176	\$ 324	\$ 673	\$ 1,547
Central America	\$ 197	\$ 655	\$ 808	\$ 1,015	\$ 1,287	\$ 713	\$ 713	\$ 1,015	\$ 1,287	\$ 713	\$ 1,234	\$ 2,307	\$ 4,731
Brazil	\$ 37	\$ 90	\$ 112	\$ 144	\$ 188	\$ 120	\$ 120	\$ 144	\$ 188	\$ 120	\$ 232	\$ 477	\$ 1,036
Rest of South America	\$ 58	\$ 297	\$ 353	\$ 424	\$ 514	\$ 431	\$ 431	\$ 514	\$ 651	\$ 431	\$ 651	\$ 1,074	\$ 1,956
Northern Africa	\$ 45	\$ 189	\$ 245	\$ 323	\$ 431	\$ 416	\$ 416	\$ 431	\$ 431	\$ 416	\$ 728	\$ 1,347	\$ 2,708
Western Africa	\$ 27	\$ 803	\$ 956	\$ 1,137	\$ 1,343	\$ 3,373	\$ 3,373	\$ 1,137	\$ 1,343	\$ 3,373	\$ 4,798	\$ 6,981	\$ 10,360
Eastern Africa	\$ 11	\$ 260	\$ 307	\$ 365	\$ 437	\$ 714	\$ 714	\$ 437	\$ 437	\$ 714	\$ 1,054	\$ 1,668	\$ 2,866
South Africa	\$ 7	\$ 43	\$ 56	\$ 73	\$ 96	\$ 115	\$ 115	\$ 73	\$ 96	\$ 115	\$ 204	\$ 385	\$ 788
Western Europe	\$ 380	\$ 626	\$ 805	\$ 1,062	\$ 1,423	\$ 581	\$ 581	\$ 1,062	\$ 1,423	\$ 581	\$ 1,140	\$ 2,494	\$ 5,900
Central Europe	\$ 247	\$ 258	\$ 324	\$ 412	\$ 534	\$ 165	\$ 165	\$ 412	\$ 534	\$ 165	\$ 327	\$ 704	\$ 1,613
Turkey	\$ 160	\$ 414	\$ 544	\$ 731	\$ 997	\$ 583	\$ 583	\$ 731	\$ 997	\$ 583	\$ 1,125	\$ 2,334	\$ 5,179
Ukraine region	\$ 71	\$ 137	\$ 173	\$ 221	\$ 283	\$ 175	\$ 175	\$ 221	\$ 283	\$ 175	\$ 301	\$ 546	\$ 1,066
Kazakhstan region	\$ 11	\$ 288	\$ 335	\$ 390	\$ 451	\$ 428	\$ 428	\$ 390	\$ 451	\$ 428	\$ 613	\$ 887	\$ 1,294
Russia	\$ 80	\$ 160	\$ 196	\$ 244	\$ 304	\$ 173	\$ 173	\$ 244	\$ 304	\$ 173	\$ 280	\$ 481	\$ 890
Middle East	\$ 16	\$ 101	\$ 126	\$ 162	\$ 210	\$ 187	\$ 187	\$ 162	\$ 210	\$ 187	\$ 320	\$ 591	\$ 1,201
India	\$ 526	\$ 3,855	\$ 4,520	\$ 5,329	\$ 6,312	\$ 4,802	\$ 4,802	\$ 5,329	\$ 6,312	\$ 4,802	\$ 7,013	\$ 11,038	\$ 18,987

SI Table 4-5: MAGNET land rent in look-up table derived from three selected stylized linear agricultural reduction scenarios. (continued)

year	2010			2050			2100		
	percentage agricultural reduction.	baseline	4%	8%	12%	baseline	10%	20%	30%
Korea region	\$ 2,569	\$ 4,291	\$ 5,448	\$ 6,949	\$ 8,881	\$ 1,131	\$ 2,543	\$ 5,908	\$ 14,004
East Asia	\$ 260	\$ 1,114	\$ 1,423	\$ 1,827	\$ 2,354	\$ 189	\$ 444	\$ 1,107	\$ 2,849
Southeast Asia	\$ 319	\$ 1,157	\$ 1,367	\$ 1,627	\$ 1,952	\$ 1,192	\$ 1,943	\$ 3,299	\$ 6,054
Indonesia	\$ 452	\$ 2,125	\$ 2,518	\$ 3,005	\$ 3,612	\$ 1,845	\$ 2,878	\$ 4,813	\$ 8,904
Japan	\$ 1,670	\$ 663	\$ 1,015	\$ 1,679	\$ 2,926	\$ 50	\$ 151	\$ 1,108	\$ 6,193
Oceania	\$ 14	\$ 71	\$ 85	\$ 105	\$ 129	\$ 78	\$ 123	\$ 206	\$ 376
Rest India	\$ 526	\$ 3,855	\$ 4,520	\$ 5,329	\$ 6,312	\$ 4,802	\$ 7,013	\$ 11,038	\$ 18,987
Rest Southern Africa	\$ 7	\$ 43	\$ 56	\$ 73	\$ 96	\$ 115	\$ 204	\$ 385	\$ 788

SI Table 4-6: Conversion and monitoring costs for 2010, 2050 and 2100.

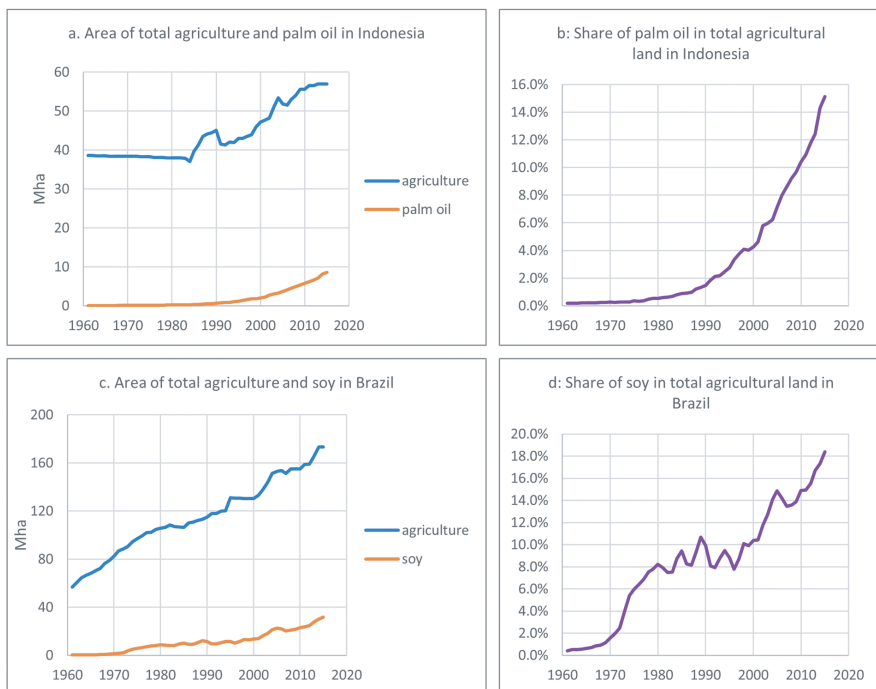
year	2010		2050		2100	
	Conversion costs (2010 US\$/ha)	Monitoring costs (2010 US\$/ha)	Conversion costs (2010 US\$/ha)	Monitoring costs (2010 US\$/ha)	Conversion costs (2010 US\$/ha)	Monitoring costs (2010 US\$/ha)
Canada	\$ 1,531	\$ 4.92	\$ 2,418	\$ 7.77	\$ 3,817	\$ 12.26
USA	\$ 1,634	\$ 5.25	\$ 2,585	\$ 8.30	\$ 3,436	\$ 11.04
Mexico	\$ 983	\$ 3.16	\$ 1,731	\$ 5.56	\$ 3,127	\$ 10.05
Central America	\$ 908	\$ 2.92	\$ 1,621	\$ 5.21	\$ 3,275	\$ 10.52
Brazil	\$ 930	\$ 2.99	\$ 1,582	\$ 5.08	\$ 2,481	\$ 7.97
Rest of South America	\$ 915	\$ 2.94	\$ 1,610	\$ 5.17	\$ 2,694	\$ 8.66
Northern Africa	\$ 866	\$ 2.78	\$ 1,485	\$ 4.77	\$ 2,430	\$ 7.81
Western Africa	\$ 832	\$ 2.67	\$ 1,389	\$ 4.46	\$ 2,606	\$ 8.37
Eastern Africa	\$ 826	\$ 2.66	\$ 1,350	\$ 4.34	\$ 2,330	\$ 7.49
South Africa	\$ 931	\$ 2.99	\$ 1,666	\$ 5.35	\$ 2,725	\$ 8.76
Western Europe	\$ 1,513	\$ 4.86	\$ 2,401	\$ 7.72	\$ 4,078	\$ 13.10
Central Europe	\$ 991	\$ 3.18	\$ 1,785	\$ 5.74	\$ 2,912	\$ 9.36
Turkey	\$ 967	\$ 3.11	\$ 1,761	\$ 5.66	\$ 2,947	\$ 9.47
Ukraine region	\$ 864	\$ 2.78	\$ 1,492	\$ 4.79	\$ 2,336	\$ 7.51
Kazakhstan region	\$ 856	\$ 2.75	\$ 1,527	\$ 4.91	\$ 2,300	\$ 7.39
Russia	\$ 938	\$ 3.01	\$ 1,684	\$ 5.41	\$ 2,537	\$ 8.15
Middle East	\$ 939	\$ 3.02	\$ 1,581	\$ 5.08	\$ 2,452	\$ 7.88
India	\$ 837	\$ 2.69	\$ 1,442	\$ 4.63	\$ 2,338	\$ 7.51
Korea region	\$ 1,105	\$ 3.55	\$ 2,163	\$ 6.95	\$ 3,522	\$ 11.32
East Asia	\$ 890	\$ 2.86	\$ 1,882	\$ 6.05	\$ 2,965	\$ 9.53

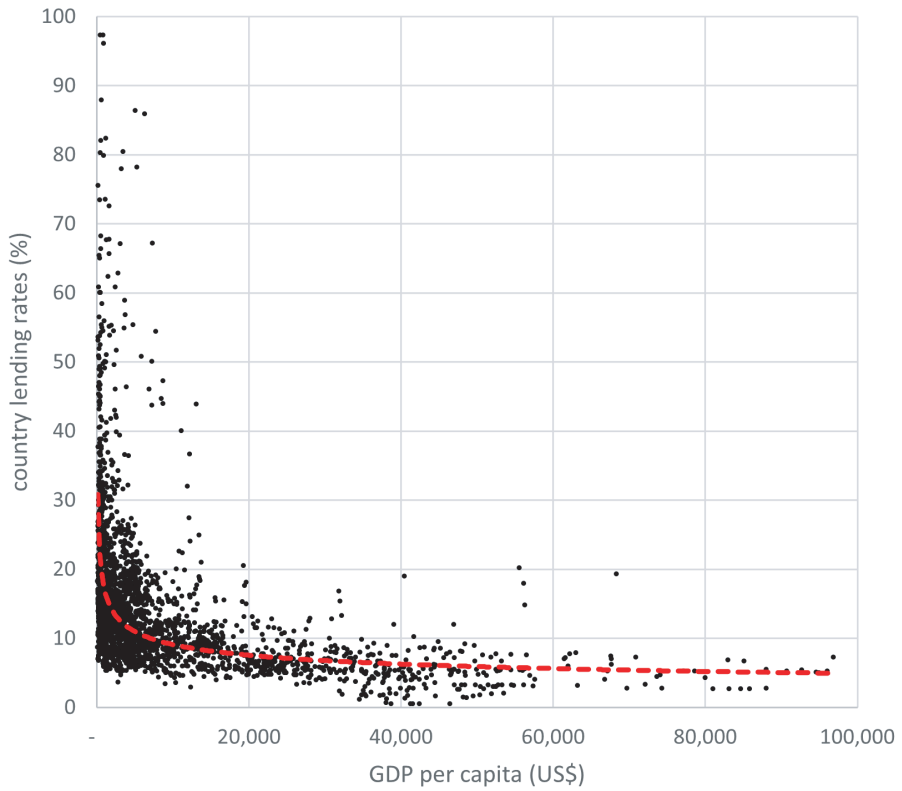
SI Table 4-6: Conversion and monitoring costs for 2010, 2050 and 2100. (continued)

year	2010		2050		2100	
	Conversion costs (2010 US\$/ha)	Monitoring costs (2010 US\$/ha)	Conversion costs (2010 US\$/ha)	Monitoring costs (2010 US\$/ha)	Conversion costs (2010 US\$/ha)	Monitoring costs (2010 US\$/ha)
Southeast Asia	\$ 862	\$ 2.77	\$ 1,495	\$ 4.80	\$ 2,464	\$ 7.92
Indonesia	\$ 850	\$ 2.73	\$ 1,547	\$ 4.97	\$ 2,690	\$ 8.64
Japan	\$ 1,547	\$ 4.97	\$ 2,436	\$ 7.83	\$ 4,045	\$ 13.00
Oceania	\$ 1,435	\$ 4.61	\$ 2,348	\$ 7.54	\$ 3,793	\$ 12.19
Rest India	\$ 830	\$ 2.67	\$ 1,365	\$ 4.39	\$ 2,207	\$ 7.09
Rest Southern Africa	\$ 835	\$ 2.68	\$ 1,375	\$ 4.42	\$ 2,500	\$ 8.03

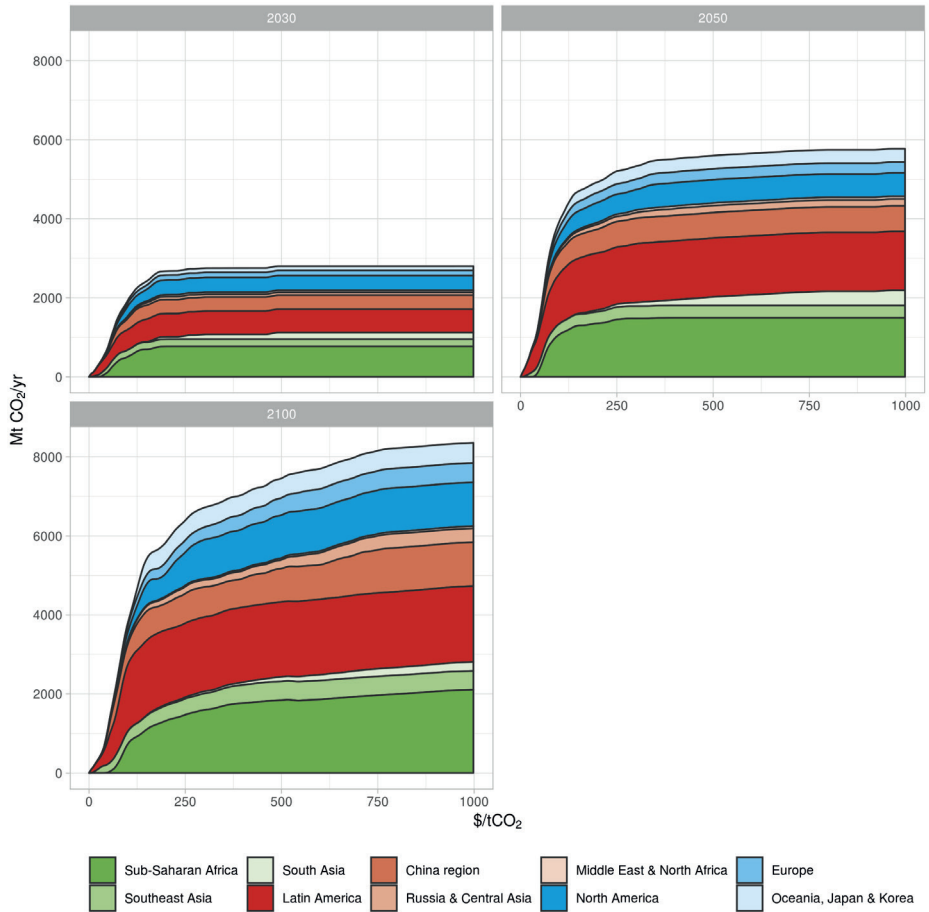
SI Table 4-7: Parameter change for sensitivity analysis.

	-	default	+
Discount rate	Lowest region-specific discount rates in all regions (USA in 2010, applied throughout scenario period)	Region-specific discount rates (SI table 1)	Highest region-specific discount rates in all regions (Eastern Africa in 2010, applied throughout scenario period)
Time horizon	10 years	30 years	50 years
Conversion and monitoring costs	Lowest region-specific conversion and monitoring costs in all regions (Eastern Africa in 2010, applied throughout scenario period)		Highest region-specific conversion and monitoring costs in all regions (USA in 2010, applied throughout scenario period)
Afforestation rate	0.2%/yr	0.4%/yr	0.6%/yr
Climate	Climate change without CO ₂ fertilization	No climate change	Climate change with CO ₂ fertilization

**SI Figure 4-1:** FAO data from 1961-2015 on a) area of palm oil and total agricultural land in Indonesia, b) the share of palm oil relative to total agricultural land in Indonesia, c) the area of soy and total agricultural land in Brazil and d) the share of soy relative to total agricultural land in Brazil (FAOSTAT, 2017).

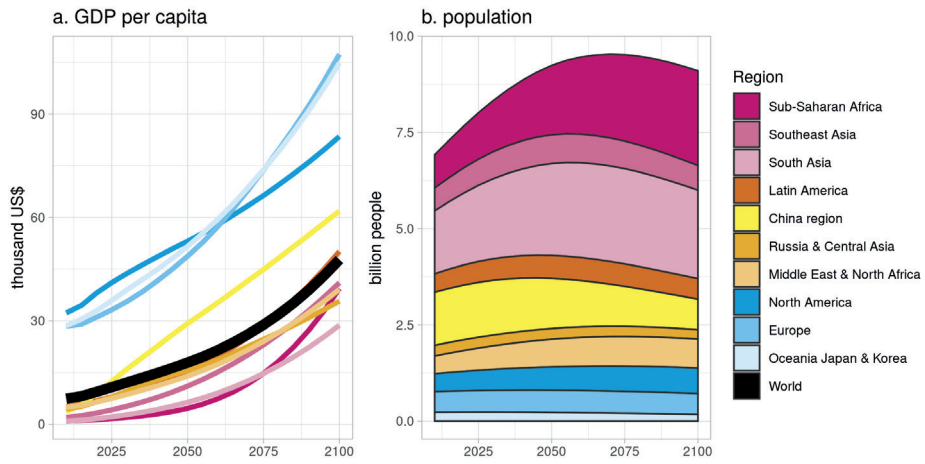


SI Figure 4-2: Scatter plot of country data for GDP per capita and lending rates with a fitted exponential relation.



SI Figure 4-3: Marginal abatement cost curves of carbon sequestration through afforestation in 10 aggregated regions (SI Table 4-1) in years 2030, 2050 and 2100. Based on stylized linear CO_2 price trajectories that increase from $\$/tCO_2$ in 2020 to CO_2 price as shown on the Y-axis.

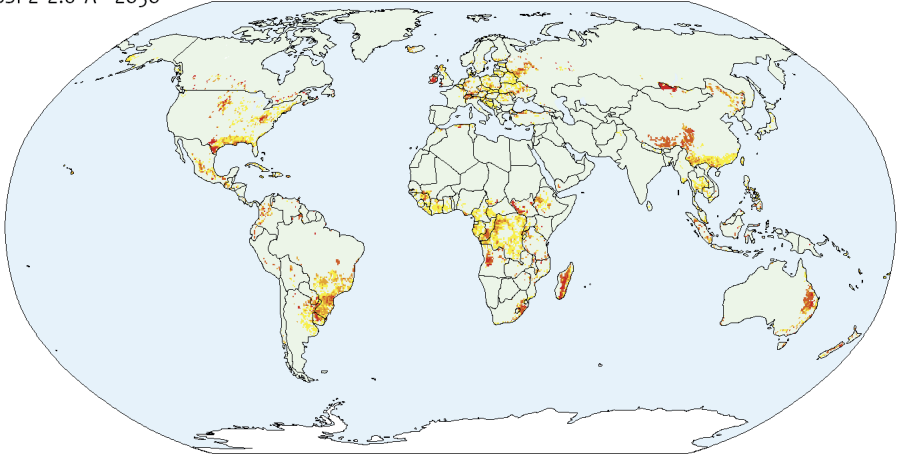
A



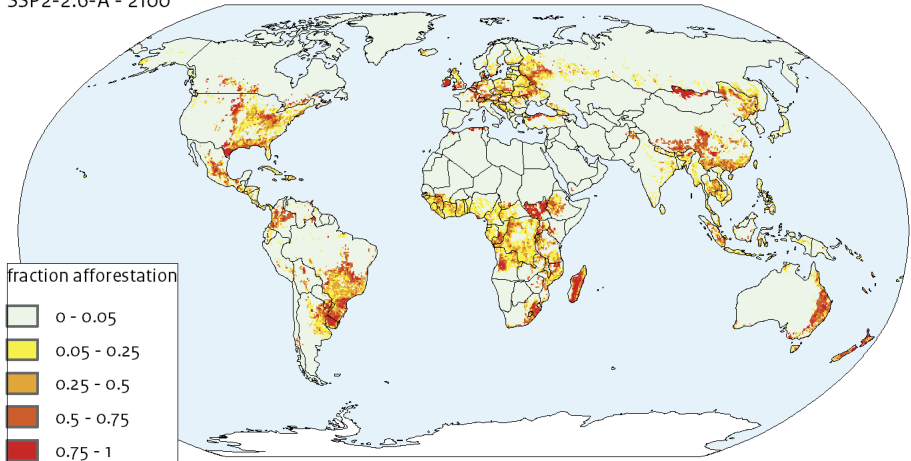
SI Figure 4-4: Regional a) GDP per capita (Dellink et al., 2017) and b) population in the SSP2 baseline scenario (KC and Lutz, 2017).

Fraction per gridcell afforested

SSP2-2.6-A - 2050

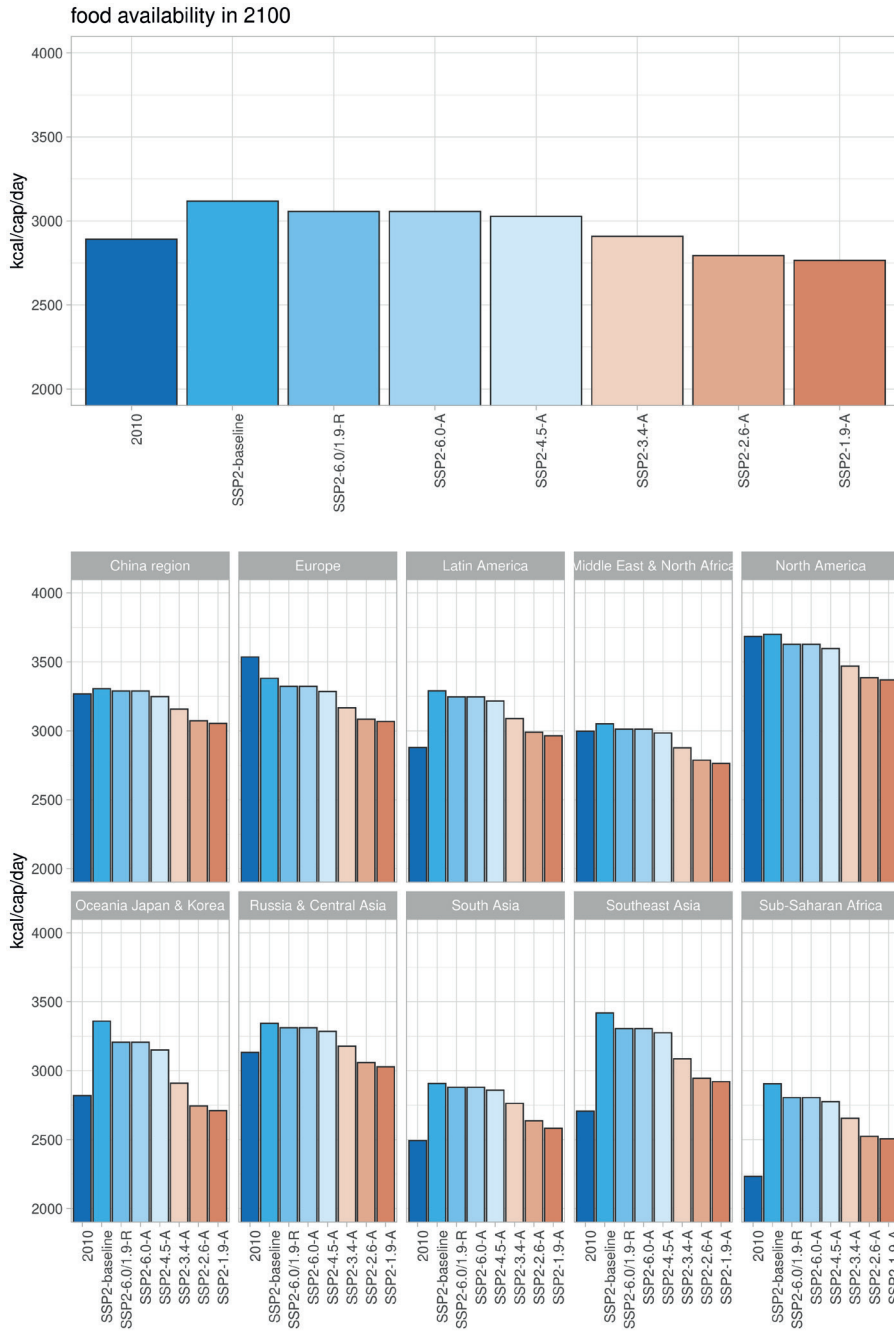


SSP2-2.6-A - 2100

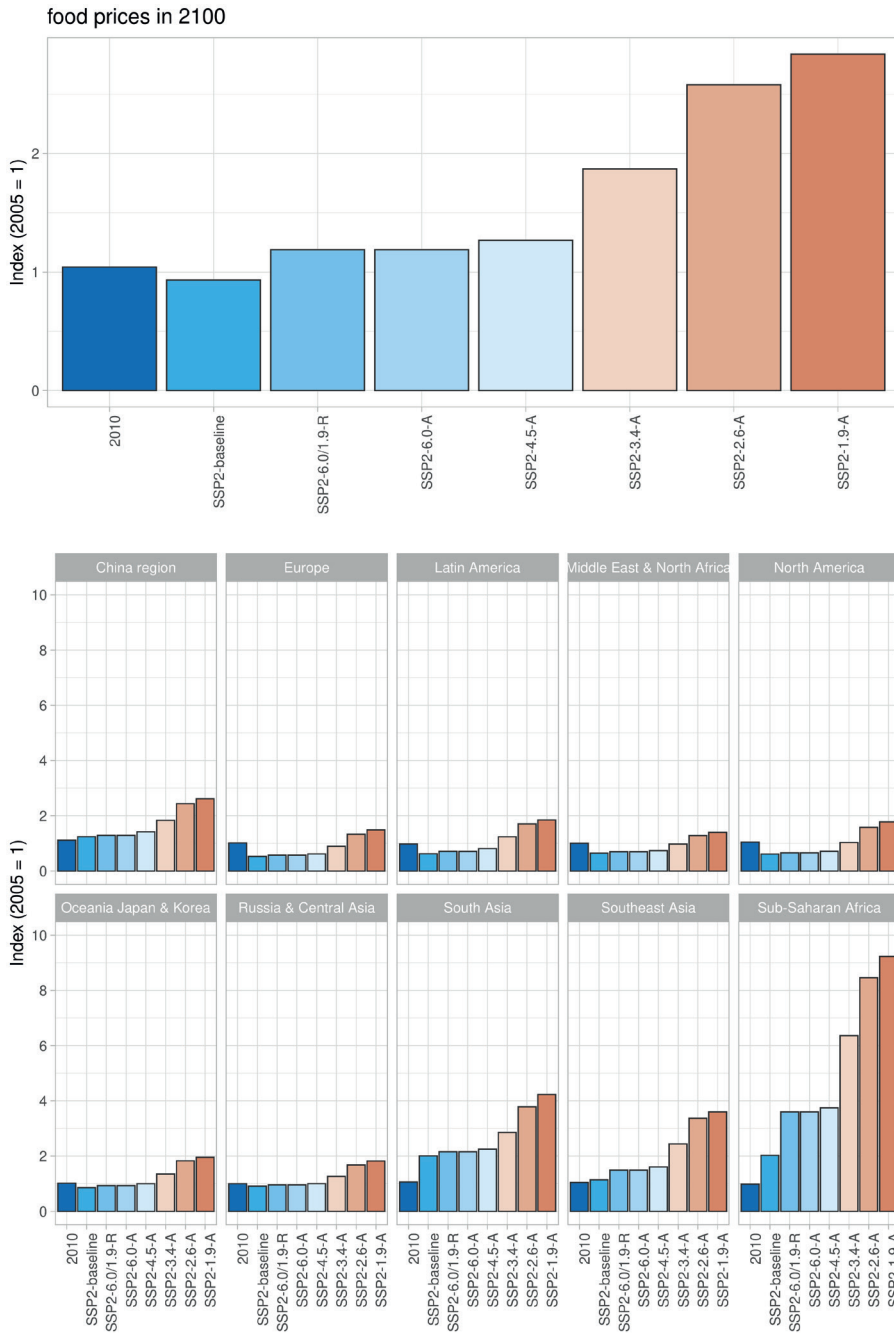


SI Figure 4-5: Map of afforestation fractions in SSP2-2.6-A showing the locations and extent of afforestation in 2050 and 2100.

A



SI Figure 4-6: Food availability in 2010 and 2100 on the global and regional level shown in kcal/cap/day.

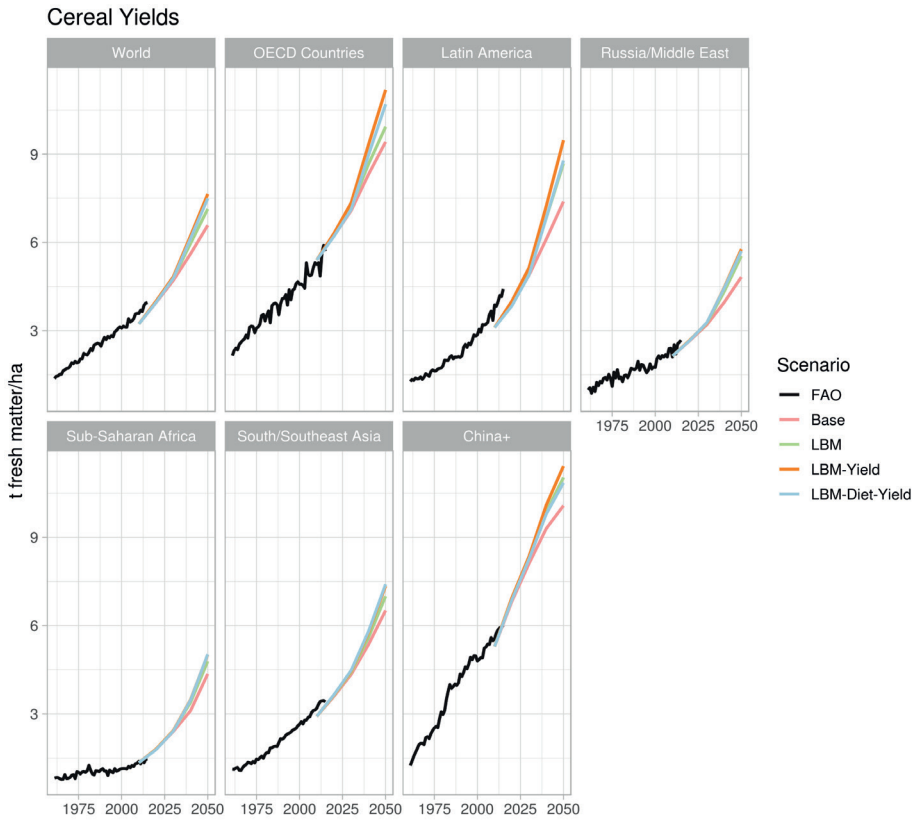


SI Figure 4-7: Food prices in 2010 and 2100 on the global and regional level shown as an index normalized to 1 in 2005.

S5. Making the Paris Agreement climate targets consistent with food security objectives

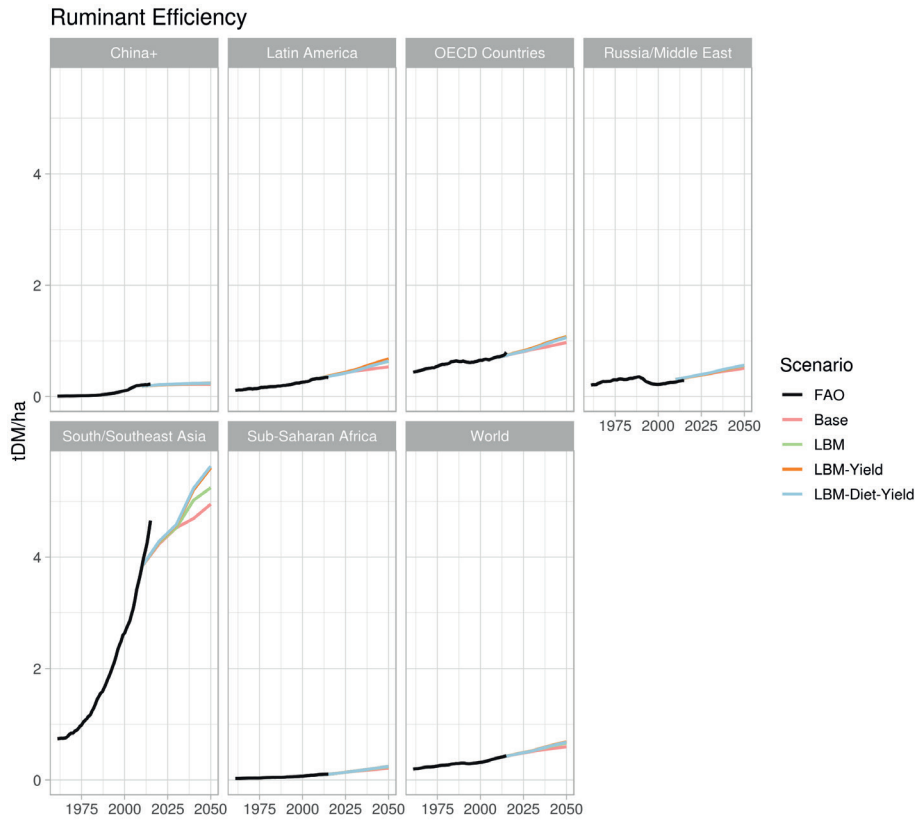
SI Table 5-1: Aggregation of MAGNET/IMAGE regions as used in this paper (see for map of IMAGE regions SI Figure 3-1).

MAGNET/IMAGE region	Aggregated region
Canada	OECD countries
USA	OECD countries
Mexico	Latin America
Rest Central America	Latin America
Brazil	Latin America
Rest South America	Latin America
Northern Africa	Russia/Middle East
Western Africa	Sub-Saharan Africa
Eastern Africa	Sub-Saharan Africa
South Africa	Sub-Saharan Africa
OECD Europe	OECD countries
Eastern Europe	OECD countries
Turkey	Russia/Middle East
Ukraine +	Russia/Middle East
Asia-Stan	Russia/Middle East
Russia +	Russia/Middle East
Middle East	Russia/Middle East
India	South/Southeast Asia
Korea	OECD countries
China +	China
South-East Asia	South/Southeast Asia
Indonesia +	South/Southeast Asia
Japan	OECD countries
Oceania	OECD countries
Rest South Asia	South/Southeast Asia
Rest Southern Africa	Sub-Saharan Africa

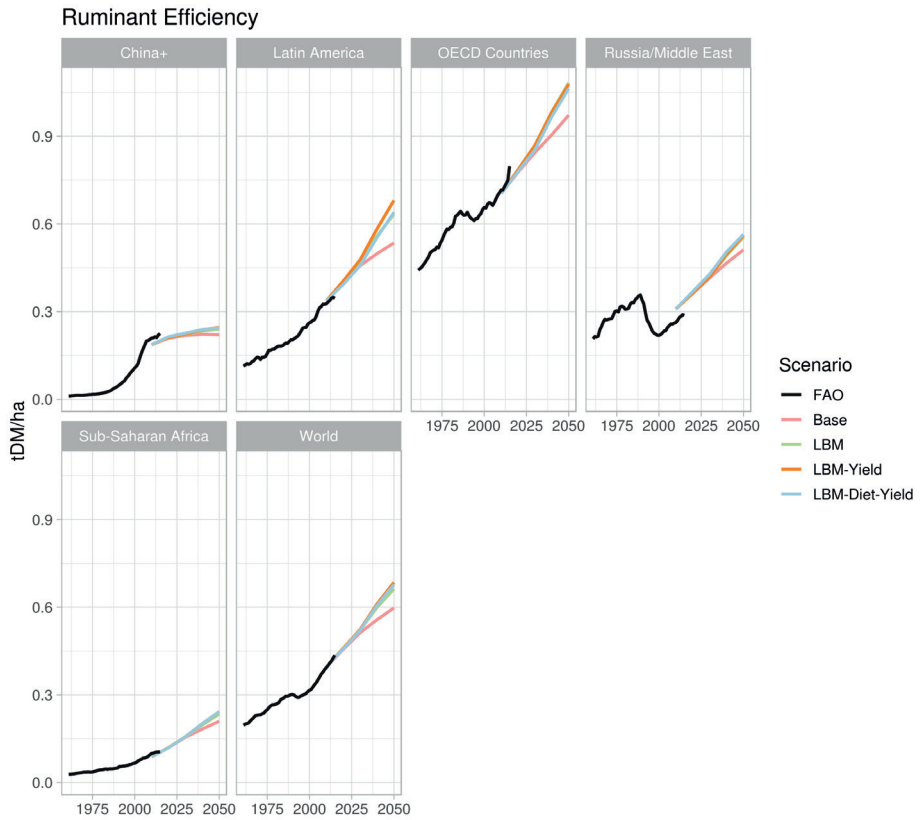


SI Figure 5-1: Cereal yields for historical period based on FAO and scenario period for four scenarios.

A



SI Figure 5-2: Ruminant efficiency (ruminant meat and dairy production divided by grassland area) for historical period based on FAO and scenario period for four scenarios.

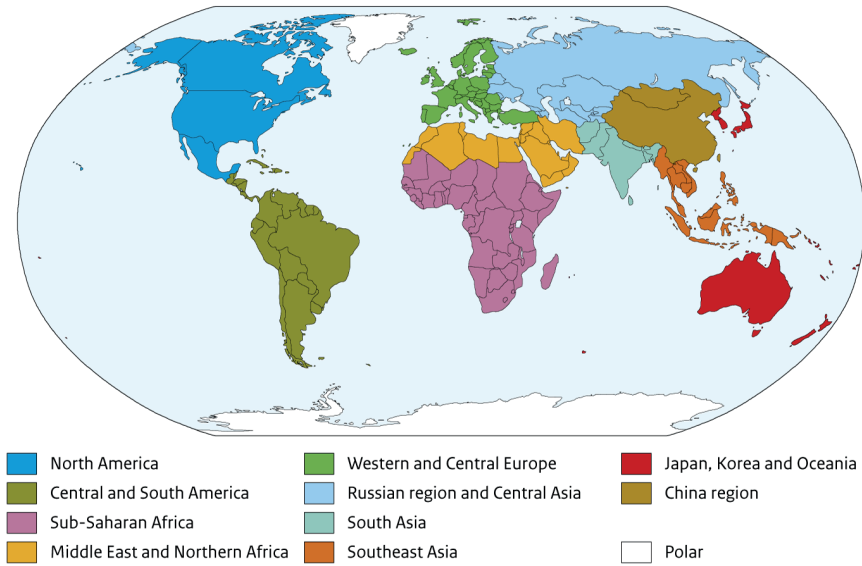


SI Figure 5-3: Ruminant efficiency (ruminant meat and dairy production divided by grassland area) for historical period based on FAO and scenario period for four scenarios, South/Southeast Asia is excluded for clarity.

S6. Quantifying synergies and trade-offs in the global water-land-food-climate nexus using a multi-model scenario approach

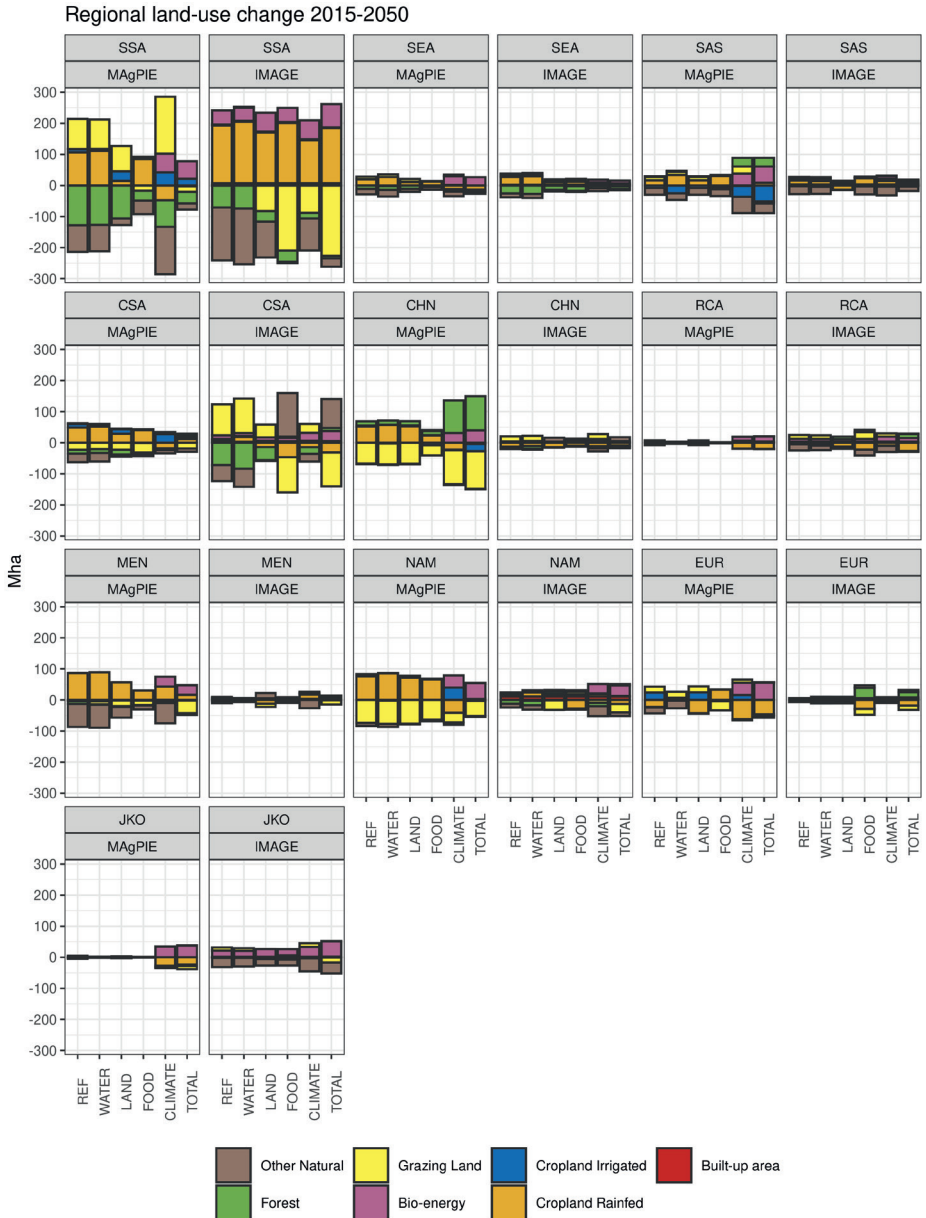
S6.1 Supplementary material figures

The 10 IMAGE regions used in this report



Source: PBL

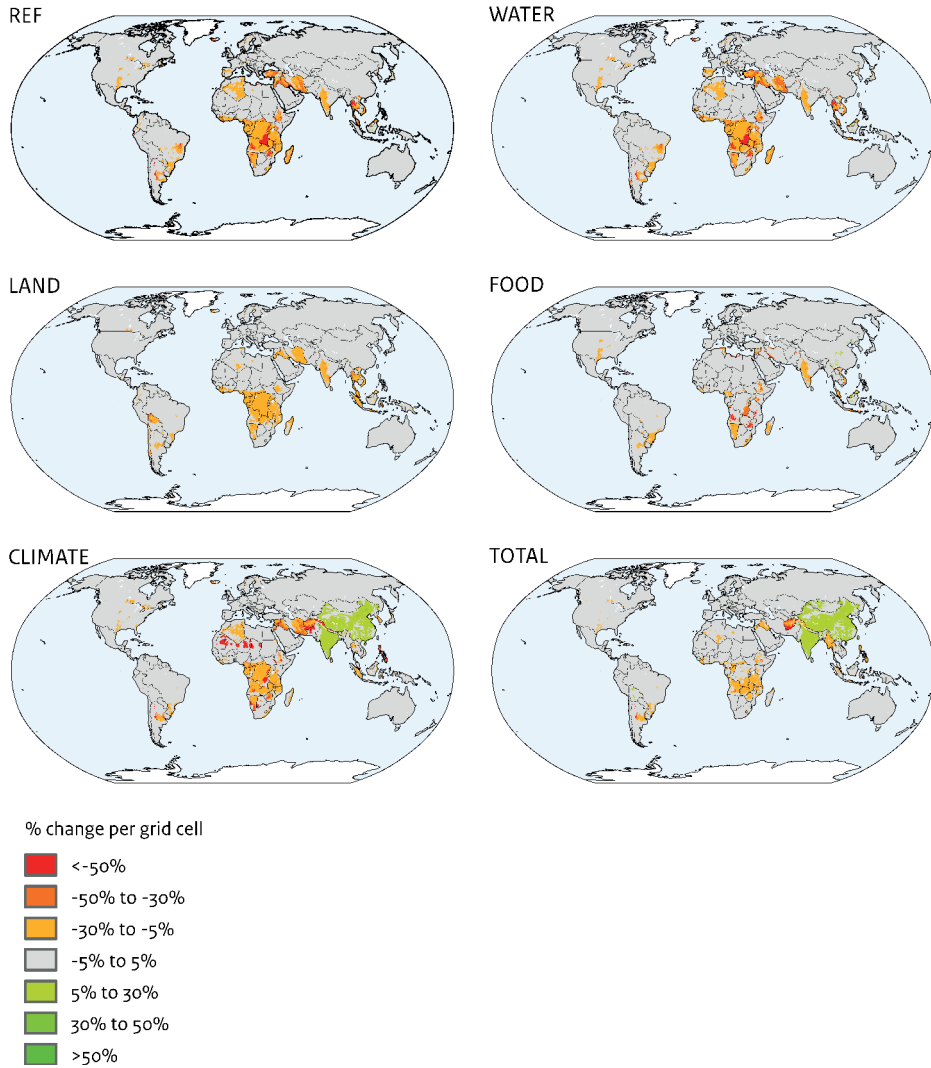
SI Figure 6-1: Ten aggregated regions used in this study.



SI Figure 6-2: Regional land-use change in IMAGE and MagPIE in the 2015-2050 period for all scenarios for 7 land-use categories. Negative values indicate area reduction in a land-use category, positive values indicate area expansion of a land-use category for different regions (high-income: Japan, Korea and Oceania (JKO), North America (NAM), Western and Central Europe (EUR); middle-income: Middle East, and Northern Africa (MEN), Russia and Central Asia (RCA), China region (CHN) Central and South America (CSA); low-income: Sub-Saharan Africa (SSA), South Asia (SAS), Southeast Asia (SEA))

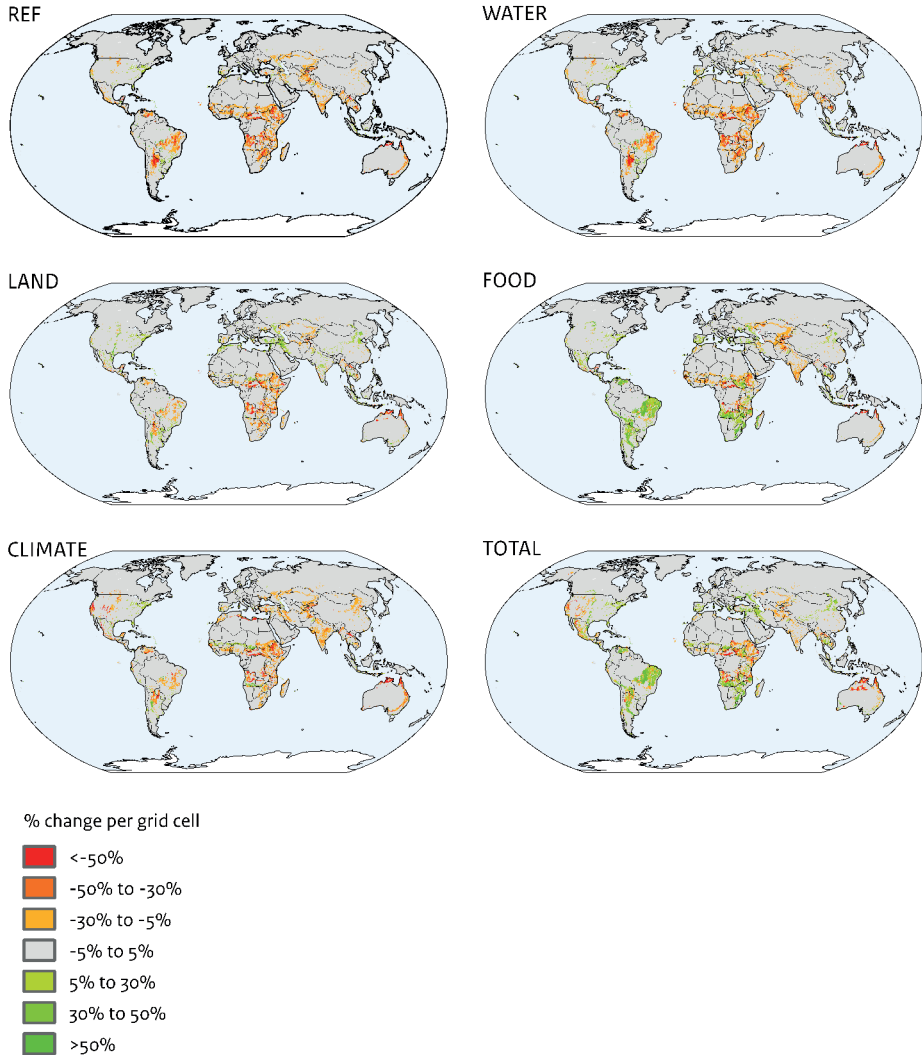
A

Natural land share change 2015-2050 per grid cell - MAgPIE

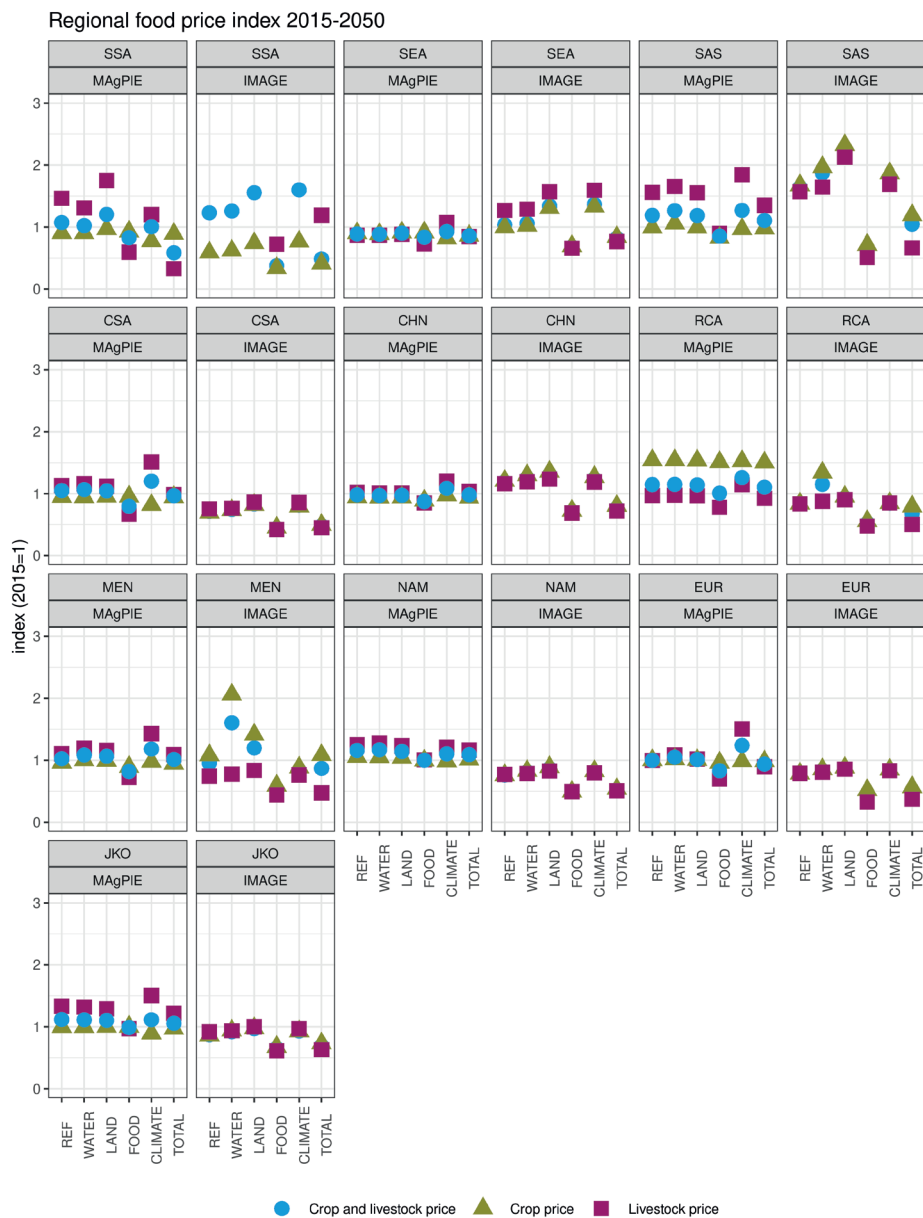


SI Figure 6-3: Percentage change in natural land share per grid cell in the 2015-2050 period in MAgPIE in the six scenarios.

Natural land share change 2015-2050 per grid cell - IMAGE

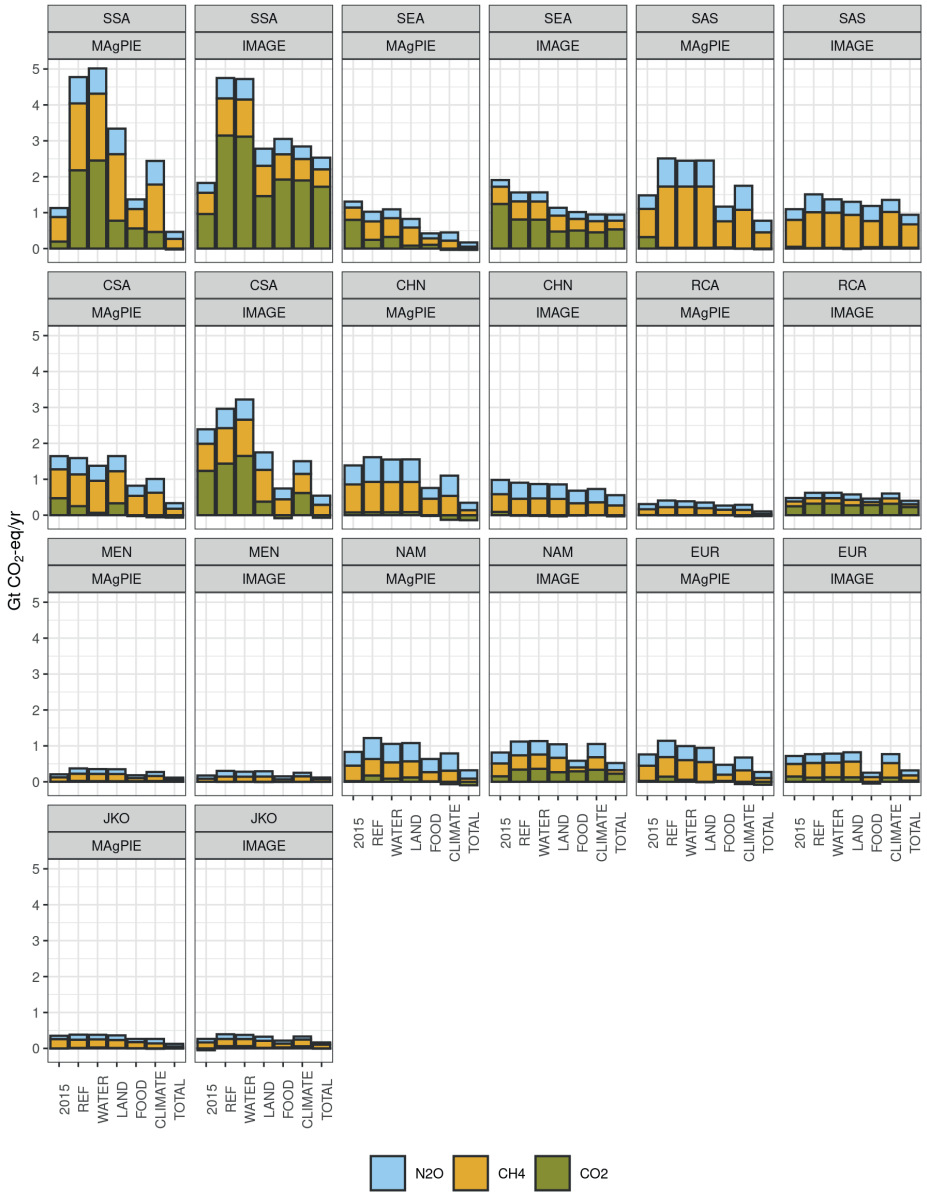


SI Figure 6-4: Percentage change in natural land share per grid cell in the 2015-2050 period in IMAGE in the six scenarios.



SI Figure 6-5: Regionally averaged food price index in IMAGE and MAGPIE for crops, livestock, and crops and livestock combined for the 2015-2050 period for different regions (high-income: Japan, Korea and Oceania (JKO), North America (NAM), Western and Central Europe (EUR); middle-income: Middle East, and Northern Africa (MEN), Russia and Central Asia (RCA), China region (CHN) Central and South America (CSA); low-income: Sub-Saharan Africa (SSA), South Asia (SAS), Southeast Asia (SEA). For clarity, the Y-axis are limited to 3 which excludes 4 outlying values for livestock in IMAGE in SSA (7.0-9.1).

Regional AFOLU GHG emissions in 2015 and 2050



SI Figure 6-6: Regional CO₂, CH₄ and N₂O emissions in IMAGE and MAgPIE in 2015 and in 2050 for all scenarios for the AFOLU sector for different regions (high-income: Japan, Korea and Oceania (JKO), North America (NAM), Western and Central Europe (EUR); middle-income: Middle East, and Northern Africa (MEN), Russia and Central Asia (RCA), China region (CHN) Central and South America (CSA); low-income: Sub-Saharan Africa (SSA), South Asia (SAS), Southeast Asia (SEA)).

A

S6.2 Extended model description MAgPIE

The Model of Agricultural Production and Its Impact on the Environment (MAgPIE) is a global recursive dynamic partial equilibrium model that simulates future scenarios of the land system (Dietrich et al., 2019). It derives optimal land-use patterns and land-use change under different future scenarios considering both spatially-explicit biogeophysical as well as different socioeconomic constraints on country- and world-region level. This modular open-source land-systems modelling framework¹⁰ is flexible in its application to different spatial and temporal scales (Dietrich et al., 2019). In this study, the simulation period spans from 1995 to 2100 and the model operates recursively in 5-year time steps. For computational reasons, the 0.5° inputs are aggregated to clusters based on biophysical similarity of grid cells (Dietrich et al., 2013). Certain processes, such as trade, take place on regional level (Schmitz et al., 2012). For this publication, the unit of simulation of the provided MAgPIE runs was 200 clusters and 11 world regions.

The constrained optimization follows a global production cost minimization approach. Costs include factor requirement costs, investment costs for irrigation expansion or yield-increasing technologies, transportation costs, land conversion costs, and, in the case of mitigation, costs for GHG emissions and costs for technical mitigation (Dietrich et al., 2014; Popp et al., 2017, 2011; Wang et al., 2020). The objective is to meet global food (Bodirsky et al., 2020), feed (Weindl et al., 2017b, 2017a), material and bioenergy demand (Popp et al., 2011) while taking resource constraints (land and water availability), biophysical conditions and possible future socioeconomic scenarios into account. Global agricultural production as well as the optimal spatial distribution of cropland, pasture land, and natural land are projected under different future scenarios and policies on food provision, GHG emissions, agricultural production patterns and food prices can be analysed (Popp et al., 2017). MAgPIE obtains spatial-explicit (0.5° spatial resolution) information on available water, crop water requirements and potential yields under different climatic conditions from the global vegetation model LPJmL (Bondeau et al., 2007; Müller and Robertson, 2014).

Available water resources in MAgPIE are derived from cellular runoff (precipitation that enters water bodies). It only includes renewable water resources and does not consider alternative water sources such as fossil groundwater, melting glaciers or desalination. Water resource use is restricted to the water available in the growing period. MAgPIE focuses on agricultural water demand and treats water demand from all other sectors as exogenous assuming a certain fraction to be reserved for these purposes. Irrigation water demand for crop and livestock production is calculated endogenously taking spatially differing crop-specific irrigation water requirements (provided by LPJmL) and livestock water demand (derived from FAO data) into account. Irrigation efficiencies vary by region depending on the development

10 The MAgPIE modular framework code is open-source and can be found on GitHub: <https://github.com/magpiemodel/magpie>. The code is comprehensively documented under <https://rse.pik-potsdam.de/doc/magpie/4.3/> and a model description is available in the model description article published in Geosci. Model Dev. (<https://gmd.copernicus.org/articles/12/1299/2019/>).

state (Rohwer et al., 2007). In the first timestep, areas equipped for irrigation are initialized to data provided by FAO (Siebert et al., 2007). In the following simulation time steps, MAgPIE can endogenously expand irrigated areas taking unit costs per hectare for irrigation equipment into account that are derived from the World Bank (Jones, 1995).

Land productivity is determined by biophysical conditions. Irrigated and rainfed crop yields, carbon densities, water availability and crop water irrigation requirements are provided at a 0.5° spatial resolution by the global dynamic vegetation crop water model LPJmL (Lund Potsdam-Jena model) (Bondeau et al., 2007; Müller and Robertson, 2014). In the initialization period, yields are calibrated to meet regional crop area (FAOSTAT, 2020). Climate change impacts as simulated by LPJmL affect agricultural production and land-use patterns via impacts on attainable yields and available water. Using LPJmL inputs from different climate scenarios and different Representative Concentration Pathways (RCPs) with various climate futures, their impacts and adaptation can be included in the analysis. Depending on costs and potential yields, MAgPIE can invest into yield-enhancing technologies or expand cropland to increase crop production (Dietrich et al., 2014). The model thereby simulates an equilibrium between cropland expansion, crop intensification and relocating production to more productive areas within and between world regions.

Future food demand is driven by population (KC and Lutz, 2017) and economic growth (Dellink et al., 2017) projections. Food consumption patterns depend not only on the absolute number of people populating the planet, but as well on the sex and age structure as well as the physical activity level (Bodirsky et al., 2020). Feed demand is determined by regionally- and livestock-specific feed baskets. Depending on cultural particularities, past productivity improvements and income projections, feed baskets as well as livestock productivity differ in line with the general scenario storyline (Weindl et al., 2017b, 2017a). Besides endogenous food and feed demand for MAgPIE's 17 crop types, bioenergy demand for climate change mitigation is a major driver of land-use change. The model differentiates first and second generation bioenergy. In future time steps, first generation bioenergy is gradually replaced by second generation bioenergy up until 2050 from which onwards only second generation bioenergy crops and residues are used for bioenergy production.

Agricultural production is a major contributor to GHG emissions (CO₂ through land-use change, e.g. deforestation; CH₄ from livestock and rice farming; N₂O from crop fertilization). In MAgPIE, GHG emissions arise as a consequence of agricultural production resulting from the transformation of natural land or forests into cropland or pasture land as well as from livestock (methane emissions) and cropland production (nitrogen application). CH₄ emissions from enteric fermentation are based on the Tier-II approach of IPCC (2006) and feed baskets of Weindl et al (2017b), while CH₄ from animal waste management and flooded rice are estimates based on the Tier-I approach. CO₂ emissions are based on endogenously estimated land-use change, and carbon densities from the LPJmL model (Popp et al., 2014). It includes CO₂ emissions from removed vegetation as estimated by LPJmL, as well as a loss of soil

organic matter after conversion based on IPCC (2006). N₂O emissions are accounted in the Nitrogen (N) flow module (Bodirsky et al., 2014, 2012) that transforms all biomass flows into N flows. Cropland nitrogen budgets include harvested crops, crop residues (aboveground and belowground), fertilizers (organic, inorganic, (non)-symbiotic nitrogen-fixation), soil organic matter depletion and atmospheric deposition. Nitrogen losses (the difference between N inputs and harvested N) depend on the nitrogen uptake efficiency (NUE). For future projections, we use a scenario approach.

Available land is divided into urban areas, natural vegetation, forests (primary, secondary), cropland and pastureland. From all land that is suitable for agricultural purposes (excluding e.g. urban areas, mountainous areas, glaciers), certain areas can be additionally protected from human uses by various protection scenarios. In MAGPIE, natural vegetation includes primary forest, secondary forest and other natural land. Besides upholding the NDCs with respect to natural area protection, climate change mitigation is included via marginal abatement cost curves (MACCs) and GHG prices. Prices for GHG enter the model as an exogenous input from integrated assessment models or energy system models like REMIND and affect land-use change, mainly by making deforestation less attractive (Klein et al., 2014; Popp et al., 2014).

S6.3 Extended model description IMAGE

IMAGE 3.2 is an integrated assessment modelling framework¹¹ that simulates the interactions between human activities and the environment (Stehfest et al., 2014) to explore long-term global environmental change and policy options in the areas of climate, land, and sustainable development. IMAGE consists of various sub-models describing land use, agricultural economy, the energy system, natural vegetation, hydrology, and the climate system. Socioeconomic processes are modelled at the level of 26 regions. Most environmental processes are modelled on the grid-level at 30 or 5 arc-minutes resolution with upscaling and downscaling functions used to couple the different resolutions. Data exchange takes place either through hard-coupling with an annual exchange of data or soft-coupling using an iterative approach of scenario data exchange.

Agriculture, forestry, and land-use dynamics are modelled on the IMAGE-LandManagement model's grid-level (Doelman et al., 2018). Demand for crop and livestock products, trends in agricultural intensification, and trade dynamics are provided by the economic general equilibrium model MAGNET (Woltjer et al., 2014). Gridded land-use dynamics are implemented in the dynamic global vegetation model LPJmL to model effects on the carbon and hydrological cycle (Müller et al., 2016; Schaphoff et al., 2018b) and to the global nutrient model (GNM) to model the nitrogen and phosphorus cycles (Beusen et al., 2015). LPJmL provides data on potential crop and grass yields, land-use change emissions, and irrigation water use. The simulation model TIMER represents the energy system with high

¹¹ For more information on the IMAGE model visit the online documentation: <http://models.pbl.nl/image>.

technological detail for 12 primary energy carriers, including bioenergy. Land use for the production of bioenergy as determined by TIMER is implemented on the grid-level in IMAGE-LandManagement. GHG emissions from energy, industry, and land use are inputs to the simple climate model MAGICC, which emulates complex climate models to calculate global mean temperature change (Meinshausen et al., 2011). Finally, the climate policy model FAIR-SimCAP uses MAC curves to determine cost-optimal emission pathways to achieve specific climate targets (den Elzen et al., 2008).

The Modular Applied General Equilibrium Tool (MAGNET)(Woltjer et al., 2014) is based on the standard GTAP model (Hertel, 1997). This is a multi-regional, static, applied computable general equilibrium (CGE) model based on neoclassical economic theory. It covers all sectors of the economy (agriculture, manufacturing, and services) and all regions and major countries globally. The agricultural sector is represented in great detail compared to standard CGE models. Land is modelled as an explicit production factor described by a land-supply curve. This curve specifies the relation between total agricultural land supply and the real land price given constraints related to biophysical availability (potential area of suitable land) and institutional factors (agricultural and urban policy, conservation of nature). The land supply curve is constructed with land availability data provided by IMAGE (Dixon et al., 2016; van Meijl et al., 2006). Food demand in MAGNET is endogenously determined by income changes, relative prices, and the dynamic income elasticities of food demand (van Meijl et al., 2020). These price feedbacks can arise from price changes due to increases in total demand (resulting from population growth or higher income) or changes in the supply side, e.g., from reduced availability of suitable land due to nature protection or the impacts of climate change on agriculture as modelled by IMAGE-land and LPJmL (van Meijl et al., 2018). Food demand can be prescribed in the model to test the effects of dietary change.

The dynamic global vegetation model LPJmL is an integral part of IMAGE (Müller et al., 2016) and simulates crop yields, grassland productivity, vegetation dynamics, and carbon and water cycles on a 30 arc-minute geographic grid. LPJmL is based on the concept of multiple plant functional types (PFTs) categorized according to biophysical characteristics. Both natural and crop PFTs are represented. LPJmL also includes a full hydrological model with a river routing module that calculates river discharge, with lakes and reservoirs as additional water stores. It accounts for both “blue” water (water from rivers, lakes, aquifers, and dams) and “green” water (precipitation used by plants directly). Irrigated crop production is a management option for all crop PFTs calculating water withdrawals and consumption estimates depending on the irrigation system efficiency (surface, sprinkler, or drip)(Jägermeyr et al., 2015). Water withdrawal for irrigation or other uses (e.g., energy and industry) can be restricted to account for environmental flow requirements, affecting crop productivity in irrigated agriculture (Pastor et al., 2014). The effects of climate change are dynamically included in LPJmL as spatial-explicit data on changing temperature and precipitation drive the model, affecting many key processes such as crop yields, water availability, crop water use efficiency and forest growth (Jägermeyr et al., 2021; Schaphoff et al., 2018b).

IMAGE-LandManagement determines the area and location of irrigated and rainfed cropland on a 5 arc-minute geographical grid required to fulfil the demand for production of 16 crop categories (wheat, rice, maize, tropical cereals, other temperate cereals, pulses, soybeans, temperate oil crops, tropical oil crops, temperate roots & tubers, tropical roots & tubers, sugar crops, oil palm, vegetables & fruits, other non-food, luxury crops, spices, plant-based fibres). The historical locations and areas of cropland and grazing land are based on the HYDE database (Klein Goldewijk et al., 2017) which is based on regional FAOSTAT data (FAOSTAT, 2020). For each region in each time step crop production is calculated using gridded potential yields from LPJmL, locations of cropland in the previous time step and a regional management factor (calibrated to historical yields from FAO and future yield trends according to MAGNET). If production is higher than demand, cropland is abandoned on the least productive locations. If production is lower than demand, cropland is expanded following empirically-based statistical suitability layers derived from ESA-CCI land-use change data (Cengic et al., 2023). IMAGE-LandManagement also calculates livestock production for five categories (beef, dairy, pigs, poultry, sheep and goats) for 26 regions in intensive and extensive systems taking into account variations between regions in feed composition, feed efficiency, genetic animal productivity and age at slaughter (Bouwman et al., 2005; Lassaletta et al., 2019). The livestock production module determines the amount of feed crops and grass required to fulfil demand for livestock production as calculated by MAGNET. Expansion or abandonment of grazing land depends on demand for grass and follows the same allocation procedure as cropland. IMAGE-LandManagement also computes timber production in four forest management systems: clear cut, selective cut (conventional or reduced impact logging) and wood plantations (Arets et al., 2011).

IMAGE includes a detailed description of land-use greenhouse gas emissions. Land-use CO₂ emissions are calculated in LPJmL where the emissions from land-use conversion for agriculture and timber harvest are determined, as well as the uptake of CO₂ in vegetation following regrowth of vegetation. In addition, CO₂ emissions from degraded peatland are included based on gridded information on peatland extent and CO₂, N₂O and CH₄ emissions factors (IPCC, 2014a; Stoorvogel et al., 2017). A large number of non-CO₂ gasses is included (CH₄, N₂O, CO, NH₃, NO_x, SO_x, NMVOC, BC, OC) based on a variety of activity data such as total number of livestock, manure production, rice production, land-use conversion, vegetation burning and more (Doelman et al., 2018). These activity data are combined with calibrated emission factors mostly based on the EDGAR database and a number of other sources (Doelman et al., 2018; JRC/PBL, 2012).

The GNM model is a global, spatially explicit model that calculates the nitrogen and phosphorus balance at a spatial resolution of 30 arc-minutes (Beusen et al., 2015). For nitrogen discussed explicitly in this study, GNM calculates the nitrogen balance account for incoming flows from synthetic fertilizer, animal manure, synthetic fertilizer, N fixation, and N deposition, and for outgoing flows such as uptake by vegetation, leaching, denitrification, erosion, and ammonia volatilization. The nutrient balance is used in combination with

hydrological data to calculate water quality. An important policy measure that can be implemented is improved fertilizer efficiency, which reduces the amount of excess nitrogen implemented on the land resulting in better water quality and reduced N₂O emissions. Future N inputs are determined by the N use efficiency (NUE, $NUE = N \text{ removal} / \text{total N input}$). N yields are calculated from the scenario-specific crop production expressed in N using N contents for each of the 160 crops reported by FAO (Lassaletta et al., 2014). For a given NUE, total inputs can be calculated as $N \text{ yield} / NUE$. Fertilizer use is the difference between total N inputs, manure, biological N fixation and deposition. Biological N fixation is from production of leguminous crops according to (Salvagiotti et al., 2008). Atmospheric deposition and manure production and attribution to cropland and grassland are calculated by the IMAGE-LandManagement module.

S6.4 Extended description of modelling procedures and key model differences

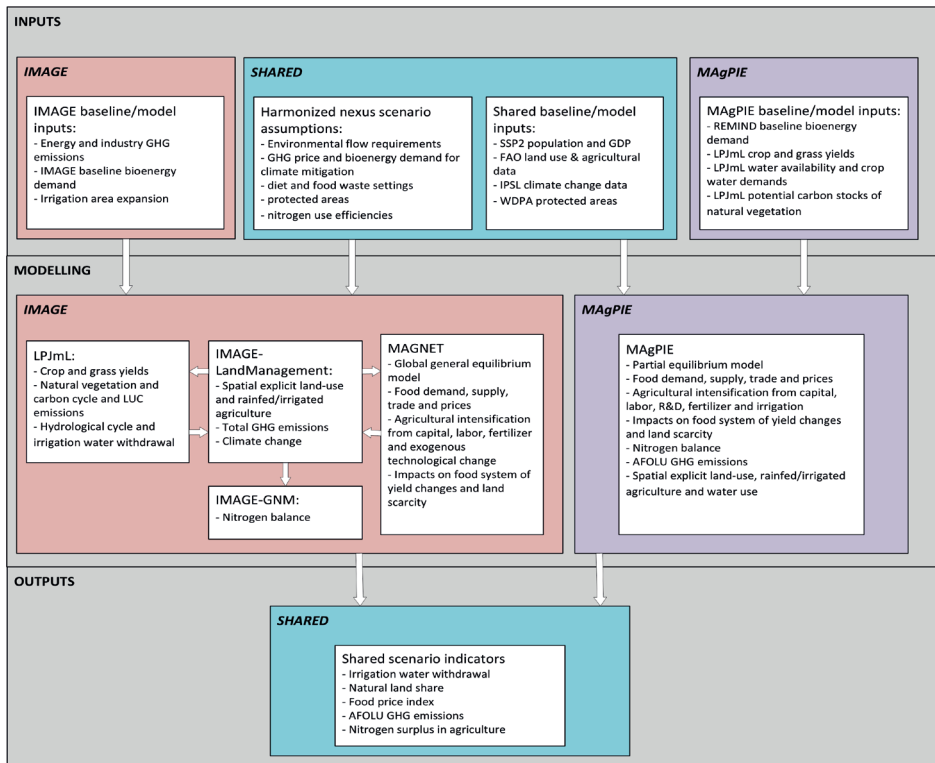
In this study the models MAgPIE and IMAGE implement the same set of scenarios with harmonized scenario assumptions and inputs. The models both cover the Water-Land-Food-Climate nexus in detail, but differ substantially in their model setups and philosophy and therefore make an interesting model intercomparison case. SI Figure 6-7 shows a schematic visualization of the modelling procedures applied in this study, highlighting crucial differences and similarities between MAgPIE and IMAGE.

On the input side, a harmonized set of assumptions is made on environmental flow requirements (EFRs), GHG prices and bioenergy demand for climate change mitigation, diet and food waste assumptions, protected areas and nitrogen use efficiencies (NUEs) that are described in detail in Section 6.2.2. The models partly use the same data for inputs for the baseline scenario, for example GDP and population data from the SSP2 scenario, statistics from the FAO on land use, agricultural consumption, production and more, climate change data from the IPSL-CM5a-LR model as processed by the ISIMIP project, and current day protected areas from the world database on protected areas. Some inputs in the baselines differ, such as bioenergy demand which is provided by the respectively coupled energy models: REMIND for MAgPIE and TIMER for IMAGE. IMAGE also uses data on energy and industry emissions from TIMER to calculate total emissions and resulting climate change, whereas MAgPIE only considers emissions from the AFOLU sector. In addition, IMAGE uses a predefined irrigated area expansion as input while in MAgPIE irrigation area expansion is endogenously determined.

The LPJmL model has an important role in both models. For MAgPIE, gridded data from LPJmL on crop and grass yields, water availability and crop water demand, and potential carbon stocks is provided as exogenous input to the model. For IMAGE, LPJmL is an integral component of the model system and is hard-coupled to grid-based land allocation modelling in IMAGE-LandManagement, which uses data on crop and grass yields, vegetation carbon stocks, land-use change emissions and irrigation water use. Changes in carbon stocks and irrigation water use are directly modelled by LPJmL in the IMAGE setup. While LPJmL is

implemented very differently in the two models, it means that the same model is used to estimate crop yields, water availability as well as crop water requirements, and carbon cycle dynamics. As dynamic vegetation models, crop models and hydrological models can differ widely in their estimates (Krause et al., 2018; Rosenzweig et al., 2014; Wada et al., 2013) this limits the range of model variation covered in this study.

A key difference between the two models is the economic modelling approach that is used. MAgPIE uses a recursive dynamic partial equilibrium approach covering the food, agriculture and land-use systems. IMAGE uses a global general equilibrium approach as modelled by MAGNET which covers the complete global economy, however with relatively high detail on the food, agriculture and land-use sectors. Another key difference regards the handling of spatially-explicit land use: IMAGE operates at the grid-scale using empirically based statistical suitability layers for land-use allocation, while MAgPIE operates at sub-regional spatial units with similar biophysical characteristic where land-use allocation follows a cost minimization approach. Both models represent food demand, supply, trade and prices. Nevertheless, model dynamics are very different as a result of, among others, different sector aggregations, elasticities, and trade modelling. The approach to agricultural intensification is also a key difference: MAGNET has an exogenous assumption on technological change, and can furthermore substitute between capital, labour and fertilizer use to increase agricultural production. MAgPIE has an endogenous approach to technological improvement through investment in research and development, and can furthermore substitute between capital, labour, fertilizer and irrigation. Additionally, MAgPIE has an endogenous representation of gridded land use and nitrogen balance, while IMAGE-LandManagement is soft-coupled to the MAGNET model from which trends in land use and agricultural production are adopted and downscaled on the grid level. The nitrogen balance for IMAGE is calculated in the IMAGE-GNM model which is also soft-coupled, implying that assumptions on the nitrogen use efficiency do not feed back into the economic modelling of MAGNET. Finally, both models calculate all indicators considered in this study allowing for a consistent comparison between model results.



SI Figure 6-7: Schematic description of shared and differentiated inputs, modelling and outputs implemented.

S6.5 Extended information scenario assumptions

S6.5.1 Climate mitigation

SI Table 6-1: GHG price and bioenergy demand implemented in CLIMATE and TOTAL scenario.

	2010	2020	2030	2040	2050
GHG price (US2010\$/tCO ₂ -eq)	0.0	0.0	54.8	73.8	86.7
Bioenergy demand (Ej/yr)	49.3	59.4	75.5	138.4	167.2

Both models use GHG prices from the FAIR-SimCAP module which is part of IMAGE. In MAGPIE the GHG prices implemented in the CLIMATE and TOTAL scenarios have an effect on consumer prices not only via the increased costs, but also via passing on the tax payments for unmitigated emissions from producers to consumers. This is different from the IMAGE implementation, where the effects of GHG pricing are implemented in MAGNET through reduced availability of land due to for example forest protection (Doelman et al., 2018). As the tax income in MAGPIE does not only increase prices, but can also be recycled to consumers or to reduce other taxes, we ex-post excluded the tax revenue from the reported price index. Without the correction, MAGPIE results could not be compared to IMAGE results.

The resulting food price index as calculated from MAGPIE is a consumption weighted Laspeyres index of agricultural prices, with the quantity weight being harmonized across the scenarios on the food basket of the REFERENCE scenario (SSP2, no mitigation) in 2015. The emission tax income from agricultural emissions is subtracted from food expenditure. Emission costs are calculated from the emission tax rate t and emissions E in the reported year 2050. This leads to the following equation for the price index I :

$$I_{scen,i,2050} = \frac{\sum_c p_{scen,i,c,2050} \cdot q_{ref,i,c,2015} - E_{scen,i,2050} \cdot t_{scen,i,2050}}{\sum_c p_{ref,i,c,2015} \cdot q_{ref,i,c,2015}}$$

with p being the price of each commodity c in USD, q demand for each commodity c in kcal per year, resulting in $\sum_c p_{scen,i,c,2050} \cdot q_{ref,i,c,2015}$ being the total food demand in USD per year for the food basket of the reference year 2015. The index $scen$ represents the current scenario, ref the reference scenario, c : the commodity, i the region.

The Index can be reported for the entire food basket or for livestock and crop products separately. For the separate reporting, emission costs are weighted with the food products share to attribute the emission costs across livestock and crops.

$$EmissionCost_{scen,k,i,2050} = \frac{p_{ref,i,k,2015} \cdot q_{ref,i,k,2015}}{\sum_c p_{ref,i,c,2015} \cdot q_{ref,i,c,2015}} \cdot (E_{scen,i,2050} \cdot t_{scen,i,2050})$$

with k being a subset of c .

S6.5.2 Food demand

In MAGPIE, the food demand module estimates income-dependent food intake, dietary composition and food waste (Bodirsky et al., 2020). In the FOOD and TOTAL scenarios, diets shift gradually towards healthy and sustainable patterns until 2050, following the recommendations of the EAT Lancet commission proposing low consumption of meat and processed foods such as sugar and a high contribution of legumes, nuts, fruits and vegetables (Willett et al., 2019). In addition, healthy total calorie intake is estimated based on the anthropometric equations assuming healthy body weight in all population sub-groups. Food waste is reduced to a maximum of 20% of food intake (Note: this is equivalent to about 50% of food waste currently observed in high-income countries). The implemented Flexitarian diet results in a global kilocalorie intake from animal products of 251 kcal/cap/day (ranging between 161 kcal/cap/day and 344 kcal/cap/day depending on the region) in 2050 that is much lower than the animal product food intake in the business-as-usual scenario (with global average kilocalorie intake of 788 kcal/cap/day [582 – 1062 kcal/cap/day depending on the region]).

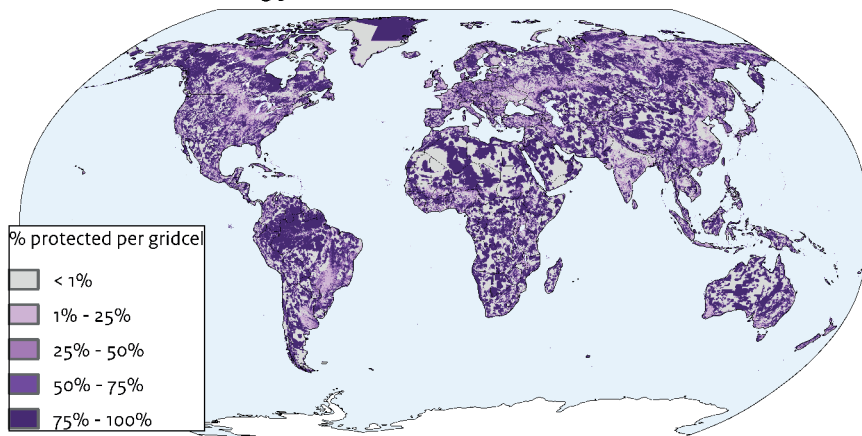
For IMAGE, in the standard approach food demand is endogenously calculated in MAGNET based on income changes, relative prices, and dynamic income elasticities of food demand (van Meijl et al., 2020). For the FOOD and TOTAL scenarios alternative consumption patterns are implemented based on the definitions of the EAT-Lancet commission (Willett et al., 2019). Following the Springmann et al. (2018) implementation and adapted for MAGNET food group aggregations, several targets are implemented: a maximum level of 275 kcal/cap/day for animal products, a minimum level of 900 kcal/cap/day vegetables, fruits, nuts, legumes and vegetable oils, and a maximum level of 110 kcal/cap/day for sugars. Any baseline outcomes below maximum levels or above minimum levels were not adjusted. The final restriction was set for cereals to let the full diet reach the recommended target of 2100 kcal/cap/day as average diet. In addition, a 50% reduction of food waste is implemented by reducing losses in processing, transport & retail, and consumption.

S6.5.3 Natural land protection

The protected area map used in the LAND scenario in this study (SI Figure 6-8) is developed by Kok et al. (2020). The approach is based on Dinerstein et al. (2017) and aims to protect 50% of all terrestrial area per ecoregion where natural land is still available, where the definition of ecoregions is based on the RESOLVE Ecoregion2017 project (Resolve, 2017). Remaining natural land was derived from the satellite-based ESA-CCI land cover dataset for the year 2015 (ESA, 2017) to obtain potential locations for nature protection. Then a nature protection claim of 50% per ecoregion is allocated. First, current protected areas retrieved from the World Database on Protected Areas (WDPA) are assumed to remain protected. Second, Key Biodiversity Areas (UNEP/KBA) and Intact Forest Landscapes (IFL) are allocated to be protected up to 2050. Third, additional remaining natural land is allocated to be protected with a higher priority for locations with high range size rarity index (IUCN).

In MAGPIE and IMAGE, in the REF scenario the protection of areas reported in the World Database on Protected Areas (WDPA) of the International Union for Conservation of Nature (IUCN) is implemented. In MAGPIE, in addition national protection policies (NPIs) based on climate policy are included. The half earth natural land protection map is gradually implemented in both IMAGE and MAGPIE: One third of the final protected area is assumed by 2030, two thirds by 2040, and the full protection by 2050.

Protected areas conserving 50% of terrestrial area



SI Figure 6-8: Fraction protected area per grid cell to achieve 50% protection of terrestrial area per ecoregion.

S6.5.4 Nitrogen use efficiency

MAGPIE uses the concept of “soil nutrient uptake efficiency”, which is defined as the share of nitrogen taken up by plant biomass from the soil (i.e. nitrogen in crop biomass minus biological fixation minus nitrogen inputs from seed) divided by the soil N inputs (organic and inorganic fertilizer, nitrogen deposition, organic matter loss, residues, fish and pasture-fed livestock products) (Bodirsky et al., 2014) and is updated with recent data (Zhang et al., 2021). The regional (and global) values for this parameter (SNuPE) are shown in SI Table 6-2 in the appendix.

For this publication, the reference nitrogen use efficiency (NUE) scenario starts off from regionally specific historical NUE in 2015 and converges to an efficiency of 60% by 2050 in the REF scenario. In the CLIMATE scenario where a moderate increase in nitrogen use efficiency is assumed, NUE reaches 65% by 2050 in all regions. In the LAND and WATER scenarios where a strong increase in fertilizer efficiency is assumed, NUE reaches 70% by 2050 in all regions. In the TOTAL scenario where a very strong increase is assumed fertilizer efficiency reaches 75% in 2050 in all regions. All scenarios start their trajectory from regional values in 2010.

The GNM model which is part of IMAGE calculates the nitrogen balance account for incoming flows from synthetic fertilizer, animal manure, synthetic fertilizer, N fixation, and N deposition, and for outgoing flows such as uptake by vegetation, leaching, denitrification, erosion, and ammonia volatilization (Bouwman et al., 2017). Future N inputs are determined by the N use efficiency (NUE, $NUE = N \text{ removal} / \text{total N input}$). For a given NUE, total inputs can be calculated as $N \text{ yield} / NUE$. Fertilizer use is the difference between total N inputs, manure, biological N fixation and deposition. In the REF scenario, the historical ratio between NUE change and yield change for the period 1980 – 2015 is used in combination with the future yield change to calculate the NUE change for the period 2015-2050. NUE values do not exceed those for SSP1 (Beusen et al., 2022). Where NUE had a negative trend in the recent past (Eastern Africa, China, and Korea) the future NUE is assumed to decline by < 5% for the period 2015-2050. For China a constant NUE of 0.38 is assumed after 2015 as increased application of synthetic fertilizer is prohibited.

In the scenarios with improved fertilizer use efficiency, a convergence towards maximum achievable NUE values as proposed by (Zhang et al., 2015) on a regional basis is applied (SI Table 6-2). In the CLIMATE scenario where a moderate increase in nutrient use efficiency is assumed plus 50% of the difference between the 2015 values and the assumed maximum achievable NUEs is reached in 2050. In the LAND and WATER scenarios where a strong increase in nutrient use efficiency is assumed plus 70% of the difference between the 2015 values and the assumed maximum achievable NUEs is reached in 2050. In the TOTAL scenario where a very strong increase is assumed plus 80% of the difference between the 2015 values and the assumed maximum achievable NUEs is reached. NUE values > 0.70 for 2015 exceed the target values for 2050, are assumed to point to soil N depletion, and consequently NUE values decline and converge with the Zhang et al. values.

SI Table 6-2a: Nitrogen use efficiency for the historical period (2015) and the scenario period (2050) for all scenarios in MAgPIE

MAgPIE	REF - 2015	REF - 2050	WATER - 2050	LAND - 2050	FOOD - 2050	CLIMATE - 2050	TOTAL - 2050
North America	0.72	0.60	0.70	0.70	0.60	0.65	0.75
Central and South America	0.56	0.60	0.70	0.70	0.60	0.65	0.75
Middle East and Northern Africa	0.60	0.60	0.70	0.70	0.60	0.65	0.75
Sub-Saharan Africa	0.55	0.60	0.70	0.70	0.60	0.65	0.75
Europe	0.69	0.60	0.70	0.70	0.60	0.65	0.75
Russia and Central Asia	0.62	0.60	0.70	0.70	0.60	0.65	0.75
South Asia	0.49	0.60	0.70	0.70	0.60	0.65	0.75
China	0.48	0.60	0.70	0.70	0.60	0.65	0.75
Southeast Asia	0.56	0.60	0.70	0.70	0.60	0.65	0.75
Japan, Korea and Oceania	0.66	0.60	0.70	0.70	0.60	0.65	0.75

SI Table 6-2b: Nitrogen use efficiency for the historical period (2015) and the scenario period (2050) for all scenarios in IMAGE

IMAGE	REF - 2015	REF - 2050	WATER - 2050	LAND - 2050	FOOD - 2050	CLIMATE - 2050	TOTAL - 2050
North America	0.59	0.62	0.70	0.70	0.61	0.67	0.71
Central and South America	0.70	0.68	0.69	0.69	0.68	0.68	0.69
Middle East and Northern Africa	0.36	0.39	0.60	0.60	0.38	0.53	0.63
Sub-Saharan Africa	0.41	0.53	0.61	0.61	0.57	0.55	0.65
Europe	0.62	0.67	0.70	0.70	0.67	0.68	0.72
Russia and Central Asia	0.64	0.66	0.67	0.67	0.64	0.66	0.67
South Asia	0.31	0.29	0.51	0.51	0.29	0.45	0.54
China	0.32	0.38	0.51	0.51	0.38	0.46	0.54
Southeast Asia	0.66	0.60	0.60	0.60	0.60	0.60	0.60
Japan, Korea and Oceania	0.48	0.48	0.62	0.62	0.48	0.58	0.64

References

- Abdalla, M., Hastings, A., Truu, J., Espenberg, M., Mander, Ü., Smith, P., 2016. Emissions of methane from northern peatlands: a review of management impacts and implications for future management options. *Ecol Evol* 6, 7080–7102. <https://doi.org/https://doi.org/10.1002/ece3.2469>
- Albrecht, T.R., Crootof, A., Scott, C.A., 2018. The Water-Energy-Food Nexus: A systematic review of methods for nexus assessment. *Environmental Research Letters* 13, 43002.
- Alcamo, J., Leemans, R., Kreileman, E., 1998. Global change scenarios of the 21st century: Results from the IMAGE 2.1 model.
- Alexander, P., Moran, D., Rounsevell, M.D.A., Smith, P., 2013. Modelling the perennial energy crop market: the role of spatial diffusion. *J R Soc Interface* 10, 20130656.
- Alexandratos, N., Bruinsma, J., 2012. World agriculture towards 2030/2050.
- Alkama, R., Cescatti, A., 2016. Biophysical climate impacts of recent changes in global forest cover. *Science* (1979) 351, 600–604.
- Alkemade, R., van Oorschot, M., Miles, L., Nellemann, C., Bakkenes, M., ten Brink, B., 2009. GLOBIO3: A Framework to Investigate Options for Reducing Global Terrestrial Biodiversity Loss. *Ecosystems* 12, 374–390. <https://doi.org/10.1007/s10021-009-9229-5>
- Anderson, K., Peters, G., 2016. The trouble with negative emissions. *Science* (1979) 354, 182–183.
- Arets, E., van der Meer, P.J., Verwer, C.C., Hengeveld, G.M., Tolkamp, G.W., Nabuurs, G.J., van Oorschot, M., 2011. Global wood production: assessment of industrial round wood supply from forest management systems in different global regions. Alterra, Wageningen-UR.
- Armington, P.S., 1969. A theory of demand for products distinguished by place of production. *Staff Papers* 16, 159–178.
- Asseng, S., Ewert, F., Rosenzweig, C., Jones, J.W., Hatfield, J.L., Ruane, A.C., Boote, K.J., Thorburn, P.J., Rötter, R.P., Cammarano, D., 2013. Uncertainty in simulating wheat yields under climate change. *Nat Clim Chang* 3, 827–832.
- Azar, C., Lindgren, K., Obersteiner, M., Riahi, K., van Vuuren, D.P., den Elzen, K.M.G.J., Möllersten, K., Larson, E.D., 2010. The feasibility of low CO₂ concentration targets and the role of bio-energy with carbon capture and storage (BECCS). *Clim Change* 100, 195–202.
- Bajželj, B., Richards, K.S., Allwood, J.M., Smith, P., Dennis, J.S., Curmi, E., Gilligan, C.A., 2014. Importance of food-demand management for climate mitigation. *Nat Clim Chang* 4, 924.
- Barbarossa, V., Bosmans, J., Wanders, N., King, H., Bierkens, M.F.P., Huijbregts, M.A.J., Schipper, A.M., 2021. Threats of global warming to the world's freshwater fishes. *Nat Commun* 12, 1701. <https://doi.org/10.1038/s41467-021-21655-w>
- Bastin, J.-F., Finegold, Y., Garcia, C., Mollicone, D., Rezende, M., Routh, D., Zohner, C.M., Crowther, T.W., 2019. The global tree restoration potential 365, 76–79. <https://doi.org/10.1126/science.aax0848> %J Science
- Benítez, P.C., McCallum, I., Obersteiner, M., Yamagata, Y., 2007. Global potential for carbon sequestration: Geographical distribution, country risk and policy implications. *Ecological Economics* 60, 572–583. <https://doi.org/https://doi.org/10.1016/j.ecolecon.2005.12.015>
- Berntal, F., Dowdeswell, E., Luo, J., Attard, D., Vellinga, P., Karimanzira, R., 1990. Climate Change: The IPCC Response Strategies.
- Beusen, A.H.W., Bouwman, A.F., van Beek, L.P.H., Mogollón, J.M., Middelburg, J.J., 2016. Global riverine N and P transport to ocean increased during the 20th century despite increased retention along the aquatic continuum. *Biogeosciences* 13, 2441–2451. <https://doi.org/10.5194/bg-13-2441-2016>
- Beusen, A.H.W., Doelman, J.C., van Beek, L.P.H., van Puijenbroek, P.J.T.M., Mogollón, J.M., van Grinsven, H.J.M., Stehfest, E., van Vuuren, D.P., Bouwman, A.F., 2022. Exploring river nitrogen and phosphorus loading and export to global coastal waters in the Shared Socio-economic pathways. *Global Environmental Change* 72, 102426. <https://doi.org/https://doi.org/10.1016/j.gloenvcha.2021.102426>

- Beusen, A.H.W., van Beek, L.P.H., Bouwman, A.F., Mogollón, J.M., Middelburg, J.J., 2015. Coupling global models for hydrology and nutrient loading to simulate nitrogen and phosphorus retention in surface water – description of IMAGE-GNM and analysis of performance. *Geosci Model Dev* 8, 4045–4067. <https://doi.org/10.5194/gmd-8-4045-2015>
- Biemans, H., Siderius, C., Mishra, A., Ahmad, B., 2016. Crop-specific seasonal estimates of irrigation-water demand in South Asia. *Hydrol. Earth Syst. Sci.* 20, 1971–1982. <https://doi.org/10.5194/hess-20-1971-2016>
- Bijl, D.L., Biemans, H., Bogaart, P.W., Dekker, S.C., Doelman, J.C., Stehfest, E., van Vuuren, D.P., 2018. A global analysis of future water deficit based on different allocation mechanisms. *Water Resour Res.*
- Bijl, D.L., Bogaart, P.W., Dekker, S.C., Stehfest, E., de Vries, B.J.M., van Vuuren, D.P., 2017. A physically-based model of long-term food demand. *Global Environmental Change* 45, 47–62.
- Bijl, D.L., Bogaart, P.W., Kram, T., de Vries, B.J.M., van Vuuren, D.P., 2016. Long-term water demand for electricity, industry and households. *Environ Sci Policy* 55, 75–86.
- Billen, G., Lassaletta, L., Garnier, J., 2015. A vast range of opportunities for feeding the world in 2050: trade-off between diet, N contamination and international trade. *Environmental Research Letters* 10, 25001.
- Bobbink, R., Hicks, K., Galloway, J., Spranger, T., Alkemade, R., Ashmore, M., Bustamante, M., Cinderby, S., Davidson, E., Dentener, F., Emmett, B., Erisman, J.-W., Fenn, M., Gilliam, F., Nordin, A., Pardo, L., de Vries, W., 2010. Global assessment of nitrogen deposition effects on terrestrial plant diversity: a synthesis. *Ecological Applications* 20, 30–59. <https://doi.org/https://doi.org/10.1890/08-1140.1>
- Bodirsky, B.L., Dietrich, J.P., Martinelli, E., Stenstad, A., Pradhan, P., Gabrysch, S., Mishra, A., Weindl, I., le Mou  l, C., Rolinski, S., 2020. The ongoing nutrition transition thwarts long-term targets for food security, public health and environmental protection. *Sci Rep* 10, 1–14.
- Bodirsky, B.L., Popp, A., Lotze-Campen, H., Dietrich, J.P., Rolinski, S., Weindl, I., Schmitz, C., M  ller, C., Bonsch, M., Humpen  der, F., Biewald, A., Stevanovic, M., 2014. Reactive nitrogen requirements to feed the world in 2050 and potential to mitigate nitrogen pollution. *Nat Commun* 5, 3858. <https://doi.org/10.1038/ncomms4858>
- Bodirsky, B.L., Popp, A., Weindl, I., Dietrich, J.P., Rolinski, S., Scheffele, L., Schmitz, C., Lotze-Campen, H., 2012. Current state and future scenarios of the global agricultural nitrogen cycle. *Biogeosciences Discussions* 9, 2755.
- Bonan, G.B., 2016. Forests, Climate, and Public Policy: A 500-Year Interdisciplinary Odyssey. *Annu Rev Ecol Evol Syst* 47, 97–121. <https://doi.org/10.1146/annurev-ecolsys-121415-032359>
- Bond, T.C., Streets, D.G., Yarber, K.F., Nelson, S.M., Woo, J., Klimont, Z., 2004. A technology-based global inventory of black and organic carbon emissions from combustion. *Journal of Geophysical Research: Atmospheres* 109.
- Bondeau, A., Smith, P.C., Zaehle, S  n., Schaphoff, S., Lucht, W., Cramer, W., Gerten, D., Lotze-Campen, H., M  LLer, C., Reichstein, M., Smith, B., 2007. Modelling the role of agriculture for the 20th century global terrestrial carbon balance. *Glob Chang Biol* 13, 679–706. <https://doi.org/10.1111/j.1365-2486.2006.01305.x>
- Bonsch, M., Humpen  der, F., Popp, A., Bodirsky, B., Dietrich, J.P., Rolinski, S., Biewald, A., Lotze-Campen, H., Weindl, I., Gerten, D., 2016. Trade-offs between land and water requirements for large-scale bioenergy production. *GCB Bioenergy* 8, 11–24.
- Bonsch, M., Popp, A., Biewald, A., Rolinski, S., Schmitz, C., Weindl, I., Stevanovic, M., H  gner, K., Heinke, J., Ostberg, S., Dietrich, J.P., Bodirsky, B., Lotze-Campen, H., Humpen  der, F., 2015. Environmental flow provision: Implications for agricultural water and land-use at the global scale. *Global Environmental Change* 30, 113–132. <https://doi.org/https://doi.org/10.1016/j.gloenvcha.2014.10.015>
- Bouwman, A.F., Beusen, A.H.W., Lassaletta, L., van Apeldoorn, D.F., van Grinsven, H.J.M., Zhang, J., Ittersum van, M.K., 2017. Lessons from temporal and spatial patterns in global use of N and P fertilizer on cropland. *Sci Rep* 7, 40366. <https://doi.org/10.1038/srep40366>

- Bouwman, A.F., Boumans, L.J.M., Batjes, N.H., 2002. Modeling global annual N₂O and NO emissions from fertilized fields. *Global Biogeochem Cycles* 16.
- Bouwman, A.F., van der Hoek, K.W., Eickhout, B., Soenario, I., 2005. Exploring changes in world ruminant production systems. *Agric Syst* 84, 121–153.
- Braakhekke, M.C., Doelman, J.C., Baas, P., Müller, C., Schaphoff, S., Stehfest, E., van Vuuren, D.P., 2019. Modeling forest plantations for carbon uptake with the LPJmL dynamic global vegetation model. *Earth System Dynamics* 10, 617–630. <https://doi.org/10.5194/esd-10-617-2019>
- Bremer, L.L., Farley, K.A., 2010. Does plantation forestry restore biodiversity or create green deserts? A synthesis of the effects of land-use transitions on plant species richness. *Biodivers Conserv* 19, 3893–3915.
- Brown, C., Seo, B., Rounsevell, M., 2019. Societal breakdown as an emergent property of large-scale behavioural models of land use change. *Earth System Dynamics* 10, 809–845. <https://doi.org/10.5194/esd-10-809-2019>
- Busch, J., Engelmann, J., Cook-Patton, S.C., Griscom, B.W., Kroeger, T., Possingham, H., Shyamsundar, P., 2019. Potential for low-cost carbon dioxide removal through tropical reforestation. *Nat Clim Chang* 9, 463–466. <https://doi.org/10.1038/s41558-019-0485-x>
- Calvin, K., Wise, M., Kyle, P., Patel, P., Clarke, L., Edmonds, J., 2014. Trade-offs of different land and bioenergy policies on the path to achieving climate targets. *Clim Change* 123, 691–704.
- Canadell, J.G., Raupach, M.R., 2008. Managing forests for climate change mitigation. *Science* (1979) 320, 1456–1457.
- CBD, 2010. COP Decision X/2. Strategic plan for biodiversity 2011–2020 and the Aichi Biodiversity Targets.
- Cengic, M., Steinmann, Z.J.N., Defourny, P., Doelman, J.C., Lamarche, C., Stehfest, E., Schipper, A.M., Huijbregts, M.A., 2023. Global Maps of Agricultural Expansion Potential at a 300 m Resolution. *Land* (Basel) 12.
- Chapman, M., Walker, W.S., Cook-Patton, S.C., Ellis, P.W., Farina, M., Griscom, B.W., Baccini, A., 2020. Large climate mitigation potential from adding trees to agricultural lands. *Glob Chang Biol* 26, 4357–4365. <https://doi.org/https://doi.org/10.1111/gcb.15121>
- Ciais, P., Sabine, C., Bala, G., Bopp, L., Brovkin, V., Canadell, J., Chhabra, A., DeFries, R., Galloway, J., Heimann, M., 2014. Carbon and other biogeochemical cycles, in: *Climate Change 2013: The Physical Science Basis. Contribution of Working Group I to the Fifth Assessment Report of the Intergovernmental Panel on Climate Change*. Cambridge University Press, pp. 465–570.
- Clarke, D., McGugin, S., Schmirer, G., Towers, S., 2008. Project Plan for Carbon Sequestration through Afforestation in the Lower Mississippi Alluvial Valley. Laboratory for Sustainable Business, Massachusetts Institute of Technology.
- Clarke, L., Jiang, K., Akimoto, K., Babiker, M., Blanford, G., Fisher-Vanden, K., Hourcade, J.-C., Krey, V., Kriegler, E., Löschel, A., 2014. Assessing transformation pathways.
- Crezee, B., Dargie, G.C., Ewango, C.E.N., Mitchard, E.T.A., Emba B., O., Kanyama T., J., Bola, P., Ndjango, J.-B.N., Girkin, N.T., Bocko, Y.E., Ifo, S.A., Hubau, W., Seidensticker, D., Batumike, R., Imani, G., Cuní-Sánchez, A., Kiahtipes, C.A., Lebamba, J., Wotzka, H.-P., Bean, H., Baker, T.R., Baird, A.J., Boom, A., Morris, P.J., Page, S.E., Lawson, I.T., Lewis, S.L., 2022. Mapping peat thickness and carbon stocks of the central Congo Basin using field data. *Nat Geosci*. <https://doi.org/10.1038/s41561-022-00966-7>
- Dagnachew, A.G., Hof, A.F., Lucas, P.L., van Vuuren, D.P., 2020. Scenario analysis for promoting clean cooking in Sub-Saharan Africa: Costs and benefits. *Energy* 192, 116641. <https://doi.org/https://doi.org/10.1016/j.energy.2019.116641>
- Dagnachew, A.G., Lucas, P.L., Hof, A.F., van Vuuren, D.P., 2018. Trade-offs and synergies between universal electricity access and climate change mitigation in Sub-Saharan Africa. *Energy Policy* 114, 355–366.
- Daiglou, V., 2016. The role of biomass in climate change mitigation: Assessing the long-term dynamics of bioenergy and biochemicals in the land and energy systems. Utrecht University, Utrecht.

- Daioğlu, V., Doelman, J.C., Stehfest, E., Müller, C., Wicke, B., Faaij, A., van Vuuren, D.P., 2017. Greenhouse gas emission curves for advanced biofuel supply chains. *Nat Clim Chang* 7, 920–924. <https://doi.org/10.1038/s41558-017-0006-8>
- Daioğlu, V., Doelman, J.C., Wicke, B., Faaij, A., van Vuuren, D.P., 2019. Integrated assessment of biomass supply and demand in climate change mitigation scenarios. *Global Environmental Change* 54, 88–101. <https://doi.org/https://doi.org/10.1016/j.gloenvcha.2018.11.012>
- Daioğlu, V., Stehfest, E., Wicke, B., Faaij, A., van Vuuren, D.P., 2016. Projections of the availability and cost of residues from agriculture and forestry. *GCB Bioenergy* 8, 456–470. <https://doi.org/https://doi.org/10.1111/gcbb.12285>
- Daioğlu, V., van Ruijven, B.J., van Vuuren, D.P., 2012. Model projections for household energy use in developing countries. *Energy* 37, 601–615.
- Dargie, G.C., Lewis, S.L., Lawson, I.T., Mitchard, E.T.A., Page, S.E., Bocko, Y.E., Ifo, S.A., 2017. Age, extent and carbon storage of the central Congo Basin peatland complex. *Nature* 542, 86–90. <https://doi.org/10.1038/nature21048>
- de Janvry, A., Fafchamps, M., Sadoulet, E., 1991. Peasant household behaviour with missing markets: some paradoxes explained. *The Economic Journal* 101, 1400–1417.
- de Lima, C.Z., Buzan, J.R., Moore, F.C., Baldos, U.L.C., Huber, M., Hertel, T.W., 2021. Heat stress on agricultural workers exacerbates crop impacts of climate change. *Environmental Research Letters* 16, 44020. <https://doi.org/10.1088/1748-9326/abeb9f>
- de Vos, L., Biemans, H., Doelman, J.C., Stehfest, E., van Vuuren, D.P., 2021. Trade-offs between water needs for food, utilities, and the environment—a nexus quantification at different scales. *Environmental Research Letters* 16, 115003. <https://doi.org/10.1088/1748-9326/ac2b5e>
- Dellink, R., Chateau, J., Lanzi, E., Magné, B., 2017. Long-term economic growth projections in the Shared Socioeconomic Pathways. *Global Environmental Change* 42, 200–214.
- den Elzen, M.G.J., Lucas, P.L., van Vuuren, D.P., 2008. Regional abatement action and costs under allocation schemes for emission allowances for achieving low CO₂-equivalent concentrations. *Clim Change* 90, 243–268.
- Dietrich, J.P., Bodirsky, B.L., Humpenöder, F., Weindl, I., Stevanović, M., Karstens, K., Kreidenweis, U., Wang, X., Mishra, A., Klein, D., 2019. MAGPIE 4—a modular open-source framework for modeling global land systems. *Geosci Model Dev* 12, 1299–1317.
- Dietrich, J.P., Popp, A., Lotze-Campen, H., 2013. Reducing the loss of information and gaining accuracy with clustering methods in a global land-use model. *Ecol Modell* 263, 233–243. <https://doi.org/https://doi.org/10.1016/j.ecolmodel.2013.05.009>
- Dietrich, J.P., Schmitz, C., Lotze-Campen, H., Popp, A., Müller, C., 2014. Forecasting technological change in agriculture—An endogenous implementation in a global land use model. *Technol Forecast Soc Change* 81, 236–249. <https://doi.org/https://doi.org/10.1016/j.techfore.2013.02.003>
- Dinerstein, E., Olson, D., Joshi, A., Vynne, C., Burgess, N.D., Wikramanayake, E., Hahn, N., Palminteri, S., Hedao, P., Noss, R., Hansen, M., Locke, H., Ellis, E.C., Jones, B., Barber, C.V., Hayes, R., Kormos, C., Martin, V., Crist, E., Sechrest, W., Price, L., Baillie, J.E.M., Weeden, D., Suckling, K., Davis, C., Sizer, N., Moore, R., Thau, D., Birch, T., Potapov, P., Turubanova, S., Tyukavina, A., de Souza, N., Pintea, L., Brito, J.C., Llewellyn, O.A., Miller, A.G., Patzelt, A., Ghazanfar, S.A., Timberlake, J., Klöser, H., Shennan-Farpon, Y., Kindt, R., Lillesø, J.-P.B., van Breugel, P., Graudal, L., Voge, M., Al-Shammari, K.F., Saleem, M., 2017. An Ecoregion-Based Approach to Protecting Half the Terrestrial Realm. *Bioscience* 67, 534–545. <https://doi.org/10.1093/biosci/bix014>
- Dixon, P., van Meijl, H., Rimmer, M., Shutes, L., Tabeau, A., 2016. RED versus REDD: Biofuel policy versus forest conservation. *Econ Model* 52, 366–374.
- Doelman, J.C., Stehfest, E., Tabeau, A., van Meijl, H., 2019. Making the Paris agreement climate targets consistent with food security objectives. *Glob Food Sec* 23, 93–103. <https://doi.org/https://doi.org/10.1016/j.gfs.2019.04.003>

- Doelman, J.C., Stehfest, E., Tabeau, A., van Meijl, H., Lassaletta, L., Gernaat, D.E.H.J., Hermans, K., Harmsen, M., Daioglou, V., Biemans, H., van der Sluis, S., van Vuuren, D.P., 2018. Exploring SSP land-use dynamics using the IMAGE model: Regional and gridded scenarios of land-use change and land-based climate change mitigation. *Global Environmental Change* 48, 119–135. <https://doi.org/10.1016/j.gloenvcha.2017.11.014>
- Doelman, J.C., Stehfest, E., van Vuuren, D.P., Tabeau, A., Hof, A.F., Braakhekke, M.C., Gernaat, D.E.H.J., van den Berg, M., van Zeist, W.J., Daioglou, V., van Meijl, H., Lucas, P.L., 2020. Afforestation for climate change mitigation: Potentials, risks and trade-offs. *Glob Chang Biol* 26. <https://doi.org/10.1111/gcb.14887>
- Dutschke, M., 2001. Permanence of CDM forests or non-permanence of land use related carbon credits? HWWA discussion paper.
- Edelenbosch, O., van den Berg, M., de Boer, H.-S., Chen, H., Daioglou, V., Dekker, M., Doelman, J., den Elzen, M., Frinking, V., Harmsen, M., Hof, A., Mikropoulos, E., van Sluisveld, M., Tagomori, I., van Vuuren, D., 2022. Mitigating greenhouse gas emissions in hard-to-abate sectors. The Hague.
- Eitelberg, D.A., van Vliet, J., Verburg, P.H., 2015. A review of global potentially available cropland estimates and their consequences for model-based assessments. *Glob Chang Biol* 21, 1236–1248. <https://doi.org/10.1111/gcb.12733>
- Eker, S., Reese, G., Obersteiner, M., 2019. Modelling the drivers of a widespread shift to sustainable diets. *Nat Sustain* 2, 725–735. <https://doi.org/10.1038/s41893-019-0331-1>
- Ellis, E.C., Ramankutty, N., 2008. Putting people in the map: anthropogenic biomes of the world. *Front Ecol Environ* 6, 439–447. <https://doi.org/10.1890/070062>
- Erb, K.H., Lauk, C., Kastner, T., Mayer, A., Theurl, M.C., Haberl, H., 2016. Exploring the biophysical option space for feeding the world without deforestation. *Nat Commun* 7. <https://doi.org/10.1038/pj.2016.37>
- 10.1038/ncomms11382
- ESA, 2017. Climate Change Initiative (ESA-CCI), v2.07 [WWW Document].
- FAO, 2018a. Global Forest Resource Assessment 2020 - Terms and Definitions. Rome.
- FAO, 2018b. The future of food and agriculture: Alternative Pathways to 2050. Food and Agriculture Organization of the United Nations, Rome.
- FAO, 2015. Global Forest Resource Assessment. Rome.
- FAO, 2008. FAO methodology for the measurement of food deprivation updating the minimum dietary energy requirements. FAO, Rome.
- FAO, 1996. Rome Declaration on World Food Security.
- FAOSTAT, 2022. FAOSTAT, Food and Agriculture Organization of the United Nations [WWW Document]. URL <http://www.fao.org/faostat> (accessed 12.21.22).
- FAOSTAT, 2020. FAOSTAT, Food and Agriculture Organization of the United Nations [WWW Document]. URL <http://www.fao.org/faostat>
- FAOSTAT, 2017. FAOSTAT, Food and Agriculture Organization of the United Nations [WWW Document]. URL <http://www.fao.org/faostat>
- FAOSTAT, 2013. FAOSTAT, Food and Agriculture Organization of the United Nations [WWW Document]. URL www.fao.org/faostat
- Fischer, G., Nachtergaele, F., Prieler, S., van Velthuizen, H.T., Verelst, L., Wiberg, D., 2008. Global agro-ecological zones assessment for agriculture (GAEZ 2008). IIASA, Laxenburg, Austria and FAO, Rome, Italy 10.
- Fischer, R.A., Byerlee, D., Edmeades, G., 2014. Crop yields and global food security. ACIAR: Canberra, ACT.
- Foley, J.A., Defries, R., Asner, G.P., Barford, C., Bonan, G., Carpenter, S.R., Chapin, F.S., Coe, M.T., Daily, G.C., Gibbs, H.K., Helkowski, J.H., Holloway, T., Howard, E.A., Kucharik, C.J., Monfreda, C., Patz, J.A., Prentice, I.C., Ramankutty, N., Snyder, P.K., 2005. Global consequences of land use. *Science* (1979) 309, 570–574. <https://doi.org/10.1126/science.1111772>

- Foley, J.A., Ramankutty, N., Brauman, K.A., Cassidy, E.S., Gerber, J.S., Johnston, M., Mueller, N.D., O'Connell, C., Ray, D.K., West, P.C., Balzer, C., Bennett, E.M., Carpenter, S.R., Hill, J., Monfreda, C., Polasky, S., Rockstrom, J., Sheehan, J., Siebert, S., Tilman, D., Zaks, D.P., 2011. Solutions for a cultivated planet. *Nature* 478, 337–342. <https://doi.org/10.1038/nature10452>
- Frank, S., Gusti, M., Havlík, P., Lauri, P., DiFulvio, F., Forsell, N., Hasegawa, T., Krisztin, T., Palazzo, A., Valin, H., 2021. Land-based climate change mitigation potentials within the agenda for sustainable development. *Environmental Research Letters* 16, 24006. <https://doi.org/10.1088/1748-9326/abc58a>
- Frank, S., Havlík, P., Soussana, J.-F., Levesque, A., Valin, H., Wollenberg, E., Kleinwechter, U., Fricko, O., Gusti, M., Herrero, M., 2017. Reducing greenhouse gas emissions in agriculture without compromising food security? *Environmental Research Letters* 12, 105004.
- Frank, S., Havlík, P., Stehfest, E., van Meijl, H., Witzke, P., Pérez-Domínguez, I., van Dijk, M., Doelman, J.C., Fellmann, T., Koopman, J.F.L., Tabeau, A., Valin, H., 2019. Agricultural non-CO₂ emission reduction potential in the context of the 1.5 °C target. *Nat Clim Chang* 9, 66–72. <https://doi.org/10.1038/s41558-018-0358-8>
- Fricko, O., Havlík, P., Rogelj, J., Klimont, Z., Gusti, M., Johnson, N., Kolp, P., Strubegger, M., Valin, H., Amann, M., 2017. The marker quantification of the Shared Socioeconomic Pathway 2: A middle-of-the-road scenario for the 21st century. *Global Environmental Change* 42, 251–267.
- Friedlingstein, P., Jones, M.W., O'Sullivan, M., Andrew, R.M., Bakker, D.C.E., Hauck, J., le Quéré, C., Peters, G.P., Peters, W., Pongratz, J., Sitch, S., Canadell, J.G., Ciais, P., Jackson, R.B., Alin, S.R., Anthoni, P., Bates, N.R., Becker, M., Bellouin, N., Bopp, L., Chau, T.T.T., Chevallier, F., Chini, L.P., Cronin, M., Currie, K.I., Decharme, B., Djeutchouang, L.M., Dou, X., Evans, W., Feely, R.A., Feng, L., Gasser, T., Gilfillan, D., Gkritzalis, T., Grassi, G., Gregor, L., Gruber, N., Gürses, Ö., Harris, I., Houghton, R.A., Hurtt, G.C., Iida, Y., Ilyina, T., Luijckx, I.T., Jain, A., Jones, S.D., Kato, E., Kennedy, D., Klein Goldewijk, K., Knauer, J., Korsbakken, J.I., Körtzinger, A., Landschützer, P., Lauvset, S.K., Lefèvre, N., Lienert, S., Liu, J., Marland, G., McGuire, P.C., Melton, J.R., Munro, D.R., Nabel, J.E.M.S., Nakaoka, S.-I., Niwa, Y., Ono, T., Pierrot, D., Poulter, B., Rehder, G., Resplandy, L., Robertson, E., Rödenbeck, C., Rosan, T.M., Schwinger, J., Schwingshackl, C., Séférian, R., Sutton, A.J., Sweeney, C., Tanhua, T., Tans, P.P., Tian, H., Tillbrook, B., Tubiello, F., van der Werf, G.R., Vuichard, N., Wada, C., Wanninkhof, R., Watson, A.J., Willis, D., Wiltshire, A.J., Yuan, W., Yue, C., Yue, X., Zaehle, S., Zeng, J., 2022. Global Carbon Budget 2021. *Earth Syst Sci Data* 14, 1917–2005. <https://doi.org/10.5194/essd-14-1917-2022>
- Frieler, K., Lange, S., Piontek, F., Reyer, C.P.O., Schewe, J., Warszawski, L., Zhao, F., Chini, L., Denvil, S., Emanuel, K., Geiger, T., Halladay, K., Hurtt, G., Mengel, M., Murakami, D., Ostberg, S., Popp, A., Riva, R., Stevanovic, M., Suzuki, T., Volkholz, J., Burke, E., Ciais, P., Ebi, K., Eddy, T.D., Elliott, J., Galbraith, E., Gosling, S.N., Hattermann, F., Hickler, T., Hinkel, J., Hof, C., Huber, V., Jägermeyr, J., Krysanova, V., Marcé, R., Müller Schmied, H., Mouratiadou, I., Pierson, D., Tittensor, D.P., Vautard, R., van Vliet, M., Biber, M.F., Betts, R.A., Bodirsky, B.L., Deryng, D., Frolking, S., Jones, C.D., Lotze, H.K., Lotze-Campen, H., Sahajpal, R., Thonicke, K., Tian, H., Yamagata, Y., 2017. Assessing the impacts of 1.5 °C global warming – simulation protocol of the Inter-Sectoral Impact Model Intercomparison Project (ISIMIP2b). *Geosci. Model Dev.* 10, 4321–4345. <https://doi.org/10.5194/gmd-10-4321-2017>
- Fritz, S., See, L., van der Velde, M., Nalepa, R.A., Perger, C., Schill, C., McCallum, I., Schepaschenko, D., Kraxner, F., Cai, X., Zhang, X., Ortner, S., Hazarika, R., Cipriani, A., di Bella, C., Rabia, A.H., Garcia, A., Vakolyuk, M., Singha, K., Beget, M.E., Erasmí, S., Albrecht, F., Shaw, B., Obersteiner, M., 2013. Downgrading recent estimates of land available for biofuel production. *Environ Sci Technol* 47, 1688–1694. <https://doi.org/10.1021/es303141h>
- Fujimori, S., Hasegawa, T., Krey, V., Riahi, K., Bertram, C., Bodirsky, B.L., Bosetti, V., Callen, J., Després, J., Doelman, J., Drouet, L., Emmerling, J., Frank, S., Fricko, O., Havlík, P., Humpenöder, F., Koopman, J.F.L., van Meijl, H., Ochi, Y., Popp, A., Schmitz, A., Takahashi, K., van Vuuren, D., 2019. A multi-model assessment of food security implications of climate change mitigation. *Nat Sustain* 2, 386–396. <https://doi.org/10.1038/s41893-019-0286-2>

- Fujimori, S., Hasegawa, T., Masui, T., Takahashi, K., 2014. Land use representation in a global CGE model for long-term simulation: CET vs. logit functions. *Food Secur* 6, 685–699.
- Fujimori, S., Hasegawa, T., Rogelj, J., Su, X., Havlik, P., Krey, V., Takahashi, K., Riahi, K., 2018. Inclusive climate change mitigation and food security policy under 1.5°C climate goal. *Environmental Research Letters* 13, 74033.
- Gernaat, D.E.H.J., Bogaart, P.W., Vuuren, D.P. van, Biemans, H., Niessink, R., 2017. High-resolution assessment of global technical and economic hydropower potential. *Nat Energy* 2, 821–828. <https://doi.org/10.1038/s41560-017-0006-y>
- Gernaat, D.E.H.J., Calvin, K., Lucas, P.L., Luderer, G., Otto, S.A.C., Rao, S., Strefler, J., van Vuuren, D.P., 2015. Understanding the contribution of non-carbon dioxide gases in deep mitigation scenarios. *Global Environmental Change* 33, 142–153. <https://doi.org/10.1016/j.gloenvcha.2015.04.010>
- Gernaat, D.E.H.J., de Boer, H.S., Daioglou, V., Yalaw, S.G., Müller, C., van Vuuren, D.P., 2021. Climate change impacts on renewable energy supply. *Nat Clim Chang* 11, 119–125. <https://doi.org/10.1038/s41558-020-00949-9>
- Gerten, D., Hoff, H., Rockström, J., Jägermeyr, J., Kummu, M., Pastor, A. v., 2013. Towards a revised planetary boundary for consumptive freshwater use: role of environmental flow requirements. *Curr Opin Environ Sustain* 5, 551–558. <https://doi.org/https://doi.org/10.1016/j.cosust.2013.11.001>
- Grand-Clement, E., Anderson, K., Smith, D., Luscombe, D., Gatis, N., Ross, M., Brazier, R.E., 2013. Evaluating ecosystem goods and services after restoration of marginal upland peatlands in South-West England. *Journal of Applied Ecology* 50, 324–334. <https://doi.org/https://doi.org/10.1111/1365-2664.12039>
- Grassini, P., Eskridge, K.M., Cassman, K.G., 2013. Distinguishing between yield advances and yield plateaus in historical crop production trends. *Nat Commun* 4.
- Griscom, B.W., Adams, J., Ellis, P.W., Houghton, R.A., Lomax, G., Miteva, D.A., Schlesinger, W.H., Shoch, D., Siikamäki, J. v, Smith, P., Woodbury, P., Zganjar, C., Blackman, A., Campari, J., Conant, R.T., Delgado, C., Elias, P., Gopalakrishna, T., Hamsik, M.R., Herrero, M., Kiesecker, J., Landis, E., Laestadius, L., Leavitt, S.M., Minnemeyer, S., Polasky, S., Potapov, P., Putz, F.E., Sanderman, J., Silvius, M., Wollenberg, E., Fargione, J., 2017. Natural climate solutions 114, 11645–11650. <https://doi.org/10.1073/pnas.1710465114> %J Proceedings of the National Academy of Sciences
- Gumbricht, T., Roman-Cuesta, R.M., Verchot, L., Herold, M., Wittmann, F., Householder, E., Herold, N., Murdiyarto, D., 2017. An expert system model for mapping tropical wetlands and peatlands reveals South America as the largest contributor. *Glob Chang Biol* 23, 3581–3599. <https://doi.org/https://doi.org/10.1111/gcb.13689>
- Gustavsson, J., Cederberg, C., Sonesson, U., van Otterdijk, R., Meybeck, A., 2011. Global food losses and food waste. Food and Agriculture Organization of the United Nations, Rom.
- Hall, J.M., van Holt, T., Daniels, A.E., Balthazar, V., Lambin, E.F., 2012. Trade-offs between tree cover, carbon storage and floristic biodiversity in reforesting landscapes. *Landsc Ecol* 27, 1135–1147.
- Hansen, M.C., Potapov, P. v, Moore, R., Hancher, M., Turubanova, S.A., Tyukavina, A., Thau, D., Stehman, S. v, Goetz, S.J., Loveland, T.R., Kommareddy, A., Egorov, A., Chini, L., Justice, C.O., Townshend, J.R., 2013. High-resolution global maps of 21st-century forest cover change. *Science* (1979) 342, 850–853. <https://doi.org/10.1126/science.1244693>
- Hanssen, S. v, Daioglou, V., Steinmann, Z.J.N., Doelman, J.C., van Vuuren, D.P., Huijbregts, M.A.J., 2020. The climate change mitigation potential of bioenergy with carbon capture and storage. *Nat Clim Chang* 10, 1023–1029. <https://doi.org/10.1038/s41558-020-0885-y>
- Harmesen, J.H.M., van Vuuren, D.P., Nayak, D.R., Hof, A.F., Höglund-Isaksson, L., Lucas, P.L., Nielsen, J.B., Smith, P., Stehfest, E., 2019. Long-term marginal abatement cost curves of non-CO2 greenhouse gases. *Environ Sci Policy* 99, 136–149. <https://doi.org/https://doi.org/10.1016/j.envsci.2019.05.013>
- Harris, N.L., Brown, S., Hagen, S.C., Saatchi, S.S., Petrova, S., Salas, W., Hansen, M.C., Potapov, P. v, Lotsch, A., 2012. Baseline map of carbon emissions from deforestation in tropical regions. *Science* (1979) 336, 1573–1576.

- Hasegawa, T., Fujimori, S., Havlík, P., Valin, H., Bodirsky, B.L., Doelman, J.C., Fellmann, T., Kyle, P., Koopman, J.F.L., Lotze-Campen, H., Mason-D'Croz, D., Ochi, Y., Pérez Domínguez, I., Stehfest, E., Sulser, T.B., Tabeau, A., Takahashi, K., Takakura, J., van Meijl, H., van Zeist, W.-J., Wiebe, K., Witzke, P., 2018. Risk of increased food insecurity under stringent global climate change mitigation policy. *Nat Clim Chang* 8, 699–703. <https://doi.org/10.1038/s41558-018-0230-x>
- Hasegawa, T., Fujimori, S., Ito, A., Takahashi, K., Masui, T., 2017. Global land-use allocation model linked to an integrated assessment model. *Science of The Total Environment* 580, 787–796. <https://doi.org/https://doi.org/10.1016/j.scitotenv.2016.12.025>
- Hasegawa, T., Fujimori, S., Shin, Y., Tanaka, A., Takahashi, K., Masui, T., 2015a. Consequence of climate mitigation on the risk of hunger. *Environ Sci Technol* 49, 7245–7253.
- Hasegawa, T., Fujimori, S., Takahashi, K., Masui, T., 2015b. Scenarios for the risk of hunger in the twenty-first century using Shared Socioeconomic Pathways. *Environmental Research Letters* 10, 14010.
- Hasegawa, T., Sands, R.D., Brunelle, T., Cui, Y., Frank, S., Fujimori, S., Popp, A., 2020. Food security under high bioenergy demand toward long-term climate goals. *Clim Change* 163, 1587–1601. <https://doi.org/10.1007/s10584-020-02838-8>
- Hausfather, Z., Peters, G.P., 2020. Emissions—the ‘business as usual’ story is misleading.
- Havlík, P., Schneider, U.A., Schmid, E., Böttcher, H., Fritz, S., Skalský, R., Aoki, K., Cara, S. de, Kindermann, G., Kraxner, F., Leduc, S., McCallum, I., Mosnier, A., Sauer, T., Obersteiner, M., 2011. Global land-use implications of first and second generation biofuel targets. *Energy Policy* 39, 5690–5702. <https://doi.org/10.1016/j.enpol.2010.03.030>
- Havlík, P., Valin, H., Herrero, M., Obersteiner, M., Schmid, E., Rufino, M.C., Mosnier, A., Thornton, P.K., Böttcher, H., Conant, R.T., 2014. Climate change mitigation through livestock system transitions. *Proceedings of the National Academy of Sciences* 201308044.
- Havlík, P., Valin, H., Mosnier, A., Obersteiner, M., Baker, J.S., Herrero, M., Rufino, M.C., Schmid, E., 2012. Crop Productivity and the Global Livestock Sector: Implications for Land Use Change and Greenhouse Gas Emissions. *Am J Agric Econ* 95, 442–448. <https://doi.org/10.1093/ajae/aas085>
- Hayman, G.D., Comyn-Platt, E., Huntingford, C., Harper, A.B., Powell, T., Cox, P.M., Collins, W., Webber, C., Lowe, J., Sitch, S., House, J.I., Doelman, J.C., van Vuuren, D.P., Chadburn, S.E., Burke, E., Gedney, N., 2020. Regional variation in the effectiveness of methane-based and land-based climate mitigation options. *Earth Syst. Dynam. Discuss.* 2020, 1–41. <https://doi.org/10.5194/esd-2020-24>
- Herrero, M., Havlík, P., Valin, H., Notenbaert, A., Rufino, M.C., Thornton, P.K., Blümmel, M., Weiss, F., Grace, D., Obersteiner, M., 2013. Biomass use, production, feed efficiencies, and greenhouse gas emissions from global livestock systems. *Proceedings of the National Academy of Sciences* 110, 20888–20893.
- Herrero, M., Henderson, B., Havlík, P., Thornton, P.K., Conant, R., Smith, P., Wirsenius, S., Hristov, A.N., Gerber, P., Gill, M., Butterbach-Bahl, K., Valin, H., Garnett, T., Stehfest, E., 2016. Greenhouse gas mitigation potentials in the livestock sector. *Nat Clim Chang* 6, 9. <https://doi.org/10.1038/nclimate2925>
- Hertel, T.W., 1997. *Global trade analysis: modeling and applications*.
- Hertel, T.W., de Lima, C.Z., 2020. Viewpoint: Climate impacts on agriculture: Searching for keys under the streetlight. *Food Policy* 95, 101954. <https://doi.org/https://doi.org/10.1016/j.foodpol.2020.101954>
- Hiederer, R., Köchy, M., 2011. Global soil organic carbon estimates and the harmonized world soil database. *EUR* 79, 10–2788.
- Hilderink, H., Lucas, P., ten Hove, A., Kok, M., de Vos, M., Janssen, P.C.M., Meijer, J., Faber, A., Ignaciuk, A., Petersen, A.C., 2008. *Towards a global Integrated sustainability model: GISMO1. 0 status report*.
- Hoff, H., 2011. *Understanding the nexus: Background paper for the Bonn2011 Nexus Conference*.
- Höhne, N., den Elzen, M., Escalante, D., 2014. Regional GHG reduction targets based on effort sharing: a comparison of studies. *Climate Policy* 14, 122–147. <https://doi.org/10.1080/14693062.2014.849452>
- Hollmann, R., Merchant, C.J., Saunders, R., Downy, C., Buchwitz, M., Cazenave, A., Chuvieco, E., Defourny, P., de Leeuw, G., Forsberg, R., 2013. The ESA climate change initiative: Satellite data records for essential climate variables. *Bull Am Meteorol Soc* 94, 1541–1552.

- Hoogwijk, M., Faaij, A., de Vries, B., Turkenburg, W., 2009. Exploration of regional and global cost-supply curves of biomass energy from short-rotation crops at abandoned cropland and rest land under four IPCC SRES land-use scenarios. *Biomass Bioenergy* 33, 26–43. <https://doi.org/10.1016/j.biombioe.2008.04.005>
- Hoogwijk, M., Faaij, A., van den Broek, R., Berndes, G., Gielen, D., Turkenburg, W., 2003. Exploration of the ranges of the global potential of biomass for energy. *Biomass Bioenergy* 25, 119–133. [https://doi.org/10.1016/s0961-9534\(02\)00191-5](https://doi.org/10.1016/s0961-9534(02)00191-5)
- Hooijer, A., Page, S., Jauhainen, J., Lee, W.A., Lu, X.X., Idris, A., Anshari, G., 2012. Subsidence and carbon loss in drained tropical peatlands. *Biogeosciences* 9, 1053.
- Hoskins, A.J., Bush, A., Gilmore, J., Harwood, T., Hudson, L.N., Ware, C., Williams, K.J., Ferrier, S., 2016. Downscaling land-use data to provide global 30" estimates of five land-use classes. *Ecol Evol* 6, 3040–3055. <https://doi.org/https://doi.org/10.1002/ece3.2104>
- Howarth, R., Chan, F., Conley, D.J., Garnier, J., Doney, S.C., Marino, R., Billen, G., 2011. Coupled biogeochemical cycles: eutrophication and hypoxia in temperate estuaries and coastal marine ecosystems. *Front Ecol Environ* 9, 18–26. <https://doi.org/https://doi.org/10.1890/100008>
- Humpenöder, F., Bodirsky, B.L., Weindl, I., Lotze-Campen, H., Linder, T., Popp, A., 2022. Projected environmental benefits of replacing beef with microbial protein. *Nature* 605, 90–96. <https://doi.org/10.1038/s41586-022-04629-w>
- Humpenöder, F., Karstens, K., Lotze-Campen, H., Leifeld, J., Menichetti, L., Barthelmes, A., Popp, A., 2020. Peatland protection and restoration are key for climate change mitigation. *Environmental Research Letters* 15, 104093. <https://doi.org/10.1088/1748-9326/abae2a>
- Humpenöder, F., Popp, A., Bodirsky, B.L., Weindl, I., Biewald, A., Lotze-Campen, H., Dietrich, J.P., Klein, D., Kreidenweis, U., Müller, C., Rolinski, S., Stevanovic, M., 2018. Large-scale bioenergy production: how to resolve sustainability trade-offs? *Environmental Research Letters* 13, 24011.
- Humpenöder, F., Popp, A., Dietrich, J.P., Klein, D., Lotze-Campen, H., Bonsch, M., Bodirsky, B.L., Weindl, I., Stevanovic, M., Müller, C., 2014. Investigating afforestation and bioenergy CCS as climate change mitigation strategies. *Environmental Research Letters* 9, 64029. <https://doi.org/10.1088/1748-9326/9/6/064029>
- Hurrell, J.W., Holland, M.M., Gent, P.R., Ghan, S., Kay, J.E., Kushner, P.J., Lamarque, J.-F., Large, W.G., Lawrence, D., Lindsay, K., Lipscomb, W.H., Long, M.C., Mahowald, N., Marsh, D.R., Neale, R.B., Rasch, P., Vavrus, S., Vertenstein, M., Bader, D., Collins, W.D., Hack, J.J., Kiehl, J., Marshall, S., 2013. The Community Earth System Model: A Framework for Collaborative Research. *Bull Am Meteorol Soc* 94, 1339–1360. <https://doi.org/10.1175/BAMS-D-12-00121.1>
- Hurt, G.C., Chini, L.P., Frohking, S., Betts, R.A., Feddema, J., Fischer, G., Fisk, J.P., Hibbard, K., Houghton, R.A., Janetos, A., Jones, C.D., Kindermann, G., Kinoshita, T., Klein Goldewijk, K., Riahi, K., Shevliakova, E., Smith, S., Stehfest, E., Thomson, A., Thornton, P., van Vuuren, D.P., Wang, Y.P., 2011. Harmonization of land-use scenarios for the period 1500–2100: 600 years of global gridded annual land-use transitions, wood harvest, and resulting secondary lands. *Clim Change* 109, 117–161. <https://doi.org/10.1007/s10584-011-0153-2>
- IEA, 2017. World Energy Balances 2017. https://doi.org/https://doi.org/10.1787/world_energy_bal-2017-en
- Immerzeel, D.J., Verweij, P., Hilst, F., Faaij, A.P.C., 2014. Biodiversity impacts of bioenergy crop production: a state-of-the-art review. *GCB Bioenergy* 6, 183–209.
- IPBES, 2019. Summary for policymakers of the global assessment report on biodiversity and ecosystem services of the Intergovernmental Science-Policy Platform on Biodiversity and Ecosystem Services. IPBES Secretariat, Bonn, Germany.
- IPCC, 2022. Climate Change 2022, Mitigation of Climate Change: Working Group III contribution to the Sixth Assessment Report of the Intergovernmental Panel on Climate Change. Cambridge University, Cambridge.

- IPCC, 2021. IPCC, 2021: Summary for Policymakers. In: *Climate Change 2021: The Physical Science Basis. Contribution of Working Group I to the Sixth Assessment Report of the Intergovernmental Panel on Climate Change*, in: Masson-Delmotte, V., Zhai, P., Pirani, A., S.L. Connors, C. Péan, S. Berger, N. Caud, Y. Chen, L. Goldfarb, M.I. Gomis, M. Huang, K. Leitzell, E. Lonnoy, J.B.R. Matthews, T.K. Maycock, T. Waterfield, O. Yelekçi, R. Yu, B. Zhou (Eds.), . Cambridge University, Cambridge, UK, and New York, USA. <https://doi.org/10.1017/9781009157896>.
- IPCC, 2019a. IPCC, 2019: *Climate Change and Land: an IPCC special report on climate change, desertification, land degradation, sustainable land management, food security, and greenhouse gas fluxes in terrestrial ecosystems*.
- IPCC, 2019b. IPCC, 2019: *Climate Change and Land: an IPCC special report on climate change, desertification, land degradation, sustainable land management, food security, and greenhouse gas fluxes in terrestrial ecosystems - summary for policymakers*. Cambridge University Press, Cambridge, UK and New York, NY, USA.
- IPCC, 2018. *Summary for Policymakers*. In: *Global warming of 1.5°C. An IPCC Special Report on the impacts of global warming of 1.5°C above pre-industrial levels and related global greenhouse gas emission pathways, in the context of strengthening the global response to the threat of climate change, sustainable development, and efforts to eradicate poverty*. World Meteorological Organization, Geneva, Switzerland.
- IPCC, 2014a. 2013 supplement to the 2006 IPCC guidelines for national greenhouse gas inventories: *Wetlands*. IPCC, Switzerland.
- IPCC, 2014b. *Climate Change 2014: Synthesis Report. Contribution of Working Groups I, II and III to the Fifth Assessment Report of the Intergovernmental Panel on Climate Change*. IPCC, Switzerland.
- IPCC, 2006. *IPCC guidelines for national greenhouse gas inventories*. Institute for Global Environmental Strategies (IGES) , Hayama, Japan.
- IPCC, 2000a. *Special Report on Emissions Scenarios* . Cambridge University Press, Cambridge.
- IPCC, 2000b. *Land Use, Land-Use Change, and Forestry. A Special Report of the Intergovernmental Panel on Climate Change*. Cambridge University Press, Cambridge.
- IUCN, U.-W., 2015. *The World Database on protected Areas [WWW Document]*. URL www.protectedplanet.net
- Iyer, G.C., Clarke, L.E., Edmonds, J.A., Flannery, B.P., Hultman, N.E., McJeon, H.C., Victor, D.G., 2015. Improved representation of investment decisions in assessments of CO₂ mitigation. *Nat Clim Chang* 5, 436.
- Jackson, R.B., Randerson, J.T., Canadell, J.G., Anderson, R.G., Avissar, R., Baldocchi, D.D., Bonan, G.B., Caldeira, K., Diffenbaugh, N.S., Field, C.B., 2008. Protecting climate with forests. *Environmental Research Letters* 3, 44006.
- Jaenicke, J., Wösten, H., Budiman, A., Siebert, F., 2010. Planning hydrological restoration of peatlands in Indonesia to mitigate carbon dioxide emissions. *Mitig Adapt Strateg Glob Chang* 15, 223–239. <https://doi.org/10.1007/s11027-010-9214-5>
- Jägermeyr, J., Gerten, D., Heinke, J., Schaphoff, S., Kumm, M., Lucht, W., 2015. Water savings potentials of irrigation systems: global simulation of processes and linkages. *Hydrol Earth Syst Sci* 19, 3073–3091.
- Jägermeyr, J., Müller, C., Ruane, A.C., Elliott, J., Balkovic, J., Castillo, O., Faye, B., Foster, I., Folberth, C., Franke, J.A., Fuchs, K., Guarin, J.R., Heinke, J., Hoogenboom, G., Iizumi, T., Jain, A.K., Kelly, D., Khabarov, N., Lange, S., Lin, T.-S., Liu, W., Mialyk, O., Minoli, S., Moyer, E.J., Okada, M., Phillips, M., Porter, C., Rabin, S.S., Scheer, C., Schneider, J.M., Schyns, J.F., Skalsky, R., Smerald, A., Stella, T., Stephens, H., Webber, H., Zabel, F., Rosenzweig, C., 2021. Climate impacts on global agriculture emerge earlier in new generation of climate and crop models. *Nat Food* 2, 873–885. <https://doi.org/10.1038/s43016-021-00400-y>
- Janse, J.H., van Dam, A.A., Hes, E.M.A., de Klein, J.J.M., Finlayson, C.M., Janssen, A.B.G., van Wijk, D., Mooij, W.M., Verhoeven, J.T.A., 2019. Towards a global model for wetlands ecosystem services. *Curr Opin Environ Sustain* 36, 11–19. <https://doi.org/https://doi.org/10.1016/j.cosust.2018.09.002>

- Janzen, H.H., van Groenigen, K.J., Powlson, D.S., Schwinghamer, T., van Groenigen, J.W., 2022. Photosynthetic limits on carbon sequestration in croplands. *Geoderma* 416, 115810. <https://doi.org/https://doi.org/10.1016/j.geoderma.2022.115810>
- Jia, G., Shevliakova, E., Artaxo, P., de Noblet-Ducoudré, N., Houghton, R., House, J., Kitajima, K., Lennard, C., Popp, A., Sirin, A., Sukumar, R., Verchot, L., 2019. Land–climate interactions. In: *Climate Change and Land: an IPCC special report on climate change, desertification, land degradation, sustainable land management, food security, and greenhouse gas fluxes in terrestrial ecosystem*, in: P.R. Shukla, J. Skea, E. Calvo Buendia, v. Masson-Delmotte, H.-O. Pörtner, D.C. Roberts, P. Zhai, R. Slade, S. Connors, R. van Diemen, M. Ferrat, E. Haughey, S. Luz, S. Neogi, M. Pathak, J. Petzold, J. Portugal Pereira, P. Vyas, E. Huntley, K. Kissick, M. Belkacemi, J. Malley (Eds.), . Cambridge University Press, Cambridge, UK and New York, NY, USA.
- Jiang, L., O'Neill, B.C., 2017. Global urbanization projections for the Shared Socioeconomic Pathways. *Global Environmental Change* 42, 193–199.
- Johnson, N., Burek, P., Byers, E., Falchetta, G., Flörke, M., Fujimori, S., Havlik, P., Hejazi, M., Hunt, J., Krey, V., 2019. Integrated solutions for the Water-Energy-Land Nexus: Are global models rising to the challenge? *Water (Basel)* 11, 2223.
- Jones, A.D., Calvin, K. v, Collins, W.D., Edmonds, J., 2015. Accounting for radiative forcing from albedo change in future global land-use scenarios. *Clim Change* 131, 691–703. <https://doi.org/10.1007/s10584-015-1411-5>
- Jones, C.D., Ciais, P., Davis, S.J., Friedlingstein, P., Gasser, T., Peters, G.P., Rogelj, J., van Vuuren, D.P., Canadell, J.G., Cowie, A., 2016. Simulating the Earth system response to negative emissions. *Environmental Research Letters* 11, 95012.
- Jones, W.I., 1995. *World Bank and Irrigation*. Washington, D.C.
- Joosten, H., 2010. *The Global Peatland CO2 Picture: peatland status and drainage related emissions in all countries of the world.*, The Global Peatland CO2 Picture: peatland status and drainage related emissions in all countries of the world. Wetlands International, Ede.
- JRC/PBL, 2012. *Emission database for global atmospheric research (EDGAR)*.
- Karlberg, L., Hoff, H., Amsalu, T., Andersson, K., Binnington, T., Flores-López, F., de Bruin, A., Gebrehiwot, S.G., Gedif, B., Johnson, O., 2015. Tackling complexity: understanding the food-energy-environment nexus in Ethiopia's Lake tana sub-basin. *Water Alternatives* 8.
- Kartha, S., Dooley, K., 2016. *The risks of relying on tomorrow's 'negative emissions' to guide today's mitigation action*. Stockholm Environmental Institute, Somerville, Aug.
- KC, S., Lutz, W., 2017. The human core of the shared socioeconomic pathways: Population scenarios by age, sex and level of education for all countries to 2100. *Global Environmental Change* 42, 181–192.
- Keenan, R.J., 2015. Climate change impacts and adaptation in forest management: a review. *Ann For Sci* 72, 145–167. <https://doi.org/10.1007/s13595-014-0446-5>
- Kindermann, G., Obersteiner, M., Sohngen, B., Sathaye, J., Andrasko, K., Rametsteiner, E., Schlamadinger, B., Wunder, S., Beach, R., 2008. Global cost estimates of reducing carbon emissions through avoided deforestation. *Proc Natl Acad Sci U S A* 105, 10302–10307. <https://doi.org/10.1073/pnas.0710616105>
- Kissinger, G.M., Herold, M., de Sy, V., 2012. *Drivers of deforestation and forest degradation: a synthesis report for REDD+ policymakers*.
- Klein, D., Luderer, G., Kriegler, E., Strefler, J., Bauer, N., Leimbach, M., Popp, A., Dietrich, J.P., Humpenöder, F., Lotze-Campen, H., Edenhofer, O., 2014. The value of bioenergy in low stabilization scenarios: an assessment using REMIND-MAGPIE. *Clim Change* 123, 705–718. <https://doi.org/10.1007/s10584-013-0940-z>
- Klein Goldewijk, K., Beusen, A., Doelman, J., Stehfest, E., 2017. Anthropogenic land use estimates for the Holocene - HYDE 3.2. *Earth Syst Sci Data* 9, 927–953. <https://doi.org/10.5194/essd-9-927-2017>
- Klein Goldewijk, K., Beusen, A., Janssen, P., 2010. Long-term dynamic modeling of global population and built-up area in a spatially explicit way: HYDE 3.1. *Holocene* 20, 565–573. <https://doi.org/10.1177/0959683609356587>

- Klein Goldewijk, K., Beusen, A., van Drecht, G., de Vos, M., 2011. The HYDE 3.1 spatially explicit database of human-induced global land-use change over the past 12,000 years. *Global Ecology and Biogeography* 20, 73–86. <https://doi.org/10.1111/j.1466-8238.2010.00587.x>
- Kok, M.T.J., Meijer, J.R., van Zeist, W.-J., Hilbers, J.P., Immovilli, M., Janse, J.H., Stehfest, E., Bakkenes, M., Tabeau, A., Schipper, A.M., Alkemade, R., 2020. Assessing ambitious nature conservation strategies within a 2 degree warmer and food-secure world. *bioRxiv* 2020.08.04.236489. <https://doi.org/10.1101/2020.08.04.236489>
- Konapala, G., Mishra, A.K., Wada, Y., Mann, M.E., 2020. Climate change will affect global water availability through compounding changes in seasonal precipitation and evaporation. *Nat Commun* 11, 3044. <https://doi.org/10.1038/s41467-020-16757-w>
- Krause, A., Pugh, T.A.M., Bayer, A.D., Doelman, J.C., Humpenöder, F., Anthoni, P., Olin, S., Bodirsky, B.L., Popp, A., Stehfest, E., Arneth, A., 2017. Global consequences of afforestation and bioenergy cultivation on ecosystem service indicators. *Biogeosciences* 14, 4829–4850. <https://doi.org/10.5194/bg-14-4829-2017>
- Krause, A., Pugh, T.A.M., Bayer, A.D., Li, W., Leung, F., Bondeau, A., Doelman, J.C., Humpenöder, F., Anthoni, P., Bodirsky, B.L., Ciais, P., Müller, C., Murray-Tortarolo, G., Olin, S., Popp, A., Sitch, S., Stehfest, E., Arneth, A., 2018. Large uncertainty in carbon uptake potential of land-based climate-change mitigation efforts. *Glob Chang Biol* 24, 3025–3038. <https://doi.org/https://doi.org/10.1111/gcb.14144>
- Kreidenweis, U., Humpenöder, F., Stevanović, M., Bodirsky, B.L., Kriegler, E., Lotze-Campen, H., Popp, A., 2016. Afforestation to mitigate climate change: impacts on food prices under consideration of albedo effects. *Environmental Research Letters* 11, 85001.
- Kriegler, E., Bauer, N., Popp, A., Humpenöder, F., Leimbach, M., Strefler, J., Baumstark, L., Bodirsky, B.L., Hilaire, J., Klein, D., Mouratiadou, I., Weindl, I., Bertram, C., Dietrich, J.-P., Luderer, G., Pehl, M., Pietzcker, R., Piontek, F., Lotze-Campen, H., Biewald, A., Bonsch, M., Giannousakis, A., Kreidenweis, U., Müller, C., Rolinski, S., Schultes, A., Schwanitz, J., Stevanovic, M., Calvin, K., Emmerling, J., Fujimori, S., Edenhofer, O., 2017. Fossil-fueled development (SSP5): An energy and resource intensive scenario for the 21st century. *Global Environmental Change* 42, 297–315. <https://doi.org/https://doi.org/10.1016/j.gloenvcha.2016.05.015>
- Kyle, G.P., Luckow, P., Calvin, K. v, Emanuel, W.R., Nathan, M., Zhou, Y., 2011. GCAM 3.0 agriculture and land use: data sources and methods. Pacific Northwest National Laboratory (PNNL), Richland, WA (US).
- la Viña, A.G.M., de Leon, A., Barrer, R.R., 2016. History and future of REDD+ in the UNFCCC: Issues and challenges. *Research handbook on REDD-Plus and international law* 11–29.
- Laclau, J.-P., Ranger, J., Deleporte, P., Nouvellon, Y., Saint-André, L., Marlet, S., Bouillet, J.-P., 2005. Nutrient cycling in a clonal stand of Eucalyptus and an adjacent savanna ecosystem in Congo: 3. Input-output budgets and consequences for the sustainability of the plantations. *For Ecol Manage* 210, 375–391. <https://doi.org/https://doi.org/10.1016/j.foreco.2005.02.028>
- Lambin, E.F., 2012. Global land availability: Malthus versus Ricardo. *Glob Food Sec* 1, 83–87. <https://doi.org/10.1016/j.gfs.2012.11.002>
- Lambin, E.F., Meyfroidt, P., 2011. Global land use change, economic globalization, and the looming land scarcity. *Proc Natl Acad Sci U S A* 108, 3465–3472. <https://doi.org/10.1073/pnas.1100480108>
- Lassaletta, L., Billen, G., Grizzetti, B., Anglade, J., Garnier, J., 2014. 50 year trends in nitrogen use efficiency of world cropping systems: the relationship between yield and nitrogen input to cropland. *Environmental Research Letters* 9, 105011.
- Lassaletta, L., Estellés, F., Beusen, A.H.W., Bouwman, L., Calvet, S., van Grinsven, H.J.M., Doelman, J.C., Stehfest, E., Uwizeye, A., Westhoek, H., 2019. Future global pig production systems according to the Shared Socioeconomic Pathways. *Science of The Total Environment* 665, 739–751. <https://doi.org/https://doi.org/10.1016/j.scitotenv.2019.02.079>
- Latka, C., Kuiper, M., Frank, S., Heckelee, T., Havlík, P., Witzke, H.-P., Leip, A., Cui, H.D., Kuijsten, A., Geleijnse, J.M., van Dijk, M., 2021. Paying the price for environmentally sustainable and healthy EU diets. *Glob Food Sec* 28, 100437. <https://doi.org/https://doi.org/10.1016/j.gfs.2020.100437>

- Lauri, P., Havlík, P., Kindermann, G., Forsell, N., Böttcher, H., Obersteiner, M., 2014. Woody biomass energy potential in 2050. *Energy Policy* 66, 19–31.
- Leclère, D., Obersteiner, M., Barrett, M., Butchart, S.H.M., Chaudhary, A., De Palma, A., DeClerck, F.A.J., Di Marco, M., Doelman, J.C., Dürauer, M., Freeman, R., Harfoot, M., Hasegawa, T., Hellweg, S., Hilbers, J.P., Hill, S.L.L., Humpenöder, F., Jennings, N., Krisztin, T., Mace, G.M., Ohashi, H., Popp, A., Purvis, A., Schipper, A.M., Tabeau, A., Valin, H., van Meijl, H., van Zeist, W.-J., Visconti, P., Alkemade, R., Almond, R., Bunting, G., Burgess, N.D., Cornell, S.E., Di Fulvio, F., Ferrier, S., Fritz, S., Fujimori, S., Grooten, M., Harwood, T., Havlík, P., Herrero, M., Hoskins, A.J., Jung, M., Kram, T., Lotze-Campen, H., Matsui, T., Meyer, C., Nel, D., Newbold, T., Schmidt-Traub, G., Stehfest, E., Strassburg, B.B.N., van Vuuren, D.P., Ware, C., Watson, J.E.M., Wu, W., Young, L., 2020. Bending the curve of terrestrial biodiversity needs an integrated strategy. *Nature* 585, 551–556. <https://doi.org/10.1038/s41586-020-2705-y>
- Lehmann, J., Cowie, A., Masiello, C.A., Kammann, C., Woolf, D., Amonette, J.E., Cayuela, M.L., Camps-Arbestain, M., Whitman, T., 2021. Biochar in climate change mitigation. *Nat Geosci* 14, 883–892. <https://doi.org/10.1038/s41561-021-00852-8>
- Lehner, B., Döll, P., 2004. Development and validation of a global database of lakes, reservoirs and wetlands. *J Hydrol (Amst)* 296, 1–22.
- Leifeld, J., Menichetti, L., 2018. The underappreciated potential of peatlands in global climate change mitigation strategies. *Nat Commun* 9, 1071. <https://doi.org/10.1038/s41467-018-03406-6>
- Leifeld, J., Wüst-Galley, C., Page, S., 2019. Intact and managed peatland soils as a source and sink of GHGs from 1850 to 2100. *Nat Clim Chang* 9, 945–947. <https://doi.org/10.1038/s41558-019-0615-5>
- Lele, U., Masters, W.A., Kinabo, J., Meenakshi, J. v., Ramaswami, B., Tagwireyi, J., BELL, W.F.L., Goswami, S., 2016. Measuring food and nutrition security: An independent technical assessment and user's guide for existing indicators. Food Security Information Network.
- Leng, L.Y., Ahmed, O.H., Jalloh, M.B., 2019. Brief review on climate change and tropical peatlands. *Geoscience Frontiers* 10, 373–380. <https://doi.org/https://doi.org/10.1016/j.gsf.2017.12.018>
- Leskinen, P., Cardellini, G., González-García, S., Hurmekoski, E., Sathre, R., Seppälä, J., Smyth, C., Stern, T., Verkerk, P.J., 2018. Substitution effects of wood-based products in climate change mitigation. *From Science to Policy* 7.
- Lewis, S.L., Wheeler, C.E., Mitchard, E.T.A., Koch, A., 2019. Restoring natural forests is the best way to remove atmospheric carbon.
- Liu, J., You, L., Amini, M., Obersteiner, M., Herrero, M., Zehnder, A.J.B., Yang, H., 2010. A high-resolution assessment on global nitrogen flows in cropland. *Proceedings of the National Academy of Sciences* 107, 8035–8040. <https://doi.org/10.1073/pnas.0913658107>
- Loisel, J., Yu, Z., Beilman, D.W., Camill, P., Alm, J., Amesbury, M.J., Anderson, D., Andersson, S., Bochicchio, C., Barber, K., Belyea, L.R., Bunbury, J., Chambers, F.M., Charman, D.J., de Vleeschouwer, F., Fiałkiewicz-Kozielec, B., Finkelstein, S.A., Gałka, M., Garneau, M., Hammarlund, D., Hinchcliffe, W., Holmquist, J., Hughes, P., Jones, M.C., Klein, E.S., Kokfelt, U., Korhola, A., Kuhry, P., Lamarre, A., Lamentowicz, M., Large, D., Lavoie, M., MacDonald, G., Magnan, G., Mäkilä, M., Mallon, G., Mathijssen, P., Mauquoy, D., McCarroll, J., Moore, T.R., Nichols, J., O'Reilly, B., Oksanen, P., Packalen, M., Peteet, D., Richard, P.J.H., Robinson, S., Ronkainen, T., Rundgren, M., Sannel, A.B.K., Tarnocai, C., Thom, T., Tuittila, E.-S., Turetsky, M., Väliranta, M., van der Linden, M., van Geel, B., van Bellen, S., Vitt, D., Zhao, Y., Zhou, W., 2014. A database and synthesis of northern peatland soil properties and Holocene carbon and nitrogen accumulation. *Holocene* 24, 1028–1042. <https://doi.org/10.1177/0959683614538073>
- Lotze-Campen, H., Müller, C., Bondeau, A., Rost, S., Popp, A., Lucht, W., 2008. Global food demand, productivity growth, and the scarcity of land and water resources: a spatially explicit mathematical programming approach. *Agricultural Economics* 39, 325–338. <https://doi.org/10.1111/j.1574-0862.2008.00336.x>

- Lucas, P.L., Hilderink, H.B.M., Janssen, P.H.M., Kc, S., van Vuuren, D.P., Niessen, L., 2019. Future impacts of environmental factors on achieving the SDG target on child mortality—A synergistic assessment. *Global Environmental Change* 57, 101925. <https://doi.org/https://doi.org/10.1016/j.gloenvcha.2019.05.009>
- Lucas, P.L., van Vuuren, D.P., Olivier, J.G.J., den Elzen, M.G.J., 2007. Long-term reduction potential of non-CO₂ greenhouse gases. *Environ Sci Policy* 10, 85–103. <https://doi.org/10.1016/j.envsci.2006.10.007>
- Lunt, M.F., Palmer, P.I., Feng, L., Taylor, C.M., Boesch, H., Parker, R.J., 2019. An increase in methane emissions from tropical Africa between 2010 and 2016 inferred from satellite data. *Atmos Chem Phys* 19, 14721–14740. <https://doi.org/10.5194/acp-19-14721-2019>
- Lutz, F., Herzfeld, T., Heinke, J., Rolinski, S., Schaphoff, S., von Bloh, W., Stoorvogel, J.J., Müller, C., 2019. Simulating the effect of tillage practices with the global ecosystem model LPJmL (version 5.0-tillage). *Geosci Model Dev* 12, 2419–2440. <https://doi.org/10.5194/gmd-12-2419-2019>
- Mandryk, M., Doelman, J.C., Stehfest, E., 2015. Assessment of global land availability. FOODSECURE technical working paper no. 7.
- McDermott, J.J., Staal, S.J., Freeman, H.A., Herrero, M., van de Steeg, J.A., 2010. Sustaining intensification of smallholder livestock systems in the tropics. *Livest Sci* 130, 95–109.
- Meinshausen, M., Raper, S.C.B., Wigley, T.M.L., 2011. Emulating coupled atmosphere-ocean and carbon cycle models with a simpler model, MAGICC6 – Part 1: Model description and calibration. *Atmos Chem Phys* 11, 1417–1456. <https://doi.org/10.5194/acp-11-1417-2011>
- Miettinen, J., Hooijer, A., Shi, C., Tollenaar, D., Vernimmen, R., Liew, S.C., Malins, C., Page, S.E., 2012. Extent of industrial plantations on Southeast Asian peatlands in 2010 with analysis of historical expansion and future projections. *GCB Bioenergy* 4, 908–918. <https://doi.org/https://doi.org/10.1111/j.1757-1707.2012.01172.x>
- Minasny, B., Berglund, Ö., Connolly, J., Hedley, C., de Vries, F., Gimona, A., Kempen, B., Kidd, D., Lilja, H., Malone, B., McBratney, A., Roudier, P., O'Rourke, S., Rudiyanto, Padarian, J., Poggio, L., ten Caten, A., Thompson, D., Tuve, C., Widyatmanti, W., 2019. Digital mapping of peatlands – A critical review. *Earth Sci Rev* 196, 102870. <https://doi.org/https://doi.org/10.1016/j.earscirev.2019.05.014>
- Molden, D., 2007. Water for food. Water for life. A comprehensive assessment of water management in agriculture. International Water Management Institute (IWMI) and FAO.
- Mueller, N.D., Gerber, J.S., Johnston, M., Ray, D.K., Ramankutty, N., Foley, J.A., 2012. Closing yield gaps through nutrient and water management. *Nature* 490, 254–257. <https://doi.org/10.1038/nature11420>
- Muhammad, A., Seale, J.L., Meade, B., Regmi, A., 2011. International evidence on food consumption patterns: an update using 2005 international comparison program data.
- Müller, C., Elliott, J., Chryssanthacopoulos, J., Deryng, D., Folberth, C., Pugh, T.A.M., Schmid, E., 2015. Implications of climate mitigation for future agricultural production. *Environmental Research Letters* 10, 125004. <https://doi.org/10.1088/1748-9326/10/12/125004>
- Müller, C., Robertson, R.D., 2014. Projecting future crop productivity for global economic modeling. *Agricultural Economics* 45, 37–50. <https://doi.org/https://doi.org/10.1111/agec.12088>
- Müller, C., Stehfest, E., van Minnen, J.G., Strengers, B., von Bloh, W., Beusen, A.H.W., Schaphoff, S., Kram, T., Lucht, W., 2016. Drivers and patterns of land biosphere carbon balance reversal. *Environmental Research Letters* 11, 44002. <https://doi.org/10.1088/1748-9326/11/4/044002>
- Nachtergaele, F., van Velthuisen, H., Verelst, L., 2012. Harmonized World soil database version 1.2. Food and agriculture organization of the United Nations (FAO). International Institute for Applied Systems Analysis (IIASA), ISRIC-World Soil Information, Institute of Soil Science–Chinese Academy of Sciences (ISSCAS), Joint Research Centre of the European Commission (JRC).
- Nelson, A., 2008. Travel time to major cities: A global map of Accessibility.

- Nelson, G.C., Valin, H., Sands, R.D., Havlik, P., Ahammad, H., Deryng, D., Elliott, J., Fujimori, S., Hasegawa, T., Heyhoe, E., Kyle, P., von Lampe, M., Lotze-Campen, H., Mason d’Croz, D., van Meijl, H., van der Mensbrugghe, D., Muller, C., Popp, A., Robertson, R., Robinson, S., Schmid, E., Schmitz, C., Tabeau, A., Willenbockel, D., 2014. Climate change effects on agriculture: economic responses to biophysical shocks. *Proc Natl Acad Sci U S A* 111, 3274–3279. <https://doi.org/10.1073/pnas.1222465110>
- Nemet, G.F., Callaghan, M.W., Creutzig, F., Fuss, S., Hartmann, J., Hilaire, J., Lamb, W.F., Minx, J.C., Rogers, S., Smith, P., 2018. Negative emissions—Part 3: Innovation and upscaling. *Environmental Research Letters* 13, 63003.
- Neumann, K., Stehfest, E., Verburg, P.H., Siebert, S., Müller, C., Veldkamp, T., 2011. Exploring global irrigation patterns: A multilevel modelling approach. *Agric Syst* 104, 703–713. <https://doi.org/10.1016/j.agsy.2011.08.004>
- Neumann, K., Verburg, P.H., Stehfest, E., Müller, C., 2010. The yield gap of global grain production: A spatial analysis. *Agric Syst* 103, 316–326. <https://doi.org/10.1016/j.agsy.2010.02.004>
- Nilsson, M., Griggs, D., Visbeck, M., 2016. Policy: map the interactions between Sustainable Development Goals. *Nature News* 534, 320.
- Obersteiner, M., Walsh, B., Frank, S., Havlík, P., Cantele, M., Liu, J., Palazzo, A., Herrero, M., Lu, Y., Mosnier, A., 2016. Assessing the land resource–food price nexus of the Sustainable Development Goals. *Sci Adv* 2, e1501499.
- OECD, 2017. The Land-Water-Energy Nexus. <https://doi.org/doi:https://doi.org/10.1787/9789264279360-en>
- Oke, T.R., 1982. The energetic basis of the urban heat island. *Quarterly Journal of the Royal Meteorological Society* 108, 1–24.
- O’Neill, B.C., Kriegler, E., Ebi, K.L., Kemp-Benedict, E., Riahi, K., Rothman, D.S., van Ruijven, B.J., van Vuuren, D.P., Birkmann, J., Kok, K., 2017. The roads ahead: narratives for shared socioeconomic pathways describing world futures in the 21st century. *Global Environmental Change* 42, 169–180.
- Orlov, A., Daloz, A.S., Sillmann, J., Thiery, W., Douzal, C., Lejeune, Q., Schleussner, C., 2021. Global Economic Responses to Heat Stress Impacts on Worker Productivity in Crop Production. *Econ Disaster Clim Chang* 5, 367–390. <https://doi.org/10.1007/s41885-021-00091-6>
- Overmars, K.P., Stehfest, E., Tabeau, A., van Meijl, H., Beltrán, A.M., Kram, T., 2014. Estimating the opportunity costs of reducing carbon dioxide emissions via avoided deforestation, using integrated assessment modelling. *Land use policy* 41, 45–60. <https://doi.org/10.1016/j.landusepol.2014.04.015>
- Page, S.E., Hooijer, A., 2016. In the line of fire: the peatlands of Southeast Asia. *Philosophical Transactions of the Royal Society B: Biological Sciences* 371, 20150176. <https://doi.org/10.1098/rstb.2015.0176>
- Page, S.E., Rieley, J.O., Banks, C.J., 2011. Global and regional importance of the tropical peatland carbon pool. *Glob Chang Biol* 17, 798–818. <https://doi.org/https://doi.org/10.1111/j.1365-2486.2010.02279.x>
- Pastor, A. v, Ludwig, F., Biemans, H., Hoff, H., Kabat, P., 2014. Accounting for environmental flow requirements in global water assessments. *Hydrol Earth Syst Sci* 18, 5041–5059.
- Pimm, S.L., Jenkins, C.N., Li, B. v, 2018. How to protect half of Earth to ensure it protects sufficient biodiversity. *Sci Adv* 4, eaat2616.
- Poore, J., Nemecek, T., 2018. Reducing food’s environmental impacts through producers and consumers. *Science* (1979) 360, 987–992.
- Popp, A., Calvin, K., Fujimori, S., Havlik, P., Humpenöder, F., Stehfest, E., Bodirsky, B.L., Dietrich, J.P., Doelmann, J.C., Gusti, M., Hasegawa, T., Kyle, P., Obersteiner, M., Tabeau, A., Takahashi, K., Valin, H., Waldhoff, S., Weindl, I., Wise, M., Kriegler, E., Lotze-Campen, H., Fricko, O., Riahi, K., van Vuuren, D.P., 2017. Land-use futures in the shared socio-economic pathways. *Global Environmental Change* 42, 331–345. <https://doi.org/10.1016/j.gloenvcha.2016.10.002>
- Popp, A., Dietrich, J.P., Lotze-Campen, H., Klein, D., Bauer, N., Krause, M., Beringer, T., Gerten, D., Edenhofer, O., 2011. The economic potential of bioenergy for climate change mitigation with special attention given to implications for the land system. *Environmental Research Letters* 6, 34017. <https://doi.org/10.1088/1748-9326/6/3/034017>

- Popp, A., Humpenöder, F., Weindl, I., Bodirsky, B.L., Bonsch, M., Lotze-Campen, H., Müller, C., Biewald, A., Rolinski, S., Stevanovic, M., 2014. Land-use protection for climate change mitigation. *Nat Clim Chang* 4, 1095–1098.
- Popp, A., Rose, S.K., Calvin, K., van Vuuren, D.P., Dietrich, J.P., Wise, M., Stehfest, E., Humpenöder, F., Kyle, P., van Vliet, J., Bauer, N., Lotze-Campen, H., Klein, D., Kriegler, E., 2013. Land-use transition for bioenergy and climate stabilization: model comparison of drivers, impacts and interactions with other land use based mitigation options. *Clim Change* 123, 495–509. <https://doi.org/10.1007/s10584-013-0926-x>
- Posa, M.R.C., Wijedasa, L.S., Corlett, R.T., 2011. Biodiversity and Conservation of Tropical Peat Swamp Forests. *Bioscience* 61, 49–57. <https://doi.org/10.1525/bio.2011.61.1.10>
- Prestele, R., Alexander, P., Rounsevell, M.D.A., Arneth, A., Calvin, K., Doelman, J., Eitelberg, D.A., Engström, K., Fujimori, S., Hasegawa, T., Havlik, P., Humpenöder, F., Jain, A.K., Krisztin, T., Kyle, P., Meiyappan, P., Popp, A., Sands, R.D., Schaldach, R., Schüngel, J., Stehfest, E., Tabeau, A., van Meijl, H., van Vliet, J., Verburg, P.H., 2016. Hotspots of uncertainty in land-use and land-cover change projections: a global-scale model comparison. *Glob Chang Biol* 22, 3967–3983. <https://doi.org/https://doi.org/10.1111/gcb.13337>
- Quérel, C. le, Andrew, R.M., Canadell, J.G., Sitch, S., Korsbakken, J.I., Peters, G.P., Manning, A.C., Boden, T.A., Tans, P.P., Houghton, R.A., 2016. Global Carbon Budget 2016. *Earth Syst Sci Data* 8, 605–649.
- Resolve, 2017. Global map of 846 global ecoregions nested within 14 terrestrial biomes.
- Riahi, K., van Vuuren, D.P., Kriegler, E., Edmonds, J., O'Neill, B.C., Fujimori, S., Bauer, N., Calvin, K., Dellink, R., Fricko, O., Lutz, W., Popp, A., Cuaresma, J.C., KC, S., Leimbach, M., Jiang, L., Kram, T., Rao, S., Emmerling, J., Ebi, K., Hasegawa, T., Havlik, P., Humpenöder, F., da Silva, L.A., Smith, S., Stehfest, E., Bosetti, V., Eom, J., Gernaat, D., Masui, T., Rogelj, J., Strefler, J., Drouet, L., Krey, V., Luderer, G., Harmsen, M., Takahashi, K., Baumstark, L., Doelman, J.C., Kainuma, M., Klimont, Z., Marangoni, G., Lotze-Campen, H., Obersteiner, M., Tabeau, A., Tavoni, M., 2017. The shared socioeconomic pathways and their energy, land use, and greenhouse gas emissions implications: an overview. *Global Environmental Change* 42, 153–168. <https://doi.org/10.1016/j.gloenvcha.2016.05.009>
- Ritson, J.P., Bell, M., Brazier, R.E., Grand-Clement, E., Graham, N.J.D., Freeman, C., Smith, D., Templeton, M.R., Clark, J.M., 2016. Managing peatland vegetation for drinking water treatment. *Sci Rep* 6, 36751. <https://doi.org/10.1038/srep36751>
- Robinson, S., Mason-D'Croz, D., Sulser, T., Islam, S., Robertson, R., Zhu, T., Gueneau, A., Pitois, G., Rosegrant, M.W., 2015. The international model for policy analysis of agricultural commodities and trade (IMPACT): model description for version 3.
- Rochedo, P.R.R., Soares-Filho, B., Schaeffer, R., Viola, E., Szklo, A., Lucena, A.F.P., Koberle, A., Davis, J.L., Rajão, R., Rathmann, R., 2018. The threat of political bargaining to climate mitigation in Brazil. *Nat Clim Chang* 8, 695–698. <https://doi.org/10.1038/s41558-018-0213-y>
- Rockström, J., Steffen, W., Noone, K., Persson, Å., Chapin, F.S., Lambin, E.F., Lenton, T.M., Scheffer, M., Folke, C., Schellnhuber, H.J., Nykvist, B., de Wit, C.A., Hughes, T., van der Leeuw, S., Rodhe, H., Sörlin, S., Snyder, P.K., Costanza, R., Svedin, U., Falkenmark, M., Karlberg, L., Corell, R.W., Fabry, V.J., Hansen, J., Walker, B., Liverman, D., Richardson, K., Crutzen, P., Foley, J.A., 2009. A safe operating space for humanity. *Nature* 461, 472–475. <https://doi.org/10.1038/461472a>
- Roe, S., Streck, C., Beach, R., Busch, J., Chapman, M., Daioglou, V., Deppermann, A., Doelman, J., Emmet-Booth, J., Engelmann, J., Fricko, O., Frischmann, C., Funk, J., Grassi, G., Griscom, B., Havlik, P., Hanssen, S., Humpenöder, F., Landholm, D., Lomax, G., Lehmann, J., Mesnildrey, L., Nabuurs, G.-J., Popp, A., Rivard, C., Sanderman, J., Sohngen, B., Smith, P., Stehfest, E., Woolf, D., Lawrence, D., 2021. Land-based measures to mitigate climate change: Potential and feasibility by country. *Glob Chang Biol* 27, 6025–6058. <https://doi.org/https://doi.org/10.1111/gcb.15873>

- Roe, S., Streck, C., Obersteiner, M., Frank, S., Griscom, B., Drouet, L., Fricko, O., Gusti, M., Harris, N., Hasegawa, T., Hausfather, Z., Havlík, P., House, J., Nabuurs, G.-J., Popp, A., Sánchez, M.J.S., Sanderman, J., Smith, P., Stehfest, E., Lawrence, D., 2019. Contribution of the land sector to a 1.5 °C world. *Nat Clim Chang* 9, 817–828. <https://doi.org/10.1038/s41558-019-0591-9>
- Rogelj, J., Hare, W., Lowe, J., van Vuuren, D.P., Riahi, K., Matthews, B., Hanaoka, T., Jiang, K., Meinshausen, M., 2011. Emission pathways consistent with a 2°C global temperature limit. *Nat Clim Chang* 1, 413.
- Rogelj, J., Popp, A., Calvin, K. v., Luderer, G., Emmerling, J., Gernaat, D., Fujimori, S., Streffer, J., Hasegawa, T., Marangoni, G., Krey, V., Kriegler, E., Riahi, K., van Vuuren, D.P., Doelman, J., Drouet, L., Edmonds, J., Fricko, O., Harmsen, M., Havlík, P., Humpenöder, F., Stehfest, E., Tavoni, M., 2018. Scenarios towards limiting global mean temperature increase below 1.5° C. *Nat Clim Chang* 8, 325. <https://doi.org/10.1038/s41558-018-0091-3>
- Rohwer, J., Gerten, D., Lucht, W., 2007. Development of functional irrigation types for improved global crop modelling. Potsdam.
- Rosenzweig, C., Elliott, J., Deryng, D., Ruane, A.C., Muller, C., Arneth, A., Boote, K.J., Folberth, C., Glotter, M., Khabarov, N., Neumann, K., Piontek, F., Pugh, T.A., Schmid, E., Stehfest, E., Yang, H., Jones, J.W., 2014. Assessing agricultural risks of climate change in the 21st century in a global gridded crop model intercomparison. *Proc Natl Acad Sci U S A* 111, 3268–3273. <https://doi.org/10.1073/pnas.1222463110>
- Ruesch, A., Gibbs, H.K., 2008. New IPCC Tier-1 global biomass carbon map for the year 2000 [WWW Document]. URL http://cdiac.ornl.gov/epubs/ndp/global_carbon/carbon_documentation.html
- Saarimaa, M., Aapala, K., Tuominen, S., Karhu, J., Parkkari, M., Tolvanen, A., 2019. Predicting hotspots for threatened plant species in boreal peatlands. *Biodivers Conserv* 28, 1173–1204. <https://doi.org/10.1007/s10531-019-01717-8>
- Salvagiotti, F., Cassman, K.G., Specht, J.E., Walters, D.T., Weiss, A., Dobermann, A., 2008. Nitrogen uptake, fixation and response to fertilizer N in soybeans: A review. *Field Crops Res* 108, 1–13.
- Sandbag, 2021. Tracking the European Union Emissions Trading System carbon market price day-by-day [WWW Document]. URL <https://sandbag.be/index.php/carbon-price-viewer/>
- Sasaki, N., Asner, G.P., Pan, Y., Knorr, W., Durst, P.B., Ma, H.O., Abe, I., Lowe, A.J., Koh, L.P., Putz, F.E., 2016. Sustainable Management of Tropical Forests Can Reduce Carbon Emissions and Stabilize Timber Production. *Front Environ Sci* 4. <https://doi.org/10.3389/fenvs.2016.00050>
- Sathaye, J., Makundi, W., Dale, L., Chan, P., Andrasko, K., 2006. GHG mitigation potential, costs and benefits in global forests: a dynamic partial equilibrium approach. *The Energy Journal* 127–162.
- Schaeffer, M., Eickhout, B., Hoogwijk, M., Strengers, B., van Vuuren, D., Leemans, R., Opsteegh, T., 2006. CO₂ and albedo climate impacts of extratropical carbon and biomass plantations. *Global Biogeochem Cycles* 20, n/a-n/a. <https://doi.org/10.1029/2005gb002581>
- Schaphoff, S., Forkel, M., Müller, C., Knauer, J., von Bloh, W., Gerten, D., Jägermeyr, J., Lucht, W., Rammig, A., Thonicke, K., Waha, K., 2018a. LPJmL4 – a dynamic global vegetation model with managed land – Part 2: Model evaluation. *Geosci Model Dev* 11, 1377–1403. <https://doi.org/10.5194/gmd-11-1377-2018>
- Schaphoff, S., von Bloh, W., Rammig, A., Thonicke, K., Biemans, H., Forkel, M., Gerten, D., Heinke, J., Jägermeyr, J., Knauer, J., 2018b. LPJmL4—a dynamic global vegetation model with managed land—Part 1: Model description. *Geosci Model Dev* 11, 1343–1375.
- Scharlemann, J.P.W., Tanner, E.V.J., Hiederer, R., Kapos, V., 2014. Global soil carbon: understanding and managing the largest terrestrial carbon pool. *Carbon Manag* 5, 81–91. <https://doi.org/10.4155/cmt.13.77>
- Schipper, A.M., Hilbers, J.P., Meijer, J.R., Antão, L.H., Benítez-López, A., de Jonge, M.M.J., Leemans, L.H., Scheper, E., Alkemade, R., Doelman, J.C., 2020. Projecting terrestrial biodiversity intactness with GLOBIO 4. *Glob Chang Biol* 26, 760–771. <https://doi.org/10.1111/gcb.14848>
- Schmidt, H.-P., Kammann, C., Hagemann, N., Leifeld, J., Bucheli, T.D., Sánchez Monedero, M.A., Cayuela, M.L., 2021. Biochar in agriculture – A systematic review of 26 global meta-analyses. *GCB Bioenergy* 13, 1708–1730. <https://doi.org/https://doi.org/10.1111/gcbb.12889>

- Schmitz, C., Biewald, A., Lotze-Campen, H., Popp, A., Dietrich, J.P., Bodirsky, B., Krause, M., Weindl, I., 2012. Trading more food: Implications for land use, greenhouse gas emissions, and the food system. *Global Environmental Change* 22, 189–209. <https://doi.org/https://doi.org/10.1016/j.gloenvcha.2011.09.013>
- Schmitz, C., van Meijl, H., Kyle, P., Nelson, G.C., Fujimori, S., Gurgel, A., Havlik, P., Heyhoe, E., d’Croz, D.M., Popp, A., Sands, R., Tabeau, A., van der Mensbrugghe, D., von Lampe, M., Wise, M., Blanc, E., Hasegawa, T., Kavallari, A., Valin, H., 2014. Land-use change trajectories up to 2050: insights from a global agro-economic model comparison. *Agricultural Economics* 45, 69–84. <https://doi.org/10.1111/agec.12090>
- Searchinger, T., Heimlich, R., Houghton, R.A., Dong, F., Elobeid, A., Fabiosa, J., Tokgoz, S., Hayes, D., Yu, T.-H., 2008. Use of U.S. Croplands for Biofuels Increases Greenhouse Gases Through Emissions from Land-Use Change. *Science* (1979) 319, 1238–1240. <https://doi.org/10.1126/science.1151861>
- Searchinger, T.D., Beringer, T., Strong, A., 2017. Does the world have low-carbon bioenergy potential from the dedicated use of land? *Energy Policy* 110, 434–446.
- Seppelt, R., Arndt, C., Beckmann, M., Martin, E.A., Hertel, T.W., 2020. Deciphering the Biodiversity–Production Mutualism in the Global Food Security Debate. *Trends Ecol Evol* 35, 1011–1020. <https://doi.org/https://doi.org/10.1016/j.tree.2020.06.012>
- Shabman, L., Zepp, L., Wainger, L., King, D., 2002. Incentives for reforestation of agricultural land: What will a market for carbon sequestration credits contribute? *American journal of alternative agriculture* 17, 116–124.
- Shukla, P.R., Skea, J., Slade, R., al Khourdajie, A., van Diemen, R., 2022. *Climate Change 2022: Mitigation of Climate Change. Contribution of Working Group III to the Sixth Assessment Report of the Intergovernmental Panel on Climate Change*. Cambridge University Press, Cambridge, UK and New York, NY, USA.
- Siebert, S., Döll, P., Feick, S., Hoogeveen, J., Frenken, K., 2007. *Global Map of Irrigation Areas version 4.0.1*. Johann Wolfgang Goethe University, Frankfurt am Main, Germany / Food and Agriculture Organization of the United Nations, Rome, Italy.
- Sitch, S., Smith, B., Prentice, I.C., Arneth, A., Bondeau, A., Cramer, W., Kaplan, J.O., Levis, S., Lucht, W., Sykes, M.T., 2003. Evaluation of ecosystem dynamics, plant geography and terrestrial carbon cycling in the LPJ dynamic global vegetation model. *Glob Chang Biol* 9, 161–185.
- Smakhtin, V., Revenga, C., Döll, P., 2004. A Pilot Global Assessment of Environmental Water Requirements and Scarcity. *Water Int* 29, 307–317. <https://doi.org/10.1080/02508060408691785>
- Smith, P., 2013. Chapter 11: Agriculture, Forestry and Other Land Use (AFOLU). IPCC WGIII AR5.
- Smith, P., Davis, S.J., Creutzig, F., Fuss, S., Minx, J., Gabrielle, B., Kato, E., Jackson, R.B., Cowie, A., Kriegler, E., 2016. Biophysical and economic limits to negative CO₂ emissions. *Nat Clim Chang* 6, 42–50.
- Smith, P., Gregory, P.J., van Vuuren, D., Obersteiner, M., Havlik, P., Rounsevell, M., Woods, J., Stehfest, E., Bellarby, J., 2010. Competition for land. *Philos Trans R Soc Lond B Biol Sci* 365, 2941–2957. <https://doi.org/10.1098/rstb.2010.0127>
- Soergel, B., Kriegler, E., Weindl, I., Rauner, S., Dirnhaichner, A., Ruhe, C., Hofmann, M., Bauer, N., Bertram, C., Bodirsky, B.L., Leimbach, M., Leininger, J., Levesque, A., Luderer, G., Pehl, M., Wingens, C., Baumstark, L., Beier, F., Dietrich, J.P., Humpenöder, F., von Jeetze, P., Klein, D., Koch, J., Pietzcker, R., Strefler, J., Lotze-Campen, H., Popp, A., 2021. A sustainable development pathway for climate action within the UN 2030 Agenda. *Nat Clim Chang* 11, 656–664. <https://doi.org/10.1038/s41558-021-01098-3>
- Sohnngen, B., Sedjo, R., 2006. Carbon sequestration in global forests under different carbon price regimes. *The Energy Journal* 109–126.
- Springmann, M., Clark, M., Mason-D’Croz, D., Wiebe, K., Bodirsky, B.L., Lassaletta, L., de Vries, W., Vermeulen, S.J., Herrero, M., Carlson, K.M., Jonell, M., Troell, M., DeClerck, F., Gordon, L.J., Zurayk, R., Scarborough, P., Rayner, M., Loken, B., Fanzo, J., Godfray, H.C.J., Tilman, D., Rockström, J., Willett, W., 2018. Options for keeping the food system within environmental limits. *Nature*. <https://doi.org/10.1038/s41586-018-0594-0>

- Stape, J.L., Binkley, D., Ryan, M.G., Fonseca, S., Loos, R.A., Takahashi, E.N., Silva, C.R., Silva, S.R., Hakamada, R.E., Ferreira, J.M. de A., Lima, A.M.N., Gava, J.L., Leite, F.P., Andrade, H.B., Alves, J.M., Silva, G.G.C., Azevedo, M.R., 2010. The Brazil Eucalyptus Potential Productivity Project: Influence of water, nutrients and stand uniformity on wood production. For Ecol Manage 259, 1684–1694. <https://doi.org/https://doi.org/10.1016/j.foreco.2010.01.012>
- Steffen, W., Richardson, K., Rockström, J., Cornell, S.E., Fetzer, I., Bennett, E.M., Biggs, R., Carpenter, S.R., de Vries, W., de Wit, C.A., 2015. Planetary boundaries: Guiding human development on a changing planet. *Science* (1979) 347.
- Stehfest, E., Bouwman, L., van Vuuren, D.P., den Elzen, M.G.J., Eickhout, B., Kabat, P., 2009. Climate benefits of changing diet. *Clim Change* 95, 83–102. <https://doi.org/10.1007/s10584-008-9534-6>
- Stehfest, E., van Vuuren, D., Kram, T., Bouwman, L., Alkemade, R., Bakkenes, M., Biemans, H., Bouwman, A., den Elzen, M., Janse, J., Lucas, P., van Minnen, J., Müller, C., Prins, A., 2014. Integrated Assessment of Global Environmental Change with IMAGE 3.0. Model description and policy applications, PBL Netherlands Environmental Assessment Agency. The Hague.
- Stehfest, E., van Zeist, W.-J., Valin, H., Havlik, P., Popp, A., Kyle, P., Tabeau, A., Mason-D’Croz, D., Hasegawa, T., Bodirsky, B.L., Calvin, K., Doelman, J.C., Fujimori, S., Humpenöder, F., Lotze-Campen, H., van Meijl, H., Wiebe, K., 2019. Key determinants of global land-use projections. *Nat Commun* 10, 2166. <https://doi.org/10.1038/s41467-019-09945-w>
- Stenzel, F., Greve, P., Lucht, W., Tramberend, S., Wada, Y., Gerten, D., 2021. Irrigation of biomass plantations may globally increase water stress more than climate change. *Nat Commun* 12, 1512. <https://doi.org/10.1038/s41467-021-21640-3>
- Stevanović, M., Popp, A., Bodirsky, B.L., Humpenöder, F., Müller, C., Weindl, I., Dietrich, J.P., Lotze-Campen, H., Kreidenweis, U., Rolinski, S., Biewald, A., Wang, X., 2017. Mitigation Strategies for Greenhouse Gas Emissions from Agriculture and Land-Use Change: Consequences for Food Prices. *Environ Sci Technol* 51, 365–374. <https://doi.org/10.1021/acs.est.6b04291>
- Stoorvogel, J.J., 2014. S-World: A global map of soil properties for modelling’. *GlobalSoilMap: Basis of the global spatial soil information system* 227.
- Stoorvogel, J.J., Bakkenes, M., Temme, A.J.A.M., Batjes, N.H., ten Brink, B.J.E., 2017. S-World: A Global Soil Map for Environmental Modelling. *Land Degrad Dev* 28, 22–33. <https://doi.org/https://doi.org/10.1002/ldr.2656>
- Strengers, B.J., Leemans, R., Eickhout, B., de Vries, B., Bouwman, L., 2004. The land-use projections and resulting emissions in the IPCC SRES scenarios as simulated by the IMAGE 2.2 model. *GeoJournal* 61, 12.
- Strengers, B.J., van Minnen, J.G., Eickhout, B., 2007. The role of carbon plantations in mitigating climate change: potentials and costs. *Clim Change* 88, 343–366. <https://doi.org/10.1007/s10584-007-9334-4>
- Szogs, S., Arneith, A., Anthoni, P., Doelman, J.C., Humpenöder, F., Popp, A., Pugh, T.A.M., Stehfest, E., 2017. Impact of LULCC on the emission of BVOCs during the 21st century. *Atmos Environ* 165, 73–87. <https://doi.org/https://doi.org/10.1016/j.atmosenv.2017.06.025>
- Tabeau, A., van Meijl, H., Overmars, K.P., Stehfest, E., 2017. REDD policy impacts on the agri-food sector and food security. *Food Policy* 66, 73–87. <https://doi.org/https://doi.org/10.1016/j.foodpol.2016.11.006>
- Tanneberger, F., Tegetmeyer, C., Busse, S., Shumka, S., Joosten, H., 2017. The peatland map of Europe. *Mires and Peat* 19.
- ten Brink, B., van der Esch, S., Kram, T., van Oorschot, M., Arets, E., 2010. Rethinking global biodiversity strategies: exploring structural changes in production and consumption to reduce biodiversity loss. *Netherlands Environmental Assessment Agency*.
- Tilman, D., Clark, M., Williams, D.R., Kimmel, K., Polasky, S., Packer, C., 2017. Future threats to biodiversity and pathways to their prevention. *Nature* 546, 73–81. <https://doi.org/10.1038/nature22900>
- Tokarick, S., 2006. Does Import Protection Discourage Exports?
- UN, D., 2019. World Population Prospects 2019: Volume 1, Comprehensive Tables. DESA/Population Division.

- UN, G.A., 2015. Transforming our world: The 2030 agenda for sustainable development. A/RES/70/1, 21 October.
- UN, G.A., 1994. United Nations Framework Convention on Climate Change : resolution / adopted by the General Assembly.
- UNCCD, 2017. Global Land Outlook - First Edition. Secretariat of the United Nations Convention to Combat Desertification, Bonn.
- UNEP, 2022. Global Peatlands Assessment – The State of the World’s Peatlands: Evidence for action toward the conservation, restoration, and sustainable management of peatlands. Nairobi.
- UNEP, 2019. Global Environment Outlook – GEO-6: Healthy Planet, Healthy People. Nairobi. <https://doi.org/10.1017/9781108627146>
- UNFCCC, 2015. Paris Agreement.
- USDA-ERS, 2022a. International Agricultural Productivity [WWW Document]. URL <https://www.ers.usda.gov/data-products/international-agricultural-productivity/> (accessed 12.19.22).
- USDA-ERS, 2022b. Feedgrains Sector at a Glance [WWW Document]. URL <https://www.ers.usda.gov/topics/crops/corn-and-other-feedgrains/feedgrains-sector-at-a-glance/> (accessed 8.23.22).
- van Asselen, S., Verburg, P.H., 2013. Land cover change or land-use intensification: simulating land system change with a global-scale land change model. *Glob Chang Biol* 19, 3648–3667. <https://doi.org/10.1111/gcb.12331>
- van den Berg, N.J., van Soest, H.L., Hof, A.F., den Elzen, M.G.J., van Vuuren, D.P., Chen, W., Drouet, L., Emmerling, J., Fujimori, S., Höhne, N., Köberle, A.C., McCollum, D., Schaeffer, R., Shekhar, S., Vishwanathan, S.S., Vrontisi, Z., Blok, K., 2020. Implications of various effort-sharing approaches for national carbon budgets and emission pathways. *Clim Change* 162, 1805–1822. <https://doi.org/10.1007/s10584-019-02368-y>
- van den Born, G.J., Kragt, F., Henkens, D., Rijken, B., van Bommel, B., van der Sluis, S., Polman, N., Bos, E.J., Kuhlman, T., Kwakernaak, C., others, 2016. Dalende bodems, stijgende kosten: mogelijke maatregelen tegen veenbodemdaling in het landelijk en stedelijk gebied: beleidsstudie. Den Haag.
- van der Esch, S., Sewell, A., Bakkenes, M., Berkhout, E., Doelman, J., Stehfest, E., Langhans, C., Bouwman, A., ten Brink, B., Fleskens, L., 2022. The global potential for land restoration: Scenarios for the Global Land Outlook 2. The Hague.
- van der Hilst, F., 2018. Location, location, location. *Nat Energy* 3, 164–165. <https://doi.org/10.1038/s41560-018-0094-3>
- van Dijk, M., Gramberger, M., Laborde, D., Mandryk, M., Shutes, L., Stehfest, E., Valin, H., Faradsch, K., 2020. Stakeholder-designed scenarios for global food security assessments. *Glob Food Sec* 24, 100352. <https://doi.org/https://doi.org/10.1016/j.gfs.2020.100352>
- van Ittersum, M.K., Cassman, K.G., Grassini, P., Wolf, J., Tittonell, P., Hochman, Z., 2013. Yield gap analysis with local to global relevance—A review. *Field Crops Res* 143, 4–17. <https://doi.org/10.1016/j.fcr.2012.09.009>
- van Ittersum, M.K., van Bussel, L.G.J., Wolf, J., Grassini, P., van Wart, J., Guilpart, N., Claessens, L., de Groot, H., Wiebe, K., Mason-D’Croz, D., 2016. Can sub-Saharan Africa feed itself? *Proceedings of the National Academy of Sciences* 113, 14964–14969.
- van Meijl, H., Havlik, P., Lotze-Campen, H., Stehfest, E., Witzke, P., Domínguez, I.P., Bodirsky, B.L., van Dijk, M., Doelman, J., Fellmann, T., 2018. Comparing impacts of climate change and mitigation on global agriculture by 2050. *Environmental Research Letters* 13, 64021. <https://doi.org/10.1088/1748-9326/aabdc4>
- van Meijl, H., Tabeau, A., Stehfest, E., Doelman, J., Lucas, P., 2020. How food secure are the green, rocky and middle roads: food security effects in different world development paths. *Environ Res Commun* 2, 31002. <https://doi.org/10.1088/2515-7620/ab7aba>
- van Meijl, H., van Rheenen, T., Tabeau, A., Eickhout, B., 2006. The impact of different policy environments on agricultural land use in Europe. *Agric Ecosyst Environ* 114, 21–38. <https://doi.org/10.1016/j.agee.2005.11.006>

- van Minnen, J.G., Strengers, B.J., Eickhout, B., Swart, R.J., Leemans, R., 2008. Quantifying the effectiveness of climate change mitigation through forest plantations and carbon sequestration with an integrated land-use model. *Carbon Balance Manag* 3, 1.
- van Soest, H.L., van Vuuren, D.P., Hilaire, J., Minx, J.C., Harmsen, M.J.H.M., Krey, V., Popp, A., Riahi, K., Luderer, G., 2019. Analysing interactions among sustainable development goals with integrated assessment models. *Glob Transit* 1, 210–225.
- van Vliet, M.T.H., Jones, E.R., Flörke, M., Franssen, W.H.P., Hanasaki, N., Wada, Y., Yearsley, J.R., 2021. Global water scarcity including surface water quality and expansions of clean water technologies. *Environmental Research Letters* 16, 24020. <https://doi.org/10.1088/1748-9326/abbfc3>
- van Vliet, M.T.H., Wiberg, D., Leduc, S., Riahi, K., 2016. Power-generation system vulnerability and adaptation to changes in climate and water resources. *Nat Clim Chang* 6, 375–380. <https://doi.org/10.1038/nclimate2903>
- van Vuuren, D.P., 2007. Energy systems and climate policy-long-term scenarios for an uncertain future.
- van Vuuren, D.P., Bijl, D.L., Bogaart, P., Stehfest, E., Biemans, H., Dekker, S.C., Doelman, J.C., Gernaat, D.E.H.J., Harmsen, M., 2019. Integrated scenarios to support analysis of the food–energy–water nexus. *Nat Sustain* 2. <https://doi.org/10.1038/s41893-019-0418-8>
- van Vuuren, D.P., Deetman, S., van Vliet, J., van den Berg, M., van Ruijven, B.J., Koelbl, B., 2013. The role of negative CO₂ emissions for reaching 2 °C—insights from integrated assessment modelling. *Clim Change* 118, 15–27. <https://doi.org/10.1007/s10584-012-0680-5>
- van Vuuren, D.P., Edmonds, J., Kainuma, M., Riahi, K., Thomson, A., Hibbard, K., Hurtt, G.C., Kram, T., Krey, V., Lamarque, J.-F., Masui, T., Meinshausen, M., Nakicenovic, N., Smith, S.J., Rose, S.K., 2011. The representative concentration pathways: an overview. *Clim Change* 109, 5–31. <https://doi.org/10.1007/s10584-011-0148-z>
- van Vuuren, D.P., Hof, A.F., van Sluisveld, M.A.E., Riahi, K., 2017a. Open discussion of negative emissions is urgently needed. *Nat Energy* 2, 902.
- van Vuuren, D.P., Kok, M., Lucas, P.L., Prins, A.G., Alkemade, R., van den Berg, M., Bouwman, L., van der Esch, S., Jeuken, M., Kram, T., 2015. Pathways to achieve a set of ambitious global sustainability objectives by 2050: explorations using the IMAGE integrated assessment model. *Technol Forecast Soc Change* 98, 303–323.
- van Vuuren, D.P., Riahi, K., Moss, R., Edmonds, J., Thomson, A., Nakicenovic, N., Kram, T., Berkhout, F., Swart, R., Janetos, A., Rose, S.K., Arnell, N., 2012. A proposal for a new scenario framework to support research and assessment in different climate research communities. *Global Environmental Change* 22, 21–35. <https://doi.org/10.1016/j.gloenvcha.2011.08.002>
- van Vuuren, D.P., Stehfest, E., Gernaat, D., de Boer, H.-S., Daioglou, V., Doelman, J.C., Edelenbosch, O., Harmsen, M., van Zeist, W.-J., van den Berg, M., 2021. The 2021 SSP scenarios of the IMAGE 3.2 model. The Hague. <https://doi.org/10.31223/X5CG92>
- van Vuuren, D.P., Stehfest, E., Gernaat, D.E.H.J., Berg, M., Bijl, D.L., Boer, H.S., Daioglou, V., Doelman, J.C., Edelenbosch, O.Y., Harmsen, M., Hof, A., Sluisveld, M.A.E., 2018. Alternative pathways to the 1.5 °C target reduce the need for negative emission technologies. *Nat Clim Chang* 8, 391–397. <https://doi.org/10.1038/s41558-018-0119-8>
- van Vuuren, D.P., Stehfest, E., Gernaat, D.E.H.J., Doelman, J.C., van den Berg, M., Harmsen, M., de Boer, H.S., Bouwman, L.F., Daioglou, V., Edelenbosch, O.Y., Girod, B., Kram, T., Lassaletta, L., Lucas, P.L., van Meijl, H., Müller, C., van Ruijven, B.J., van der Sluis, S., Tabeau, A., 2017b. Energy, land-use and greenhouse gas emissions trajectories under a green growth paradigm. *Global Environmental Change* 42, 237–250. <https://doi.org/10.1016/j.gloenvcha.2016.05.008>
- van Zeist, W.-J., Stehfest, E., Doelman, J.C., Valin, H., Calvin, K., Fujimori, S., Hasegawa, T., Havlik, P., Humpenöder, F., Kyle, P., 2020. Are scenario projections overly optimistic about future yield progress? *Global Environmental Change* 64, 102–120. <https://doi.org/10.1016/j.gloenvcha.2020.102120>

- Verburg, P.H., van de Steeg, J., Veldkamp, A., Willemsen, L., 2009. From land cover change to land function dynamics: a major challenge to improve land characterization. *J Environ Manage* 90, 1327–1335. <https://doi.org/10.1016/j.jenvman.2008.08.005>
- von Lampe, M., Willenbockel, D., Ahammad, H., Blanc, E., Cai, Y., Calvin, K., Fujimori, S., Hasegawa, T., Havlik, P., Heyhoe, E., Kyle, P., Lotze-Campen, H., Mason d’Croz, D., Nelson, G.C., Sands, R.D., Schmitz, C., Tabeau, A., Valin, H., van der Mensbrugge, D., van Meijl, H., 2014. Why do global long-term scenarios for agriculture differ? An overview of the AgMIP Global Economic Model Intercomparison 45, 3–20. <https://doi.org/doi:10.1111/agec.12086>
- Vörösmarty, C.J., McIntyre, P.B., Gessner, M.O., Dudgeon, D., Prusevich, A., Green, P., Glidden, S., Bunn, S.E., Sullivan, C.A., Liermann, C.R., 2010. Global threats to human water security and river biodiversity. *Nature* 467, 555–561.
- Wada, Y., van Beek, L.P.H., van Kempen, C.M., Reckman, J.W.T.M., Vasak, S., Bierkens, M.F.P., 2010. Global depletion of groundwater resources. *Geophys Res Lett* 37, n/a-n/a. <https://doi.org/10.1029/2010gl044571>
- Wada, Y., Wisser, D., Eisner, S., Flörke, M., Gerten, D., Haddeland, I., Hanasaki, N., Masaki, Y., Portmann, F.T., Stacke, T., Tessler, Z., Schewe, J., 2013. Multimodel projections and uncertainties of irrigation water demand under climate change. *Geophys Res Lett* 40, 4626–4632. <https://doi.org/10.1002/grl.50686>
- Wang, X., Dietrich, J.P., Lotze-Campen, H., Biewald, A., Stevanović, M., Bodirsky, B.L., Brümmer, B., Popp, A., 2020. Beyond land-use intensity: Assessing future global crop productivity growth under different socioeconomic pathways. *Technol Forecast Soc Change* 160, 120208. <https://doi.org/https://doi.org/10.1016/j.techfore.2020.120208>
- Ward, K., Lauf, S., Kleinschmit, B., Endlicher, W., 2016. Heat waves and urban heat islands in Europe: A review of relevant drivers. *Science of The Total Environment* 569–570, 527–539. <https://doi.org/https://doi.org/10.1016/j.scitotenv.2016.06.119>
- Watson, R.T., Noble, I.R., Bolin, B., Ravindranath, N.H., Verardo, D.J., Dokken, D.J., 2000. *Land Use, Land-Use Change and Forestry*. IPCC, Cambridge, UK.
- Weindl, I., Bodirsky, B.L., Rolinski, S., Biewald, A., Lotze-Campen, H., Müller, C., Dietrich, J.P., Humpenöder, F., Stevanović, M., Schaphoff, S., Popp, A., 2017a. Livestock production and the water challenge of future food supply: Implications of agricultural management and dietary choices. *Global Environmental Change* 47, 121–132. <https://doi.org/https://doi.org/10.1016/j.gloenvcha.2017.09.010>
- Weindl, I., Popp, A., Bodirsky, B.L., Rolinski, S., Lotze-Campen, H., Biewald, A., Humpenöder, F., Dietrich, J.P., Stevanović, M., 2017b. Livestock and human use of land: Productivity trends and dietary choices as drivers of future land and carbon dynamics. *Glob Planet Change* 159, 1–10. <https://doi.org/https://doi.org/10.1016/j.gloplacha.2017.10.002>
- Willett, W., Rockström, J., Loken, B., Springmann, M., Lang, T., Vermeulen, S., Garnett, T., Tilman, D., DeClerck, F., Wood, A., Jonell, M., Clark, M., Gordon, L.J., Fanzo, J., Hawkes, C., Zurayk, R., Rivera, J.A., de Vries, W., Majele Sibanda, L., Afshin, A., Chaudhary, A., Herrero, M., Agustina, R., Branca, F., Lartey, A., Fan, S., Crona, B., Fox, E., Bignet, V., Troell, M., Lindahl, T., Singh, S., Cornell, S.E., Srinath Reddy, K., Narain, S., Nishtar, S., Murray, C.J.L., 2019. Food in the Anthropocene: the EAT–Lancet Commission on healthy diets from sustainable food systems. *The Lancet*. [https://doi.org/https://doi.org/10.1016/S0140-6736\(18\)31788-4](https://doi.org/https://doi.org/10.1016/S0140-6736(18)31788-4)
- Wilson, D., Blain, D., Couwenberg, J., Evans, C.D., Murdiyarto, D., Page, S.E., Renou-Wilson, F., Rieley, J.O., Sirin, A., Strack, M., Tuittila, E.-S., 2016. Greenhouse gas emission factors associated with rewetting of organic soils. *Mires and Peat* 17.
- Wilson, E.O., 2016. *Half-earth: our planet’s fight for life*. WW Norton & Company.
- Winsemius, H.C., van Beek, L.P.H., Jongman, B., Ward, P.J., Bouwman, A., 2013. A framework for global river flood risk assessments. *Hydrol Earth Syst Sci* 17, 1871–1892. <https://doi.org/10.5194/hess-17-1871-2013>
- Winsten, J., Walker, S., Brown, S., Grimland, S., 2011. Estimating carbon supply curves from afforestation of agricultural land in the Northeastern U.S. *Mitig Adapt Strateg Glob Chang* 16, 925–942. <https://doi.org/10.1007/s11027-011-9303-0>

- Wise, M., Calvin, K., Kyle, P., Luckow, P., Edmonds, J., 2014. Economic and physical modeling of land use in GCAM 3.0 and an application to agricultural productivity, land, and terrestrial carbon. *Clim Chang Econ* (Singap) 5, 1450003.
- Wisser, D., Frohling, S., Douglas, E.M., Fekete, B.M., Vörösmarty, C.J., Schumann, A.H., 2008. Global irrigation water demand: Variability and uncertainties arising from agricultural and climate data sets. *Geophys Res Lett* 35. <https://doi.org/https://doi.org/10.1029/2008GL035296>
- Woltjer, G.B., Kuiper, M., Kavallari, A., van Meijl, H., Powell, J.P., Rutten, M.M., Shutes, L.J., Tabeau, A.A., 2014. The MAGNET model: Module description. LEI Wageningen UR.
- Wu, Y., Chan, E., Melton, J.R., Versegny, D.L., 2017. A map of global peatland distribution created using machine learning for use in terrestrial ecosystem and earth system models. *Geoscientific Model Development Discussions* 1–21.
- Xu, J., Morris, P.J., Liu, J., Holden, J., 2018. PEATMAP: Refining estimates of global peatland distribution based on a meta-analysis. *Catena* (Amst) 160, 134–140. <https://doi.org/https://doi.org/10.1016/j.catena.2017.09.010>
- Yang, Y.C.E., Ringler, C., Brown, C., Mondal, M.A.H., 2016. Modeling the agricultural water–energy–food nexus in the Indus River Basin, Pakistan. *J Water Resour Plan Manag* 142, 4016062.
- Yu, Z., Loisel, J., Brosseau, D.P., Beilman, D.W., Hunt, S.J., 2010. Global peatland dynamics since the Last Glacial Maximum. *Geophys Res Lett* 37. <https://doi.org/https://doi.org/10.1029/2010GL043584>
- Zalasiewicz, J., Williams, M., 2012. *The Goldilocks Planet: The 4 billion year story of Earth's climate*. Oxford University Press, Oxford.
- Zhang, X., Davidson, E.A., Mauzerall, D.L., Searchinger, T.D., Dumas, P., Shen, Y., 2015. Managing nitrogen for sustainable development. *Nature* 528, 51–59.
- Zhang, X., Zou, T., Lassaletta, L., Mueller, N.D., Tubiello, F.N., Lisk, M.D., Lu, C., Conant, R.T., Dorich, C.D., Gerber, J., Tian, H., Bruulsema, T., Maaz, T.M., Nishina, K., Bodirsky, B.L., Popp, A., Bouwman, L., Beusen, A., Chang, J., Havlík, P., Leclère, D., Canadell, J.G., Jackson, R.B., Heffer, P., Wanner, N., Zhang, W., Davidson, E.A., 2021. Quantification of global and national nitrogen budgets for crop production. *Nat Food*. <https://doi.org/10.1038/s43016-021-00318-5>
- Zhao, C., Liu, B., Piao, S., Wang, X., Lobell, D.B., Huang, Y., Huang, M., Yao, Y., Bassu, S., Ciais, P., Durand, J.-L., Elliott, J., Ewert, F., Janssens, I.A., Li, T., Lin, E., Liu, Q., Martre, P., Müller, C., Peng, S., Peñuelas, J., Ruane, A.C., Wallach, D., Wang, T., Wu, D., Liu, Z., Zhu, Y., Zhu, Z., Asseng, S., 2017. Temperature increase reduces global yields of major crops in four independent estimates. *Proceedings of the National Academy of Sciences* 114, 9326–9331. <https://doi.org/10.1073/pnas.1701762114>

Acknowledgements

Nearly ten years ago when I first visited PBL, then still located at the RIVM premises in the forests of Bilthoven, I could not have imagined that I would one day get a PhD in integrated assessment modelling. It took some perseverance at times, but I am incredibly happy and grateful to have reached this milestone. I would certainly not have made it this far without the support of colleagues, family and friends.

First of all, my gratitude goes out to Elke, my co-promotor. You gave me the opportunity to get to know the IMAGE work, even though as a fresh graduate in physical geography I had barely any modelling experience. I have learned a great deal from you, your support and critical feedback have been essential in my professional development, and I admire your passion for science. A big thank you of course goes to Detlef, my promotor. Thanks for your inspiration and motivation, and your unwavering enthusiasm for every dimension of our research. I am grateful for the many opportunities you gave me to participate in interesting scientific collaborations, and your capacity to provide high-quality feedback at the oddest of hours does not cease to amaze me.

I have always experienced working as part of the IMAGE team as a great privilege thanks to the wonderful colleagues. Liesbeth, your skill to code Fortran ‘even while sleeping’ has been crucial for the successful finalization of this thesis, and the endless stories about your dogs and horses were a healthy distraction from the day-to-day work. Willem-Jan, working together on IMAGE and MAGNET was always great fun, and your move to WEcR was a great win for Wageningen and a big loss for PBL. Fortunately, that didn’t prevent us from collaborating closely, both professionally and during the *borrels* where every evening was bound to end with an excessively alcoholic stout or barley wine. Maarten, our co-supervision of various interns was always a great pleasure and I am happy you agreed to be paranymp at my PhD defense. David and Mathijs, it took lots of reruns to finally get those IMAGE 3.0 SSP scenarios perfect (thanks again for your patience to teach me the ins and outs of the IMAGE train and the one-click), but in the end we cooperated like a well-oiled machine. Of course I want to thank the entire IMAGE team, with a big risk of forgetting some people (sorry!). The IMAGE-land team *oude garde* (Tom, Rineke, Kees, Jelle, Peter, Coen, Frits, Maryia, Maarten B.) as well as the more recent generation (Lotte, Willem, Astrid, Ge, Hermen, Carlijn), the TIMER team (Vassilis, Harmen-Sytze, Oreane, Mariesse, Anteneh, Nicole, Kaj-Ivar, Hsing-Hsuan, Isabela, Rik, Mark) and of course the climate policy team (Andries, Michel, Heleen, Mark, Kendall, Ioannis, Elena).

As described at length in this thesis, land is central to many environmental and societal challenges. My work on land allowed me to cooperate with many people throughout PBL. For the productive and enjoyable cooperations I would like to thank Lex, Arthur, Luis and Peter (global nutrient cycles), Arno and Willem (water), Henk (food), Paul (health), Frank and Bas (urbanization), Maria and Jan (nexus), and the entire GLOBIO team (Aafke, Mark, Rob,

Clara, Michel, Jelle, Marcel, Harry, Alexandra, Machteld). A big thanks also to the Global Land Outlook team for the challenging but interesting work we did on desertification and land degradation for the UNCCD (Stefan, Annelies, Willem, Christoph, Michel, Ben, Ezra, Sophie). Finally I would like to thank the management of PBL who have supported me throughout the process of finishing this thesis, especially Martine and Tom.

A number of colleagues beyond PBL also contributed enormously to this thesis. I want to specifically thank the MAGNET team from Wageningen Economic Research. The close collaboration between IMAGE and MAGNET has proven very successful over the years, but this would not have been possible without the very pleasant personal connection with Andrzej, Hans and Jason (and nowadays Willem-Jan). Also the collaboration with Hester from Wageningen Environmental Research on water modelling with LPJmL has been very enjoyable over the years. An important note of thanks also goes out to the developers of LPJmL at PIK in Potsdam, especially to Christoph who is always supportive of the close link between our two models. I am also grateful for the many wonderful international collaborations that I could participate in as part of various European projects, most importantly LUC4C, SIM4NEXUS and the AgCLIM projects. A special note of thanks to the MAGPIE team at PIK who contributed to Chapter 6 and various joint project deliverables over the years (Alex, Florian, Benni and Feli). Finally, I want to thank Utrecht University, my alma mater. After finishing both my Bachelor and Master degrees in Utrecht, it feels perfectly natural to also earn my PhD degree at UU.

Of course I want to thank my friends for so many great memories: the Skifahrers, Cullieboys, Ijsstrijkers, JCU batties and echte bosjesmannen. I bet many of you are happy to see that, in essence, I just continued my MSc hobby of counting trees (see Chapter 4).

A special word goes out to my uncle and paranymp, Leo. From a young age I found your job in which you were 'saving the world' highly intriguing, although the IPCC work was also rather incomprehensible to me. This changed in the third grade of high school, when you took me on a *snuffelstage* to one of the UN organizations in Bonn where you were presenting the Montreal Protocol. I vividly remember you explained to me the essence of the protocol and the chemistry behind ozone depletion, while travelling on the train. I still thought it was very complicated, but it did feel like I could one day maybe work on such a topic. That became a reality when you introduced me to Elke at PBL, and this thesis is the result. Very importantly, I also want to thank my wonderful aunt Pien for supporting me, and for introducing Leo into our family.

Of course I want to thank my dear parents who have always been so supportive and interested in my professional and academic career, even though their own academic backgrounds do not match the contents of this thesis very well. I would never have been able to get this far without your help. An extra big thanks goes out to my dad for providing the Dutch translation of this thesis (Chapter 8). I also want to thank my sister Marieke and her husband Thijs for their love and support.

Last but not least, I want to thank my love Barbara for always being there for me, and for putting up with me when I was yet again fussing about another dreadful review round. Achieving this milestone would definitely not have been possible without you in my life, and I am looking forward to the next chapters in our lives with our lovely daughters.

And with that being said, I now close this book...

Curriculum Vitae

Jonathan Doelman was born on the 22nd of March 1989 in Amsterdam, the Netherlands. He spent his childhood in Landsmeer, Nijmegen and Culemborg. In 2007 he graduated from secondary school in Culemborg (VWO). From 2007 to 2010 he attended University College Utrecht where he studied liberal arts and sciences majoring in earth, environmental and climate sciences with a minor in human geography. During his bachelor he participated in an exchange program at the University of Iceland in Reykjavík where he studied geology. Subsequently he did a master studies in Physical Geography at Utrecht University where he graduated in 2013. His thesis was on the topic of hyperspectral remote sensing of Mediterranean vegetation. In addition he did an internship on satellite observation of tropical deforestation in the Amazon rainforest with Greenpeace in Manaus, Brazil. After graduating he worked part-time as an assistant teacher at the department of physical geography at UU. In addition, he started as an intern with the IMAGE-team at PBL on agricultural land-use allocation. In 2014, he started a full-time job at PBL funded by the European research project LUC4C focusing on land-based climate change mitigation measures and the development of land use scenarios, most notably the SSPs. In 2017 he worked for three months at Wageningen Economic Research in the MAGNET-team on agro-economic impacts of climate change and climate change mitigation measures as part of the JRC-funded AgCLIM50-II project. Subsequently he returned to PBL to work on the development and application of the IMAGE model with a focus on land in various projects such as SIM4NEXUS and the second Global Land Outlook report for the UNCCD. He continues to work at PBL with the IMAGE model framework and in various Horizon Europe projects such as LAMASUS, BrightSpace and ForestPaths as well as for UNEPs seventh Global Environmental Outlook report.

List of publications

This thesis

- Doelman, J. C.**, Beier, F. D., Stehfest, E., Bodirsky, B. L., Beusen, A. H. W., Humpenöder, F., Mishra, A., Popp, A., van Vuuren, D. P., de Vos, L., Weindl, I., van Zeist, W.-J., & Kram, T. (2022). Quantifying synergies and trade-offs in the global water-land-food-climate nexus using a multi-model scenario approach. *Environmental Research Letters*, 17(4), 045004. <https://doi.org/10.1088/1748-9326/ac5766>
- Doelman, J. C.**, Stehfest, E., Tabeau, A., & van Meijl, H. (2019). Making the Paris agreement climate targets consistent with food security objectives. *Global Food Security*, 23, 93–103. <https://doi.org/https://doi.org/10.1016/j.gfs.2019.04.003>
- Doelman, J. C.**, Stehfest, E., Tabeau, A., van Meijl, H., Lassaletta, L., Gernaat, D. E. H. J., Hermans, K., Harmsen, M., Daioglou, V., Biemans, H., van der Sluis, S., & van Vuuren, D. P. (2018). Exploring SSP land-use dynamics using the IMAGE model: Regional and gridded scenarios of land-use change and land-based climate change mitigation. *Global Environmental Change*, 48, 119–135. <https://doi.org/10.1016/j.gloenvcha.2017.11.014>
- Doelman, J. C.**, Stehfest, E., van Vuuren, D. P., Tabeau, A., Hof, A. F., Braakhekke, M. C., Gernaat, D. E. H. J., van den Berg, M., van Zeist, W.-J., Daioglou, V., van Meijl, H., & Lucas, P. L. (2020). Afforestation for climate change mitigation: Potentials, risks and trade-offs. *Global Change Biology*, 26(3). <https://doi.org/10.1111/gcb.14887>

Other publications

- Alexander, P., Prestele, R., Verburg, P. H., Arneith, A., Baranzelli, C., e Silva, F., Brown, C., Butler, A., Calvin, K., Dendoncker, N., **Doelman, J. C.**, Dunford, R., Engström, K., Eitelberg, D., Fujimori, S., Harrison, P. A., Hasegawa, T., Havlik, P., Holzhauser, S., ... Rounsevell, M. D. A. (2017). Assessing uncertainties in land cover projections. *Global Change Biology*, 23(2), 767–781. <https://doi.org/https://doi.org/10.1111/gcb.13447>
- Beusen, A. H. W., **Doelman, J. C.**, van Beek, L. P. H., van Puijenbroek, P. J. T. M., Mogollón, J. M., van Grinsven, H. J. M., Stehfest, E., van Vuuren, D. P., & Bouwman, A. F. (2022). Exploring river nitrogen and phosphorus loading and export to global coastal waters in the Shared Socio-economic pathways. *Global Environmental Change*, 72, 102426. <https://doi.org/https://doi.org/10.1016/j.gloenvcha.2021.102426>
- Bijl, D. L., Biemans, H., Bogaart, P. W., Dekker, S. C., **Doelman, J. C.**, Stehfest, E., & van Vuuren, D. P. (2018). A Global Analysis of Future Water Deficit Based On Different Allocation Mechanisms. *Water Resources Research*, 54(8), 5803–5824. <https://doi.org/https://doi.org/10.1029/2017WR021688>
- Braakhekke, M. C., **Doelman, J. C.**, Baas, P., Müller, C., Schaphoff, S., Stehfest, E., & van Vuuren, D. P. (2019). Modeling forest plantations for carbon uptake with the LPJmL dynamic global vegetation model. *Earth System Dynamics*, 10(4), 617–630. <https://doi.org/10.5194/esd-10-617-2019>
- Cengic, M., Steinmann, Z. J. N., Defourny, P., **Doelman, J. C.**, Lamarche, C., Stehfest, E., Schipper, A. M., & Huijbregts, M. A. (2023). Global Maps of Agricultural Expansion Potential at a 300 m Resolution. *Land*, 12(579).
- Daioglou, V., **Doelman, J. C.**, Stehfest, E., Müller, C., Wicke, B., Faaij, A., & van Vuuren, D. P. (2017). Greenhouse gas emission curves for advanced biofuel supply chains. *Nature Climate Change*, 7(12), 920–924. <https://doi.org/10.1038/s41558-017-0006-8>
- Daioglou, V., **Doelman, J. C.**, Wicke, B., Faaij, A., & van Vuuren, D. P. (2019). Integrated assessment of biomass supply and demand in climate change mitigation scenarios. *Global Environmental Change*, 54, 88–101. <https://doi.org/https://doi.org/10.1016/j.gloenvcha.2018.11.012>
- Doelman, J. C.**, & Stehfest, E. (2022). The risks of overstating the climate benefits of ecosystem restoration. *Nature*, 609(7926), E1–E3. <https://doi.org/10.1038/s41586-022-04881-0>

- de Vos, L., Biemans, H., **Doelman, J. C.**, Stehfest, E., & van Vuuren, D. P. (2021). Trade-offs between water needs for food, utilities, and the environment—a nexus quantification at different scales. *Environmental Research Letters*, 16(11), 115003. <https://doi.org/10.1088/1748-9326/ac2b5e>
- Edelensbosch, O., van den Berg, M., de Boer, H.-S., Chen, H., Daioglou, V., Dekker, M., **Doelman, J. C.**, den Elzen, M., Frinking, V., Harmsen, M., Hof, A., Mikropoulos, E., van Sluisveld, M., Tagomori, I., & van Vuuren, D. (2022). Mitigating greenhouse gas emissions in hard-to-abate sectors.
- Eitelberg, D. A., van Vliet, J., **Doelman, J. C.**, Stehfest, E., & Verburg, P. H. (2016). Demand for biodiversity protection and carbon storage as drivers of global land change scenarios. *Global Environmental Change*, 40, 101–111. <https://doi.org/https://doi.org/10.1016/j.gloenvcha.2016.06.014>
- Fitton, N., Alexander, P., Arnell, N., Bajzelj, B., Calvin, K., **Doelman, J. C.**, Gerber, J. S., Havlik, P., Hasegawa, T., Herrero, M., Krisztin, T., van Meijl, H., Powell, T., Sands, R., Stehfest, E., West, P. C., & Smith, P. (2019). The vulnerabilities of agricultural land and food production to future water scarcity. *Global Environmental Change*, 58. <https://doi.org/10.1016/j.gloenvcha.2019.101944>
- Frank, S., Havlík, P., Stehfest, E., van Meijl, H., Witzke, P., Pérez-Domínguez, I., van Dijk, M., **Doelman, J. C.**, Fellmann, T., Koopman, J. F. L., Tabeau, A., & Valin, H. (2019). Agricultural non-CO₂ emission reduction potential in the context of the 1.5 °C target. *Nature Climate Change*, 9(1), 66–72. <https://doi.org/10.1038/s41558-018-0358-8>
- Fujimori, S., Hasegawa, T., Krey, V., Riahi, K., Bertram, C., Bodirsky, B. L., Bosetti, V., Callen, J., Després, J., **Doelman, J. C.**, Drouet, L., Emmerling, J., Frank, S., Fricko, O., Havlik, P., Humpenöder, F., Koopman, J. F. L., van Meijl, H., Ochi, Y., ... van Vuuren, D. (2019). A multi-model assessment of food security implications of climate change mitigation. *Nature Sustainability*, 2(5), 386–396. <https://doi.org/10.1038/s41893-019-0286-2>
- Fujimori, S., Wu, W., **Doelman, J. C.**, Frank, S., Hristov, J., Kyle, P., Sands, R., van Zeist, W.-J., Havlik, P., Domínguez, I. P., Sahoo, A., Stehfest, E., Tabeau, A., Valin, H., van Meijl, H., Hasegawa, T., & Takahashi, K. (2022). Land-based climate change mitigation measures can affect agricultural markets and food security. *Nature Food*, 3(2), 110–121. <https://doi.org/10.1038/s43016-022-00464-4>
- Gidden, M. J., Riahi, K., Smith, S. J., Fujimori, S., Luderer, G., Kriegler, E., van Vuuren, D. P., van den Berg, M., Feng, L., Klein, D., Calvin, K., **Doelman, J. C.**, Frank, S., Fricko, O., Harmsen, M., Hasegawa, T., Havlik, P., Hilaire, J., Hoesly, R., ... Takahashi, K. (2019). Global emissions pathways under different socioeconomic scenarios for use in CMIP6: a dataset of harmonized emissions trajectories through the end of the century. *Geoscientific Model Development*, 12(4), 1443–1475. <https://doi.org/10.5194/gmd-12-1443-2019>
- Gil, J. D. B., Daioglou, V., van Ittersum, M., Reidsma, P., **Doelman, J. C.**, van Middelaar, C. E., & van Vuuren, D. P. (2019). Reconciling global sustainability targets and local action for food production and climate change mitigation. *Global Environmental Change*, 59. <https://doi.org/10.1016/j.gloenvcha.2019.101983>
- Hanssen, S. v., Daioglou, V., Steinmann, Z. J. N., **Doelman, J. C.**, van Vuuren, D. P., & Huijbregts, M. A. J. (2020). The climate change mitigation potential of bioenergy with carbon capture and storage. *Nature Climate Change*, 10(11), 1023–1029. <https://doi.org/10.1038/s41558-020-0885-y>
- Harper, A. B., Powell, T., Cox, P. M., House, J., Huntingford, C., Lenton, T. M., Sitch, S., Burke, E., Chadburn, S. E., Collins, W. J., Comyn-Platt, E., Daioglou, V., **Doelman, J. C.**, Hayman, G., Robertson, E., van Vuuren, D., Wiltshire, A., Webber, C. P., Bastos, A., ... Shu, S. (2018). Land-use emissions play a critical role in land-based mitigation for Paris climate targets. *Nature Communications*, 9(1), 2938. <https://doi.org/10.1038/s41467-018-05340-z>
- Hasegawa, T., Fujimori, S., Havlík, P., Valin, H., Bodirsky, B. L., **Doelman, J. C.**, Fellmann, T., Kyle, P., Koopman, J. F. L., Lotze-Campen, H., Mason-D’Croz, D., Ochi, Y., Pérez Domínguez, I., Stehfest, E., Sulser, T. B., Tabeau, A., Takahashi, K., Takakura, J., van Meijl, H., ... Witzke, P. (2018). Risk of increased food insecurity under stringent global climate change mitigation policy. *Nature Climate Change*, 8(8), 699–703. <https://doi.org/10.1038/s41558-018-0230-x>

- Hayman, G. D., Comyn-Platt, E., Huntingford, C., Harper, A. B., Powell, T., Cox, P. M., Collins, W., Webber, C., Lowe, J., Sitch, S., House, J. I., **Doelman, J. C.**, van Vuuren, D. P., Chadburn, S. E., Burke, E., & Gedney, N. (2020). Regional variation in the effectiveness of methane-based and land-based climate mitigation options. *Earth Syst. Dynam. Discuss.*, 2020, 1–41. <https://doi.org/10.5194/esd-2020-24>
- Hof, A. F., Esmeijer, K., de Boer, H. S., Daioglou, V., **Doelman, J. C.**, Elzen, M. G. J. den, Gernaat, D. E. H. J., & van Vuuren, D. P. (2022). Regional energy diversity and sovereignty in different 2 °C and 1.5 °C pathways. *Energy*, 239, 122197. <https://doi.org/https://doi.org/10.1016/j.energy.2021.122197>
- Hurttt, G. C., Chini, L., Sahajpal, R., Frolking, S., Bodirsky, B. L., Calvin, K., **Doelman, J. C.**, Fisk, J., Fujimori, S., Klein Goldewijk, K., Hasegawa, T., Havlik, P., Heinemann, A., Humpenöder, F., Jungclaus, J., Kaplan, J. O., Kennedy, J., Krisztin, T., Lawrence, D., ... Zhang, X. (2020). Harmonization of global land use change and management for the period 850–2100 (LUH2) for CMIP6. *Geosci. Model Dev.*, 13(11), 5425–5464. <https://doi.org/10.5194/gmd-13-5425-2020>
- Khan, Z., Abraham, E., Aggarwal, S., Ahmad Khan, M., Arguello, R., Babbar-Sebens, M., Bereslawski, J. L., Bielicki, J. M., Campana, P. E., Silva Carrazzone, M. E., Castanier, H., Chang, F.-J., Collins, P., Conchado, A., Dagan, K. R., Daher, B., Dekker, S. C., Delgado, R., Diuana, F. A., **Doelman, J. C.**, ... Yue, Q. (2022). Emerging Themes and Future Directions of Multi-Sector Nexus Research and Implementation. *Frontiers in Environmental Science*, 10. <https://doi.org/10.3389/fenvs.2022.918085>
- Klein Goldewijk, K., Beusen, A., **Doelman, J. C.**, & Stehfest, E. (2017). New anthropogenic land use estimates for the Holocene: HYDE 3.2. *Earth System Science Data*, 9(2), 927–953. <https://doi.org/10.5194/essd-9-927-2017>
- Krause, A., Pugh, T. A. M., Bayer, A. D., **Doelman, J. C.**, Humpenöder, F., Anthoni, P., Olin, S., Bodirsky, B. L., Popp, A., Stehfest, E., & Arneth, A. (2017). Global consequences of afforestation and bioenergy cultivation on ecosystem service indicators. *Biogeosciences*, 14(21), 4829–4850. <https://doi.org/10.5194/bg-14-4829-2017>
- Krause, A., Pugh, T. A. M., Bayer, A. D., Li, W., Leung, F., Bondeau, A., **Doelman, J. C.**, Humpenöder, F., Anthoni, P., Bodirsky, B. L., Ciais, P., Müller, C., Murray-Tortarolo, G., Olin, S., Popp, A., Sitch, S., Stehfest, E., & Arneth, A. (2018). Large uncertainty in carbon uptake potential of land-based climate-change mitigation efforts. *Global Change Biology*, 24(7), 3025–3038. <https://doi.org/https://doi.org/10.1111/gcb.14144>
- Lassaletta, L., Estellés, F., Beusen, A. H. W., Bouwman, L., Calvet, S., van Grinsven, H. J. M., **Doelman, J. C.**, Stehfest, E., Uwizeye, A., & Westhoek, H. (2019). Future global pig production systems according to the Shared Socioeconomic Pathways. *Science of The Total Environment*, 665, 739–751. <https://doi.org/https://doi.org/10.1016/j.scitotenv.2019.02.079>
- Leclère, D., Obersteiner, M., Barrett, M., Butchart, S. H. M., Chaudhary, A., de Palma, A., DeClerck, F. A. J., di Marco, M., **Doelman, J. C.**, Dürauer, M., Freeman, R., Harfoot, M., Hasegawa, T., Hellweg, S., Hilbers, J. P., Hill, S. L. L., Humpenöder, F., Jennings, N., Krisztin, T., ... Young, L. (2020). Bending the curve of terrestrial biodiversity needs an integrated strategy. *Nature*, 585(7826), 551–556. <https://doi.org/10.1038/s41586-020-2705-y>
- Li, W., Ciais, P., Stehfest, E., van Vuuren, D., Popp, A., Arneth, A., di Fulvio, F., **Doelman, J. C.**, Humpenöder, F., Harper, A. B., Park, T., Makowski, D., Havlik, P., Obersteiner, M., Wang, J., Krause, A., & Liu, W. (2020). Mapping the yields of lignocellulosic bioenergy crops from observations at the global scale. *Earth System Science Data*, 12(2), 789–804. <https://doi.org/10.5194/essd-12-789-2020>
- Littleton, E. W., Shepherd, A., Harper, A. B., Hastings, A. F. S., Vaughan, N. E., **Doelman, J. C.**, van Vuuren, D. P., & Lenton, T. M. (2023). Uncertain effectiveness of *Miscanthus* bioenergy expansion for climate change mitigation explored using land surface, agronomic and integrated assessment models. *GCB Bioenergy*, 15(3), 303–318. <https://doi.org/https://doi.org/10.1111/gcbb.12982>
- Ma, L., Hurttt, G. C., Chini, L. P., Sahajpal, R., Pongratz, J., Frolking, S., Stehfest, E., Klein Goldewijk, K., O’Leary, D., & **Doelman, J. C.** (2020). Global rules for translating land-use change (LUH2) to land-cover change for CMIP6 using GLM2. *Geoscientific Model Development*, 13(7), 3203–3220. <https://doi.org/10.5194/gmd-13-3203-2020>

- Mandryk, M., **Doelman, J. C.**, & Stehfest, E. (2015). Assessment of global land availability. FOODSECURE Technical Working Paper No. 7.
- Marquardt, S. G., **Doelman, J. C.**, Daioglou, V., Tabeau, A., Schipper, A. M., Sim, S., Kulak, M., Steinmann, Z. J. N., Stehfest, E., Wilting, H. C., & Huijbregts, M. A. J. (2021). Identifying regional drivers of future land-based biodiversity footprints. *Global Environmental Change*, 69, 102304. <https://doi.org/https://doi.org/10.1016/j.gloenvcha.2021.102304>
- Molotoks, A., Henry, R., Stehfest, E., **Doelman, J. C.**, Havlik, P., Krisztin, T., Alexander, P., Dawson, T. P., & Smith, P. (2020). Comparing the impact of future cropland expansion on global biodiversity and carbon storage across models and scenarios. *Philosophical Transactions of the Royal Society B: Biological Sciences*, 375(1794). <https://doi.org/10.1098/rstb.2019.0189>
- Popp, A., Calvin, K., Fujimori, S., Havlik, P., Humpenöder, F., Stehfest, E., Bodirsky, B. L., Dietrich, J. P., **Doelman, J. C.**, Gusti, M., Hasegawa, T., Kyle, P., Obersteiner, M., Tabeau, A., Takahashi, K., Valin, H., Waldhoff, S., Weindl, I., Wise, M., ... van Vuuren, D. P. (2017). Land-use futures in the shared socio-economic pathways. *Global Environmental Change*, 42, 331–345. <https://doi.org/10.1016/j.gloenvcha.2016.10.002>
- Prestele, R., Alexander, P., Rounsevell, M. D. A., Arneth, A., Calvin, K., **Doelman, J. C.**, Eitelberg, D. A., Engström, K., Fujimori, S., Hasegawa, T., Havlik, P., Humpenöder, F., Jain, A. K., Krisztin, T., Kyle, P., Meiyappan, P., Popp, A., Sands, R. D., Schaldach, R., ... Verburg, P. H. (2016). Hotspots of uncertainty in land-use and land-cover change projections: a global-scale model comparison. *Global Change Biology*, 22(12), 3967–3983. <https://doi.org/https://doi.org/10.1111/gcb.13337>
- Riahi, K., van Vuuren, D. P., Kriegler, E., Edmonds, J., O'Neill, B. C., Fujimori, S., Bauer, N., Calvin, K., Dellink, R., Fricko, O., Lutz, W., Popp, A., Cuaresma, J. C., KC, S., Leimbach, M., Jiang, L., Kram, T., Rao, S., Emmerling, J., ..., **Doelman, J. C.**, ..., Tavoni, M. (2017). The shared socioeconomic pathways and their energy, land use, and greenhouse gas emissions implications: an overview. *Global Environmental Change*, 42, 153–168. <https://doi.org/10.1016/j.gloenvcha.2016.05.009>
- Roe, S., Streck, C., Beach, R., Busch, J., Chapman, M., Daioglou, V., Deppermann, A., **Doelman, J. C.**, Emmet-Booth, J., Engelmann, J., Fricko, O., Frischmann, C., Funk, J., Grassi, G., Griscom, B., Havlik, P., Hanssen, S., Humpenöder, F., Landholm, D., ... Lawrence, D. (2021). Land-based measures to mitigate climate change: Potential and feasibility by country. *Global Change Biology*, 27(23), 6025–6058. <https://doi.org/https://doi.org/10.1111/gcb.15873>
- Rogelj, J., Popp, A., Calvin, K. v., Luderer, G., Emmerling, J., Gernaat, D., Fujimori, S., Strefler, J., Hasegawa, T., Marangoni, G., Krey, V., Kriegler, E., Riahi, K., van Vuuren, D. P., **Doelman, J. C.**, Drouet, L., Edmonds, J., Fricko, O., Harmsen, M., ... Tavoni, M. (2018). Scenarios towards limiting global mean temperature increase below 1.5° C. *Nature Climate Change*, 8(4), 325. <https://doi.org/10.1038/s41558-018-0091-3>
- Rose, S. K., Popp, A., Fujimori, S., Havlik, P., Weyant, J., Wise, M., van Vuuren, D., Brunelle, T., Cui, R. Y., Daioglou, V., Frank, S., Hasegawa, T., Humpenöder, F., Kato, E., Sands, R. D., Sano, F., Tsutsui, J., **Doelman, J. C.**, Muratori, M., ... Yamamoto, H. (2022). Global biomass supply modeling for long-run management of the climate system. *Climatic Change*, 172(1), 3. <https://doi.org/10.1007/s10584-022-03336-9>
- Schipper, A. M., Hilbers, J. P., Meijer, J. R., Antão, L. H., Benítez-López, A., de Jonge, M. M. J., Leemans, L. H., Scheper, E., Alkemade, R., & **Doelman, J. C.** (2020). Projecting terrestrial biodiversity intactness with GLOBIO 4. *Global Change Biology*, 26(2), 760–771. <https://doi.org/10.1111/gcb.14848>
- Seneviratne, S. I., Wartenburger, R., Guillod, B. P., Hirsch, A. L., Vogel, M. M., Brovkin, V., van Vuuren, D. P., Schaller, N., Boysen, L., Calvin, K. v., **Doelman, J. C.**, Greve, P., Havlik, P., Humpenöder, F., Krisztin, T., Mitchell, D., Popp, A., Riahi, K., Rogelj, J., ... Stehfest, E. (2018). Climate extremes, land-climate feedbacks and land-use forcing at 1.5°C. *Philosophical Transactions of the Royal Society A: Mathematical, Physical and Engineering Sciences*, 376(2119), 20160450. <https://doi.org/10.1098/rsta.2016.0450>

- Stehfest, E., van Zeist, W.-J., Valin, H., Havlik, P., Popp, A., Kyle, P., Tabeau, A., Mason-D'Croz, D., Hasegawa, T., Bodirsky, B. L., Calvin, K., **Doelman, J. C.**, Fujimori, S., Humpenöder, F., Lotze-Campen, H., van Meijl, H., & Wiebe, K. (2019). Key determinants of global land-use projections. *Nature Communications*, 10(1), 2166. <https://doi.org/10.1038/s41467-019-09945-w>
- Szogs, S., Arneth, A., Anthoni, P., **Doelman, J. C.**, Humpenöder, F., Popp, A., Pugh, T. A. M., & Stehfest, E. (2017). Impact of LULCC on the emission of BVOCs during the 21st century. *Atmospheric Environment*, 165, 73–87. <https://doi.org/https://doi.org/10.1016/j.atmosenv.2017.06.025>
- van der Esch, S., Sewell, A., Bakkenes, M., Berkhout, E., **Doelman, J. C.**, Stehfest, E., Langhans, C., Bouwman, A., ten Brink, B., & Fleskens, L. (2022). The global potential for land restoration: Scenarios for the Global Land Outlook 2.
- van Meijl, H., Havlik, P., Lotze-Campen, H., Stehfest, E., Witzke, P., Domínguez, I. P., Bodirsky, B. L., van Dijk, M., **Doelman, J. C.**, & Fellmann, T. (2018). Comparing impacts of climate change and mitigation on global agriculture by 2050. *Environmental Research Letters*, 13(6), 64021. <https://doi.org/10.1088/1748-9326/aabdc4>
- van Meijl, H., Tabeau, A., Stehfest, E., **Doelman, J. C.**, & Lucas, P. (2020). How food secure are the green, rocky and middle roads: food security effects in different world development paths. *Environmental Research Communications*, 2(3), 31002. <https://doi.org/10.1088/2515-7620/ab7aba>
- van Vuuren, D. P., Bijl, D. L., Bogaart, P., Stehfest, E., Biemans, H., Dekker, S. C., **Doelman, J. C.**, Gernaat, D. E. H. J., & Harmsen, M. (2019). Integrated scenarios to support analysis of the food–energy–water nexus. *Nature Sustainability*, 2(12), 1132–1141. <https://doi.org/10.1038/s41893-019-0418-8>
- van Vuuren, D. P., Stehfest, E., Gernaat, D. E. H. J., Berg, M., Bijl, D. L., Boer, H. S., Daioglou, V., **Doelman, J. C.**, Edelenbosch, O. Y., Harmsen, M., Hof, A., & Sluisveld, M. A. E. (2018). Alternative pathways to the 1.5 °C target reduce the need for negative emission technologies. *Nature Climate Change*, 8(5), 391–397. <https://doi.org/10.1038/s41558-018-0119-8>
- van Vuuren, D. P., Stehfest, E., Gernaat, D. E. H. J., **Doelman, J. C.**, van den Berg, M., Harmsen, M., de Boer, H. S., Bouwman, L. F., Daioglou, V., Edelenbosch, O. Y., Girod, B., Kram, T., Lassaletta, L., Lucas, P. L., van Meijl, H., Müller, C., van Ruijven, B. J., van der Sluis, S., & Tabeau, A. (2017). Energy, land-use and greenhouse gas emissions trajectories under a green growth paradigm. *Global Environmental Change*, 42, 237–250. <https://doi.org/10.1016/j.gloenvcha.2016.05.008>
- van Vuuren, D. P., Stehfest, E., Gernaat, D., de Boer, H.-S., Daioglou, V., **Doelman, J. C.**, Edelenbosch, O., Harmsen, M., van Zeist, W.-J., & van den Berg, M. (2021). The 2021 SSP scenarios of the IMAGE 3.2 model. <https://doi.org/10.31223/X5CG92>
- van Zeist, W.-J., Stehfest, E., **Doelman, J. C.**, Valin, H., Calvin, K., Fujimori, S., Hasegawa, T., Havlik, P., Humpenöder, F., & Kyle, P. (2020). Are scenario projections overly optimistic about future yield progress? *Global Environmental Change*, 64, 102–120. <https://doi.org/10.1016/j.gloenvcha.2020.102120>
- Westhoek, H., **Doelman, J. C.**, Muilwijk, H., & Stehfest, E. (2021). Commentary: Food choices and environmental impacts: Achievements and challenges. *Global Environmental Change*, 71, 102402. <https://doi.org/https://doi.org/10.1016/j.gloenvcha.2021.102402>

